ISSN 0386-5878
Technical Memorandum
of PWRI No.4075

UJNR

TSUKUBA 2007

PROCEEDINGS OF THE 39TH JOINT MEETING OF U.S. - JAPAN PANEL ON WIND AND SEISMIC EFFECTS UJNR

May 14 - 16, 2007

Tsukuba, Japan

Public Works Research Institute

Copyright © (2007) by P.W.R.I.
All rights reserved. No part of this book may be reproduced by any means, nor transmitted, nor translated into a machine language without the written permission of the Chief Executive of P.W.R.I.
この報告書は、土木研究所理事長の承認を得て刊行したものである。したがって、本報告書の全部又は一部の転載、複製は、土木研究所理事長の文書による承認を得ずしてこれを行ってはならない。

Technical Memorandum
of PWRI No. 4075

PROCEEDINGS OF THE 39TH JOINT MEETING OF U.S.-JAPAN PANEL ON WIND AND SEISMIC EFFECTS UJNR

Edited by

Osamu Matsuo, Secretary-General
Japan-side Panel on Wind and Seismic Effects

Synopsis

This publication contains the proceedings of the 39th Joint Meeting of the U.S.-Japan Panel on Wind and Seismic Effects, UJNR. The meeting was held at the National Institute for Land and Infrastructure Management, Tsukuba, Japan during May 14-16, 2007. Thirty-two technical papers were authored for the meeting, which were organized into eight themes; Transportation Systems, Storm Surge and Tsunami, Sustainable Design, for Buildings and Infrastructure - Focus on Natural Disaster Prevention, Dams, Fire Performance of Structures, Geotechnical Engineering and Ground Motion, Next-Generation Building and Infrastructure Systems, Wind Engineering.

Keywords: *wind engineering, earthquake engineering, sustainable design, natural disaster prevention, UJNR*

PREFACE

This publication contains the proceedings of the 39th Joint Meeting of the U.S.-Japan Panel on Wind and Seismic Effects, UJNR. The meeting was held at the National Institute for Land and Infrastructure Management, Tsukuba, Japan during May 14-16, 2007. The proceedings include the program, list of members, task committee reports, and technical papers submitted to the Joint Panel Meeting, and a summary of the technical site visits.

BACKGROUND

Responding to the need for improving engineering and scientific practices through exchange of technical data and information, research personnel and research equipments, the United States and Japan created the U.S.-Japan Cooperative Science Program in 1961. The U.S.-Japan Cooperative Program in Natural Resources (UJNR) was created in January 1964. The objective of UJNR is to exchange information on research results and scientists and engineers in natural resources of benefit of both countries. UJNR is of 18 Panels each responsible for specific technical subjects.

The Panel on Wind and Seismic Effects was established in 1969. Seventeen U.S. and eight Japanese agencies currently participate to develop and exchange technologies aimed at reducing damage from high winds, earthquakes, storm surge, and tsunamis. This work is produced through collaboration between U.S. and Japanese member researchers working in five Task Committees. Each Task Committee focuses on specific technical issues, e.g., geotechnical engineering and ground motion. The Panel provides the vehicle to exchange technical date and information on design and construction of civil engineering infrastructures, buildings, and to exchange high wind and seismic measurement records. Annual Joint Panel Meetings alternate in the U.S. and Japan. These one-week technical meetings including technical site visits provide the forum to discuss on-going research and research results.

The National Institute of Standards and Technology (NIST) provides the U.S.-side chairman and secretary-general. The Public Works Research Institute (PWRI) provides the Japan-side chairman and secretary-general.

These annual Joint Panel Meetings provide the mechanism for interaction with U.S. and Japanese researchers in wind and earthquake engineering which provides opportunities to gain valuable information and to engage in cooperative research. Through these opportunities the Panel member organizations have realized important advances in building and structure technology.

The Panel provides the vehicle to exchange technical data and information on design and construction of civil engineering lifelines, buildings, waterfront, and coastal structures. The data produced by the

Panel influence on-going structural engineering research and contribute to the revision and creation of U.S. building codes and standards. Examples of Panel benefits include:

- Created and exchanged digitized earthquake records used as the basis of design and research for Japan and the U.S.
- Produced full-scale test data that advanced seismic design standards for buildings.
- Translated into English a Port and Harbour Research Institute handbook on *Liquefied Remediation of Reclaimed Land*, A. A. Balkema, The Netherlands, publisher that provided general guidance for the US design profession on remediation of liquefiable soils.
- In collaboration with Japan's Geotechnical Society translated into English a report from the Port and Harbour Research Institute, *Remedial Measures Against Soil Liquefaction: From Investigation and Design to Implementation*, A. A. Balkema, The Netherlands, 1998, publisher that served as background and guidance for the Corps of Engineers in performing dam remediation at Clemson University.
- Developed a protocol for testing bridge columns subjected to earthquake loads that facilitated the exchange of experimental data between both countries. The protocol serves as a basis for FHWA's development of new seismic design criteria for bridge columns.
- Facilitated an USACE Team to Kobe within days after the Kobe Earthquake that allowed access to data and information through performing post disaster investigations. This investigation would not have been possible without the Panel's endorsement.
- Performed joint post disaster investigations whose findings influenced revisions to and development of new seismic design and rehabilitation criteria in the US.
- Accessed a large US and Japan database that helped develop an USACE Guidance Criteria in Geotechnical Engineering.
- Provided access to data to help characterize gravely soils in determining the seismic instability of gravely soils for dams and were used to improve USACE construction criteria.
- Through a Japan Guest Researcher from the Port and Harbour Research Institute working at ERDC/WES, Vicksburg geotechnical research findings were transferred into USACE documents.
- Created a database comparing Japanese and US standard penetration tests to improve prediction of soil liquefaction.
- Influenced the creation of a NIST base isolation research program using data from translated Japan reports into English on base isolation systems.
- Increased awareness of wind engineering practice, problems, and breakthroughs in Japan and the U.S.
- Improved cross-discipline research among wind engineers/meteorologists/sociologists in each country.
- Increased the dissemination of latest research findings in wind engineering, especially post-storm events (typhoons/hurricanes) to each country.
- Stimulated interest to create Joint quick-response storm survey teams with interdisciplinary research thrusts to examine storm damage in both countries.

- Developed field test data for use in aerodynamic retrofit of bridge structures.
- Produced data that advanced retrofit techniques for bridge structures.
- Advanced technology for repairing and strengthening reinforced concrete, steel, and masonry structures, improved in-situ measurement methods for soil liquefaction and stability under seismic loads.
- Created database on storm surge and tsunamis and verified mathematical models of tsunami and storm surge warning systems.
- Established a library resource of current research on wind and earthquake engineering and on storm surge and tsunamis.
- Exchanged more than 200 guest researchers between Japan and the US that has resulted in advancing their respective organizations mission research, advanced the state-of-technology, and provided career growth opportunities for these guest researchers.
- Performed joint research in more than 10 collaborative research projects that resulted in new US seismic design criteria for buildings and bridges.
- Published proceedings of Panel meetings, Task Committee Workshops, and special publications such as List of Panel Publications, translated two-volume series on earthquake resistant construction using base isolation systems, newsletter, website of Panel activities, and more.
- Gained better knowledge of both countries research, design and construction capabilities from in-depth visits to host country's laboratories and building and public works projects. Results of such visits contribute to creation of new Task Committees, agendas for Joint Panel meetings and task committee workshops, special visits of US-Japan researchers, and joint collaborative research.

The Panel's efforts are exemplary of effective joint research and of technology delivery between researchers in the U.S. and Japan. Since its creation, about 2000 papers were presented in 38 Joint Panel Meetings and Task Committee Workshops and over 250 guest researchers were exchanged. The Panel provides important information about the U.S. and Japan's civil engineering thrusts which influence both countries' research and provide the basis for improvements in building and structure codes and standards.

TABLE OF CONTENTS

PREFACE i

AGENDA OF JOINT MEETING AND TECHNICAL SITE VISITS 1

LIST OF PANEL MEMBERS 11

RESOLUTIONS 25

STRATEGIC PLAN 31

PAPERS 41

THEME 1. Transportation Systems 43

FHWA Seismic Retrofitting of Highway Truss Bridges
W. Phillip Yen*, Charles Seim, and Jerome S. O'Connor 45

Bridge Seismic Response Experiment Program Using E-Defense
Kazuhiko Kawashima*, Hiromichi Ukon, and Koichi Kajiwara 57

Integral Connection Seismic Performance Between Precast Girders and Cast-in-Place Bent Caps
Kevin Almer and David Sanders* 67

THEME 2. Storm Surge and Tsunami 79

The Storm Surges in the Seto Inland Sea Caused by Typhoon Chaba (0416) in Japan
Nadao Kohno*, Kazuo Kamakura, and Hiroaki Minematsu 81

Report on Field Survey of Solomon Islands Earthquake Tsunami in April 2007
Takashi Tomita*, Taro Arikawa, Daisuke Tatsumi, Kazuhiko Honda, Hiroshi Higashino, Kazuya Watanabe, and Shigeo Takahashi 90

US National Tsunami Research Plan
Eddie Bernard, Lori Dengler, and Solomon Yim* 96

Storm Surge Forecast System for Floodfighting Warning
Masaya Fukuhama* and Fuminori Kato 105

Analysis of Spillover Process and Development of Estimation Methods of Tsunami Damage in Ports and Surrounding Areas
Katsuya Oda*, Osamu Okamoto, and Kentaro Kumagai 116

THEME 3. Sustainable Design for Buildings and Infrastructure - Focus on Natural Disaster Prevention 129

Development of Safe Infrastructures against Global Changes of Natural Disasters
Masanori Hamada* 131

Grand Challenges for Disaster Reduction – an Overview
Noël Raufaste* 141

Toward the Establishment of a Regional Society that is Safe and Secure from Disasters
Tsuneyoshi Mochizuki*, NILIM "Safe and Secure" Project Team 152
State of the Art Review for Sustainable Building Design and Innovation Technologies
William Roper* 164
Earthquake disaster mitigation policy in Japan
Koji Ikeuchi* and Nobuharu Isago 190
The Public Health Perspective on Hazard Reductions in Indoor Environments
Fuyuen Yip*, Paul Garbe, and Josephine Malilay 197
Quick report on damage to infrastructures and buildings by the 2007 Noto Hanto Earthquake
NILIM, PWRI, BRI and PARI reconnaissance team for the 2007 Noto Hanto Earthquake
(Presented by Keiichi Tamura*) 204

THEME 4. Dams 217

Seismic Design and Evaluation of Concrete Dams – An Engineering Manual
Yusof Ghanaat*, and Anjana K. Chudgar 219
Outline of "Guidelines for Seismic Performance Evaluation of Dams during Large Earthquakes (Draft)"
Nario Yasuda, Kazuhito Shimamoto*, Yoshikazu Yamaguchi, and Takashi Sasaki 236
Lessons Learned from Analysis of the New Orleans Hurricane Protection System
Michael K. Sharp* 248
Calculation Method of Hydrodynamic Pressure in Seismic Response Analysis of Gates
Takashi Sasaki, Tomoya Iwashita*, and Yoshikazu Yamaguchi 265
3D Nonlinear Transient Analysis of Concrete Dams
Victor Saouma*, Yoshihisa Uchita, and Yoshinori Yagome 279

THEME 5. Fire Performance of Structures 295

Ultimate Temperature of Steel Columns subject to Thermal Elongations of Adjacent Beams at Fire
Fuminobu Ozaki* 297
Recent Advances in Fire-Structure Analysis
Dat Duthinh, Kevin McGrattan, and Abed Khaskia (Presented by Joseph Main*) 310
Numerical Analysis of Fire Resistance Tests of Press-formed Steel Columns (BCP325)
Takeshi Okabe* and Mamoru Kohno 320
Fire Resistance Proficiency Testing of Gypsum/Steel-Stud Wall Assemblies
William Grosshandler (Presented by H. S. Lew*) 334

THEME 6. Geotechnical Engineering and Ground Motion 345

Correlation between aspects of slope failures and surface displacement triggered
by the 2005 northern Pakistan earthquake
Hiroshi P. Sato*, Hiroshi Une, and Mikio Tobita 347
Response Health Monitoring of Buildings Using Threshold Drift Ratios - Now an Established Method
Mehmet Celebi* 352
Development of seismic design criteria for river facilities against large earthquakes

Hideki Sugita* and Keiichi Tamura 361

Extraction of Damages by Tsunami from ALOS Image at South Java in 2006
Mayumi Noguchi, Keiko Suzuki, and Toshio Kitahara 369

THEME 7. Next-Generation Building and Infrastructure Systems 373

Damping Ratio Estimation of an Existing 8-story Building Considering Soil-Structure Interaction Using Strong Motion Observation Data
Koichi Morita* 375

Smart Sensing Technology: A New Paradigm for Structural Health Monitoring
Bill F. Spencer Jr., T. Nagayama, Jennifer Rice*, and G.A. Agha 383

THEME 8. Wind Engineering 407

Comparative Inter-Laboratory Study of Wind Loading on Low Industrial Buildings
Bogusz Bienkiewicz , Munehito Endo, Joseph Main*, and William Fritz 409

Damage to Buildings Induced by Tatsumakis in Nobeoka City, Miyazaki and Saroma Town, Hokkaido in 2006
Yasuo Okuda*, Hitomitsu Kikitsu, and Tomonori Murakami 418

Parametric Study of Flutter Derivatives of Bridge Cross Sections and Their Implications on the Aeroelastic Stability of Flexible Bridges
Partha Sarkar*, Luca Caracoglia, and Fred Haan 432

APPENDIX 451

TASK COMMITTEE REPORTS 453

TECHNICAL SITE VISITS 471

AGENDA OF JOINT MEETING AND TECHNICAL SITE VISITS

JOINT MEETING

National Institute for Land and Infrastructure Management
May 14-16, 2007

May 13 (Sunday)

Arrival of U.S.-side Delegation
Hotel: Okura Frontier Hotel Tsukuba Epochal
Phone/Fax: +81-(0)29-860-7700/+81-(0)29-860-7701

May 14 (Monday)

10:00 **Opening Ceremonies** [8F Conference Room]

Call to order by Osamu Matsuo, Secretary-General, Japan-side Panel

Opening remarks by Hiroaki Taniguchi, Vice-Minister for Engineering Affairs, Ministry of Land, Infrastructure and Transport

Remarks by Joyce Rabens, Minister-Counselor for Environment, Science and Technology Affairs, Embassy of the United States of America

Remarks by Takashi Kato, Director, International Science and Technology Affairs Division, Science and Technology Policy Bureau, Ministry of Education, Culture, Sports, Science and Technology

Remarks by Tadahiko Sakamoto, Chairman, Japan-side Panel on Wind and Seismic Effects, Chief Executive, Public Works Research Institute

Remarks by H. S. Lew, Acting Chairman, U.S.-side Panel on Wind and Seismic Effects, Building and Fire Research Laboratory, National Institute of Standards and Technology, Department of Commerce

Introduction of Japan-side Members by Japan-side Panel Chairman

Introduction of U.S.-side Members by U.S.-side Panel Chairman

Elect Joint Panel Meeting Chairman

Adopt Agenda

Adjourn

11:10	Group Photograph
11:30	**Technical Session 1 - Transportation Systems** Chairman – Dr. H. S. Lew
11:30	*FHWA Seismic Retrofitting of Highway Truss Bridges*, W. Phillip Yen*, FHWA; Charles Seim, Consulting Engineer, and Jerome S. O'Connor, MCEER
11:45	*Bridge Seismic Response Experiment Program Using E-Defense*, Kazuhiko Kawashima*, Tokyo Institute of Technology; Hiromichi Ukon and Koichi Kajiwara, NIED
12:00	*Integral Connection Seismic Performance Between Precast Girders and Cast-in-Place Bent Caps*, Kevin Almer and David Sanders*, University of Nevada at Reno
12:15	Discussion
12:30	Lunch [1F Conference Room]
13:30	**Technical Session 2- Storm Surge and Tsunami** Chairman – Dr. H. S. Lew
13:30	*The Storm Surges in the Seto Inland Sea Caused by Typhoon Chaba (0416) in Japan*, Nadao Kohno*, MRI; Kazuo Kamakura, Hiroaki Minematsu, JMA
13:45	*Report on Field Survey of Solomon Islands Earthquake Tsunami in April 2007*, Takashi Tomita*, Taro Arikawa, Daisuke Tatsumi, Kazuhiko Honda, Hiroshi Higashino, Kazuya Watanabe, and Shigeo Takahashi, PARI
14:00	*US National Tsunami Research Plan*, Eddie Bernard, NOAA; Lori Dengler, Humboldt State University; and Solomon Yim*, Oregon State University
14:15	*Storm Surge Forecast System for Floodfighting Warning*, Masaya Fukuhama* and Fuminori Kato, NILIM
14:30	*Analysis of Spillover Process and Development of Estimation Methods of Tsunami Damage in Ports and Surrounding Areas*, Katsuya Oda* and Osamu Okamoto, Kentaro Kumagai, NILIM
14:45	Discussion
15:10	Break

15:30	**Task Committee Meetings**	
	A: Geotechnical Engineering and Ground Motion	[Room #524]
	B: Next-Generation Building and Infrastructure Systems	[8F Conference Room]
	C: Dams	[Room #532]
	D: Wind Engineering	[Room #616]
	G: Transportation Systems	[Room #617]
	H: Storm Surge and Tsunami	[8F Conference Room]
	I: Fire Performance of Structures	[8F Conference Room]
17:00	Conclusion of Day 1	
18:30	Japan-side Panel Hosted Reception (Okura Frontier Hotel Tsukuba)	

May 15 (Tuesday)

9:00	**Technical Session 3 - Sustainable Design for Buildings and Infrastructure - Focus on Natural Disaster Prevention I** Chairman – Dr. Tadahiko Sakamoto
9:00	*Development of Safe Infrastructures against Global Changes of Natural Disasters*, Masanori Hamada*, Waseda University
9:15	*Grand Challenges for Disaster Reduction – an Overview*, Noël Raufaste*, NIST
9:30	*Toward the Establishment of a Regional Society that is Safe and Secure from Disasters*, Tsuneyoshi Mochizuki*, NILIM "Safe and Secure" Project Team
9:45	Discussion
10:00	Break
10:15	**Technical Session 4 - Sustainable Design for Buildings and Infrastructure - Focus on Natural Disaster Prevention II** Chairman – Dr. Tadahiko Sakamoto
10:15	*State of the Art Review for Sustainable Building Design and Innovation Technologies*, William Roper*, George Mason University
10:30	*Earthquake disaster mitigation policy in Japan*, Koji Ikeuchi*, Nobuharu Isago, Cabinet Office
10:45	*The Public Health Perspective on Hazard Reductions in Indoor Environments*, Fuyuen Yip*, Paul Garbe, and Josephine Malilay, Centers for Disease Control and Prevention
11:00	*Quick report on damage to infrastructures and buildings by the 2007 Noto Hanto Earthquake*, NILIM, PWRI, BRI and PARI reconnaissance team for the 2007 Noto Hanto Earthquake (Presented by Keiichi Tamura*, NILIM)

11:15 Discussion

11:35 Break

11:50 **Technical Session 5 – Dams I**
Chairman –Dr. Tadahiko Sakamoto

11:50 *Seismic Design and Evaluation of Concrete Dams – An Engineering Manual*, Yusof Ghanaat*, Quest Structures, Inc.; and Anjana K. Chudgar, Corps

12:05 *Outline of "Guidelines for Seismic Performance Evaluation of Dams during Large Earthquakes (Draft)"*, Nario Yasuda, Kazuhito Shimamoto*, NILIM; Yoshikazu Yamaguchi, Takashi Sasaki, PWRI

12:20 Discussion

12:30 Lunch [1F Conference Room]

13:20 **Technical Session 6 – Dams II**
Chairman –Dr. Tadahiko Sakamoto

13:20 *Lessons Learned from Analysis of the New Orleans Hurricane Protection System*, Michael K. Sharp*, Corps

13:35 *Calculation Method of Hydrodynamic Pressure in Seismic Response Analysis of Gates*, Takashi Sasaki, Tomoya Iwashita* and Yoshikazu Yamaguchi, PWRI

13:50 *3D Nonlinear Transient Analysis of Concrete Dams*, Victor Saouma*, University of Colorado; Yoshihisa Uchita, and Yoshinori Yagome, Tokyo Electric Power Service Company

14:05 Discussion

14:20 Break

14:35 **Technical Session 7 - Fire Performance of Structures**
Chairman –Dr. Tadahiko Sakamoto

14:35 *Ultimate Temperature of Steel Columns subject to Thermal Elongations of Adjacent Beams at Fire*, Fuminobu Ozaki*, Tokyo University of Science

14:50 *Recent Advances in Fire-Structure Analysis*, Dat Duthinh and Kevin McGrattan, NIST; and Abed Khaskia, Mallett Technology (Presented by Joseph Main*, NIST)

15:05 *Numerical Analysis of Fire Resistance Tests of Press-formed Steel Columns (BCP325)*, Takeshi Okabe*, Graduate School of Science and Technology; and Mamoru Kohno, NILIM

15:20 *Fire Resistance Proficiency Testing of Gypsum/Steel-Stud Wall Assemblies*, William Grosshandler, NIST (Presented by H. S. Lew*, NIST)

15:35 Discussion

15:55 Break

16:10 **Strategic Planning Session**

17:10 Conclusion of Day 2

18:30 Individual Japan-side Members Hosted Dinners

May 16 (Wednesday)

9:00 **Technical Session 8 - Geotechnical Engineering and Ground Motion**
Chairman – Dr. H. S. Lew

9:00 *Correlation between aspects of slope failures and surface displacement triggered by the 2005 northern Pakistan earthquake*, Hiroshi P. Sato*, Hiroshi Une and Mikio Tobita, GSI

9:15 *Response Health Monitoring of Buildings Using Threshold Drift Ratios - Now an Established Method*, Mehmet Celebi*, USGS

9:30 *Development of seismic design criteria for river facilities against large earthquakes*, Hideki Sugita*, PWRI; and Keiichi Tamura, NILIM

9:45 Discussion

10:00 Break

10:15 **Technical Session 9 - Next-Generation Building and Infrastructure Systems**
Chairman – Dr. H. S. Lew

10:15 *Damping Ratio Estimation of an Existing 8-story Building Considering Soil-Structure Interaction Using Strong Motion Observation Data*, Koichi Morita*, BRI

10:30 *Smart Sensing Technology: A New Paradigm for Structural Health Monitoring*, Bill F. Spencer Jr., University of Illinois at Urbana-Champaign; T. Nagayama, University of Tokyo; Jennifer Rice* and G.A. Agha, University of Illinois at Urbana-Champaign

10:45 Discussion

10:55 Break

11:10 **Technical Session 10 - Wind Engineering**
Chairman – Dr. H. S. Lew

11:10 *Comparative Inter-Laboratory Study of Wind Loading on Low Industrial Buildings*, Bogusz Bienkiewicz and Munehito Endo, CSU; Joseph Main*, NIST; and William Fritz, Wells Fargo Bank

11:25	*Damage to Buildings Induced by Tatsumakis in Nobeoka City, Miyazaki and Saroma Town, Hokkaido in 2006*, Yasuo Okuda*, Hitomitsu Kikitsu, and Tomonori Murakami, BRI
11:40	*Parametric Study of Flutter Derivatives of Bridge Cross Sections and Their Implications on the Aeroelastic Stability of Flexible Bridges*, Partha Sarkar*, Iowa State University; Luca Caracoglia, Northeastern University; and Fred Haan, Iowa State University
11:55	Discussion
12:10	Lunch [1F Conference Room]
13:00	**Workshop and Task Committee Reports** Chairman – Dr. Tadahiko Sakamoto
14:20	Break
14:40	**Adoption of Final Resolutions** Chairman – Dr. Tadahiko Sakamoto
15:40	Break
15:50	**Closing Ceremonies** Call to order by Osamu Matsuo, Secretary-General, Japan-side Panel Remarks by H. S. Lew, Acting Chairman, U.S.-side Panel on Wind and Seismic Effects Remarks by Tadahiko Sakamoto, Chairman, Japan-side Panel on Wind and Seismic Effects
16:20	Conclusion of 39th Joint Panel Technical Sessions
18:30	U.S.-side Panel Hosted Reception (Restaurant ESPOIR, Epochal Tsukuba International Congress Center)

TECHNICAL SITE VISITS

May 17, Thursday

8:15--10:30	Move to Ohashi Office of Metropolitan Expressway Co Ltd (Meguro, Tokyo) by bus
10:30--12:00	Introduction of operation and maintenance for Metropolitan Expressway
	Fatigue retrofit of steel bridge at Ikejiri on Met Expwy Route 3, Shibuya Line
12:00--15:00	Move to Western Construction Office of Tokyo Metropolitan Government Waterworks Bureau by bus
	Have lunch along the way
15:00--16:30	Seismic retrofit of earthfill dam at Lower Murayama Reservoir
16:30--18:00	Move to hotel by bus
	Stay at Royal Park Shiodome Tower (Shinbashi, Tokyo)

May 18, Friday

9:30--10:00	Move to Shinagawa Intercity by bus
10:00--11:30	Building vibration control system against strong wind (Obayashi Co)
11:30--12:00	Move to Tokyo Terminal by bus
12:36--15:42	Move to Shin-Hanamaki by Bullet train (Yamabiko 53, Have lunch on train)
16:00--18:30	Move to Kamaishi by bus
	Visit Karematsusawa Bridge, one of the largest arch bridges in Japan, along the way
	Stay at Kamaishi Bay City Hotel (Kamaishi City)

May 19, Saturday

8:00-- 8:10	Move to Kamaishi Port Office
8:10--10:00	Visit Tsunami Breakwater, deepest construction water depth in the world, by boat
10:00--14:30	Move to Morioka Station by bus
	Visit Jodo-ga-hama, scenic spot in the Rikuchu Kaigan National Park
	Have lunch along the way
14:40--17:08	Move to Tokyo by Bullet train (Hayate 18)
	Stay at Royal Park Shiodome Tower (Shinbashi, Tokyo)

May 20, Sunday

Departure of US-side Delegation

LIST OF PANEL MEMBERS

U.S.-SIDE DELEGATION

Dr. H. S. Lew
Acting-Chairman, U.S.-side Panel
Materials and Construction Research Division
Building and Fire Research Laboratory
National Institute of Standards and Technology

Mr. Stephen A. Cauffman
Secretary-General, U.S.-side Panel
Leader, Structures Group
Materials and Construction Research Division
Building and Fire Research Laboratory
National Institute of Standards and Technology

Dr. Luca Caracoglia
Assistant Professor
Department of Civil and Environmental Engineering
Northeastern University

Dr. Mehmet K. Celebi
Research Civil Engineer
U.S. Geological Survey
U.S. Department of the Interior

Dr. Anjana Chudgar
U.S. Army Corps of Engineers

Dr. Douglas Foutch
Program Director
Structural Systems and Hazard Mitigation of Structures (SSHM)
National Science Foundation

Dr. Yusof Ghanaat, President
Quest Structures

Dr. Robert L. Hall
Chief, Geosciences and Structures Division
Geotechnical and Structures Laboratory
US Army Engineer Research and Development Center

Dr. Joseph Main
Research Engineer
Building and Fire Research Laboratory
National Institute of Standards and Technology

Dr. Josephine Malilay
Associate Director for Science
Division of Environmental Hazards and Health Effects
National Center for Environmental Health
Centers for Disease Control and Prevention

Mr. Noël Raufaste
NIST Emeritus and Guest Researcher
Building and Fire Research Laboratory
National Institute of Standards and Technology

Ms. Jennifer Rice
Graduate Student
University of Illinois,Champaign

Dr. William E. Roper
School of Computational Sciences
Center for Earth Observing and Space Research
George Mason University

Dr. David Sanders
Professor
Civil and Environmental Engineering Department
University of Nevada, Reno

Dr. Victor E. Saouma
Professor Structural Engineering and mechanics
Department of Civil, Environmental & Architectural Engineering
University of Colorado

Dr. Partha P. Sarkar
Professor and Wilson Chair
Director of Wind Simulation and Testing Laboratory
Department of Aerospace Engineering
Iowa State University

Dr. Michael Sharp
Director, Centrifuge Research Center
Geotechnical and Structures Laboratory
US Army Engineer Research and Development Center

Dr. W. Phillip Yen
Program Manager
Seismic Hazard Mitigation Program
Office of Infrastructure, R&D
Federal Highway Administration

Dr. Solomon C. Yim
Professor
Structural and Ocean Engineering
Oregon State University

Dr. Fuyuen Yip
Epidemiologist
Air Pollution and Respiratory Health Branch,
Division of Environmental Hazards and Health Effects, National Center for Environmental Health,
Centers for Disease Control and Prevention

U.S.-SIDE PANEL ON WIND AND SEISMIC EFFECTS
MEMBERSHIP LIST

Mr. Stephen A. Cauffman
Secretary-General, U.S.-side Panel
Leader, Structures Group
Materials and Construction Research Division
Building and Fire Research Laboratory
National Institute of Standards and Technology

Dr. Kharaiti L. Abrol
Principal Structural Engineering Consultant
Department of Veterans Affairs

Dr. Jon Ake
Geophysicist
Seismotectonics and Geophysics Section
Bureau of Reclamation
U.S. Department of the Interior

Mr. John Baals
Seismic Safety Coordinator
Bureau of Reclamation
U.S. Department of the Interior

Dr. Eddie N. Bernard
Director, Pacific Marine Environmental Laboratory
National Oceanic and Atmospheric Administration
U.S. Department of Commerce

Dr. David M. Boore
U.S. Geological Survey

Dr. Roger D. Borcherdt
U.S. Geological Survey
U.S. Department of the Interior

Dr. Mehmet K. Celebi
Research Civil Engineer
U.S. Geological Survey
U.S. Department of the Interior

Dr. C.Y. Chen
Senior Civil/Geotechnical Engineer
Office of Foreign Buildings
Department of State

Dr. Ken Chong
Program Director
Mechanics and Materials
Engineering Directorate
National Science Foundation

Dr. Anjana Chudgar
Structural Engineer
U.S. Army Corps of Engineers

Ronald T. Eguchi, President
ImageCat, Inc.
Union Bank of California Building

Dr. Amr Elnashai
Director, Mid-America Earthquake Center
Professor of Civil Engineering
University of Illinois

Dr. Douglas Foutch
Program Director
Structural Systems and Hazard Mitigation of
Structures (SSHM)
National Science Foundation

Mr. John Gaynor
Director, Office of Weather and Air Quality
Office of Oceanic and Atmospheric Research
National Oceanic and Atmospheric Administration

Dr. Hamid Ghasemi
Bridge Safety, Reliability and Security
Office of Infrastructure and Security
Office of Infrastructure R&D
Federal Highway Administration

Dr. John Gross
Research Structural Engineer
Materials and Construction Research Division
Building and Fire Research Laboratory
National Institute of Standards and Technology

Dr. William Grosshandler
Chief, Fire Research Division
Building and Fire Research Laboratory
National Institute of Standards and Technology

Dr. Robert L. Hall
Chief, Geosciences and Structures Division
Geotechnical and Structures Laboratory
US Army Engineer Research and Development
Center

Dr. Mary Ellen Hynes
Chief, Earthquake Engineering and Geophysics
Branch
Geotechnical Laboratory
US Army Engineer Research and Development
Center

Dr. Nicholas P. Jones
Dean, Whiting School of Engineering
Johns Hopkins University

Mr. Michael Keever
Chief, Earthquake Engineering Office
Division of Engineering Services
California Department of Transportation

Dr. George C. Lee
Task Director, Multidisciplinary Center for
Earthquake Engineering Research (MCEER)
University at Buffalo

Dr. H.S. Lew
Senior Research Structural Engineer
Materials and Construction Research Division
Building and Fire Research Laboratory
National Institute of Standards and Technology

Mr. Michael Mahoney
Physical Scientist
Federal Emergency Management Agency

Dr. Josephine Malilay
Associate Director for Science (Acting)
Division of Environmental Hazards and Health
Effects
National Center for Environmental Health
Centers for Disease Control and Prevention

Dr. Enrique E. Matheu
Dams Sector Lead
Infrastructure Protection/Risk Management Division
Preparedness Directorate
US Department of Homeland Security

Dr. Vilas Mujumdar
Director, Engineering Research Centers Program
Division of Engineering Education and Centers
(EEC)
National Science Foundation

Mr. Noel Raufaste
NIST Emeritus and Guest Researcher
Building and Fire Research Laboratory
National Institute of Standards and Technology

Dr. William E. Roper
School of Computational Sciences
Center for Earth Observing and Space Research
George Mason University

Dr. Michael Sharp
Technical Director, Civil Works Infrastructure
Geotechnical and Structures Laboratory
US Army Engineer Research and Development
Center

Dr. Charles E. Smith
Senior Technical Advisor
Accident Investigation Board
U. S. Minerals Management Service

Mr. Steven Sweeney
Seismic and Structural Engineering Group
Construction Engineering Research Laboratory
US Army Engineer Research and Development
Center

Dr. Maria I. Todorovska
Research Professor
Department of Civil & Environmental Engineering
University of Southern California

Dr. David Wald
Supervisory Research Geophysicist
Central Geologic Hazards Team
Denver Federal Center
U.S. Geological Survey

Dr. W. Phillip Yen
Program Manager
Seismic Hazard Mitigation Program
Office of Infrastructure, R&D
Federal Highway Administration

Dr. Solomon C. Yim
Professor
Structural and Ocean Engineering
Oregon State University

JAPAN-SIDE PANEL ON WIND AND SEISMIC EFFECTS
MEMBERSHIP LIST

STEERING COMMITTEE MEMBERS

Dr. Tadahiko Sakamoto
Chairman, Japan-side Panel on Wind and Seismic Effects
Chief Executive, Public Works Research Institute

Mr. Osamu Matsuo
Secretary-General, Japan-side Panel on Wind and Seismic Effects
Director, Earthquake Disaster Prevention Research Group
Public Works Research Institute

Mr. Koichi Abe
Director, Office for Disaster Reduction Research
Research and Development Bureau
Ministry of Education, Culture, Sports, Science and Technology

Mr. Jiro Fukui
Director, Structures Research Group
Public Works Research Institute

Mr. Yoshikazu Fukushima
Director, Geographic Department
Geographical Survey Institute
Ministry of Land, Infrastructure and Transport

Dr. Hiroshi Fukuyama
Chief Research Engineer and Research Coordinator
Department of Structural Engineering
Building Research Institute

Mr. Yoshifumi Hara
Director, Disaster Risk Management Division
River Bureau
Ministry of Land, Infrastructure and Transport

Mr. Kinji Hasegawa
Director, Disaster Prevention Office
Coast Administration and Disaster Prevention Division
Ports and Harbors Bureau
Ministry of Land, Infrastructure and Transport

Dr. Hiromichi Higashihara
Director, Earthquake Mitigation Research Center (EDM),
National Research Institute for Earth Science and Disaster Prevention

Dr. Masanori Iiba
Research Coordinator for Disaster Mitigation of Buildings
Research Center for Disaster Risk Management
National Institute for Land and Infrastructure Management
Ministry of Land, Infrastructure and Transport

Dr. Takashi Iijima
President, Civil Engineering Research Laboratory

Mr. Koji Ikeuchi
Director, Earthquake, Volcanic and Catastrophic Flood Disaster Management
Disaster Management Bureau
Cabinet Office

Mr. Jun Inomata
Director, Planning and Research Administration Department
National Institute for Land and Infrastructure Management
Ministry of Land, Infrastructure and Transport

Mr. Yasuyuki Kajiwara
Director, Road Risk Management
Road Bureau
Ministry of Land, Infrastructure and Transport

Mr. Takashi Kaminosono
Director, Structural Engineering Department
Building Research Institute

Dr. Naohito Kawai
Chief Research Engineer, Department of Structural Engineering
Building Research Institute

Prof. Kazuhiko Kawashima
Professor, Department of Civil Engineering
Tokyo Institute of Technology

Dr. Mamoru Kohno
Research Coordinator for Quality Control of Building
Building Department
National Institute for Land and Infrastructure Management
Ministry of Land, Infrastructure and Transport

Mr. Tsuneyoshi Mochizuki
Director-General, National Institute for Land and Infrastructure Management
Ministry of Land, Infrastructure and Transport

Mr. Shigeo Mori
Director, Seismological and Volcanology Research Department
Meteorological Research Institute
Japan Meteorological Agency

Mr. Jun Murakoshi
Team Leader, Bridge Research Team
Structures Research Group
Public Works Research Institute

Dr. Masayoshi Nakashima
Director, Hyogo Earthquake Engineering Center
National Research Institute for Earth Science and Disaster Prevention

Prof. Shinsuke Nakata
Professor, Infrastructure System Engineering Course
Kochi University of Technology

Dr. Jun-ichi Nishikawa
Director, Cold-Region Construction Engineering Research Group
Civil Engineering Research Institute for Cold Region
Public Works Research Institute

Dr. Isao Nishiyama
Director, Building Department,
National Institute for Land and Infrastructure Management

Dr. Hisashi Okada
Director, Research and Testing Laboratory
Japan Housing and Wood Technology Center

Dr. Izuru Okawa
Senior Research Fellow
Department of Structural Engineering
Building Research Institute

Dr. Yasuo Okuda
Chief Research Engineer, Department of Structural Engineering
Building Research Institute

Dr. Hiroshi Sato
Executive Research Coordinator
Public Works Research Institute

Ms. Teruko Sato
Head, Outreach Division
Strategic Planning Department
National Research Institute for Earth Science and Disaster Prevention

Mr. Yasuhiro Shoji
Head, Earthquake Disaster Prevention Division
Research Center for Disaster Risk Management
National Institute for Land and Infrastructure Management
Ministry of Land, Infrastructure and Transport

Dr. Hideki Sugita
Team Leader, Ground Vibration Research Team
Earthquake Disaster Prevention Research Group
Public Works Research Institute

Mr. Hiroki Sunohara
International Codes and Standards
Building Guidance Division
Housing Bureau
Ministry of Land, Infrastructure and Transport

Dr. Kei-ichi Tamura
Research Coordinator for Earthquake Disaster Prevention
Research Center for Disaster Risk Management
National Institute for Land and Infrastructure Management
Ministry of Land, Infrastructure and Transport

Mr. Masaaki Togashi
Director, Typhoon Research Department
Meteorological Research Institute
Japan Meteorological Agency

Dr. Takashi Tomita
Tsunami Research Director
Tsunami Research Center
Port and Airport Research Institute

Mr. Yuichi Toya
Director, Disaster Risk Management Office
Coast Administration and Disaster Reduction Division
Port and Harbors Bureau
Ministry of Land, Infrastructure and Transport

Dr. Shigeki Unjoh
Team Leader, Earthquake Engineering Research Team
Earthquake Disaster Prevention Research Group
Public Works Research Institute

Dr. Yoshikazu Yamaguchi
Team Leader, Dam Structure Research Team
Hydraulic Engineering Research Group
Public Works Research Institute

Mr. Naoyuki Yamane
Director, International Division for Infrastructure
Policy Bureau
Ministry of Land, Infrastructure and Transport

Dr. Hiroyuki Yamanouchi
Chief Executive, Building Research Institute

Mr. Hiroshi Yokoyama
Senior Assistant for Research and Development
Planning Division
Administration Department
Japan Meteorological Agency

Prof. Koichi Yokoyama
Professor, Department of Urban and Civil Engineering
Ibaraki University

Mr. Hitoshi Yoshida
Director, Hydraulic Engineering Research Group
Public Works Research Institute

SECRETARIES COMMITTEE MEMBERS

Mr. Osamu Matsuo
Secretary-General, Japan-side Panel on Wind and Seismic Effects
Director, Earthquake Disaster Prevention Research Group
Public Works Research Institute

Mr. Jiro Fukui
Director, Structures Research Group
Public Works Research Institute

Mr. Yasuhiro Fukushima
Head, Planning Division, Geographic Department
Geographical Survey Institute
Ministry of Land, Infrastructure and Transport

Dr. Hiroshi Fukuyama
Chief Research Engineer and Research Coordinator
Department of Structural Engineering
Building Research Institute

Mr. Hiroyuki Ishikawa
Team Leader, Cold-Region Structure Research Team
Civil Engineering Research Institute for Cold Region
Public Works Research Institute

Dr. Mamoru Kohno
Research Coordinator for Quality Control of Building
Building Department
National Institute for Land and Infrastructure Management
Ministry of Land, Infrastructure and Transport

Dr. Shin Koyama
Chief Research Engineer
Department of Structural Engineering
Building Research Institute

Mr. Akiyoshi Mukai
Head, Structural Standard Division
Building Department
National Institute for Land and Infrastructure Management
Ministry of Land, Infrastructure and Transport

Mr. Jun Murakoshi
Team Leader, Bridge Structure Research Team
Structures Research Group
Public Works Research Institute

Mr. Shoichi Nakatani
Team Leader, Foundation Engineering Team
Structures Research Group
Public Works Research Institute

Dr. Tetsuo Nakazawa
Head, The Second Research Laboratory
Typhoon Research Department
Meteorological Research Institute
Japan Meteorological Agency
Ministry of Land, Infrastructure and Transport

Mr. Tomohiro Naruse
Head, Fire Standards Division
Building Department
National Institute for Land and Infrastructure Management
Ministry of Land, Infrastructure and Transport

Dr. Yasuo Okuda
Chief Research Engineer, Department of Structural Engineering
Building Research Institute

Ms. Teruko Sato
Head, Outreach Division
Strategic Planning Department
National Research Institute for Earth Science and Disaster Prevention

Mr. Yasuhiro Shoji
Head, Earthquake Disaster Prevention Division
Research Center for Disaster Risk Management
National Institute for Land and Infrastructure Management
Ministry of Land, Infrastructure and Transport

Dr. Hideki Sugita
Team Leader, Ground Vibration Research Team
Earthquake Disaster Prevention Research Group
Public Works Research Institute

Dr. Kei-ichi Tamura
Research Coordinator for Earthquake Disaster Prevention
Research Center for Disaster Risk Management
National Institute for Land and Infrastructure Management
Ministry of Land, Infrastructure and Transport

Dr. Takashi Tomita
Tsunami Research Director
Tsunami Research Center
Port and Airport Research Institute

Dr. Shigeki Unjoh
Team Leader, Earthquake Engineering Research Team
Earthquake Disaster Prevention Research Group
Public Works Research Institute

Dr. Yoshikazu Yamaguchi
Team Leader, Dam Structure Research Team
Hydraulic Engineering Research Group
Public Works Research Institute

TEMPORARY MEMBERS

Mr. Masaya Fukuhama	National Institute for Land and Infrastructure Management
Prof. Masanori Hamada	Waseda University
Mr. Tomoya Iwashita	Public Works Research Institute
Mr. Nadao Kohno	Meteorological Research Institute
Dr. Koichi Morita	Building Research Institute
Mr. Katsuya Oda	National Institute for Land and Infrastructure Management
Prof. Takeshi Okabe	Kumamoto University
Dr. Fuminobu Ozaki	Tokyo University of Science
Dr. Hiroshi P. Sato	Geographical Survey Institute
Mr. Kazuhito Shimamoto	National Institute for Land and Infrastructure Management

ASSOCIATE MEMBERS

Mr. Tomomitsu Fujii	Foundation of River Basin Integrated Communications
Dr. Minoru Fujiwara	Strait Crossing Highway Research Association
Dr. Masami Fukuoka	Manegement System Assessment Center
Prof. Masaya Hirosawa	Kogakuin University
Prof. Shiro Ibukiyama	Kogyokusha College of Technology
Dr. Kaoru Ichihara	Central Consultant Inc.
Dr. Takashi Iijima	Civil Engineering Research Laboratory
Mr. Yasutake Inoue	Fukuda Corporation
Dr. Toshio Iwasaki	Public Works Research Center
Mr. Shunichiro Kamijo	KICTEC Inc.
Mr. Kenji Kawakami	Kubota Corporation
Prof. Eiichi Kuribayashi	Professor Emeritus, Toyohashi University of Technology
Mr. Mitsuru Nagao	Japan Construction Mechanization Association
Prof. Kiyoshi Nakano	Nakano Architectural and Engineering Associate
Prof. Shinsuke Nakata	Kochi University of Technology
Dr. Kazuto Nakazawa	Formerly, Public Works Research Center
Dr. Nobuyuki Narita	Public Works Research Center
Dr. Hisashi Okada	Japan Housing and Wood Technology Center
Dr. Michio Okahara	Advanced Construction Technology Center
Dr. Shin Okamoto	P. S. Mitsubishi Construction Co. Ltd.
Mr. Kei-ichi Ohtani	Formerly, National Research Institute for Earth Science and Disaster Prevention
Mr. Yoshijiro Sakagami	Japan Development Construction Corporation
Dr. Yasushi Sasaki	Japan Institute of Construction Engineering
Dr. Yukihiko Sumiyoshi	Central Consultant Inc.
Mr. Jiro Taguchi	Construction Research Institute
Dr. Masateru Tominaga	Public Works Research Center
Dr. Hajime Tsuchida	Echo Corporation
Mr. Seizo Tsuji	Japan Utility Subway Company Inc.
Prof. Koichi Yokoyama	Ibaraki University

TASK COMMITTEE MEMBERS

* denotes Task Committee Chair.

A. Geotechnical Engineering and Ground Motion

Mehmet K. Celebi*	USGS
Michael K. Sharp*	USACE-ERDC
David M. Boore	USGS
Roger D. Borcherdt	USGS
Harish Chander	DOE
Mary E. Hynes	USACE-ERDC
Joseph P. Koester	USACE-ERDC
Richard S. Olsen	USACE-ERDC
Erdal Safak	USGS
Donald E. Yule	USACE-ERDC
Keiichi Tamura*	National Institute for Land and Infrastructure Management
Takahiro Sugano*	Port and Airport Research Institute
Hiroyuki Fujiwara	National Research Institute for Earth Science and Disaster Prevention
Shin Koyama	Building Research Institute
Osamu Matsuo	Public Works Research Institute
Chikahiro Minowa	National Research Institute for Earth Science and Disaster Prevention
Shoichi Nakatani	Public Works Research Institute
Satoshi Nishimoto	Public Works Research Institute
Atsushi Nozu	Port and Airport Research Institute
Izuru Okawa	Building Research Institute
Yasuhiro Shoji	National Institute for Land and Infrastructure Management
Hideki Sugita	Public Works Research Institute
Hideki Uehara	NTT Access Network Service Systems Laboratories

B. Next-Generation Building and Infrastructure Systems

George C. Lee*	MCEER
Douglas Foutch*	NSF
Fu-Kuo Chang	Stanford University
Mete A. Sozen	Purdue University
B. F. Spencer	University of Illinois
K. Thirumalai	DOT
Ming Wang	University of Illinois
Hiroshi Fukuyama*	Building Research Institute
Masayoshi Nakashima*	National Research Institute for Earth Science and Disaster Prevention
Namihiko Inoue	Building Research Institute
Yoshihiro Iwata	Building Research Institute
Takashi Kaminosono	Building Research Institute
Koichi Kusunoki	Yokohama National University
Chikahiro Minowa	National Research Institute for Earth Science and Disaster Prevention
Koichi Morita	Building Research Institute
Akiyoshi Mukai	National Institute for Land and Infrastructure Management
Isao Nishiyama	National Institute for Land and Infrastructure Management
Taiki Saito	Building Research Institute
Hitoshi Shiobara	University of Tokyo
Masaomi Teshigawara	Nagoya University
Shigeki Unjoh	Public Works Research Institute
Akira Wada	Tokyo Institute of Technology

C. Dams

Robert L. Hall*	USACE-ERDC
Enrique E. Matheu*	Louisiana State University
Anjuna Chudgar	USACE
Richard C. Dove	USACE-ERDC

Ziyad H. Duron	Harvey Mudd College
Larry K. Nuss	U.S. Bureau of Reclamation
Richard S. Olsen	USACE-ERDC
Rick Poeppelman	USACE
Donald E. Yule	USACE-ERDC
Yoshikazu Yamaguchi*	Public Works Research Institute
Noriaki Hakoishi	Public Works Research Institute
Takashi Ikeda	Japan Dam Engineering Center
Tomoya Iwashita	Public Works Research Institute
Hideharu Norimatsu	Japan Water Agency
Tatsuo Ohmachi	Tokyo Institute of Technology
Yoshio Ohne	Aichi Institute of Technology
Wataru Ohnishi	Japan Institute of Construction Engineering
Hiroyuki Satoh	Public Works Research Institute
Choshiro Tamura	University of Tokyo
Nario Yasuda	National Institute for Land and Infrastructure Management
Hitoshi Yoshida	Public Works Research Institute

D. Wind Engineering

John Gaynor*	NOAA
Nicholas P. Jones*	Johns Hopkins University
Earl J. Baker	Florida State University
Bogusz Bienkiewicz	Colorado State University
Harold Bosch	FHWA
Donald Burgess	NOAA
Ahsan Kareem	University of Notre Dame
Joseph Main	NIST
Mark D. Powell	NOAA
Liz Ritchie	University of New Mexico
Partha Sarkar	Iowa State University
Emil Simiu	NIST
Yasuo Okuda*	Building Research Institute
Jun Murakoshi*	Public Works Research Institute
Hiroshi Katsuchi	Yokohama National University
Hiromasa Kawai	Kyoto University
Hitomitsu Kikitsu	Building Research Institute
Kichiro Kimura	Kyushu Institute of Technology
Masao Mikami	Meteorological Research Institute
Hisashi Okada	Japan Housing and Wood Technology Center
Hiromichi Shirato	Kyoto University
Tetsuro Tamura	Tokyo Institute of Technology
Yukio Tamura	Tokyo Institute of Polytechnics
Masaaki Togashi	Meteorological Research Institute
Yasushi Uematsu	Tohoku University
Ikuo Yamada	Honshu-Shikoku Bridge Expressway Company Limited

G. Transportation Systems

W. Phillip Yen*	FHWA
Hamid Ghasemi	FHWA
Harold Bosch	FHWA
Michel Bruneau	MCEER
Nicholas P. Jones	Johns Hopkins University
David H. Sanders	University of Nevada
Peter Chang	University of Maryland
Jiro Fukui *	Public Works Research Institute
Yozo Fujino	University of Tokyo
Kensaku Hata	Honshu-Shikoku Bridge Expressway Company Limited
Yasuo Inokuma	Central Nippon Expressway Company Limited
Hiroyuki Ishikawa	Public Works Research Institute
Yasushi Josen	Public Works Research Institute

Kazuhiko Kawashima	Tokyo Institute of Technology
Motoki Kazama	Tohoku University
Osamu Matsuo	Public Works Research Institute
Jun Murakoshi	Public Works Research Institute
Toshihiko Naganuma	Hanshin Expressway Company Limited
Shoichi Nakatani	Public Works Research Institute
Atsushi Nozu	Port and Airport Research Institute
Katsuya Oda	National Institute for Land and Infrastructure Management
Naoyuki Odagiri	Metropolitan Expressway Company Limited
Masahiro Shirato	Public Works Research Institute
Takahiro Sugano	Port and Airport Research Institute
Takeshi Sugimoto	Public Works Research Institute
Hideki Sugita	Public Works Research Institute
Akihiro Takahashi	Public Works Research Institute
Takashi Tamakoshi	National Institute for Land and Infrastructure Management
Keiichi Tamura	National Institute for Land and Infrastructure Management
Shigeki Unjoh	Public Works Research Institute
Koichi Yokoyama	Ibaraki University
Shigeji Yoshida	Honshu-Shikoku Bridge Expressway Company Limited

H. Storm Surge and Tsunami

Solomon C. Yim*	OSU
Eddie Bernard*	NOAA
Michael Briggs	USACE
Frank Gonzalez	NOAA
Laura Kong	ITIC
Harry Yeh	OSU
Philip Liu	Cornell University
Takashi Tomita*	Port and Airport Research Institute
Koji Fujima	National Defense Academy of Japan
Masaya Fukuhama	National Institute for Land and Infrastructure Management
Fumihiko Imamura	Tohoku University
Hiroyasu Kawai	Port and Airport Research Institute
Katsuya Oda	National Institute for Land and Infrastructure Management

I. Fire Performance of Structures

William Grosshandler*	NIST
John Gross*	NIST
Paul DesJardin	University at Buffalo
Jay Gore	Purdue University
Mamoru Kohno*	National Institute for Land and Infrastructure Management
Ichiro Hagiwara*	Building Research Institute
Tomohiro Naruse	National Institute for Land and Infrastructure Management

RESOLUTIONS

RESOLUTIONS OF THE THIRTY-NINTH JOINT MEETING U.S.-JAPAN PANEL ON WIND AND SEISMIC EFFECTS (UJNR)

National Institute for Land and Infrastructure Management, Tsukuba, Japan
14-16 May, 2007

The following resolutions are hereby adopted:

1. The Thirty-ninth Joint Panel Meeting provided the forum to exchange valuable technical information that is beneficial to both countries. In view of the importance of cooperative programs on the subject of wind and seismic effects, the continuation of Joint Panel Meetings is considered essential. Both sides agreed to follow the recommendations of the Panel's 2nd Five-Year Strategic Plan and will give emphasis to identifying opportunities, primarily through the seven Task Committees, and to share and develop technologies that lead to new design and construction practices, and provide users with improved procedures.

2. The following activities have been conducted since the Thirty-eighth Joint Meeting:

   a. Technology Exchanges. Technical experts and technical documents have been exchanged. These exchanges have contributed to the development of new research and enhanced ongoing research programs in both countries.

   b. Task Committee Workshops. The Panel held five workshops:
      1) Task Committee (A), 4th Workshop on Soil-Structure Interaction, 28-30 March 2007, Tsukuba, Japan
      2) Task Committee (B), Workshop on Next Generation Buildings, 25-26 February 2007, Hawaii, U.S.
      3) Task Committee (D), 4th Workshop on Wind Engineering, New Challenges for Reduction of High-Wind Disasters, 20-22 July 2006, Tsukuba, Japan
      4) Task Committee (G), 22nd U.S.-Japan Bridge Engineering Workshop, 23-25 October 2006, Seattle, US.
      5) Task Committee (H), 3 rd International Workshop on Coastal Disaster Prevention, 12-13 February 2007, Colombo, Sri Lanka.

   c. Major Products. The Panel members produced or made significant contributions to the following major products:
      1) Task Committee (A) Japan members contributed to issuing the Japan Guidelines on Seismic Performance Verification of River Facilities (Draft) which include geotechnical works.

2) The Workshop of Task Committee (B) resulted in a process to develop a five-year strategic research plan that addresses high-performance buildings' abilities to better resist the effects from extreme wind, earthquakes, and fire loads and to effect informed decisions about design procedures that incorporate environmental quality and sustainability of occupant health and life cycle systems.
3) Task Committee (C) conducted collaborative research on non-linear analysis of concrete dams.
4) Task Committee (G) developed seismic performance testing guidelines for bridge piers.
5) Task Committee (H), through several US-side members, developed the US National Tsunami Research Plan.

3. The Panel accepted the Task Committee reports presented during the Thirty-ninth Joint Panel Meeting. Each report included objectives, scope of work, accomplishments and future plans.

4. The Panel continues to work toward streamlining its structure and encouraging the collaboration of researchers in both countries.

5. The Panel conducted its annual Strategic Planning Session. Based on its 2nd Five-Year Strategic Plan, the Panel evaluated its accomplishments and Task Committees activities and recommended the following actions:
   a. More broadly and quickly disseminate and share TC publication
   b. Facilitate the use of e-mail and the Panel's eNewsletter, and Web Site for information sharing and dissemination.
   c. Encourage partnering opportunities identified by respective Task Committee

6. The Panel endorses the following four proposed Task Committee Workshops during the coming year:
   a. Task Committee (B), 2nd Workshop on Next Generation Infrastructure Systems, 2007
   b. Task Committee (C), 4th US – Japan Workshop on Advanced Research for Dams, 17 May 2007, Tsukuba
   c. Task Committee (G), 23rd US – Japan Bridge Engineering Workshop, fall 2007, Japan
   d. Task Committee (H), 4 th International Workshop on Coastal Disaster Prevention, Fall 2007, Colombo, Sri Lanka.

In the event that T/C co-chairs recommend conducting a joint meeting or workshop

prior to the next annual meeting, that is not included in the above list, the T/C co-chairs will make a request to conduct the meeting through their respective Secretary-General for approval by the Joint Panel Chairmen.

7. The Panel encourages continued cooperative research interactions between the National Science Foundation's Network for Earthquake Engineering Simulation (NSF/NEES) and Ministry of Education, Culture, Sports, Science and Technology/National Research Institute for Earth Science and Disaster Prevention's E-Defense (MEXT/NIED).

8. The U.S. and Japan sides will plan and conduct, as appropriate, joint investigations following earthquake, wind, and fire disasters in the U.S. and Japan.

9. The results of the Panel's work should be widely disseminated to improve the quality of life globally. The Panel will make use of the internet to the extent possible to disseminate its accumulated and timely information.

10. The Fortieth Joint Panel Meeting of the UJNR Panel on Wind and Seismic Effects will be organized by the U.S.-side Panel, to be held at NIST in May 2008. The U.S.-side secretariat will propose dates, program, location, and itinerary with the concurrence of the Japan-side Panel.

STRATEGIC PLAN

ADDENDUM 1
Panel Expectations During 2006-2010

STRATEGIC PLAN
U.S.-JAPAN JOINT PANEL ON WIND AND SEISMIC EFFECTS
(May 2006)

1. INTRODUCTION

This document is Addendum 1 of the Strategic Plan for the US-Japan Panel on Wind and Seismic Effects 2001-2005 (attachment). The Panel's 2001 Strategic Plan serves as the base of the Panel's operations and structure. This Addendum 1 provides a roadmap of outlined technical approaches for the Panel's operations during the next five-year period 2006-2010. As background, the Panel's Charter, developed in 1987 at the 19th Joint Panel Meeting, is to:

a. Encourage, develop, and implement the exchange of wind and seismic technology between appropriate US and Japanese organizations to share scientific and technological knowledge.
b. Develop strong technical links of scientific and engineering researchers between the two countries and encourage exchanges of guest researchers.
c. Conduct joint research in areas of winds and seismic technology including exchange of available research equipment and facilities in both countries. Publish findings from joint research efforts.
d. Conduct cooperative programs to improve engineering design and construction practices and other wind and earthquake hazard mitigation practices. Publish results from cooperative programs.

2. Panel Approaches During 2006-2010

The Panel's operational procedure is defined in the attached Strategic Plan (2001-2005). Annually the Panel performs a self-evaluation during a Strategic Planning session held during its May Joint Panel Meeting. Based on the Panel's evaluation, incremental modifications are carried out to enhance the Panel's operations and to bring 'value-added' to its users.

2.1 Panel Mission and Vision for 2006-2010

1. Continue performing post disaster investigations and reconnaissance and sharing findings with Panel members and others as was carried out for:
   a) Earthquakes: (2004 Niigata, 2004 Indonesia, 2005 Pakistan, and others)
   b) Typhoons and Hurricanes: (2005 Katrina and Rita, 2004 Typhoon)
2. Share US and Japan National Disaster Mitigation Plan among the Panel members such as:
   a) USA. NSTC/SDR: *Grand Challenge for Disaster Prevention- a 10-year strategy*

for disaster reduction through science and technology; *Windstorm Impact Reduction Implementation Plan*; the NEHRP Annual Plan.

b) Japan. *Central Disaster Prevention Council: Reduction by half of human damage and economic damage in coming 10 years*, Technology Development Plan at "Council for Science and Technology"

3. Identify methods that support each countries efforts in disaster mitigation through cooperation between the US and Japan and explore opportunities for joint research projects.
4. During 2006-2010 the Panel will focus on topics such as:
   a) Continue to understand causes and effects of wind and seismic hazards and pursue the accumulation and interpretation of data
   b) Evaluate and estimate risk of natural hazards
   c) Improve/develop disaster mitigation technology and methodology, and dissemination of disaster response technology into practical applications
   d) Promote attention to increase research that considers societal implications of natural disasters
   e) Integrate technology development and the viewpoint of social/civil engineering by increasing the importance of the cooperative works between related UJNR Panels, the Panel's Task Committees, and the private sector and academia
   f) Create methods to better integrate comprehensive technology information as a base for transmitting information throughout the Panel member's organizations
   g) Contribute to dissemination of cooperative products that will facilitate global standardization of related civil engineering technologies

2.2. Evaluate Task Committees. The Panel operates under seven Task Committees; an optimum number for Panel management and productivity. The Task Committees serve as the heart of the Panel's operations:

Task Committee A. Geotechnical Engineering and Ground Motion
Task Committee B. Next Generation Building and Infrastructure Systems
Task Committee C. Dams
Task Committee D. Wind Engineering
Task Committee G. Transportation Systems
Task Committee H. Storm Surge and Tsunami
Task Committee I. Fire Performance of Structures

Findings from Task Committees' evaluations will help the Task Committees 1) measure achievements, productivity, and impact on contributions to improving design and construction practices, 2) identify opportunities for making contributions and addressing emerging technical challenges, and 3) assess when they completed their mission and are ready for retirement. Task Committee Evaluation Criteria includes: 1) one or more workshop conducted

at least every three-years, 2) implementing recommendations from workshops, 3) publications and other outreach, and 4) collaborations beyond their Task Committee.

The Panel will encourage its respective Task Committees to identify thematic focuses requiring technology sharing and joint collaborations. These Themes will be discussed at annual Panel Meetings. The Panel will consider the merits of creating new Task Committees that meet special needs and eliminating Task Committees that have completed their mission or can be strengthened through consolidation with other Task Committee(s).

2.3. Partnering Opportunities. Identify partnering opportunities through clustering appropriate Panel's Task Committees, collaborating with other UJNR Panels, and working together with the private sector and academia. Clustering provides Task Committee optimization of resources (human and financial). Partnering and clustering will be discussed at annual Panel Meetings including increasing participation from the private sector and academia.

2.4. Joint Research. Perform joint research initiated by the Panel and its Task Committees. The Task Committees are encouraged to identify key joint-research opportunities to improve the state-of-knowledge or to consider engaging in a significant long-term research funded from one or more sponsoring organizations. For the latter, below are the Panel Cooperative Research Projects performed during the past 27-years that improved design and construction practices for both countries.

1. Reinforced Concrete Structures (1979-1987), accomplishments include testing six-story full scale buildings which led to improve seismic design methods of reinforced concrete buildings.
2. Seismic Performance of Lifeline Facilities (1982-1989); accomplishments included development of improved seismic design methods of bridge columns.
3. *In-situ* Testing Methods for Soil Liquefaction (1983-1986); accomplishments include development of rationale for Standard Penetration Test (SPT) data based on energy ratio.
4. Masonry Structures (1984-1988); accomplishments include development of strength-based design guidelines for reinforced masonry buildings.
5. Steel-Frame Structures (1985-1987); accomplishments include testing of a full-scale five-story building to confirm prediction of performance based on components and subassemblages.
6. Bridge Hybrid Control Systems (1990-1994); accomplishments include development of hybrid control algorithms that require less energy for controlling bridge response.
7. Precast Seismic Structural Systems (1991-1992); accomplishments include development of strength-based design guidelines.
8. Seismic Performance of Composite and Hybrid Structures (1993-1998);

accomplishments include development of design guidelines for composite and hybrid system, and development of new materials.

9. Countermeasures for Soil Liquefaction (1994-2004); accomplishments include contributions on the revision of design guidelines for building foundations and formulation of soil experiment plans using E-Defence.
10. Development of Smart Structural Systems (1998-2003); accomplishments include development of structural performance detection technology and structural members using intelligent materials.
11. Develop Comparative Analysis of Seismic Performance Testing Guidelines for Bridge Piers (1999-2006); accomplishments included a joint publication on the comparative analysis of US and Japan bridge piers.

The respective Task Committees will identify candidate joint research for discussion at annual Panel meetings.

2.5. Panel Communications. More broadly disseminate Panel's activities, accomplishments, and impacts including findings from post-disaster investigations using the Panel's eNewsletter, a more active Web Site, Task Committee publications, and identify Panel accomplishments and impacts. The Panel will increase information sharing among its member organizations and include links to related organizations in both countries. Task Committees will serve as a knowledge base of information on their respective themes and share their information to users following methods described above.

3. Conclusion

This Addendum represents the Panel's focus to address panel's activities of the next five-years. The strategic plan is annually evaluated during its annual May Meetings.

U.S.-Japan Joint Panel on Wind and Seismic Effects
Strategic Plan
(May 2001)

1. Introduction

1.1 Context

The U.S. and Japan must maintain an awareness of international developments in earthquake and wind mitigation technology. The international exchange of information is achieved through a combination of formal and informal mechanisms, including: attendance at conferences and workshops; cooperative research projects and programs; and exchange of scientists and engineers. There is a long-established tradition of joint research activities between Japan and the United States. The U.S.-Japan Cooperative Program in Natural Resources (UJNR) Panel on Wind and Seismic Effects (WSE Panel) provides a formal government-to-government mechanism for cooperation between the two countries in the area of earthquake and wind mitigation technology.

At the 32nd Joint Panel Meeting, a resolution was passed to establish a joint Ad-Hoc Committee for the purpose of developing a strategic plan for the WSE Panel. The catalyst for this effort was the need to address immediate issues related to cost and participation. While the Panel recognized the importance of addressing these immediate issues, it also realized that an opportunity existed to strengthen the WSE Panel's focus on its core mission and foster greater collaboration between researchers in the U.S. and Japan while streamlining the overall operation of the Panel. It was with this goal in mind that the ad-hoc committee developed the strategic plan contained in this document.

1.2 Approach

Before meeting to develop the strategic plan, each side held domestic panel meetings and conducted one-on-one meetings with participating agencies to identify issues that needed to be addressed by the strategic plan and to understand which features of the Panel and its operation should be retained and which needed to be changed or adapted to meet current and future needs. Each side developed a concept paper to capture these ideas. The concept papers, however, tended to focus on addressing the immediate issues rather than positioning the Panel to address the needs and challenges of the future. Through the exchange of the concept papers and subsequent discussion, the two sides moved close to agreement on near-term changes to the Panel's operation. Thus, the strategic plan emphasizes longer-term goals for the operation and growth of the Panel and a time-phased approach to implementation of steps to achieve these goals.

The strategic plan is intended to establish a course for the WSE Panel over the next 5-10 years. It recognizes that there are many ways in which the Panel may work to achieve the goals identified, and so while some steps in the implementation process are clear, others are left open to be determined through experimentation. However, the Panel believes working toward the goals identified will strengthen its role in engineering and scientific communities of the U.S. and Japan and will allow our countries to make more efficient use of resources to conduct research and disseminate results to the benefit of both countries.

2. ROLE OF THE PANEL

2.1 Guide Research Agendas

As a government-to-government mechanism for collaboration, the WSE Panel is in a unique position to guide the development and execution of each country's research agenda. Currently, each country defines its own research priorities, projects are formulated in a fragmented manner, and results are reported through vehicles such as the Annual Joint Panel

Meeting. By strengthening its ties to industry and academia, the Panel will be able to identify specific research needs and align those with government priorities. The Panel shall work toward a coordinated research agenda that permits the efficient use of human resources, funding, and research facilities to achieve mutual research objectives.

The new Task Committees formed through implementation of this strategic plan shall work to identify areas where joint research projects can be established and conducted as a part of a coordinated research agenda. Joint research projects may include participation by university or industry researchers in addition to member agency researchers.

2.2 Leverage Resources

The U.S. and Japan each possess significant expertise in the fields of earthquake and wind engineering and have a substantial investment in equipment and facilities to perform testing and measurements in support of research in these fields. Historically, the WSE Panel has facilitated the exchange of researchers between the U.S. and Japan but has not made a concerted effort to leverage the resources of the two countries. There is an opportunity for the Panel to coordinate research activities to efficiently utilize testing and measurement facilities in both countries to address mutual research needs and avoid duplication. This is an area in which the Panel can significantly strengthen its efforts and provide a tangible benefit to each country by working to establish strong partnerships for coordinated research.

2.3 Foster Cooperation

From its founding, the WSE Panel has promoted cooperation between the U.S. and Japan through annual Joint Panel Meetings, Task Committee activities, and exchange of researchers. One of the hallmarks of success for the WSE Panel through the years has been the high level of cooperation. The model these cooperative efforts have been built around, however, is one of information exchange. While the exchange of information and research results is an important facet of the WSE Panel's work, there is the opportunity to greatly expand the scope and importance of cooperative efforts to leverage resources (people, funding, facilities) through joint research projects of bilateral importance. Additionally, the Panel should look beyond the government agencies that participate to be more inclusive of universities and the private sector. At a minimum, this will include broadening participation in the Joint Panel Meetings to include industry and university participants. As industry and universities become more engaged, exchanges of researchers among government, university, and industry participants may be possible. Joint programs that include participation by government, industry, and university partners shall also be considered. These activities would broaden the reach of the Panel and provide a means for more rapid diffusion of research results into practice.

2.4 Technical Exchange

The WSE Panel has, throughout its history, been an effective mechanism for the exchange of technical information between Japan and the United States. Further, the WSE Panel has provided a means for disseminating measurements and research results to other nations affected by earthquake, wind, tsunami, and storm surge hazards. Annual Joint Panel Meetings, Task Committee Meetings and Workshops, researcher exchange programs, and personal relationships among researchers have fostered this exchange. The Panel recognizes this as one of its strengths and should seek to broaden its reach to include participation by researchers in other nations. The Panel should explore means of increasing collaboration with other countries through inclusion of representatives from other nations in Joint Panel Meetings, encouraging joint projects through the Task Committees that include partners outside the U.S. and Japan, and through the exchange of researchers with other countries.

2.5 Engage Private Sector

The WSE Panel has engaged the private sector to a limited extent in its activities during its history, although the work of the Panel and the participating agencies can have a direct benefit to industry and ultimately the public in our respective countries. Further, some larger companies have research capabilities and programs that could enrich the Panel. More

actively engaging the private sector will provide a means for obtaining input in setting priorities and for more rapidly diffusing the results of research activities into practice within Japan and the United States. The involvement of the private sector may include participation in the development of coordinated research agendas and dissemination of information perhaps through special sessions at the annual Joint Panel Meetings. The Panel should also consider involving the private sector in research projects coordinated at the Task Committee level that will have broad-based benefits to industry in both countries. Longer-term, the involvement of the private sector will facilitate dialogue between practicing engineers and builders in Japan with their counterparts in the U.S. The Joint Panel will examine ways to increase industry participation, initially by inviting key industry representatives to participate in Joint Panel Meetings and to speak about the work of their company or organization and explore possibilities for greater collaboration.

2.6 Web Page Development

The Joint Panel will explore ways to increase utilization of the Internet as a means of communication both among Panel members and with outside organizations. The Japan-side has offered to take the lead in developing an Internet presence for the Joint Panel and has begun work on an initial concept for the site. Once the site is established, the Task Committees will be relied on to provide, maintain, and update content related to their activities. The Joint Panel will also explore ways of using Internet resources as a means of facilitating communication among researchers as well as the exchange and dissemination of information and research results.

3. IMPLEMENTATION

3.1 Strategic Plan Development and Approval

This strategic plan was prepared through the efforts of the Joint Ad-Hoc Committee appointed by the Chairmen following the 32nd Joint Panel Meeting. The Joint Panel shall work toward approval of the Strategic Plan during the 33rd Joint Panel Meeting May 28-30, 2001. The approved document will reflect comments received from Panel members on the draft. Implementation of the strategic plan will begin with approval and require 12-24 months for full implementation.

3.2 Task Committee Charters and Recommended Committees

The US- and Japan-side Panels have agreed on the following seven themes around which Task Committees may be formed:

- Theme A: Geotechnical Engineering and Ground Motion
- Theme B: Buildings
- Theme C: Dams
- Theme D: Wind
- Theme E: Lifelines
- Theme F: Seismic Information and IT
- Theme G: Transportation
- Theme H: Storm Surge and Tsunami
- Theme I: Public Health

Task Committee formed to address one of these themes will be approved by the Joint Panel on annual basis, provided that the Task Committee remains active. The criteria for active Task Committees are following:

a) Conducts joint workshops or technical meetings on a regular basis for the purpose of exchanging technical information, research results, or data for the mutual benefit of both countries.

b) Engages in frequent exchange of researchers for the purpose of technical interchange and collaboration on research.
c) Conducts one or more joint research projects having clearly defined technical objectives, finite duration, and shared responsibility for producing technical results.

Task Committees will report results through papers presented during the joint panel meeting and through task committee reports. The Joint Panel will review task committee results and future plans on an annual basis and will approve task committees for the next year based on this information.

For this year, new task committees may be established by requesting approval through the Secretary-Generals at any time before the 34th Joint Panel Meeting.

3.3 Transition to New Annual Panel Meeting Format

A number of alternative formats for the annual Joint Panel Meeting were considered. Based upon the input received from Panel members, the basic format of the Joint Panel Meeting be retained. Session topics will be principally driven by the Task Committees. Each Task Committee would be given one session during which it would be able to present research results. This Task Committee-driven format should strengthen the role of the Task Committees and is intended to stimulate greater cooperation among researchers in each country. This format will foster the exchange of information that many have expressed is a desirable feature of the Joint Panel Meeting.

The Joint Panel meeting will be shortened by one day (from 4 days to 3 days). The shorter meeting, coupled with a shorter Technical Site Tour will reduce the time commitment for participants to one week. This is intended to encourage greater participation in the Panel Meetings and Site Tours, particularly by members of the visiting Panel.

Finally, the Joint Panel will explore streamlining the Joint Panel Meeting to maximize the opportunity for technical exchange.

The shortened Panel Meeting/Technical Site Tour format is implemented for the first time at the 33rd Joint Panel Meeting. The Task Committee-driven technical meeting format will be implemented at a later date when the revised Task Committee organization is in place.

4. CONCLUSION

The plan outlined above represents a strategic plan for positioning the Joint Panel to meet the challenges of the future, while retaining those aspects that have contributed to its success through it 32 year history. This plan is intended to address the current realities of the Panel, as well as increase the value and contribution of the Panel to the U.S. and Japan. Full implementation of the strategic plan will take approximately two years.

PAPERS

THEME 1

Transportation Systems

FHWA Seismic Retrofitting of Highway Truss Bridges

by

W. Phillip Yen, Ph.D. P.E.[1]; Charles Seim, P.E.[2]; and Jerome S. O'Connor, P.E.[3]

ABSTRACT

This paper presents a summary of the recently released document entitled *Seismic Retrofitting Guidelines for Complex Steel Truss Highway Bridges* (referred to here as the Guidelines). The Federal Highway Administration (FHWA), commissioned MCEER (formally known as the Multidisciplinary Center for Earthquake Engineering) to develop guidelines for seismic retrofitting of steel truss highway bridges as part of a larger research project. The Guidelines list various types and articulations of trusses and define bridge performance levels under the actions of a lower-level (LL) and an upper-level (UL) earthquake. The Guidelines present methods of structural analysis, from simple linear-elastic to dynamic non-linear, time-history, to determine demand on the structure. Methods are presented for determining the capacities of the truss members and there are several examples of retrofit strategies.

KEYWORDS: bridge, truss, retrofit, retrofitting, seismic.

1.0 INTRODUCTION

The AASHTO Standard Specifications cover seismic design and construction for ordinary highway bridges with spans less than 150 m and a 75-year design life. No present specifications cover the seismic retrofit of highway truss bridges with design life over 75 years; with spans longer than 150 m; with multiple truss spans, unusual geometry, or unusual mass and stiffness distribution. The Guidelines are specifically written to include both the seismic retrofit of these complex truss bridges and the seismic retrofit of standard truss bridges.

Seismic Retrofitting Guidelines for Complex Steel Truss Highway Bridges *was produced by MCEER at the University at Buffalo under the sponsorship of the FHWA. It extends the state of practice for seismically retrofitting steel truss bridges on the highway system within the United States, using research advances in seismic engineering and recent experiences from steel truss highway bridge seismic retrofitting projects.*

During the last century, trusses were the bridges of choice for highway structures requiring long, high, or multi-spanned crossings. Throughout the USA, truss bridges were built in a variety of types and configurations, and in locations varying from very high to very low seismicity. Although the number of this type of structure is falling as they are replaced by more contemporary styles, there were still 14,334 truss bridges remaining as of 2004. Researchers and practitioners have learned from studying bridge performance during recent earthquakes, from analytical studies, and from laboratory testing, that truss bridges may be vulnerable to damage and collapse in an earthquake. Structural deterioration from rust can accentuate the problem.

1 Seismic Research Program Manager & Senior Research Structural Engineer, Federal Highway Administration, McLean, VA 22101 USA, wen-huei.yen@fhwa.dot.gov

2 Consulting Engineer, San Francisco, CA 94111 USA, cjseim@pacbell.net

3 Senior Program Officer, Transportation Research, MCEER, University at Buffalo, State University of New York, Buffalo, New York 14261 USA, jso7@buffalo.edu

An important new document on bridge retrofitting is the two-part *Seismic Retrofitting Manual for Highway Structures.* It also was developed by MCEER with the sponsorship of FHWA. It is based on a previous edition of the manual, but updated with information on recent seismic research and professional practice. This new document was issued in late 2006. Part 1 of this Manual is titled *Seismic Retrofitting Manual for Highway Bridges, Part 1: Bridges* and focuses on the seismic retrofitting of conventional highway bridges. It is intended to be applicable nation-wide in the USA for all levels of seismic hazards and for conventional concrete substructures and steel and concrete girder-type highway bridges with spans less than 150 m (500 ft) and a design life limited to 75 years. Suspension bridges, cable-stayed bridges, arches, long-span trusses, and movable bridges are not covered; however, many of the procedures and techniques presented can be applied to these types of structures, if appropriate judgment is used.

Seismic Retrofitting Truss Highway Bridges, which is the subject of this paper, specifically extends the seismic retrofit provisions of the *Seismic Retrofitting Manual for Highway Structures, Part 1: Bridges* to cover the seismic retrofit of both ordinary steel truss highway bridges and of seismically-complex and long-span steel truss highway bridges.

The truss Guidelines are divided into the following sections.
(1) Introduction - presenting the seismic characteristics of steel truss highway bridges.
(2) Philosophy and Procedures - covering the approaches to and the methods of seismic retrofitting of steel truss highway bridges.
(3) Screening and Prioritization - presenting methods of determining seismically deficient highway truss bridges and prioritizing the scheduling of bridges requiring retrofitting.
(4) Analysis
(5) Design Parameters
(6) Evaluation Methods – which gives methods of analysis to determine seismic demands and capacities, ranging from simple calculations to non-linear, dynamic analyses.
(7) Retrofit Measures – providing several overall retrofit strategies which consist of evaluating several retrofit approaches, and selecting specific retrofit measures to modify the structural members.
(8) Case Histories
(9) Glossary
(10) References and Bibliography

2.0 BRIDGE SEISMIC RETROFITTING IN THE USA

The major turning point of modern seismic engineering of bridges in the United States began with the 1971 earthquake in the San Fernando Valley of California. In 1973, the California Department of Transportation responded to public outcry to make highway bridges safe from earthquake collapse by issuing new seismic design criteria for bridges in California. This was the first attempt in the US to relate peak ground accelerations, as are shown on seismic hazard maps, to different soil types at bridge sites; to the dynamic-response characteristics of the structure; and to force-reduction factors that account for inelastic behavior. This FHWA-backed seismic design criteria formed the basis for the seismic provisions in the 1977 AASHTO Standard Specifications for Highway Bridges.

In 1978, the FHWA awarded a contract to the Applied Technology Council (ATC) to develop improved seismic design guidelines for highway bridges that are applicable to all regions of the USA. The product of this effort was the ATC-6 Seismic Design Guidelines for Highway Bridges published in 1981.

FHWA followed this pioneering work by publishing, in 1983, Report No. FHWA/RD-83/007, *Seismic Retrofitting Guidelines for Highway Bridges*. This was the first document that focused exclusively on providing nationally-applicable guidance to the bridge design profession for seismic evaluation and retrofitting of highway bridges. In 1987, FHWA published Report No. FHWA-IP-87-6, *Seismic Design and Retrofit Manual for Highway Bridges*, which updated and expanded the 1983

work into a manual for the design and retrofit of highway bridges.

The 1987 document was followed, in 1995, by the FHWA Publication No. FHWA-RD-94-052, *Seismic Retrofitting Manual for Highway Bridges*. This 1995 Manual incorporated the experience gained from use of the 1987 publication, new knowledge gained from analytical and laboratory research, and reconnaissance trips to earthquake-devastated areas to review structural damage. The 1995 Manual was developed as an interim document with the expectation that it would be revised and updated in a few years.

The FHWA 1995 Manual has now been revised, updated, and expanded by MCEER as the two-volume *Seismic Retrofitting Manual for Highway Structures. Part 1, Bridges* (referred to here as the Bridge Retrofitting Manual), incorporates the experience gained from recent earthquakes and the intense seismic-research effort that has recently been developed and conducted in several structural testing laboratories. *Part 2* is completely new material pertaining to retaining structure, slopes, tunnels, culverts, and roadways. This two volumes manual were published in November, 2006.

3.0 GUIDELINES SECTION 1 - INTRODUCTION

The most prolific bridge type constructed in the last 100 years or more for highway structures, in the span range of about 50-m to 350-m, is the steel truss. Most of these 14,334 truss bridges were designed to much lower seismic requirements than seismic design specifications require today. The public demanded earthquake-safe bridges after experiencing the bridge failures in the 1989 Loma Prieta and the 1994 Northridge earthquakes. In the New Madrid seismic zone alone, there are 2618 trusses and of these, 69% are considered structurally deficient.

Steel truss highway bridges are generally defined as a framework of straight steel members forming triangular patterns that are connected together to form a primary load-supporting system, called a truss. The triangle is the characteristic basic unit of a truss bridge configuration because a triangle is the most inherently stable geometric figure. Generally, two primary trusses are spaced apart by floor beam members framed into the vertical posts, or into the apex of the diagonals. The floor beams support longitudinal stringers, which support the concrete deck on which vehicles travel.

Secondary members fulfill important functions, such as forming a lateral bracing system in a horizontal plane at the upper and lower chord level, and the lateral bracing system acts to carry transverse wind and seismic loads longitudinally to the truss supports. Secondary cross bracing in the vertical plane at the panel points acts to space the trusses apart to match the floor beam spacing and to fulfill the important function of stiffening the rectangular cross-section against sway distortions.

3.1 Types of steel truss bridges

Trusses are classified by the position of the deck within the cross section of the bridge. If the deck is in the plane of the top chords, the bridge is referred to as a deck truss; when the deck is in the plane of the lower chord, the bridge is referred to as a through truss. If the deck is between the top and bottom chords, the bridge is called a half-through truss. In 2003, there were 13,563 through trusses and 770 deck trusses in the National Bridge Inventory.

3.2 Steel truss articulation

Trusses can also be classified by the articulation of the truss at its support points and at the inter-span hinged points. The articulation of a truss is determined by the type and location of its support points.

A single span, supported by bearings at each end, is called a Simple Span Truss. A Cantilever Truss refers to the construction method in which the truss in erected by balanced-cantilevering out from each of the two center towers. A

suspended span is usually connected to the tips of the cantilever arms by eye bars or by hanger plates and it functions as a simple span.

A Continuous Truss is, as it name implies, continuous over each of the piers that support the truss. Continuous Trusses are generally limited to four spans. The position of the deck, as denoted by the terms "through" with the deck positioned in the plane of the lower chord, or "deck" with the deck positioned in the plane of the upper chord, is usually placed after the truss classification term, i.e., Simple Span Deck Truss, or Cantilever Through Truss.

3.3 Structural Classifications of Steel Trusses Used for Highway Bridges

Most steel truss highway bridges can be classified into the following truss types and articulation methods:

- Steel Truss Types
  - Through Truss
  - Half-through Truss
  - Deck Truss
  - Pony Truss
  - Bow- String Trusses
- Articulation Methods
  - Simple Span
  - Cantilever
  - Gerber
  - Continuous
  - Combination

3.4 Lateral load resisting systems

Most trusses have stiff sway-frames, called portals or portal frames, at each support point of the truss. The function of the portal frames is to carry wind loads from the lateral bracing system in the plane of the upper chord down to the bridge bearings that support the truss at each support point. However, in a seismic event, the portal frames will perform the same function as they do for wind: carrying the seismic lateral forces down to the truss bearings.

Trusses are usually supported on structural steel bearings, sometimes called "shoes," that carry vertical gravity loads and lateral wind and seismic loads to the substructure. Rockers and nested rollers are usually used for bearings that are designed to move to accommodate thermal movements. Bearings that are rigidly connected to the substructure fix the truss from longitudinal movement. The bearings are the last link in the lateral load-resisting system as they connect to the substructure, which must then have its own separate force-resisting load path to the ground.

An important seismic characteristic of most highway truss bridges is that the center of mass of the superstructure is well above the support bearings. In an earthquake, the high position of the mass of the superstructure generates inertia forces that produce large overturning moments in the bearings at the support points of the truss.

3.5 Concrete Decks

Often the concrete decks of truss bridges have joints supported by the floor beams every three or four panel points. The function of these joints is to reduce the lateral load-carrying participation of the concrete deck through composite action with the truss chords under live load flexure. These joints also reduce the participation of the concrete deck through composite action with the truss chords in resisting wind and seismic lateral loads. The concrete decks of trusses are connected to the abutment roadway slabs or to adjacent trusses, in multi-span truss arrangements, by thermal joints that accommodate temperature movements.

3.6 Seismic classification of truss bridges

3.6.1 Seismically-Ordinary Truss Bridges

In the AASHTO LRFD Standard Specifications for Highway Bridges for both Allowable Stress Design (ASD) and for Load Factor Design (LFD), the Introduction states, "[these specifications] apply to ordinary highway bridges, and supplemental specifications may be required for unusual types and for bridges with spans longer than 150 m (500 ft)". Thus the AASHTO, ASD and LFD bridge design specifications recognize that there are both long-

span and unusual types of bridges that are not covered within the AASHTO specifications for the design of ordinary bridges, and that unusual types of bridges require special supplemental specifications for their design. The Guidelines classify these special truss bridges as Seismically Complex Truss Bridges (SC Bridges).

3.6.2 Seismically-Complex Truss Bridges

Damage to bridges from recent earthquakes and seismic investigations and analyses of bridge structures have demonstrated that there are also unusual configurations of steel truss highway bridges that behave under seismic excitation in a manner that is not covered by the AASHTO standard bridge specifications. These unusual configurations of truss bridges are classified as SC Bridges. A Seismically-Complex Truss Bridge is defined as meeting one or more of the truss bridge configurations listed below.

- A truss span exceeding 150 m.
- Deck-trusses or double-deck trusses.
- A series of truss spans creating a long bridge with multiple supports exceeding seven spans.
- A series of truss spans creating a long bridge with a total length exceeding 500 m.
- Truss bridges that have unusual geometry or alignment, skews exceeding 20 degrees, or unusual mass or stiffness distribution.
- Movable bridges that swing, lift, or tilt open with truss superstructures.

4.0 GUIDELINES SECTION 2 - SEISMIC RETROFIT PHILOSOPHY AND PROCESS

4.1 Retrofit philosophy for truss bridges

The basic concepts for retrofitting truss bridges, presented in the Guidelines, are based on the following concepts.

- Minimize loss of life and serious injury to the traveling public from unacceptable bridge performance.
- These provisions for high, moderate, and low seismicity should be applicable to all regions of the United States.
- Bridge designers should not be restricted from using new and innovative concepts and approaches in the seismic retrofit or seismic design of bridges.

4.2 Performance criteria and Performance Levels

Owners, with the help of bridge engineers, should decide which one of four performance levels that their retrofitted truss bridge should meet. The Life Safety performance level (PL-1) is to prevent bridge collapse and loss of life, although the bridge may need extensive repairs or replacing. For bridges on lifeline routes, the performance level must be set to provide full service soon after a seismic event, including the maximum expected event.

Performance Levels for the seismic retrofitting of an existing bridge are given below:

4.2.1 Damage Definitions

Minimal damage includes minor inelastic response and narrow flexural cracking in concrete. Permanent deformations are not apparent and repairs can be made under non-emergency conditions with the possible exception of superstructure expansion joints, which may need removal and temporary replacement or bridge over with temporary steel plates immediately after the seismic event.

Significant damage includes permanent offsets and cracking, yielded reinforcement, major spalling of concrete, which may require a bridge closure to repair. Partial or complete replacement of columns may be required. Foundations should not be damaged except in the event of large lateral flows due to liquefaction, in which case inelastic deformation in piles is permitted.

4.3 Earthquake levels

The *lower level* (LL) earthquake is the largest earthquake that has a reasonable probability of occurrence within the lifetime of the bridge, i.e. it represents a relatively small but likely event. Accordingly, the lower level earthquake was selected with a return period of about 100 years. The *upper level* (UL) earthquake is an earthquake that has a finite, but remote, probability of occurrence within the life of the bridge, i.e. it represents a large and rare event and a return period of about 1000 years was selected.

4.4 Bridge importance

The Guidelines define two classes of bridge importance: Essential Bridges and Standard Bridges. In the Guidelines, all essential truss bridges are classified as Seismically Complex (SC) Bridges, because, by definition, they are non-standard truss bridges. All other truss bridges are classified as Seismically Standard Truss Bridges (SS Bridges).

4.5 Anticipated service life

An important factor in deciding the extent to which a complex bridge should be seismically retrofitted is the anticipated service life (ASL) of the structure. Seismic retrofitting of a complex bridge with a short service life may be difficult to justify in view of the very low likelihood that the design earthquake will occur during the remaining service life of the structure.

Complex truss bridges usually have anticipated service life much longer than ordinary AASHTO truss bridges of 75 years. Although these types of bridges may have been designed according to an AASHTO bridge design specification that implies a design life of 75 years, many of these types of complex truss bridges do, in fact have longer service life. This is because some of these SC Bridges are generally more costly to design and construct so that there is a large investment in the facility.

4.6 Selection of minimum performance level

Minimum performance levels for SC Bridges are given in Table 2 according to earthquake size and service life category. All SC are classified as Essential Bridges. These are minimum recommended levels. If retrofitting to these levels cannot be justified economically, the owner may choose a lower level. The owner may also choose a higher level than that recommended here for certain classes of bridges. Examples are bridges on the National Highway Network, which are critically important to the operation of national or regional transportation routes.

5.0 GUIDELINES SECTION 3 - SCREENING AND PRIORITIZATION

5.1 Screening of truss bridges

The first step in implementing a screening method for truss bridges is to compile a bridge inventory to obtain the following basic information:

- The structural characteristics of each bridge to determine vulnerability rating
- The soil conditions and seismicity at the bridge site to determine a seismic hazard rating
- The truss bridge performance level, its importance to the transportation system and its value to the socio-economics of the community

The bridges classified as SS Bridges from the first-screening level need to be further screened in a second- screening level that determines if any of these standard truss bridges meet the physical definition of SC Bridges.

Prioritization of SC truss bridges:

The objective of a prioritization program is to determine the order of retrofitting a population of of truss bridges that were found to be SC by the screening program. A number of factors must be considered in any prioritization program:

- The bridge as a symbol and an economic link to the community
- Bridge importance

- Physical condition of the truss and of the substructure supporting the truss
- Serviceability of the truss. Many truss bridges were built with two narrow lanes, light truck loading, or low clearance levels
- Anticipated Service Life. A bridge in poor physical condition, or one that is already scheduled for structural or functional rehabilitation, may be given a higher priority for seismic retrofitting.
- Cost of seismic retrofit. If the cost of the seismic retrofitting approaches about 75 percent of the cost of a new bridge, bridge replacement should be considered.

6. GUIDELINES SECTIONS 4, 5, & 6 – ANALYSIS, DESIGN PARMETERS, AND EVALUATION METHODS

There are several methods for the seismic analysis of truss bridges and also several different ways in which to express their capacity. These lead to a matrix of possibilities for the capacity/demand evaluation of truss bridges. The matrix of possibilities considered in the Guidelines are shown in Table 3. Examples of "subsystems" of a truss bridge are a portal frame at the end of a span, a sway frame, or a support tower.

Also indicated in parentheses in Table 3 is the general equivalence to the methods of analysis described in the Bridge Retrofitting Manual. Demands may be calculated using either elastic or inelastic analysis methods.

The capacity of members can be expressed either in terms of force – the strength of the member, or deformations - the ductility of the member. A force approach will be suitable for most problems. Only for members subjected to inelastic demands, will it be necessary to consider the ductility of the member. Members which are particularly likely to be subjected to inelastic demands are those occurring in support towers, for example.

6.1 Methods of analysis

The three methods of analysis for the seismic analysis of truss bridges are, in increasing order of complexity:

- Elastic modal analysis with response spectrum input
- Elastic time history analysis with ground motion input
- Inelastic time history analysis with ground motion input

The choice of method depends on both the level of seismic hazard, and on the complexity and importance of the structure. The dependence on seismic hazard is perhaps more clear; an inelastic analysis would only be warranted if the demands are large enough to produce inelastic response. A complex detail or an important structure might warrant a time history analysis to obtain simultaneous force demands in order to realize an efficient retrofit or a more accurate evaluation that would make it possible to avoid a retrofit altogether. Analysis may also be required to obtain the displacement capacity of portal frames, sway frames, support towers, or other subsystems of truss bridges. The displacement capacity may be obtained from a pushover analysis of a model of the subsystem.

6.2 Modeling techniques

6.2.1 Global Modeling

Seismic analysis of truss bridges may be generally accomplished using three-dimensional finite element analysis, as for other bridge structures. Although truss members primarily resist tension and compression, it is usually preferable to model them using three-dimensional beam elements with flexural properties.

6.2.2 Properties of Built-Up Members

The section properties of built-up members may be computed by integration over the cross-section, using the same mechanics of materials approach as for solid sections. Laces used to connect different elements of a cross-section together usually do not contribute to the axial or the flexural stiffness of the section. The laces do contribute to the shear and torsional stiffness of a built-up member, however. Indeed, the laces are the major

component of the shear and torsional stiffness of many members.

6.2.3 Modeling of Tension Only Members (Eyebars)

Eyebars and similar members constructed from flat plates may be unable to resist compression forces. Typically, these members are under dead load tension, and the issue of their compression capacity—or lack thereof—only arises if the dynamic force in a member exceeds its initial tension. In this case, an elastic analysis will predict a net compression in the member, which is not physically realizable.

6.2.4 Modeling of Buckling of Compression Members

It may occur that the predicted compression force in a compression member exceeds its compression capacity, which is usually limited by buckling. The behavior is likely to be inelastic—either straightforward yielding or inelastic buckling—with the formation of a plastic hinge near the middle of the member. Possibly, a small overstress may be considered acceptable, if the member in question is compact and able to withstand inelastic straining without too much degradation of response. In cases of significant overstress, or if a member is not compact, it's probably better to model its inelastic response.

6.2.5 Inelastic Response of Built-Up Members

The ability of the cross-section to sustain inelastic strains depends on its compactness—on the compactness of its individual components in the case of a built-up member. Testing of large-scale models is a reliable method of proving the capability of a member. However, useful results can also be obtained by inelastic finite element analysis, if this is performed by experienced engineer. Such an analysis may need to include such refinements as: geometric nonlinearity, inelastic material, initial imperfections, and residual stresses, in order to obtain meaningful results.

7. GUIDELINES SECTION 7 – RETROFIT MEASURES

7.1 Definition of terms

When a bridge is evaluated and found to be seismically deficient, the next step is to decide what retrofit strategy, if any, should be used to correct the deficiencies. Decision-making may be formalized by exploring different retrofit strategies and comparing the cost estimates and other implications of each. A *Retrofit Strategy* is the overall plan for the seismic retrofit of a bridge. This plan can employ more than one retrofit approach and thus several different retrofit measures. *Retrofit Approach* is a method of improving or correcting the seismic deficiencies of the bridge. Strengthening and isolation are examples of a retrofit approach. *Retrofit Measure* is the physical modification of a component in a bridge for the purpose of improving or correcting seismic deficiencies of the bridge.

7.2 The Do-nothing, Retrofit, and Replacement options

The three retrofit performance levels should be weighed against the 'do-nothing' option, incurring loss of service after an event, and with the higher costs of a full-service replacement option. The decision to do nothing will be relatively straightforward if life-safety is the only performance requirement, and if the expected damage, such as total span-collapse, is not a threat to life-safety and the loss of bridge.

7.3 Members

The two general approaches are the addition of stiffeners to decrease the slenderness of any longitudinal plates, and the addition of cover plates to increase the strength.

7.3.1 Stiffener Retrofit

If the plates that make up a member are slender, the strength of the member may be limited by local buckling of those plates. The addition of appropriately designed stiffeners will reduce the width-to-thickness ratio of the plates to which they

are applied. An example of stiffening a member to improve is ductility is shown in Figure 2-1:

8.3.2 Cover Plate Retrofit

Cover plates may be added to strengthen a member in both tension and compression. An example is shown in Figure 2-2:

7.3.3 Connections

Truss bridges constructed before the Second World War used riveted connections between the truss members and the gusset plates. After the war, rivets continued to be used, but high strength bolts were developed which could be tightened with an easy-to-use pneumatic wrench, so bolts gradually replaced rivets.

7.3.4 Existing Connections and Splices

Existing connections and splices, between or within members having a ductility demand-to-capacity ratio greater than unity shall be strengthened, if necessary, so that their nominal capacity is at least 25% greater than the nominal capacity of the members they connect. Riveted connections may be readily strengthened by replacing the rivets with high strength bolts.

8. SUMMARY

This paper presents a synopsis of the role of the FHWA and the MCEER in seismic research and in the development and the publication of research papers and standards of practice, such as these truss Guidelines. The Guidelines list the various types of trusses, defines distinct performance levels and levels of earthquakes with short and long return periods. It presents methods of structural analysis from simple linear-elastic to dynamic, non-linear, time-history, and it presents design criteria to determine the capacity of truss members for determining demand-capacity ratios. The Guidelines include examples of retrofit measures. The document is available for purchase at http://mceer.buffalo.edu as is the new *Seismic Retrofitting Manual for Highway Structures*.

9 ACKNOWLEDGEMENTS & DISCLAIMER

The Guidelines were produced by MCEER's research team under FHWA Contract DTFH61-98-C-00094. The contents are the sole responsibility of the authors and do not constitute official policy. It is presented to researchers and practitioners for interest only. The authors gratefully acknowledge the work of T. Y. Lin International Inc., and especially Dr. Tom Ho, P.E. who assembled a team of practicing engineers to author the Guidelines.

10 REFERENCES

1. American Association of State Highway and Transportation Officials, (2002). *Standard Specifications for Highway Bridges, 17th Ed.*

2. Applied Technology Council, (1996). *Improved Seismic Design Criteria for California Bridges: Provisional Recommendations*, Report ATC-32, Redwood City, CA.

3. Buckle, Ian, et al., *Seismic Retrofitting Manual for Highway Structures, Part I: Bridges*, Multidisciplinary Center for Earthquake Engineering Research, 90% Draft, November, 2003.

4. Kulak, G.L., Fisher, J.W., & Struik, J.H.A. (1987). *Guide to Design Criteria for Bolted and Riveted Joints,* John Wiley & Sons

5. Structural Stability Research Council, Galambos, T. V. Ed. (1988). *Guide to Stability Design Criteria for Metal Structures 4th Ed.*, John Wiley & Sons

TABLE 1
BRIDGE PERFORMANCE LEVELS

Performance Level	Damage
PL- 0	No minimum level of performance is specified.
PL-1 Life Safety	Sustained damage is significant after a large earthquake and service is significantly disrupted, but life safety is assured. The Bridge may need to be replaced after a large earthquake.
PL-2 Operational	Sustained damage is minimal and limited service for emergency vehicles is available after inspection and clearance of debris. The Bridge is repairable, but with restrictions on traffic flow during repair.
PL-3 Fully Operational	Sustained damage is negligible and full service to all traffic is available after inspection and clearance of debris. Damage that does occur is repairable without interruption to traffic flow. Negligible damage may include evidence of small movement and minor damage to non-structural components, but no evidence of inelastic response in structural members or permanent deformations of any kind.

TABLE 2
MINIMUM PERFORMANCE LEVEL

	Service Life Category (Essential Bridges)		
Earthquake	**ASL 1**	**ASL 2**	**ASL 3**
Lower Level	PL 1	PL 2	PL 3
Upper Level	PL 1	PL 1	PL 3
Fault Rupture	PL 1	PL 1	PL 1

TABLE 3
APPROACHES TO DEMAND ANALYSIS AND CAPACITY EVALUATION

Demand Analysis		Capacity Evaluation		
		Member		Subsystem
		Strength	Ductility	Displacement
Elastic	Modal	XX (C)		XX (D2)
	Time History	X		X
Inelastic	Time History	X	XX (E)	XX

An X in the table indicates a feasible combination of analysis method and approach to capacity evaluation. The most sensible and/or common combinations are indicated with XX.

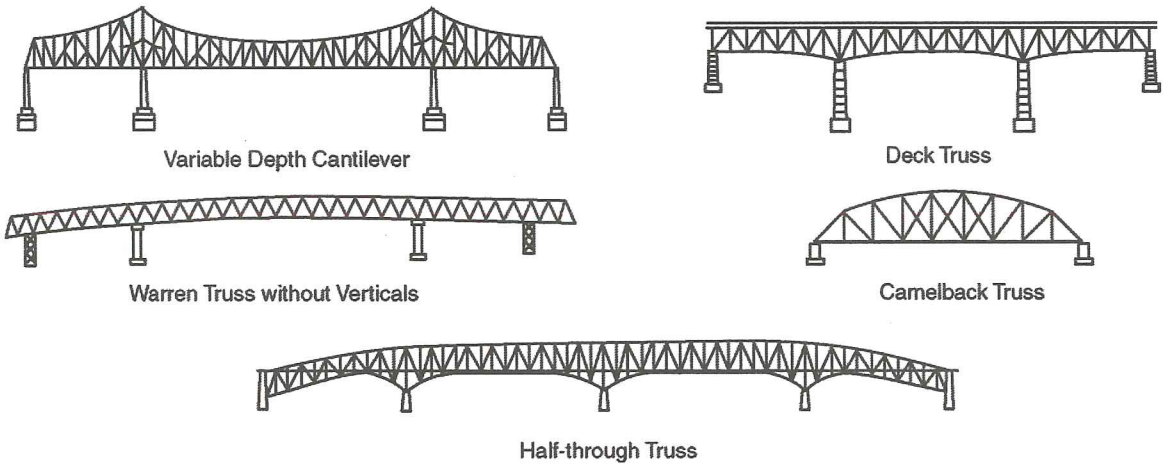

Figure 1 Examples of Continuous Truss Highway Bridges

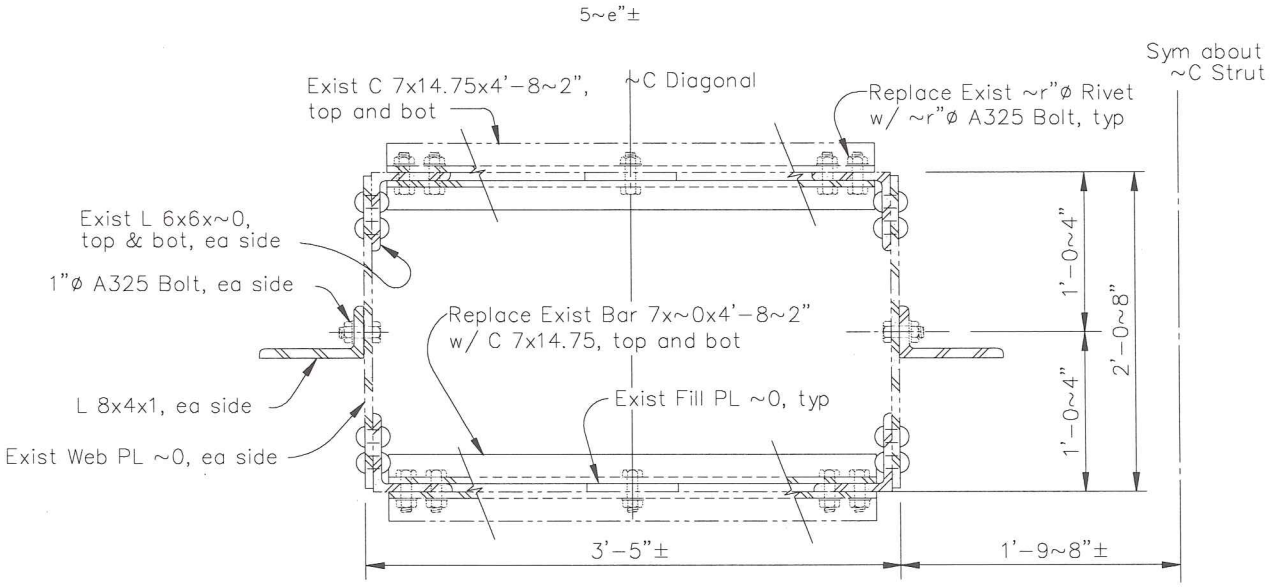

Figure 2-1 **Plate Retrofit with Stiffeners**

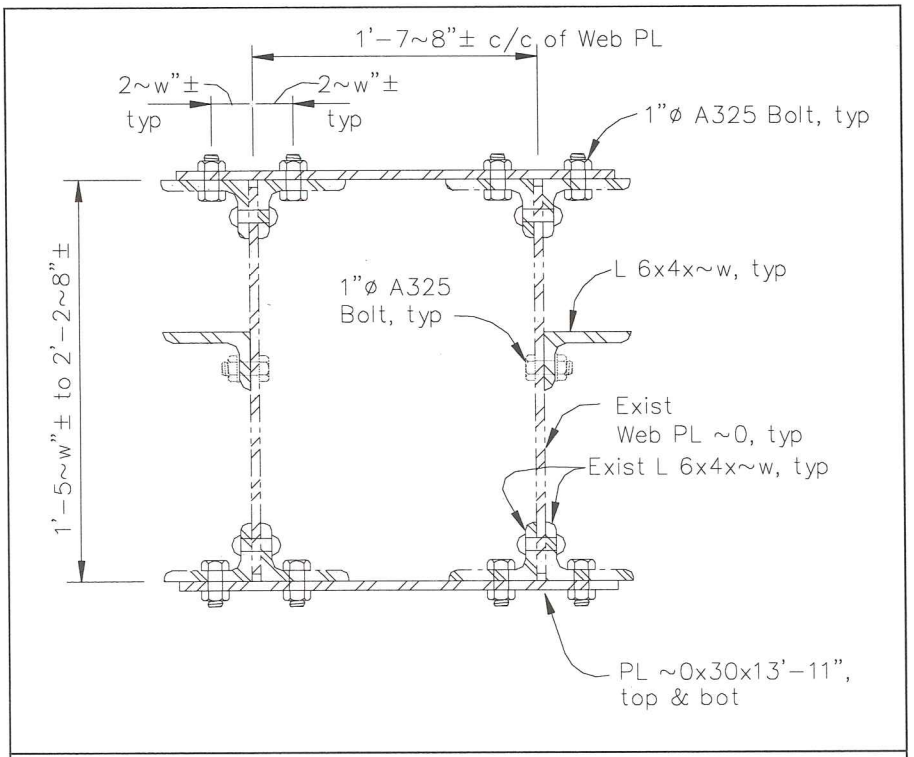

Figure 2-2 Cover Plate Retrofit

Bridge Seismic Response Experiment Program using E-Defense

by

Kazuhiko Kawashima[1], Hiromichi Ukon[2], Kouichi Kajiwara[3]

ABSTRACT

This paper introduces a large scale shake table experimental program on bridge structures using E-Defense. The bridge program was formulated by Japan and US researchers as one of the US-Japan cooperative research program based on NEES and E-Defense collaboration. Component model (C1 model) and system model (C2 model) are included in the program. Objectives of C1 model is to clarify the failure mechanism of reinforced concrete bridge piers using as large models as possible to eliminate barriers of scale and loading rate effect. C2 model is to study the complex system behavior of bridges to failure. Background, objectives, proposed models and tests cases are briefly introduced.

KEYWORDS: Seismic design, Seismic retrofit, Bridges, US-Japan cooperative research, E-Defense, NEES

1. INTRODUCTION

E-Defense is the world largest shake table of National Research Institute for Earth Science and Disaster Prevention (NIED), Japan [1]. The table is 20 m long and 15 wide with the maximum payload of 1,200 tf. Peak acceleration, velocity and displacement which can be excited by E-Defense under full load are 0.9 g, 2 m/s, +/- 1 m, respectively, in the two lateral directions, and 1.5 g, 0.7 m/s and +/- 0.5 m in the vertical direction.

It was built to advance the scientific knowledge in earthquake engineering as a consequence of the extensive damage of urban infrastructures in the 1995 Kobe, Japan earthquake. "why did structures suffer such extensive damage during the Kobe earthquake?," "what were the mechanism of failure?," and "what extend do structures fail under near-field ground motions?" are the basic motivations of constriction of E-Defense.

A large scale shake table test on bridge structures was identified as one of the high priority research areas using E-Defense. A large scale bridge experimental program as well as two other programs (steel buildings and information technology) was initiated in 2005 as one of the US-Japan cooperative research programs based on NEES and E-Defense collaboration. The project is coordinated by US-Japan Joint Technical Coordinating Committee.

Since E-Defense was built for clarifying the extensive damage of structures during the 1995 Kobe earthquake, breakthrough experiments which are significantly important as a benchmark test for clarifying the failure mechanism and/or enhancing the seismic performance of structures are expected.

2. FORMULATION OF EXPERIMENTAL PROGRAM

Program on large-scale shake table test on bridge structures was formulated based on discussions among Japan and US researchers. It was extremely valuable to formulate the program from conceptual stage of the project based on discussion. Outline of the past discussion is briefly presented in the following.

[1] Professor, Department of Civil Engineering, Tokyo Institute of Technology, Meguro, Tokyo, Japan

[2] Research Fellow, Hyogo Earthquake Engineering Research Center, National Research Institute for Earth Science and Disaster Prevention, Miki, Hyogo, Japan

[3] Senior Researcher, ditto

The 1st planning meeting was held in April 2004 in Shin-Kobe with participation of nearly 50 researchers from Japan and US. Through discussion on research needs in earthquake engineering, it was agreed that high priority of mutual interest to Japan and US researchers included bridge structures, steel buildings and information technology [1, 3]. Both bridges and buildings were seriously damaged during the Loma Prieta, Northridge and Kobe earthquakes, and considerable research based on component testing was conducted following these earthquakes to develop new design recommendations. It was thought highly profitable for both Japan and US to assess system level behavior of structures designed using these new recommendations, and to explore the seismic performance of similar structural systems that were not yet researched [3].

Research needs of bridge structures included progressive failure, soil foundation structure interaction, liquefaction-induced lateral displacement and forces, retrofit strategies and measures, protective systems and responses to spatially varying ground motions.

The 2nd and 3rd planning meetings were held in Arlington in July 2004 and Miki in January 2005, respectively. Besides discussion on the general framework of the NEES and E-Defense collaboration and budget, research needs for bridge structures were discussed.

An extremely important occasion to research community on bridges was two day US-Japan Workshop on Large-scale Testing on the Seismic Performance of Bridges in February, 2005 in San Francisco. Twelve Japanese and seventeen US researchers attended the workshop as shown in Fig. 1. Discussion was directed to research plan and scheduling of the large-size shake table experiments using E-defense and NEES as well as the research needs and current research activities related to bridge earthquake engineering. Among a number of research items discussed were clarification of the failure mechanism, evaluation and development of effective seismic retrofit measures, performance evaluation of current bridges under extreme ground motions, and further enhancement of the seismic performance of bridges. High priority research targets for large-scale shake table experiments using E-Defense supported with NEES facilities were identified to include;

- performance evaluation and retrofit & repair of reinforced concrete columns under combinations of loading,
- progressive collapse of bridge system,
- new technologies, and
- seismic response modifications.

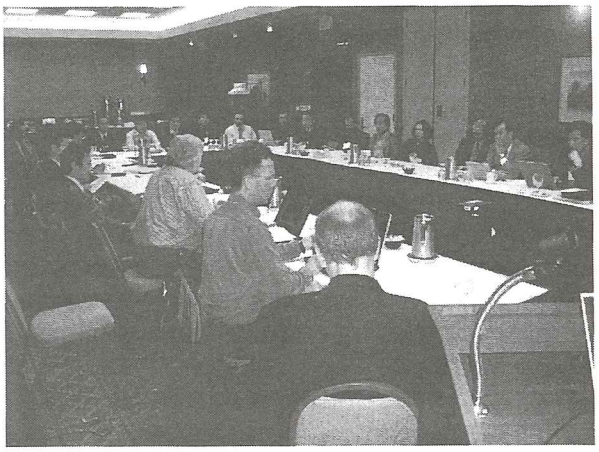

Fig. 1 US-Japan Workshop on Large-scale Testing on the Seismic Performance of Bridges, February, 2005, San Francisco, USA

In the WS, group discussion was conducted for 1) RC columns, and 2) progressive collapse and isolation. Following are the outline of proposed programs.

RC columns:

Because failure of RC columns was one of the most major mechanisms of the damage of 1998 Loma Prieta, 1994 Northridge and 1995 Kobe earthquakes, study on RC columns is a high priority research area. The points of discussion were as follows;

- Integrated experimental strategy and program on reinforced concrete columns should be

established so that large-scale experiments using E-Defense and medium-size experiments in both the US and Japan are complementary.

- Large-scale experiments on reinforced concrete columns should be conducted using as large models as possible to clarify and solve the problems inherent to small & medium-size experiments.
- Experimental and analytical research on failure mechanisms, seismic retrofit, performance evaluation under extreme ground motions and further enhancement of the seismic performance of columns should be conducted.
- Japan-side plan is to start experiment on the failure mechanisms of RC columns with insufficient development at cut-off, followed by experiments on seismic retrofit and the performance evaluation of columns designed based on current seismic design codes. Scheduling of experiments will be confirmed among Japan and US researchers after preliminary design of models and catch system in Japan and research funding allocation in the US.
- Pre-NEES research programs which were funded in US in 2004 should be incorporated in this research collaboration. Possible involvement of Japanese researchers in the pre-NEES program was discussed.
- Catch and setup system should be as flexible as possible to enable wider range of experiments including but not limited to single columns, bents or multiple span models.

Progressive failure and isolation:

Due to limitation of table size and loading capacity, realistic shake table test on bridge system response consisting of various structural members could not be conducted in the past. This is one of the breakthrough experiments which are required to advance the current knowledge on bridge performance under destructive near-field ground motions. Possible programs discussed on progressive failure are as follows;

- Progressive collapse testing should involve seismic response of a whole bridge system (piers, bearings, superstructure, spans, abutments, unseating devices, etc.) with sequential or progressive failure modes of structural components
- Industry (agencies, corporations, designers, owners/operators, etc.) has a strong interest and high need for better knowledge on system behavior related to progressive collapse, and for analysis tools to accurately and reliably capture this system response
- US-Japan collaboration can be highly successful and integrated because there is a strong shared interest in all of the various aspects of progressive collapse
- Because of the high complexity and costs of system-level tests, the E-Defense and NEES tests should be planned to be modular and to allow the greatest possible flexibility
- Areas of collaboration include
  - ✓ Innovative and advanced structural control technologies (for bearings, energy dissipation systems, 3D response and pounding, interaction of various systems, etc.)
  - ✓ New testing procedures to simulate broader system behavior (e.g. hybrid testing with substructuring, distributed tests, etc.)
  - ✓ Development of new type sensors for progressive collapse that can measure information needed (for testing, and eventually health monitoring purposes)
  - ✓ Development of analysis and design tools to achieve the above purposes

On the occasion of 4th planning meeting in August 2005 in Miki, Japan and US researchers agreed to conduct shake table test using E-Defense on two type models; 1) component models and 2) system models. They are called C1 test (C1 models) and C2 test (C2 models), respectively.

C1. Component experiments (single columns)

Component experiments on single RC column models with as large sections as possible was

proposed as shown in Fig. 2 to provide test data so that they could be used as a bench mark test for clarifying the scale effect and 2D/3D excitation effect. It was agreed among Japan and US researchers that both Japan and US contributed to C2 test.

The objectives of the C1 test is to

- clarify the failure mechanism of RC columns which failed during 1995 Kobe earthquake,
- clarify effectiveness of the standard seismic retrofit measures for existing RC columns ,
- clarify the seismic performance of RC columns designed based on the current design requirements under the current design ground motions,
- clarify the seismic performance of RC columns designed based on the current design requirements under stronger than the current design ground motions, and
- clarify the effect of damper technology.

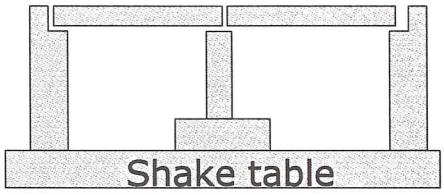

Fig. 2 Component Model (C1 Model)

Clarification on failure mechanism of premature shear failure at cut-off due to insufficient development is important for Japan because it was one of the most extensive failures during 1995 Kobe earthquake [2]. It is also interesting to study the effect of composite materials jacket for seismic retrofit because it is well implemented to columns as well as steel jacket.

C2. System experiments (progressive collapse)

System experiment is proposed to clarify system failure mechanism of a bridge consisting of a deck, columns, abutments, bearings, expansion joints, and unseating prevention devices as shown in Fig. 3 under various loading conditions. The objectives of C2 test are;

- clarify progressive failure modes of a bridge system due to combination of poundings and rupture of expansion joints, bearings, restrainers and columns
  - ✓ Effect lock of failed bearings & expansion joints
  - ✓ Interaction of failed structural components
- Advanced and critical columns
  - ✓ High ductility columns
  - ✓ Re-centering columns
  - ✓ Rocking seismic isolation
  - ✓ C-bent columns
  - ✓ Interlocking spiral columns
  - ✓ Square columns with cross bars
  - ✓ Columns subjected to combined flexure, axial force and torsion
- Advanced dampers and energy dissipating units
- Advanced unseating prevention devices

To achieve the objectives, proposed are modular models in which a part of structural components can be replaced to enable repeated experiments under various conditions. Thus, experiments are expected for straight, skewed and curved bridges which are supported by various type columns and foundations (single cantilever columns, multi-column bents, re-centering columns, interlocking spiral columns, inverted L (C-bent) columns, moment-resisting frame piers, lightly reinforced wall piers, high performance columns, circular and rectangular, solid and hollow, rocking isolation, columns with different heights, etc.). Tests for C2 model accommodated with advanced dampers, energy dissipators and unseating prevention devices are also proposed.

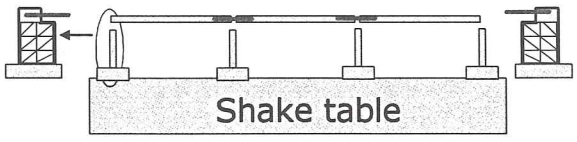

Fig. 3 System Model (C2 Model)

Table 1 Test Program on Component Models (C1) and System Models (C2)

Fiscal Year	Test Programs
2005	Preliminary tests & analyses; ● Pushover, cyclic and hybrid loading tests on premature shear failure ● 3D shake table tests ● Progressive failure
2006	Preliminary tests & analyses; ● Pushover, cyclic and hybrid loading tests on flexure and premature shear failure ● Shake table and cyclic loading tests using NEES facility ● Shake table test using scaled models ● Progressive failure
2007	Large-scale tests on component models (C1 models) using E-Defense; ● Test on flexural failure using a column build in 1970-1980s ● Test on premature shear failure using a column built in 1970-1980s
2008	Large-scale tests on component models (C1 models) using E-Defense; ● Test on steel jacket retrofit using a column build in 1970-1980s ● Test on carbon fiber sheet retrofit using a column build in 1970-1980s ● Test on a column designed based on the current code
2009	Large-scale tests on system models (C2 models) using E-Defense; ● Tests on progressive failure ● Tests on advanced technologies

A bridge program meeting was held to accelerate planning of the bridge program in December 2005 in San Francisco. The test program proposed at the US-Japan workshop on large-scale testing on the seismic performance of bridges, February 2005, San Francisco and 4th Planning Meeting, August 2005, Miki were reviewed and reaffirmed. Research needs were reviewed and agreed as follows:

- clarification of the failure mechanism,
- evaluation and development of effective seismic retrofit measures,
- performance evaluation of bridge columns designed based on current design codes under extreme ground motions, and
- further enhancement of the seismic performance of bridges.

3. PROPOSED MODELS AND TEST CASES

Based on discussions prevented in the previous chapter, an experimental program consisting of C1 and C2 models was formulated as shown in Table 1. Preliminary experiments and analysis as well as design of C1 and C2 models are conducted in 2005 and 2006. Tests using E-Defense are scheduled in 2007-2009.

Five tests are planned for C1 models at this stage. Two C1 model tests are scheduled in 2007; one is a column which fails in flexure, and the other is a column which fails in premature shear failure. They are typical columns built in 1970-1980s and collapsed during 1995 Kobe earthquake.

Verification of seismic retrofit for shear using steel jacket and carbon fiber jacket is scheduled in 2008. Two C1 models designed so as to fail in premature shear failure are retrofitted. Experiments on two C1 models designed based on the current seismic design criteria are also scheduled in 2008 to clarify the seismic performance under the design ground motions and further redundancy under stronger than the design ground motions. Several tests are planned using module C2 model in 2009. However, the test program

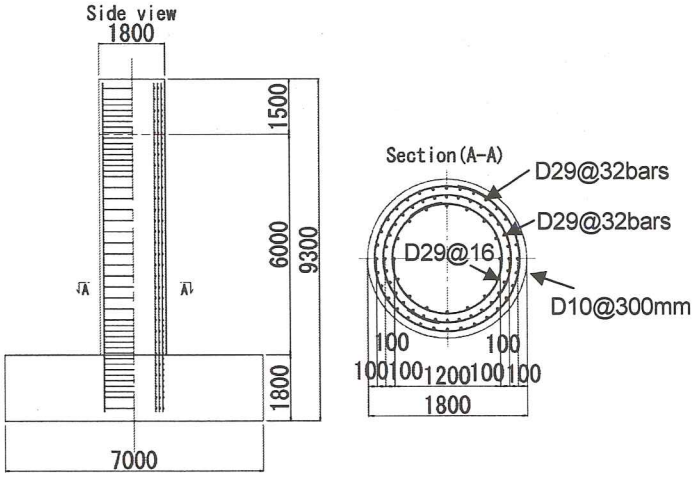

Fig. 4 C1 Column Built in 1960-1970s which fails

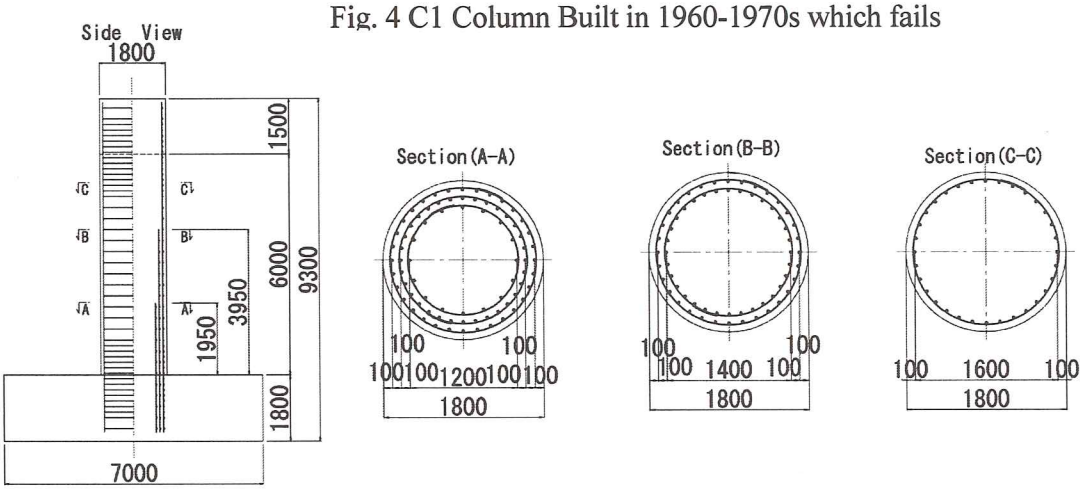

Unit: mm

Fig. 5 C1 Column Built in 1960-1970s which fails

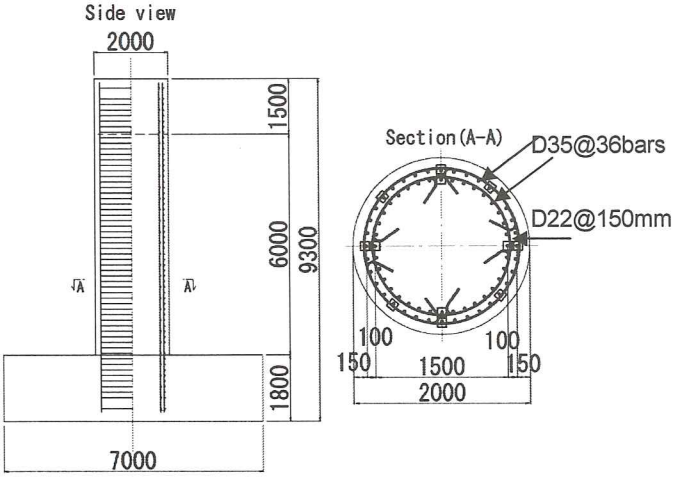

Fig. 6 C1 Column Built based on the Current

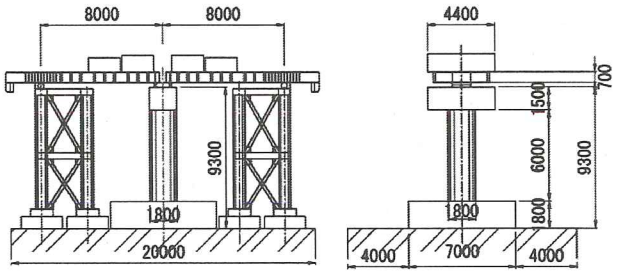

(a) Support System

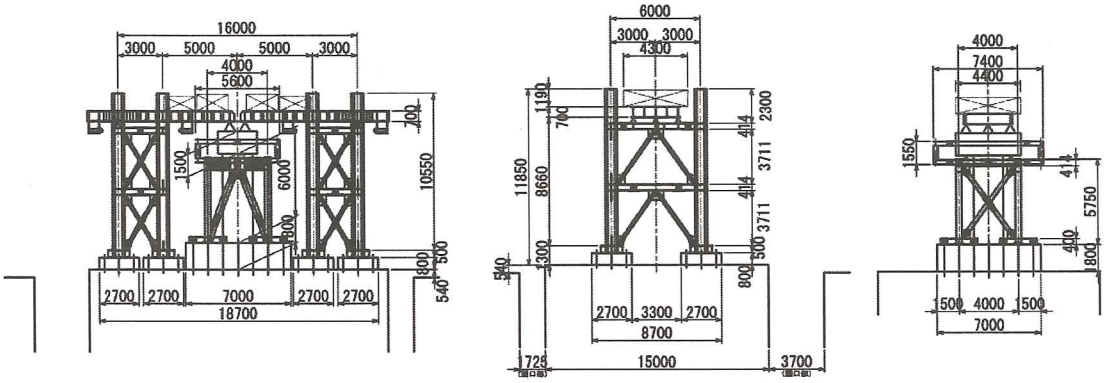

(b) Support and Catch Systems

Fig. 7 Support and catch Systems

will be subjected to modification based on experiments in 2007 and preliminary experiments and analyses.

Figs. 4 and 5 are show C1 model columns built in 1960-1970s which fails in flexure and shear, respectively and Fig. 6 shows C1 model column built based on the current design codes. They are 7.5 m tall circular columns with 1.8m and 2m diameter, supported by 1.8 m thick footing. Two simple decks with steel masses are pin connected to a C1 model. Total weight of a deck with mass is 21t+147t=168t. The decks are not for representing real decks but for supporting 2@147t masses. The decks are supported by steel columns with high stiffness and strength at both ends using movable bearings. Inertia force of two decks and masses are imposed to model column in the longitudinal direction. A certain friction force develops at the movable bearings, but it is limited. However because end columns contribute to support

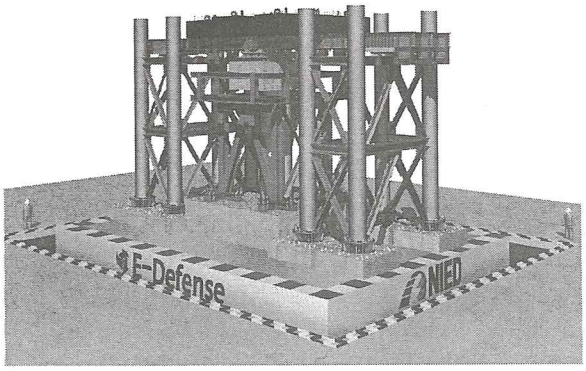

Fig. 8 Component Model (C1 Model)

the inertia force of two decks and masses through the movable bearings (movable in the longitudinal direction, but pin connected in the transverse

direction) in the transverse excitation, the masses on decks are set as close to model column as possible.

Because mass of the column with footing and the two decks with steel masses is 310.5 t and 336 t, respectively, total mass of a model is 646.5 t. Thus total weight including catch system as shown in Fig. 7 is 900.5 t. However 50% mass is further added on decks for clarifying redundancy of C1 model designed based on current code, the maximum mass of C1 model is 1,068.5 t including catch system. Fig. 8 shows anticipated model and catch system for C1 models.

4. PRELIMINARY TESTS AND ANALYSES

Following four preliminary tests and analyses were conducted for clarifying testing procedure and proving comparative data, based on request of NIED in 2005 and 2006.

Shake table test on three circular columns with 600 mm diameter was conducted at the Public Works Research Institute in 2005 and 2006 as shown in Fig. 9. Two columns tested in 2006 were 1/3 scaled model of C1 columns scheduled to be excited in 2007. One was column which failed in flexure and the other was column which failed in shear. Loading setup and catch system which were closed to the real systems for E-Defense experiment were used. Experimental results can be directly compared to E-Defense experiment on C1 models [4, 5].

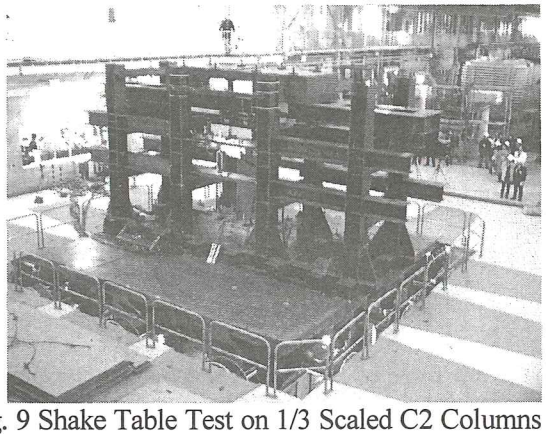

Fig. 9 Shake Table Test on 1/3 Scaled C2 Columns at Public Works Research Institute

A series of pushover, cyclic, and hybrid loading was conducted on 8 circular columns with 400 mm diameter at Tokyo Institute of Technology in 2005 and 2006 as shown in Fig. 10. They had two cut-offs with insufficient development so they failed in premature shear. They were 2/9 scaled model of C1 model scheduled to be tested in 2007. Flexure and shear failure mechanism was clarified by varying shear and flexural strength ratios. Loading protocol dependence of failure modes was also studied [6, 7].

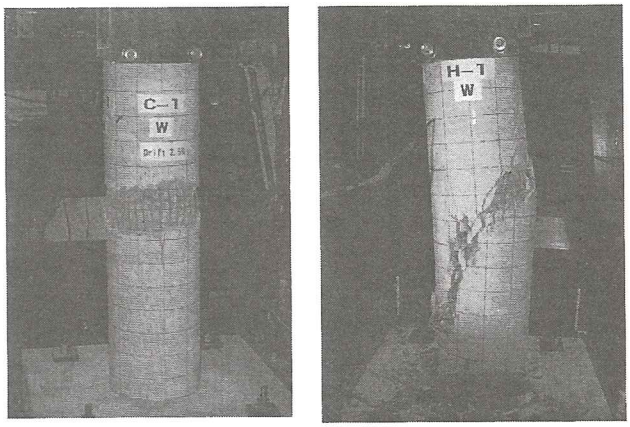

(a) (b)

Fig. 10 Loading test on 2/9 Scaled C2 Models under (a) Cyclic Loading and (b) Hybrid Loading using Near-Field Ground Motion at Tokyo Institute of Technology

Shake table experiment was conducted as shown in Fig. 11 on two interlocking spiral columns and two rectangular columns jointly by Pacific Earthquake Engineering Research Center, University of California, Berkeley and Tokyo Institute of Technology in 2006. Interlocking spiral columns had two interlocking spirals and had a section of 400x280 mm and 440x280 mm. Rectangular columns had two cross bars and had the same sections with the interlocking spiral columns. They were excited by yield and design level table accelerations several times to failure. Comparative evaluation on the

seismic performance of interlocking spiral columns and rectangular columns was conducted.

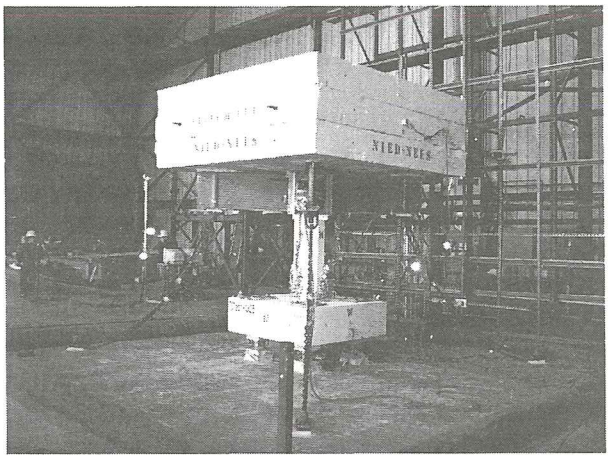

Fig. 11 Shake Table Experiment on Interlocking Spiral and Rectangular Columns (University of California, Berkeley)

An international hybrid simulation with two experimental components at Kyoto University and University of California, Berkeley was conducted in 2006 to evaluate seismic response of a bridge with a C-bent and a single RC and a steel piers. Fig. 12 shows testing set-up. Numerical analysis was also conducted [8, 9, 10].

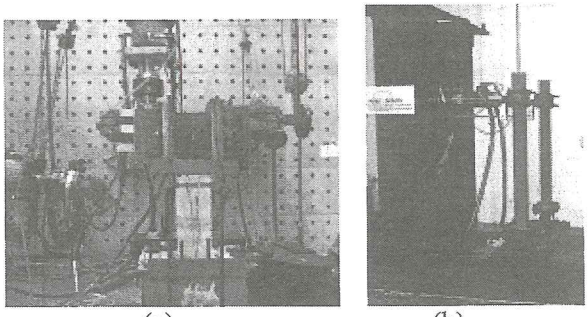

(a) (b)

Fig. 12 Experimental Set-up at (a) Kyoto University and (b) University of California, Berkeley

5. COCLUDING REMARKS

Extensive effort has been devoted to reveal deficiency of design practice and to develop seismic design technologies of structures whenever significant damage occurred in past earthquakes. However it was difficult in the past to accumulate real data on structural failure and to verify adequacy of seismic design technologies of structures because of long recurrent time of significant earthquakes. Small scale experiments were insufficient to provide realistic seismic performance data of bridge components and systems inherent to problems of small scaled experiments.

E-Defense enables researchers to conduct large scale experiments on bridge structures so that limitations inherent to small scaled experiment can be eliminated for breaking through disputed problems. US-Japan cooperative research can be highly successful by integrating the efforts in both sides to experimental strategy and programs on bridge structures using E-Defense and NEES in a complementary manner. The authors wish to contribute for enhancing seismic design technology of bride structures in this program by dissolving critical problems which cannot be studied based on small scale experiment.

ACKNOWLEDGEMENTS

The large-scale bridge program is supported by a number of researchers in Japan and US. In particular, the authors express their sincere appreciation to Professor Ian Buckle, University of Nevada, Reno and Professor Stephen Mahin, University of California, Berkeley for their continuing support for the program. The joint shake table experiment on four columns at PEER was conducted in collaboration with Professor Stephen Mahin. Strong and kind support of staff members at PEER laboratory in the University of California, Berkeley was greatly appreciated. Dr. Shigeki Unjoh and Dr. Jyun-ichi Sakai provided invaluable support to the entire research program. The international hybrid loading experiment was conducted by Associate Professor Yoshikazu Takahasi, Kyoto University and Professors Gregory L. Fenves, and Stephen Mahin, University of

California, Berkeley. Kind guidance and discussion of Reviewing Committee (Chaired by Professor Hirokazu Iemura, Kyoto University) and Executing Committee of Large-scale Bridge Experimental Program (Chaired by Kazuhiko Kawashima, Tokyo Institute of Technology) is greatly appreciated.

REFERENCES

1. Katayama, T., (2005), "Construction of E-defense-a large-sized 3-dimensional shake table," Proc. 1st International Conference on Advances in Experimental Structural Engineering, pp. 29-38, 2005, Nagoya, Japan
2. Kawashima, K. and Unjoh, S., (1997), "The damage of highway bridges in the 1995 Hyogo-ken nanbu earthquake and its impact on Japanese seismic design," Journal of Earthquake Engineering, 1(3), pp. 505-542.
3. Mahin, S., (2005), "Future directions in earthquake simulation," Proc. 1st International Conference on Advances in Experimental Structural Engineering, pp. 39-49, 2005, Nagoya, Japan
4. Sakai, J. and Unjoh, S. (2006), "Earthquake simulation test of reinforced concrete bridge column under multidirectional loading," Proc. 4th International Workshop on Seismic Design and Retrofit of Transportation Facilities, CD-ROM, San Francisco, CA, USA.
5. Sakai, J. and Unjoh, S. (2006), "Earthquake simulation test of circular reinforced concrete bridge column under multidirectional seismic excitation," Earthquake Engineering and Engineering Vibration, Vol. 5, No. 1, pp. 103-110
6. Sasaki, T., Kawashima, K., Watanabe, G., Nagata, S. and Tharin, K. (2006), "Shear failure of reinforced concrete bridge piers with termination of reinforcements with insufficient development," Proc. 4th International Workshop on Seismic Design asnd Retrofit of Transportation Facilities, pp. 1-11, MCEER 06-SP03 (CD-ROM).
7. Sasaki, T., Kawashima, K., Watanabe, G., Nagata, S., Tharin, K., Ukon, H. and Kajiwara, K. (2007), "Effect of loading protocols on premature shear failure of reinforced concrete bridge piers with termination of main reinforcements," Journal of Structural Engineering, Vol. 53A, pp. 449-460, JSCE
8. Schellenberg, A. Kim, H., Takahashi, Y., Fenves, G.L. and Mahin, S., (2006), "OpenFresco framework for hybrid simulation: installation and example guide, Ver.2.0," NEESit, 2006.
9. Takahashi, Y. Iemura, H. Mahin, S. and Fenves, G. L., (2007), "International distributed hybrid experiments on bridge system," Structural Congress, ASCE, 2007.
10. Takahashi, Y., Nakano, Y., Iemura, H., Mahin, S., Fenves, G. L., (2007), "US-Japan distributed hybrid simulation of bridge system," JSCE Journal of Earthquake Engineering, 2007 (in Japanese).

Integral Connection Seismic Performance between Precast Girders and Cast-in-Place Bent Caps

By

Kevin Almer[1] and David H. Sanders[2]

ABSTRACT

Widening of existing bridge structures or new bridge construction in heavily congested areas has become a necessity due to the increasing traffic demands on Nevada's highway systems. The purpose of this study is to develop and examine integral connection details of precast superstructures with cast-in-place bent caps subjected to longitudinal seismic loading. Analytical modeling and experimental testing of four, 40 percent precast "U" girder specimens will be used to develop a design methodology. The main parameters of this study are the magnitude of post-tensioning and the connection reinforcement.

KEYWORDS: bridge engineering, seismic, precast, post-tension, integral connection

1.0 INTRODUCTION

Bridge structures are an integral part of the nation's highway infrastructure. As the infrastructure continues to age, existing bridges may need to be widened, retrofitted due to increasing traffic demands, or new bridges may need to be added. Often, widening or replacing of existing bridges or new bridge construction occurs in heavily congested areas where traffic delays and public safety are of major concerns. This is especially true in seismic regions where bridges are typically continuous, cast-in-place concrete superstructures that are integral with cast-in-place concrete substructures in order to transfer high seismic moment and shear forces. The monolithic bridge construction provides good continuity for transfer of seismic forces; however, falsework over the traffic lanes is needed while the superstructure is cast. This falsework can potentially create significant traffic delays due to reduced number of lanes provided for the public or unsafe driving conditions, unsafe working conditions for construction workers, and reduced bridge clearance.

Using precast concrete girders for the superstructure eliminates the need for falsework over traffic lanes and also allows for accelerating the construction time needed to place the superstructure, thereby reducing the traffic delay to the public and reducing the danger to the construction workers. This construction process has great advantages and applications when widening and retrofitting existing bridges as well as new bridge construction in highly congested areas. However, the uncertainty in behavior of the precast girder connections to cast-in-place bent caps for transferring seismic forces has led designers and agencies not to use this construction and design method. The purpose of this study is to investigate the seismic behavior of the integral connection between precast concrete girders and cast-in-place concrete and develop design guidelines based on analytical and experimental testing for the Nevada Department of Transportation.

2.0 PREVIOUS RESEARCH

The only prior experimental research pertaining to the integral connection in the longitudinal direction was conducted at the University of California at San Diego La Jolla, California in the late 1990's (Holombo 2000). This study investigated the continuity of a post-tensioned

[1] Graduate Student, Dept. of Civil and Environmental Eng., University of Nevada, Reno, Reno, NV 89557, USA

[2] Professor, Dept. of Civil and Environmental Eng., University of Nevada, Reno, Reno, NV 89557, USA

spliced precast girder system subjected to longitudinal seismic forces. Two 40% scaled bridge models featuring bulb-tee girders and bathtub girders that represented typical bridge construction in California were tested. In both tests, the superstructure was designed to perform elastically while the inelastic behavior was to occur in the column. Negative moment continuity was provided by post-tensioning of the girders over the bent cap and positive moment continuity was provided through splicing the extended bars and strands at the bottom of the girder. The results of the test indicated good ductility performance of the integral connection with only minor strength degradation. The superstructure was able to remain essentially elastic with only minor cracks occurring that closed after the removal of seismic loading. Another important conclusion the researches reported was the proportion of the column seismic moment to be resisted over the width of the superstructure. They concluded that the moment should be proportioned according to the relative stiffness of the integral system, or roughly two-thirds of column moment to be resisted by the two adjacent girders and the other one-third to be resisted by the remaining girders. Another important detail they recommended was to extend the column longitudinal reinforcement as far as possible into the bent cap for better transfer of the seismic forces.

3.0 ANALYTICAL PARAMETER STUDY

To establish the most important parameters for the integral connection, a prototype U-Girder representative of NDOT U-Girders was developed and is shown in Figure 1. This girder section was analyzed using the moment-curvature program XTRACT (2002) to determine the strength and ductility characteristics. Based on this information, a scaled version of the prototype girder was chosen and the most favorable connection details determined from a survey given to Department of Transportation agencies and literature search were applied. Ultimately, a 40% scale of the prototype was developed using post-tensioning for negative moment continuity and spliced mild steel for positive moment continuity. The 40% girder cross-section at the bent cap is shown in Figure 2.

3.1 GIRDER TO BENT-CAP CONNECTION

Post-tensioning over the bent cap is advantageous because this allows the section to have a high negative moment capacity without having to increase the amount of reinforcement in the composite deck. However, when the post-tensioning is part of the system, it introduces positive secondary moments that reduce the negative dead load moment effect. These secondary moments can be minimized and controlled through the tendon configuration. The post-tensioning also contributes significantly to positive moment capacity, which again will reduce the amount reinforcement needed in the bottom flange of the section at the face of the bent-cap. Therefore, adjusting the amount of post-tensioning significantly affects the negative and positive moment capacities as well as the curvature ductility of the section making post-tensioning a very advantageous and important parameter in this study.

Mild reinforcement and untensioned strands are both commonly used for the positive moment connection between the girder and the bent-cap. Mild reinforcement was chosen due to its more ductile characteristics and ease of application. All of the details using strands required some sort of mechanical connection or welding anchors to the end, whereas the mild reinforcement could just be lap spliced.

3.2 STRUT-AND-TIE MODELS

Another important aspect of the project includes using strut-and-tie models to describe the force transfer between the substructure and the superstructure. A widely used model consists of using joint stirrups outside the column core region to transfer the forces (external joint transfer model) (Priestley et al. 1996) shown in Figure 3 (a). Note that the T designates ties (tension) where C designates struts (compression). More recently, research on the transverse loading of bridge tee joints by

Sritharan (2005) was conducted. Sritharan's research suggested that the joint design based on Priestley et al. models was conservative when the joint was prestressed and unconservative when the joint did not include prestressing. Therefore he suggested a modified external strut and tie force transfer model. Figure 3 (c) shows a model that requires joint stirrups on both sides of the joint for one direction of loading when prestressing is not included. Figure 3 (b) and 3(d) show models for when the joint is prestressed and partially prestressed respectively. Notice the prestressed joint doesn't require joint stirrups for the force transfer while the partially prestressed joint only requires a small amount. Hence only nominal joint reinforcement would be required. These models were verified through experimental testing. Based on these models, similar models will be developed based on the experimental results of the program detailed above.

4.0 EXPERIMENTAL PROGRAM

The objective of testing the girder shown in Figure 2 is to assess the ability to distribute the column moment using the positive and negative continuity connections until failure. This will show the dominate failure mode of the connection and allow for the development of more specific design guidelines. A total of four specimens will be tested at the University of Nevada, Reno Large-Scale Structures Laboratory. The feasibility of two different testing methods was investigated. The first method consisted of testing the system using the UNR shake tables. An inelastic dynamic analysis was performed using SAP2000 (2005) subjected to different ground motions. The results of this analysis indicated that a larger scale specimen could be loaded under cyclic loading compared to on the shake table... Therefore, the set-up shown in Figure 4 was adopted, where actuators push on one end and pull on the other end. . Mass was added to the superstructure in order to model the scaled dead load of the prototype correctly.

4.1 Specimen Design

The prevailing design code for the specimens was the AASHTO Bridge Specifications (1998). The span lengths on either side of the bent cap of the scale model are half of the prototype span length in order to get the desired seismic shear across the joint. Since failure of the superstructure connection detail is desired, the column was designed to yield but not experience significant levels of inelastic behavior. The 40% scale U-Girder was selected primarily for two reasons, first, scaling smaller than 40% produced webs that were extremely small and problems such as cracking could occur when transporting and placing the girders with the equipment available. Secondly, a smaller scale would require mild reinforcement below #3 rebar. Therefore, if a smaller scale than 40% is to be used, then bars would have to manually deformed and treated until they were representative of actual field conditions.

The bent cap was designed using Caltrans (2004) specifications since AASHTO (1998) does not provide a clear design procedure for joint design where seismic forces are transferred between the substructure and superstructure. The details contained in the Caltrans specifications are similar to those given in the book *Seismic Design and Retrofit of Bridges* (Priestly et al. 1996) and Prestressed Concrete Institute (PCI 2003). This method was used in the experimental study done at the University of California, San Diego and the bent cap performed adequately. Caltrans uses the idea of external joint stirrups to transfer the column tension into the superstructure. Figure 5 shows these external joint stirrups. It is important to note that since the column was over-designed, the amount of joint stirrups provided was based on the actual column moment required to produce failure of the specimen, not the nominal capacity of the columns required by Caltrans.

The column-footing connection was designed as a two-way hinge using a methodology developed from research conducted at UNR (Cheng et al. 2006). The study found that shear friction theory either overestimated or underestimated the hinge shear strength. A new method was developed based on observed shear failure mechanisms. Using a base hinge reduced the column seismic shear force required to develop the superstructure

moments as compared to a fixed case. Since recommendations for contributory superstructure (Holombo 2000) stiffness to resist the column moment were made from the researchers at University of California at San Diego, it was felt one girder on either side of the bent cap would be sufficient.

4.2 Experimental Results

At the time this paper was written, one of the four specimens had been tested. The first two specimens were designed to test the effect of post-tensioning. The first specimen (UGHP) contained eight strands while the second specimen contained 25% less post-tensioning than the first (six strands). The third and fourth specimens will be determined after the results of the first two specimens are analyzed. The pushover curves for the first two specimens are shown in Figure 6. Sap2000 (2005) was used to generate the curves; the cut-off points for the curve are the maximum force values, in other words, the drop in the load after the max strength was reached is not depicted on this curve.

4.2.1 UGHP Results

The loading protocol for UGHP consisted of reverse cyclic loading as shown in Figure 7. The cycles up to ¾ of the yield displacement were run in force control, where after the cycles were in displacement control. The actual hysteresis curve is shown in Figure 8. From the analytical work, it was predicted plastic hinges would form in both the positive and negative moment regions on either side of the bent-cap and the specimen would ultimately fail with concrete crushing at the top of the girder/bent-cap connection. Strain data from the girders, see Figure 9, indicated that inelastic behavior did indeed occur on both sides of the joint and redistribution of forces were possible. Ultimately, the specimen failed as predicted, see Figures 10 and 11. Another important observation to be made was that the joint (bent-cap) was relatively undamaged suggesting that the joint was over-designed.

The results presented above suggest that less joint reinforcement could be used to transfer the forces in integral connections when post-tensioning is utilized. The effect post-tensioning has on the joint will be better quantified after the results of the second experiment (UGLP) are acquired. Based on the experimental observations and analytical work completed to date, the following options for the third and fourth test consist of

- reduce amount of joint reinforcement to produce failure in joint instead of girder/bent-cap interface,
- remove post-tensioning from system.

From these specimens and analytical work, design details and strut-and-tie models similar to those presented will be developed for design of integral connections.

5.0 SUMMARY

This paper presents research conducted on integral connections between precast bridge girders and cast-in-place bent-caps. Analytical and experimental work on four 40% U-Girder specimens will be used to develop design guidelines for integral connections. Based on research conducted to date, current design methods over-design the joint regions when post-tensioning is used. By using post-tensioning for the negative moment region and lap spliced mild-reinforcement for the positive moment region of girders, the full moment capacity of the precast girders could be obtained.

6.0 REFERENCES

AASHTO (1998), *LRFD Bridge Design Specification, second edition*, American Association of State Highway and Transportation officials, Washington , D.C.

Caltrans, *Seismic Design Criteria*, Version 1.3, California Department of Transportation, Sacramento, CA, 2004.

Cheng, Z., Saiidi, M., and Sanders, D. (2006), "Development of Seismic Design Method for Reinforced Concrete Two-Way Bridge Column Hinges," Center for Civil Engineering Earthquake Research, Department of Civil Engineering, University of Nevada, Reno, Nevada, Report No CCEER-06-01.

Holombo, J., Priestley, M.J.N., and Seible, F, "Continuity of Precast Prestressed Spliced-Girder Bridges Under Seismic Loads," *PCI Journal*, 45(2), 40–63, March-April, 2000.

PCI, 2003, *Precast Prestressed Concrete Bridge Design Manual, second edition*, Precast /Prestressed Concrete Institute, Chicago, IL.

Priestley, M.J.N., Seible, F., and Calvi, G.M., *Seismic Design and Retrofit of Bridges*, John Wiley and Sons, Inc., New York, 1996.

Sap2000, Version Advanced 9.1.1, Computers and Structures, Inc., Berkeley, CA 2005.

Sritharan, Sri, "Strut-and-Tie Analysis of Bridge Tee Joints Subjected to Seismic Actions," *Journal of Structural Engineering,* Vol. 131, No.9, September 1, 2005.

XTRACT, Version 2.6.2, Imbsen Software Systems, Sacramento, CA, 2002.

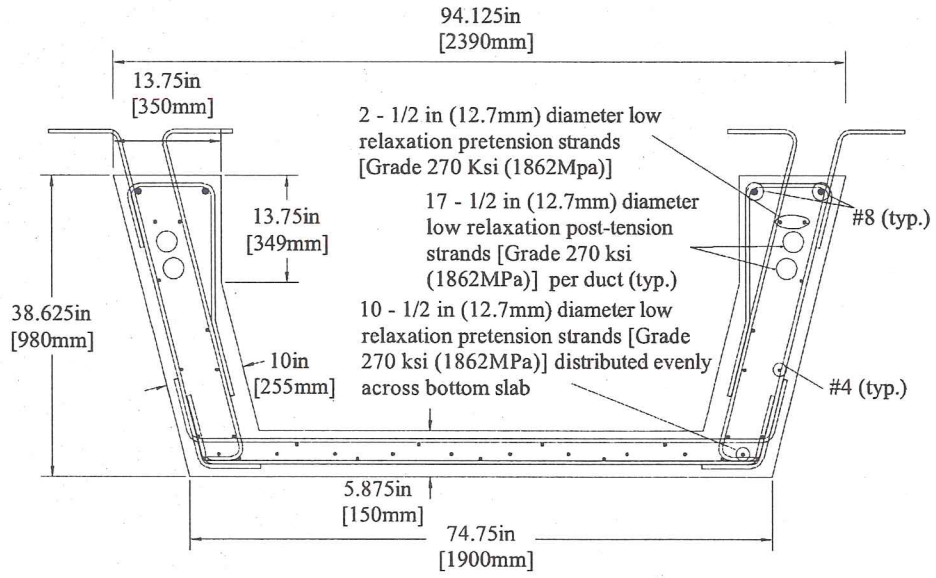

All mild reinforcement crosses the Girder/Bent-Cap interface. All pretension strands terminated at interface and all post-tensioning strands continue across the interface.

Figure 1: NDOT Prototype U-Girder Cross-Section

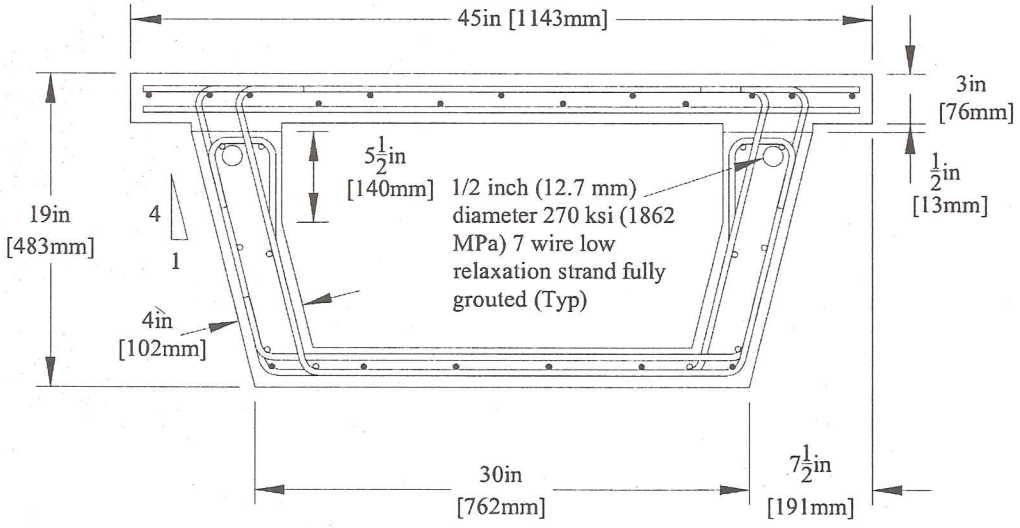

Note: All rebar is #3 unless otherwise noted. The non-solid reinforcement terminates at the bentcap interface. The post-tensioning strands continue through the bent-cap.

Figure 2: 40% Scale U-Girder and Deck at Girder/Bent-Cap Interface

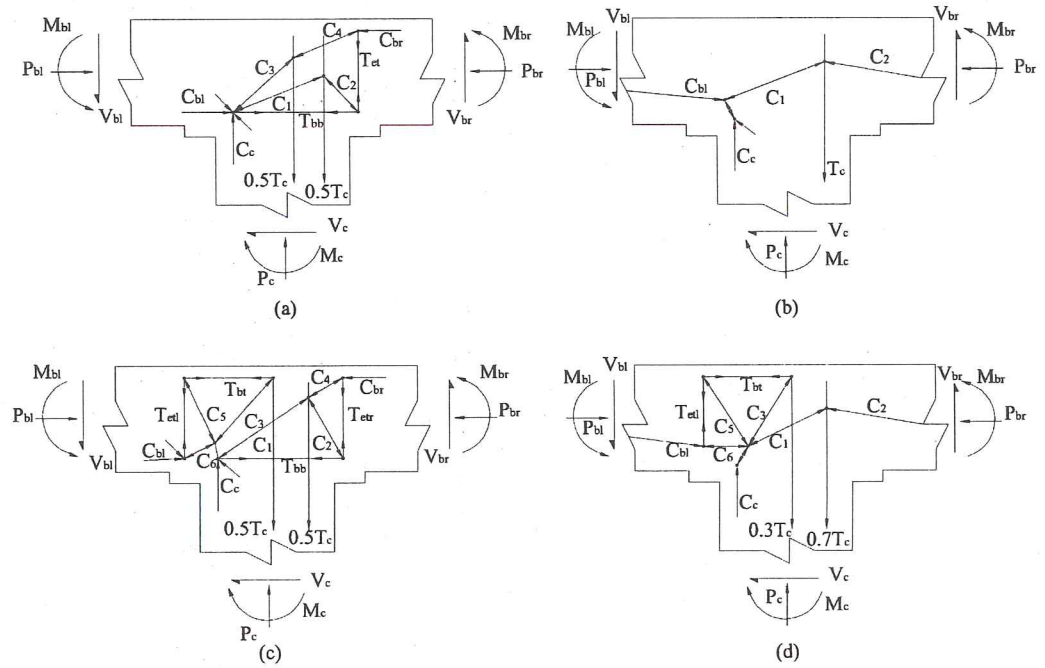

Figure 3: Previously Developed Strut and Tie Models, (a) Priestley et al. (1996), (b)-(d) Sritharan (2005)

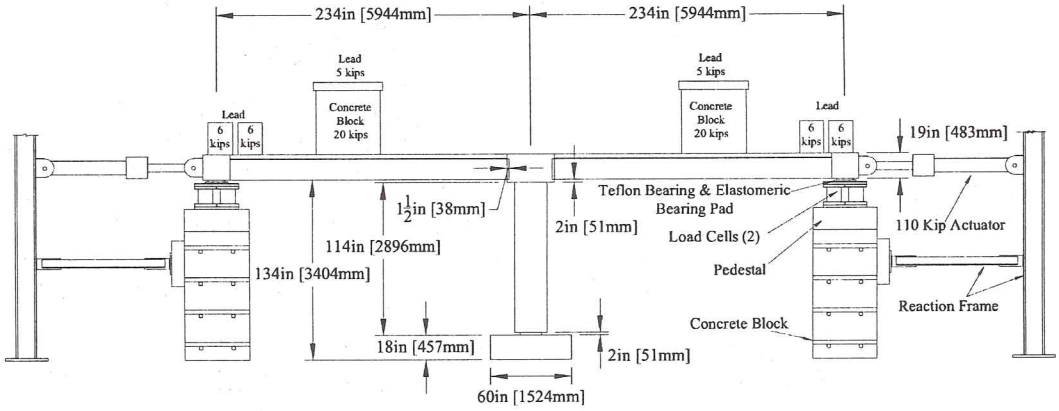

Figure 4: Experimental Test Set-Up

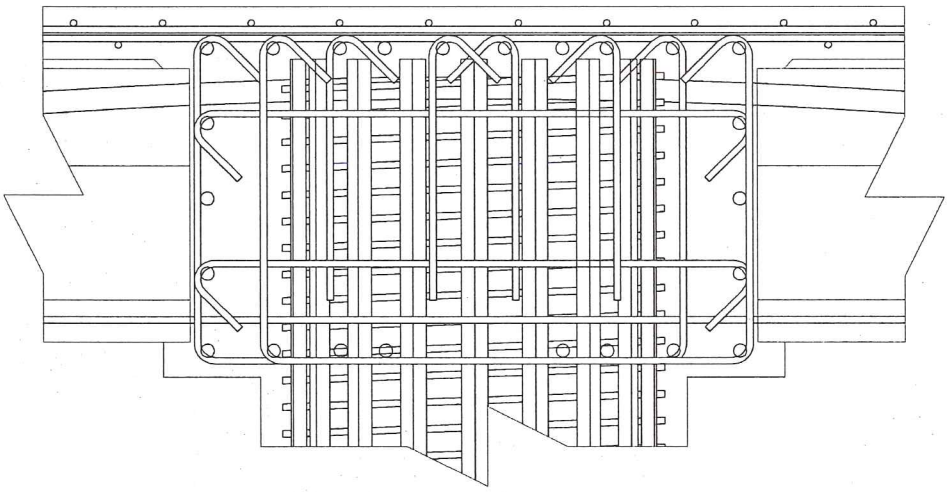

Figure 5: Bent-Cap Joint Reinforcement

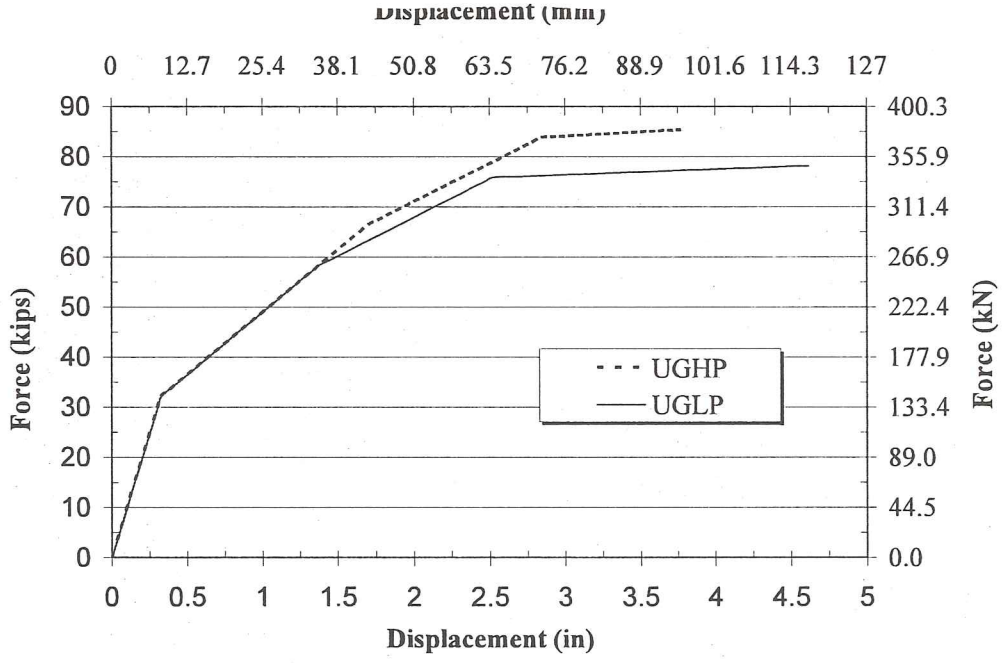

Figure 6: Pushover Curve for Specimens UGHP and UGLP

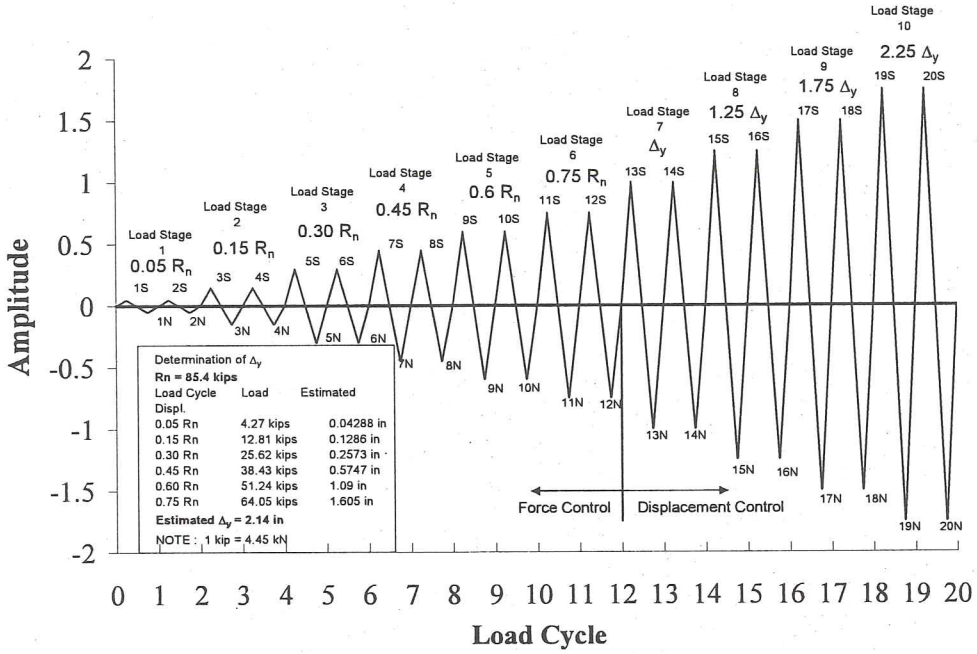

Figure 7: UGHP Reverse Cyclic Lateral Load History

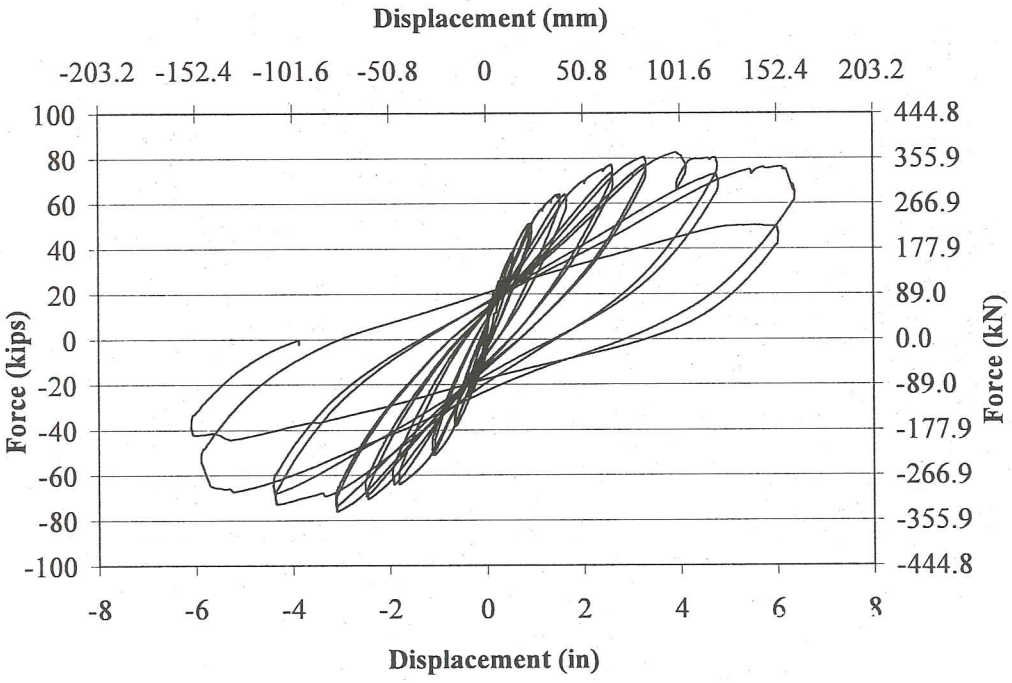

Figure 8. Experimental Hysteresis for Specimen UGHP

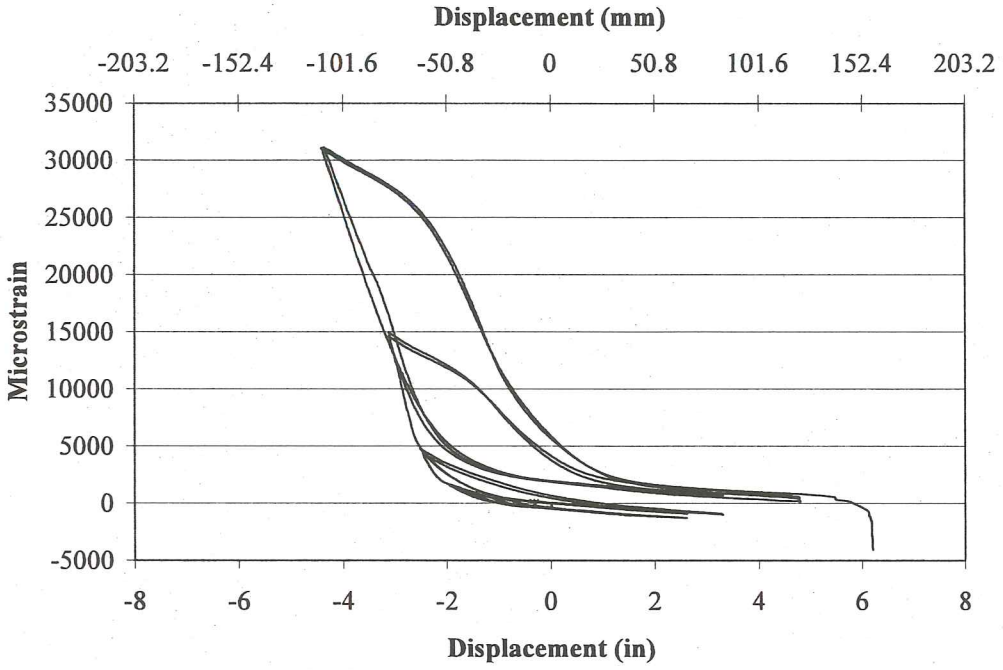

(a)

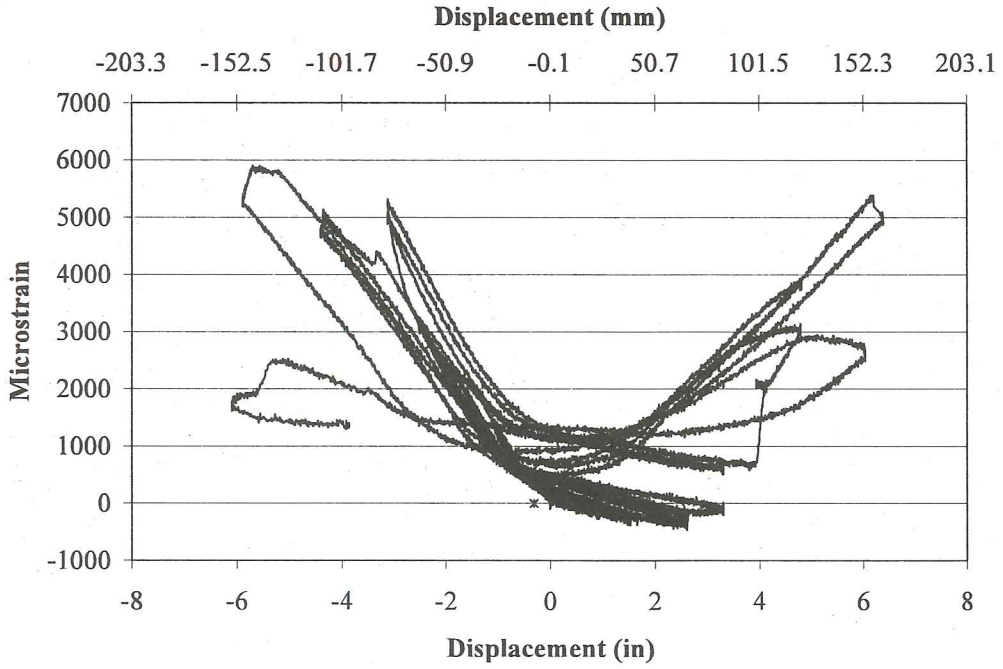

(b)

Figure 9: Strain Gauge Data for Girder Reinforcement, (a) top, (b) bottom, at Bent-Cap/Girder Interface.

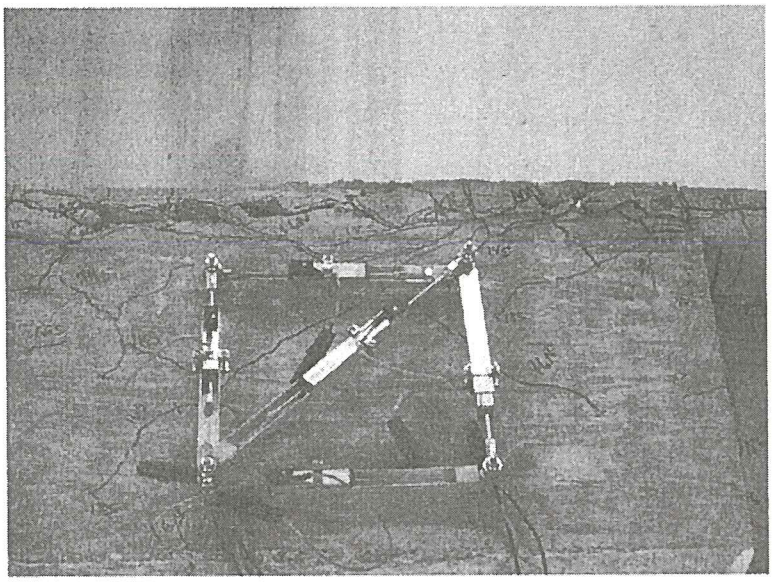

Figure 10: Crushing of Concrete at Top of Girder and Joint.

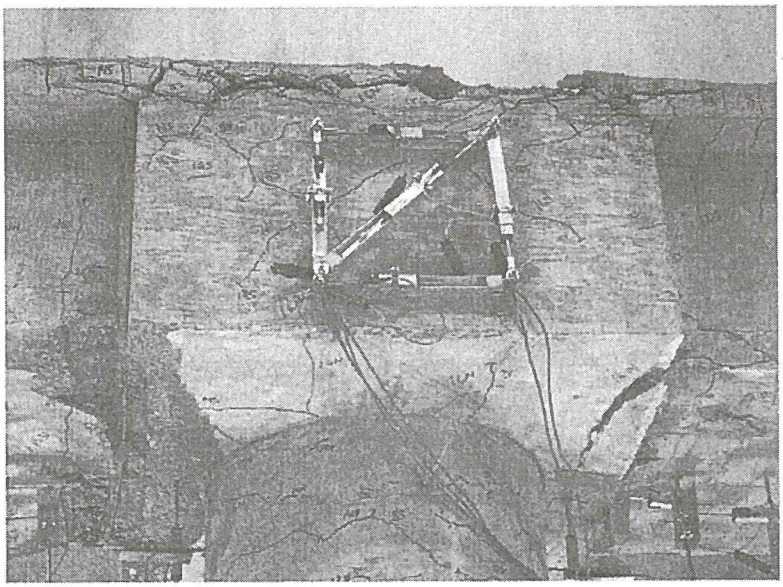

Figure 11: Plastic Hinging of Girders.

THEME 2

Storm Surge and Tsunami

The Storm Surges in the Seto Inland Sea Caused by Typhoon Chaba (0416) in Japan

by

Nadao Kohno[1], Kazuo Kamakura[2], Hiroaki Minematsu[3]

ABSTRACT

Typhoon Chaba in 2004 made landfall on the southeastern Kyushu and went through Chugoku (western part of Japan's Main Island) on 30 August, causing large storm surges in the Seto Inland Sea (SIS). The high tide records were broken at tide stations in Takamatsu and Uno Ports. We analyzed the tidal data and simulated this case with a numerical storm surge model.

The results revealed that the wind set-up basically played a key role in causing the large storm surges. However, the maximum storm surge (MSS) in Takamatsu did not occur when the typhoon was the nearest to the city, but about 2 hours later. Since the time of MSS approximately corresponds to the high spring tide time, the record breaking storm tide was observed there.

KEYWORDS: Storm Surge, Typhoon Chaba, timing of warning

1. INTRODUCTION

Storm surges generated by typhoons have often brought large disasters in the coast of Japan. Especially, in the case of Typhoon (TY) Vera, which caused 5,098 dead or missing in 1959, most of the casualties were brought by the storm surges. The countermeasures to storm surges have developed progressively after this disaster. However, serious storm surges still occurred. In 1991, large storm surges were generated in the western part of the Seto Inland Sea (SIS; shown in Fig.1) by TY Mireille[1, 2]. However, severe disaster did not occur since the maximum storm surge (MSS) occurred just in low tide. In 1999, the storm surges by TY Bart led to serious disasters; 13 people were directly killed by storm surges in Yatsushiro Sea, and Yamaguchi-Ube airport in the Suoh-Nada (western part of the SIS) was unavailable by inundation[3, 4]. The tracks of these two typhoons are almost the same and both of them generated large storm surges in Yatsushiro Sea. Recently, intense typhoons have frequently hit Japan since 2000, and serious disasters sometimes happened. In 2004, as many as ten named tropical cyclones made landfall on Japan, which is quite extraordinary since usual number is two or three. Several tropical cyclones brought disasters due to storm surges. Especially,

TY Chaba generated large storm surges in the SIS, and the coincidence of MSS with the peak time of high tide caused the highest storm tide records at Takamatsu and Uno (central part of the SIS). More than 8,300 houses are inundated above the floor level only in Kagawa Prefecture, and total damages were quite

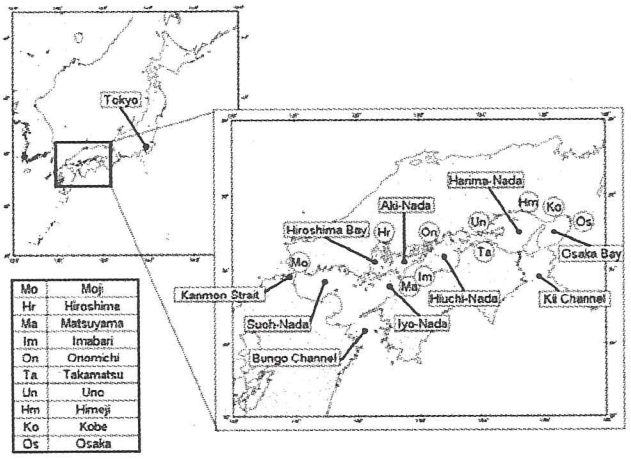

Fig. 1 Map of the western part of Japan and the Seto Inland Sea (SIS)
The whole area of the Seto Inland Sea from the Suoh-Nada to the Osaka Bay is an inland sea. The points of tide stations are also shown.

[1] Senior Researcher, Typhoon Research Department, Meteorological Research Institute, Tsukuba-shi, Ibaraki-ken 305-0052 Japan

[2] Forecaster, Takamatsu Local Observatory, Takamatsu -shi, Kagawa-ken 761-8071 Japan

[3] Takamatsu Local Observatory , ditto (Present affiliation: Marine Division, Japan Meteorological Agency, Chiyoda-ku, Tokyo-to 100-8122 Japan)

enormous as 16,799 houses inundated above the floor level.

Although large storm surges sometimes occurred in the SIS due to typhoon passages as mentioned above, most cases happened in the Suoh-Nada (western part of the SIS) or the Osaka-Bay (eastern part of the SIS), and they rarely occurred in the central part of the SIS. TY Chaba is applicable to the latter case. This case is also characterized by the fact that the MSS occurred a few hours later than the time when the typhoon was nearest. Therefore we have investigated the mechanism of this storm surge with a concern to the effects of sea topography and the sequence of typhoon position, mainly based on a numerical model.

TY Chaba and storm surges in the SIS are described in section 2, and the results are provided in section 3. Section 4 focuses on the factors that may mainly contribute to storm surges, and the conclusion is summarized in section 5

2. TY CHABA(0416) AND STORM SURGES IN THE SIS

2.1 TY Chaba (0416)

A tropical depression (TD) was formed in the sea around the Caroline Islands at 06UTC (all times are expressed in UTC hereafter) on 18 August 2004. It moved slowly westward and developed into a Tropical Storm Chaba at 12UTC on 19 August. Chaba continued to move westward and was upgraded into a Typhoon at 18UTC on 21 August. Then it turned toward the northwest at the southwestern edge of sub-tropical high on 23 August. The typhoon continuously intensified during this period and developed to the strongest level as central pressure of 910hPa and the maximum wind speed of 56m/s at 18UTC on 23 August.

The typhoon kept its intensity till 18UTC on 26 August, moving to northwest and gradually weakened. The typhoon moved to west again in the sea east of the Nansei Inlands and turned to the north-northeast in the sea south of Kyushu.

The typhoon made landfall at Kushikino at about 00UTC on 30 August, with central pressure 950hPa, the maximum wind speed 41m/s, and the radius of storm wind extended to 230km east (Fig. 2). The typhoon passed through Kyushu and moved northward in the Suoh-Nada, and made landfall again at around Hohfu. As the TY Chaba approaching, Chugoku, Shikoku, northern and central part of Kinki were gradually covered by storm winds. The typhoon passed Tottori at about 12UTC with slightly

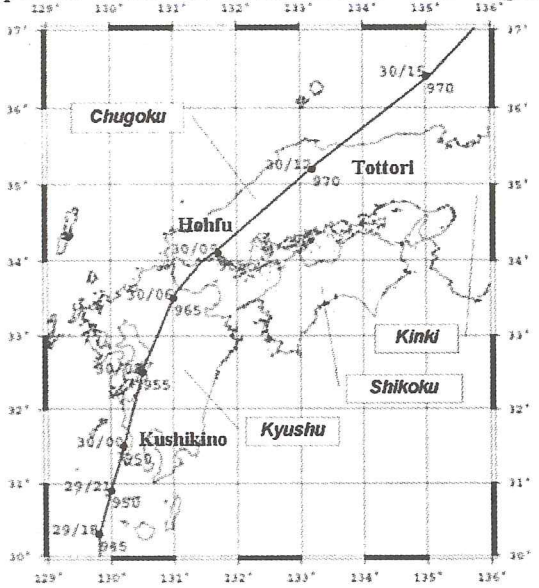

Fig. 2 Best track of TY Chaba (0416)
The circles on the path indicate the positions of the typhoon every 3 hours. Days and hours (UTC) are plotted to the upper left and central pressures (hPa) to the lower right of each point.

weakened intensity (central pressure 960hPa and the maximum wind speed of 31m/s), and became to move faster in the Sea of Japan. The typhoon made landfall again at Hakodate at 03UTC on 31 August, and transformed into an extratropical cyclone in the east of Hokkaido at 06UTC.

Strong winds were observed in the areas the typhoon passed nearby. In Okayama, the maximum wind of 21.1m/s (SW) and the maximum gust of 38.5m/s (SW) were observed at 15:20 and 12:51UTC on 30 August, respectively; those were the highest records there.

2.2 Storm Surges in the SIS by TY Chaba

The main storm surges in the SIS by TY Chaba occurred from 30 to 31 August. Fig. 3 shows the time series of hourly storm surges (the each

storm surge is defined by detracting astronomical tide from observed sea level) observed at tide stations. The magnitudes of the MSSs are generally about 1-1.5m.

The more east the observation point is located, the later the MSS was observed. (Table 1). For example, in the western part of the SIS, the MSS of 1.33m in Moji was observed at 06:36. The MSSs in Hiroshima and Matsuyama occurred at 09:35 (1.49m) and 08:49 (1.40m), respectively. MSSs in Takamatsu and Uno were observed after 13UTC, 4 hours later than that in Matsuyama. The MSS of 1.33m was observed at 13:23 in Takamatsu, and 1.37m at 13:16 in Uno. In Kobe and Osaka, that are in the eastern part of the SIS, the MSSs were observed just before 15UTC: 1.34m at 14:42 in Kobe and 1.32m at 14:30 in Osaka.

Fig. 4 shows the water levels at several tide stations. The magnitudes of the storm surges are not so different among these points, but the magnitudes of the storm tides are different each other because the timing of the astronomical tides are different each other. Since the time of MSSs were the same as that of low tide in Moji, storm tides did not become so high; the maximum tides were observed about 6 hours earlier than the time of MSS (around 00:30), this was mostly contributed by high tide, not the storm surge. The maximum storm tides of 2.58m (Matsuyama) and 2.69m (Hiroshima) were observed at 11:56 and 12:56 respectively, 2-3 hours earlier than the high tides. The maximum storm tide there results from combination of storm surge and astronomical tide. The maximum storm tides were observed in Takamatsu and Uno at 13:42 and 13:47, respectively, only 30 minutes later than MSS. Moreover, since it was period of spring tide, water levels at high water were higher than usual. This also led to the highest record of maximum tides as 2.46m (Takamatsu) and 2.54m (Uno). This extraordinary high storm tide caused enormous disasters, and more than 12,000 houses were flooded to over floor level in these coastal areas. The maximum storm tides were observed at 12:24 in both Kobe and Osaka to the east of Takamatsu, which was about 2 hours earlier than the time of MSSs.

In order to investigate the relation of storm surges to the relative position of typhoon, the time of MSS and the time when the minimum sea level pressure (MSLP) was observed, which corresponds to the time when the typhoon mostly approached, are listed in Table 1. The easterly wind was predominant in the western part of the SIS as the typhoon was approaching, and the sea level became higher from early stage in the Suoh-Nada. Around the Suoh-Nada area, the times of MSSs were almost the same as the time of the MSLP, since the typhoon passed through the Suoh-Nada. For example, in Moji, the time of MSS (1.33m) was only 6 minutes later than MSLP time. After the typhoon passed and made landfall at Chugoku region, the predominant wind turned to westerly in the wake of typhoon, and large storm surge area shifted to the eastern part of the SIS gradually.

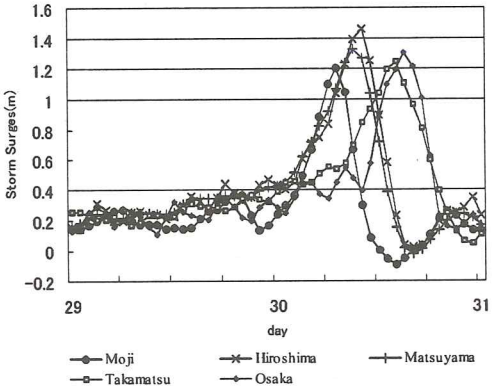

Fig. 3 Storm surges observed at several tide stations in the Seto Inland Sea.

Table 1 The maximum storm surges (MSS), the minimum sea level pressures (MSLP) and the difference of time

Tide station	MSS (m) and time (UTC)	MSLP (hPa) and time(UTC)	difference of time (min.)
Moji	1.33 (06:36)	969.5 (06:30)	6
Hiroshima	1.49 (09:35)	972.1 (10:16)	-41
Matsuyama	1.40 (08:49)	972.8 (08:49)	—
Uno	1.37 (13:16)	978.1 (10:48)	148
Takamatsu	1.33 (13:23)	978.1 (11:01)	132
Himeji	1.57 (14:50)	982.7 (13:13)	97
Kobe	1.34 (14:42)	987.5 (14:05)	37
Osaka	1.32 (14:30)	988.1 (13:42)	48

The MSS was observed at almost the same time of MSLP in Matsuyama, but was 41 minutes earlier in Hiroshima. At the points to the east of Matsuyama, the MSSs were observed later than the time of the MSLP.

It is notable that the times of MSS in Takamatsu and Uno were more than 2 hours later than the times of the MSLPs, but in Himeji and Osaka, located in further east of Uno, the difference of times between MSS and MSLP became smaller again. This indicates that the storm surge area did not move monotonously to east while the typhoon was simply leaving northward.

3. SIMULATION RESULTS

Fig. 5 (a) shows the simulated storm surge distributions as well as the surface winds used in the calculations. The observation of winds is not

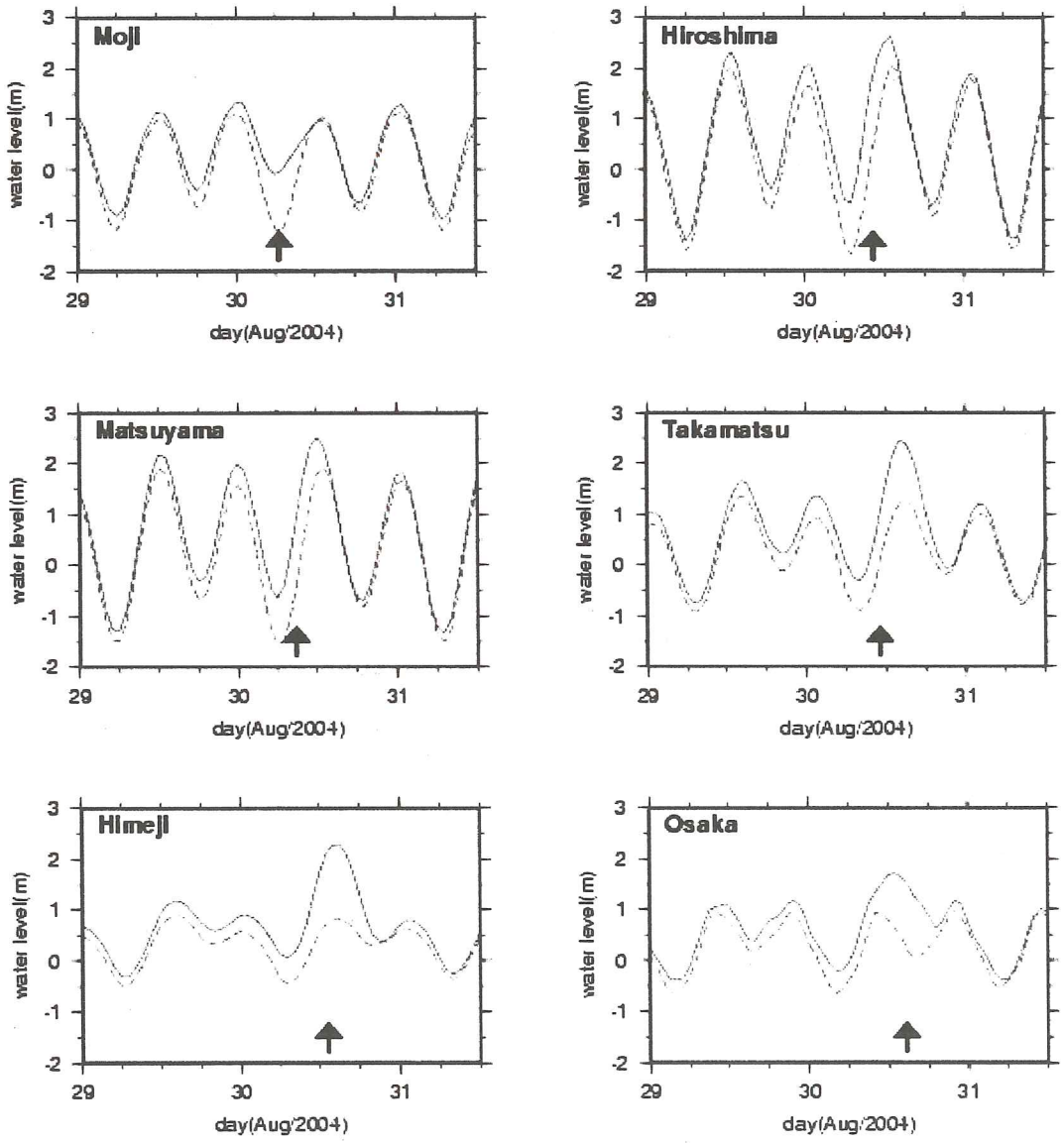

Fig. 4 The observed sea levels at several tide stations in the Seto Inland Sea
The observed sea levels are indicated by a solid line; the broken line represents the astronomical tide. The arrows show the time of the minimum surface pressure.

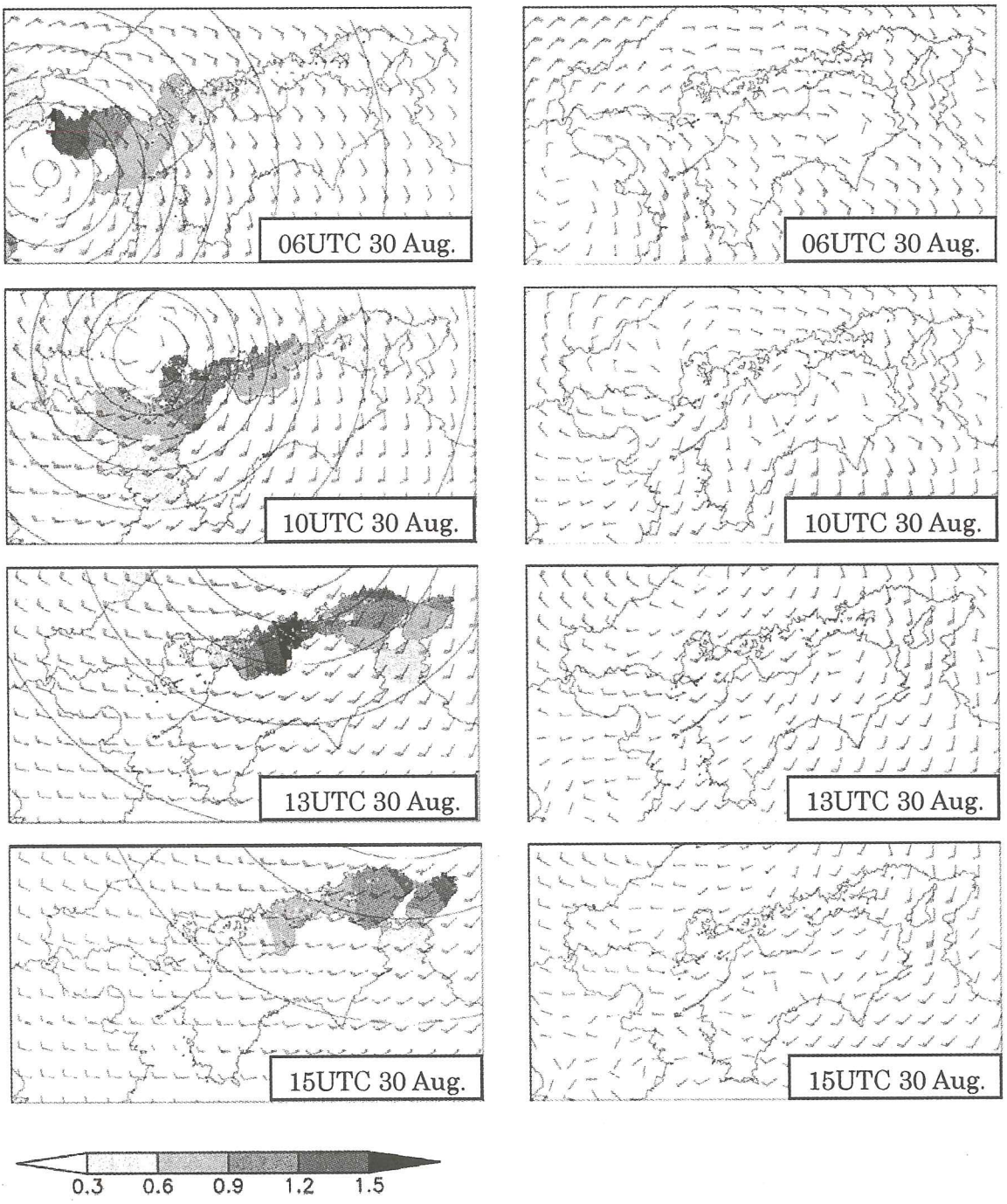

Fig. 5 Horizontal distribution of (a)the simulated storm surge and the model wind, and (b) the surface wind of the hourly objective analyses.
The shades indicate simulated storm surges (m), and the contours in the left column show the model surface pressure. The barbs in both columns show the winds (long fletching is 10m/s, and short 5m/s)

so dense in this area, especially in the sea, for intensive comparison. Therefore, the surface winds of the hourly objective analysis, which is based on the operational Meso-Scale Model (MSM) prediction as a first guess and modified with the wind profiler observation, is shown in

Fig. 5 (b).

Storm surges are little detected in the whole area before the typhoon reached Kyushu and a gale wind started. In the Suoh-Nada, large storm surge area is generated by strong easterly wind ahead of the approaching typhoon (06UTC on 30 August). As the typhoon had passed the Suoh-Nada and moved northeastward, the wind turned to westerly, which led the large storm surge area to move eastward (10UTC). Around 13UTC, although the typhoon had already moved away northward, a large storm surge is notable in the central sea to the west of a narrow straight (just where Takamatsu and Uno exist). After that, although the typhoon continued to leave further, westerly wind continued to blow, and storm surge shifted eastward, to the Osaka Bay around 15UTC on 30 August.

The calculated MSSs at several points are listed in Table 2, and Fig. 6 shows the time series at Takamatsu: Observed and calculated storm surges, observed sea level pressures as well as those used in the model. According to Tables 1 and 2, all the calculated MSSs are favorably compared with observation and every error are within 0.30m. However, there are almost 1 hour differences in peak time at some points. This may mainly come from the error of meteorological data input, e.g. assumed pressure field, since the time of minimum surface

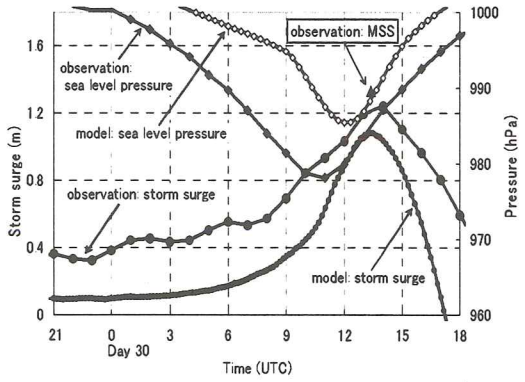

Fig. 6 The time series at Takamatsu

pressure given to the model is different from that of observation as shown in Fig. 6. The difference of pressure fields may also lead to the error of wind fields, but the wind fields in the time of MSS at Takamatsu was preferably estimated as shown in Fig. 5.

4. DISCUSSION

Generally speaking, storm surges are mainly caused by two factors: the inverted barometric effect and the wind set-up. Both of the effects are easily estimated to some extent by assuming the static balance. In addition, it is known that the dynamical effects such as resonance of the moving speed of meteorological disturbance and

Table 2 The results of three calculations

Simulated magnitudes of the maximum storm surges (MSS), given MSLP with the occurrence time in parenthesis. Contribution ratio of the wind set-up in the MSS, CR, defined as the MSS in II divided by that in I is also listed.

Tide station	MSS(m) in I	MSLP (hPa)	MSS (m) in II	MSS (m) in III	CR
Moji	1.61 (05:40)	969 (07:20)	1.35 (05:20)	0.52 (08:40)	84%
Hiroshima	1.44 (10:10)	969 (10:20)	1.01 (08:50)	0.70 (11:10)	66%
Matsuyama	1.15 (10:30)	978 (10:00)	0.70 (10:20)	0.50 (11:00)	60%
Uno	1.19 (12:40)	983 (12:00)	0.89 (12:20)	0.49 (14:00)	74%
Takamatsu	1.08 (13:30)	985 (12:00)	0.76 (12:50)	0.47 (14:20)	69%
Himeji	1.47 (13:50)	985 (13:20)	1.16 (13:30)	0.46 (15:20)	78%
Kobe	1.40 (14:30)	990 (13:40)	1.11 (14:20)	0.36 (15:50)	79%
Osaka	1.62 (14:40)	991 (14:00)	1.35 (14:30)	0.37 (15:50)	82%

surface water movement as ocean long wave may cause large storm surges[5].

Since the numerical simulation model enables to include such dynamical effects without any simplification of topography, we will be able to proceed to discuss how the two main effects functioned in the simulation.

To detect these effects, we carried out two additional simulations: One is that only the wind effects are considered by setting the pressure force is set to 0 (hereafter we refer to as the "wind calculation"), and the other is that only the pressure effects are considered by setting the wind stress to 0 (hereafter we refer to as the "pressure calculation"). We represent I as the control calculation, II as the "wind calculation", and III as the "pressure calculation". The MSSs by every calculation are listed in Table
The MSSs by every calculation are listed in Table 2.

4.1 The Inverted Barometric Effect

The results of III show that all the MSSs appeared after the time when the typhoon was nearest; especially the delay became large in the Hiuchi-Nada and the Osaka Bay, that is, Uno, Takamatsu, Himeji, Kobe and Osaka. The reason is supposed that the eastward movement of water piled up in the western part of the SIS was prevented at the narrow part of the east channel surrounded by the ellipse in Fig. 7 (a). In order to verify this hypothesis, a calculation with an experimental topography as shown in Fig. 7 (b) was conducted. (The channel part is enlarged and changed to the sea with 20m depth.) The result showed that the times of the MSS in the west of the Iyo-Nada were hardly changed. On the one hand, those in the east of the Iyo-Nada became earlier and the delay of time decreased (not shown). For example, the time became earlier about 20 minutes in Takamatsu and Uno, and about 40 minutes in the Hiuchi-Nada at most.

If the static balance ($\fallingdotseq$1cm/hPa) is assumed, the amount of surge by inverted barometric effect can be estimated to be 30 - 40cm from the minimum surface pressure, that are generally 10cm smaller than the MSSs of III. The reason of this difference may be that sea water was preferably piled up, due to the inertia of sea water and the narrow strait as an "obstacle". Therefore, the dynamical inverted barometric effect with an influence of sea topography is likely to give larger MSS than only static one would give in this area.

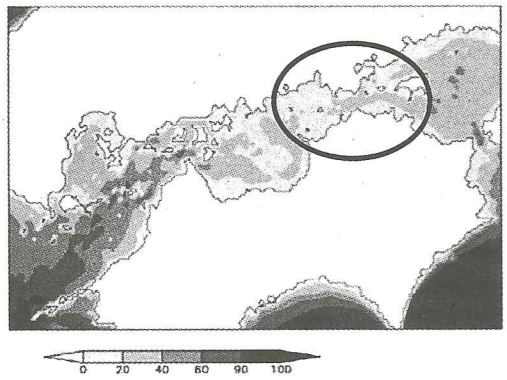

(a)

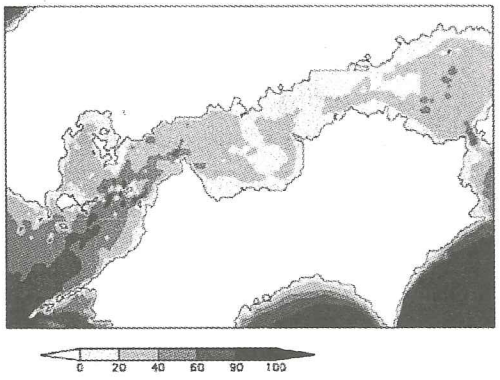

(b)

Fig. 7 (a) The original topography, (b) The test one where the east channel is extended.

4.2 The Wind Set-up

The wind set-up is the major effect of the large storm surges. The "contribution ratio" of the wind set-up in the MSS defined as the MSS in II divided by that in I, (hereafter CR) was calculated in several tide station points. CR shows high value in every point as 70 - 80% (except Matsuyama of 60%). This indicates that the wind change along with a moving typhoon had an important role.

4.3 The Characteristic Differences among Local Seas

Fig. 8 shows the amplitudes of the MSS at every grid point and surface wind corresponding to the occurrence time of the calculation I. This

distribution reveals several clusters of large storm surge area and wind direction. The storm surge in each area behaves as if the area is a bay, where large storm surge is generated in the most inner part by an inflow wind. By considering this characteristic, we divide the SIS into 6 local seas as shown in Fig. 8.

① the sea opening to east with the Kanmon Straight as a wall (the Suoh-Nada)

The wind set-up is extremely predominant due to its shallow water depth. The inflow of sea water from the Bungo Chanel also influences on the storm surges.

② the sea opening to south with the north coast of Hiroshima (the Hiroshima Bay)

Since the typhoon passed nearby and the duration of southerly wind was long, the wind set-up continued longer than other areas.

③ the sea opening to southwest, closed by islands around Imabari (the Iyo-Nada and the Aki-Nada)

The wind set-up is not so predominant due to deep water. However, the coincidence of the time of the maximum inverted barometric effect and that of the wind set-up causes large storm surge.

④ the sea opening to west, closed by the narrow channels (the Hiuchi-Nada)

The peak of inverted barometric effect appeared after the typhoon approached to the nearest because of the pile up of the sea water in the Aki-Nada. The coincidence of the time of the maximum inverted barometric effect and that of the wind set-up causes large storm surge similar to the Iyo-Nada.

⑤ the sea opening to south with the north coast of Himeji (the Harima-Nada)

The wind set-up functioned well since the sea opens to south and southwest and water depth is shallow.

⑥ the sea opening to south with the north coast of Osaka (the Osaka Bay)

The character is almost same as those of the Harima-Nada.

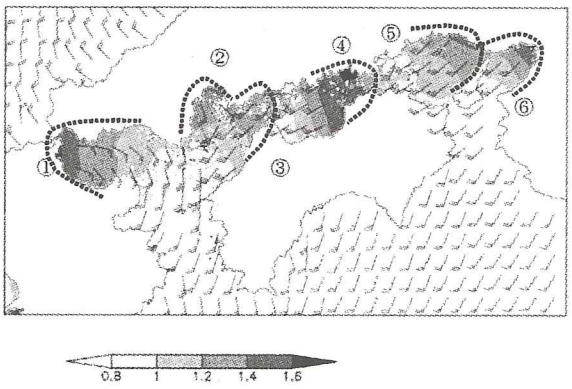

Fig. 8 The maximum storm surges (m) calculated in every grid and wind at same time

5. CONCLUSIONS

The mechanism of the storm surges in the SIS caused by TY Chaba in 2004 was investigated and our conclusions are summarized as follows:

(1) The storm surges by TY Chaba are mainly caused by the wind set-up effect, since the water depth in the SIS is generally shallow.
(2) The SIS is divided into six areas in terms of the characteristics of the storm surge caused by TY Chaba. Each area is characterized by the preferred wind direction, relative importance of wind set-up effect and piling up of the sea water.
(3) The time of the MSS was different among the areas. The time is almost the same as the time when the typhoon was nearest in the western part, although it delayed in the eastern part, especially the delay of time in the Hiuchi-Nada was over 2 hours. This indicates that storm surges in the SIS have good chances to occur after a typhoon passing away by the influence of sea topography. The timing of MSS was also influenced by the change of wind directions along with the typhoon movement.
(4) The fact that storm surges in the SIS occurred after a typhoon passing away, should be strongly kept in mind for adequate timing of warning.

Since it is rather common for a typhoon to pass along the same course as TY Chaba, that made landfall in Kyushu and passed into the Sea

of Japan, it is likely that similar storm surges also happen frequently. Therefore we will research other storm surge cases to detect the mechanism as well.

6. REFERENCES

1. Konishi, T.: Storm surges in the western part of the Inland Sea, caused by Typhoon 9119 –analyses of tidal records, documents on flooding and field inspection-, Umi to Sora (SEA AND SKY), 70, 1995 (in Japanese)
2. Konishi, T. and Y. Tsuji: Analyses of Storm Surges in the western part of the Seto Inland Sea of Japan caused by Typhoon 9119, Continental Shelf Res., 15, 1995
3. JMA:Repot on the storm surges by Typhoon Bart (No.9918) in September 1999, Japan, Technical Report of JMA, 122, 2000. (in Japanese)
4. Kohno, N.: The mechanism of storm surges caused by TY BART (9918) in 1999, KAIYO MONTHLY, 32, 2000. (in Japanese)
5. Arakawa, H. and M. Yoshitake: Report on the 'Muroto Taifu' in 1934, 1935. (in Japanese)

Report on Field Survey of Solomon Islands Earthquake Tsunami in April 2007

by

Takashi Tomita[1], Taro Arikawa[2], Daisuke Tatsumi[3], Kazuhiko Honda[3], Hiroshi Higashino[4]
Kazuya Watabnabe[4], and Shigeo Takahashi[5]

ABSTRACT
On 2 April 2007 a tsunami following an M8.1 earthquake caused serious disasters in western islands of the Solomon Islands. The tsunami killed more than fifty people and destroyed some coastal villages. To investigate the characteristics of the tsunami striking the islands and the induced damage, we conducted a field survey around Simbo Island, Ghizo Island, Ranongga Islands, Vella Lavella Island and New Georgia Island near the epicenter. A 9.03 m runup height above the sea level at the event was measured on a hill surface of Simbo Island, another 5.63 m runup height was on a hill along a southern coast of Ghizo Island. The northern village of Tapurai in Simbo Island, and Titiana and Malakerava in Ghizo Island suffered serious damage such as almost houses were swept away. According to inhabitants, many people evacuated after they watched the tsunami coming to coasts where they lived. The reason why they were able to evacuate successfully from the tsunami is that hills to escape from the tsunami are located near the affected low-lying areas. Another mitigation of tsunami disaster is traditional houses on stilts. Almost of these house damaged less by the earthquake remained after the tsunami. Some people escape to such houses from the tsunami flooding.

KEYWORDS: Disaster, Field Survey, Inundation, Rununp, Solomon Islands, Trace Height, Tsunami

1. INTRODUCTION

A big undersea earthquake whose magnitude was 8.1 occurred near the Solomon Islands around 7:40 in the morning on 2 April 2007 in local time (20:40 on 1 April in the coordinated universal time). The earthquake created a tsunami causing serious disasters along coasts of the western islands of the Solomon Islands. The Government of Solomon Island reported on 30 April that 52 people had been confirmed dead by the disaster. In order to investigate the characteristics of the tsunami and the feature of the induced damage, the Port and Airport Research Institute dispatched three researchers to the affected areas for nine days from 9 April 2007, which was one week after the disaster occurrence.

The Solomon Islands lie northeast of Australia in the South Pacific Ocean as shown in Fig. 1, and consist of approximately 1,000 mountainous islands and coral atolls, including the six main islands of New Georgia, Choiseul, Santa Isabel, Guadalcanal, Malaita, and San Cristóbal. Their land area is approximately 29,000 km^2, and the population is estimated to be approximately 480,000 people. The capital is Honiara in Guadalcanal Island. In rural islands, people live in some villages, and there are few hundred residents in a big village. The unity of each village is strong, because such a village is the minimum unit of life.

According to USGS[1], the location of epicenter is 8.481°S and 156.978°E, and is 40 km away from Gizo Town, which is the second largest town of the Solomon Islands, 345 km from Honiara. In the islands near the epicenter, for example, Simbo Island, Ghizo Island, Ranongga Islands, Vella Lavella Island and so on, is felt big ground shaking motion.

1. Tsunami Research Director, Tsunami Research Center, Port and Airport Research Institute, 3-1-1 Nagase Yokosuka, 239-0826, Japan.
2. Senior Researcher, Marine Environment and Engineering Department, Port and Airport Research Institute, ditto.
3. Researcher, Tsunami Research Center, Port and Airport Research Institute, ditto.
4. Special Researcher, Tsunami Research Center, Port and Airport Research Institute, ditto.
5. Executive Researcher, Port and Airport Research Institute, ditto.

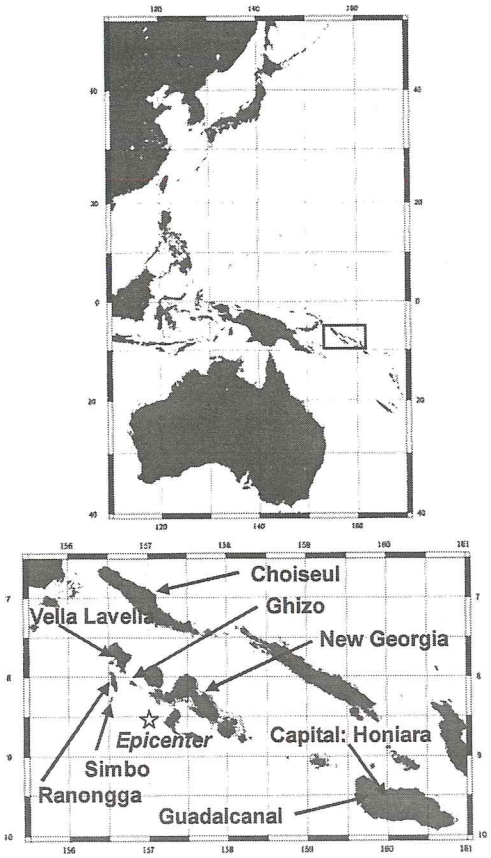

Figure 1: Location of Solomon Islands and epicenter of the earthquake on 2 April 2007.

2. NUMERICAL SIMULATION

Before carried out the field survey on the tsunami, some cases of numerical simulation were conducted to figure out the tsunami in perspective. Figures 2 and 3 show an initial form of the tsunami and a snap shot of the tsunami propagating, respectively. Figure 4 indicates the distribution of the maximum tsunami height. These results are based on the fault data, Version 0.2, by Prof. Yuji Yagi, Tsukuba University [2], which is used to calculate the initial form of tsunami. In his result, earthquake moment M_o is 3.2 x 10**21 Nm, and strike, dip and rake angles are 300°, 19° and 72°, respectively. The location of the epicenter depends on the USGS data in which latitude = -8.481°, longitude = 156.978°, and depth = 15 km. Based on other sets of fault model parameters, other numerical simulations of the tsunami are also carried out.

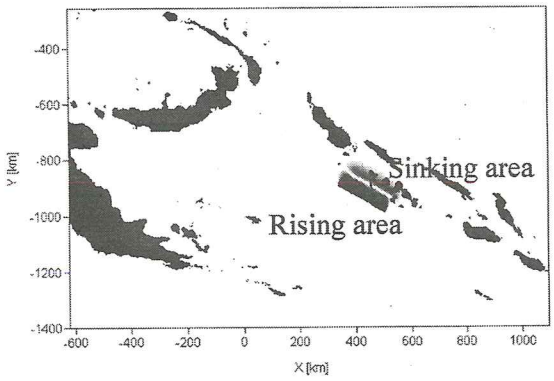

Figure 2: An initial form of the tsunami.

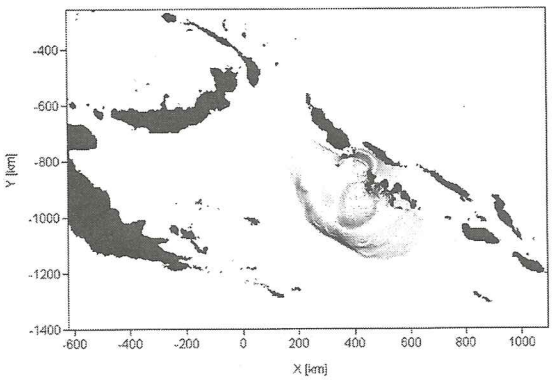

Figure 3: A snap shot of the tsunami propagating 10 minutes after the earthquake occurrence.

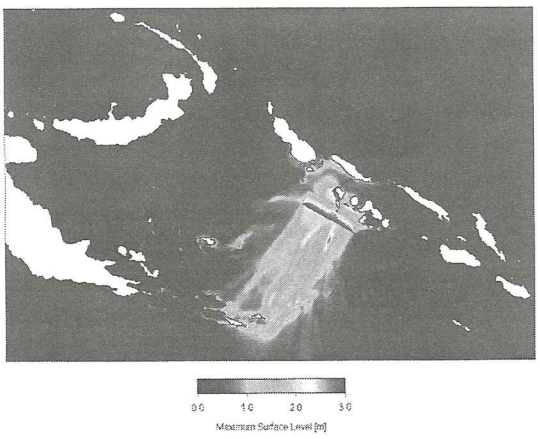

Figure 4: Distribution of the maximum tsunami height.

The numerical simulation of tsunami indicated that a higher tsunami stroke along coasts of the Ghizo, Simbo and Choiseul Islands, since these islands are in a direction perpendicular to the strike of the fault, in which the higher tsunami

energy is radiated. From such simulation results, we estimated that bigger damage was occurred along the coasts of these islands. The simulation result also showed that on the coasts of the islands near the epicenter the tsunami reached within several minutes after the quake occurrence. The other numerical simulations with the different fault parameters also showed similar results.

Actually mass media reported that the Ghizo and Simbo Islands suffered severe damage, and that the Sasamunga Village around the middle of the southern coast of the Choiseul Island was also struck by a destructive tsunami.

3. PROCEDURE OF FIELD SURVEY

Based on the results of numerical simulation and information from media and inhabitants, the locations for the field survey were selected as follows: Gizo, Titiana, New Manra, Marakerava and Sagheraghi in Ghizo Island, Tapurai and Vellaveli in Simbo Islands, Paramata, Reona, Iringgira and Vonunu in Vella Lavella Island, Keara and Pienuna in Ranongga Island, and Munda in New Georgia Island.

In the field survey, tsunami inundation heights as well as runup heights were measured from the sea surface, and then they were converted into the heights above the sea level at the tsunami striking. For the conversion, the astronomical tides at Gizo at the measurements and the event were calculated with harmonic components of tide.

To investigate the feature of the tsunami striking, tsunami arrival time after the quake, the number of tsunami waves, time interval between waves, incident direction of each wave, and tsunami front form were heard from inhabitants.

4. RESULTS OF FIELD SURVEY

4.1 Trace Height

Figure 5 shows the tsunami trace heights measured in the field survey. The trace height is divided into inundation height and runup height. As shown in Figure 6, the inundation height is, for example, the height of the water mark remaining on a wall of house on the ground. The

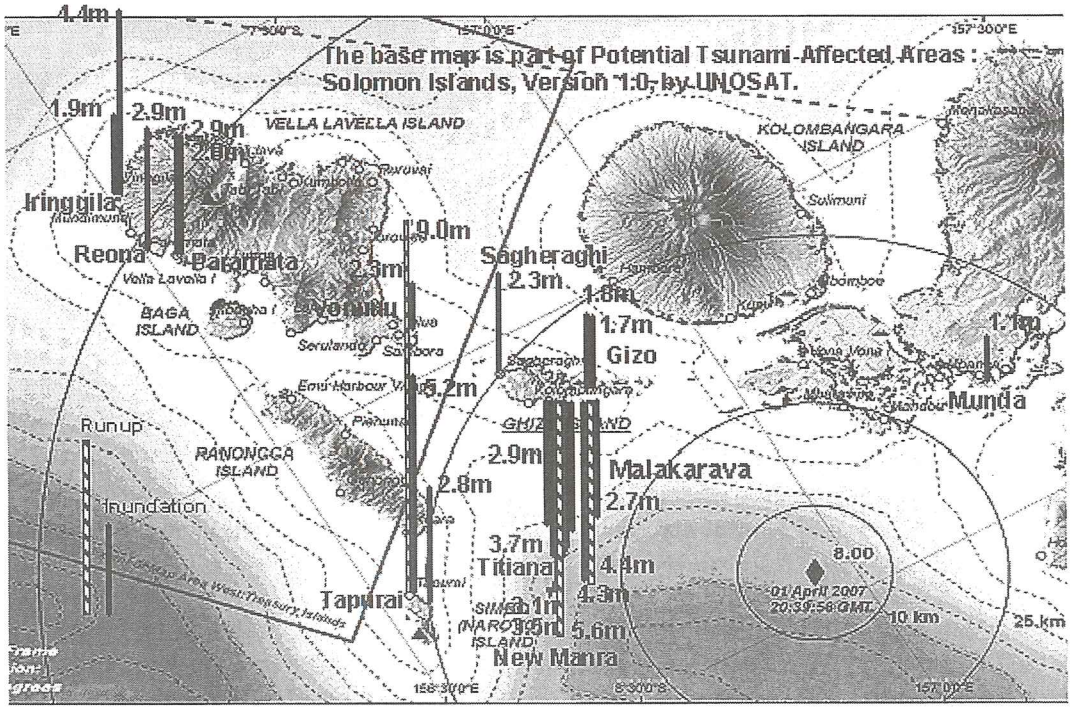

Figure 5: Tsunami trace heights above the sea level at the tsunami striking

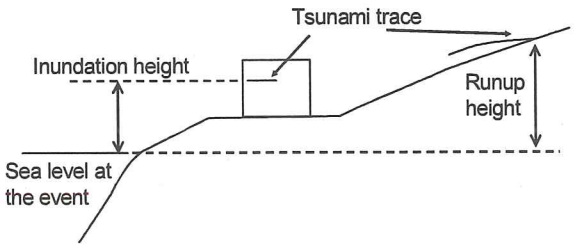

Figure 6: Definitions of inundation height and runup height

runup height is the height of the water mark on a hill.

Form the field survey results, it is confirmed that the higher tsunami struck along coasts of Simbo Island and southern coast of Ghizo Island. The trace heights are more than 5 m locally.

4.2 Tsunami and Damage in Each Island

4.2.1 Ghizo Island

On the southern coasts of Ghizo Island, the tsunami with 4 m approximately struck. At Marakerava on the southern coast, the tsunami climbed up to 5.63 m on a hill surface. According to eyewitness, the first tsunami receded and then the sea water rose in whole, which was not like a water wall. Some inhabitants said that they watched the tsunami coming to the coast and then they evacuated to the hill behind their village. A 14-year-old boy told us that he and his 5-year-old friend were swept by the tsunami in a house, and he helped his friend to escape from a window and then he got out from a breach of a house wall that was made by the tsunami flow. The inundation depth there measured was 1.43 m on the ground. Another person said the first tsunami came a few minutes after the quake and another two tsunamis struck after that. The duration time of three tsunami waves was within 10 minutes. The tsunami destroyed completely houses in the first and second rows from a beach, and the third-row houses remained but suffered severe damage as shown in Picture 1.

In Titiana Village, almost houses were swept by the tsunami higher than 3 m, as shown in Picture 2. However, some houses on stilts remained in the affected area as shown in Picture 3. When we visited there, no persons were in the village because they took refuge on the hill and did not return to the coastal side.

In New Manra, the inundation height of 3.50 m was measured on an inside wall of a house. Beach erosion whose depth was 1 m was found there.

In Sagheraghi Village on the western coast of the Ghizo Island, some houses on stilts were floated away and some main bodies of house sit on the ground and other houses were collapsed.



Picture 1: Swept and remained houses in Marakerava.

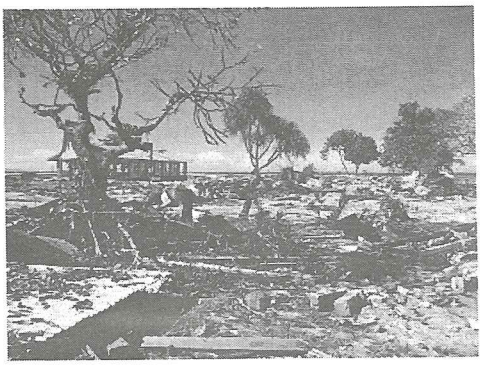

Picture 2: Tsunami damage in Titiana.

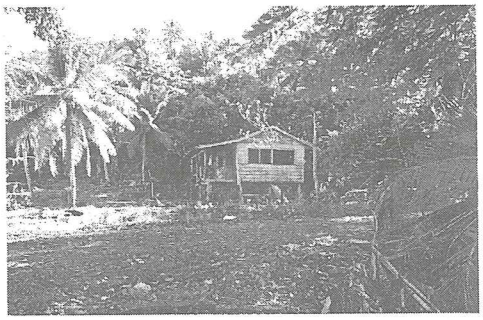

Picture 3: House on stilts remained after the tsunami in Titiana.

4.2.2 Simbo Island

A runup height of 9.03 m was found on a hill slope as a clear border of dead vegetation by salty water, as shown in Picture 4. In Titiana Village, there were more than 100 houses, and the houses were completely swept by the tsunami as shown in Picture 5, but a house on stilts remained at the innermost part of the village along the hill edge. Since many wrecks of destroyed houses were twined around the stilts of the house, the tsunami inundation depth was lower than the length of the stilts. The inundation height there was 5.20 m. Church on a hill also remained.

Inhabitants said that the first tsunami came from north and the second tsunami reached from south. They encountered each other in the sea in front of the village and went away from the island. This feature seems the coming of diffracted tsunamis by the island. The diffracted tsunamis by the island encountered each other behind the island resulting in the higher tsunami striking the village.



Picture 4: Tsunami runup in Tapurai.

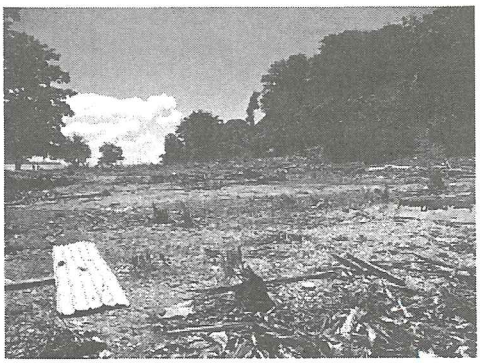

Picture 5: Tsunami damage in Taprai.

4.2.3 Vella Lavella Island

In Vella Lavella Island, four villages were investigated. Especially in Iringgira on the western coast of the island, higher inundation height of 4.46 m was measured. A local area in the village was struck by the higher tsunami and a lot of houses were swept away, as shown in Picture 6. However, other parts of the village were also inundated by the tsunami but many houses remained. According to eyewitness, firstly the sea in front of a beach of the village was separated into right and left. After that the seawater came reversely from the right and left sides into the area that the seawater retreated and then the tsunami struck the village. Part of the tsunami climbed a river and hit the village from behind. The tsunami striking this village seems to be effected highly by bathymetry, topography and geometry. To understand the tsunami feature there, we should conduct the numerical simulation with detailed bathymetry, topography and geometry data.

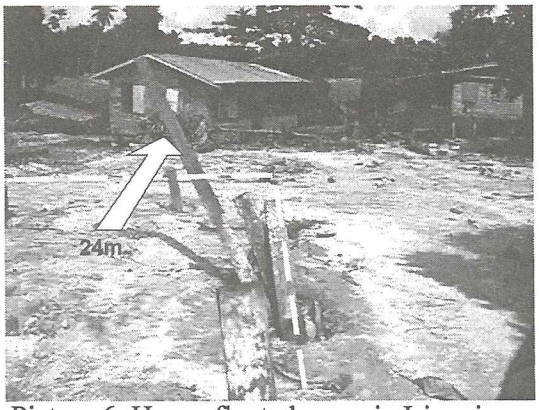

Picture 6: House floated away in Iringgira.

4.2.4 Ranongga Island

At locations we visited in Ranongga Island there were less damages by the tsunami. Especially, in Pienuna on the eastern cost of the island, the tsunami did not overflow the land, because the land was raised 2m from the original level by the displacement due to the earthquake. As the result, coral reef appeared above the sea surface as shown in Picture 7.

At other places of the island, landsides were caused by the earthquake motion. An example is shown in Picture 8.



Picture 7: Coral reef appearing above the sea surface in Pienuna.

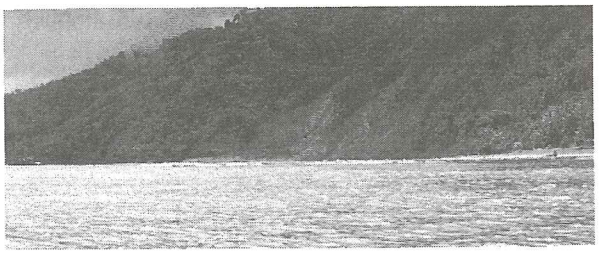

Picture 8: Landslide in Ranongga Island.

5. DISCUSSIONS

Although the high tsunami whose height was more than 3 m struck coastal low-lying areas in the Solomon Islands, many people could evacuate to save their lives. There are four key points to achieve successful evacuation;

1) The earthquake occurred around 7:40 in the morning. Therefore, many people could recognize the tsunami coming visually.

2) The coming tsunami was not like a wave, and the sea surface was raised like a fast tide. Therefore, the water flow by the tsunami was not as fast as a supercritical flow whose speed is faster than an ordinal tsunami speed of $\sqrt{gh}$. Some people could run in the flow of tsunami

3) There were hills to evacuate from the tsunami near coasts. Therefore, many people could climb the heights to escape from the tsunami as soon as watching the tsunami.

4) A tale in which you should escape to a hill when you see an abnormal low tide helped some people to do quick evacuation. The lessons from the 2004 Indian Ocean Tsunami Disasters was also effective for some persons' evacuation after the earthquake.

Another mitigation of tsunami disaster is traditional houses on stilts. If such a house suffered less damage by the earthquake, almost of them remained. On the other hand, many houses on stilts were broken by the earthquake motion, because such a structure was vulnerable to quake motions. A house on stilts that is strong against quake motion is a good measure against tsunamis as well as earthquakes. Moreover, it is better that such a house is built on a place which is as high as possible.

6. SUMMARY

The field survey on the Solomon Islands Earthquake Tsunami on 2 April 2007 was conducted by PARI. The tsunami trace heights were measured in Ghizo, Simbo, Vella Lavella and New Georgia Islands. The maximum trace height was 9 m on the hill slope of Simbo Island which was the runup height.

Because the hills to escape from the tsunami are near the coasts, many people could climb the hills to save their lives quickly after they watched the tsunami. The traditional houses on stilts are effective for tsunami disaster reduction.

ACKNOWLEDGEMENT

We would like to express our gratitude to National Disaster Council National Disaster Management Office, Mr. Yukio SATO, and Mr. Yoshiyuki SATO of the Solomon Islands, and related departments of the Ministry of Foreign Affairs and the Ministry of Land, Infrastructure and Transport. For our field survey on the tsunami, we have received their assistance.

REFERENCES

1 URL of USGS: http://earthquake.usgs.gov/eqcenter/eqinthenews/2007/us2007aqbk/

2 URL of Prof. Yagi: http://www.geo.tsukuba.ac.jp/press_HP/yagi/EQ/20070401/ (in Japanese).

US National Tsunami Research Plan

by

Eddie Bernard[1] and Lori Dengler[2], and Solomon C. Yim[3]

ABSTRACT

This paper summarizes the events that led to the development and completion as well as the main points of the US National Tsunami Research Plan (Reference 1) under a project jointly supported by the United State National Science Foundation and the National Oceanographic and Atmospheric Administration. The Office of Science and Technology released a report in 2005 that called for a review of tsunami research needed to reduce tsunami vulnerability in the United States. An Organizing Committee was appointed by the Chair of the U.S. National Tsunami Hazard Mitigation Program (NTHMP) to develop a Strategic Plan for tsunami research. The Committee assembled a group of tsunami experts to review the current state of knowledge in areas essential to tsunami risk reduction and a workshop was held 25–26 July 2006 to develop a consensus on priority research needs. The focus of the effort was to define the basic research in areas of technology, geosciences, oceanography, engineering, and social sciences needed to develop, promote, and institutionalize tsunami-resilient communities in the United States. The group agreed to fifteen recommendations in tsunami hazard assessment, tsunami warnings, and tsunami preparedness and education. The Organizing Committee combined these recommendations into six synthesized high-priority areas for tsunami research. The synthesized plan was approved by the NTHMP Steering Committee on 1 November 2006. The final report reflects the comments for the NTHMP Steering Committee and workshop participants. Serendipitously, the U.S. Congress passed the Tsunami Warning and Education Act which President Bush signed into law on 20 December 2006. The Research Plan and the Tsunami Act are amazingly consistent and compatible and lay the foundation for a successful implementation of the Research Plan through a multi-agency effort.

KEYWORDS: tsunami; United States; national; planning; research; warning; education.

1.0 INTRODUCTION

Tsunamis have been recognized as a significant hazard in the United States since the mid-twentieth century when major tsunamis caused significant damage in Hawaii, Alaska, and the West Coast of the United States. The 2004 Indonesian earthquake and tsunami has led to increased concern about tsunami hazards in the United States and a reassessment of risk and mitigation programs. As part of this assessment effort, the December 2005 release of the Office of Science and Technology Policy report "Tsunami Risk Reduction for the United States: A

[1] Director, Pacific Marine Environmental Laboratory, NOAA, Seattle, WA 98115, USA
[2] Professor and Chair, Dept. of Geology, Humboldt State University, Arcata, CA 95521, USA
[3] Professor, Dept. of Civil Engineering, Oregon State University, Corvallis, OR 97331, USA

Framework for Action" called for scientists to perform a "review of tsunami research and develop a strategic plan for tsunami research in the United States" (Reference 2). An Organizing Committee was appointed by the Chair of the National Tsunami Hazard Mitigation Program (NTHMP), Dr. John Jones of NOAA, to develop a Strategic Plan for Tsunami Research and write an initial draft Plan by 1 November 2006.

The focus of the effort was to define the basic research in areas of technology, geosciences, oceanography, engineering, and social sciences needed to develop, promote, and institutionalize tsunami-resilient communities in the United States.

2.0 ORGANIZING COMMITTEE AND WORKSHOP

An Organizing Committee (OC) was formed consisting of Dr. Eddie Bernard, Director of the NOAA Pacific Marine Environmental Laboratory (PMEL), Professor Lori Dengler, Humboldt State University, and Professor Solomon Yim, Oregon State University. A framework was developed to include all areas of tsunami risk assessment and mitigation that are essential to creating tsunami-resilient communities:

- Hazard Assessment: characterization of local and distant sources, determination of tsunami recurrence, estimation of tsunami impact using field, laboratory, and model data, and evaluation of the threat to lives, community infrastructure, and the natural environment.
- Warning Guidance: development, installation, and maintenance of monitoring systems to detect and forecast tsunamis in real time, timely dissemination of these warnings to save lives, and improving products received by the end users of warning information.
- Preparedness and Response: developing, implementing, assessing, and institutionalizing programs to reduce the long-term risk to human life and property based on hazard assessment, and preparing threatened communities through education, land use management, and other legislative and incentive policies.

Each OC member was responsible for one area of the framework, with Bernard on Warning Guidance, Dengler on Preparedness and Response, and Yim on Hazard Assessment. Dr. Bernard is the Director of NOAA/PMEL, former Director of the Pacific Tsunami Warning Center, and the founding Chairman of the National Tsunami Hazard Mitigation Program. Dr. Dengler is Professor and Chair of the Geology Department at Humboldt State University. She developed the Strategic Implementation Plan for tsunami mitigation projects in the NTHMP, and has been involved with tsunami community mitigation, education, and outreach activities. Dr. Yim has been conducting numerical and experimental research on tsunami effects on coastal infrastructure. He is the Principal Investigator (PI) of the National Science Foundation (NSF) Tsunami Wave Basin Construction Project and the PI of the NSF Site Operation and Management Project at Oregon State University.

Professor Yim wrote a proposal to NSF and Dr. Bernard provided matching NOAA funds to jointly sponsor the NSF/NOAA workshop, which had three objectives:

1. To review: (a) past tsunami research plans, (b) current tsunami research, (c) Federal agency plans for future tsunami research, (d) research needs resulting from the 2004 Indian Ocean tsunami, and (e) experimental research capabilities in the U.S.
2. To develop a Strategic Research Framework for the development of tsunami-resilient communities based on the reviews above and input from all participants, including Federal and State agencies, academic researchers, and private sector practitioners.
3. To document and disseminate the resulting review and strategic research framework to the tsunami research community.

The OC assembled a group of tsunami experts to review and report on the current state of knowledge in areas essential to tsunami risk reduction, and chose the workshop format to develop recommendations. After the workshop, the OC met to synthesize the reports and recommendations to

constitute the Plan.

3.0 PRE-WORKSHOP PREPARATION

Experts from academic institutions, governmental agencies, and the private sector were selected based on balancing scientific discipline, ethnic, gender, research experience, and geographical diversity. Approximately half of the participants were from government and state agencies with responsibilities for research planning, funding, and implementation (NSF, NOAA, Federal Emergency Management Agency (FEMA), Nuclear Regulatory Commission (NRC), United States Army Corps of Engineers (USACE), and United States Geological Survey (USGS)). The other half were academic faculty and private sector representatives involved with research in a number of areas, including wave propagation, inundation, coastal structures, experiments, numerical modeling, instrumentation and sensor technology, education and outreach, social psychology, social and natural sciences, and oceanography. A balance of junior- and senior-level researchers was maintained by having similar numbers of junior (assistant—5 and associate—2 professors) and senior (full professors—9) faculty from the academics. The participants were geographically diverse and included the east coast (Pennsylvania, Florida, D.C., New Jersey, New York, Virginia, Maryland), south (Georgia, Mississippi, Texas) mid-west (Illinois), central (Colorado), and west coast (California, Oregon, Washington, Alaska, Hawaii).

Every participant was assigned a "state of the science" topic and asked to write a report for a particular sub-element of the three framework categories, Hazard Assessment, Warning Guidance, and Preparedness and Response. They were also asked to vet their summary with colleagues in their field and identify areas of needed research (see Appendix C of Reference 1 for assignment letter, submitted reports, and recommendations). Federal Agency representatives were asked to provide a summary of tsunami activity and expenditures for Fiscal Year 2005. A description of agency activity and funding for tsunami activities for Fiscal Year 2005 was provided by the NSF, NOAA, National Aeronautics and Space Administration (NASA), USGS, FEMA, and US-ACE (see Appendix D, Reference 1) and Federal Agency expenditures on tsunami research is summarized in Section 4 below.

Once the participants had agreed to participate and provide advanced written material, the OC created an agenda with invited and Federal agency presenters. The OC used the "state of the science" reports to compile a preliminary draft research plan that contained 65 research recommendations and was available to workshop participants.

A workshop to develop consensus for tsunami research strategic planning was held 25–26 July 2006, in Corvallis, Oregon. Appendix B has a complete list of the 48 participants.

4.0 FEDERAL AGENDA SUMMARY

Table 1 provides a Federal Agency funding profile for the U.S. tsunami risk reduction effort (extracted from Appendix D, Reference 1). Five agencies spent $54.4M in FY05 to reduce the impact of tsunamis to U.S. coastlines. NOAA and the USGS contributed about 80% of the effort, while NSF contributed 12%. The agencies reported their expenditures in four categories: Research, Hazard Assessment, Warnings, and Preparedness. About 60% of the effort went into warnings, while Research represented a respectable 20% of the total. Tsunami assessment was the third largest category, while Preparedness was the smallest category at 7%. Preparedness efforts funded at the State or local level are not included in this report. It is, therefore, incorrect to infer that Preparedness is the lowest priority in the total Federal effort.

5.0 WORKSHOP PROCESS

Presenters gave overviews of the "state of the science" and agency activities to plenary sessions of all the workshop participants. Following each presentation, discussions were held to elaborate on and clarify the issues. On the second day of the meeting, participants were divided into three focus groups

based on the framework areas: hazard assessment, warning guidance, and preparedness and response. Each Focus Group was asked to formulate five recommendations in their respective areas. A plenary discussion of all the participants was held to combine and refine the focus groups' recommendations. After extensive discussion and debate, workshop participants agreed to recommendations listed in the section: Fifteen Workshop Recommendations.

A major concern that emerged from the discussion was how will this Plan offer an opportunity to actually conduct tsunami research? The group wanted to have a tsunami research program established that would receive proposals and provide a fair review process. Serendipitously, the Tsunami Warning and Education Act (see Appendix E, Reference 1) was passed by Congress and signed by the President on 20 December 2006. Section 6 of the law states

> "The Administrator shall, in consultation with other agencies and academic institutions, and with the coordinating committee established under section 5(b), establish or maintain a tsunami research program to develop detection, forecast, communication and mitigation science and technology, including advanced sensing techniques, information and communication technology, data collection, analysis, and assessment for tsunami tracking and numerical forecast modeling. Such research program shall—
>
> (1) consider other appropriate research to mitigate the impact of tsunami;
>
> (2) coordinate with the National Weather Service on technology to be transferred to operations;
>
> (3) include social science research to develop and assess community warning, education, and evacuation materials; and
>
> (4) ensure that research and findings are available to the scientific community."

A limitation of this authorization act is that the research program described in the law is about $2M/year for the fiscal years 2008–2012. Examining Table 1 reveals that in FY2005, research expenditures exceeded $10M. The Tsunami Act research program would represent about 20% of the national tsunami research effort. The Act research program may be the basis for a multi-agency research program that includes NSF, NOAA, FEMA, and USGS. This Tsunami Research Plan could serve as the starting point to establish an interagency research program that could be supported by several agencies. One option would be for NSF to serve as lead agency with other agencies providing annual contributions to support basic tsunami research as suggested by the Research Plan.

Participants were allowed to study the 15 recommendations and provide comments to the OC until 15 September 2006.

6.0 POST-WORKSHOP PROCESSING

On 4 and 5 October 2006 the OC met to synthesize the preliminary report and workshop recommendations. It was a concern of the OC and many workshop participants that, while dividing the framework into the areas of hazard assessment, warning guidance, and preparedness/response simplified organization, it did not recognize the inherent overlaps in the three areas. To develop a more integrated approach, the OC chose to organize the recommendations from the perspective of "a person on the beach," and define the essential needs to reduce the risks to this individual and his/her community. The 15 recommendations were distilled into 6 recommendations that are presented in the Strategic Tsunami Research Plan section.

7.0 FIFTEEN WORKSHOP RECOMMANDATIONS

7.1. Improve identification and understanding of tsunami sources (earthquakes, landslides, volcanoes,

asteroids, others (explosion)—Source physics, geophysics, and geology. Includes paleotsunami studies to identify and define sources and their recurrence (needed for prioritizing by coast and state), and to test source models for consistency with coseismic land-level change and geodetic observations.

7.2. Quantitative analysis of shore impacts—Improvements in hydrodynamic modeling of propagation and inundation, structural response, vulnerability (population, infrastructure in harm's way). Methods of using tsunami deposits to validate inundation models. Bathymetric focusing and defocusing, including problems with modeling for fringing reefs. Flow in built environments. Social science. Regional damage and loss assessment methods (Hazards U.S. (HAZUS) analog). Modeling standards and benchmarks. (HAZUS-MH, or Hazards U.S. Multi-Hazard, is FEMA's Geographic Information System- (GIS-)based multi-hazard loss estimation software program. It currently covers earthquake, hurricane winds, and flood inundation.)

7.3. Develop probabilistic methods—subsumes deterministic and parametric studies; inundation maps, impact forces, national and community-specific tsunami hazard maps (to be consistent with earthquake maps, FEMA FIRM (flood insurance rate maps)).

7.4. Improve data acquisition, archiving, and retrieval—field observations and instruments; experiments; numerical computations, including tsunami simulation results (inputs and outputs); remote sensing. Topography and bathymetry—submarine landslides identified this way; also basic to identifying recently active faults.

7.5. Improve tsunami warning products, including forecasts of tsunami arrival times, amplitudes, period, duration, and "all clear" advisories through tsunami imaging.

- Requires new tsunami monitoring methodology, including rapid earthquake magnitude estimation, spaceborne and oceanic tsunami imaging, and new instruments for measuring the tsunami flow regime flooding.

7.6. Design scalable multi-purpose observational networks for timeliness, accuracy, precision, and sustainability for both local and distant tsunami sources and tsunami dynamics.

a. Explore use and accessibility of existing observational networks such as real-time Global Positioning System (GPS) networks, or enhanced GPS remote sensing technologies for atmospheric, ionospheric, and ocean surface disturbance mapping;

b. Evaluate non-seismic source networks.

7.7. Develop tsunami forecasting models and data assimilation and analysis techniques.

a. Requires operational standards and calibration,

b. Requires improvements in rapid seismic and other tsunamigenic source characterization,

c. Requires high-resolution global bathymetry and topography,

d. Requires continued bench-mark simulations based on laboratory and tsunami field observations.

7.8. Develop interoperable communications protocols

a. To better exploit data, and

b. To disseminate information using standardized text and visual products that requires social and behavioral science research.

7.9. Quantify the impact and interaction of tsunamis on structures and the built environment and develop design guidelines (include demonstration projects and possible tsunami-resistant building code criteria).

7.10. Describe the effects of tsunamis on the natural environment (sediment transport, liquefaction, debris, etc.).

7.11. Develop risk quantification measures,

including economic loss analysis—such as an enhanced HAZUS module that includes ecosystem economic losses/value.

7.12. Assess how different population segments respond to official and natural warnings, evacuation behavior—and how we promote appropriate behavior (including framework for local officials to assess alternative warning and evacuation mechanisms).

7.13. Develop scenario-based guidelines for the response (evacuation), recovery, and mitigation planning processes (exercises).

7.14. Address how building codes and land-use planning can be incorporated into design and construction practices for a tsunami-resilient community.

7.15. Establish standards for tsunami education based on evaluation and assessment to define best practices with regards to signage, curriculum, door-to-door campaigns, print and video products, drills, and other outreach programs.

8.0 FINALSTAGES OF PLAN DEVELOPMENT

The OC presented the October 2006 draft version of the Plan during the annual meeting of the NTHMP in Washington, D.C. on 1 November 2006. Based on the feedback from the NTHMP, the revised Plan was disseminated to all participants for final review by 31 December 2006. Following a 2-week vetting process, the final plan was published.

9.0 STRATEGIC TSUNAMI RESEARCH PLAN

9.1 Recommendation 1: Enhance and sustain tsunami education

Societal Need

Education is the core of any effective tsunami mitigation effort. The vulnerable individual on the beach must recognize both natural and official warnings and respond quickly and appropriately, often with little official guidance. Education is identified by the Strategic Implementation Plan for Mitigation Activities in the U.S. Tsunami Hazard Mitigation Program as the first of five planning elements. The first recommendation of the California Seismic Safety Commission report on California's tsunami risk (2005) was to "Improve education about tsunami issues in the State," but even with the heightened concern about tsunamis produced by the December 2004 Indian Ocean tsunami, tsunami education and outreach programs have not seen an increase in support commensurate with the scientific and engineering aspects of warning systems.

Research Need

Research is needed to understand how individuals process warning information, whether it is an official warning issued by the warning centers or natural indicators such as ground shaking or drawdown. There has been little analysis of what constitutes effective tsunami educational materials and little coordination among states to define messages in terms of different user groups and desired outcomes. Few studies have examined how individuals identify what they consider a credible source of tsunami information and what prompts them to evacuate.

9.2 Recommendation 2: Improved warning system

Societal Need

As the populations of the U.S. continue to migrate to coastal areas, the need for timely, accurate, and effective tsunami warnings is essential for coastal populations to function efficiently. Failure to warn effectively as in the case of the 2004 Indian Ocean tsunami can lead to catastrophic loss and public outcry. Over warning diminishes confidence in the system, and involves economic costs. For example, the economic losses of evacuation for a nondestructive tsunami can be as high as $70M for a city like Honolulu, Hawaii. At the other extreme, the economic impact of closing the port of Los Angeles for 6 months due to a destructive tsunami could be in the billions of doilars. Hence, the need for accurate tsunami information to the right person at the right time is vital to our coasts' physical and economic

survival.

Research Need

Research is needed to improve tsunami warning products and effectiveness, including forecasts of tsunami arrival times, amplitudes, period, duration, and "all clear" advisories for specific coastal locations. It is also essential to assess how people respond to natural and official tsunami warnings. Such research will require new instrumentation, evacuation behavior studies, and standard communication protocols to ensure compatibility with various state and federal dissemination systems. Research is also needed to design scalable, multi-purpose observational networks for timeliness, accuracy, precision, and sustainability for both local and distant tsunami sources and tsunami dynamics, including existing and non-seismic networks.

9.3 Recommendation 3: Understand the impacts of tsunamis at the coast

Societal Need

No effective tsunami mitigation program can be undertaken without an understanding of the coastal impacts of tsunamis. In order to establish evacuation zones and routes, design for tsunami-resistant construction, estimate likely losses, and develop education programs, coastal communities must understand what areas are at risk, the likely water heights and flow velocities, and how tsunamis interact with the built and natural environment.

Research Need

Research is needed to improve hydrodynamic modeling of propagation and inundation that includes not only expected water heights but also characterizes the distribution of flow velocities and duration of the tsunami event. Instrumentation needs to be developed and deployed to measure tsunami currents at the coast and in harbors to validate modeling results. Credible fragility models and laboratory data are needed to understand the interaction of tsunamis with the built and natural environment. Methodology for using tsunami deposits and other paleoindicators of past tsunami events should be expanded to validate inundation models. Modeling standards and benchmarks must be established to provide credibility to numerical modeling results.

9.4 Recommendation 4: Develop effective mitigation and recovery tools

Societal Need

Mitigation taken in the broadest context includes all activities taken before an event to reduce vulnerability, such as tsunami-resistant design and construction, land-use planning, response and recovery planning, and benefit-cost analyses of potential impacts and mitigation activities. The construction, design, and layout of buildings and other infrastructure will affect damage, evacuation, and recovery. In the United States, regulations comparable to those of other hazards such as earthquake ground shaking or hurricane hazards have not been incorporated into building codes or land use zoning decisions.

While many State and community recovery plans are multi-hazard in nature, many of these plans do not specifically address the tsunami hazard in sufficient detail. Hurricane Katrina demonstrated that the United States faces significant problems in both response and recovery for catastrophic disasters. While major tsunami events have been included in FEMA planning exercises, there has been little research specific to tsunamis, or efforts that incorporate the lessons from Katrina into tsunami response and recovery plans.

Longer-term tsunami recovery plans are non-existent. Analyses of the potential costs and benefits of mitigation measures can stimulate both government and the private sector to take action to reduce vulnerability.

Research Need

Research is needed to develop design and construction practices and guidelines for land use planning decisions, designation of vertical evacuation shelters, and realistic loss estimates. Research must be conducted to identify both the unique issues involved with tsunami events and those in common with other disasters. Research is needed to develop a framework for the tsunami recovery and

reconstruction process that incorporates both sustain-ability and reducing vulnerability from future tsunami events.

9.5 Recommendation 5: Improve characterization of tsunami sources

Societal Need

Tsunami hazard mapping and coastal impacts depend upon an accurate analysis of potential tsunami sources and their recurrence. Zoning that addresses hazards such as the FEMA Flood Insurance Rate Maps (FIRM) require a definition of 100-year and 500-year hazard zones. An accepted methodology for probabilistic tsunami hazard mapping has not been developed for the United States. Tsunamis cannot be addressed in a manner comparable to other natural hazards until this methodology is developed.

Research Need

Research is needed to better identify and understand tsunami sources, including earthquakes, subaerial and submarine landslides, volcanic eruptions, and impacts. It is necessary to develop a probabilistic framework for characterization of tsunami sources that includes recurrence so that tsunami hazards can be incorporated into planning efforts in a manner comparable to other hazards such as earthquakes and flooding.

9.6 Recommendation 6: Develop a tsunami data acquisition, archival, and retrieval system

Societal Need

All recommendations listed above require basic data infrastructure to conduct tsunami research efficiently and with consistency. The 2004 Indian Ocean tsunami exposed many shortcomings in our past practice of "ad hoc" approach to tsunami data collection and archiving. While the world was clamoring for accurate data on past tsunamis to evaluate potential threats to coastal communities, many errors and inconsistencies were discovered in the existing tsunami data bases due to inadequate past investments. Without accurate, assessable data bases the tsunami research will be stymied.

Research Need

A research data acquisition system is needed—including field observations, experiments, experimental scenarios, remotely sensed data, topography, high resolution bathymetry—that is easily accessible through a web-based archival system. The system should also include a searchable bibliography to ensure publications are easily available.

10.0 ACKNOWLEDGEMENT

Financial support from the National Science Foundation (CMMI-0636344) and NOAA is gratefully acknowledged.

11.0 REFERENCES

1. Bernard, E., Dengler, L. and Yim, S.C., "National Tsunami Research Plan: Report of a Workshop Sponsored by NSF/NOAA," NOAA Technical Memorandum OAR PMEL-133, March 2007.

2. A Joint Report of the Subcommittee on Disaster Reduction and the United States Group on Earth Observations "Tsunami Risk Reduction for the United States: A Framework for Action".

Table 1: Fiscal Year 2005 Federal Agency expenditures ($M) for tsunami risk reduction.

Agency	Research	Assessment	Warnings	Preparedness	Totals	% of Totals
NSF	6.3	0.0	0.0	0.0	6.3	**12**
NOAA	0.8	1.4	20.3	3.5	26.0	**48**
USGS	3.0	2.0	12.0	0.0	17.0	**31**
USACE	0.0	4.5	0.0	0.0	4.5	**8**
FEMA	0.0	0.5	0.0	0.2	0.7	**1**
Totals	10.1	8.4	32.3	3.7	**54.5**	
% of Totals	**19**	**15**	**59**	**7**		**100**

Storm Surge Forecast System for Floodfighting Warning

by

Masaya Fukuhama[1] and Fuminori Kato[2]

ABSTRACT

This paper presents current developments in a real-time forecast system for wave runup to ensure proper floodfighting warning in coastal areas. The system consists of a typhoon model, storm surge model, wave models, and a wave runup model. A wave model for shallow water was developed through numerical tests on preciseness and time of hindcasting. The results of the tests show that an improved WAM that considers wave breaking and tides can forecast waves in inner bays with good precision in real time.

KEYWORDS: Floodfighting Warning, Real-time Forecast, Storm Surge, Wave Runup

1. INTRODUCTION

Japan's Flood Fighting Law stipulates that prefectural governors shall issue a floodfighting warning of storm surges in coast areas previously recognized as being at high risk. Floodfighting warnings are transmitted to the administrators (mayors, etc.) of floodfighting activities such as patrolling coasts and closing water gates. However, forecasts of storm surges and high waves before a typhoon approach are not sufficient information for issuing a floodfighting warning because the forecasts do not indicate if the wave runup exceeds the coastal dikes. Also, wave forecasts are not very precise, particularly near the coasts because wave models do not consider wave transformation in shallow water, such as shoaling and refraction. Therefore, we are developing a wave runup forecast system to ensure proper floodfighting warnings.

2. WAVE RUNUP FORECAST SYSTEM

As shown in Fig. 1, the system forecasts wave runup on each coast every hour for 24 hours based on storm surges and high waves estimated by the Japan Meteorological Agency (JMA). Wave runup is calculated by the Improved Imaginative Slope Method [1], a simple method often used for designing shore protection facilities in Japan. The forecasted wave runup is edited in graphs and tables, and delivered via Intranet and Internet to regional bureaus of MLIT and prefectures. The graphs that show predicted wave runup and height of coastal dikes is important information for deciding when and on which coasts a floodfighting warning is issued. The system can predict the worst-case scenario because wave runup is forecasted for five typhoon courses based on the probability circle forecasted for the typhoon. The predicted wave runup is updated every six hours.

3. DEVELOPMENT OF WAVE FORECAST MODEL

JMA forecasts waves near Japan using the Regional Wave Model, in which ocean waves forecasted by the Global Wave Model are used as boundary conditions. As of March 2007, the grid size of the Regional Wave Model is 6 min in polar coordinates (about 10 km long). The model does not consider wave transformation in shallow water, such as shoaling and refraction. Therefore, reproducibility of bathymetry and wave transformation is limited for inner seas with complicated bathymetry.

In this study, we examined wave models to precisely forecast waves in inner seas by using forecasts of the Regional Wave Model as boundary conditions, considering bathymetry and wave transformation in shallow water.

[1] Head, Coast Division, River Department, National Institute for Land and Infrastructure Management, Ministry of Land, Infrastructure and Transport (MLIT), Asahi 1, Tsukuba-shi, Ibaraki-ken 305-0804, Japan

[2] Senior Researcher, Coast Division, NILIM

3.1 Review of Wave Forecasting Model

3.1.1 Comparison of Wave Forecasting Models

WAM (WAve Model) and SWAN (Simulating WAves Nearshore) are major wave hindcasting models that can be applied for shallow water. WAM is widely used for estimating ocean waves, and its applicability to hindcasting in inner seas has been reviewed in recent years [2-5]. SWAN is a third-generation wave model the same as WAM and can also consider wave breaking. Wave transformation models, which consider not winds but reflection and wave breaking etc., are often used for designing shore protection facilities. They do not consider generation and growth of waves, but need only a short time to calculate nearshore waves.

In this study, wave models were examined for major typhoons between 1997 and 2004, in Ise Bay, Harima Sea and Ariake Sea as shown in Figs. 2-4. The computation areas are divided as shown in Table 1. Preciseness and time of hindcasting were compared between cases in which WAM (Cycle 4), SWAN (40.41), and a wave transformation model based on energy balance equation were set in each computation area as shown in Table 2. Target fields of this study are the Middle Area and the Narrow Area. WAM was used for hindcasting waves in the Wide Areas covered by JMA's Regional Wave Model forecasts. In connecting Wide Area 3 to Wide Area 2, the number of angular components was increased with expansion of frequency band to higher frequency by spline interpolation following the rule "f to the minus five". In Cases 1-4, waves in the Middle Area were calculated on grids about 1.7 km wide, using the waves in Wide Area 3 as boundary conditions, and then were used as boundary conditions for wave calculation in the Narrow Area. In Case 5, waves in the Narrow Area were calculated using the wave transformation model (10 angular components) and the waves in Wide Area 3 as boundary conditions, without wave calculation in the Middle Area. The size of calculation grids in the Narrow Area was about 0.4 km for WAM and SWAN, and 50 m for the wave transformation model because of its small calculation model amount.

Calculation was conducted using a personal computer with a Pentium IV (3.6 GHz) processor. Bathymetry data from the Central Disaster Prevention Council was used for Ise Bay and Harima Sea. As for Ariake Sea, bathymetry data was prepared based on JTOPO30 (Japan Hydrographic Association).

A gradient wind model (Cardone-Myers Hybrid Model [6]) was used to hindcast ocean winds. As for winds on inner seas, the most precise hindcast was selected for each typhoon among JMA's grid-point value (RSM), mesoscale meteorological model (ANEMOS, developed by the Japan Weather Association), and a gradient wind model (Cardone-Myers Hybrid Model [6] + MASCON Model [7]), as shown in Table 3. Note that wind speeds estimated as above were divided by the regression coefficients of those at Hamada (Ise Bay), Eigashima (Harima Sea), and Ariake Tower (Ariake Sea).

3.1.2 Results

Waves are observed at Hamada, Eigashima, and Ariake Tower. The correlation coefficients (R), root mean square of errors (E), regression equations (A: regression coefficients, y: estimated value, x: observed value), and time to calculate waves in the Harima Sea are shown in Table 4. The correlation coefficients of wave heights were higher than those of wave periods in all cases, and the difference between cases was small. The root mean square of errors was less than 0.6 m for wave heights, but was relative large for wave periods in Cases 2 and 4 in which SWAN was used. The time to calculate waves in Case 1 was 14 min for the Middle Area and 53 min for the Narrow Area, and shortest among all cases. In Case 1, the regression coefficients of wave periods were almost 1, and those of wave heights were larger than 1, which means that the model did not underestimate on the average. As shown in Fig. 4, the time series of hindcasted waves also agreed with observed waves.

For Case 1 which was shortest in calculation time, omitting non-linear wave-wave interaction in shallow water and widening calculation grids

were examined to further reduce the calculation time. Non-linear wave-wave interaction is the energy transfer between frequency components. It is important for growth and dissipation of waves but not very effective in inner seas. The results of wave hindcast without the effects of non-linear wave-wave interaction showed that estimated wave heights are almost the same as those with the effects as shown in Fig. 5, and that the calculation time was reduced by 30%. On the other hand, wave heights and wave periods hindcasted in the Middle Area almost agreed with those in the Narrow Area.

As mentioned above, WAM with 1.7-km grids can forecast waves in inner seas in a short time with good precision. Therefore, we decided to develop a real-time wave forecast system based on WAM with 1.7-km grids.

3.2 Improvement of Wave Forecasting Model

3.2.1 Model Improvement

WAM does not consider the effects of wave breaking, although water depth is relatively small in inner seas. Besides this, tides are so large in inner seas that time variation of water depth may influence waves. To consider wave breaking and tides in wave forecasts, we combined WAM with the bore model [8] and the ocean tide model (NAO.99b) [9]. The bore model used for SWAN is a method of calculating energy dissipation based on the similarity between breaking wave and bores [2].

Table 5 shows the typhoons for which waves were hindcasted by the improved models. The computation area and the number of frequency components are the same in Table 1, but RSM winds adjusted by observed wind speeds were used in Wide Area 3 and the Middle Area.

3.2.2 Review of Improved Model

As shown in Tables 6 and 7, the effects of the model improvement were very small at Hamada (Ise Bay), but were obvious in the regression coefficients and root mean square of errors at Eigashima (Harima Sea) and Ariake Tower (Ariake Sea). For example, considering wave breaking improved hindcast precision at Ariake Tower near the peak of wave height, as shown in Fig. 6. The effects of wave breaking were clear at Eigashima and Ariake Tower because the water depth was smaller than Hamada (20 m deep). Also, considering wave breaking and tides increased the calculation time by only 10%.

4. CONCLUSIONS

An improved WAM that considers wave breaking and tides can forecast waves in inner seas with good precision in real time. Information for proper floodfighting warning can be supplied by combining this system with the forecast system for wave runup at each coast.

This system will be operated in Tokyo Bay, Ise Bay, Osaka Bay and Harima Sea, and the Ariake Sea. Test operation for one typhoon course will start in August 2007. After solving operating problems, we will begin full-scale operation for five typhoon courses in August 2008.

ACKNOWLEDGMENTS

This study was conducted through discussion within a working group formed by the NILIM, Port and Airport Research Institute (PARI), and Meteorological Research Institute (MRI), in cooperation with the River Bureau and Port Bureau of the Ministry of Land, Infrastructure and Transport, and the Japan Meteorological Agency. Source codes of WAM improved by PARI were used in this study. Examination and improvement of wave hindcasting models were conducted with the Japan Weather Association. We express our appreciation for the bathymetry data on Ise Bay and the Harima Sea provided by the Cabinet Office of Japanese Government.

5. REFERENCES

1. Nakamura, M., Sasaki, Y., and Yamada, J.: Wave Runup on Compound Slopes, *Proceedings of 19th Japanese Conference on Coastal Engineering*, JSCE, 1972. (in Japanese)

2. Kawaguchi, K., Sugimoto, A., and Hashimoto, N.: Application of Third Generation Wave Models Coupled with Mesoscale Meteorological Models for Tokyo Bay, *Technical Note of The Port and Airport Research Institute*, No.1061, 2003. (in Japanese)
3. Hashimoto, N. and Kawaguchi, K.: Recent Progress in Wave Hindcasting Models and Their Applications, *Journal of Civil Engineering in the Ocean*, JSCE, Vol.19, 2003. (in Japanese)
4. Hashimoto, N., Matsumoto, H., Kawaguchi, K., Matsufuji, E., and Matsuura, K.: Development of Wave Hindcasting Database for Seto Inland Sea by Using Mesoscale Meteorological Model and Third Generation Wave Model, *Journal of Civil Engineering in the Ocean*, JSCE, 2004. (in Japanese)
5. Hashimoto, N., Kawaguchi, K., Ikegami, M., and Suzuyama K.: Study on Applicability of Third Generation Wave Model WAM for Tokyo Bay, *Journal of Civil Engineering in the Ocean*, JSCE, 2004. (in Japanese)
6. Okada, K., Hayashi, K., and Isozaki, I.: A Development of A Sea Surface Wind Estimation Method in Inland Sea, *Oceanography in Japan*, Vol.4, No.2, 1995. (in Japanese)
7. Sherman, C., A.: A Mass-consistent Model for Wind Fields over Complex Terrain, *Journal of Applied Meteorology*, Vol.17, 1978.
8. Battjes, J. A. and Janssen, J. P. F. M.: Energy Loss and Set-up due to Breaking of Random Waves, *Proceedings of the 16th International Conference on Coastal Engineering*, ASCE, 1978.
9. Matsumoto, K., Takanezawa, T. and Ooe, M.: Ocean Tide Models Developed by Assimilating TOPEX/ POSEIDON Altimeter Data into Hydrodynamical Models: A Global Model and A Regional Model around Japan, *Journal of Oceanography*, Vol. 56, 2000.

Table 1 Computation Areas

	Wide Area 1	Wide Area 2		Wide Area 3	Middle Area	Narrow Area
Computation Area	N 15.0 - 50.0 E 120.0 - 155.0	N 30.0 - 35.5 E 128.0 - 140.0	Ise Bay	N 34.0 - 35.25 E 136.5 - 137.75	N 34.4 - 35.1 E 136.5 - 137.4	N 34.55 - 34.7 E 136.5 - 136.8
			Harima Sea	N 33.5 - 35.0 E 134.0 - 135.5	N 34.1 - 34.8 E 134.1 - 135.5	N 34.6 - 34.8 E 134.7 - 135.05
			Ariake Sea	N 32.0 - 33.5 E 129.25 - 130.75	N 32.45 - 33.25 E 130.05 - 130.75	N 33.05 - 33.2 E 130.1 - 130.45
Number of Grids	71×71	49×23	Ise Bay	26×26	55×43	73×37
			Harima Sea	31×31	85×43	85×49
			Ariake Sea	31×31	43×49	73×37
Grid Size	30 minutes (app. 50 km)	15 minutes (app. 25 km)	3 minutes (app. 5 km)		1 minute (app. 1.7 km)	0.25 minutes (app. 0.4 km)
Number of Frequent Components	25 components		35 compnents			
	$f(1)\times1.10^{(i-1)}$ $(f(1)= 0.04177248)$					
Period Components	2.4 to 24 seconds		0.9 - 24 seconds			
Number of Direction Components	16 components		36 components			
Wind Data	Gradient wind model		RSM, ANEMOS, gradient wind model			

Table 2 Case Setup

Case	Middle Area	Narrow Area
1	WAM	WAM
2	WAM	SWAN
3	WAM	Wave transformation model
4	SWAN	SWAN
5	-	Wave transformation model

Table 3 Wind Models for Wave Hindcast

Ise Bay		Harima Sea		Ariake Sea	
T9807	RSM	T9708	ANEMOS	T9711	Gradient wind model
T9810	RSM	T9805	RSM	T9918	ANEMOS
T0111	RSM	T9807	RSM	T0014	ANEMOS
T0310	ANEMOS	T9810	ANEMOS	T0205	RSM
T0406	RSM	T9918	ANEMOS	T0215	Gradient wind model
		T0310	ANEMOS	T0306	ANEMOS
		T0416	RSM	T0314	RSM
		T0418	RSM	T0418	ANEMOS

Table 4 Hindcast Preciseness and Calculation Time for Harima Sea

	Hamada		Eigashima		Ariake Tower		Calculation time for 24-hours wave		
	wave height	wave period	wave height	wave period	wave height	wave period	Wide Areas	Middle Area	Narrow Area
Case 1 (WAM-WAM)	R=0.81	R=0.55	R=0.91	R=0.73	R=0.86	R=0.42	1.5 minutes	14 minutes	53 minutes
	E=0.58m	E=1.49s	E=0.34m	E=1.07s	E=0.43m	E=1.26s			
	y=1.26x	y=1.09x	y=1.08x	y=1.05x	y=1.42x	y=0.99x			
Case 2 (WAM-SWAN)	R=0.81	R=0.40	R=0.85	R=0.64	R=0.85	R=0.40		14 minutes	232 minutes
	E=0.51m	E=2.58s	E=0.40m	E=1.83s	E=0.34m	E=1.82s			
	y=1.21x	y=0.48x	y=0.96x	y=0.54x	y=1.19x	y=0.50x			
Case 3 (WAM-WTM)	R=0.74	R=0.56	R=0.92	R=0.86	R=0.88	R=0.56		14 minutes	92 minutes
	E=0.55m	E=1.23s	E=0.31m	E=0.96s	E=0.48m	E=0.96s			
	y=1.11x	y=1.02x	y=0.98x	y=0.86x	y=1.48x	y=0.90x			
Case 4 (SWAN-SWAN)	R=0.81	R=0.48	R=0.97	R=0.91	R=0.95	R=0.85		113 minutes	232 minutes
	E=0.43m	E=2.83s	E=0.40m	E=2.21s	E=0.32m	E=1.61s			
	y=1.04x	y=0.44x	y=0.84x	y=0.53x	y=0.80x	y=0.52x			
Case 5 (only WTM)	R=0.73	R=0.57	R=0.92	R=0.80	R=0.87	R=0.56		-	92 minutes
	E=0.55m	E=1.34s	E=0.32m	E=0.92s	E=0.44m	E=0.96s			
	y=1.08x	y=1.06x	y=1.02x	y=0.88x	y=1.39x	y=0.88x			

R: correlation coefficients, E: root-mean-square of error, y=Ax: regression equation
WTM: wave transformation model

Table 5 Typhoons for Model Examination

Sea	Typhoon	Maximum of significant wave height (m)	Storm period
Ise Bay	T9807	3.84	20-22 Sep. 1998
	T9810	3.08	16-18 Oct. 1998
	T9805	2.78	14-16 Sep. 1998
Harima Sea	T0416	3.94	27-31 Aug. 2004
	T9810	2.85	16-18 Oct. 1998
	T0418	2.62	4-8 Sep. 2004
Ariake Sea	T0418	2.85	4-8 Sep. 2004
	T0306	2.42	16-20 Jun. 2003
	T0415	2.08	17-19 Aug. 2004
	T0314	1.84	10-13 Sep. 2003

Table 6 Correlation between Estimated Wave Height and Observed Wave Height

Sea	Model	Regression coefficient	Correlation coefficient	Root mean square of error (m)
Ise Bay	original	1.17	0.82	0.47
	+ wave breaking	1.16	0.82	0.46
	+ tides	1.18	0.82	0.48
	+ wave breaking and tides	1.17	0.82	0.48
Harima Sea	original	1.15	0.91	0.39
	+ wave breaking	0.98	0.90	0.32
	+ tides	1.15	0.91	0.39
	+ wave breaking and tides	0.99	0.90	0.32
Ariake Sea	original	1.44	0.93	0.42
	+ wave breaking	1.23	0.92	0.33
	+ tides	1.42	0.94	0.40
	+ wave breaking and tides	1.20	0.93	0.31

Table 7 Correlation between Estimated Wave Period and Observed Wave Period

Sea	Model	Regression coefficient	Correlation coefficient	Root mean square of error (s)
Ise Bay	original	1.17	0.61	1.6
	+ wave breaking	1.17	0.62	1.5
	+ tides	1.20	0.61	1.7
	+ wave breaking and tides	1.20	0.61	1.6
Harima Sea	original	0.98	0.71	1.3
	+ wave breaking	0.97	0.71	1.3
	+ tides	1.01	0.69	1.3
	+ wave breaking and tides	1.00	0.69	1.3
Ariake Sea	original	0.91	0.55	1.3
	+ wave breaking	0.89	0.53	1.2
	+ tides	0.91	0.55	1.3
	+ wave breaking and tides	0.89	0.53	1.2

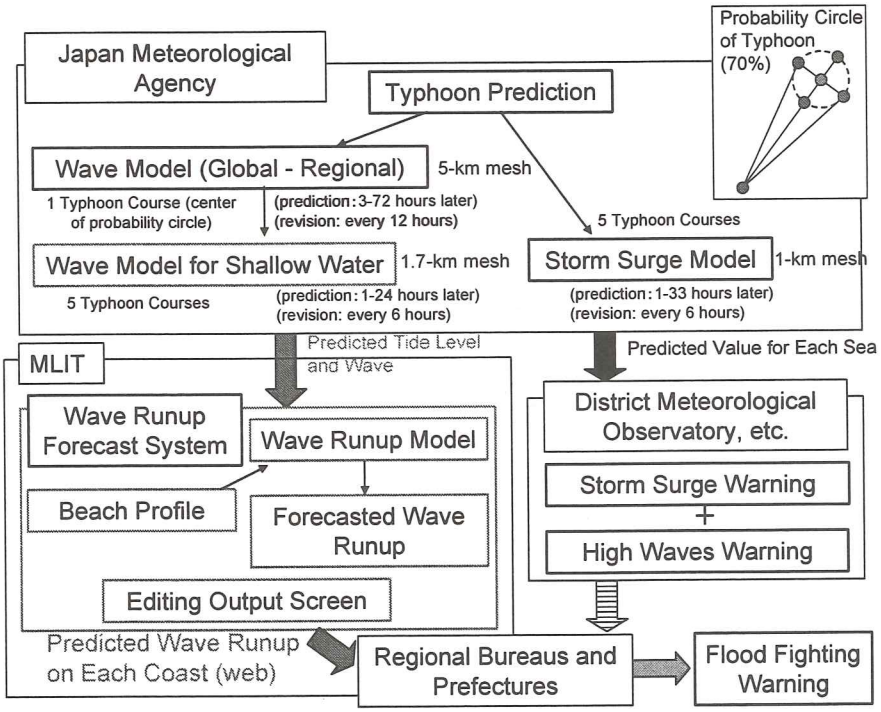

Fig.1 Constitution of the System

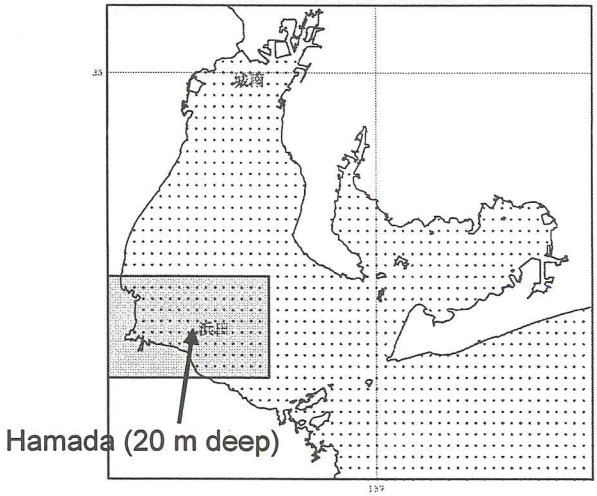

Fig. 2 Middle Area and Narrow Area (Grayed) in Ise Bay (Arrow: Wave Observatory)

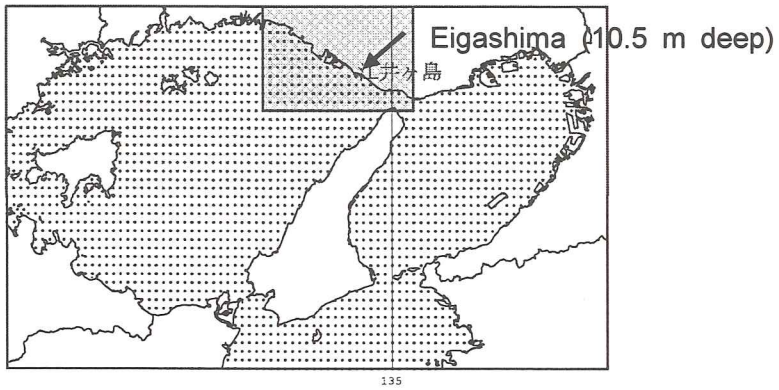

Fig. 3 Middle Area and Narrow Area (Grayed) in Harima Sea (Arrow: Wave Observatory)

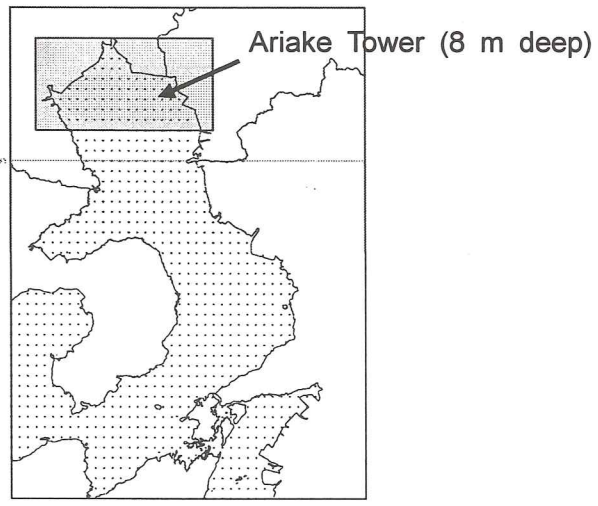

Fig. 4 Middle Area and Narrow Area (Grayed) in Ariake Sea (Arrow: Wave Observatory)

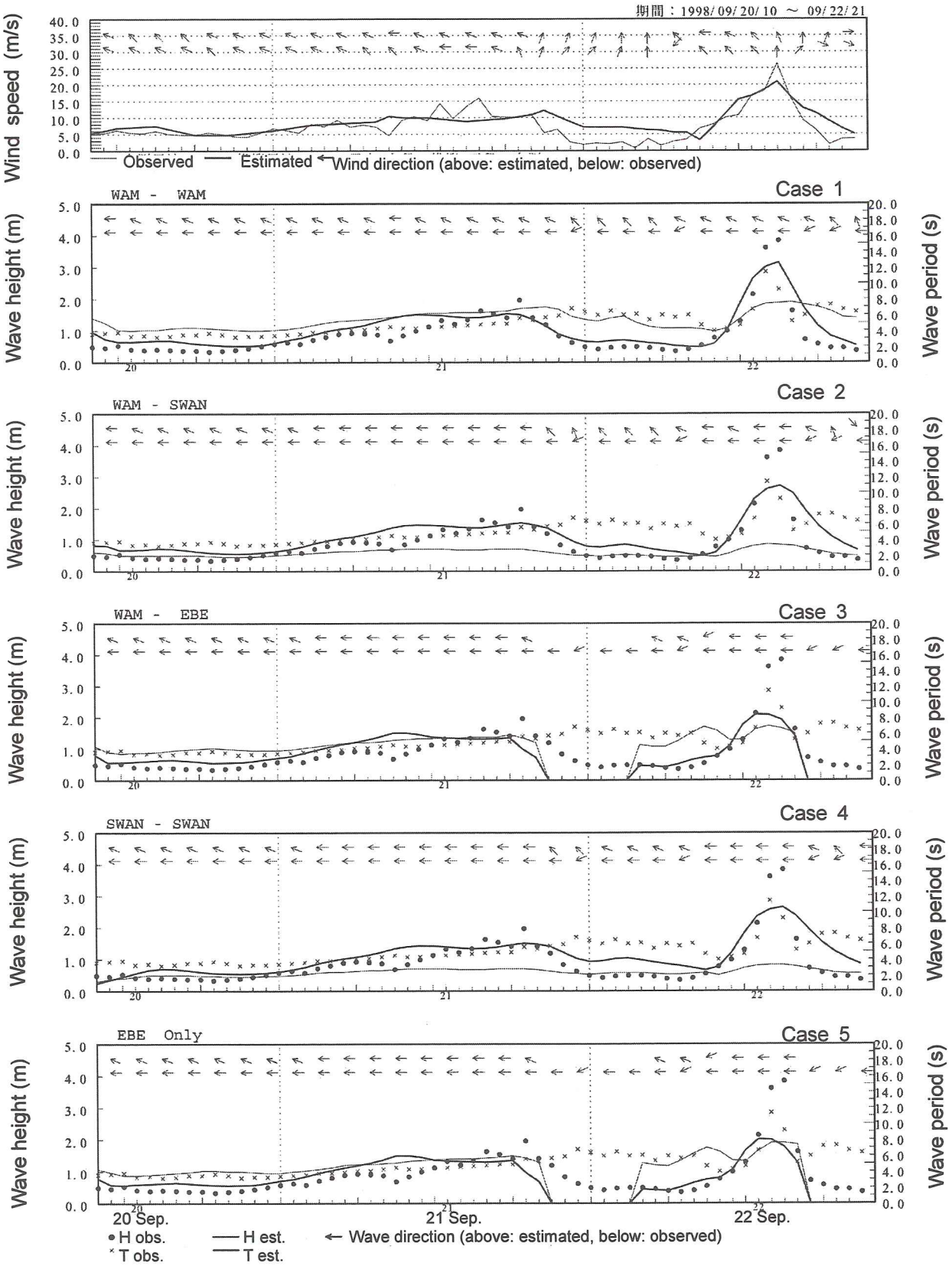

Fig. 5 Time Series of Winds and Waves in Typhoon 9807

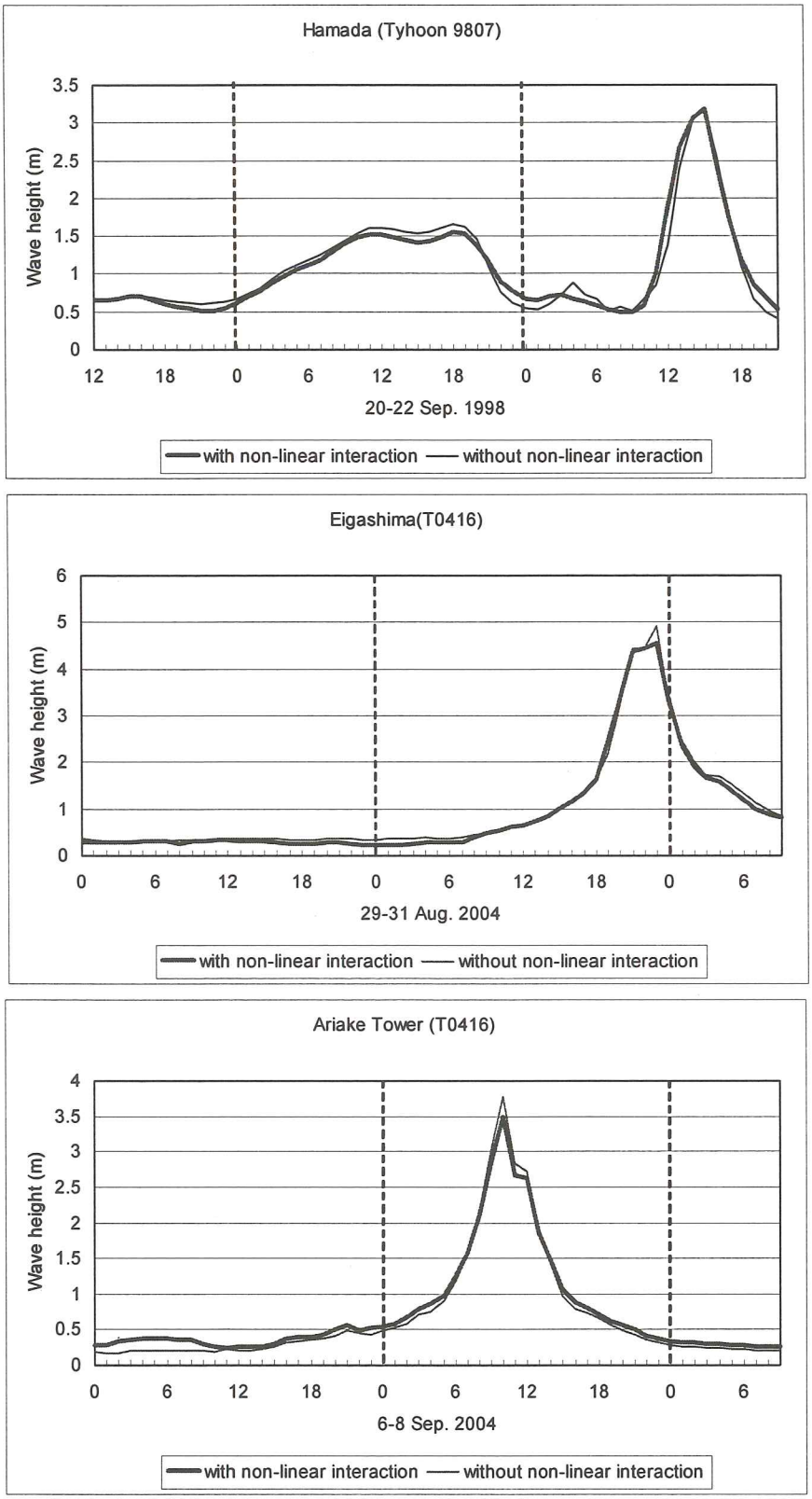

Fig. 6 Effects of Nonlinear Wave-Wave Interaction (upper: Hamada; middle: Eigashima; lower: Ariake Tower)

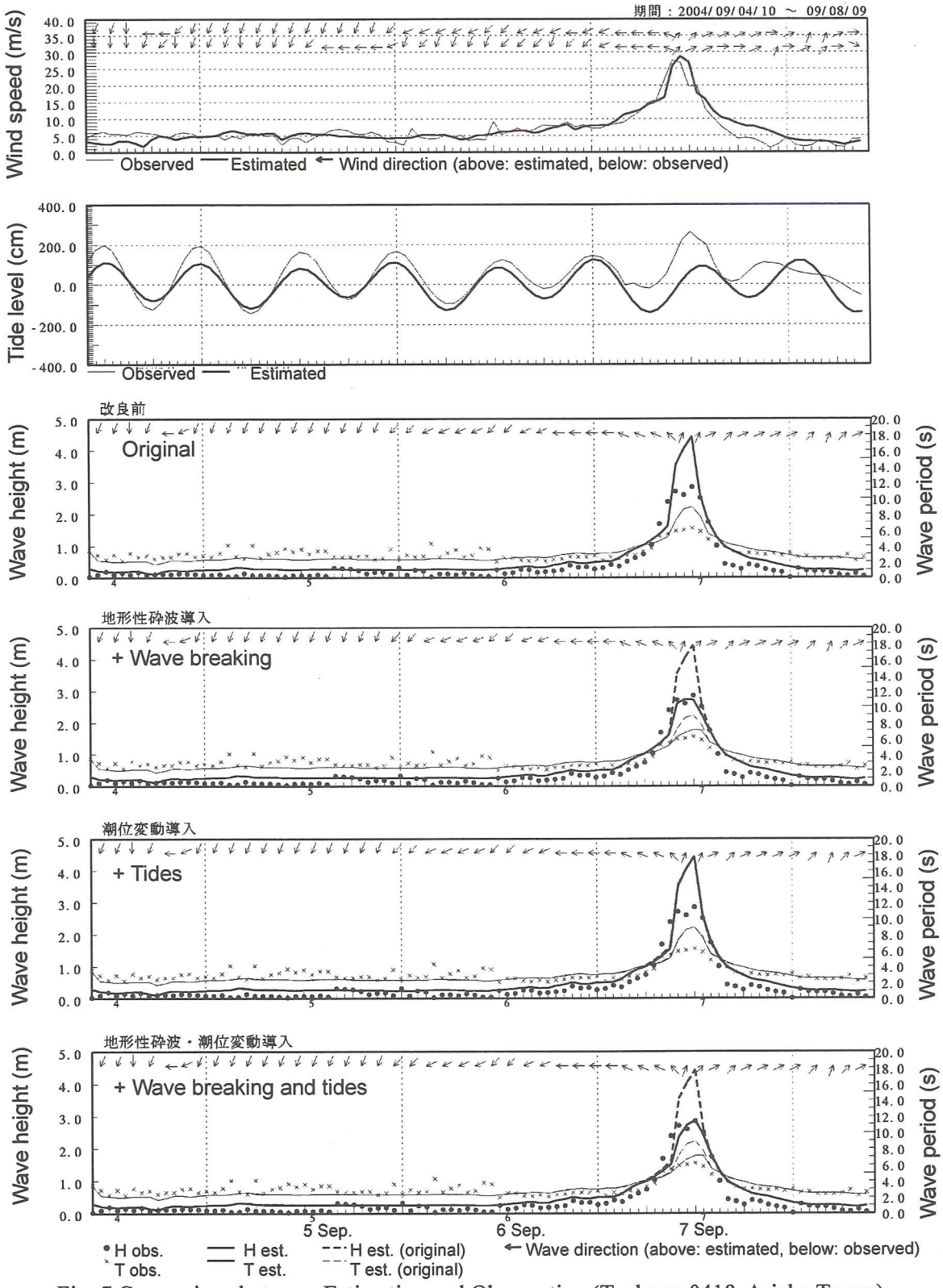

Fig. 7 Comparison between Estimation and Observation (Typhoon 0418, Ariake Tower)

Analysis of Spillover Process and Development of Estimation Methods of Tsunami Damage in Ports and Surrounding Areas

by

Katsuya Oda[1], Osamu Okamoto[2] and Kentaro Kumagai[2]

ABSTRACT

Based on the actual damage in past tsunamis that caused damage in Japan, this paper systematizes the types of tsunami damage which can be assumed to occur in coastal areas, where ports locate their centers, by classification into "direct damage" due to inundation and drifting objects and "indirect damage," in which the depression of port functions and related effects of the tsunami spill over into the surrounding region and society. Based on the results, estimation methods for tsunami damage and tsunami countermeasures in ports are proposed. The scope of research on coastal hazards of a scale exceeding the design external force (mega-risk coastal hazards) is also discussed.

KEYWORDS: Estimation method, Excess external force, Spillover process, Tsunami damage

1. INTRODUCTION

In recent years, large-scale ocean trench-type earthquakes accompanied by tsunamis have been a serious concern. Likewise, Japan is located in a seismically-active region and has experienced a number of tsunamis in the past. Based on this experience, countermeasures have been implemented, but these measures mainly involve the construction improvement of coastal protection facilities such as dikes revetments and similar works. At present, adequate study has not been given to countermeasures for wharfs and basins which lie outside of these works.

On the other hand, population and property are concentrated in coastal areas, and diverse facilities exist in these areas, including ports which serve as bases for logistics and passenger transport and coastal facilities which are important for not only disaster prevention but also conservation of environment and proper use of shore, and. In the event of a tsunami accompanying a large-scale earthquake, which is considered imminent in many parts of Japan, the damage will not be limited to "direct damage" due to inundation and other direct effects, but will also include a wide range of "indirect damage" due to reduction of port functions and the like. This means that tsunami hazards in coastal regions will have serious and wide-ranging socioeconomic effects. Therefore, as a new research topic, in addition to direct damage due to inundation, etc., it is also necessary to analyze the spillover process of tsunami damage, which includes indirect damage, and to study estimation methods for tsunami damage in ports and surrounding areas.

Considering the fact that ports play a crucial role in the social infrastructure, in this paper, damage to ports by tsunamis was systemized based on past examples, and tsunami damage was analyzed using a model port. Tsunami countermeasures in the model port were studied, and the basic concepts of tsunami countermeasures in ports were summarized.

2. ANALYSIS OF TSUNAMI DAMAGE

2.1 Systemization of Examples of Tsunami Damage

A total of 11 major earthquakes accompanied by tsunami damage have occurred in Japan since 1945, including the Showa Nankai Earthquake, Niigata Earthquake, Tokachi-oki Earthquakes, Hokkaido- Nansei-Oki Earthquake, and others. Table 1 summarizes the main tsunami damage in ports and their hinterland areas since 1964.

[1] Head, Coastal Disaster Prevention Division, National Institute for Land and Infrastructure Management (NILIM), Ministry of Land, Infrastructure and Transport(MLIT), Yokosuka-shi, Kanagawa-ken 239-0826 Japan

[2] Senior Researcher, ditto

Table 1 Damage Caused By Major Tsunami Ports and Surrounding Areas (Hinterland) Since 1964

Name, date, and magnitude (M)	Direct damage in port/hinterland				Indirect damage such as reduction of port functions, etc.
	Damage to protective facilities, mooring facilities, etc.	Inundation damage	Drift damage	Human injury (no. of persons; including injury due to earthquake)	
Niigata Earthquake Tsunami, June 6, 1964, M7.5		Inundation of products stored in warehouses, loss of value of products	Spill/fire of hazardous materials from oil tanks, drift of timber	26	Economic damage to commerce and industry due long-term inundation of hinterland
Tokachi-Oki Earthquake Tsunami, May 16, 1968, M7.9		Inundation of buildings	Drift of ships	52	
Nihonkai-Chubu Earthquake Tsunami, May 26, 1983, M7.7	Sliding/overturning of training dike, bulkhead of reclaimed land, etc.	Inundation/damage of fishery facilities, inundation of factories and houses in hinterland	Drift of timber, drift of fishing boats	104: Large number of port construction workers and port visitors were killed by tsunami.	Port activity suspended due to closure of port for collection and removal of timber
Hokkaido-Nansei-Oki Earthquake Tsunami, July 12, 1993, M7.8	Sliding/overturning of breakwater, seawall, etc.	Inundation/damage of ferry terminal, inundation/damage of fishery facilities, fire in houses in hinterland	Drift of automobiles, drift of fishing boats, drift of housing wreckage	230	Suspension of ferry service for collection and removal of drifting objects
Hokkaido-Toho-Oki Earthquake Tsunami, Oct. 4, 1994, M8.2				10 *Injury on Iturup Island	
Tokachi-Oki Earthquake Tsunami, Sept. 26, 2003, M8.0		Inundation of ferry terminal, inundation/damage of cargo handling equipment	Drift of containers, drift of fishing boats	2	Long-term stoppage of cement supply/substitution by nearby port

According to this table, damage to protective facilities/mooring facilities such as breakwaters, seawalls, which were affected by external forces due to tsunamis took the form of sliding or overturning. In the ports, inundation damage affected various port facilities such as transit sheds including stored products, ferry terminals, fishery facilities, cargo handling equipment. In the hinterland, factories, residence and others suffered inundation damage and sometimes fires occurred. Drift damage involving timber, fishing boats, automobiles, wreckage from houses, cargo containers, hazardous materials and other debris also occurred. Human injury, including injury due to the earthquake, was not limited to injury in the port, and in many cases, scores of persons were affected. In particular, there are cases in which a large number of port construction workers and visitors were injured or killed. Indirect damage also occurred due to long-term inundation of the hinterland area and reduction of port functions, such as port closure, etc. Other hazards that can be predicted to occur as a result of a tsunami, such as drifting of pleasure boats were also identified separately by referring to examples of storm surge due to typhoons.

Damage due to a tsunami can be classified as human injury, damage to facilities and other property due to run-up of the tsunami on the land, and drift damage due to debris which were transported from water basins onto the land or vice versa. The locations where damage occurs were classified as damage in the port area, including wharfs, basins, etc., and damage in urban areas in the hinterland of the port. The results of the analysis of these kinds of tsunami damage are shown in Table 2.

Table 2 Classification of Tsunami Damage

Class of tsunami damage		Damage item
Human injury		Loss of life of port construction workers, port visitors, etc.
Damage due to inundation	Damage in port area	Inundation and damage of ferry terminal facilities
		Damage of goods in warehouses, sheds, etc.
		Damage of cargo handling equipment by inundation
	Damage in hinterland	Stop of industrial activity due to inundation by tsunami
		Long-term inundation due to damage of pump stations
Damage due to drift	Damage in port area	Drift of vehicles, pulpwood, containers, ships, etc. into port
		Capsizing, stranding of ships on quays, etc.
		Drift of pleasure boats
		Drift of tankers
	Damage in hinterland	Damage to houses by fishing boats and other drifting objects
		Fire damage due to oil spill

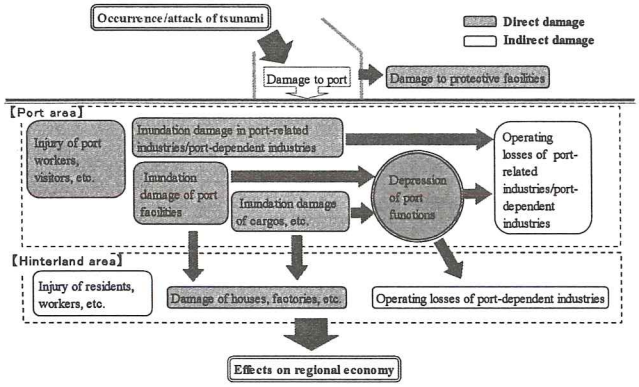

Fig.1 Schematic Diagram of Spillover Process of Tsunami Damage

2.2 Spillover Process of Tsunami Damage

Because the areas fronting onto the sea are utilized in logistics and other port functions, it is a distinctive feature of ports that the larger part of the port area is located outside the tsunami or storm surge defense line. Therefore, if a tsunami attacks, the damage is not limited to direct damage (see Table 2); indirect damage due to depression of port function also occurs over a wide area. In other words, as shown in Fig.1, when a tsunami attacks a port, it causes direct damage, and as a result, the facilities affected by the damage can no longer fulfill full essential roles. This lead to a depression of the functions of logistics and passenger transportation, and causes reduction of business activities and operating losses of business affecting not only industries with bases located in the port area, but also industries that depend on the port. In addition, because the tsunami also causes direct damage in the hinterland of the port, the activity of industries in the surrounding area is reduced, with a negative impact on the regional economy as a whole. The spillover process of tsunami damage in the port and hinterland, which was systematized considering the interrelationship of these various forms of damage, is shown in Fig.2. The temporal/spatial relationship of direct damage and indirect damage was systematized in this diagram of the spillover process, while continuing to focus on the classes of damage to port facilities such as protective facilities and mooring facilities, inundation damage, drift damage and human injury.

2.3 Simulation of Tsunami in Model Port

A numerical simulation of a tsunami in a model port was performed in order to analyze the behavior of tsunamis in ports and the damage which can be assumed to occur in the event of a tsunami. In this numerical simulation of a tsunami, the range of inundation on land and maximum inundation depth, tsunami arrival time, and rates of rise/fall of the water level and flow velocity vectors in water basins were calculated. The conditions used in the simulation are shown in Table 3. The earthquake applied to this case study was the maximum design earthquake in the model port as proposed by the Central Disaster Management Council.

Among the results of the simulation, Fig.3 shows the inundation range/inundation depth on land. In area ① in Fig.3, inundation becomes remarkable at the deepest part of the wharfs due to the increase in the water level at the extreme back of the berth, which is surrounded by the wharfs. It was also confirmed in area ② in Fig.2 that the tsunami run-up in the river flooded over the river levees.

Fig.4 shows the distribution of maximum flow velocity vectors. Increases in flow velocity can be confirmed in locations with rapidly narrowing cross sections, such as the breakwater opening, mooring basins surrounded by wharfs, openings in inner jetties surrounding reservoirs. On land, flow velocities are high in locations where overflow occurs, for example, around the deepest part of berths.

2.4 Estimation Method of Tsunami Damage

(1) Inundation damage

Inundation damage was estimated from the inundation range and the inundation depth in the simulation results.

(2) Drift damage

The objects which may be swept away and drift were assumed to be fishing boats, pleasure boats, and other boats, pontoon, floating piers, cargos stored in the open, such as timber, chips, empty containers and automobiles in wharf parking lots.

For cargos stored in the open, drifting was assumed to begin from the time of inundation, and the damage rate of such cargos in the inundation area was assumed to be 1.0.

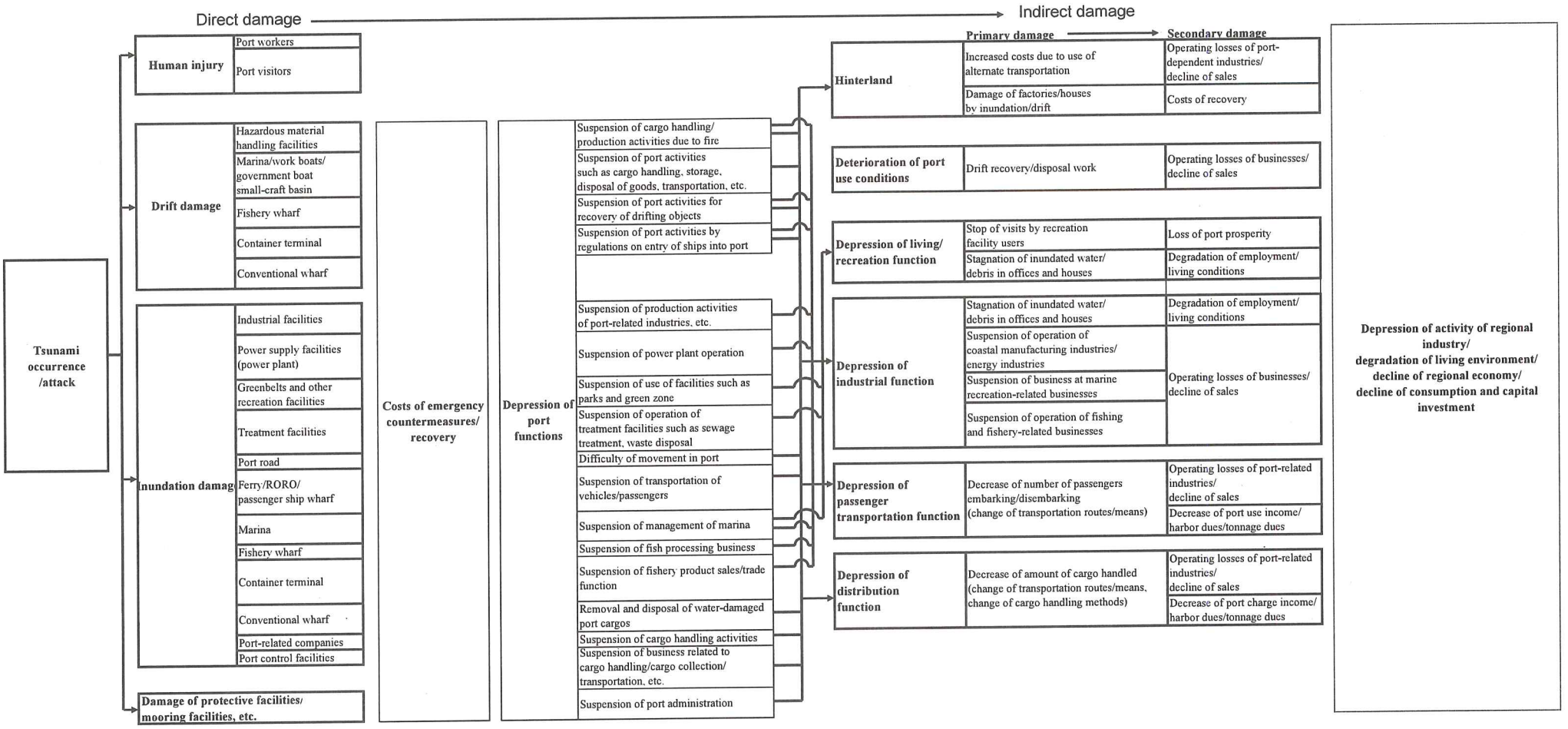

Fig.2 Spillover Process of Tsunami Damage

Table 3 Conditions of Tsunami Simulation

Calculation grid size	Minimum grid size 12.5m x 12.5m
Object earthquake	Assumed Tokai Earthquake
Uplifting of ground	Not considered.
Basic equation	Nonlinear long wave theory equation
Sea bottom friction	Manning's roughness coefficient n = 0.025m-1/3s
Ground friction	Roughness according to land use
Eddy viscosity coefficient	AH=10.0
Water level	H.W.L (T.P. +0.86m)
Calculation time	180min (3hr) after occurrence of tsunami

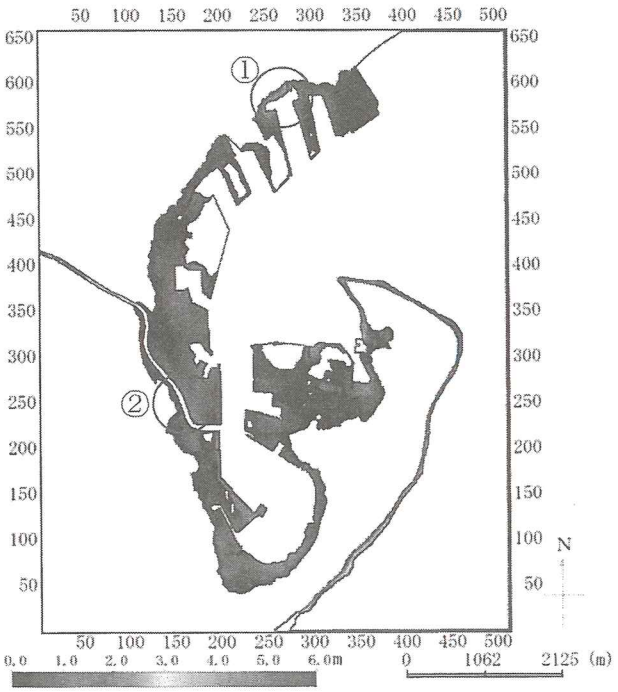

Fig.3 Inundated Area and Inundation Depth

Empty containers were assumed to be stacked four high. Based on the relationship between the buoyancy of the containers and the weight of the stacking levels, the depth of inundation required to cause the containers to drift is assumed to be 0.8m.

The drift damage rate of automobiles in wharf parking lots was assumed to be 1.0 at inundation depths of 50cm and greater, as this is the depth at which passenger automobiles float.

In determining the damage rate for boats, based on the relationship of the tsunami height and damage ratio of all fishing boats in fishing ports (Fig.5) compiled by the Japan Association of Marine Safety (JAMS), it is considered that (a) the damage rate shows a high correlation with the tsunami height, (b) damage occurs when the tsunami height exceeds approximately 1m, and (c) the damage rate increases with the tsunami height, and all vessels are damaged when the tsunami height reaches 7m or more [2]. From this, the solid line shown in Fig.5 was set as the damage rate of boats.

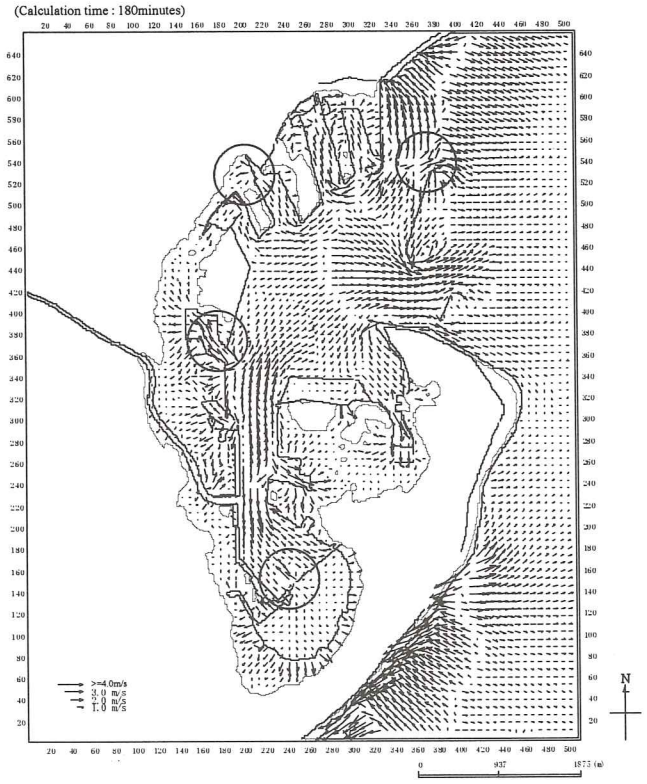

Fig.4 Distribution of Velocity Vector at the Moments When Maximum Velocity Occurs

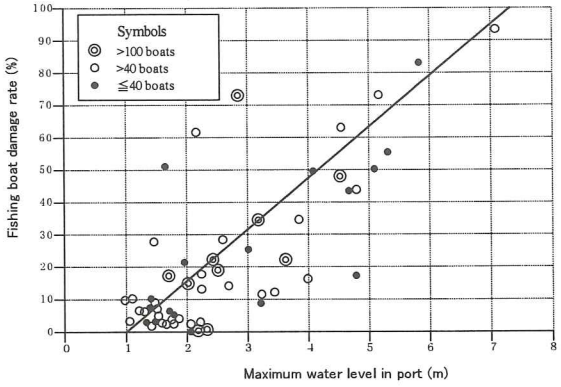

Fig.5 Damage Rate for Ships [2]

Table 4 Drift Damage Rate

Drifting Object		Drift Damage Rate
Mooring facilities (pontoon pier)		Set by tsunami water level in port(Fig.5)
Surveillance service boats (small), patrol boats		
Fishery	Fishing boats	
Cargo	Lumber, chips, etc.	When inundation depth is 0.0m or more, damage rate = 1.0
	Empty containers	When inundation depth is 0.8m or more, damage rate = 1.0
Pleasure boats		Set by tsunami water level in port(Fig.5)
General ships in port		
Automobiles		When inundation depth is 0.5m or more, damage rate = 1.0

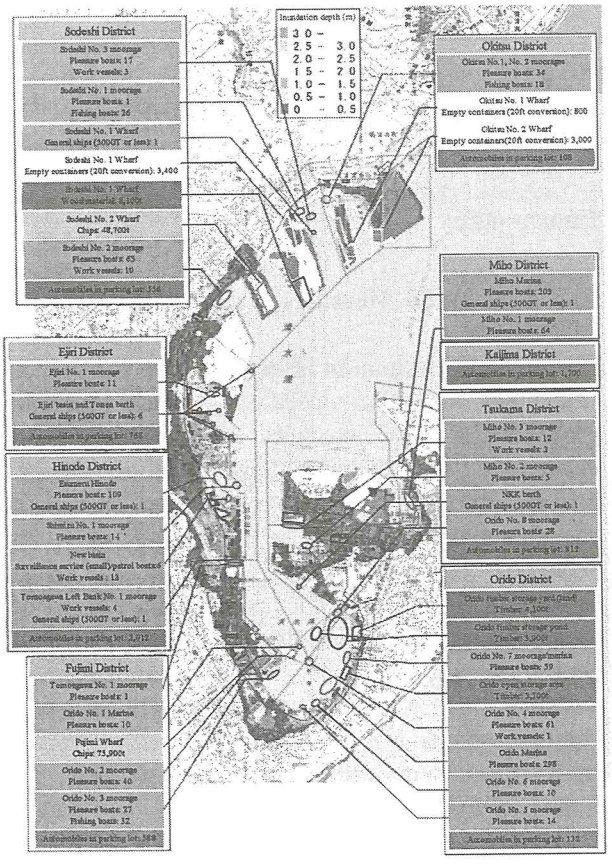

Fig.6 Amount and Location of Drifting Cargos

The drift damage rates of drifting objects are shown in Table 4. The position and amount of drifting objects in the model port were determined based on the field survey, as shown in Fig.6.

(3) Human injury

Fig. 7 shows the boundary between whether a person can walk safely in floodwater or not. This relationship is determined by both the inundation depth and flow velocity [3]. Using the region where it is possible to walk in water when evacuating in a flood shown in the figure as a criterion, the area where safe evacuation is difficult was set and the area affected by human injury due to a tsunami was calculated. The body height used in calculating the area where safe evacuation is difficult was assumed to be 165cm, which is the average height of the Japanese population.

The number of port workers/visitors and the area where safe evacuation is difficult in the model port are shown in Fig.8.

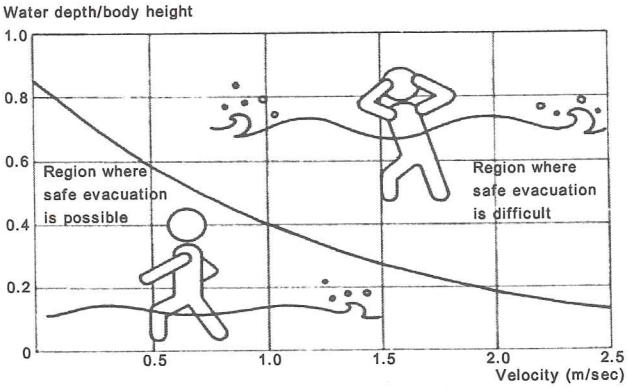

Fig.7 Criterion of Safety Evacuation; Relation between Safety Evacuation and Flood Conditions [3]

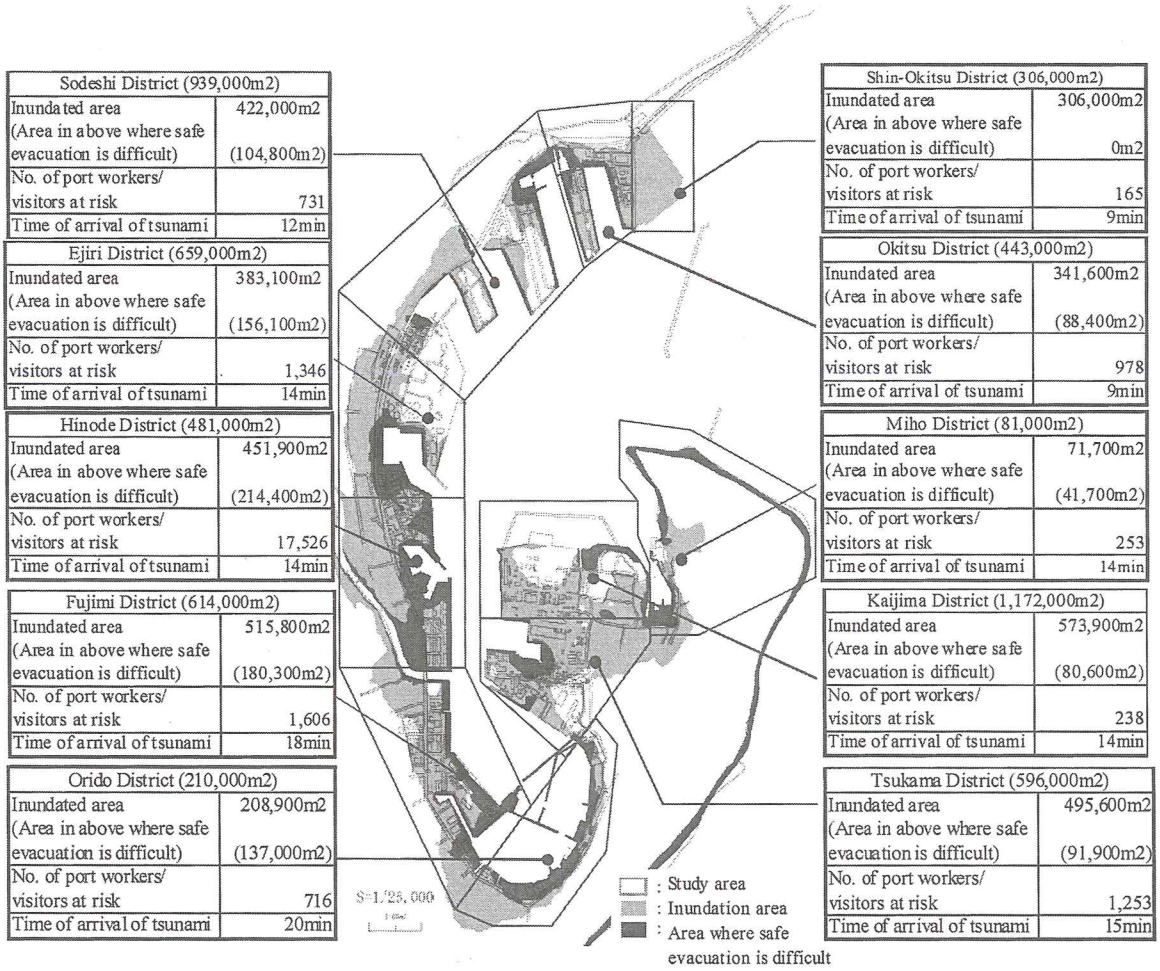

Fig.8 Area affected by human injury

3. STUDY OF COUNTERMEASURES FOR MITIGATION OF TSUNAMI DAMAGE

3.1 System of Tsunami Damage Mitigation Countermeasures in Ports

Tsunami countermeasures can be divided into preventive measures before a tsunami and recovery measures after a tsunami. Preventive measures are considered to include "evacuation measures to ensure the safety of port workers and visitors" and "preventive measures to secure port functions and mitigate property damage in ports," and can be arranged as shown in Fig.9.

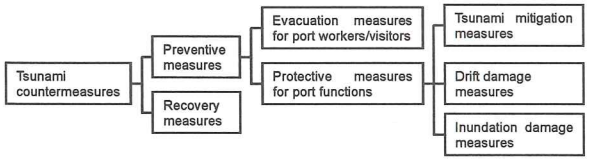

Fig.9 Classification of Tsunami Countermeasures

3.2 Evacuation Measures for Port Workers and Visitors

In areas where human injury due to a tsunami is expected, measures aimed at securing adequate safety for port workers and visitors and preventing human injury have to be developed. A procedure for consideration and establishment of these measures are shown in Fig.10. To enable prompt evacuation of port workers/visitors, quick communication of information is necessary. Establishment of communication methods such as installation of simultaneous wireless broadcasting devices and tsunami alarm bulletin board, coupled with the tsunami observation system, should be considering.

A fundamental concept for designation of refuge facilities is to select the adequate facilities from existing facilities which have earthquake resistance and tsunami resistance and enable smooth evacuation from outside. In areas where it is not possible to evacuate to refuge facilities

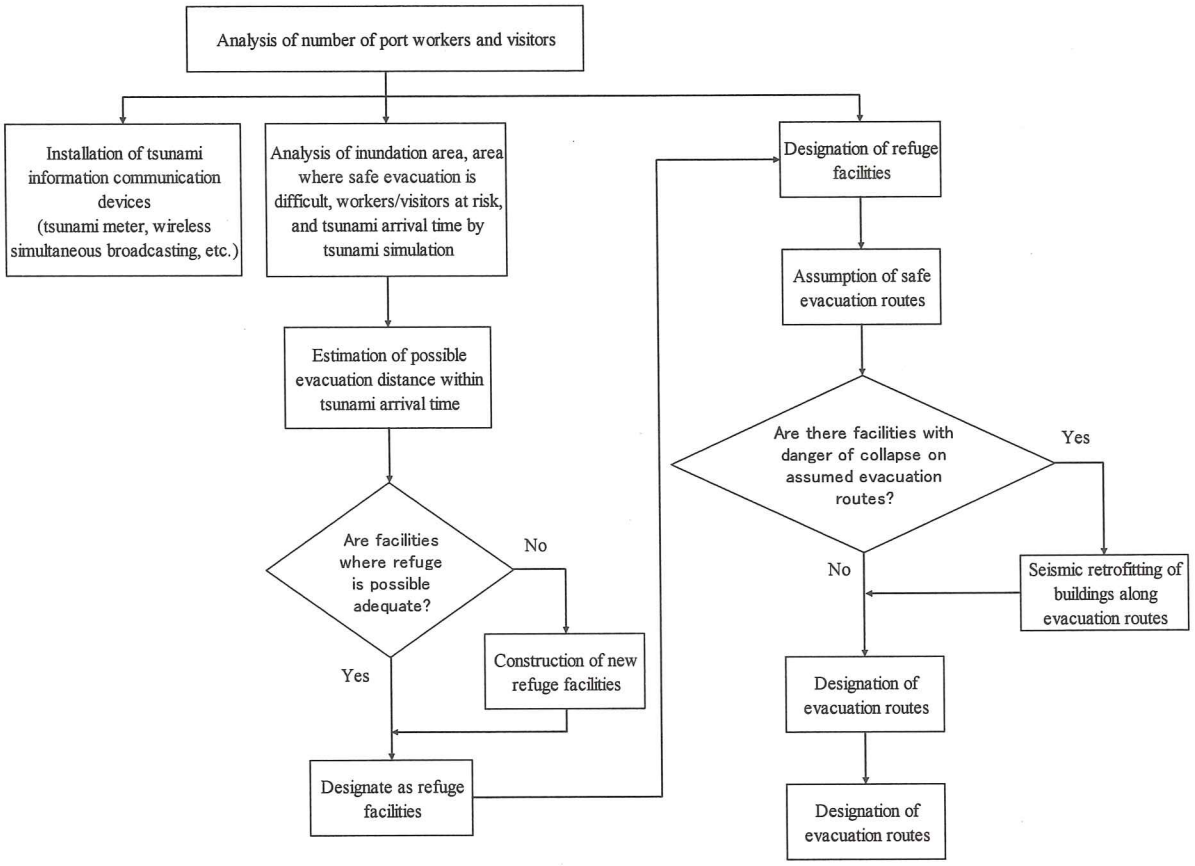

Fig.10 Planning Procedures of measures for safety evacuation and prevention of human injury

by the tsunami arrival time, it is also necessary to study the construction of new refuge facilities.

Evacuation routes are designated so as to avoid buildings which may collapse. It is necessary to implement seismic retrofitting of buildings which may collapse. It is also necessary to lead a smooth evacuation of port visitors and others using evacuation route signs.

3.3 Protective Measures for Port Functions

Protective measures for port functions also should be developed, assuming protection on a priority basis of the functions which must be secured during a tsunami disaster such as emergency material transportation function, critical logistics function and reduction of damage to a degree where "functions are not impaired" or "immediate restoration of functions by emergency measures is possible."

Because the breakwater at the port entrance can be expected to reduce the energy of a tsunami and thereby have a damage mitigation effect in the port as a whole, its effect in reducing inundation in the port and reducing flow velocities should be studied. As tsunami mitigation measures at the waterfront, it is also necessary to consider improvement of seawalls such as raising the height.

In areas where inundation damage was identified establishment of measures for inundation in land areas is necessary. These measures include increasing the ground height, raising the level of floors, constructing watertight doors, waterproof walls, waterproofing or raising the floor level of power supply facilities, etc.

As measures for drift, in areas where there is a possibility that cargos, small boats, and automobiles may drift, it is necessary to study construction of drift prevention fences, while continuing to consider use under normal conditions, and to strengthen countermeasures for automobiles and small boats, etc. which are left unattended and may possibly drift in a tsunami.

3.4 Recovery Measures

The aim of recovery measures is to enable appropriate emergency response/recovery after a disaster, thereby minimizing spillover to indirect damage due to direct damage, and early recovery of port functions. It is considered that sharing disaster information regarding the damage such as status of port facilities, drift/scattering of cargos and other objects, whether the quays are in service or not with related organizations will contribute to smoothing the recovery work. Furthermore, it is also important to calculate in advance the time required to remove the debris which were stranded on lands or washed away into basins based on the expected amount of drifting objects and the capability to collect and remove drifting objects in the port.

4. USE OF RESEARCH RESULTS

This research has analyzed the potential damage of a tsunami on ports and the spillover damage from the affected port to the surrounding area by classifying and systematizing the modes of damage caused by tsunamis in ports and the tsunami damage spillover process. Methods of quantifying tsunami damage in ports were also proposed by studying the tsunami damage in a model port. It is thought that these results will be useful in evaluating the effects of countermeasures in future studies of tsunami countermeasures for ports.

In the study of tsunami countermeasures, it is possible to define the viewpoint of countermeasures and clarify the objects for which effects can be obtained by systematizing the countermeasures and proposing countermeasures which correspond to respective purposes. However, it is difficult to achieve the purposes of countermeasures and eliminate tsunami damage by implementing single countermeasures. For this reason, in tsunami countermeasures, it is important to implement comprehensive countermeasures in ports, including nonstructural soft countermeasures.

The Port and Harbor Bureau of the Ministry of Land, Infrastructure and Transport (MLIT) is compiling the research results introduced in this paper for the purpose of publication as "Basic Concepts of Tsunami Countermeasures in Ports." It is hoped that tsunami countermeasures will be implemented at all ports based on these "Basic Concepts" through cooperation mainly of the national government, port administrators, related businesses, and other stakeholders.

5. PREPARATIONS AGAINST MEGA-RISK COASTAL HAZARDS

5.1 What are Mega-Risk Coastal Hazards?

In a tsunami, storm surge, or other natural disaster affecting a coastal area, there is a possibility that the event may exceed the design external force used for planning and design of protection works such as seawalls, dikes and other structural countermeasures using coastal conservation. This is due to uncertainty in the assumptions related to earthquakes which cause tsunamis, limitations on past typhoon data used in probabilistic evaluations, the effects of global warming, and other factors. The probability of occurrence of a gigantic tsunami or storm surge exceeding design external forces is low, but the damage if such a disaster occurs, the effects can be catastrophic. In other words, in spite of the low frequency of such events, the risk of damage is large.



Photo1 Damage in Sri Lanka resulting from the Indian Ocean Tsunami (Courtesy of Penta-Ocean Construction Co., Ltd.)

The disaster caused by the Indian Ocean Tsunami which struck the coastlines of the nations on the Indian Ocean in December 2004 (Photo1) can be termed a infrequent mega-risk coastal disaster. Likewise, Hurricane Katrina,

which made landfall near New Orleans in the United States on August 29, 2005, caused damage that was said to be the worst in US history due to a natural disaster. Because a substantial part of New Orleans lies at or below sea level, the city suffered devastating damage after the levees were breached by the storm surge accompanying the hurricane (Photo–2).

What is the situation in Japan? Estimates of damage by giant earthquakes and tsunamis accompanying these earthquakes have been published for Tokai, Tonankai/Nankai earthquakes, earthquakes in the areas of the Japan Trench and Kuril Trench, and others where occurrence is considered imminent. However, because these damage estimates are based on given scenarios, such as the setting of the scale of the earthquake, the location and dimensions of the fault and so on, there is a possibility of damage on a scale exceeding these damage estimates. Furthermore, there is also concern regarding larger and more frequent typhoons striking Japan. Over the long term, an increase in damage due to rising sea levels is also feared. Because the population and city functions are heavily concentrated in areas lying below sea level in major Japanese cities, that is, in the so-called zero-meter region, an enormous effect on society and the economy is feared in the event of a storm surge exceeding the planned level of protection works in such areas, which are particularly vulnerable to coastal disaster.

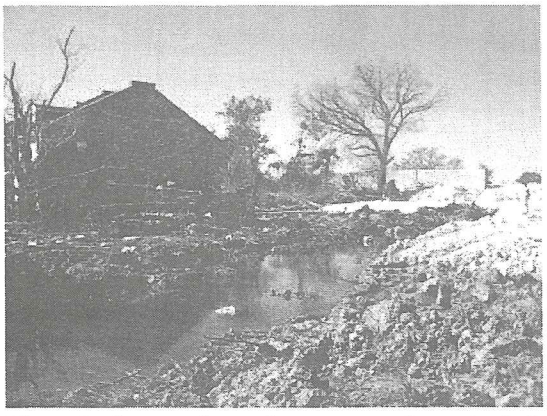

Photo2 Area where levee was breached in New Orleans (photo by the authors)

5. 2 Countermeasures for Infrequent Mega-Risk Coastal Hazards

Because endangered areas have long depended on hard countermeasures against infrequent mega-risk coastal hazards, the cost of investment is enormous. Even assuming that various types of hard countermeasures against infrequent mega-risk coastal hazards are implemented, the disaster-mitigating effect is not apparent as long as a major disaster does not occur, and criticism as excessive measures/wasted investment is possible. Therefore, proposals of measures which are effective in mitigating damage during a disaster and also have social utility under ordinary conditions have been demanded.

A wide range of concrete countermeasures are conceivable. These can be broadly divided into measures which diminish the energy or delay the arrival time of a tsunami, etc. by using existing port and harbor facilities such as wharfs, sheds, and warehouses and buildings, forests, aforestation, and plantation sited in the front line, and land use planning and layout planning by introducing regulations and inducement mechanisms for land use which considers disaster mitigation, for example, by arranging promenades and greenbelts which have the function of dikes/refuge areas when redeveloping or converting the use of idle land in coastal areas. Fig.11 shows an image of these countermeasures.

5.3 Efforts by NILIM

Based on the background described above, the National Institute for Land and Infrastructure Management (NILIM) is engaged in "Research on Evaluation Method of Countermeasures with Various Utilities against Infrequent Mega-Risk Type Coastal Hazards" as a project research, which has been promoted on a priority basis since FY2006. In this research, NILIM will propose countermeasures which are effective in mitigating damage in the event of a disaster and also have social utility under non-disaster (normal) conditions as countermeasures for infrequent mega-risk coast hazards, and will also construct an evaluation method for such multi-utility countermeasures and a method of building a consensus between local residents,

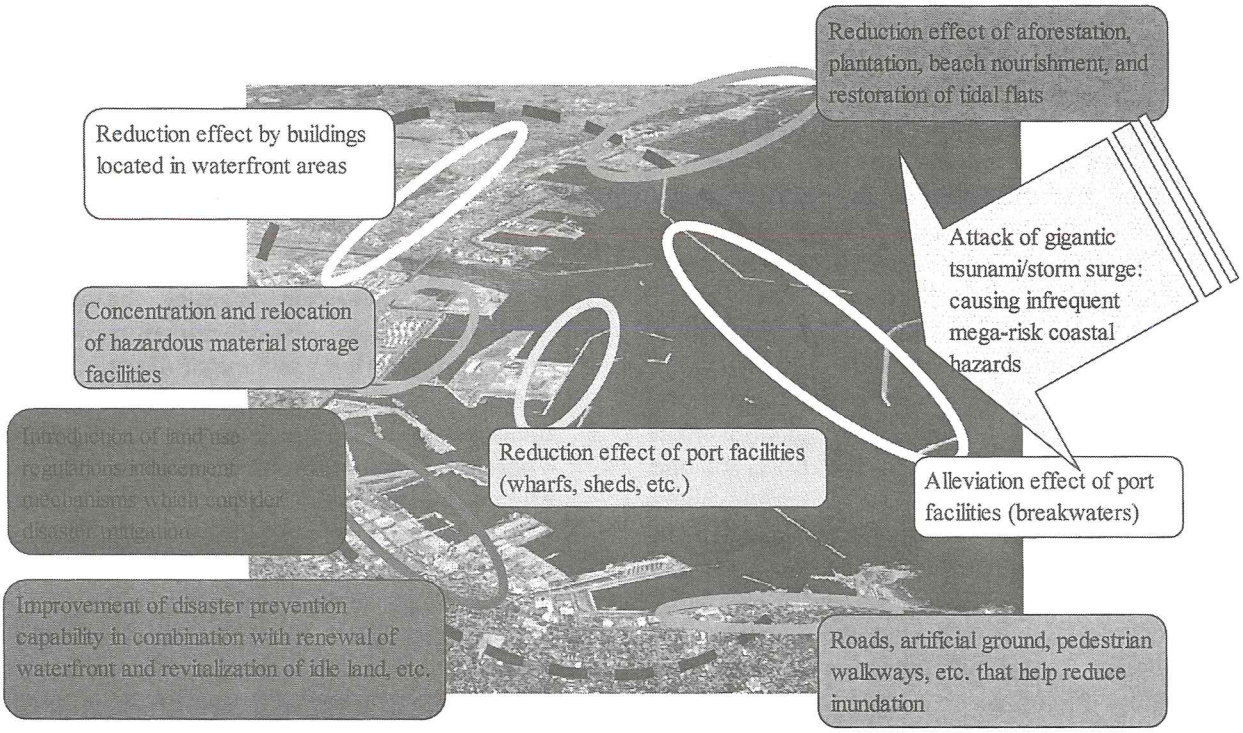

Fig.11 Image of multi-utility countermeasures

administrative authorities and other stakeholders. The objective is to propose guidelines for planning based on the results of these efforts. A facility management system and its operating measures based on life cycle management of storm surge and high wave countermeasure facilities will be proposed. In addition, NILIM will study measures for the construction of a system which integrates risk management in coastal regions, enabling joint use of facility management for storm surge and high wave countermeasure facilities and other infrastructure having a disaster-mitigating effect. NILIM is currently carrying out a study related to the establishment of scenarios for infrequent mega-risk coast hazards, and verification of the disaster mitigation effects of port and harbor facilities and other structures by numerical simulation and experiments. Normally, a 2-dimensional model which expresses shore and land topography using only ground height is employed as a simulation model for estimating tsunami/storm surge inundation behavior. However, in order to verify the disaster mitigation effects of port and harbor facilities, buildings, and others, it is necessary to use a more detailed topographical model which considers the 3-dimensional nature of the shapes of the facilities, as shown in Fig.12.

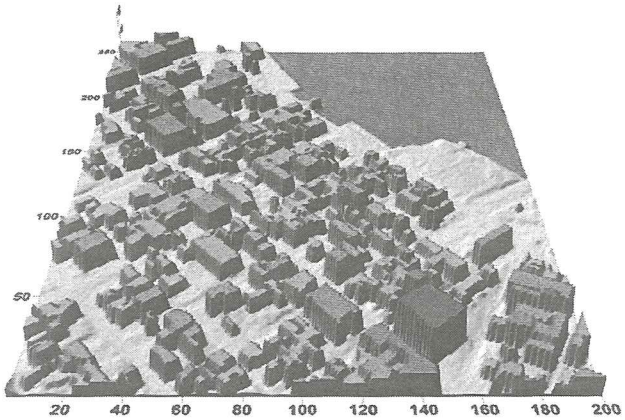

Fig.12 Example of topography in three-dimensional model

5.4 No Regret Policy

The objective of the No Regret Policy advocated in this research is to ensure that there are no regrets in the future to the effect that "preparations were lax" in the event that a major disaster occurs due to external forces exceeding the protective levels of existing countermeasures, and at the same time, there are no regrets about

"wasted investment" if a disaster does not occur during the service life of the facilities and equipment. From this viewpoint, we would like to inquire widely about the validity of the No Regret Policy in countermeasures against infrequent mega-risk coastal hazards.

If the results of this research are applied practically, the following effects can be expected: (a) diversification of countermeasures to large-scale tsunamis and other disasters based on the features of the region (expansion of the options of the region), (b) enhanced safety and resilience of the coastal hazard-prone areas and restoration of the coastal environment and urban/residential environments, (c) improvement of accountability for investments in disaster prevention/mitigation, (d) early manifestation of the effects of disaster prevention/mitigation projects by smooth project implementation.

6. REFERENCES

1. Okamoto, O., Oda, K., Kumagai, K.; "A Tsunami Damage Influence Process Including the Indirect Damage and the Evaluation Method in Ports Harbor and Rear Area, Technical Note of National Institute for Land and Infrastructure Management, Ministry of Land, Infrastructure and Transport, No. 306, June 2006(in Japanese).
2. Japan Association of Marine Safety: "Report of Research on Securing Ship Safety in Expected Tsunamis," March 2004(in Japanese).
3. Ministry of Land, Infrastructure and Transport: "Guidelines for Inundation Countermeasures in Underground Space and Commentary (Technical Documents), March 2002(in Japanese).

THEME 3

Sustainable Design
for Buildings and Infrastructure
- Focus on Natural Disaster Prevention

Development of Safe Infrastructures against Global Changes of Natural Disasters

by
Masanori HAMADA
Professor, Dept. of Civil and Environment Engineering
Waseda University, Tokyo, Japan

1. Introduction

The natural environmental changes such as global warming, heat island phenomena in mega cities, the decrease of the forest, desertification and erosion of rivers, are resulting in extremely heavy rains and snows, huge typhoons and hurricanes, abnormally high temperature, and high tidal waves. In addition to the change of natural environment, our social environment is also changing and it is becoming fragile against natural disasters. Those are highly congested urban areas, depopulation of rural areas, human habitation on disaster-prone lands, lack of cooperation and communication among recent urban societies, and insufficient infrastructures for disaster mitigation. The characteristics of the natural disasters are changing due to the changes of the natural and social environment.

This paper briefly reviews the recent natural disasters in the world and associated subjects. Furthermore, the author discusses the basic concept of the policies for the natural disaster mitigation and the roles of civil engineers.

2. Natural Disasters and Climate Change in the World

2.1 Recent Earthquake and Tsunami Disasters in the World

During recent few years, the disastrous earthquakes and tsunamis have attacked the Asian countries. The 2004 Sumatra earthquake and consequent tsunami killed more than 2 hundred thousand people in the areas around the Indian Ocean[1]. In the same year, a devastating earthquake caused serious damage to Niigata Prefecture, Japan[2] due to extensive slope failures in mountainous areas. In 2005, about 70 thousand people were killed in Pakistan[3], and last year, a disastrous earthquake attacked the Java Island, Indonesia.

Figure 1 shows the number of earthquakes and tsunamis with more than one thousand casualties in each five years period during the last 60 years in the world. The number of events has drastically increased in the last two decades.

The number of earthquakes with magnitudes more than 7.0 and more than 6.0 in the world during the last 60 years is shown in Figure 2. On the contrary of the increase of the earthquake and tsunami disasters, the number of

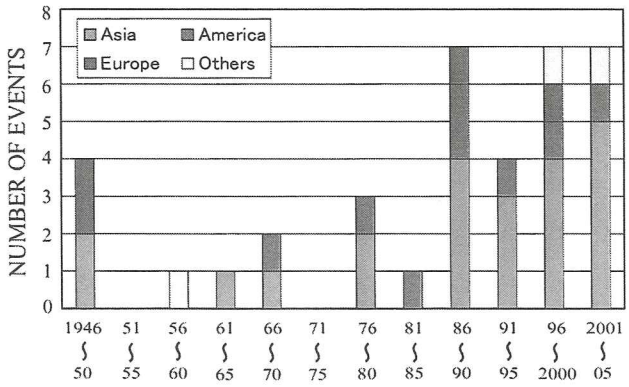

Figure 1 Damaging Earthquakes and Tsunamis in the World in the Last 60 Years (Events with more than 1000 casualties)

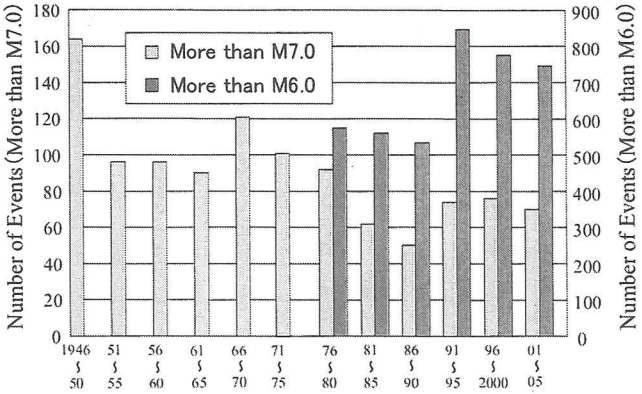

Figure 2 Number of Earthquakes with Magnitudes More than 7 and More than 6

occurrences of earthquakes with magnitudes more than 7.0 has been decreasing during the last 60 years. The number of the earthquakes with more than 6.0 slightly increased during the last decade, but was not consistent with the rapid increase of the number of the earthquake and tsunami disasters. This suggests that the reason of the increase of the earthquake and tsunami disasters is the increase of the vulnerability of our human societies. The regional ratio of the number of the earthquake and tsunami disasters and of the number of causalities during the last two decades is shown in Figure 3. 25 earthquake and tsunami disasters occurred in the world. Among them, 16 events were in Asian region. About five hundred thousands people, which are almost 90% of the total number of casualties in the world were killed in Asian region.

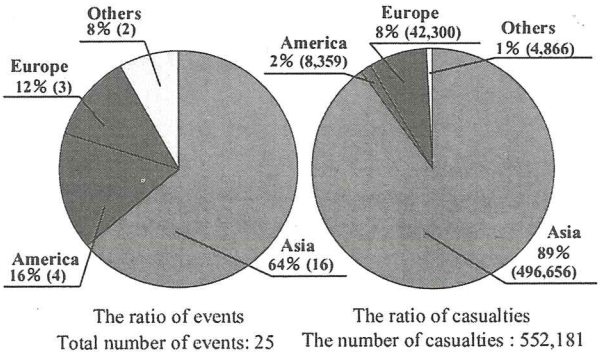

Figure 3 Regional Ratio of Earthquake Tsunami Events and Casualties (1986–2005 Events with More than 1000 Casualties)

2.2 Recent Storm and Flood Disasters in the World

Storm and flood disasters also have suffered the people in the world in recent years. During the last decade, 21 disasters killed one hundred thousands people. Most of the storm and flood disasters were concentrated in the Asian region and Central America. In 2005, Hurricane Katrina attacked Louisiana in United States, and killed more than 1 thousand people. In 2004, the Asian countries such as Japan, Philippines, India and Bangladesh suffered from many typhoons and heave rains, and about four thousand lives were lost.

Figure 4 shows the number of storm and flood disasters with more than one thousands casualties in each five years period during the last 60 years. The storm and flood disasters in the world have also increased during the last two decades. And, the disasters in Asia are dominant. The regional ratio of the number of the storm and flood disasters and the number of causalities is shown in Figure 5. 31 events occurred during the last two decades in the world, and 23 events, which was about three quarters of the total number, attacked the Asian region. About two hundred thousand lives, which is almost 80% of the total causalities were lost by storm and flood disasters in the Asian region.

There may be two main reasons for the increase of the flood and storm disasters. One is the increase of the vulnerability of the human societies against disasters, which is particularly remarkable in the Asian countries. Another reason may be the global climate change. Figure 6 illustrates the change of air temperature and seawater temperature in the world during the last 40 years. The air temperature raised about 0.5 degree in centigrade and the sea water temperature raised 0.3 degree. The rise of seawater temperature can be considered to be one of causes of the occurrence of huge typhoons and hurricanes, and high tidal waves.

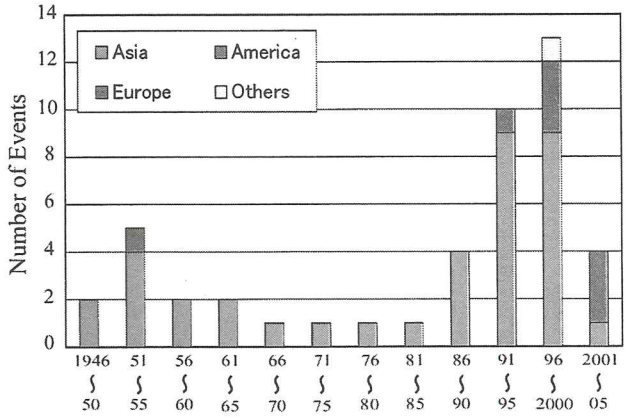

Figure 4 Damaging Storms and Floods in the World during the Last Half Century (Events with more than 1000 casualties)

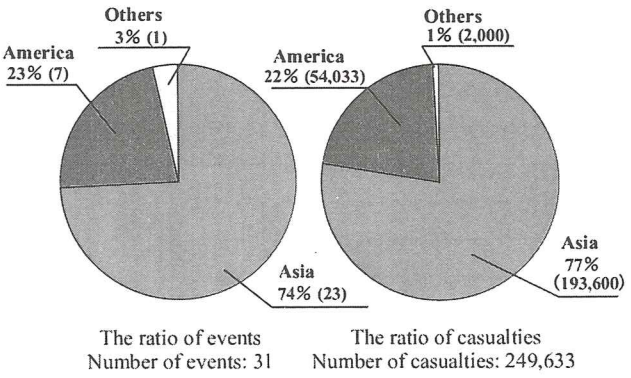

Figure 5 Regional Ratio of Storm and Flood and Associated Casualties (1986–2005, Events with More than 1000 Casualties)

2.3 Recent Natural Disasters and Climate Change in Japan

The locations of earthquake disasters after the 1995 Kobe earthquake are shown in Figure 7. The total 6 thousand and five hundred lives were lost, including the Kobe earthquake. We have learned new lessons from each past earthquake. From the Kobe earthquake, we learned lack of earthquake resistance of concrete bridges, subway structures and buildings against the strong earthquake ground motions in the near field of the earthquake fault. A large man-made island reclaimed from the sea extensively was liquefied resulting in severe damage to structures such as storage tanks, and quaywalls.

The Niigata earthquake in 2004 taught us new lessons, one of which was an overlap of different natural disasters. Three days before the earthquake a huge typhoon attacked the same area with heavy rains. The slopes in the mountainous area and embankments were saturated. The earthquake ground motion caused huge landslides and embankment failures. Liquefaction also caused severe damage to lifeline systems, and strong ground motion in the vicinity of the fault derailed the bullet train, Shinkansen. This derailment of Shinkansen exposed a serious social subject, which is how to balance the risk with a large benefit of the high-speed train for the society and the people.

The recent flood and storm disasters in Japan are shown in Figures 9 and 10. Flood and storm disasters with casualties meaningfully occurred twice a year, and about 5 hundred lives were lost during the last decade. Last year, a huge mudflow, which was caused by a heavy rain, attacked residential area in Nagano Prefecture, and killed 12 people. In 2004, Itsukushima shrine, one of national treasures was severely damaged by high tidal wave and strong wind by a large-scale typhoon. In 2005, a downpour with 100 mm rain per hour flooded a wide area of the downtown of Tokyo. This is considered to be caused by the heat island phenomena in highly urbanized mega cities.

Figure 11 shows the change of the temperature and the rain falls in Japan. The mean temperature in whole area of Japan raised about 0.7°C during the last 30 years, and 1.0°C in Tokyo. The number of the rainfalls with more than 100 mm per hour in Japan

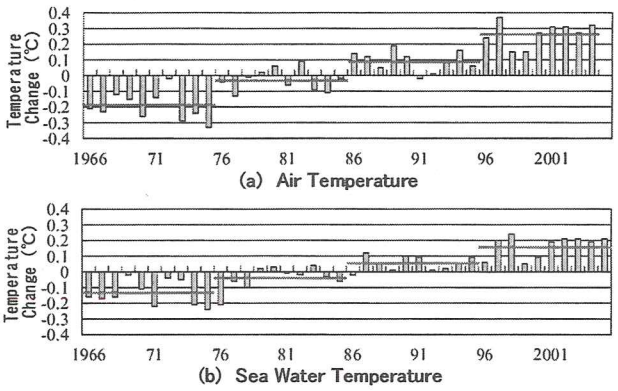

Figure 6 Temperature Change of Air and Sea Water in the World [4)]

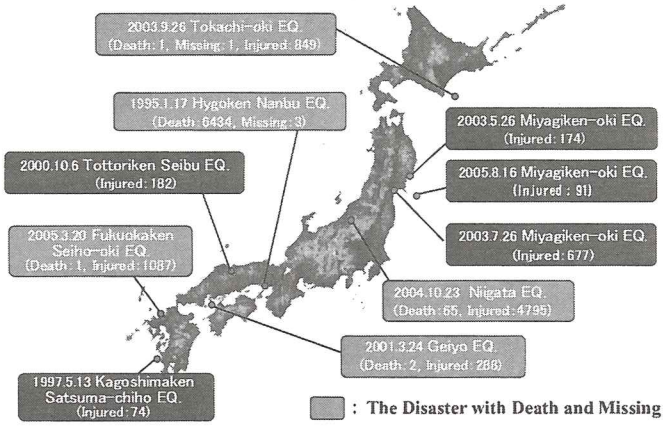

Figure 7 Recent Earthquake Disasters in Japan (1995–) (The Number of Death and Missing : 6507)

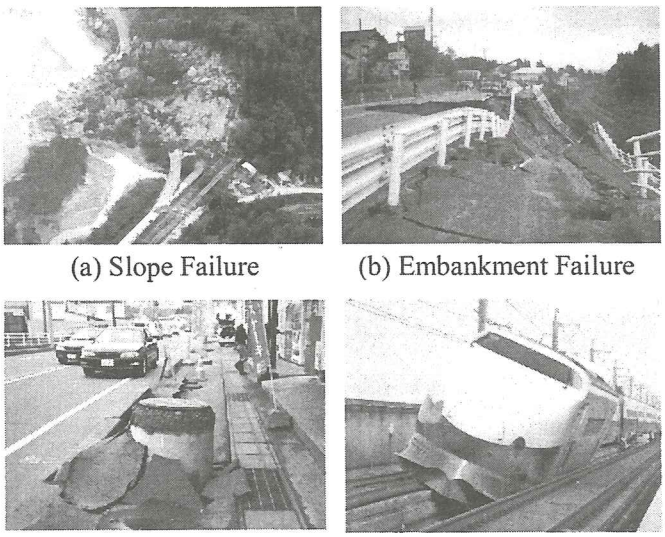

(a) Slope Failure (b) Embankment Failure

(c) Uplift of Sewage Manholes (d) Derailment of Shinkanse (Bullet Train)

Figure 8 Disaster by the 2004 Niigata Earthquake

has been increasing during the last decade.

3. Basic Concepts of the Policy against Future Disasters under the Change of Natural and Social Environments

The natural environment is changing. Those changes are global warning, heat Island phenomena in urbanized area, deforestation, desertification and erosion of river and seashore. The change of natural environment is increasing natural disasters. Those are extremely heavy rains and snows, huge typhoons, hurricanes and cyclones, drought, abnormally high temperature and high tidal waves due to the rising of sea water level. In addition to the change of natural environment, our social environment is also changing, becoming fragile against natural disasters. Those are too congested urban areas, depopulation of rural area, human habitations on fragile ground, lack of cooperation and communication among the recent urban societies, budget deficit of central and rural governments, and finally poverty. The poverty is the most important factor for the increase of the natural disasters in the Asian countries. The poverty is expanding the disaster, and the disaster is worsening the poverty.

The characteristics of natural disaster are changing due to the change of natural and social environments. What is the basic policy against these kind of natural disasters? The key point for the measures against future disasters is how to prepare unexpected natural phenomena and against external forces largely exceeding the design level. In another word, how to prepare against natural disasters with a huge scale,

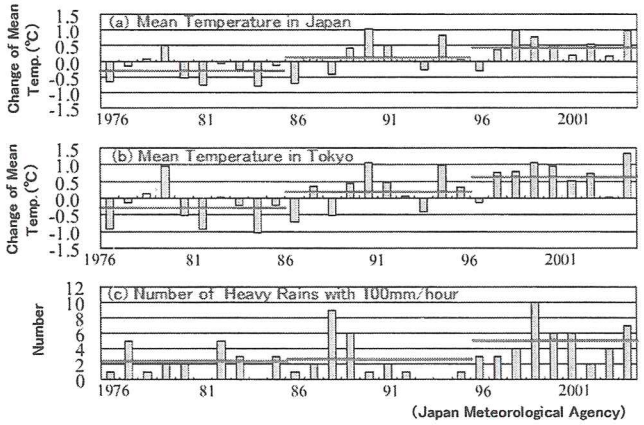

Figure 11 Change of Mean Temperature and Rain Falls in Japan [4] (1976–2004)

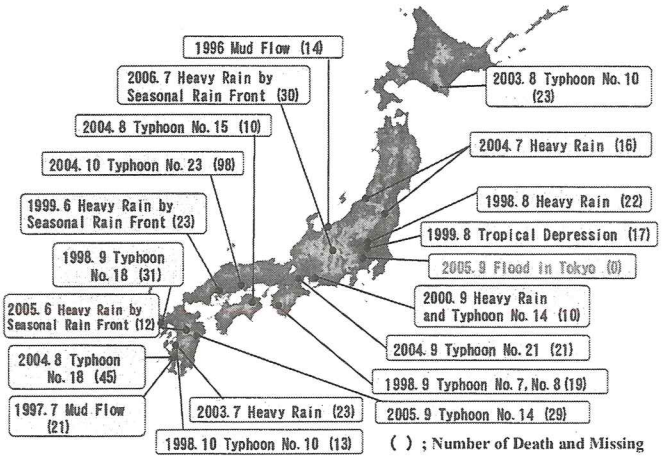

Figure 9 Recent Floods and Storm Disasters in Japan (1996–) (The Number of Death and Missing : 477)



(a) 2006 Mud Flow by Heavy Rain (Nagano)

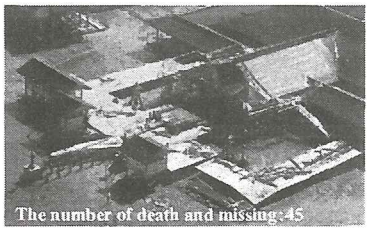

(b) 2004 Itsukushima-shrine which was Destroyed by Typhoon No.18 (Hiroshima)

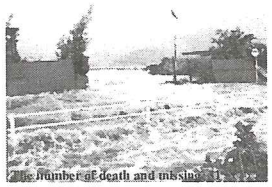

(c) 1999 Tidal Wave by Typhoon No.18 (Kumamoto)

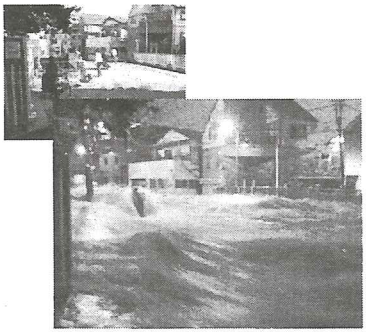

(d) 2005 Flood by Heavy Rain (Tokyo)

Figure 10 Recent Flood and Storm Disaster in Japan

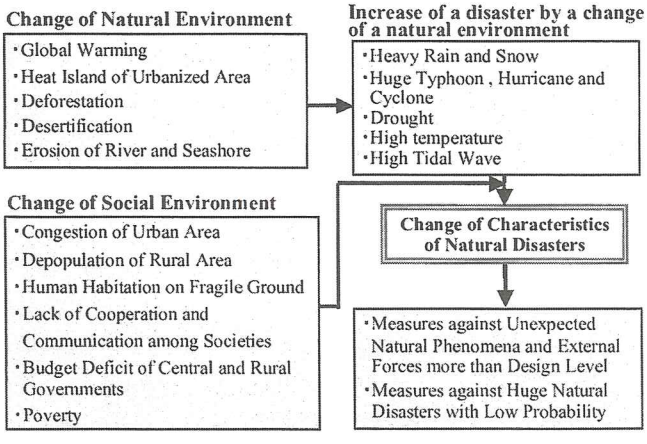

Figure 12 Basic Concepts of the Policy against Future Disasters under the Changes of Natural and Social Environment

but low probability of occurrence.

Figure 13 illustrates a basic concept for the measures against huge natural disasters with low probability of occurrence. That is a combination of hardware measures and software measures. Hardware measures mean, for an example, reinforcement of dikes against floods, and the soft ware measures are evacuation systems during flood and the education of people. Moderate disasters with medium probability are prevented mainly by hardware measures. However, against huge disasters with low probability, the disaster is reduced both by hardware and software measures.

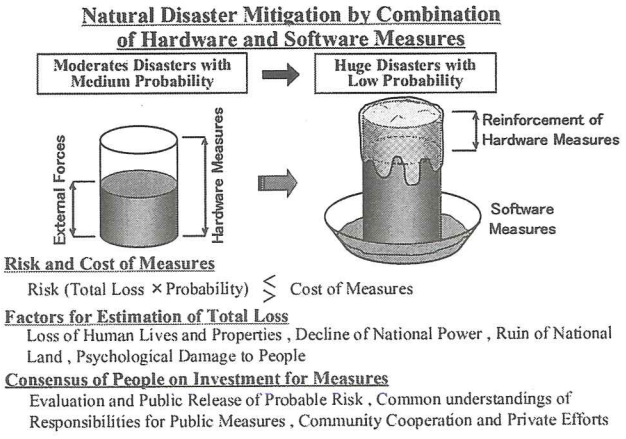

Figure 13 Measures against Huge Natural Disasters with Low Probability

The problem is how to determine the rational level of the investment for disaster mitigation. One of methods to judge the rational level of the investment is the comparison of the risk with the cost of the measures. The risk is estimated as the product of the total loss with the probability. For the estimation of the total loss, we have to take into consideration, various factors, not only loss of human lives and properties, but also probable national power decline resulting from the disaster, ruining of national landscape and furthermore, psychological damage to people. And the consensus among the people is essential to determine the rational level of disaster mitigation measures.

4. Future Earthquakes Threatening Japanese Mega Cities

As shown in Figure 14, large earthquakes, which have high probabilities of occurrence, are threatening the Japanese mega cities such as Tokyo, Nagoya, Osaka and Sendai. Figure 14 shows the source areas of those future earthquakes. The three earthquakes along the Nankai trough in the Pacific Ocean, Tokai, Tonankai and Nankai earthquakes have large magnitudes of 8 or more. The probabilities of the occurrence of these earthquakes are predicted to be very high. In the case of Tokai earthquake, the probability of occurrence in the next thirty years is more than 80%.

The northern Tokyo Bay earthquake with a magnitude of 7.3 has also high probability, 70% within next thirty years. In the case of Miyagi earthquake with a magnitude of 7.5, which is threatening the Sendai City, the probability is estimated as 99%. As shown in the figure, many mega cities of Japan are under the threat of being hit by disastrous earthquakes in very near future.

Table 1 shows the result of the damage assessment by the Northern Tokyo Bay earthquake by the National Council of Disaster Prevention of Japan under a condition, that is, the wind speed is 15m/s. If the earthquake did

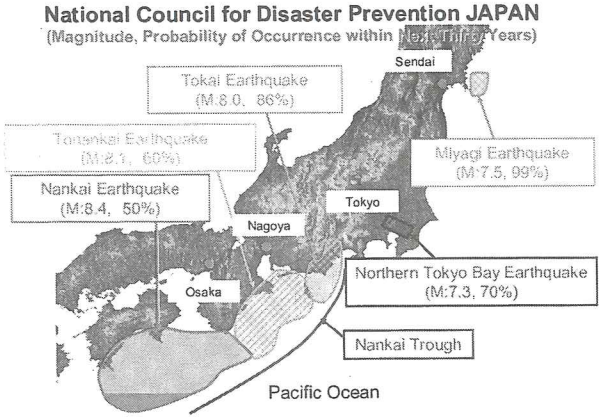

Figure 14 Future Earthquakes with High Probabilities to Hit The Mega Cities in Japan [5)]

Table 1 Assessment of Damage by the Northern Tokyo Bay Earthquake [5)]

- Tokyo and The Neighboring Three Prefectures - (Wind Speed 15 m/s)

Items		5:00 AM	6:00 PM	Kobe Earthquake
Number of Collapsed or Burnt House and Buildings	Ground Motion	150,000	150,000	110,000
	Fire	160,000	650,000	7,000
	Liquefaction, Slope Sliding, etc	35,000	50,000	46
	Total	360,000	850,000	117,000
Death	Collapse of Houses	4,200	3,100	4,915
	Fire	400	6,200	550
	Slope Sliding	1,000	900	37
	Total	5,600	11,000	5,520
Number of People unable to go home (12:00AM)			6,500,000	
Refugees			4,600,000	237,000
Economic Loss			$ 1.1 Trillion	$ 110 Billion

occur at 6 PM, the Council estimated the number of collapsed or burnt houses and building as about 850,000 in Tokyo area, including the neighboring three prefectures, that would be about seven times of the damage caused by the Kobe earthquake. The resulting fires would burn more than 650,000 houses and buildings. The total number of the death is estimated as 11,000, and among them about 6,000 people would be killed by the fire after the earthquake. Furthermore, if the earthquake occurred at noon, 6.5 million people could not go home on the day of occurrence of the earthquake due to the destructive damage to the transportation systems. And the number of refugees is estimated to be 4.6 million, which is about 20 times of the number in the case of the Kobe earthquake. The total economic loss reaches over 1.1 trillion US dollars, which is almost 1.5 times of the total amount of national budget of Japan.

5. Roles of Civil Engineers for Natural Disaster Mitigation

The first role of civil engineers for the natural disaster mitigation is the development of technologies for enhancement of infrastructures, such as technologies for the improvement of soft soil, high-performance structures, and warning and rescue systems. The second role is actual construction of infrastructures with high natural disaster resistance. The third role of civil engineers is the involvement in the rescue operation, and restoration and reconstruction works after natural disasters.

A large number of infrastructures such as highways, railways, port-harbor facilities have been constructed on improved soft alluvial and man-made ground along the seaside of the Tokyo Bay. Various kinds of methods for improvement of soft alluvial and artificial ground have been developed. Technologies such as passive and active control systems have been developed to reduce the dynamic effects on buildings and bridges during earthquakes, and have been applied to a large number of structures.

The 1995 Kobe earthquake destroyed a huge amount of infrastructures. Therefore, Reinforcement of existing infrastructures against future earthquakes has been one of most important roles of civil engineers after the Kobe earthquake. A numerous number of infrastructures such as railway and highway bridges, and subway stations have been reinforced.

The real time earthquake warning system has been developed and applied to some practical uses as shown in Figure 16. In this system, the magnitude and the epicenter of earthquakes will be judged by the ground motion records in the vicinity of earthquake faults, and if the earthquake has such a large magnitude as to cause serious damage, the warning will be sent to various organizations before the arrival of the main ground motion of the earthquake. Based on the warning, the high-speed trains will be stopped, and the road and air traffic will be carefully controlled. The operation of the various kinds of plants will be shutdown, and the water gates will be closed against the tsunami. In the case of Tokai earthquake, the time allowance before arrival of the main shocks is estimated as about 50 seconds in Tokyo area.

In low land areas in Tokyo, which has lower elevation than river water level, so-called "super levee" has been

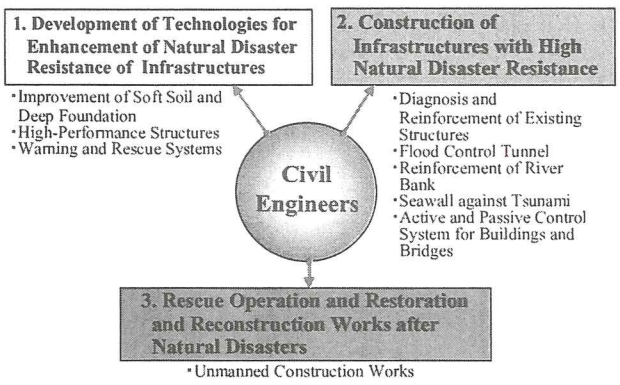

Figure 15 Roles of Civil Engineers for Natural Disaster Mitigation

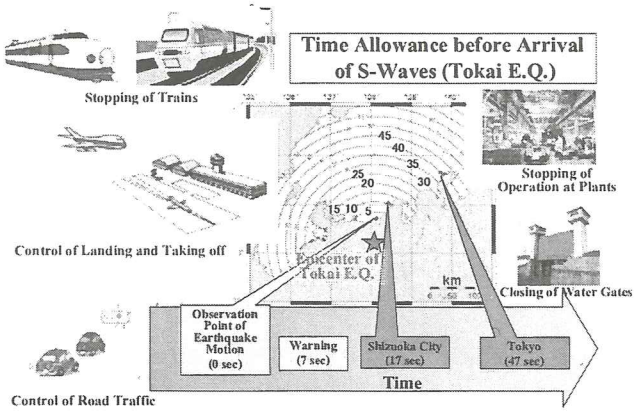

Figure 16 Real Time Earthquake Warning System

constructed against future earthquakes and for development of the areas with high natural disaster resistance, as shown in Figure 17. New banking behind the original riverbank elevated a wide area and the area was redeveloped to enhance the natural disaster resistance, by creating open spaces for the rescue operation and by constructing high earthquake resistant buildings.

6. Cooperation and Collaboration of Civil Engineers in the Asia-Pacific Region for Natural Disaster Mitigation

As mentioned previously, natural disasters are increasing, and the environments are destructed, particularly in Asian countries. The roles and the responsibilities of civil engineers are increasing. The transfer of the technologies for natural disaster mitigation and environment protection should be strongly promoted, and furthermore, we civil engineers should work together on the education of the people for natural disaster mitigation, and should more actively participate to the technical support activities for reconstruction and restoration of the areas damaged by natural disasters. For these activities, we have to further advance the cooperation and collaboration among our civil engineers societies in the Asia-Pacific region.

JSCE is encouraging its members to participate to the technical assistance activities for the areas damaged by natural disasters and to the education for natural disaster mitigation. JSCE and its members have continued to provide assistances and aid activities in Northern Sumatra after tsunami disasters. In response to the request from the Indonesian Government, JSCE prepared a technical recommendations on the plan of reconstruction of the road along the west coast of north Sumatra, most of which had been washed away by the tsunami. JSCE also proposed a regional tsunami warning system. This is the request from the state government. The student members of JSCE have been educating children in Sumatra on the earthquake and tsunami disaster mitigation.

Figure 18 illustrates the basic concept of a regional tsunami warning system for Sumatra Island, proposed by JSCE. In this warning system, the epicenter and the magnitude of the earthquake will be estimated from the seismic records at the stations along the west coast of Sumatra. The warning, which will be transmitted from the tsunami-warning center to the regional mosques through the satellites, is conveyed to the people. One of the characteristic points of this warning system is utilization of mosques, which are closely associated with the regional people, and have comparatively high resistance against tsunami and earthquake motions.

The student members of JSCE are carrying on education programs for children of Banda Ache and other areas in the northern Sumatra. They are teaching the mechanism of the occurrence of earthquakes and tsunamis and how to save lives from the future disasters. Japanese students are conducting their activities under a close corporation

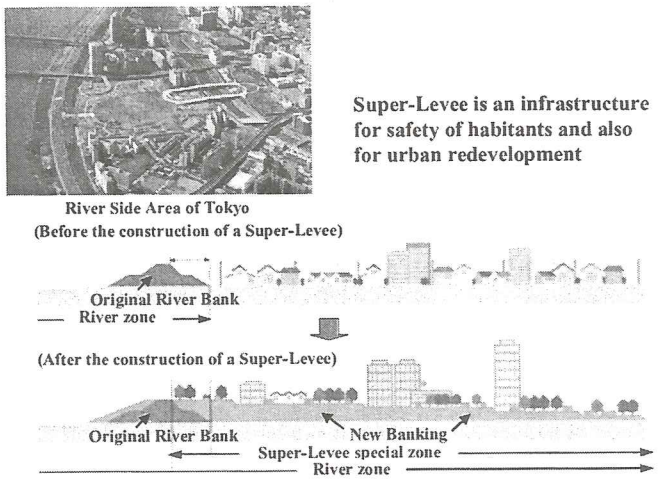

Figure 17 Construction of the Super-Levee in Low Land Area of Tokyo against Future Earthquake

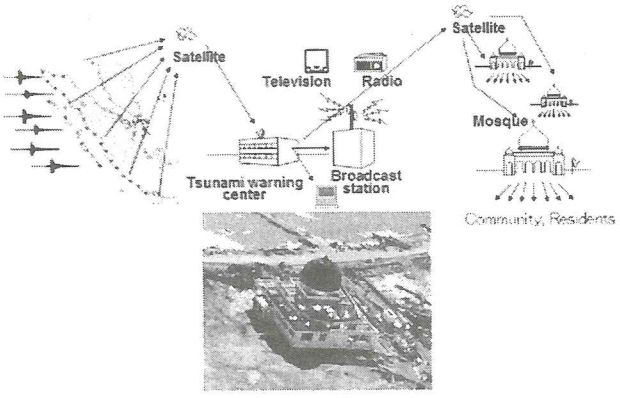

Figure 18 Plan for Regional Tsunami Warning System by JSCE (For North Sumatra Provincial Government)

with Indonesian student groups. These young civil engineers' activities are expanding internationally. The technical assistances by JSCE have been carried out in Indonesia and Pakistan for the areas attacked the recent disasters. In Nias Island, Indonesia, technical seminars for temporary restoration of bridges damaged by liquefaction have been held, while In Pakistan, the members of JSCE held conferences on the reconstruction of damaged structures, under a cooperation with the Pakistani engineers. In these conferences, JSCE introduced the reconstruction procedures based on the experiences gained from Kobe earthquake.

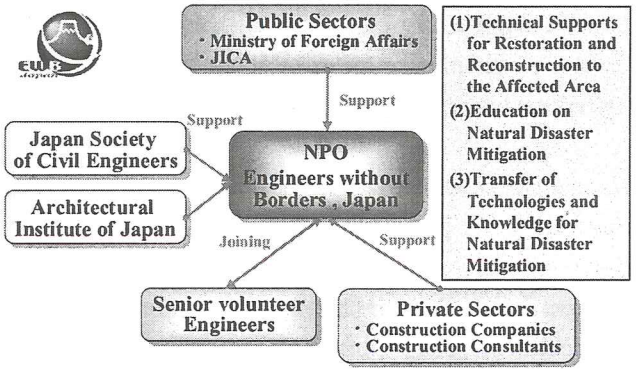

Figure 19 NPO : Engineers without Borders , Japan

Recently, members of JSCE and Architectural Institute of Japan established a NPO, named "Engineers without Borders, Japan". The objectives of this NPO are to provide technical supports for restoration and reconstruction of the damaged areas, and to carry out education on disaster mitigation. Another important role of this NPO is the transfer of the technologies and knowledge for natural disaster mitigation. JSCE is going to strongly promote assistance and aid activities under a close cooperation with this newly established organization.

7. Conclusions

Natural disasters such as earthquakes and tsunami, and storm and flood disasters have been increasing during last two decade, particularly in the Asian countries. Furthermore, due to the change of natural and social environments, the scale of the natural disasters is expanding. For the mitigation of the future natural disasters, the roles and the responsibilities of civil engineers are increasing. Furthermore, the cooperation and collaboration of civil engineers in the world are essential to accomplish these errands.

JSCE and the other organizations of civil engineers in the world have been in a good partnership during decades, and have served people for the safe living and welfare. However, the recent natural disasters into world taught us again that the development and application of technologies and knowledge for natural disaster mitigation are the urgent subject for civil engineers. We have to strengthen and to further advance the cooperation between two societies.

References

1) Japan Society of Civil Engineers : The Damage Induced by Sumatra Earthquake and Associated Tsunami of December 26, 2004, 2005.8.
2) Japan Society of Civil Engineers and Architectural Institute of Japan : A Quick Report on Kashimir Earthquake, 2005.11.
3) Japan Society of Civil Engineers : General Investigation about the Damage of Social Infrastructure Systems due to the 2004 Niigata Earthquake / Result of Investigations and Urgent Proposals, 2004.11.
4) Japan Meteorological Agency : A Report on Abnormal Weather 2005, 2005.10.
5) Cabinet Office, Government of Japan : White Paper on Disaster Prevention, 2006.

Creation of Safe and Secure Society against Global Change of Natural Disasters
- A Special Task Committee of the Science Council of Japan -

by
Masanori HAMADA
Professor, Dept. of Civil and Environment Engineering
Waseda University, Tokyo, Japan
President of Japan Society of Civil Engineers

1. Introduction

The natural environmental changes such as global warming, heat island phenomena in mega cities, decrease of forest, desertification and erosion of rivers, are resulting in extremely heavy rains and snows, huge typhoons and hurricanes, abnormally high temperature, and high tidal waves. In addition to the changes of natural environment, our social environment is also changing and is becoming more fragile against natural hazards. The fragility results from highly congested urban areas, depopulation of rural areas, human habitation on disaster-prone lands, lack of cooperation and communication among recent urban communities, and insufficient infrastructures for disaster mitigation. The Science Council of Japan organized a special task committee to discuss how to create safer and more secure society against the global change of natural disasters, and prepared political and scientific proposals to the Japanese government.

2. The Special Task Committee and Its Subject

The committee has three sub-groups with their own themes. The first sub-group, which consists of natural scientists, has a role to forecast natural hazards resulting in future disasters, on basis of studies on global change of natural environments. The second sub-group, which mainly consists of engineers and researchers in civil engineering has a role to evaluate the vulnerability in the national land use and of infrastructures, and to discuss policies and measures for improvement and reinforcement of infrastructures against future natural disasters. The third sub-group, which consists of researchers in sociology is required to evaluate the social hazards in societal systems, which will enlarge disasters.

The Minister of Land, Infrastructure and Transport of Japan requested the president of SCJ for advisory on basic policies of infrastructure development for disaster mitigation under global changes of natural hazards in June, 2006. The president instructed the committee to submit a report on the request for the advisory.

3. Summary of the discussions at the committee

The discussions at the committee were carried out according to the flow chart shown in Figure 1.

(1) Forecast of natural hazards resulting in disasters, such as earthquake and tsunami, volcano eruption, storm, storm surge, high wave, etc.
(2) Evaluation of hazards in land-use and societal systems, such as overpopulation in urbanized area and depopulation in rural areas, declining birth rate, aged society, globalization of politics and economy, information society, lack of revenue for natural disaster mitigation.
(3) Forecast of future natural disasters under the changes of natural and social environments.
(4) Proposal for basic policies how to create and more secure society against future natural disasters, and how to build consensus from the people.
(5) Proposals for measures for the improvement of national land-use and societal systems, and measures for development of infrastructures.

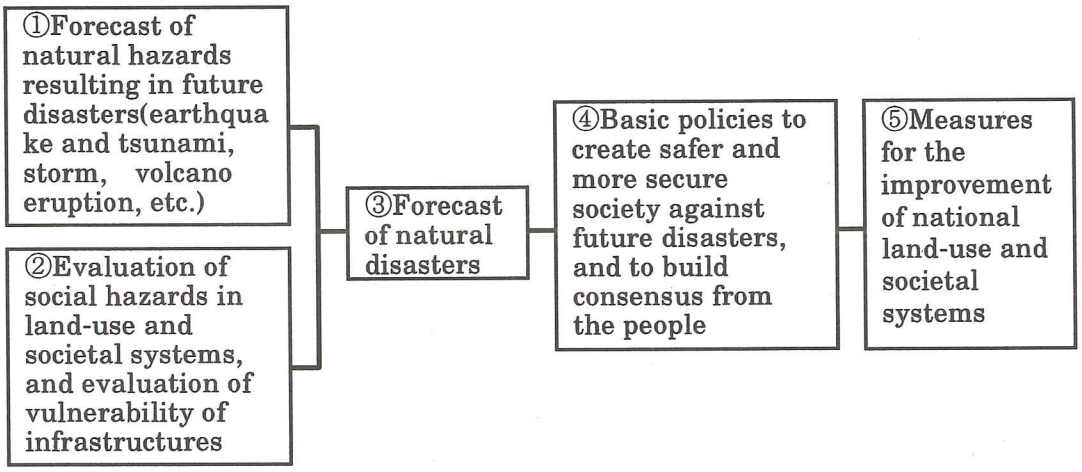

Figure 1 The flow chart of the discussions at the committee

4. Proposals from SCJ

The committee presented the following proposals for the creation of disaster-proof country and community to the central government, prefectural and municipal governments, and other organizations concerned with natural disaster mitigation.

(1) Paradigm change from short-period view of efficiency of economics to long-term view of creation of safe and secure society is required.

(2) Long-term and stable tax spending for the measures for the improvement of national land-use and societal systems, and for reinforcement of infrastructures is required.

(3)The national land-use should be reformed by decentralization of population and properties, establishment of a back-up system for maintenance of the capital function of the metropolitan Tokyo. Transport systems should be reinforced for rescue, recovery and reconstruction works after the disasters.

(4) Improvement of both hardware and software measures are required against huge natural disasters with low probability of occurrence. The hardware measures involve reinforcement of infrastructures, buildings and houses, while the software measures involve establishment of the rescue system, disaster-information system, education and so on.

(5) Comprehensive and total policies among ministries and governmental offices concerned with natural disaster mitigation are required. The cooperation among local governments and financial and personnel supports from central government to local governments are necessary for the measures against large-scale disasters over a wide area.

(6) So-called disaster-awarness society should be created by education of people, particularly of children, and by transfer of knowledge and experiences of disasters over generations.

(7) NPO and NGO's activities should be encouraged for disaster preparedness, and for rescue and recovery. Financial supports from central and local governments is required to NPO and NGO.

(8) International cooperation and assistances are essential for natural disaster mitigation in the developing countries, and promotion of international cooperative researchers and investigations on the technologies and knowledge for disaster mitigation should be strongly prompted.

The committee also claimed strong and long-term promotion of overarching researches among academic societies including fields of natural science, engineering, life science and human science as the roles and the responsibilities of SCJ for the natural disaster mitigation.

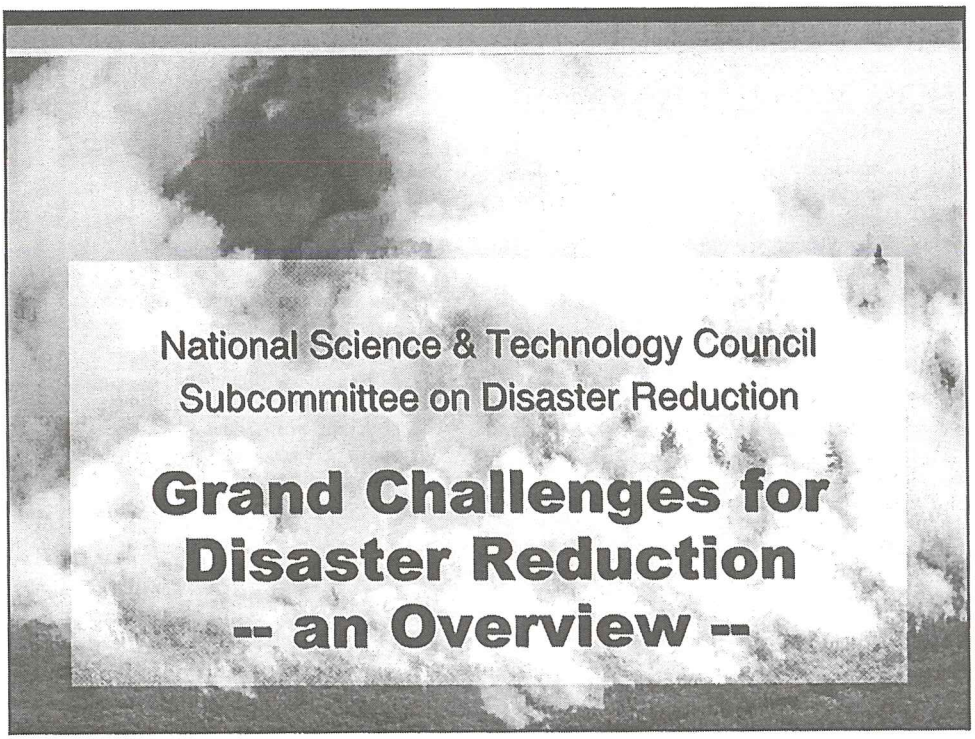

U.S. Subcommittee on Disaster Reduction

- The U.S. Subcommittee on Disaster Reduction (SDR) is part of the President's National Science & Technology Council charged with establishing national goals for Federal science and technology investments in disaster reduction.
- Promotes interagency cooperation for natural and technological hazards and disaster planning.
- Facilitates interagency approaches to identification and assessment of risk, and to disaster reduction.
- Advises the Administration about resources and the work of SDR member agencies.
- Provides policy recommendations to the President and Congress about disaster reduction approaches.

SDR Member Agencies

- Centers for Disease Control and Prevention
- Department of Defense
- Department of Energy
- Department of Homeland Security
- Department of Housing & Urban Development
- Department of the Interior
- Department of State
- Department of Transportation
- Environmental Protection Agency
- Federal Emergency Management Agency
- National Aeronautics & Space Administration
- National Geospatial-Information Agency
- National Guard Bureau
- National Institute of Standards and Technology
- National Oceanic & Atmospheric Administration
- National Science Foundation
- U.S. Agency for International Development
- U.S. Army Corps of Engineers
- U.S. Coast Guard
- U.S. Department of Agriculture
- U.S. Forest Service
- U.S. Geological Survey
- U.S. Public Health Commissioned Corps



3

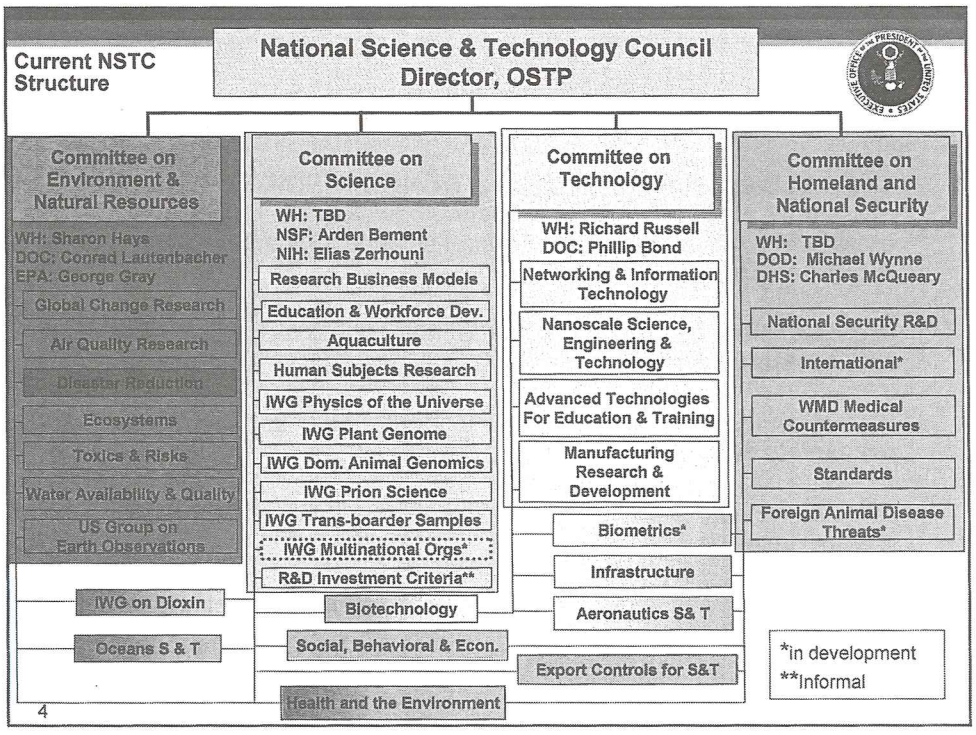

4

Some SDR Reports

Effective Disaster Warnings (November 2000)

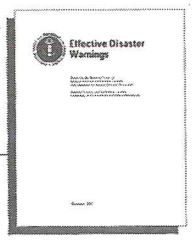

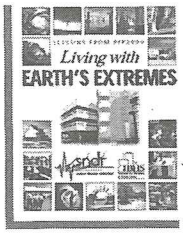

Living with Earth's Extremes (September 2001)

Reducing Disaster Vulnerability Through Science and Technology (July 2003)

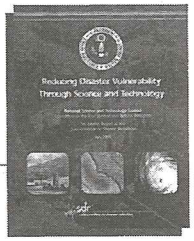

5

SDR Reports (continued)

Grand Challenges for Disaster Reduction (June 2005)

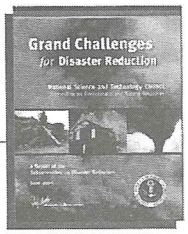

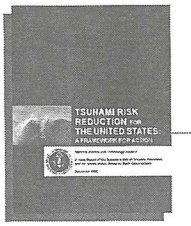

Tsunami Risk Reduction for the United States (December 2005)

Windstorm Impact Reduction Implementation Program (April 2006)

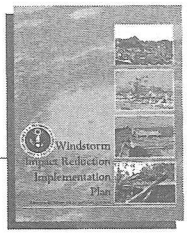

6

The Grand Challenges for Disaster Reduction

Objective: To enhance disaster resilience by developing a ten-year agenda for science and technology activities that will produce a dramatic reduction in the loss of life and property from natural and technological disasters.

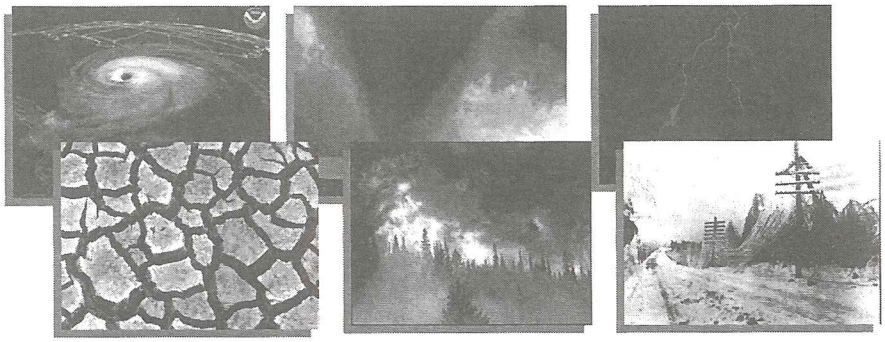

7

A framework for prioritizing disaster-related Federal investments in science and technology

Published by the SDR in June 2005 and available at www.sdr.gov

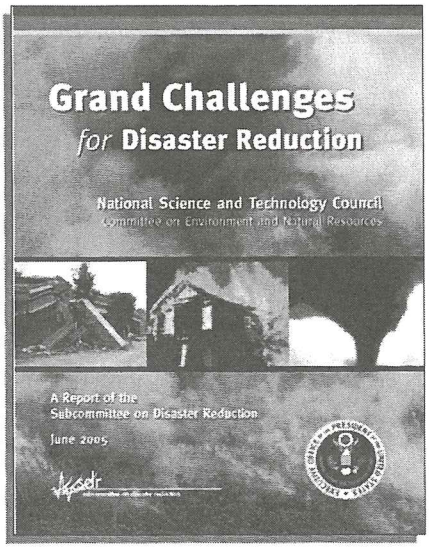

8

Grand Challenge #1 Provide Hazard and Disaster Information Where and When It Is Needed (identify and anticipate the hazards that threaten communities, develop methods to collect data and interpret information and data in real-time for scientists/engineers, emergency managers, first responders, policy makers, general public)

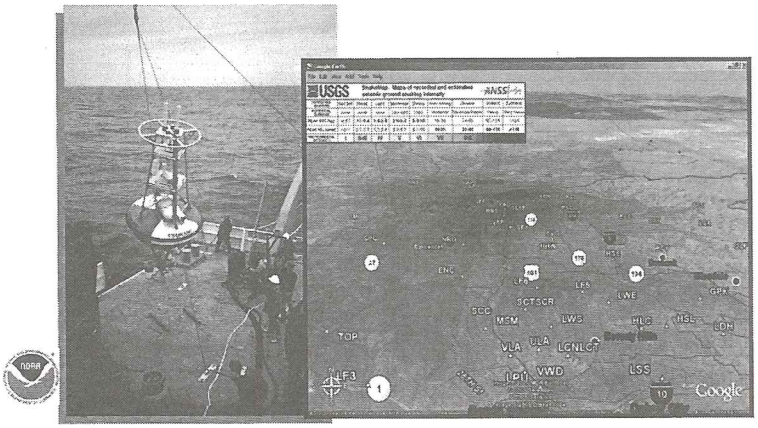

9

Grand Challenge #2 Understand the Natural Processes That Produce Hazards (improve forecasting and predictions, pursue basic research on the natural processes that produce hazards and understand how and when natural processes become hazardous).

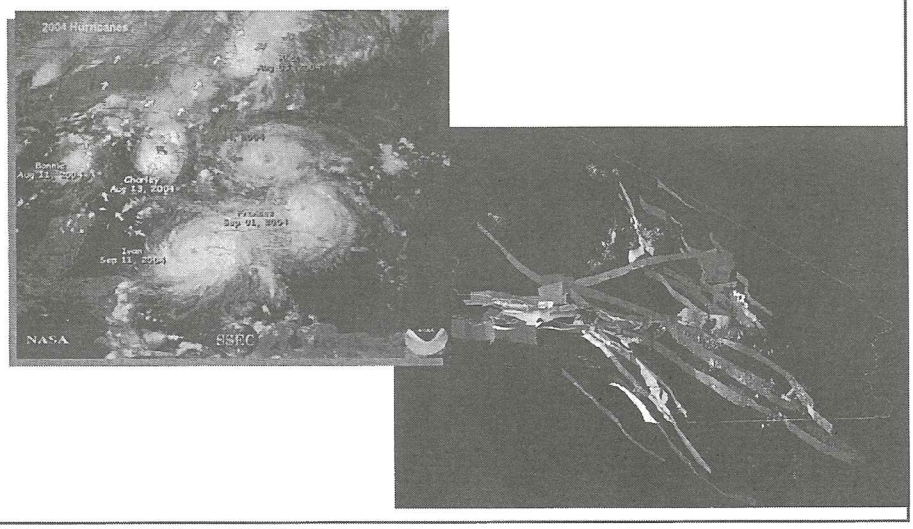

10

Grand Challenge #3 Develop Hazard Mitigation Strategies and Technologies (develop and implement cost effective hazard mitigation strategies including land-use planning and zoning laws that recognize the risks of natural hazards and disaster-resilient design and materials and smart-structures that respond to changing conditions).

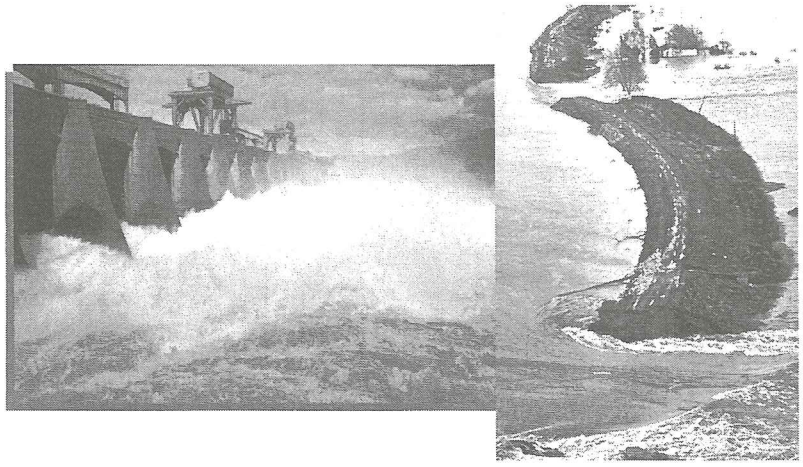

11

Grand Challenge #4 Recognize and Reduce Vulnerability of Interdependent Critical Infrastructure (identify and address the interdependencies of lifelines at a systems level, develop risk assessment tools to determine impacts of planned developments, rapidly assess public health conditions to minimize impact on the community).



12

Grand Challenge #5 Assess Disaster Resilience (collaborate with Federal, State, local agencies, academia, and the private sector to develop effective standards and metrics that assess disaster resilience, perform risk assessments for decision tools, develop 'Report Cards', assess impact of natural and technological hazards on the environment).



13

Grand Challenge #6 Promote Risk-Wise Behavior (effect communications, trust, and understanding within the community, bring about emergency communication systems, seek public response to hazards, facilitate research in social sciences to promote individual mitigation actions).

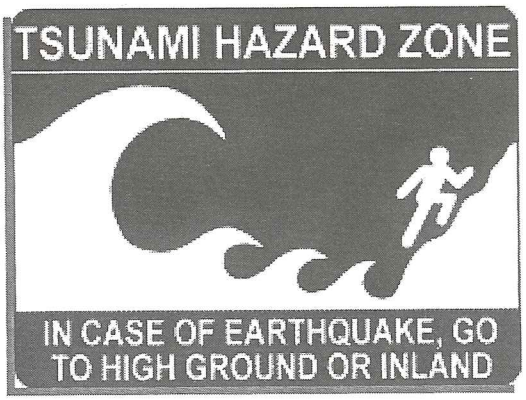

14

Implementing the Grand Challenges

The implementation strategy for the Grand Challenges are outlined in a series of documents describing the science and technology agenda for 15 hazards and cross-cutting topics:

- Coastal Inundation
- Drought
- Earthquake
- Environmental/Public Health Hazards
- Fire
- Flood
- Hurricane
- Infrastructure
- Landslide
- Natural Resource Impacts
- Space Weather
- Technological Hazards
- Tornado
- Volcano
- Winter Storms



15

S & T Agenda (Proposed Format)

Vision
Benefits

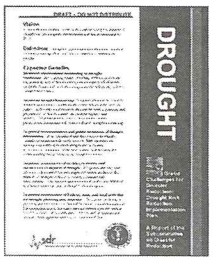

What's at Stake (definition, background, and impacts)

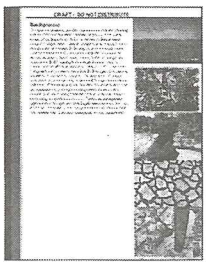

Grand Challenges

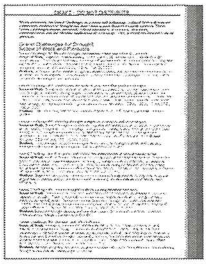

Implementation Actions

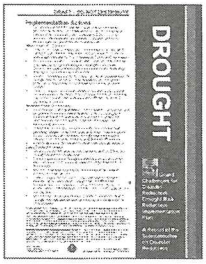

16

Vision and Benefits

- Defines enhancements to disaster resilience.
- Defines the hazard.
- Lists broad improvements in disaster reduction science and technology that will result from meeting the Grand Challenges for this hazard type.
- Describes major benefits.

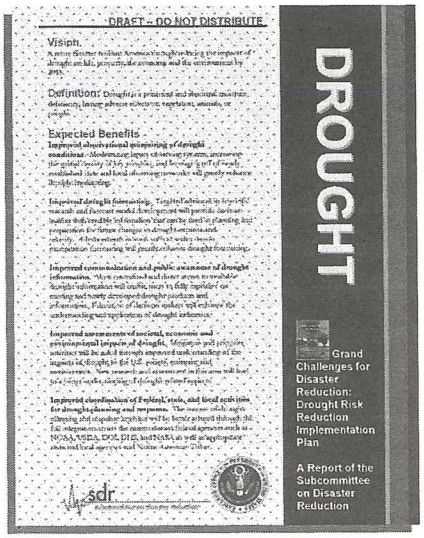

Background (What's at Stake)

- Background on impacts of the hazard including expected costs to the nation.

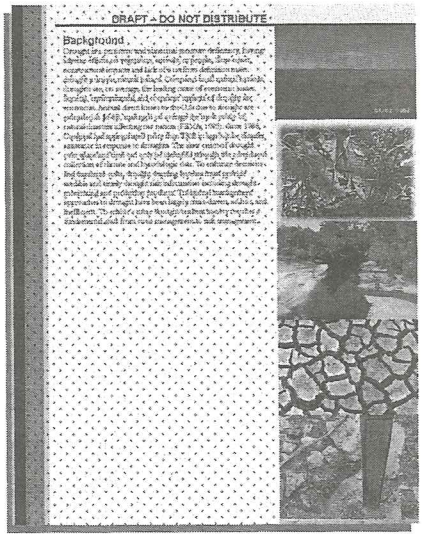

Grand Challenges

- Applies the six Grand Challenges published in June 2005 to the specific hazard described in the plan.
- Describes broad task areas included in each Challenge and products/technologies expected to result from meeting each Challenge. Includes a list of agencies responsible (primary and contributing).

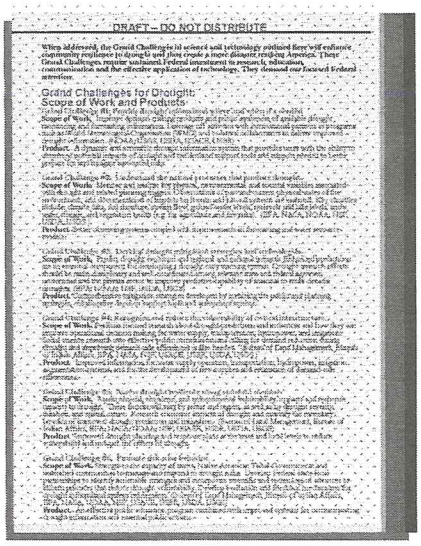
DRAFT – DO NOT DISTRIBUTE

Grand Challenges for Drought:
Scope of Work and Products

19

Implementation Actions

- Identifies **Short** (1-2 years), **Medium** (2-5) and **Long Term** (5+ years) actions.
- Brief description of actions needed to be performed by Federal, State, and local governments, the private sector, and academia to implement the Grand Challenges described in the plan.

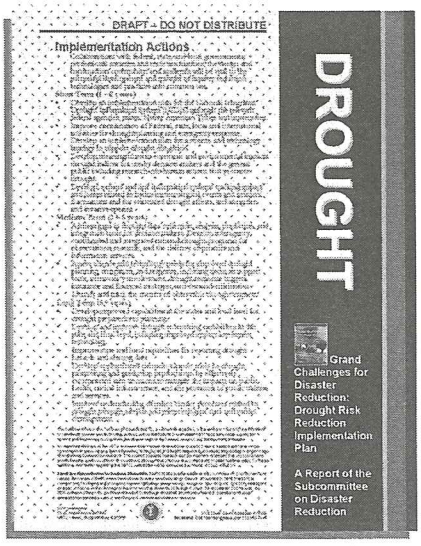

20

US Government Approval

GCs Implementation Strategies approval process (fall 2006 through spring 2007):

- 23 SDR Federal Member Agencies
- National Science and Technology Council
- Office of Science and Technology Policy
- Office of Management and Budget
- Other reviewers selected by the White House

21

More Information

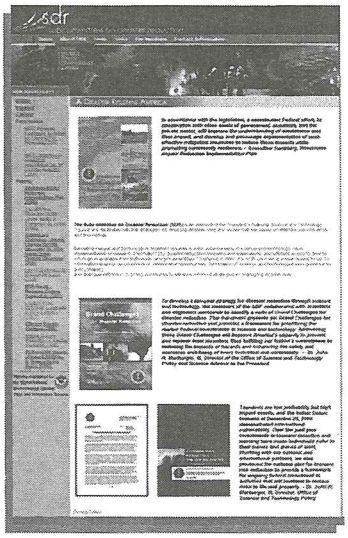

http://www.sdr.gov

22

Toward the Establishment of a Regional Society that is Safe and Secure from Disasters

by

Mochizuki Tsuneyoshi[1], NILIM "Safe and Secure" Project Team

ABSTRACT

Disaster protection measures that have been taken in Japan have primarily been individual measures such as construction of structures designed hypothesizing the external forces of each disaster and providing information during disasters etc. In recent years, the forms of natural disasters and the natural and social environments in which they occur have been transformed. This report presents policies guiding initiatives that should be taken in Japan based on our awareness that we must take comprehensive measures hypothesizing overall society and implement a PDCA based management cycle constantly focused on actual conditions in order to build a society that is safe and secure from natural disasters.

KEYWORDS: Evaluation Indices, Natural Disaster, PDCA Cycle, Safe and Secure Societies, Social Capital

1. INTRODUCTION

As a nation that has often suffered and recovered from natural disasters of many kinds, Japan has striven continuously to ensure its safety in numerous areas and bodies, contributing greatly to the safety of Japanese society.

But nearly every year, Japan continues to experience disasters that extract a heavy toll in human suffering and destruction of property, as it faces new phenomena impeding and restricting our efforts to ensure a safe and secure society.

Enhancing Japan's capacity to withstand dangerous phenomena and creating ways to construct a safe and secure society whose people can enjoy rich and high standard lives is our generation's mission, and we must deemphasize the pursuit of economic efficiency to begin working to create a safe and secure society as its top priority.

The Science Council of Japan established the "Committee to Construct the Foundations of a Society that is Safe and Secure From Global Scale Natural Disasters" in February 2006, and this committee is undertaking a study in response to an inquiry entitled "Effective Ways to Reduce Damage Caused by Changing Global Scale Natural Disasters (June 2006)" from the Ministry of Land, Infrastructure and Transport and plans to issue a report and response in May 2007.

Aware that, under these circumstances, instead of individual measures such as constructing facilities designed to deal with the external force of individual disasters and providing information in the event of a disaster as has been done until now, we must now undertake comprehensive initiatives guided by an overall vision of human society that permits the establishment of a society safe and secure from natural disasters including self-help and mutual support and that

[1] Director-General, National Institute for Land and Infrastructure Management

we must take measures premised on smooth restoration after a disaster has occurred, we have prepared a tentative plan that presents ways to achieve these goals in Japan.

2. PRESENT STATUS RELATED TO NATURAL DISASTERS

We must be fully aware of present problems that have appeared as a consequence of the great changes to the environment that are now occurring on a global scale so we can consider how to ensure a safe and secure society, and we must find ways to appropriately diagnose and prescribe curative measures for such scenarios to prevent people from needlessly feeling fear and anxiety about a variety of scenarios whose likelihood of occurring have not been clarified.
The following are noteworthy recent changes in the natural and social environments in Japan that we must consider.

(1) Growing power of dangerous phenomena
Frequent large-scale disasters occurring around the world are continuously presenting us with new forms of disasters that we must prepare for. In Japan we fear increasingly severe local meteorological events linked to global warming such as rising tides or more frequent and more severe torrential rainfall. We are also fearful that an intraplate earthquake directly under Tokyo or the Tokai, Tonankai, Nankai, or other devastating undersea earthquakes and the tsunami they would trigger will strike Japan in the near future.

(2) Decline of regional capacity to fight disasters
The aging, depopulation, and transformation of regional communities, the deterioration of their flood fighting squads and other social systems, the disappearance of empirical knowledge formerly handed down within the regions, the establishment of an urban residential consciousness isolated from nature, and other factors, have all contributed to the appearance of a deterioration of the disaster fighting capacity and the social capital that have been maintained by each region.

(3) The weakness inherent in the expansion, increasing sophistication, and rising complexity of urban systems
As urban systems expand, are concentrated, and become increasingly sophisticated and complex, these linked trends may contribute to an underlying weakening of a society's ability to withstand dangerous phenomena. This weakness might be revealed in the unstable behavior and collapse of individual systems under particularly unpredictable external forces, and in the chain reaction and radiating expansion of damage caused by the simultaneous collapse of such individual systems.

(4) Expanding weakness of infrastructure facilities and organizations etc.
We must strive to take measures, obtain resources, and train personnel needed to prevent the deterioration of the functions of disaster protection systems and disaster protection facilities from reducing safety, even from changing external conditions described above. We also face the challenge of training experts in disaster prevention and social infrastructure and of fighting the decline of regional industries that support their recovery from disasters.

3. BASIC CONDITIONS FOR REGIONAL SOCIETIES THAT ARE SAFE AND SECURE FROM DISASTERS

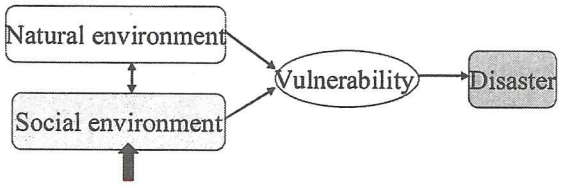

Image of a (region) society safe and secure from natural disasters

Figure 1. Vulnerability of the Environment and Natural Disasters

Natural disasters are related to vulnerability created by the interrelationship of the natural environment and the social environment (Fig. 1), although, as stated above, both have been undergoing major transformations in recent years.

The Intergovernmental Panel on Climate Change (IPCC) announced the fourth report of its First Working Group on February 2007. This report stated that the future rise of the sea level will be seriously impacted by changes in the ice-covered regions such as Greenland and Antarctica. The second Working Group report announced in April states that it is important to not only construct protection structures; but to also introduce wide area adaptations extending into the social and economic spheres.

Therefore, assuming that it is important to clarify the entire social environment that can be artificially controlled as an "image of regional societies safe and secure from natural disasters", with reference to the initiatives taken under the "Grand Challenges for Disaster Reduction" in the U.S., we have considered the directions of initiatives to be taken in Japan based on our fundamental awareness of the following issues.

□ Comprehensively establishing the essential conditions for a safe and secure society as those which, including public demands for their achievement, must be achieved by adopting a posture of exhaustively observing overall regional societies.

□ While creating a common awareness shared by related organizations of all kinds, establishing a process of constantly evolving and deepening bonds in response to actual conditions.

The first step is to list conditions that should be achieved, maintained, and encouraged as basic essential conditions to answer the question, "What is a society safe and secure from disasters?" As a result we have organized the four fields shown in Figure 2 (knowledge, social capital, information systems, and resistance to and ability to recover from disasters). Then, the specific contents of the fundamental essential conditions that have been categorized and organized in this way are explained, aware of each participant: individuals, companies, infrastructure related companies, disaster protection organizations. The details are presented in Reference 1.

Table 2 shows the results of abstracting and listing the activities that disaster protection organizations should undertake to achieve these essential conditions, and similarly categorizing and organizing them under four categories. Disaster protection organizations are not only municipalities and other organizations that bear direct responsibility for disaster protection, but research organizations who support these activities and other public bodies that manage and maintain infrastructure. Table 1 and Table 2 present the relationships between all items with codes. (For example, it is necessary for disaster protection organizations to continue to take activities a-1, a-2, and a-3 in order to achieve A-1.)

(1) Knowledge ---- Advance understanding

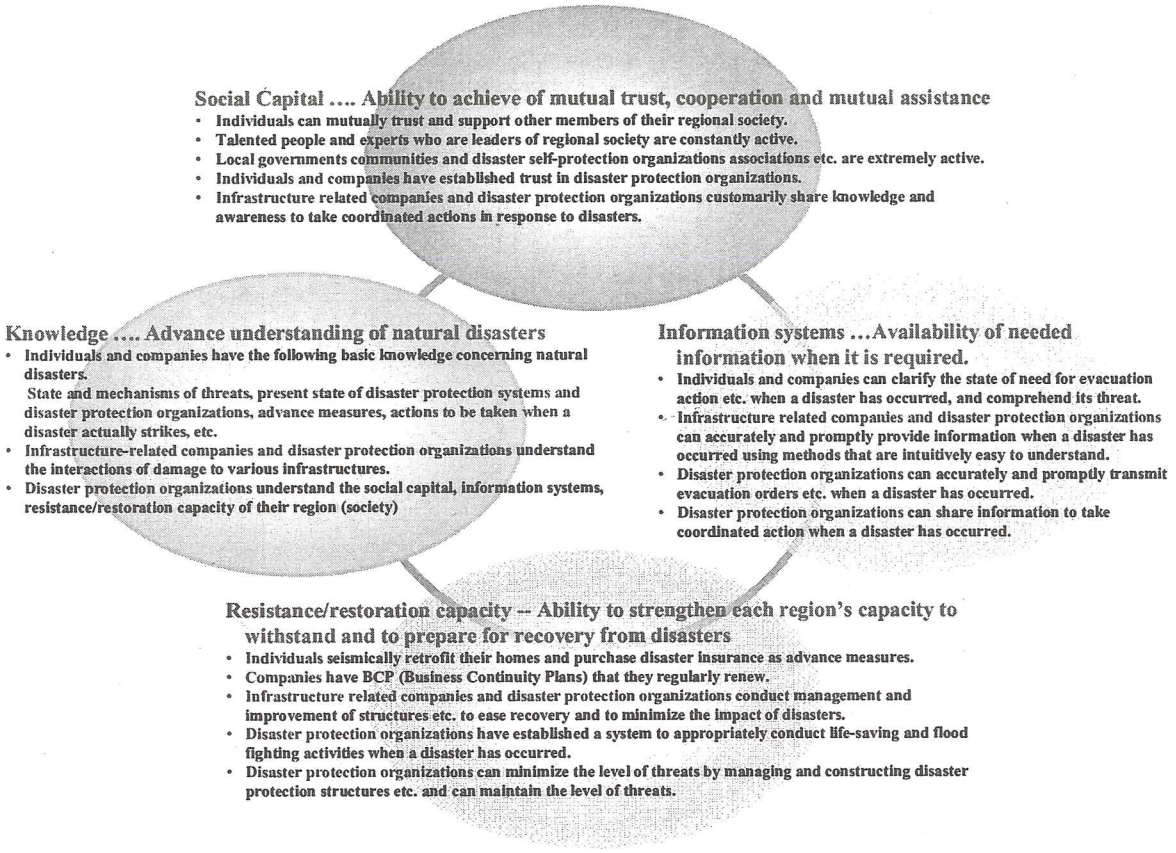

Figure 2. Image of a (Region) Society Safe and Secure from Natural Disasters

of natural disasters.

We assume that each body and organization has fundamental knowledge of natural disasters including the action that it should take in an emergency according to its own roles and responsibilities, and that it reflects this knowledge in its actions as a premise for the existence of a safe and secure society. Therefore, disaster protection organizations must continuously collect and analyze data concerning dangerous phenomena, the capacity of disaster protection facilities to withstand disasters, the mechanisms of the occurrence of dangerous phenomena, the impact of disasters on society and the economy, and crisis management and cost of damage.

(2) Social capital --- Possibility of mutual trust, cooperation and mutual assistance.

Social Capital is defined as, for example, "Characteristics of social organization featuring trust, norms, and networks that can increase the efficiency of a society by enlivening cooperative human activities" (Putnam, Quality of Life Policy Bureau, Prime Minister's Office), and we assume that it plays a particularly important role in increasing a region's disaster protection capacity.

It is necessary that in addition to residents of a region trusting and supporting each other, disaster protection organizations also earn the trust of residents by communicating with them and by providing them with easily understood information at all times, and that concerned organizations build trusting relationships.

(3) Information systems --- Availability of needed information when it is required.

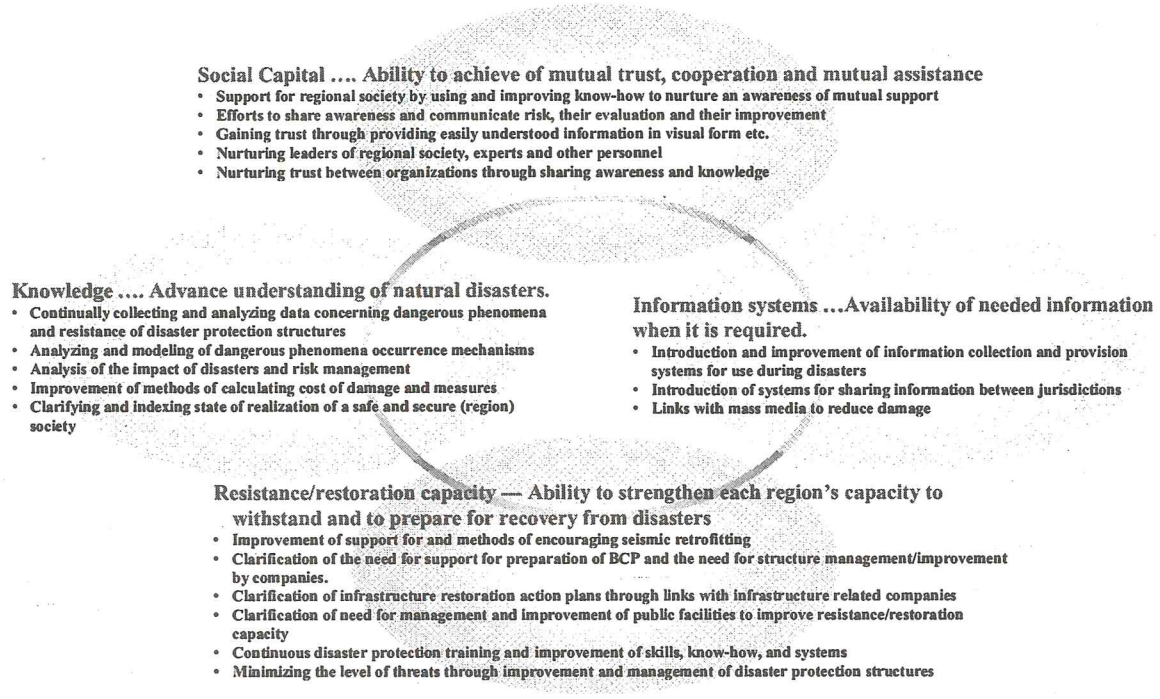

Figure 3. Actions that Disaster Protection Organizations Should Take toward Realization

When necessary, for example, a disaster has occurred, each body and organization must continually clarify constantly changing circumstances, understand the nature of its threat and take prompt and appropriate action in response. This means that disaster protection organizations must establish systems that, in addition to collecting and providing information, share information with other jurisdictions. It is also essential to build systems that enable members of the local media to fill their roles properly.

(4) Resistance to and ability to recover from disasters --- Ability to strengthen each region's capacity to withstand and to prepare for recovery from disasters

Organizations must constantly provide both non-physical and physical infrastructures that increase a region's capacity to withstand and to recover from disaster damage in order to lay the foundations for a regional society that is safe and secure from disasters. The provision and maintenance of disaster protection facilities and advance measures taken by both individuals and by companies that have been carried out in the past have been categorized as part of this category.

Concerning particularly large scale disasters, disaster protection organizations must recognize the importance of partially preventing the impact of such disasters and simplifying recovery, and continue to index and clarify the status of elements that should be considered in order to be able to take appropriate measures that combine physical and non-physical means to minimize the level of the threat to a level acceptable to society.

4. Action that disaster protection organizations should take and verification of each dangerous phenomenon

It is necessary for disaster protection organizations to take continuous initiatives to

achieve regional societies that are safe and secure from natural disasters. Figure 3 selects and lists actions that should be specifically taken and similarly categorizes these into four groups, and details are shown in Reference 2. Disaster protection organizations include, not only cities, towns, and villages and other organizations that are directly responsible for disaster protection but also research organizations that support their activities and public bodies that manage and construct infrastructures.

Actions that disaster protection organizations should take including research activities of the NILIM, are broken down for each dangerous phenomena regarding items in Reference 2, because the specific action that should be taken in response to each dangerous phenomenon such as flood, sediment-related disaster, or earthquake varies. This has been prepared by repeated brain storming by concerned members and by meetings to air and compare views with concerned research departments as a "Grand Framework" of research activities concerning disaster protection at the NILIM. In the future, we wish to conduct specific research activities in line with this framework and at the same time, to broaden the objects of dangerous phenomena and further evolve specific actions through the PDCA management cycle that is described below.

5. ESTABLISHMENT OF A MANAGEMENT CYCLE TO REALIZE SAFE AND SECURE REGIONAL SOCIETIES

The states that should be realized, maintained, and strengthened as the essential conditions for regional society safe and secure from natural disasters (Fig. 2), must be constantly clarified in each field and by each body, and their improvement must be undertaken by disaster protection organizations. This can be realized as a management cycle based on PDCA. (Fig. 4)
Table 1 shows the major contents of essential conditions for a regional society shown in Figure 2, by body. In this process, important roles of disaster protection organizations that they must fill are to constantly clarify conditions in four areas—knowledge, social capital, information systems, and resistance/restoration capacity —at each acting body. Reference 1 shows an example of evaluation indices to achieve this, but important future challenges are research and development of methods and evaluation indices to be applied to evaluate levels of knowledge, social capital, etc. that have a big impact on, for

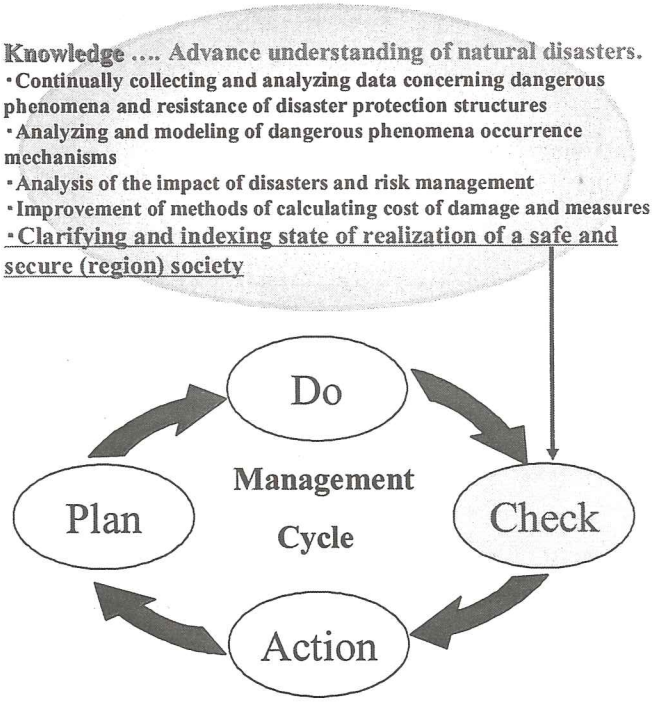

Figure 4. Management Cycle in Activities of Disaster Protection Organizations

example, people's evacuation action in the face of dangerous phenomena.

6. FUTURE INITIATIVES

These initiatives will, as their fundamental understanding, be implemented with constant reference to a process of continual evolution and deepening of relationships in response to actual situations through nurturing of a common awareness between concerned organizations of all kinds (Management cycle based on PDCA). So guided by an awareness that it is necessary to form links with concerned organizations centered on the Ministry of Land, Infrastructure and Transport, it includes policies concerning actions and initiatives that regional development bureaus take to approach other concerned organizations.

In the future, we will deepen and organize our discussions on the directions of initiatives taken to deal with each dangerous phenomenon discussed above and to promote projects in cooperation with other disaster protection related organizations, regional development bureaus and other concerned organizations in the field.

And we wish to advance this proposal based on actual conditions while repeating the PDCA cycle by selecting issues that are worth researching but have not been yet been studied at the NILIM, setting priorities, circulating technologies including those at regional development bureaus and other organizations in the field, training experts, and deepening links with concerned organizations.

7. REFERENCES

1. Grand Challenges for Disaster Reduction , Committee on Environment and Natural

Table 1. "Image of a Regional Society Safe and Secure from Natural Disasters" Categorized by Concerned Actor

	Advance understanding of natural disasters A [Knowledge]	Ability to achieve mutual trust, cooperation and mutual assistance B [Social capital]	Availability of needed information when it is required C [Information systems]	Ability to strengthen each region's capacity to withstand and to prepare for recovery from disasters D [Resistance/restoration capacity]
Individual/region	●Have basic knowledge of natural disasters and know what action to take when a disaster occurs	●Can trust and mutually assist other members of regional society ●Disaster protection leaders, experts etc. are constantly active ● Already trusts disaster protection organizations	● Can clarify state necessary for evacuation action and gain understanding when a disaster occurs.	● Seismically retrofit homes and purchase disaster insurance
Companies	●Have basic knowledge of natural disasters and know the social mission and roles of companies and industries when a disaster occurs	●Can take part in volunteer activities and provide assets, products etc. in its possession when a disaster occurs ● Already trusts disaster protection organizations	● Can clarify state necessary for implementation of BCP and gain understanding when a disaster occurs.	●Have and regularly revise BCP
Infrastructure related companies	●Have basic knowledge of natural disasters and know the process of interaction of damage to infrastructures	● Already shares knowledge and awareness with infrastructure related companies and can take coordinated action when a disaster occurs.	● Can clarify the situation from moment to moment and provide information using intuitive easily understood methods when a disaster occurs.	●Have and regularly revise BCP to restore infrastructure ●Can manage and improve structures to ease restoration and to minimize damage by disasters
Disaster protection organizations	●Have basic knowledge of natural disasters and know the process of interaction of damage to infrastructures ●Have knowledge of the (region) society and can clarify its social capital, information and resistance/restoration capacity.	● Already shares knowledge and awareness with infrastructure related companies and disaster protection organizations, and can take coordinated action when a disaster occurs.	● Can clarify the situation from moment to moment and provide information and order evacuations using intuitive easily understood methods when a disaster occurs. ● Can share information that constantly changes with disaster protection organizations and take coordinated action when a disaster occurs.	●Have and regularly revise COOP to restore infrastructure ● Have established a system permitting appropriate life saving and flood fighting activities when a disaster has occurred ●Can manage and improve disaster protection structures etc. to minimize the level of threat of flooding and can maintain the level of threat.

Checked by disaster protection organizations based on appropriate evaluation indices.....PDCA cycle to achieve safe and secure region (society)

Resources , National Science and Technology Council , June 2005
2. Report by the Committee on Science and Technology Policies to Contribute to the Building of a Safe and secure Society , Ministry of Education, Culture, Sports, Science and Technology , April 2004
3. Junko Mimaki, Ryou Fujikura , Research on Improvement of Disaster Protection Projects in International Aid,,, Based on Cases Concerning Factors Improving Regional Disaster Protection Capabilities , International Development Research , June 2006

Reference-1

Image of a (Region) Society Safe And Secure From Disasters (Proposed)

Individuals

	Advance understanding of natural disasters A [Knowledge]	Possibility of mutual trust, cooperation and mutual assistance B [Social capital]	Availability of needed information when it is required C [Information systems]	Ability to strengthen each region's capacity to withstand and to prepare for recovery from disasters D [Resistance/restoration capacity]
State that should be achieved, maintained, and advanced	● **[A-1 Basic knowledge of natural disasters]** Individuals already possess the following as basic knowledge about natural disasters. ・ True state of threats and nearby dangerous locations ・ Mechanisms and precursor phenomena ・ Present state of and future prospects for disaster facilities and disaster protection organizations ・ Present state and future prospects of threats ・ Advance measures ・ Contents of (initial period) activities (including cooperation and mutual aid) ・ Post disaster measures etc.	● **[B-1 Trust and mutual support]** Individuals can trust and mutually support others in the regional society regarding the following matters. ・ Giving and receiving knowledge of natural disasters ・ Taking advance measures ・ Giving and receiving information during a disaster ・ Acting during a disaster ・ Supporting people who require assistance ・ Taking post-disaster measures etc. ● **[B-2 Daily activities and existence of leaders]** Municipal government and voluntary disaster protection organizations that have been formed by individuals are normally highly active and their members include leaders and experts. ● **[B-3 Contributing to society]** Individuals and companies can volunteer energetically, or can voluntarily and smoothly supply resources or products they possess when a disaster occurs. ● **[B-4 Disaster protection organizations earning people's trust]** Individuals and companies trust disaster protection organizations regarding the following matters. ・ Contents of knowledge concerning natural disasters that has been provided ・ Provision of information contributing to action when a disaster occurs and contents of this information ・ Maintaining and improving capacity to withstand and to recover from disasters by appropriately managing and improving disaster protection facilities.	● **[C-1 Clarifying present state of threats]** Individuals can clarify constantly changing conditions and understand the threat related to the following actions without being confused by rumors when a disaster has occurred. ・ Measures immediately before a disaster ・ Evacuation ・ Deployment and returning home ・ Support activities (volunteers) etc.	● **[D-1 Advance measures by individuals]** Individuals take the following actions as advance measures ・ Seismic diagnosis and seismic retrofitting of homes ・ Preparing goods necessary during disasters ・ Planning the details of actions during disasters ・ Purchasing disaster insurance, etc.
Evaluation indices (proposed)	●Participation rate in disaster protection WS etc. ●Participation rate in regional disaster protection training etc. ●Awareness of hazard maps ●State of evacuation in response to dangerous phenomena	●Percentage of people requiring care covered by a support system based on mutual assistance ●Percentage of existence of disaster protection leaders in local administrations ●Percentage of members participating in volunteer activities in local administration etc. ●Degree of trust in disaster protection organizations (questionnaire surveys etc.)	● State of acquisition of information when a disaster occurs	● Percentage of homes receiving seismic diagnosis and seismic retrofitting ● Disaster insurance purchase rate

Companies

	Advance understanding of natural disasters A [Knowledge]	Possibility of mutual trust, cooperation and mutual assistance B [Social capital]	Availability of needed information when it is required C [Information systems]	Ability to strengthen each region's capacity to withstand and to prepare for recovery from disasters D [Resistance/restoration capacity]
State that should be achieved, maintained, and advanced	● **[A-2 Basic knowledge of natural disasters]** In addition to the above items concerning all kinds of natural disasters, companies know the following from the perspective of companies and industries. ・ True state of threats and nearby dangerous locations ・ Mechanisms and precursor phenomena ・ Present state of and future prospects for disaster facilities and disaster protection organizations ・ Present state and future prospects of threats ・ Advance measures ・ Contents of (initial period) activities (including cooperation and mutual aid) ・ Post disaster measures etc. ・ Social mission and roles of companies and industries when disasters occur ・ Danger with potential impact on society (storage of hazardous materials etc.)	● **[B-3 Contributing to society]** Individuals and companies can volunteer energetically, or can voluntarily and smoothly supply resources or products they possess when a disaster occurs. ● **[B-4 Disaster protection organizations earning people's trust]** Individuals and companies trust disaster protection organizations regarding the following matters. ・ Contents of knowledge concerning natural disasters that has been provided ・ Provision of information contributing to action when a disaster occurs and contents of this information Maintaining and improving capacity to withstand and to recover from disasters by appropriately managing and improving disaster protection facilities.	● **[C-2 Clarifying present state of threats]** Corporations can understand and clarify the present situation and threats as necessary to take action based on BCP during a disaster.	● **[D-2 Advance measures by corporations and industry related organizations]** Companies have BCP and carry out successive reforms and work regularly to move or concentrate facilities that are in danger or to improve their disaster protection functions.
Evaluation indices (proposed)	● Participation rate in regional disaster protection training etc. ● State of recording in BCP of details of support for regions when a disaster occurs	● State of support for regions when a disaster occurs (percentage of supporting companies) ● State of holding consultative meetings including disaster protection organizations	● Obtaining needed information when a disaster occurs	● State of enactment of BCP

Infrastructure related companies

	Advance understanding of natural disasters A [Knowledge]	Possibility of mutual trust, cooperation and mutual assistance B [Social capital]	Availability of needed information when it is required C [Information systems]	Ability to strengthen each region's capacity to withstand and to prepare for recovery from disasters D [Resistance/restoration capacity]
State that should be achieved, maintained, and advanced	● **[A-3. Basic knowledge of natural disasters]** Infrastructure related companies and disaster protection organizations are already aware of the above items related to natural disasters from various perspectives, and also know about the following from various perspectives ・ True state of threats and nearby dangerous locations ・ Mechanisms and precursor phenomena ・ Present state of and future prospects for disaster facilities and disaster protection organizations ・ Present state and future prospects of threats ・ Advance measures ・ Contents of (initial period) activities (including cooperation and mutual aid) ・ Post disaster measures etc. ・ Social mission and roles of companies and industries when disasters occur ・ Danger with potential impact on society (storage of hazardous materials etc.) ・ Process of mutual impact between damage to various infrastructure elements	● **[B-5 Sharing information and cooperative action]** Infrastructure companies and disaster protection organizations already share knowledge, information and experiences, and maintain links enabling them to mutually supplement each other's efforts when a disaster occurs.	● **[C-3 Providing information to take appropriate action]** Concerning actions of individuals, companies, and industry related organizations during a disaster, infrastructure related companies and disaster prevention organizations can clarify constantly changing conditions and can reliably and promptly provide information that can be applied to appropriate action using methods that make it easily understood visually and through other senses.	● **[D-3 Improving capacity to reduce or restore damage]** Infrastructure related companies and disaster prevention organizations make the following preparations (improving damage reduction capacity) concerning restoration or reconstruction. ・ Setting infrastructure restoration priority ・ Ensuring human resources, materials and equipment necessary for restoration ・ Managing and improving facilities etc. in order to simplify restoration and restrict the impact of disasters. etc.
Evaluation indices (proposed)	● State of hypothesis of the process of mutual impact in BCP	● State of signing agreements between infrastructure related companies ● State of holding consultative meetings including disaster protection organizations	● Rate of provision of systems to provide information to individuals and companies ● Comprehensibility, through visual methods etc., of information provided	● State of enactment of BCP ● State of response to items recorded above in BCP

Disaster protection organizations

	Advance understanding of natural disasters A [Knowledge]	Possibility of mutual trust, cooperation and mutual assistance B [Social capital]	Availability of needed information when it is required C [Information systems]	Ability to strengthen each region's capacity to withstand and to prepare for recovery from disasters D [Resistance/restoration capacity]
State that should be achieved, maintained, and advanced	● **[A-3. Basic knowledge of natural disasters]** Infrastructure related companies and disaster protection organizations are already aware of the above items related to natural disasters from various perspectives, and also know about the following from various perspectives ・ True state of threats and nearby dangerous locations ・ Mechanisms and precursor phenomena ・ Present state of and future prospects for disaster facilities and disaster protection organizations ・ Present state and future prospects of threats ・ Advance measures ・ Contents of (initial period) activities (including cooperation and mutual aid) ・ Post disaster measures etc. ・ Social mission and roles of companies and industries when disasters occur ・ Danger with potential impact on society (storage of hazardous materials etc.) ・ Process of mutual impact between damage to various infrastructure elements ● **[A-4 State of (region) society and impact of damage]** Disaster protection organizations already know about the following. ・ Individuals, companies, infrastructure related companies and disaster protection organizations respectively, already known present status of Knowledge, Social capital, Information systems, Resistance to and ability to recover from damage. Type and degree of impact of disasters on human lives, society, and the economy in various regions etc.	● **[B-5 Sharing information and cooperative action]** Infrastructure companies and disaster protection organizations already share knowledge, information and experiences, and maintain links enabling them to mutually supplement each other's efforts when a disaster occurs.	● **[C-3 Providing information to take appropriate action]** Concerning actions of individuals, companies, and industry related organizations during a disaster, infrastructure related companies and disaster prevention organizations can clarify constantly changing conditions and can reliably and promptly provide information that can be applied to appropriate action using methods that make it easily understood visually and through other senses. ● **[C-4 Transmitting evacuation orders and instructions and confirmations]** Disaster protection organizations can reliably and promptly transmit, in addition to the above items, evacuation orders to protect human lives, instructions and confirmations etc. based on disaster protection agreements to individuals, companies, and industry related organizations during a disaster. ● **[C-5 Sharing information between disaster protection organizations]** Disaster protection organizations can share knowledge and information to take unified action during a disaster.	● **[D-3 Improving capacity to reduce or restore damage]** Infrastructure related companies and disaster prevention organizations make the following preparations (improving damage reduction capacity) concerning restoration or reconstruction. ・ Setting infrastructure restoration priority ・ Ensuring human resources, materials and equipment necessary for restoration ・ Managing and improving facilities etc. in order to simplify restoration and restrict the impact of disasters. etc. ● **[D-4 Improving emergency aid and support capacities]** Disaster prevention organizations can appropriately take actions such as the following to reduce damage during a disaster. ・ Flood fighting ・ Live saving ・ Helping victims ・ Supporting restoration ● **[D-5 Managing and improving disaster protection facilities etc.]** Disaster protection organizations can minimize the level of threats to a level acceptable to a (region) society and maintain this state by preventive preliminary conservation measures such as management and improvement of disaster prevention facilities.
Evaluation indices (proposed)	● Coverage rate and contents of hazard maps ● Clarification rate of state of disaster protection structures and percentage added to date base ● State of knowledge, social capital, information systems, resistance/restoration capacity	● State of holding consultative meetings between companies and disaster protection organizations	● Rate of provision of systems to provide information and evacuation orders to individuals and companies ● Rate of provision of systems for sharing of information among disaster protection organizations	● State of enactment of COOP ● Performance of countermeasure headquarters and fire fighting activities etc. to deal with dangerous phenomena ● Rate of achievement of management and improvement levels of disaster protection structures

Reference-2

State of Action by Disaster Protection Organizations to Achieve Goals (Draft)

	Advance understanding of natural disasters A [Knowledge]	**Possibility of mutual trust, cooperation and mutual assistance** B [Social capital]	**Availability of needed information when it is required** C [Information systems]	**Ability to strengthen each region's capacity to withstand and to prepare for recovery from disasters** D [Resistance/restoration capacity]
State that should be achieved, maintained, and advanced	● **[a-1 Dangerous phenomena and capacity of disaster protection facilities to withstand them]** Data concerning dangerous phenomena and capacity of disaster protection facilities to withstand dangerous phenomena (including degree of deterioration) are obtained by an appropriate monitoring system, and these data are saved and analyzed so that necessary data can be extracted when it is needed. ● **[a-2 Dangerous phenomena occurrence mechanisms]** Dangerous phenomena occurrence mechanisms are analyzed and appropriately modeled to improve the precision of predictions. ● **[a-3 Impact of disasters and crisis management]** Standard analysis methods are available to deal with the impacts of disasters and to perform crisis management when a disaster occurs and used to continuously accumulate experiences such as the following. ・ Process of the mutual impact of damage to infrastructure elements. ・ Process that impacts human lives, society, and the economy ・ Expertise in individual advance measures, details of actions during disasters and post disaster measures ・ Details of actions by companies during disasters and their roles in restoration. ・ Expertise and effective systems for performing crisis management by disaster protection organizations	● **[b-1 Cultivating awareness of mutual aid]** Expertise and tools (hazard maps etc.) that nurture mutual aid awareness and are applied to practice mutual aid during disasters are available, evaluated, their effectiveness is continuously improved and they are used to support the (region) society. ● **[b-2 Obtaining trust through communications]** Two-way communication with individuals, companies, industries, NPO organizations and infrastructure related companies is maintained by providing and explaining knowledge and exchanging opinions concerning natural disasters regularly or when necessary, taking part in joint disaster protection training, and making agreements to provide assets or products during disasters. ● **[b-3 Gaining trust by providing easily understood information]** Tools permitting intuitive understanding of the state of predicted threats (visual) are available, they are continuously evaluated, their effectiveness is improved and they are applied (including overseas). ● **[b-4 Cultivating leaders, experts etc.]** Adequate numbers of personnel such as leaders, experts, NPO etc. usable by every regional society are cultivated continuously.	● **[c-1 Information collection systems]** Systems that promptly and reliably clarify the state of threats that constantly change during disasters and actions taken by individuals, companies, and industry related organizations are available and are continuously improved by accumulating experiences of actual disasters. ● **[c-2 Information provision systems]** Systems that can reliably (including multiple routes that function during power failures) and promptly transmit the state of threats that continuously change during a disaster, evacuation orders etc., are provided and continuously improved by accumulating experiences of actual disasters. ● **[c-3 System for sharing information between jurisdictions]** In order to reliably and promptly make judgments and to transmit information to the public and perform restoration activities during a disaster, disaster protection organizations and infrastructures related companies possess systems that share information between jurisdictions.	● **[d-1 Support for advance measures by individuals]** For supporting advance measures by individuals and procedures for promoting seismic retrofitting are provided and are constantly improved. ● **[d-2 Support for BCP etc. of corporations]** To support the preparation of BCP of corporations and industry related organizations, knowledge and opinions are regularly exchanged and the need for facility management and improvement reflecting these views is clarified. ● **[d-3 Support for the restoration of infrastructures etc.]** By regularly exchanging views with infrastructure related companies and by accumulating experience of actual disasters, the need for execution planning to restore infrastructure is clarified. ● **[d-4 Managing and improving public facilities]** The need for management and improvement of public facilities such as disaster protection facilities or roads to simplify restoration and restrict the impact of disasters etc. is clarified. ● **[d-5 Improving countermeasure headquarters and other systems]** Skills, expertise, and systems are continuously improved by continuing disaster protection training and accumulating experience of actual disasters.

	Advance understanding of natural disasters A [Knowledge]	**Possibility of mutual trust, cooperation and mutual assistance** B [Social capital]	**Availability of needed information when it is required** C [Information systems]	**Ability to strengthen each region's capacity to withstand and to prepare for recovery from disasters** D [[Resistance/restoration capacity]
State that should be achieved, maintained, and advanced	● **[a-4 Cost of disasters]** Methods of calculating the costs of disasters and countermeasures are continuously improved. ● **[a-5 State of (region) society]** The present status of, "states that should be achieved, maintained, and improved" in each (region) society are continually indexed and clarified.	● **[b-5 Cultivating trust between infrastructure related companies and disaster prevention organizations]** Systems to share knowledge and information between infrastructure related companies and disaster protection organizations are established and used continuously to carry out two-way communications by, for example, constantly exchanging views.	● **[c-4 Contribution of the mass media]** Toward proper evacuations and damage mitigation by providing appropriate information from the mass media, agreements necessary to regularly exchange knowledge and information, and distributing images are arranged involving the local mass media.	● **[d-6 Level of improvement of disaster protection facilities]** Elements that should be considered regarding the minimization of the level of threat to an acceptable level are continuously indexed and clarified to manage and improve disaster protection facilities. ● **[d-7 Technological improvements]** Technological improvements including the material used to strengthen structures and buildings etc. against natural disasters are made continuously. ● **[d-8 Clarifying regional conditions]** The state of support according to regional conditions, such as the housing conditions of people who may be isolated or may have difficulty evacuating during a disaster are clarified to make advance study of measures necessary. ● **[d-9 Land use and population distribution]** Measures to rationalize land use and population distribution are taken continuously in order to restrict damage and to simplify restoration

STATE OF THE ART REVIEW FOR SUSTAINABLE BUILDING DESIGN AND INNOVATION TECHNOLOGIES

William E. Roper
George Mason University, Fairfax, Virginia

Abstract
The design, construction, or renovation of high-performance sustainable buildings requires careful consideration during the planning, design, construction, renovation and operation phases of the buildings life. This evaluation examines the integration of all building components and systems to determine how they best work together in a sustainable manor to save energy, reduce environment impact and provide a quality indoor environment for occupants. Components of the building process are evaluated for the planning and design process, the construction process, and operations and maintenance of buildings. Specific sustainable practices for storm water management and water efficiency are described. Economic benefits and cost analysis methods for sustainable buildings are described. Four examples of sustainable building design applications are presented from the United States and Europe. Recommendations for furthering the development of high performance sustainable buildings are presented.

Key Words: Sustainable development, energy conservation, water management, green materials, design integration, recycling, life cycle analysis and construction waste management

1. Introduction

Buildings fundamentally impact people's lives and the health of the planet. In the U.S., buildings use one third of our total energy, two-thirds of our electricity, one-eighth of our water, and transform land that provides valuable ecological services. Building atmospheric emissions from the use of energy lead to acid rain, ground-level ozone, smog, and global climate change. The goal of sustainable design is to create high-performance buildings with a small environmental footprint. This goal has evolved from a variety of concerns, experiences, and needs.....

- Energy efficiency gained importance during the 1970s oil crisis.
- Recycling efforts in the U.S. in the 1970s onward became commonplace and came to the attention of the building industry.
- In the 1980s, the "sick building syndrome" concept emerged and concern for worker health and productivity became an issue. The concern for toxic material emissions also became an issue that needed to be addressed.
- Projects in water-scarce areas began to focus on water conservation.
- Early green designs usually focused on one issue at a time, mainly energy efficiency or use of recycled materials.
- Green building architects in the 1980s and 1990s began to realize that the integration of all the factors mentioned here would produce the best results and, in essence, a "high performance" building.

The designing, constructing, or renovating of high-performance sustainable buildings requires a whole building approach. This approach differs from the traditional design/build process, as the design team examines the integration of all building components and systems and determines how they best work together in a sustainable manor to save energy and reduce environmental impact.

2. Sustainable Design of Buildings

Sustainable buildings are intended though out their life time to have a beneficial impact on their occupants and their surrounding environment. Such buildings are optimally integrated on all parameters— initial affordability, timeliness of completion, net life-cycle cost, durability, functionality for programs and persons, health, safety, accessibility,

aesthetic and urban design, maintainability, energy efficiency, and environmental sustainability. Failure on any one parameter invariably undermines other parameters of the building in question and of the system of buildings and connected service systems in the community. The benefits of sustainable design can be summarized as follows:

- The local and global environment benefits from protecting air quality, water quality, and overall biodiversity and ecosystem health.
- Economic benefits are experienced in building operations, asset value, worker productivity, and the local economy.
- Occupants benefit from health and safety features. This also relates to risk management and economics. The U.S. EPA found that average Americans spend more than 90% of their time indoors, and indoor air quality can be two to five times worse than outdoor air quality.
- Community and municipal benefits include: lessened demand for large-scale infrastructure such as landfills, water supply, stormwater sewers, and their related development and operational costs; and decreased transportation development and maintenance burden (roads) and increased economic performance of mass transit systems.

There is a good deal of uncertainty about the cost of sustainable building features. This is probably due to seven main factors: 1) compared to design and construction cost-estimating generally, environmentally sustainable cost-estimating is a relatively new field with a smaller data base; 2) there are regional cost differences, driven by local abundance/scarcity of LEED certified professionals, and as a result designers and construction contractors bid higher when they don't understand the project; 3) there are regional differences in the availability and cost of environmentally-friendly materials; 4) as discussed below, costs go up when environmental sustainability is not included at the very start of the building planning and design process; 5) as also discussed below, costs go up, for both construction and maintenance, when key stakeholders are not trained in environmentally sustainable building features; 6) upfront vs. life-cycle cost tension; and 7) uncertainty about the short- and long-term performance of "green" sustainable building materials.

Urban areas have some unique challenges that generate particular environmental issues such as; Storm water Runoff, Air Quality, Heat Island effects, Traffic and Parking problems, the need for Open Space and Recreation, creation of Urban Villages (walk-ability, live-work, quality of life), and a good quality Indoor Environment (90% of our time is indoors).

3. Integrated Building Planning and Design Process.

A critical element for a successful sustainable building policy and program is an integrated building planning and design process. Integrated building design is a process of design in which multiple disciplines and seemingly unrelated aspects of design are integrated in a manner that permits synergistic benefits to be realized. The goal is to achieve high performance and multiple benefits at a lower cost than the total for all the components combined. This process often includes integrating green design strategies into conventional design criteria for building form, function, performance, and cost. A key to successful integrated building design is the participation of people from different specialties of design: general architecture, HVAC, lighting and electrical, interior design, and landscape design. By working together at key points in the design process, these participants can often identify highly attractive solutions to design needs that would otherwise not be found. In an integrated design approach, the mechanical engineer will calculate energy use and cost very early in the design, informing designers of the energy-use implications of building orientation, configuration, fenestration, mechanical systems, and lighting options.

Consider integrated building design strategies for all aspects of sustainable design: improving energy efficiency, planning a sustainable site, safeguarding water, creating healthy indoor

environments, and using environmentally preferable materials. Major design issues should be considered by all members of the design team—from civil engineers to interior designers—who have common goals that were set in the building program. The procurement of A&E services should stress a team-building approach, and provisions for integrated design should be clearly presented in the statement of work (SOW). For example, the SOW should stipulate frequent meetings and a significant level of effort from mechanical engineers to evaluate design options.

The design and analysis process for developing integrated building designs includes:

- Establishing a base case—for example, a performance profile showing energy use and costs for a typical facility that complies with code and other measures for the project type, location, size, etc.
- Identifying a range of solutions—all those that appear to have potential for the specific project.
- Evaluating the performance of individual strategies—one by one through sensitivity analysis or a process of elimination parametrics
- Grouping strategies that are high performers into different combinations to evaluate performance.
- Selecting strategies, refining the design, and reiterating the analysis throughout the process.

Finding the right building design recipes through an integrated design process can be challenging. At first, design teams often make incremental changes that are effective and result in high-performance buildings—and often at affordable costs. However, continuing to explore design integration opportunities can sometimes yield incredible results, in which the design team breaks through the cost barrier.

Whenever one sustainable design strategy can provide more than one benefit, there is a potential for design integration. For example, windows can be highly cost-effective even when they are designed and placed to provide the multiple benefits of daylight, passive solar heating, summer-heat-gain avoidance, natural ventilation, and an attractive view. A double-loaded central corridor, common in historic buildings, provides daylight and natural ventilation to each room, and transom windows above doors provide lower levels of light and ventilation to corridors. Building envelope and lighting design strategies that significantly reduce HVAC system requirements can have remarkable results. Sometimes the most effective solutions also have the lowest construction costs, especially when they are part of an integrated design.

The building design begins with an analysis of the required spaces. With an eye toward the sustainability and energy-efficiency targets established in pre-design, the individual spaces should be clearly described in terms of their function, occupancy and use, daylight and electric light requirements, indoor environmental quality standards, acoustic isolation needs, and so on. Spaces then can be clustered by similar function, common thermal zoning, need for daylight or connection to outdoors, need for privacy or security, or other relevant criteria.

It is not only environmental performance that suffers from lack of an integrated planning and design process. All the other building parameters also suffer (initial affordability, timeliness of completion, net life-cycle cost, durability, functionality for programs and persons, health, safety, accessibility, social equity, aesthetic and urban design, maintainability, and energy efficiency). Integrated Design and construction practices that significantly reduce or eliminate the negative impact of buildings on the environment and occupants may be organized into five broad areas:

- Sustainable site planning
- Safeguarding water and water efficiency
- Energy efficiency and renewable energy
- Conservation of materials and resources
- Indoor environmental quality

An integrated building planning and design process must insure that all the stakeholders are present throughout the planning and design process, even into the construction phase. Failure to do so inevitably results in delays, change orders, higher costs, and inferior buildings. In some cases, community representatives should be brought into appropriate phases of the planning and design process.

4. Economic Benefits and Cost Analysis

Sustainable buildings can reduce project costs. Green Sustainable Building projects that are well integrated and are comprehensive in scope can result in lower or neutral project development costs. Rehabilitating an existing building can lower infrastructure and materials costs. Integrated design can use the payback from some strategies to pay for others. Energy-efficient building envelopes can reduce equipment needs – downsizing some equipment, such as chillers, or eliminating equipment, such as perimeter heating. Using pervious paving and other runoff prevention strategies can reduce the size and cost of stormwater management structures.

Economic benefits of sustainable buildings include a competitive first cost. The concept of integrated design allows for high benefit at low cost by achieving synergies between disciplines and between technologies. Sustainable Designs lead to reduced utility bills and O&M costs. Sustainable design also will optimize life cycle economic performance and reduce liabilities. Energy and water-efficient buildings have been able to reduce their operating costs significantly. Use can be cut to less than half than that of a traditional building, or even better, by employing aggressive and well-integrated green design concepts.

Disagreements about costs focus on two central issues: 1) whether environmentally sustainable buildings require an up-front design and construction premium, and if so how large; 2) how the life-cycle costs of environmentally sustainable buildings compare with those of other buildings.

Healthy indoor environments can increase employee productivity according to an increasing number of case studies. Since workers are by far the largest expense for most companies (for offices, salaries are 72 times higher than energy costs, and they account for 92% of the life-cycle cost of a building), this has a tremendous effect on overall costs (See *Green Developments* by the Rocky Mountain Institute for more information).

Studies have shown that student performance, as well as energy performance, is better in schools built according to green design principles. More than 17 million Americans suffer from asthma, and 4.8 million of them are children. Ten million school days are missed by children each year because of asthma, which is exacerbated by poor IAQ. Employees in buildings with healthy interiors have less absenteeism and tend to stay in their jobs. The Internationale Nederlanden (ING) Bank headquarters in Amsterdam uses only 10% of the energy of its predecessor and has cut worker absenteeism by 15%. The combined savings equal $3.4 million per year.

4.1 Cost Analysis

Since there will usually be a number of acceptable suitable design alternatives for any project, cost/benefit analyses help you select the ones that have the best savings potential.

- Simple Payback Analysis
- Standardized Payback Equations
- Life-Cycle Cost Analysis
- Selecting the "Best" Alternatives
- Weighing Societal Impacts

Depending on the aggressiveness of the design, experience has shown that it costs no more than 10% more to build high-performance buildings. Some high-performance buildings cost less to construct. Sometimes additional upfront costs can be justified because the investment will reduce operating costs through the life of the building. The added cost, if any, of system investment each year is compared to the cost of fuel saved each year. Total energy costs are, on average, about 50% less than those for conventionally designed buildings. In many cases, the right-sizing of mechanical systems

through passive solar design offsets the costs for additional windows or controls.

In analyzing alternative building energy efficiency improvements, conversions, or purchases, cost/benefit analysis is used to determine if and when an improvement will pay for itself through energy savings, and to set priorities among alternative improvement projects. Cost/benefit analyses may be conducted using a simple payback analysis or a more sophisticated analysis of total life-cycle costs and savings. Since most electric utility rate schedules are based on both consumption and peak demand, your analyst should be skilled at assessing the impacts of both.

Before beginning any cost/benefit analyses, you must first determine acceptable design alternatives that can meet the heating, cooling, lighting, and control requirements of the building being evaluated. The criteria for determining whether a design alternative or alternative fuel is "acceptable" should include reliability, safety, conformance with building codes, occupant comfort, noise levels, refueling issues, and even space limitations.

4.1.1 Simple Payback Analysis

A highly simplified form of cost/benefit analysis is called simple payback. In this method, the total first cost of the improvement is divided by the first-year energy cost savings produced by the improvement. This method yields the number of years required for the improvement to pay for itself. For new construction, it can be used to evaluate conventional construction to energy-efficient design alternatives.

In simple payback analysis, you are assuming that the service life of the energy efficiency measure will equal or exceed the simple payback time. Simple payback analysis provides a relatively easy way to examine the overall costs and savings potentials for a variety of project alternatives. However, it does not consider a number of factors that are difficult to predict, yet can have a significant impact on cost savings. These factors may be considered by using a more sophisticated life-cycle cost analysis.

As an example of simple payback, consider the lighting retrofit of a 10,000-square-foot commercial office building. Relamping with T-8 lamps and electronic, high-efficiency ballasts may cost around $13,300 ($50 each for 266 fixtures) and produce annual savings of around $4,800 per year (80,000 kWh at $0.06/kWh). The simple payback time for this improvement would be $13,000/$4,800 annually = 2.8 years. That is, the improvement would pay for itself in 2.8 years, a 36% simple return on the investment (1/2.8 = 0.36).

4.1.2 Standardized Payback Equations

You can take advantage of a building energy measurement and verification guideline that standardizes procedures for quantifying energy savings from energy-efficiency projects. The International Performance Measure Measurement and Verification Protocol, can be used as a guideline to reduce risk and standardize paperwork. It also enables loans to be bundled together and sold on a secondary market, like mortgages.

4.1.3 Life-Cycle Cost Analysis

Life-cycle costing (LCC) is an analysis of the total cost of a system, device, building, or other capital equipment or facility over its anticipated useful life. LCC analyses allow a comprehensive assessment of anticipated costs associated with a design alternative. Factors commonly considered in LCC analyses are initial capital cost, operating costs, maintenance costs, financing costs, the expected useful life of equipment, and future equipment salvage values. The result of the LCC analysis is generally expressed as the value of initial and future costs in today's dollars as reflected by an appropriate discount rate. The Rebuild America Life-Cycle Cost Calculator can be used to help calculate the net present value of two alternatives and compare them using this cost-benefit method.

The first step in performing an LCC analysis is to establish the general study parameters for the project, including the base date (the date to which all future costs are discounted), the service date (the date when the new system will be put into service), the study period (the life of

the project or the number of years over which the investor has a financial interest in the project), and the discount rate. When two or more design alternatives are compared or when a single alternative is compared against an existing design, the variables compared must be the same to assure that the comparison is valid. It is meaningless to compare the LCC of two or more alternatives if they are computed using different study periods or different discount rates.

4.1.4 Selecting the "Best" Alternatives

Generally, all project alternatives should be initially screened using simple payback analyses. A more detailed and costly LCC analysis should be reserved for large projects or those improvements that entail a large investment, since a detailed cost analysis would then be a small part of the overall cost. Both simple payback and LCC analyses will allow you to set priorities based on measures that represent the greatest return on investment. In addition, these analyses provide a preliminary indication of appropriate financing options:

- Energy efficiency measures that have a short payback period of 1 to 2 years are the most attractive economically and should be considered for implementation using operating reserves or other readily available internal funds.
- Energy efficiency measures that have payback periods from 3 to 5 years may be considered for funding from available internal capital investment monies, or may be attractive candidates for third-party financing through energy service companies or equipment leasing arrangements.
- Frequently, short payback measures can be combined with longer payback measures of 10 or more years to increase the number of measures that can be cost-effectively included in a project. Projects that combine short- and long-term paybacks are recommended to avoid "cream-skimming" (implementing only those measures that are highly cost effective and have quick paybacks) at the expense of other worthwhile measures. A selected set of measures with a combination of payback periods can be financed either from available internal funds or through third party alternatives.

If simple payback time is 10 or more years, economic factors are very significant and LCC analysis is recommended. In contrast, if simple payback occurs within 3 to 5 years, more detailed LCC analysis may not be necessary, particularly if price and inflation changes are assumed to be moderate. Under this assumption, a simple payback analysis will often be within 15% to 20% of the payback time estimated from a detailed LCC analysis. In general, detailed LCC analyses may not be justified if the payback of the improvement is less than five years.

In any cost analysis, it is very important to include avoided cost as part of the benefit of the retrofit. When upgrading or replacing building equipment, the avoided cost of maintaining existing equipment should be considered a cost savings provided by the improvement.

4.1.5 Weighing Societal Impacts

Some factors related to building heating, air conditioning, and lighting system design are not considered in either simple payback or LCC analyses. Examples include the thermal comfort of occupants in a building and the adequacy of task lighting, both of which affect productivity.

Conventional cost/benefit analyses also normally do not consider the societal benefits from reduced energy use (e.g., reduced carbon emissions, improved indoor air quality). In some cases, these ancillary benefits are assigned an agreed upon monetary value, but the values to be used are strongly dependent on local factors. In general, if societal benefits have been assigned appropriate monetary values by a local utility, they are considered in savings calculations. However, your team should discuss this issue with your local utility or consultants working on such values in your area.

5. Sustainability Considerations during Construction

Construction sustainability guidelines can be set to lessen the impacts of building construction on the environment. Examples of actions that can be considered include:

- Specify equipment, materials, and products based on performance, not measurements.
- Use recycled materials to reduce use of raw materials and divert material from landfills.
- Use local and regional materials as much as possible.
- Minimize site impact by specifying location of trailers, equipment, storage, traffic.
- Monitor construction site energy and water use.
- Develop a construction waste management and recycling plan.

5.1 Construction

Construction design documents define the contractor's responsibilities during construction, but they typically focus on the design elements of the finished product. They rarely set environmental guidelines to be followed during the construction phase. The integrated design team should work with the construction contractor to adopt sustainability guidelines to be followed during construction.

Contractors seldom follow environmental guidelines during the construction process unless this guidance is built in as a written part of the contract, plans, and drawings for the building. Integrating construction guidelines with other sustainability guidelines is an essential part of the whole building design process. To develop and implement the guidelines, work with the team, including the architect, engineers, and contractors. Creating the guidelines as a team is helpful for educating contractors about sustainability issues and getting their early commitment to follow sustainability guidance. Environmental guidelines for the construction process should include construction specifications, material specifications, indoor air quality (IAQ) requirements, and specific measures for reducing environmental impact and energy and water use on the site during construction.

The building's impact on energy and environment begins during the construction phase. A sustainable approach to construction leads to reduced resource use, reduced disturbance of the site, and can also lower costs. Attention to environmental issues during construction also leads to a safer, healthier working environment for those people constructing the building, and later for those who occupy it.

5.2 Construction Specifications

Include these guidelines in writing in the construction contract and incorporate the guidance into plans, drawing, and specifications.

1. Specify equipment to match the intent of the design.
2. Specify equipment, materials and products based on performance, not measurements.
    - Insulation should be specified by thermal resistance (R-Value), not by thickness.
    - Lighting equipment should match watt densities from the design analysis.
3. When purchasing materials, evaluate the life cycle costs, not just the purchase price.
4. Educate your contractor about sustainability practices through charrettes and through ongoing monitoring and communication.
5. Create a written system for evaluating and monitoring how your contractor is meeting written sustainability requirements.

5.3 Purchasing Construction Materials

Define the lowest environmental impact when specifying construction materials. Questions to ask include:

1. Where was the material shipped from?
2. What is the material made of, and can it be recycled or reused when the building is renovated or demolished?
3. Are you ordering the least amount of material necessary?
4. What is the durability and replacement cost of the material?

Material Specifications:

- Use recycled materials to reduce the use of raw materials and divert material

from landfills. Use at least 5%-10% salvaged or refurbished materials, and specify that a minimum of 25%-50% of your building materials contain at least 20% post-consumer recycled content material, or a minimum of 40% post-industrial recycled content material.

- Use local and regional materials as much as possible, in order to reduce natural resources necessary from transporting materials over long distances. Specify 20%-50% of building materials be manufactured within 500 miles of the building site.
- Use rapidly renewable materials, in order to reduce the depletion of virgin materials and reduce use of petroleum-based materials. Specify 5% of total building materials be made form rapidly renewable building materials.
- For components of the building made from wood, such as flooring and framing, use a minimum of 50% wood-based materials certified in accordance with the Forest Stewardship Council Guidelines.

Select materials with volatile organic compound (VOC) limits. Specifically:

- Select adhesives that meet or exceed the VOC limits of South Coast Air Quality Management District Rule #1168.
- Select sealants that meet or exceed the Bay Area Air Quality Management District Reg 8, Rule 51.
- Select paints and coatings that meet or exceed the VOC and chemical component limits of Green Seal requirements.
- Select carpet systems that meet or exceed the Carpet and Rug Institute Green Label Indoor Air Quality Test Program.
- Select composite wood and agrifiber products that do not contain added urea-formaldehyde resin.

5.4 Reducing the Site Environmental Impact

- Document a site's existing natural, historical, and cultural features and make specific plans to preserve them.
- Specify locations for trailers and equipment.
- Specify which areas of the site should be kept free of traffic, equipment, and storage.
- Prohibit clearing of vegetation beyond 40 feet from the building perimeter.
- Explain methods of protecting vegetation, such as designating access routes and parking.
- Require methods for clearing and grading the site that are as low impact as possible.
- Examine how runoff during construction may affect the site. Consider creating storm water management practices, such as piping systems or retention ponds or tanks, which can be carried over after the building is complete.

5.5 Indoor Air Quality During Construction

During construction, dust, VOCs, and emissions from equipment permeate the building site and the building itself. Poor indoor air quality (IAQ) can damage the health of workers and occupants of nearby buildings. It is important to take specific measures to protect IAQ on the site during construction, and after.

- Create a written plan for the contractor to use in managing air quality on the construction site.
- Put up barriers to keep noise and pollutants from migrating.
- Ventilate the site through the building's HVAC system, once installed, and with temporary exhaust systems before installation.
- Increase the amount of outside air coming into the building while under construction, to reduce pollutants.
- Create controls such as scheduling construction activities at the end of the day, to ventilate over night while site and surroundings are unoccupied.
- Be aware of air quality throughout the project, not just during times of activities that create high amounts of airborne pollutants and emissions.
- Regularly monitor IAQ with tests and inspections and adjust the ventilation

and scheduling if necessary to improve IAQ

- Prevent poor IAQ by selecting materials and products designed for less off gassing, such as low VOC paints and sealants and formaldehyde-free particle board
- Keep the site and interiors clean and free of debris, in order to keep dust down. Storing polluting materials in a specified storage area will protect the building from pollutants.
- Meet or exceed the minimum requirements of the Sheet Metal and Air Conditioning National Contractors Association (SMACNA) IAQ Guideline for Occupied Buildings Under Construction, 1995.
- Protect stored on-site or installed absorptive materials from moisture damage.
- Replace all filtration immediately prior to occupancy. Filtration should have a Minimum Efficiency Reporting Value (MERV) of 13 as determined by ASHRAE 5.2.2-1999.
- Conduct a minimum two-week building flush-out with new filtration media at 100% outside air after construction ends and before occupancy, or conduct a baseline IAQ testing procedure consistent with current EPA Protocol for Environmental requirements, Baseline IAQ and Materials, for Research Triangle Park Campus, Section 01445.

5.6 Energy and Water Use

- Monitor the contractor's energy and water use. Set limits, or place the utility and water bills in the contractor's name to encourage conservation.
- Use lighting during construction only in active areas of the site. This saves energy and protects the night sky from light pollution.
- Turn all lights off when work is at a halt. Security lighting can run on motions sensors.
- Use energy-efficient lamps such as compact fluorescents, for temporary and permanent lighting schemes.
- Use renewable energy technologies or green power, if locally available, to power equipment and vehicles.
- Use low-flow fixtures for water siphons you install for construction.
- Use rainwater or reuse greywater from the construction site.

5.7 Construction Waste Management

- Make sure the infrastructure for recycling of construction and demolition materials is in place and operating at the beginning of the project. Set up an on-site system to collect and sort waste for recycling, or for reuse, and monitor the system consistently throughout all phases of construction.
- Create a recycling plan that sets goals to recycle or salvage a minimum of 50% (by weight) of construction, demolition, and land clearing waste. Aim for a minimum of 75%.
- Select products and materials with minimal or no packaging, if possible.
- Purchase materials in the sizes you will need them, rather than cutting them to size.

Consistently track and monitor the amount of waste production during construction and measure it against pre-existing goals and guidelines.

6. Sustainability through Renovation

Renovating an existing building is often an environmentally beneficial choice. You're avoiding building on undeveloped land and you are using existing infrastructure like roads, water and sewer lines, and electrical connections.

There are many ways to incorporate sustainability concepts in building renovation projects. Renovation projects may range from a simple relighting program to gutting the building to its shell and rebuilding its interior or adding a significant new addition to an existing building. Before beginning the project, asses the orientation of the building and consider ideas on how to sustainably integrate the building renovation project with the site and to evaluate how the project may affect the site. For example, will the renovation project change the site storm water runoff characteristics?

Software simulation tools can model proposed renovations to analyze how much energy they will save. Some of the simplest ways to add energy efficiency to retrofit projects include using efficient lighting, appliances, and equipment. Improved controls can also reduce HVAC and electrical use. Working with an energy service company can help you to achieve your retrofit goals. For retrofit projects, consider:

- Day lighting strategies, such as making atria out of courtyards or adding clerestories, along with modification of the electric lighting system to ensure energy savings
- Heat control techniques, such as adding exterior shades or overhangs
- Using passive solar heating strategies to allow modification of HVAC systems—perhaps down-sizing if the passive strategies reduce energy loads sufficiently.

When renovating older buildings, determine whether passive features that have been disabled can be revitalized. Boosting wall insulation levels in existing buildings is difficult without expensive building modifications. One option for existing buildings is adding an exterior insulation and finish system (EIFS) on the outside of the current building skin. With EIFS, use only systems that include a drainage layer to accommodate small leaks that may occur over time—avoid barrier-type systems.

Roof insulation can typically be increased relatively easily during re-roofing. At the time of re-roofing, consider switching to a protected-membrane roofing system, which will allow reuse of the rigid insulation during future re-roofing—thus greatly cutting down on landfill disposal.

6.1 Example of Renovation by Saving Structural components and Reusing Building Material

This case study is one in a series developed by the Massachusetts Department of Environmental Protection (DEP) to highlight techniques for saving money and protecting the environment through reuse and recycling of construction and demolition material.

Project Description: Clarke Distribution Corporation, Milford, Massachusetts
Clarke, a wholesale distributor for several lines of luxury kitchen appliances, renovated and expanded its distribution center in 2004 (figure 1). The Center is located in a rural area in central Massachusetts. Consigli Construction Inc. was the lead contractor for the project. The Institutional Recycling Network (IRN), a commercial recycling cooperative, provided waste reduction planning assistance and managed recycling logistics.

6.1.1 Ceiling Tiles and Doors: The project recycled six tons of ceiling tiles through the Armstrong Ceiling Recycling Program. Armstrong recovers the mineral fibers from discarded ceiling tiles to use in making new tiles. Armstrong's program is available to demolition projects and to building owners who choose Armstrong ceiling systems in their renovation projects. Consigli removed the ceiling tiles, stacked them and IRN provided the transportation. Armstrong provides a "Recycling cost comparison worksheet" on its web site that allows users to compare the cost of recycling versus disposal.

Clarke also donated 20 wood doors and 20 metal doors to a non-profit organization, the Building Materials Resource Center (BMRC), a reused building materials retailer. Clarke received a tax credit for the donation, Consigli saved disposal costs and BMRC sold these products at a reduced cost to low-income homeowners for use in their homes.

6.1.2 Cost Savings: Table 1 shows a breakdown of the cost savings due to source separation and recycling:

Material	Tons	Recycling Cost	Avoided Disposal Cost*	Savings
Ceiling Tiles	6	$625	$708	$83
Asphalt	970	$2,367	$114,460	$112,093
Concrete	1,267	$4,092	$149,506	$145,414
Metal	19	$785	$2,242	$1,457
Cardboard	0.86	$105	$101	(-$4)
TOTAL	2,263	$7,974	$267,017	$259,043

Table 1: Comparison of recycling and disposal of C&D material for this project and the resulting savings by using recycling of material
**Cost that would have been paid if material were disposed, asphalt & concrete are typically recycled. Cost savings does not include reuse of 7,225 tons of ledge.*
Disposal costs based on local rates.

6.1.3 Team Approach to Waste Reduction Planning: Before construction started, staff from Clarke, Consigli and the Institutional Recycling Network walked through the facility to identify potential waste reduction opportunities. They developed a waste reduction plan that guided the entire waste reduction process from planning to development and construction. The plan identified several recycling opportunities, including:

- Clarke's CEO used his business contacts to identify a new home for a 9,000 square foot refrigeration unit that would have otherwise been disposed.
- Rather than purchasing new loading dock leveling units, weighing two tons each, Clarke authorized Consigli to reuse 6 out of 10 of the existing units.

Project Team

- *Building Owner*
  Clarke Distribution Corporation, 397 Fortune Boulevard, Milford, MA 01757
- *Contractor*
  Consigli Construction Inc., 197 Main Street, Milford, MA 01757Contacts: Tom Burns, Project Manager, and John Laperle, Superintendent
- *Recycling Services*
  Institutional Recycling Network, 7 South State Street, Suite 2, Concord NH, 03301
- *Building Material Reuse*
  Building Materials Reuse Center, 100 Terrace Street, Boston, MA 02120, Armstrong

7. Sustainable Stormwater Management Strategies

7.1 Application of Bioretention Areas

- Parking lot island landscaping features adapted to treat stormwater runoff.
- Surface runoff is directed into shallow, landscaped depressions with pollutant removal layers.
- Typically, the filtered runoff is collected in a perforated underdrain and returned to the storm drain system, but the system can be enhanced for partial exfiltration.
- The system should be sized between 5% and 10% of the impervious draining area.
- These areas can be designed to hold plowed snow.

7.2 Dry Extended Detention Pond

- Vegetated, open channel management practice
- May be an option as a snow storage facility to promote treatment of plowed snow

- Swale with engineered soil matrix and under drains to promote filtration
- Recommended for sites with a minimum drainage of 10 acres
- Least expensive stormwater treatment practice, on a cost per unit area treated
- Best long-term performance track record (least clogging problems)

7.3 Infiltration Trench (narrow and deep)

- Generally applied to sites less than five acres with relatively high impervious cover
- Soil infiltration rate ranges between 0.5 and 3 inches per hour
- Best applied to drainage areas less than 10 acres
- Soil infiltration rate should range between 0.5 and 3 inches per hour
- Can be optimized for seasonal operation and to accommodate snow melt

The design of all stormwater detention areas should be for the "dry" condition for most of the year. Stormwater retention areas should not be designed to be wet year round since that may encourage development of wetlands and/or breeding areas for pests.

8. Water Efficiency Considerations

Water efficiency is the planned management of potable water to prevent waste, overuse, and exploitation of the resource. Effective water-efficiency planning seeks to "do more with less," without sacrificing environmental performance. There are two basic approaches to potable water efficiency in the landscape:

Water Efficiency in the Landscape

- Reduce water use associated with irrigation and landscaping.
- Recycle or use water with gray water or process recycling systems.

Reduce water use associated with irrigation and landscaping. This can be accomplished to varying degrees by one or a combination of the following:

- Preserve, encourage or reintroduce native or drought-tolerant vegetation that is already optimized for naturally occurring precipitation levels.
- If plants are desired that need water, group them by similar watering and soil type needs.
- Irrigate efficiently (see irrigation tips).

Recycle or use water with graywater or process recycling systems. Reclaimed wastewater, sometimes called irrigation quality or IQ water, is another possible source for irrigation water. Reclaimed water is from a wastewater treatment plant that has been treated and can be used for nonpotable uses such as landscape irrigation, cooling tower, industrial process uses, toilet flushing, and fire protection. It must be scrupulously isolated from potable water distribution, and all IQ hose bibs must be clearly marked as "nonpotable." The following considerations can be used to improve the efficiency of irrigation applications of collected water from buildings:

- Use ultra-low-volume distribution devices.
- Irrigate after on-site inspection or electronic sensing of moisture requirements, rather than just by a time clock.
- Water requirements vary greatly by season, and as the landscape matures, less irrigation is required.
- Automatic irrigation controllers should have rain switches that override the "on" signal when sufficient rain has fallen or soils are moist.

Rainwater harvested from building roofs can be used for irrigation. Graywater is untreated wastewater generated within the facility from shower and bath, laundry, and bathroom sinks (not from toilets, urinals, kitchen sinks, or dishwashers). Graywater can be used for below-ground irrigation, but it is not recommended for above-ground irrigation.

9. Sustainable Operation and Maintenance of Buildings

When a new building is ready for occupancy, the operation and maintenance of the building will impact energy use and occupant comfort. As much care should be paid to the operation of the building as was paid to the building planning, design, and building component choices. Energy-efficient lighting is one of the most cost-effective options available for reducing energy costs in buildings.

For existing buildings, effective operation and maintenance procedures provide opportunities for energy savings. Building components can be replaced with energy-efficient models. Facilities staff can be trained to cut energy use. And performance needs to be measured.

The best efforts to reduce negative environmental impacts in the built environment are doomed to failure unless well-crafted operations and maintenance (O&M) procedures are implemented. Furthermore, even the best O&M procedures are of no use unless they are understood and followed by building O&M personnel.

Facility managers play the key role in ensuring that this happens. An "integrated team" approach can be a big help. In this process, O&M personnel are active participants in the design of a facility and the development of O&M procedures. This "integrated team" promotes useful procedures that are efficient and—most important—faithfully executed.

Building operation and maintenance programs specifically designed to enhance operating efficiency of HVAC and lighting systems can reduce energy bills by 5% to 20% without significant capital investment. The EPA and DOE want to help commercial building owners capture these savings. They have developed fifteen O&M Best Practices for Energy Efficient Buildings booklet with strategies that facility managers, energy managers, and property managers can use to integrate energy-efficient operation into their organizations' O&M programs and to obtain support from senior management.

Addressing O&M considerations at the start of a project can contribute greatly to improved working environments, higher productivity, and reduced energy and resource costs. The following sections of this guide provide a variety of O&M information on the important systems typically found in Federal facilities. Other O&M-related information also can be found in various places in the earlier sections of this guide.

There are tremendous opportunities in most existing buildings and facilities to improve O&M procedures and make them more environmentally responsible. With new buildings, there are opportunities during design and construction to facilitate easy, low-environmental-impact O&M. With all buildings there are opportunities to derive multiple benefits. Energy savings and improved indoor air quality can be achieved by tuning up older oil-fired boilers, for example. Improved indoor air quality and less hazardous effluent from a building can be achieved by switching to more benign cleaning chemicals. If implemented effectively, the multiple benefits of O&M practices should include reduced operating costs.

To create an effective O&M program, the general procedures should be followed:

- Ensure that up-to-date operational procedures and manuals are available.
- Obtain up-to-date documentation on all building systems, including system drawings.
- Implement preventive maintenance programs complete with maintenance schedules and records of all maintenance performed for all building equipment and systems.
- Create a well-trained maintenance staff and offer professional development and training opportunities for each staff member.
- Implement a monitoring program that tracks and documents building systems

performance to identify and diagnose potential problems and track the effectiveness of the O&M program. Include cost and performance tracking in this analysis.

Specific elements of an effective O&M program include:

9.1 HVAC Systems and Equipment

Energy consumption and conservation are tied heavily to O&M procedures. HVAC equipment must be well maintained for the complex array of chillers, boilers, air handlers, controls, and other hardware to function at peak performance. Easy access to HVAC systems for ongoing maintenance and repair is critical (be sure that this is considered during design). A well-thought-out, well-executed O&M program can provide huge savings in equipment and energy costs.

9.2 Indoor Air Quality (IAQ) Systems and Equipment

Air ventilation and distribution systems should be well maintained and frequently checked for optimal performance. Coordination between air distribution systems and furniture layouts is especially important. In addition, regular inspection for biological and chemical contaminants is crucial. Poor IAQ lowers productivity, can cause illness, and has resulted in numerous lawsuits.

9.3 Cleaning Equipment and Products

Using biodegradable and least-toxic cleaning products and equipment can reduce both O&M costs and pollution to air and wastewater streams while improving both indoor air quality and worker productivity. The need for chemical cleaning products can also be reduced through environmentally conscious design and material choices. New requirements for cleaning contracts must be clearly specified. The EPA Cleaning Products Pilot Project can help you find environmentally preferable cleaning products.

9.4 Materials

Facilities should maintain an attentive and proactive stance with regard to the environmental impacts of their material choices. Every day new products, systems, and equipment become available that have fewer adverse environmental impacts. All these choices should be carefully scrutinized in terms of O&M.

9.5 Water Fixtures and Systems

Routine inspections and maintenance programs for water fixtures and systems are crucial. Population growth and development have reduced the availability of high-quality, potable water in many regions of the country. Along with increased water prices, reduced supply often leads to usage restrictions. An O&M program will reduce operating costs when it verifies that fixtures and systems are functioning effectively and ensures that leaks or components are quickly repaired.

9.6 Waste Systems

Recycling and waste-reduction programs and their supporting hardware need frequent attention and maintenance in order to function at peak performance.

9.7 Landscape Maintenance

Use of native plantings can reduce landscape O&M requirements and costs significantly. Although natural vegetation may take several years to become established, once it is established there is usually less need for water. Integrated pest management can also reduce overall O&M costs by reducing the need for hazardous chemicals and pesticides.

10. Standard for Rating Sustainable Facilities. Sustainability performance standards measure the impact of a building upon the environment through its entire lifecycle and specifically upon the built and natural environment's continued ability to support healthy life. The building's life-cycle includes its *construction* (including environmental impacts through the acquisition and transportation of materials, construction methods, location, site work, etc.), *operations*

and maintenance (including environmental impacts on human health, water/air/soils, energy resources, etc.), and *demolition* (including many of the same environmental impacts listed above, together with waste management).

An performance standard is needed to objectively measure the environmental sustainability of a building's life cycle, to make the most cost-effective choice among an array of environmental investments possible in a particular building, to compare the environmental performance of different buildings, to be accountable to stakeholders for the environmental investments made in buildings, and to participate in a broader social effort (national and international) towards environmental sustainability. Energy optimization is also an integral part of environmental performance.

The LEED evaluation for sustainable commercial buildings is the most used system in the United States. The letters stand for Leadership in Energy & Environmental Design. It has become the leading system for designing, constructing, and certifying the world's greenest buildings. The LEED's model takes a whole-building approach that encourages and guides a collaborative, integrated design and construction process. The intent is to optimize environmental and economic considerations throughout the planning, design, construction and operation of a building with a life cycle viewpoint. There are four levels of LEED certification based on a point system shown below:

- LEED Certified 26 - 32 points
- Silver Level 33 - 38 points
- Gold Level 39 - 51 points
- Platinum Level 52+ points (69 possible)

11. Training

In order to plan, design, construct, maintain, and operate programs in environmentally sustainable buildings, people must be adequately trained. Having LEED-certified professionals work on the design and construction is not enough; County staff must have LEED and energy management training appropriate for their level of involvement in the buildings. Failure to do so will result in delays, cost increases, design conflicts, and higher operations and maintenance costs for the buildings. While all occupants of LEED-certified building need some level of building orientation, those more extensively involved in building design and construction should have more formal training.

12. Example High Performance Sustainable Buildings

12.1 Arlington County Virginia Sustainable Building Policy Since the early 1960s, Arlington has targeted specific areas for development using its General Land Use Plan. Concentrate high density development along Metro corridors. These areas surrounded by less densely developed suburban-type neighborhoods. This approach has proven to be a very effective planning tool. Gives Arlington its unique character - walkability, public transit accessibility, neighborhoods with distinct character and allows for economic development. Offers opportunity to work and live in the same community. Arlington's land use and develop plan for buildings and other public and private infrastructure provide easy access to transit for those commuting into DC. A large number of people also commute into Arlington as well.
Through careful land use planning this results in a dense urban high rise environment, usually mixed offices, ground level retail, apartments, and hotels around Metro, bus routes, and main roads. It also preserves quiet residential neighborhoods and a network of linear parks that follow stream valleys. There are also old train lines that have been converted to bike trails along several stream valleys. As with any urban community, Arlington is facing a variety of environmental challenges. Some of these local impacts include, stormwater runoff, heat islands in high rise areas, traffic congestion, and constant demand for parking, streams and parkland.

Currently there are six County projects that are being designed to achieve LEED silver status as sustainable buildings. The include a community center serving teens and senior citizens, a school and community center, and Parks Department

operations buildings. The Walter Reed Community Center is leading the way. The goal is to achieve Gold LEED certification. This project used an integrated design process from the beginning and involved working closely with architects, engineers, users, employees, neighbors, etc. This facility here will serve teens with a game room, ball courts, indoor gym area, and organized activities. The Center also houses a senior day program with arts and crafts, kitchen facility, nursing station, and organized activities. A further purpose is to serve as a meeting place for community groups, special events, County committees, and other County programs.

On the private sector side, the Arlington County Board is requiring all site plans for construction projects to submit a LEED Scorecard to determine how "green" projects are even if they aren't going for a high level of certification. All major projects are encouraged to meet at least a LEED Silver rating. Any construction in a metro corridor gets a point for locating near transit and most get a point for urban redevelopment. Arlington requires office buildings to include bike racks and shower facilities. The sustainable building program allows developers to apply for additional density up to .25 FAR and/or 3 stores, if they meet at least silver LEED requirements. This gives builders and building owners additional leasable space which in Arlington is a strong financial incentive. All new major construction projects are now planning for LEED silver or higher. Arlington does maintain a database that tracks overall greenness as development evolves within the county. The pressure to build and increased density levels within the county continues and there is recognition of the need to consider cumulative impacts in planning for future development.

Builders and building owners are also focusing a lot of effort on indoor environmental quality. Through the LEED certification process better use of indoor materials, efficient heating, cooling and ventilation system design, energy efficiency and generous areas of day-lighted space lead to a healthy office environment. Sustainable buildings have proven to be a good marketing tool in the competitive lease market. Arlington building owners with sustainable high performance facilities can advertise environmental friendly, healthy indoor working environments, and non-toxic space to perspective customers.

12.1 Rosslyn Center Place Project: Center Place is a million-square foot, mixed-use development in Rosslyn, Arlington County that will be LEED certified silver or better and have the first and will house the only publicly-accessible observation decks overlooking Washington's monuments. The project's principal features are two massive, tall tower structures that will be the tallest buildings in Virginia and the Washington DC area when completed (see figure 3). One will be for office space and the second for apartments. The two-level observation deck on the 28th and 29th floors of the Office tower will be a unique public amenity for Arlington residents and tourists to enjoy panoramic views of the national monuments and surrounding area from a unique vantage point (figure 4) . It's expected to draw up to 450,000 visitors annually. The deck is part of the JBG Companies' proposed Central Place project. The observation deck will be atop a commercial office tower located at Wilson Boulevard, one of two glass towers that will comprise the JBG project. The re-development will redefine Rosslyn's "Central Place". I is also a candidate for demonstration/application of new technologies and systems for the next generation of sustainable high performance buildings.

The form and materials of the two glass towers reflect a sense of transparency, lightness and quiet elegance. The glass and metal residential building will rise to 380 feet and has been designed to match the drama and quality of the office tower at the opposite end of the site. The office building will contain trophy level office space, with impressive views for the public and corporate tenants. The top 60 feet of the residential building has been reserved for the highly anticipated public observation deck, which will crown the development.

An open air landscaped park between the two towers will be approximately 18,400 square feet

in size and directly opposite the Rosslyn Metro station. The park is designed to function as a "town square," surrounded by pedestrian level retail (figure 5). Landscape Architect Michael Vergason's flexible plaza design allows for both daily enjoyment and large public events and festivals. Kathleen Webb, a JBG principal who is project manager for Central Place, says the plaza will help activate the community. It is designed to be inviting, pedestrian-friendly and easy-to-get-to. The plaza will connect N. Moore and Lynn Streets at the Moore Street level, directly across from the

Rosslyn Metro entrance, to provide east-west connectivity through the heart of Rosslyn for Metro commuters and visitors alike. The plaza will be flanked by the two soaring glass and metal towers with retail spaces opening onto the park from the base of each tower. The JBG Companies' other Rosslyn developments include new retail at International Place (1735 N. Lynn Street), 1801 N. Lynn Street, distinguished by Ned Kahn's liquid pixels artwork, and the soon-to-be-completed design work of Jim Freed at Waterview.

The project is just now completing two years of community review by the Rosslyn Working Group. Initially, In October 2004, the Arlington County Manager officially appointed a group of planners, designers, and citizens including members of the Rosslyn Renovation Urban Design Committee to review and plan the JBG project's height, architecture and urban design. Central Place is identified in the Rosslyn Sector Plan as the organizing element of Rosslyn's urban core, with a vision that it will be "hub" of pedestrian activity providing streetscape, shopping, eateries, art and open space. The JBG design incorporates key components of the Rosslyn Plan and also addresses the County-commissioned study by the Urban Land Institute. This project is intended to further develop Rosslyn as a major destination in the Washington region.

12.2 Achieving Desired Indoor Air Quality for Oklahoma City surgical suites:

St. Anthony Hospital in Oklahoma City was founded in 1898, and is a private, not-for-profit, multi-campus hospital and regional referral center. The 615-bed tertiary care facility provides general and acute care services including cardiology, oncology, behavioral medicine, surgery, kidney transplantation, orthopedics, and a variety of other disciplines. With approximately 2,600 employees, the hospital administration understood the need to update their facility and equipment to compete with other hospitals for doctors, staff, and patients. Thus a lO-year, $220 million renovation is underway to enlarge the facility and incorporate the latest in medical technologies and sustainable green technology into the renovated structure (figure 6).

The first major phase of the renovation was a complete overhaul of the surgery center. Designers worked closely with hospital personnel and design engineers to ensure the best system was installed. There was an innovative, collaborative team effort to create the best possible facility and to investigate every possible option before settling on the final approach. The desiccant technology showed the best combination of performance, operating cost, and first cost. The system has been operating for some time now and has exceeded expectations in every way. The architects and engineers working on the surgery project included the physicians and surgeons throughout the entire design process. It was important to St. Anthony's that the building's designers valued the input from the physicians, because ultimately they know what is best for them and their patients.

Humidity is a constant challenge in surgical environments. Surgeons need the operating rooms to have both a low temperature and a low relative humidity. This ensures that surgical surfaces and instruments remain free of moisture, discouraging bacteria growth. For some surgical procedures, low temperature reduces the metabolic rate to lessen the impact of the surgery. Low humidity is also required to avoid "fogging" of optic systems used in minimally invasive surgical procedures. Any failure to maintain those conditions is completely unacceptable.

Cooling-based systems are inefficient because they must cool the air to the desired dew point in order to provide the humidity required. This requires a very low leaving air temperature and low temperature refrigeration systems. Additionally, they overcool the air and require substantial reheat to keep the rooms from getting too cold. These systems are costly to operate and may not provide the desired conditions under all circumstances.

This $30 million project required a new chiller plant, boiler plant, air-handling systems, and an active desiccant system. The desiccant dehumidification system at St. Anthony provides the desired temperature and humidity without the need for special refrigeration systems and without the inefficiency of cooling and reheating. This ensures better indoor air quality and a more comfortable environment for doctors and patients. The hospital has been successfully recruiting surgeons since the completion and opening of the new surgery facility.

12.3 Simulation helps Finnish office workers stay warm in winter, cool in summer

This 150,000-sq-ft building is the headquarters for Pfizer Oy, the Finnish subsidiary of Pfizer Inc. The building was designed as a high performance green facility which uses an active chilled beam cooling system for office spaces and displacement ventilation for the lobby (figure 7). The designers were concerned about thermal comfort inside the building because of the large surface area of windows and skylights and the large atrium. While many people think of Finland as a very cool climate, the Helsinki area actually has a greater solar thermal load during the summer than Paris. Keeping the atrium warm was difficult in the winter because of the large window and skylight area and keeping the atrium cool in the summer months was challenging because skylight and windows provide a significant solar heat source to the atrium:'

To address this issue simulation results for different air distribution solutions were used to diagnose a system for air distribution that would be effective throughout the building. One general problem was that air velocities were too high for comfort in a number of occupancy zones. Temperatures were too high in certain areas of the atrium during the summer due to the large amount of solar thermal loading through the skylights. We also noticed that optimization of supply air distribution in offices was I important for thermal comfort:'

The airflow problems and the heat distribution in the atrium were addressed by evaluating a number of different diffuser configurations. Using computer simulation modeling a diffuser design was found that reduced airflow to comfortable levels while improving thermal distribution to the point that the temperature remained within an acceptable range in all occupied areas of the atrium under summer conditions. A variety of different window heating systems were also modeled to find an acceptable solution for the winter environment.

The use of computer simulation significantly improved the indoor air quality of this building while avoiding the expense that would have otherwise been required to modify the HVAC system after it had already been installed.

13. Summary

The environmental impact of buildings is very important. This is an area that needs more attention on a national and local basis. Approximately 65% of the US total electric consumption is from buildings. This represents more than 36% of the total US primary energy usage. Approximately 30% of the total US greenhouse gas submissions are from buildings. There is approximately 36 billion tons annually of construction and demolition waste generated from US buildings. This represents approximately 2.8 pounds per person per day in the US. The consumption of potable water in US buildings is approximately 36 billon gallons per day representing 78% of total treated water consumption in this country included in this is 5 billion gallons per day for toilet flushing alone.

Sustainable buildings are intended though out their life time to have a beneficial impact on their occupants and their surrounding environment. Such buildings are optimally integrated on all parameters— initial affordability, timeliness of completion, net life-cycle cost, durability, functionality for programs and persons, health, safety, accessibility, aesthetic and urban design, maintainability, energy efficiency, and environmental sustainability. Failure on any one parameter invariably undermines other parameters of the building in question and of the system of buildings and connected service systems in the community. Examples of Sustainable Building components include:

- Low-VOC paint
- Low-VOC carpet tiles
- Low-flow restroom fixtures
- Recycled content tiles
- Waterless urinals
- Motion sensors
- Green Roof

There are clear economic benefits of sustainable buildings which include a competitive first cost. The concept of integrated design allows for high benefit at low cost by achieving synergies between disciplines and between technologies. Green Designs lead to reduced utility bills and O&M costs. Sustainable design also will optimize life cycle economic performance and reduce liabilities. Energy and water-efficient buildings have been able to reduce their operating costs significantly. Use can be cut to less than half than that of a traditional building, or even better, by employing aggressive and well-integrated green design concepts.

A critical element for a successful sustainable building policy and program is an integrated building planning and design process. Integrated planning and design refers to an interactive and collaborative process in which all stakeholders are actively involved and communicate with one another throughout the design and construction practice. This allows the architect and engineer to work together to ensure that building components work synergistically. Experience across the nation shows that environmentally sustainable features are often not incorporated. In other cases they are included at much higher costs, when environmental performance issues are not considered from the very outset of the planning and design process.

It is not only environmental performance that suffers from lack of an integrated planning and design process. All the other building parameters also suffer (initial affordability, timeliness of completion, net life-cycle cost, durability, functionality for programs and persons, health, safety, accessibility, social equity, aesthetic and urban design, maintainability, and energy efficiency).

Integrated Design and construction practices that significantly reduce or eliminate the negative impact of buildings on the environment and occupants may be organized into five broad areas:

- Sustainable site planning
- Safeguarding water and water efficiency
- Energy efficiency and renewable energy
- Conservation of materials and resources
- Indoor environmental quality

Indoor air quality is also a critical part of high performance sustainable buildings. Healthy indoor environments can increase employee productivity according to an increasing number of case studies. Since workers are by far the largest expense for most companies (for offices, salaries are 72 times higher than energy costs, and they account for 92% of the life-cycle cost of a building), this has a tremendous effect on overall costs. Studies have shown that student performance, as well as energy performance, is better in schools built according to green design principles. More than 17 million Americans suffer from asthma, and 4.8 million of them are children. Ten million school days are missed by children each year because of asthma, which is exacerbated by poor IAQ. Employees in buildings with healthy interiors have less absenteeism and tend to stay in their jobs.

The LEED evaluation for sustainable commercial buildings is the most used system in the United States. The letters state for Leadership in Energy & Environmental Design. It has become the leading system for designing, constructing, and certifying the world's greenest buildings. The LEED's model takes a whole-building approach that encourages and guides a collaborative, integrated design and construction process. The intent is to optimize environmental and economic considerations throughout the planning, design, construction and operation of a building with a life cycle viewpoint.

14. Recommendations for further Development of High Performance Sustainable Buildings

1) Better define the criteria (target levels) for indoor pollution levels for human occupancy.
Develop the technical bases for creating performance based standard for risk assessments and identify action to implement new knowledge into practice (research risk identification process, how to reduce the risk once identified, containment or dilution). Build on sustainability research findings and recommendations from organizations such as the World Health Organization (WHO), the US USIDR levels, the EPA IRIS data base of human health effects from exposure to various substances in the environment, and Japanese organizations to identify technologies designed to: 1) sense hazardous pollutants, 2) mitigate these pollutants, and 3) identify pollution sources (material sources, maintenance sources).

2) Minimize energy use in new building designs and retrofitting of existing buildings by using: 1) sustainable building materials, 2) energy efficient building envelopes including green roofs, 3) reuse of energy (heat), 4) efficient appliances and equipment, 5) recycled material research to assess the characteristics of these material properties, 6) water conservation and wastewater management systems, and 7) improving building management systems for green systems for operation and maintenance.

3) Demonstrate promising materials and systems in actual buildings to facilitate the more rapid transfer of this technology into use by the building industry
Establish a strong working relationship with the building industry and conduct planned demonstrations in buildings of materials and systems that meet the sustainability needs of the building in an effective, efficient and environmentally sensitive manner. The time lag and risks of technology transfer can often be reduced through demonstration projects that involve the effected industry.

4) Develop a systems approach to address the complex set of problems and issues for the next generation of sustainable buildings
Buildings are a complex mix of materials and systems that need to work together to provide safety, comfort, and efficiency to their occupants and owners. To introduce new materials, systems and other components into the next generation of high performance sustainable buildings will require a full understanding of these interactions and the ability to model and simulate these new parameters with in the total building context.

5) Identify and quantize procedures for assessing new materials
Conduct research and development efforts to understand the mechanical, environmental and other by-products from new materials made from recycled materials. This would include understanding the burning characteristics of this new and growing family of "sustainable construction materials". The broader use and smart application of these new sustainable materials will be dependent on these studies.

6) Identify and apply technologies that meet US and Japan sustainability goals that can be used in demonstration projects
Example technologies include development of effective materials made from recycled components, improved energy efficiency devices and systems, new methods to reduce air and water pollution, elimination of toxic materials in buildings, advances in structural building materials

7) Improve the knowledge base on the service life of buildings

Developing ways to lengthen the service life of buildings is a very effect sustainability approach. New innovations and applications in this area would produce high returns.

15. References:

Bisio, Attilio, "History of Recycling", in, Encyclopedia of Energy, Technology and Environment, Wiley Brothers, 1995.

Ceiling Tiles Recycling Program, 2006, http://www.armstrong.com/commceilingsna/environmental.html

Central Place Project Plan, 2007, www.RosslynVA.org

Civic Economics, Inc., on the Web go to CITIZEN-TIMES.COM., 19 MARCH 2003.

CRRA Global Recycling Council, "What I Can Do to Work Towards Zero Waste", presented at the 2003 CRRA Annual Conference, Ontario, CA.

Cutting the Waste Stream In Half: Communities Show the Way, US EPA, 2000.

"Fighting Waste Industry Consolidation With Local Recycling Facilities". ILSR, 2002.

Fisk and Rosenfeld, 1998, "Improved Indoor Environment Could Save Billions of Dollars"

Garris, Leah B., A Smart Approach to Sustainability, Buildings Magazine, PP. 44-50, March 2007

Hathaway, Hargreaves, Thompson, and Novitsky, 1992, "A Study Into the Effects of Light on Children of Elementary School Age - A Case of Daylight Robbery," Policy and Planning Branch, Planning and Information Services Division, Alberta Education, Canada.

Heschong, 1999, "Skylighting and Retail Sales: An Investigation into the Relationship Between Daylighting and Human Performance," www.h-m-g.com/Daylighting.

Nicklas and Bailey, "Analysis of the Performance of Students in Daylit Schools," Innovative Design, Raleigh, NC, www.innovativedesign.net.

Kevin McKown, "Sustainability the Goal in City", Green Pages, Autumn 2003.

Lease, Kelly, "Impact of Consolidation on Recycling", MSW Management Magazine, June 2001.

Lenssen and Roodman, 1995, "Worldwatch Paper 124: A Building Revolution: How Ecology and Health Concerns are Transforming Construction," Worldwatch Institute.

Local Actions That Support Zero Waste, CRRA Technical Council, 2003.

National Association of Home Builders Research Center (NAHBRC), *Deconstruction – Building Disassembly and Material Salvage: The Riverdale Case Study,* Upper Marlboro, MD: National Association of Home Builders Research Center, 1997.

National Association of Home Builders, *Building with Alternatives to Lumber and Plywood*, Washington, D.C.: Home Builder Press, 1994.

National Recycling Coalition, "U.S. Recycling Economic Information Study", Washington, D.C., July 2001

National Recycling Research Agenda, 1980, prepared for the National Science Foundation by ILSR and CRRA.

Neil Seldman, "An Evaluation of Incineration Technologies", Institute for Local Self-Reliance, Washington, DC, October 1986.

Peter Anderson, Deregulation: the Fifth Horseman, ILSA, June 2004

Platt, Brenda, Beyond 25% Recycling, Institute for Local Self Reliance (ILSR), 1999

Platt, Brenda, Beyond 40% Recycling, Island Press, 1999

Platt and Seldman, Wasting in the US 2000, Grass Roots Recycling Network, 2001

Recycling and Composting Programs: Designs, Costs, Results, ILSR, 1992.

Recycling Economics, ILSR, 1990, ILSR: and Salvaging the Future, ILSR, 1989.

Richard Anthony, "Reduce, Reuse, Recycle: The Way to Zero Waste", in C. Ludwig, et al, ed., Municipal Solid Waste Management, Springer, 2003

Robin Murray, Zero Waste, Greenpeace, London, 2002

Seldman, N and Platt, B, Wasting in the US 2000, Wasting in the Us 2000, Grass Roots Recycling Network, 2001

Stacy Mitchell, "Independent Businesses, Unite!", in In Business, July/August 2003.

Stacey Mitchell, Interview in Multinational Monitor, "New Rules for the New Localism: Favoring Communities, Deterring Corporate Chains", October/November 2002

Stacey Mitchell, The Home Town Advantage: How to Defend Main Street Against Chain Stores and Why It Matters, ILSR, Washington, DC, 2002.

Townsend, T. and C. Kibert, "State Construction/Demolition Debris Issues, "Florida Advisory Committee on Solid and Hazardous Waste, May 1998

Uhlik, F. and C. Kibert, "Residential Construction/Demolition Waste Characterization," Technical Report No. 97, Building Construction Industry Advisory Committee (BCIAC), March 1997

Waste Prevention, Recycling and Composting Options: Lessons from 30 Communities, US EPA, 1994

William Leiss, The Limits to Satisfaction, McGill University, Montreal, 1988.

William McDonough and Michael Braungart, Cradle to Cradle, New Point Press, New York, 2002

U.S. Department of Energy, Energy Information Administration, March 2001, *Monthly Energy Review*

U.S. EPA Office of Air and Radiation, 1989, *Report to Congress on Indoor Air Quality, Volume II: Assessment and Control of Indoor Air Pollution.*

U.S. Department of Energy, Energy Information Administration, "Emissions of Greenhouse Gases in the United States 1999."

U.S. EPA, 1998, "Characterization of Building-Related Construction and Demolition Debris in the United States."

U.S. Geological Service, 1995 data.

40 Code of Federal Regulations (CFR) Part 61 Subpart M, National Emission Standards for Asbestos.

40 Code of Federal Regulations (CFR) Part 61 Subpart M, National Emission Standards for Asbestos, Asbestos NESHAP Clarification of Intent. July 28, 1995.

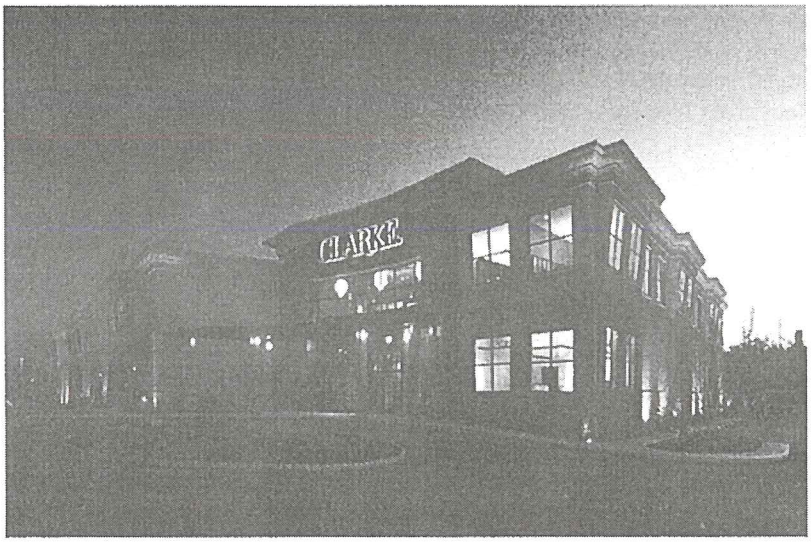

Figure 1: View of the completed Clarke Corporation structure in Milford, MA



Figure 2: View of concrete floor in the Walter Reed Community Center

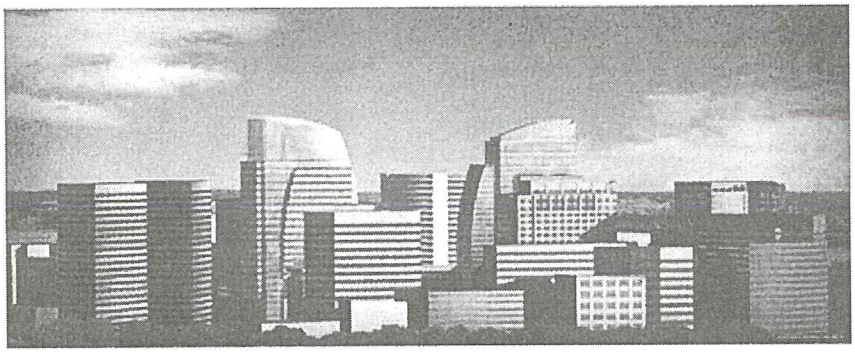

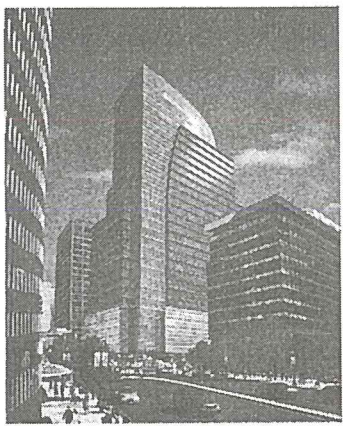

Figure 3: Central Place is illustrated here with its principal features of two tower structures that will be the tallest buildings in Virginia and the Washington DC area.

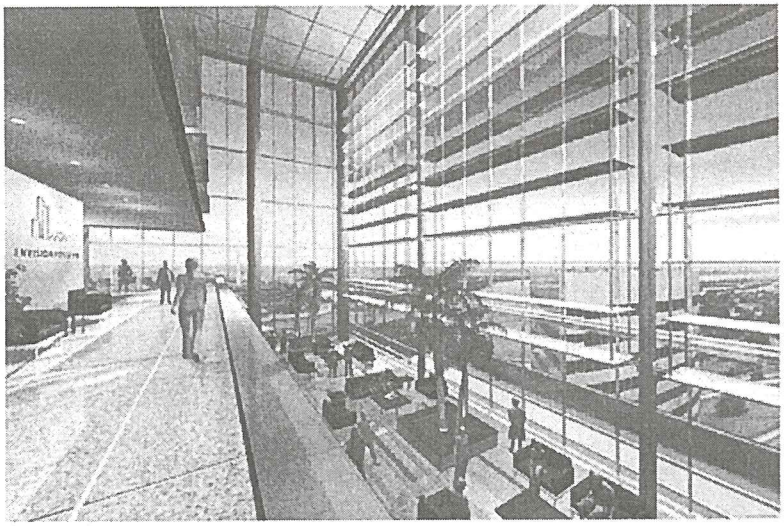

Figure 4: Illustration of the view from the two-level observation deck on the 28th and 29th floors of the Office tower



Figure 5: Landscaped park between the two towers that will be approximately 18,400

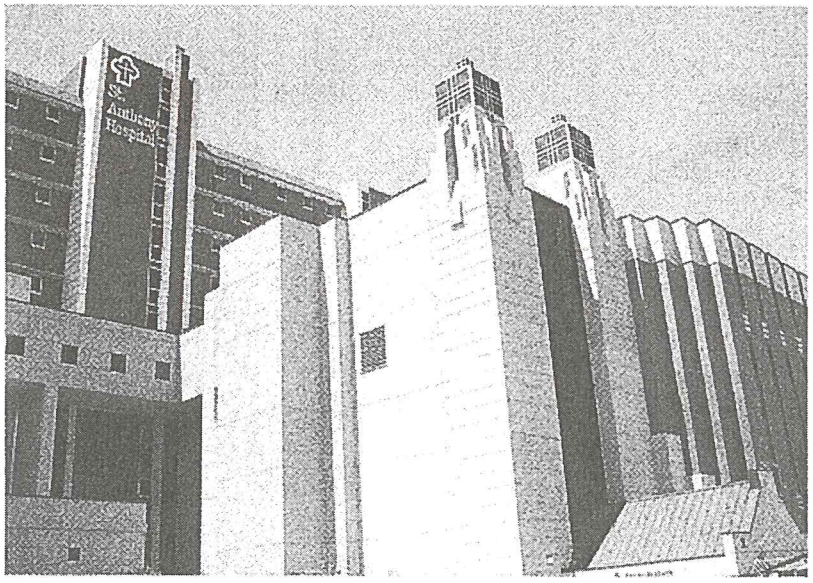

Figure 6: St. Anthony's Hospital in Oklahoma City following completion of their new surgical center



Figure 7: Headquarters building for the Finnish subsidiary of Pfizer Inc.

Earthquake Disaster Mitigation Policy in Japan

by

Koji Ikeuchi[1] and Nobuharu Isago[2]

ABSTRACT

This paper presents the state-of-the-art of earthquake disaster mitigation policy in Japan. The status that Japan is prone to have damage from earthquake is dictated. The outline of large-scale earthquake such as Tokai, Tonankai and Nankai, Japan and Chishima Trench and Tokyo Metropolitan Earthquakes, the result of estimated damage, and the countermeasures such as their general measures, disaster reduction strategy and emergency response plan are also introduced.

KEYWORDS: disaster mitigation, large-scale earthquake, the Central Disaster Management Council, Tokyo Metropolitan Earthquakes

1. INTRODUCTION

People's lives and economical property were greatly lost up to now because numerous large-scale earthquakes and tidal wave (tsunami) happened under the plate and the topographical condition. To protect national land as well as citizen's lives, livelihoods, and property from natural disasters including earthquake is an important national policy.

Along with a series of reforms of the central government system in 2001, the Cabinet Office was established to handle the general affairs which Prime Minister should be in charge. The Cabinet Office performs planning, making and executing of general and important policy. As for the area of disaster management, the Director-General for Disaster Management is mandated for the necessity of unifying the policies among related government organizations. Japan's disaster management system addressed all of the disaster phases of prevention, mitigation and preparedness, emergency response as well as recovery and rehabilitation. With clear roles and responsibilities of national and local governments, the relevant stakeholders of the public and private sectors cooperate in implementing various disaster countermeasures. The Central Disaster Management Council (CDMC) is established in the Cabinet Office based on the Disaster Countermeasures Basic Act. The council, whose chairperson is Prime Minister, promotes comprehensive disaster countermeasures including deliberating important issues on disaster reduction. In this paper, the outline of earthquake disaster mitigation policy in Japan is introduced.

2. EARTHQUAKES IN JAPAN

Figure 1 shows the plate around Japan. Japan locates the peripheral part between oceanic plate (Pacific Plate and Philippine Sea Plate) and inland plate. Pacific Plate sinks under inland plate and Philippine Sea Plate at Chishima Trough, Japan Trough and Izu-Ogasawara Trough. Also Philippine Sea Plate sinks under inland plate at south-western trough, Nankai Trough, Suruga Trough and Sagami Trough. This indicates that Japan, locating on the complex crust structure, has more earthquakes comparing with other countries and have much damage from past earthquakes. The earthquakes over 6 minus of earthquake intensity in Japanese scale happened 13 times (25 times when each aftershock was counted from the Hyogoken Nambu Earthquake in 1995 to the Noto Hanto Earthquake in 2007).

There are two types of large-scale earthquakes which heavy damages were brought. One is the type that occurs near the boundary of plate, and this is divided into the type occurred

[1] Director for Earthquake and Volcanic Disaster Management, Disaster Management Bureau, Cabinet Office, 1-2-2 Kasumigaseki, Chiyoda-ku, Tokyo 100-8969 Japan

[2] Deputy director, ditto

between the plates and the type occurred within oceanic plate. The typical example of earthquake occurred between the plates was the Kanto Earthquake in 1923 and the Nankai Earthquake in 1946. This kind of earthquake occurs when the deformation recovers after the deformation with plate's sinking in reaches its limit. Its frequency is generally said every several hundred years. The Tokai, the Tonankai and Nankai Earthquake occurred in near future are predicted as this type.

The other type is the one in inland shallow area that strain energy is accumulated by deformation of inland plate resulted from plate's sinking in and the energy is released by the disruption of underground fault. The typical example of this kind of earthquake was the Hyogoken Nambu Earthquake in 1995, the Niigataken Chuetsu Earthquake in 2004, and the Noto Hanto Earthquake in 2007.

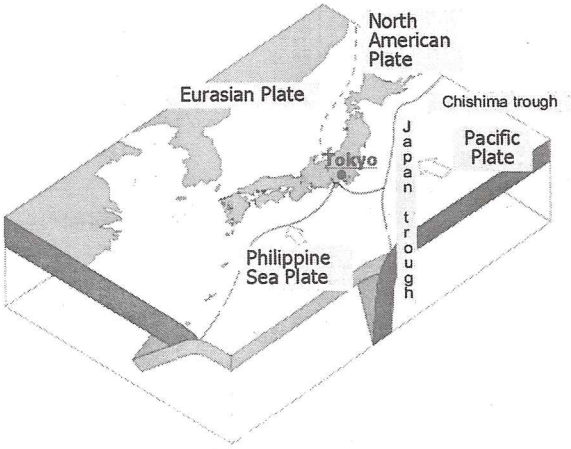

Fig.1 Plates around Japan

3. COUNTERMEASURES AGAINST LARGE-SCALE EARTHQUAKES

The main cause of many casualties in the Hyogoken Nambu Earthquake in 1995 was reported as building collapse and crushed body with it and more than 80% of casualties were resulted from it. The fire around dense area of house also added the number of casualties. In addition, some problems were reported from this disaster such as the delay of quick response to grasp the degree of disaster, that is, the number of casualties and collapsed houses because of insufficient information gathering, severe difficulty of rescue activities for evacuation, life saving and emergency transportation due to the destruction of transportation facilities and heavy traffic congestion, material conveyance, medical activity, voluntary activity, life reconstruction for people requiring assistance during disaster such as elderly.

Various policies have been executed on the basis of past experience. The CDMC has estimated the damage of earthquake and some countermeasures are proposed for the large-scale earthquakes in the next few decades, such as the Tokai Earthquake, Tonankai and Nankai Earthquake, Earthquakes around the Japan and Chishima Trenches, and Tokyo Metropolitan Earthquakes. Figure 2 shows the location of four large-scale earthquakes above mentioned. The outline of countermeasures and so on against these earthquakes is following below.

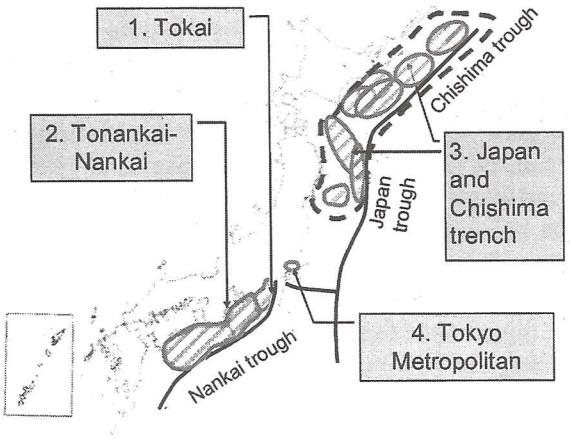

Fig.2 Outline of large-scale earthquakes

3.1 Flow of planning countermeasures against large-scale earthquakes

Figure 3 shows the planning flow of measures for earthquake in government.

Firstly, the area of epicenter and earthquake model is supposed, and the intensity and distribution of earthquake tremor and so on are estimated. Next, the damage of death person

and collapsed buildings are estimated on the basis of earthquake tremor and so on. Following, general measures, in other words, master-plan for mitigating the damage are regulated on the basis of the damage estimate results. Next, strategy by regulating quantitative damage reduction targets and the underpinning measures are decided. Finally, emergency response plan, that is, contingency operation plan for all of governments, including concrete function and the degree of backup are decided.

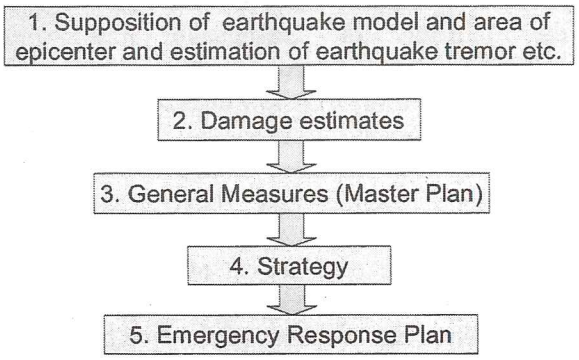

Fig.3 Flow of planning countermeasures against large-scale earthquakes

3.2 Countermeasures for Tokai Earthquake

Figure 4 shows the time history and location relating to the Tokai, the Tonankai and Nankai Earthquake. After the Ansei-Tokai Earthquake in 1854, strain on the earth's crust along Suruga Trough has been building up ever since, approximately 150 years. Therefore, it is believed that there is a high possibility of the Tokai Earthquake occurring.

Under the Act on Special Measures for Large-Scale Earthquake, the mitigation for disaster damage is aimed by designating the areas for intensified measures against the earthquake in advance, where the observation system has been reinforced and earthquake response system in the case of a prediction report being announced has been developed for the large-scale earthquake with a possibility of being predicted just before it occurs.

The Tokai Earthquake is the only one at present with a possibility of being predicted just before it occurs. Therefore, eight prefectures including Shizuoka prefecture which will have most damage in the Tokai Earthquake are designated as the areas for intensified measures under the act.

A death toll of approximately 9,200, total number of collapse or burned houses of 260 thousand and a maximum economic loss of 37 trillion JPY is estimated at the worst case when it occurs.

On the result of damage estimation, the CDMC decided the 'General Measures for Tokai Earthquake,' containing such main issues as 1) implementation of urgent upgrade of seismic resistance measures, 2) reinforcement of community capabilities against disasters, 3) establishment of a tangible disaster management system in the case of a warning declaration and 4) establishment of wide-area management system in occurrence of disaster.

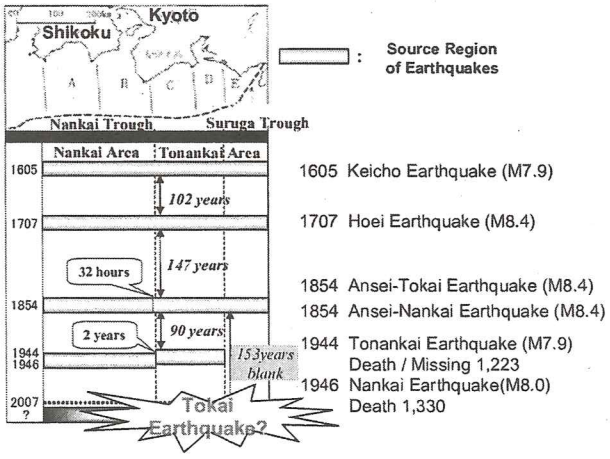

Fig.4 Time history and location relating to Tokai, Tonankai and Nankai Earthquake

As for the 'Tokai Earthquake Disaster Reduction Strategy,' the goal to halve the estimated death toll and economic loss in the next decade is set.

The CDMC also formulated the 'Guidelines for Tokai Earthquake Emergency Response Activities," and the activities of each disaster

management related organization were determined to execute rapid and proper emergency response activities in terms of each level, such as at the time of caution information, warning declaration and disaster occurrence. Furthermore, a detailed plan of action was decided to designate the content of concrete activities for emergency operations such as search and rescue, firefighting and medical activities, procurement of material, and transportation activities. In this detailed plan, two types of plan are made; one is predictive type when the prepared activities would be finished between the warning declaration and occurrence of earthquake, and the other is sudden type when no warning declaration is made and the earthquake occurs suddenly.

Start of emergency response after grasping the damage situation will be late when big disaster happens. For the Tokai Earthquake, in advance, that is, before disaster, the concrete and detailed plan of activity including the contents and volume of dispatch and material are set on the result of damage estimate to cope with that. Just after big disaster, preparing dispatch and procurement of material is started on the basis of this plan, and emergency response about rescue and medical activity is executed. Activity content will be amended after obtaining information.

3.3 Countermeasures for Tonankai and Nankai Earthquake

The Tonankai and Nankai Earthquakes with a magnitude of 8 or so have occurred at intervals of 100 to 150 years as well as the Tokai Earthquake. Most recently, it occurred in 1944 and 1946 respectively, and it is anticipated that the next ones will occur in the first half of this century.

Large damage over the wide area is predicted heavy tremor and big tsunami in the Tonankai and Nankai Earthquake. 'Act on Special Measures for Promotion of Tonankai and Nankai Earthquake Disaster Management' was regulated to advance the countermeasure for disaster management steadily.

Under the act, promoted area to advance the countermeasure for reduction of damage is designated and the set-up of the plan including the evacuation measure from tsunami and the arrangement of the facilities including observation site are regulated.

It is said that the maximum risk of death may be approximately 18,000, of which about 8,600 may be attributable to tsunamis. Total number of collapse or burned houses of 360 thousand and a maximum economic loss of 57 trillion JPY is estimated at the worst case when it occurs.

The general measures, the disaster reduction strategy and the guidelines for emergency response activities are decided. Concrete plan for activities were shown in the Secretary Organization of the CDMC in March, 2007.

3.4 Countermeasures for Trench-type Earthquakes in the Vicinity of the Japan and Chishima Trenches

There have been many large-scale earthquakes of magnitude 7 or 8 scale with plate's sinking occurring in the vicinity of the Japan Trench, extending in the oceanic areas from off of eastern Chiba to Sanriku, and in the vicinity of the Chishima Trench, extending from the areas off Sanrinku, Tokachi and Etrofu Island. There are many damages of tsunami, such as the Meiji Sanriku Earthquake in 1896 with casualties of 22 thousand and the Syowa-Sanriku Earthquake in 1933 with 3 thousands of death or missing people.

There are many type of earthquakes occurred in the vicinity of plates or inside the plate. Also, so-called 'tsunami earthquake' which did not have so heavy tremor but bring much damage by tsunami happened. The Miyagiken-oki Earthquake is said to occur at intervals of approximately 40 years and imminence of earthquake occurrence is pointed out in this area.

It is said that the maximum risk of death may be approximately 2,700 in the type of the Meiji Sanriku Earthquake, total number of collapse or burned houses of 21 thousand and a maximum

economic loss of 1.3 trillion JPY is estimated in the type of the Miyagiken-oki Earthquake. The general measures for this earthquake focusing on issues such as the promotion of tsunami disaster countermeasures, the construction of towns capable of withstanding tremors and addressing problems unique to snowy and cold areas, is decided. In addition, the guidelines for emergency response activities are decided.

3.5 Countermeasures for Tokyo Metropolitan Earthquakes

In the capital area around Tokyo, the Kanto Earthquake occurred in 1923 and brought heavy damage. The earthquake with magnitude 8 or so like the Kanto Earthquake occurs every 200 or 300 years in the boundary of plate around the Sagami Trough, extending from the Sagami Bay in southeast direction. The next earthquake with same level will be expected to occur after 100 or 200 years, however, some earthquakes with magnitude 7 or so may happen in southern Kanto area during this period.

Figure 5 shows the distribution of collapsed buildings due to seismic activity in Tokyo Metropolitan Earthquakes. In the worst case, 11 thousand of casualties, total number of collapse or burned houses of 850 thousand and a maximum economic loss of 112 trillion JPY are assumed. On the basis of the result, 'General Measures for Tokyo Metropolitan Earthquakes' for each entity's countermeasure in all of stages, from prevention stage to post-earthquake stage. In metropolitan area, the core functions such as government, administration, business are highly accumulated and a number of buildings and population are concentrated. To secure the continuity of capital functions such as politics, administration, business and economy function in essential for the countermeasure of wide-area disaster emergency response crossing over prefectures should be solved when big earthquake occurs in this area.

Figure 6 shows the outline of 'Tokyo Metropolitan Earthquakes Disaster Reduction Strategy.' Disaster reduction goal such as to halve the estimated death toll and to reduce the estimated economic loss by 40% in ten years is set through upgrade of seismic resistance of houses and buildings, fix of household furniture, improvement of densely populated urban area, nourishment of voluntary disaster management organization, reinforcement of transportation facilities and promotion of tackling business continuity.

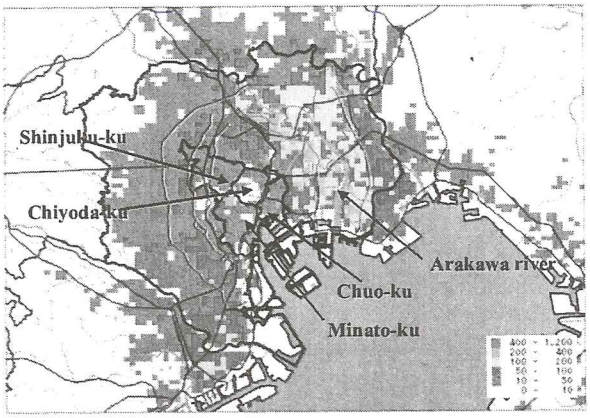

Fig.5 Distribution of collapsed buildings due to seismic activity in Tokyo Metropolitan Earthquakes

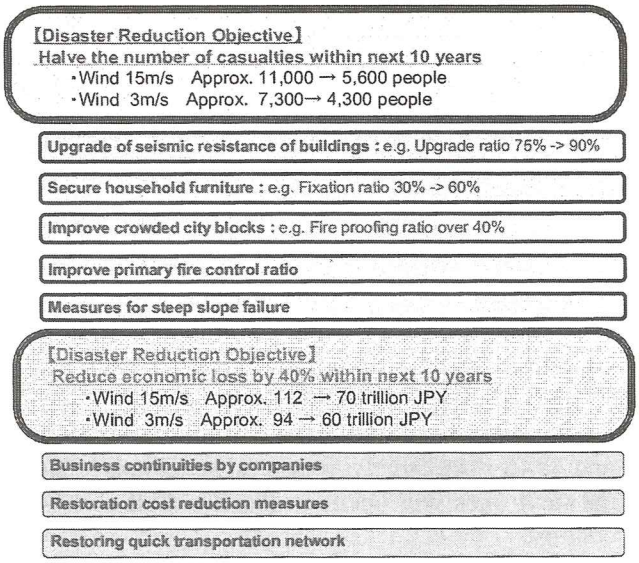

Fig.6 Outline of Tokyo Metropolitan Earthquakes Disaster Reduction Strategy

To execute emergency response activity properly and rapidly by related organizations for Tokyo Metropolitan Earthquakes, 'Guidelines for Tokyo Metropolitan Earthquakes Emergency

Response Plan' which regulates the contents for emergency activity, procedures and role for each related organization is decided. This regulates contingency operation plan for all of organizations in disaster.
The main contents are as follows;
1) Priority for setting place of establishment of emergency disaster management headquarter
2) Priority for setting place of establishment of local emergency disaster management headquarter
3) Act for maintaining business continuity for metropolitan function
4) Act for emergency rescue such as rescue, aid, medical and fire-fighting activity, procurement of food and water, and securing traffic for emergency transportation

The discussion and the examination of detailed plan of activity are in progress for the Tokyo Metropolitan Earthquakes.

Massive number of evacuees and people stranded without a means of returning home is estimated in this earthquake. In the general measures, the countermeasure is shown such as reducing evacuees to evacuation site, arrangement of evacuation system, secure of food, water and daily necessities, showing of proposal menu of emergency house and means of supporting evacuees. The measure for people stranded without a means of returning home, reducing the number of people's returning to their home is shown. Concrete countermeasure for this is stated as the problem which should be solved in near future in the disaster reduction strategy, so the committees for technical investigation on evacuation measures and so on for the Tokyo Metropolitan Earthquakes is set in the CDMC and discuss the matters.

3.6 Construction of Integrated Disaster Management Information System
Preparing the concrete measure when disaster happens is also important. In Cabinet Office, the Disaster Information Systems is arranged. This system can estimate the number of death person and complete collapsed buildings automatically on the basis of measured earthquake intensity, within 30 minutes. The result is offered to all of other ministries and this information is considered useful and important for initial response just after the occurrence of earthquake. Figure 7 shows the result of prediction of earthquake intensity distribution in the Niigataken Chuuetsu Earthquake.

Also, the 'Disaster information sharing platform' is now constructed. This system can integrate and see all of disaster information from other ministries on the common map using GIS concept. Up to now, this platform is linked with the system such as weather information, seismic intensity information, river information and lifeline status information in metropolitan area and all of the information above can be visible. The increase of the contents in coordination with other ministries such as medical information, or satellite picture will be continued. However, there are many problems to process this policy because the data in disaster is difficult to maintain their accuracy and security.

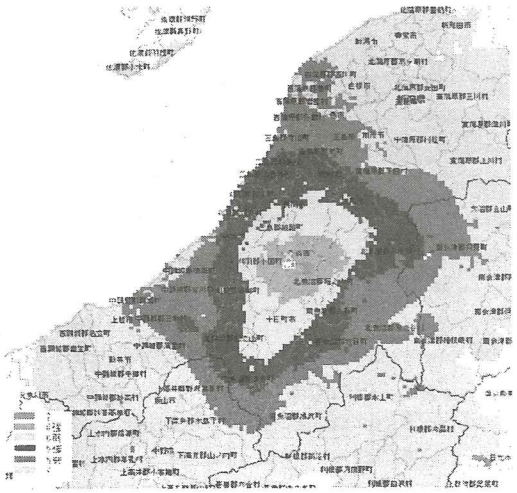

Fig.7 Result of prediction of earthquake intensity distribution in Niigataken Chuuetsu Earthquake from DIS

4. CONCLUSIONS

The outline of the disaster mitigation policy in Japan was introduced in this paper.

Large-scale earthquake may happen anytime, anywhere in Japan and everyone could have the damage from disaster. National people, community, company and government have strongly tackled with measures for safety. The countermeasure against natural disaster will be accelerated by adding the knowledge from various areas.

5. REFERENCES

1. Cabinet Office, Disaster Management in Japan. 2007

The Public Health Perspective on Hazard Reductions in Indoor Environments

by

Fuyuen Yip[1], Paul Garbe[1], and Josephine Malilay[1]

ABSTRACT

In the effort to define and develop the "Next Generation Building", a holistic approach is needed to design and develop structures that are not only capable of withstanding natural disasters and other major hazards, but can also provide an indoor environment in which the occupant is protected from injury, disease, and harmful environmental exposures. This paper describes key factors that are important in understanding the relationship between the indoor environment and human safety and health.

KEYWORDS: public health, indoor environment, safety, prevention, research

1.0 INTRODUCTION

People spend over 85% of their day indoors, and sensitive and susceptible populations spend even more time indoors[1,2]. There is compelling evidence demonstrating the relationship between the indoor environment and the health and well-being of the occupants. There has also been growing interest on the impact of the indoor environment on health at the Centers for Disease Control and Prevention (CDC) and the Office of the US Surgeon General. As part of the CDC Goals Initiative and an effort to develop a Surgeon General's *Call to Action* document on a healthy indoor environment, both agencies aim to link the importance of a healthy indoor environment with respect to factors such as prevention and eliminating health disparities. They also aim to inform the American people of the science, evidence, and data to improve their understanding of, and appreciation for, a healthy indoor environment.

The improvement of indoor environments in the "Next Generation Building" also works in concert with the Healthy Homes and Healthy Communities agenda outlined in *Healthy People 2010*, which serves as a prevention framework the US[3]. The document highlights national health objectives designed to identify the most significant preventable threats to health and to establish national goals to reduce these threats. There are specific national objectives that aim to improve office indoor air quality and to reduce exposures to indoor pollutants including allergens and radon.

The dialogue to improve the understanding of the indoor environment on human health, however, should not be confined to those in public health. It is important for all building professionals to recognize the complex linkages surrounding integrated building research, design, and human health.

2.0 HEALTHY BUILDINGS

A healthy building, from a public health perspective, can be defined as one that is sited, designed, built, maintained, and renovated to support the health of its occupants. Additionally, the sustainability of the building, in the context of potential impacts resulting from climate change, is

[1] Centers for Disease Control and Prevention, Atlanta, Georgia, 30333 USA

an important consideration. There are numerous indoor impacts and hazards that can affect people's health; three key features will be highlighted: (1) safety factors, (2) building design, and (3) environmental factors.

2.1 Safety factors

The main goal with respect to building safety factors is to prevent unintentional injuries. It is estimated that 8000 deaths[4] and 12 million nonfatal injuries occur in US housing annually[5]. Injury from fires, hypothermia and hyperthermia illness, and falls are commonly reported. It is estimated, for example, that among the nearly 400,000 US residential fires in 2005 in which the fire departments responded, 3,030 deaths resulted; the most accurate predictor of death was the absence of a smoke alarm[6,7]. Similarly, hyperthermia and hypothermia are highly preventable with the proper cooling and heating in indoor environments. Falls are also extremely preventable if buildings meet code standards. These examples of preventable unintentional injuries are intrinsically tied to building design and public awareness.

Safety factors and considerations can also include the ability of new building materials to perform and confer protection during hazard events. With the increasing demand to integrate sustainable and other new materials into construction practices, it is important to consider their safety and durability, as well as their ability to protect the occupants.

2.2 Building design

There are three critical areas of public health with respect to building design: accessibility, ventilation, and dampness.

Accessibility is directly impacted by affordability, community design, building code standards, and overall building design. It is estimated that 5.5 million people with a disability face barriers to participation in buildings because of design or absence of sidewalks[8]. Building accessibility needs to work in concert with community design and can be achieved by emphasizing the interactions between the building structure and occupant behaviors.

Ventilation is an important building characteristic as it directly affects an occupant's sense of comfort, perceived air quality, and health[9]. If not designed, installed, maintained or operated properly, ventilation can have harmful effects on the indoor environment. Some pollutant levels measured indoors are 2–10 times greater than those measured outdoors[10,11]. Recent research on building ventilation and filtration suggest that reduced infiltration of outdoor particulate matter indoors can improve health and economic gain[12]. It is also estimated that tens of thousands of premature deaths in the developed world can be reduced annually through the use of improved mechanical ventilation systems with proper supply air filtering in buildings[13].

Dampness is known to influence conditions for mold growth, which is a risk factor for health effects, especially respiratory disease[14]. In extreme hazard events, such as Hurricanes Katrina and Rita in 2005, an extraordinary growth of mold and presence of endotoxin and glucans were observed at levels associated with health effects[15]. Building materials that reduce or minimize the water-holding capacity of buildings and inadequate ventilation have been cited to strongly influence indoor

dampness. Adapting and integrating sensor technology, such as those used to monitor the structural wellness of buildings, to monitor moisture in the walls and ventilation systems can be helpful as an early detection system to prevent health effects commonly associated with indoor dampness. Use of materials that can effectively minimize or retard mold growth can also be helpful in reducing exposures and potential effects, especially during hazard events.

2.3 Environmental exposures

Occupant protection from indoor environmental exposures often fall under two categories: chemical and biologic exposures. These exposures are ubiquitous and individuals can become exposed through inhalation, ingestion, and dermal contact. Some common health symptoms often associated with these exposures include allergy-like symptoms, headaches, shortness of breath, and disease[16]. A main concern regarding these particular indoor environmental exposures is that the dose impacting health is still not clearly understood. The synergistic or additive effects of chemical mixtures and toxicity of microorganisms also need to be studied further.

2.3.1 Outdoor and indoor chemical exposures

Chemical exposures from the outdoor environment commonly enter the building through the HVAC systems or leaks in the building envelope. Outdoor pollutants including traffic emissions and biomass burning (e.g., wildfires), which constitute numerous pollutants including particulate matter, volatile organic compounds, and soot, have been shown to impact health[17,18]. A recent study in California observed that homes near heavy traffic can affect lung development in children[19]. While proximity to heavy traffic is difficult to avoid with the increasing growth of our communities, changes in siting requirements or measures to minimize outdoor air indoors may assist in reducing exposures.

Ozone is another ambient pollutant that can infiltrate into the indoor environment, but the amount of ozone that infiltrates into the indoors or other micro-environments (e.g., vehicles) is affected by factors such as the frequency in which windows are opened and the use of air conditioning. Daily inhalation intake of indoor ozone may range from 25%–60% total ozone intake[20]. Short-term exposures to ozone have been associated with an increase in daily mortality as well as cardiovascular and respiratory hospitalizations[21,22]. There is also data that suggests that excess morbidity and mortality from ozone is still occurring at and below the current US national standard[23,24]. Building design and ventilation, therefore, can play a role in reducing exposures indoors.

Sources of ozone can also be found indoors such as from laser printers and photocopiers[25]. Other common indoor sources that can also impact an occupant's exposure include products that emit irritants such as building materials and cleaning agents. Lead-based paint, pesticides, and combustion sources such as carbon monoxide, biomass burning from indoor cooking, and environmental tobacco smoke are also indoor sources that are known to elicit health effects.

Building materials can also emit chemicals. Formaldehyde, for example, is commonly emitted by pressed wood products and cleaners. It is known to cause cancer with chronic exposures[26]. These exposures can also impact the respiratory system, especially among the growing population with chemical sensitivities. Developing materials that produce little to no emissions will therefore be critical in reducing potential exposures and minimizing health effects.

2.3.2 Outdoor and indoor biologic exposures

Biologic exposures in indoor environments, including exposures to allergens, viruses, bacteria, and fungi, are also of concern as they are known to cause various health symptoms and effects. Allergens, for example, include pet dander, cockroach antigen, and pollen. It is well understood that allergens can exacerbate asthma symptoms after repeated exposures[27]. Viruses and bacteria are also of concern and these sources are primarily from building occupants. Efforts have been made to reduce transmission of exposures in the indoor environment. Fungi are also known to serve as allergens, toxins, and infectious agents[28].

An occupant's exposure to biologic and chemical sources can therefore be impacted by many factors. These factors include emission rates of specific sources and building system characteristics such as the efficiency of the HVAC system. Temperature and humidity also play an important role in one's sense of comfort as well as in promoting mold growth. Physical factors, such as furniture placement, human activities, and behaviors can also greatly influence exposures and need to be considered when designing a healthy building.

In the design process, tools such as Geographical Information Systems (GIS) can be extremely helpful in constructing the physical environment within a building. GIS can overlay biological and physical processes, as well as simulate ecosystems to predict the effects of hazards and exposures on health-related outcomes such as physical comfort and security. More specifically, GIS may assist in depicting a representation of exposures that may affect the respiratory health and safety of building occupants. For example, GIS can be used to predict indoor air quality using different ventilation systems and various air cleaning materials, chemicals, or devices. At another level, GIS applications can provide information on emissions-producing structures, highways, and landfills and their releases within a specified perimeter of a particular building over a specified time period.

3.0 RESEARCH GAPS

While there has been considerable progress in studying the relationship between specific outdoor air pollutants and health as well as exposures in occupational settings, gaps still exist in understanding the relationship between indoor environments and health. More specifically, gaps remain in characterizing dose-response relationships for exposures in indoor environments. Target levels for indoor pollution levels for occupancy need to be more clearly defined. In turn, collaborative efforts to identify methods to reduce the risk through actions such as material substitution, encapsulation, or

dilution through ventilation can then be achieved.

This process is extremely complex; considerations such as behavioral and social factors as well as individual susceptibilities need to be made. Populations who are most at risk for disease and disability from indoor hazards also need to be better addressed.

With the changing environment, there is also an urgency to evaluate the potential impacts of climate change (i.e., increasing temperatures, increasing pollen production, rising sea levels, and increasing number of severe storms) not only on the building structure, but also on the indoor environment and human health. The increased awareness of global climate change has led to a growing movement in the development of green buildings and the use of more sustainable materials. While there is encouragement to use products that emit zero to low levels of emissions, a need still remains to improve our understanding of new material properties with respect to performance, durability, and potential acute and chronic health impacts. Additionally, the impact of climate change on potential energy shortages and increasing prices can also affect the provision of ventilation, thermal control, and humidity control by mechanical systems as these features may become less reliable or less available[29].

As we find new methods to reduce energy use, it will be important to evaluate the potential impact of low energy buildings and indoor air quality on health. Sustainable design will continue to be incorporated in building practices. Accordingly, we believe that it would be important and informative to quantify the amount of gain in health as buildings improve as well as study the effect of the indoor environment over the lifetime of an individual. From this, we can learn how to create healthier environments and issues such as health and productivity can be better evaluated.

4.0 NEXT STEPS

CDC can play a key role in filling some of the gaps in understanding the relationship between the indoor environment and human health through surveillance, inter-disciplinary training and health communication; however, additional support from other building professionals including engineers, developers, and architects will also be important. For the "Next Generation Building", we are faced with the challenge to not only produce a healthy and high quality indoor environment, but an environment that can work in concert with fire, seismic, and wind safety.

There is groundwork for collaborative work to design the "Next Generation Building" through the following efforts:

- Developing sensor technology to monitor the indoor environment
- Using GIS for modeling exposures indoors which can assist in building design
- Developing and improving materials that can not only withstand outdoor environmental hazards, but can also prevent the growth or generation of indoor environmental hazards
- Creating low energy and sustainable buildings that provide a comfortable and healthy environment for its occupants.

As we continue to develop our understanding of indoor environments and its impact on human health, we find it key to foster an inter-disciplinary partnership at the international, federal, state and local level.

5.0 REFERENCES

[1] Jenkins P, Phillips T, Mulberg E, Hui S. (1992) Activity patterns of Californians. Use of and proximity to indoor pollutant sources. Atmos Environ. 26A:2141-2148.

[2] Klepis N, Nelson W, Ott W, Robinson J, et al. (2001) The National Human Activity Pattern Survey (NHAPS): A resource for assessing exposure to environmental pollutants. . J Exp Anal Environ Epidemiol. 11:231-252.

[3] http://www.healthypeople.gov/; Accessed April 9, 2007.

[4] Nagaraja I, Menkedick J, Phelan KJ, Ashley P, Zhang X and Lanphear B. (2005) Deaths from residential injuries in US children and adolescents, 1985-1987. Pediatrics 116:454-461.

[5] Phelan K, Khoury J, Kalkwarf H and Lanphear B. (2005) Residential injuries in US children and adolescents. Public Health Reports.120:63-70.

[6] Karter MJ. Fire loss in the United States during 2005. (2006) Quincy (MA): National Fire Protection Association, Fire Analysis and Research Division.

[7] Roberts I. (1996) Injury Prevention 2:263-265

[8] Hendershot G. "Building Design is Leading Barrier to Community Participation," Available at: http://www.nod.org/index.cfm?fuseaction=page.viewPage&PageID=1247. Accessed January 15, 2007.

[9] Seppanen OA, Fisk WJ. (2004) Summary of human responses to ventilation. Indoor Air. 14 Suppl 7:102-18.

[10] Wallace, L. (1987) The TEAM study: summary and analysis Vol 1. Washing DC, USEPA; EPA 600/6-87/002a, NTIS, PB 88-100060.

[11] Cyrys J, Pitz M, Bischof W, Wichmann H, Heinrich J. (2004) Relationship between indoor and outdoor levels of fine particle mass, particle number concentrations and black smoke under different ventilation conditions. J Exp Anal Environ Epidemiol.14: 275–283

[12] Sultan ZM. (2007) Estimates of associated outdoor particulate matter health risk and costs reductions from alternative building, ventilation and filtration scenarios. Sci Total Environ. 277: 1-11.

[13] Hanninen OO, Palonen J, Tuomisto JT, Yli-Tuomi T, et al. (2005) Reduction potential of urban PM2.5 mortality risk using modern ventilation systems in buildings. Indoor Air. 15: 246-56.

[14] Bornehag CG, Sundell J, Bonini S, Custovic A, Malmberg P, et al. (2004) Dampness in buildings as a risk foractor for health effects, EUROEXPO: a multidisciplinary review of the literature (1998-2000) on dampness and mite exposure in buildings and health effects. Indoor Air. 14:243-57.

[15] Rao CY, Riggs MA, Chew GL, Muilenberg ML, Thorne PS, et al. (2007) Characterization of airborn molds, endotoxins, and glucans in homes in New Orleans after Hurricanes Katrina and Rita. Appl Environ Microbiol. 73:1630-4.

[16] Samet J, Marbury M, Spengler J. (1987) Health effects and sources of air pollution. Part I. Am Rev Respir Dis. 136:1486-508.

[17] Otto D, Molhave L, Rose G, Hudnell H, House D. (1990). Neurobehavioral

and sensory irritant effects of controlled exposure to a complex mixture of volatile organic compounds. Neurotoxicol Teratol. 12:649-52.

[18] Oezkaynak H, Xue J, Weker R, Butler D, Koutrakis P. (1996) Particle TEAM (PTEAM) Study: Analysis of the Data. NASA no. 19980007226.

[19] Gauderman W, Vora H, McConnell R, Berhane K, Gilliand F, et al. (2007) Effect of exposure to traffic on lung development from 10 to 18 years of age: a cohort study. Lancet 369:571-577.

[20] Weschler CJ. (2006) Ozone's impact on public health: contribution from indoor exposures to ozone and products of ozone-initiated chemistry.

[21] Bell, ML, McDermott A, Zeger SL, Samet JM, Dominici F. (2004) Ozone and short-term mortality in 95 US urban communities, 1987-2000. JAMA. 292: 2372-8.

[22] Lipfert FW and Hammerstrom T. (1992) Temporal patterns in air pollution and hospital admissions. Environ Res. 59: 374-99.

[23] Bell ML, Peng RD, Dominici F. (2006) The exposure-response curve for ozone and risk of mortality and the adequacy of current ozone regulations. Environ Health Perspect. 111(1): p. 45-51.

[24] Vedal S, Brauer M, White R, and Petkau J, (2003) Air pollution and daily mortality in a city with low levels of pollution. Environ Health Perspect. 111(1): p. 45-51.

[25] Wolkoff P, Clausen P, Wilkins C, Nielsen G. (2000) Formation of strong airway irritants in terpene/ozone mixtures. Indoor Air. 10:82-91.

[26] International Agency for Research on Cancer. (2004). IARC Classifies Formaldehyde as Carcinogenic to Humans. Available at: http://www.iarc.fr/ENG/Press_Releases/archives/pr153a.html

[27] Leaderer B, Belanger K, Triche E, Holford T, et al. (2002) Dust mite, cockroach, cat, and dog allergen concentrations in homes of asthmatic children in the northeastern United States: impact of socioeconomic factors and population density. Environ Hlth Perspec. 110: 419-25.

[28] Hardin B, Kelman B, Saxon A. (2003) Adverse human health effects associated with molds in the indoor environment. J Occup Environ Med. 45:470-8.

[29] Levin H. Indoor Environmental Quality in "Next Generation Buildings" US-Japan Workshop, Honolulu, HI, February 2007.

Quick Report on Damage to Infrastructures and Buildings by the 2007 Noto Hanto Earthquake

NILIM, PWRI, BRI and PARI Reconnaissance Team for the 2007 Noto Hanto Earthquake

Overview of Presentation

- Earthquake and ground motions
- Damage to infrastructures
  - Slope failures and rock falls
  - Sewage system
  - Highway bridges
  - Road embankments
  - Port
- Damage to buildings
- Summary

Epicenter and Affected Region



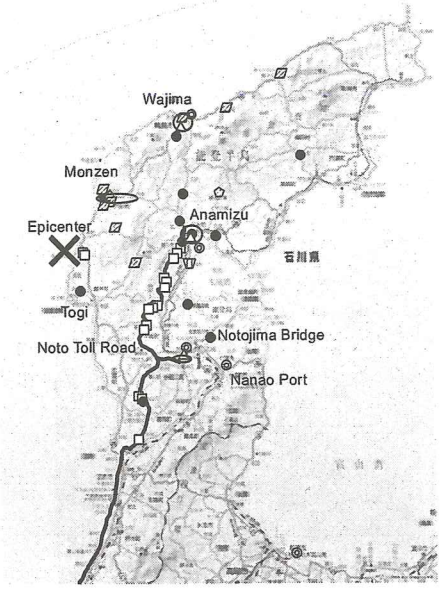

Overview of Earthquake and Damage

- Origin time: 9:42 am, March 25, 2007 (JST)
- Epicenter: West off Noto Peninsula
- Magnitude: 6.9
- Focal depth: 11km
- Maximum seismic intensity: 6 upper
- Casualty: 1, Injured: 336
- Destroyed houses: 593, Partially destroyed houses: 1,206, Partially damaged houses: 10,889

▪ Fire Defense Agency

Past Earthquakes and Probability of Occurring Seismic Intensity of 6 upper or Greater in 30 Years from 2006

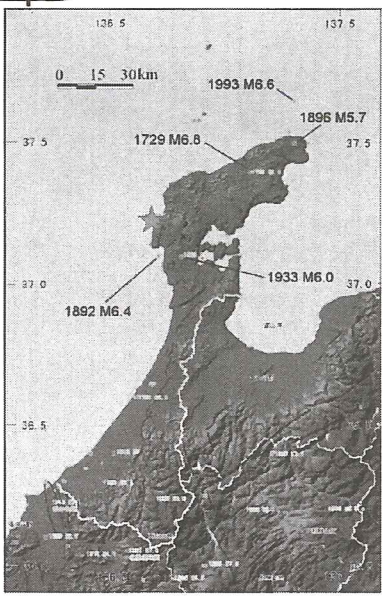

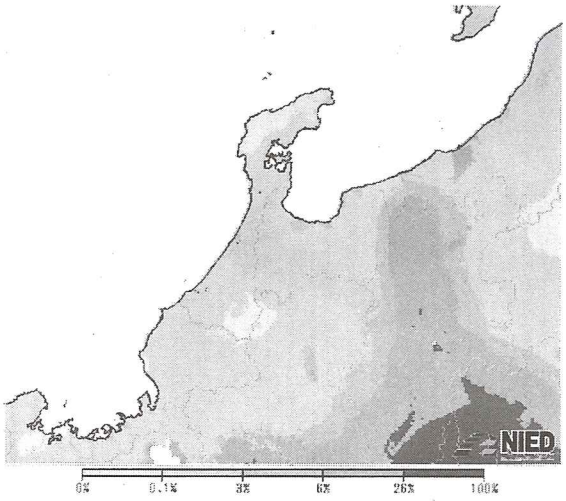

Distribution of Seismic Intensity

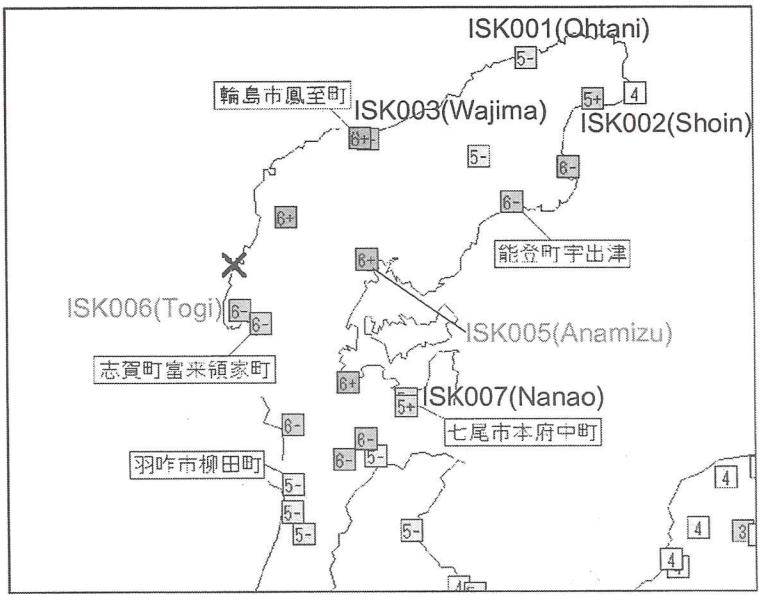

Ground Motions and Acceleration Response Spectra

ISK005(Anamizu)

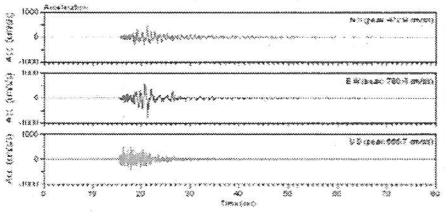

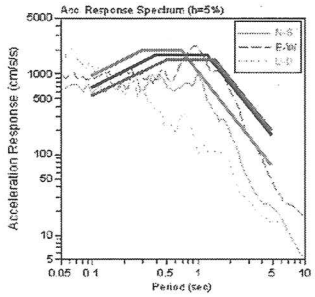

2007/03/25 09:41:47, Site: ISK005, JMA Intensity: 5.3

ISK006(Togi)

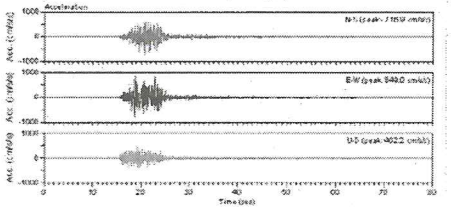

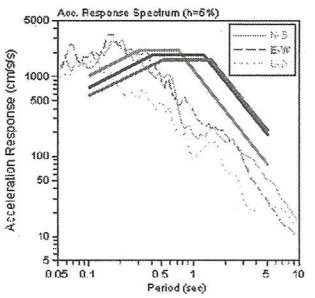

2007/03/25 09:41:45, Site: ISK006, JMA Intensity: 5.3

Rock Shed, Sosogi, National Highway Route 249

- Rock failure: 10m long x 30m wide

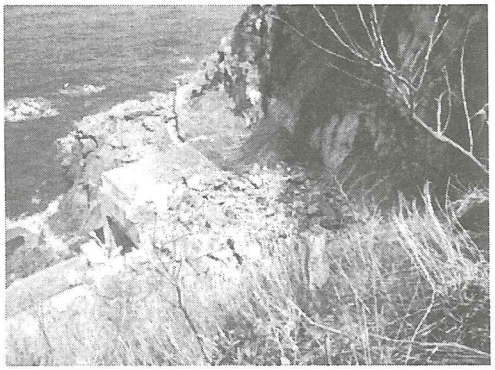

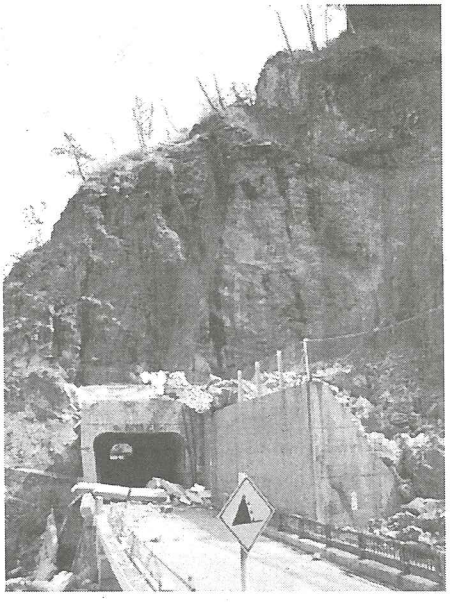

Rock Fall, Shibuta, National Highway Route 249

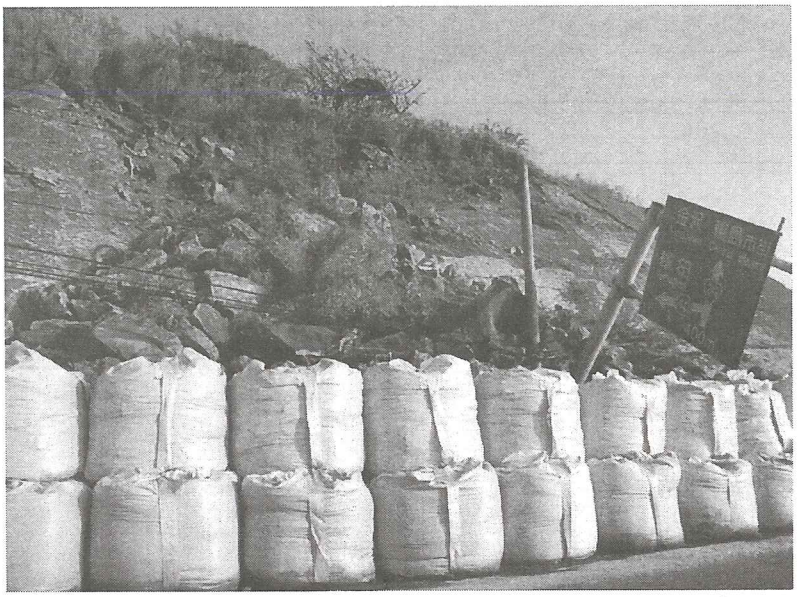

Uplift of Manhole, Monzen, Wajima City

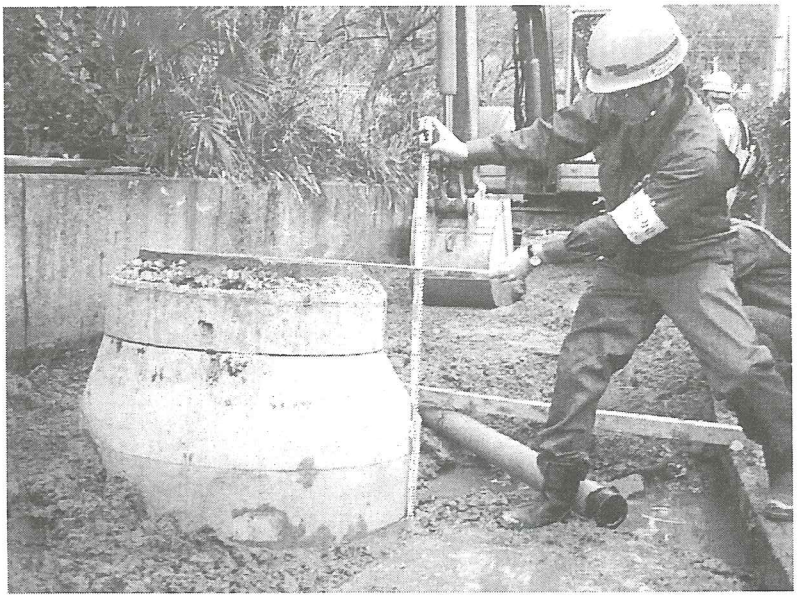

Settlement of Road Surface and Backfill of Sewage Pipe, Monzen, Wajima City

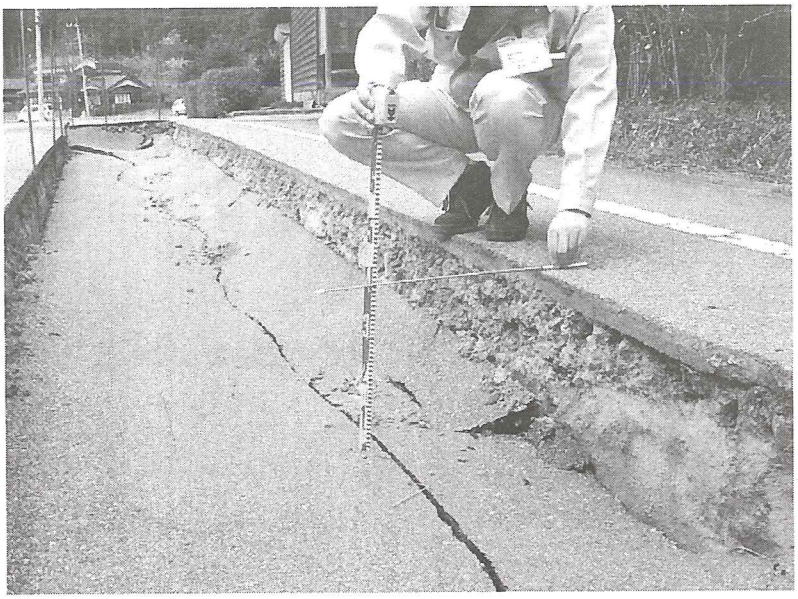

Highway Bridges

- No serious damage to threaten structural safety
- General types of damage found during past earthquakes
  - Crack and spalling-off of cover concrete of RC column
  - Failure of bearing part
  - Crack at girder end by collision
  - Settlement of backfill soil at abutment

Highway Bridge Damage - Notojima Bridge

- 3-span continuous PC frame
- 18-span PCT simply-supported girders
- Bridge length: 1,050m

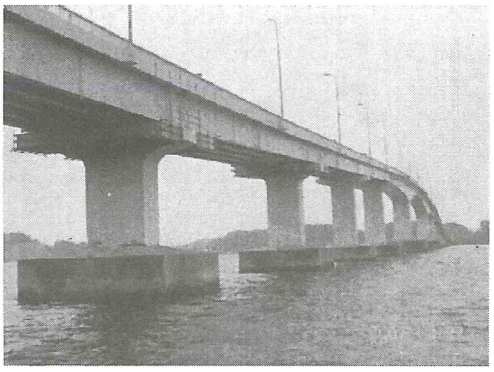



- Damage at the bottom of Pier No.7

Highway Bridge Damage - Other Damage

- Settlement of backfill soil (Noto Bridge, Right)
- Damage to expansion joint

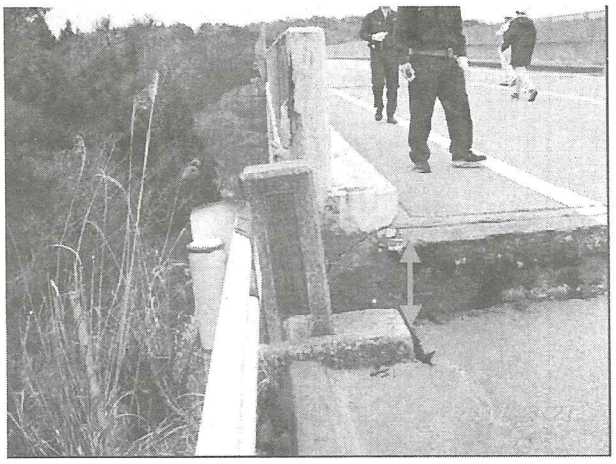

Failure of Road Embankment, Toyota (H=30m), Noto Toll Road

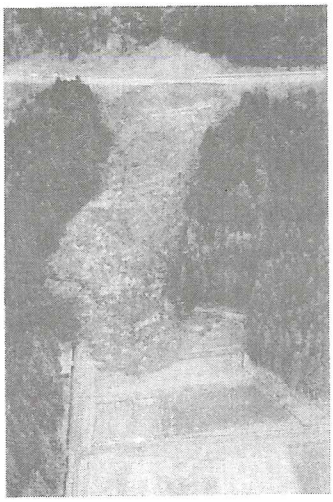

Aerial view

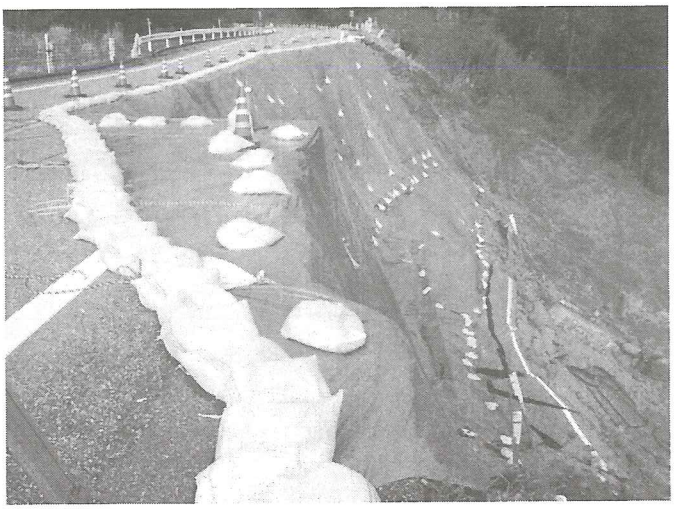

Close view

Failure of Road Embankment, Besho-dake SA (H=35m), Noto Toll Road



Aerial view



Close view

Schematic Mechanism of Earthquake-induced Flow Failure

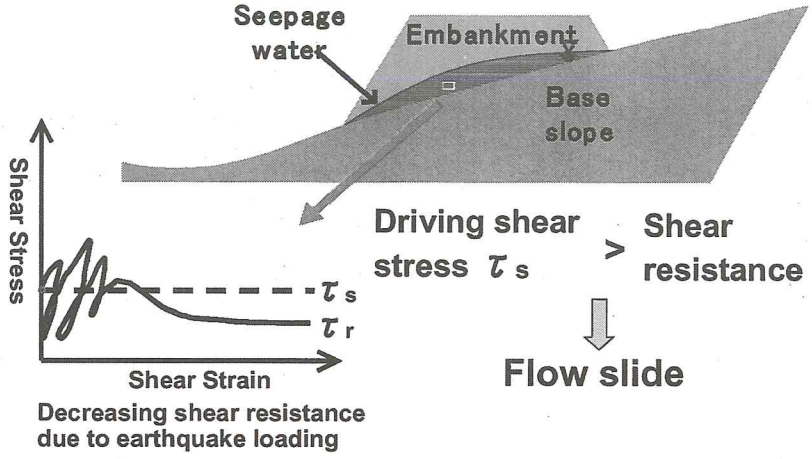

Decreasing shear resistance due to earthquake loading

factors

- Low degree of compaction
- Existence of seepage water in embankments

Nanao Port -10m Sheet Pile Quaywall



Nanao Port -10m Sheet Pile Quaywall, No.1

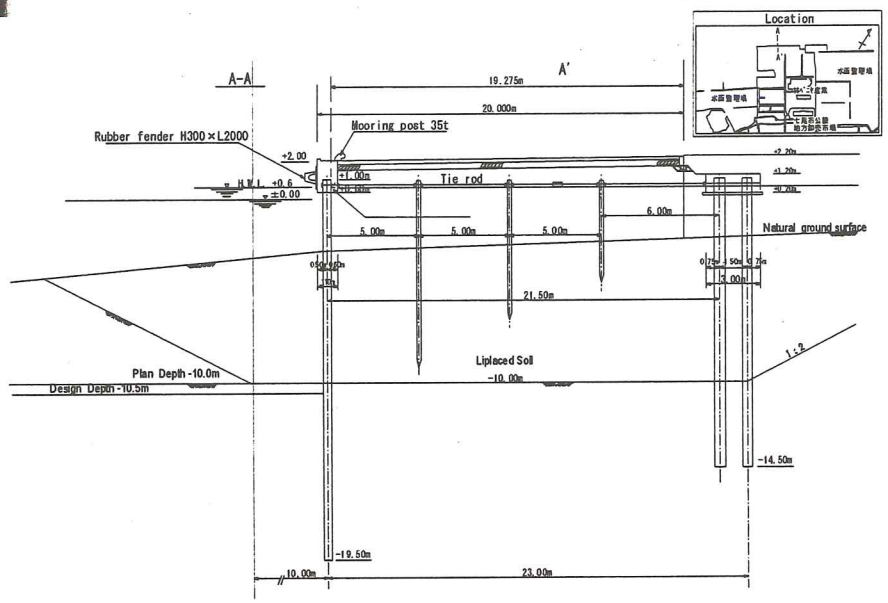

Nanao Port -10m Sheet Pile Quaywall, No.2

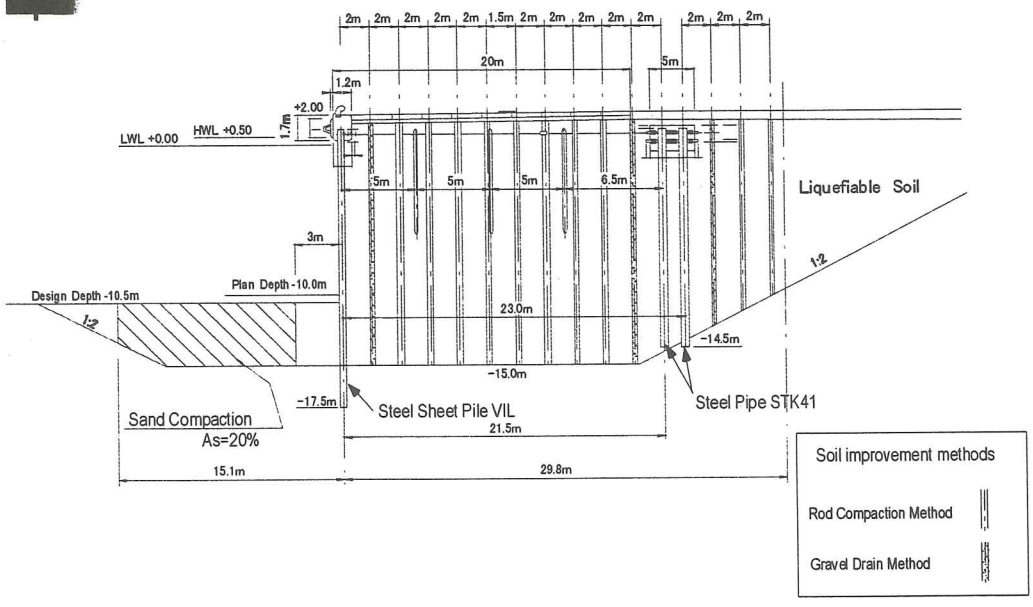

Damage to Wooden Buildings, Monzen, Wajima City

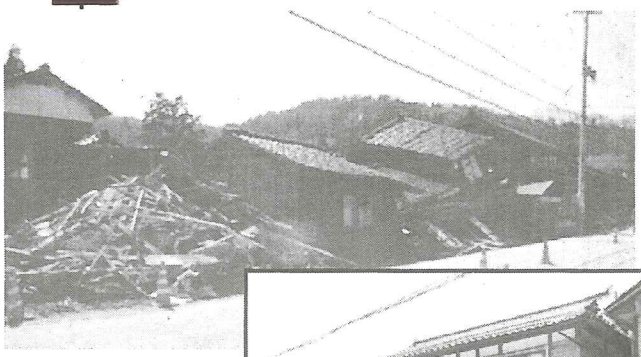



Fall of tomb stones in E-W direction



Retrofitted Monzen District Office Building, Wajima City



Retrofitted by steel braces



JMA 6+
1304 cm/s^2

Damage in office room

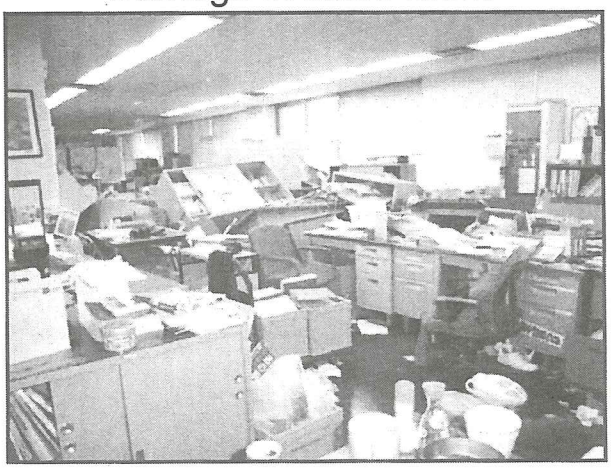

Damage to Ceiling of Gymnasium

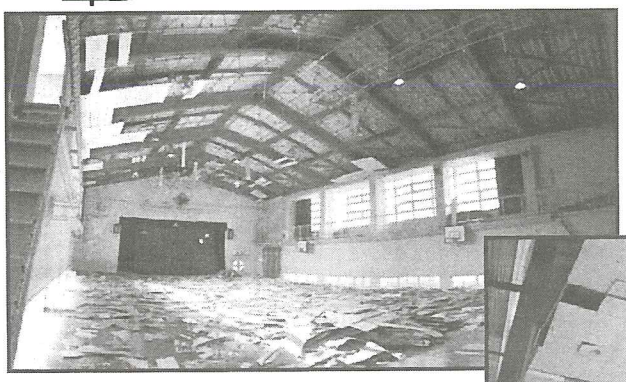

Elementary school
Noto Town
S Roof girder + RC column

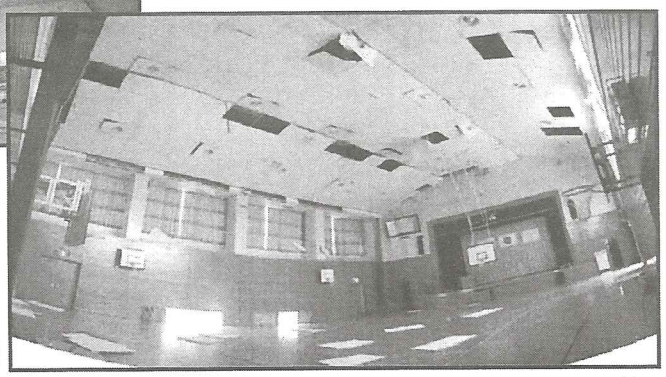

Elementary school
Shika Town
S Roof girder + RC column

Summary

- The earthquake occurred in a seismically inactive region.
- Generated strong ground motions at several locations.
- Induced numerous slope failures and rock falls.
- Among the infrastructures, road embankments constructed by filling valleys were heavily damaged.
- Liquefaction-related damage was rather limited to sewage system and a port.
- In addition to wooden buildings, ceilings of large structures were damaged.

THEME 4

Dams

Seismic Design and Evaluation of Concrete Dams – An Engineering Manual

by

Yusof Ghanaat[1] and Anjana K. Chudgar[2]

ABSTRACT

This paper provides an overview of the US Army Corps of Engineers' guidance for seismic design and evaluation of concrete dams, as presented in the Engineer Manual EM1110-2-6053. The requirements to design and evaluate concrete dams to have a predictable performance for specified levels of seismic hazard are discussed. The seismic input and performance levels associated with serviceability, damage control, and collapse prevention are defined. The analysis and evaluation procedures and acceptance criteria for each performance level are described. They consist of linear and nonlinear procedures for estimation of seismic response and acceptance criteria that use demand-capacity ratios, damage control thresholds, and irrecoverable level of movements and post-earthquake stability condition to assess dam safety. Finally, an example is provided to demonstrate the application of the manual to seismic evaluation of a concrete gravity dam.

KEYWORDS: Seismic design, seismic evaluation, concrete dams, gravity dams, arch dams, linear analysis, nonlinear analysis, joint opening, cracking, sliding displacement

1.0 INTRODUCTION

This paper provides an overview of the US Army Corps of Engineers' guidance for seismic design and evaluation of concrete hydraulic structures, as it relates to concrete dams. The Engineer Manual EM 1110-2-6053 (2007), which will be available shortly, covers seismic design and evaluation requirements for both the plain concrete structures such as dams and for the reinforced concrete structures such as navigation locks, intake/outlet towers, gravity walls, powerhouses, and spillway structures. The structures may be founded on rock, soil, or pile foundations and may or may not have backfill soil. However, only concrete gravity and arch dams will be discussed in this paper.

The manual introduces procedures that show how to design or evaluate a hydraulic structure to have a predictable performance for specified levels of seismic hazard. It states that the traditional design and evaluation procedures may still be used for feasibility and screening purposes. However, seismic design and evaluation of critical facilities should follow the procedures presented in the manual. The manual sets forth a set of requirements to prevent sudden collapse even though the structure may suffer severe damage, to limit damage to a repairable level, or to maintain functionality immediately after the earthquake.

2.0 DESIGN AND EVALUATION CRITERIA

The overall process of seismic design and evaluation of concrete dams consist of the following steps: development of design earthquakes and associated ground motions, establishment of performance levels and performance goals, analysis methodology for computation of seismic response, and interpretation and evaluation of results to assess dam safety. These steps are briefly described below followed by an example problem.

2.1 Design Earthquakes

Earthquake ground motions for the design and evaluation of the US Army Corps of Engineers' concrete hydraulic structures are the Operating Basis Earthquake (OBE) and the Maximum Design Earthquake (MDE) ground motions. Seismic forces associated with the OBE are considered unusual

[1] President, Quest Structures, 3 Altarinda Road, Suite 203, Orinda, CA 94563 USA yghanaat@QuestStructures.com
[2] Structural Engineer, US Army Corps of Engineers, Cincinnati, OH 45202 USA anjana.k.chudgar@usace.army.mil

loads. Those associated with the MDE are considered extreme loads. Earthquake loads are to be combined with other loads that are expected to be present during routine operations.

2.1.1 Operating Basis Earthquake

The OBE is a level of ground motion that is reasonably expected to occur within the service life of the project, that is, with a 50-percent probability of exceedance during the service life. (This corresponds to a return period of 144 years for a project with a service life of 100 years).

2.1.2 Maximum Design Earthquake

The MDE is the maximum level of ground motion for which a structure is designed or evaluated. As a minimum, for other than critical structures, the MDE ground motion has a 10 percent chance of being exceeded in a 100-year period, (or a 1000-year return period). For critical structures, the MDE ground motion is the same as the maximum credible earthquake (MCE) ground motion. Critical structures, by ER 1110-2-1806 definition, are structures that are part of a high hazard project and whose failure will result in loss of life. The MCE is defined as the largest earthquake that can reasonably be expected to occur on a specific source, based on seismological and geological evidence.

2.2 Performance Levels

Three performance levels are considered for evaluation of earthquake responses of dams. These include serviceability performance, damage control performance, and collapse prevention performance, as shown in Figure 1.

2.2.1 Serviceability Performance

The dam is expected to be serviceable and operable immediately following earthquakes producing ground motions up to the OBE level.

2.2.2 Damage Control Performance

Certain parts of the dam can deform beyond their elastic limits (non-linear behavior) if non-linear displacement demands are low and load resistance is not diminished when the dam is subjected to extreme earthquake events. Damage may be significant, but it is generally concentrated in discrete locations where cracking and joint opening occur. The designer should identify all potential damage regions, and be satisfied that the structure is capable of resisting static loads and if necessary can be repaired to stop further damage by non-earthquake loads. Except for unlikely MCE events, it is desirable to prevent damage from occurring in substructure elements, such as foundation, and other inaccessible structural elements.

2.2.3 Collapse Prevention Performance

Collapse prevention performance requires that the dam not collapse regardless of the level of damage. The dam may suffer unrepairable damage with nonlinear deformation greater than those associated with the damage control performance but should not result in uncontrolled release of water. If the dam does not collapse when subjected to extreme earthquake events, its resistance can be expected to decrease with increasing displacements. This can affect the post-earthquake stability condition and should be checked. Collapse prevention performance should only be permitted for unlikely MCE events. Collapse prevention analysis should be evaluated using nonlinear dynamic procedures discussed later.

2.3 Performance Goals

Both strength and serviceability must be considered in the design of dams. For concrete dams, the consequences of inadequate strength can be failure by shear, flexure, tension, or compression. Lack of adequate strength can result in loss of life and severe economic loss. Dams must also be serviceable under sustained and frequent loads. Serviceability for usual static load conditions is a matter of limiting structural displacements. For the OBE loading, the serviceability requirement is to assure the dam will function without interruption, with little or no damage.

The plain concrete structures such as dams generally show limited-ductile behavior in flexure with brittle behavior in shear. Limited ductile behavior is characterized by an elastic range and

limited plastic range that may include strain hardening or softening, followed by a complete or partial loss of strength to the residual level (see Figure 1). To properly assess this behavior it is necessary to understand the loading history, the changes in system stiffness and damping as cracking and joint opening occur, resisting loads redistribute, and response mechanisms change from the initial elastic deformation state to nonlinear sliding and rocking limit states. Under the MDE ground motions, limited ductile structures should have sufficient strength to assure performance will remain within the inelastic region where strength increases with an increase in strain (i.e. damage control region in Figure 1).

Under the MCE ground motions the dam may perform in the collapse prevention region, provided that it can be shown that the dam will remain stable without uncontrolled release of water. However, this requires the use of an appropriate nonlinear dynamic analysis with parameter sensitivity studies to assure that the dam will remain stable during and after the earthquake shaking.

2.4 Design Requirements

2.4.1 Strength Design

Strength design for dams subjected to earthquake ground motions is achieved by reducing the probability of structural collapse to an acceptable level. This is accomplished by selecting a representative design basis earthquake event to be used in combination with specific design and evaluation procedures that assure the structure will perform as intended. Seismic design and evaluation is most often based on linear-elastic response-spectrum or time-history analysis procedures, although nonlinear analysis procedures can be used for evaluation of certain nonlinear mechanisms. The design basis earthquake event used for strength evaluation is the Maximum Design Earthquake (MDE).

2.4.2 Serviceability Design

Serviceability design for dams subjected to earthquake ground motions is achieved by reducing the possibility of structural damage to a negligible level. As for strength performance, this is accomplished by selecting an appropriate design basis earthquake event to be used in combination with appropriate design and evaluation procedures. Evaluation is based on linear-elastic response spectrum analysis or time history analysis procedures. The design basis earthquake event used for serviceability evaluation is the Operating Basis Earthquake (OBE).

2.4.3 Loading Combinations

The following loading combinations establish the ultimate strength and serviceability requirements for the design and evaluation of concrete dams. The loading combinations represent the total demand (dead load + live load + earthquake) for which the structure must be designed or evaluated.

Strength design loading combination:

$$Q_{DC} = Q_D + Q_L + Q_{MDE} \quad (1)$$

Q_{DC} = Combined action of dead, live, and MDE loads for use in evaluating damage control performance

Q_D = Dead load effect

Q_L = Live load effect + uplift

Q_{MDE} = Earthquake load effect from MDE ground motions including hydrodynamic and dynamic soil pressure effects

The live load effect is the structure response to live loads such as hydrostatic, earth pressure, silt, and temperature loads. Live loads to be considered are those that are likely to be present during the design earthquake event. The earthquake load may involve multi-component ground motions with each component multiplied by +1 and -1 to account for the most unfavorable earthquake direction.

Serviceability loading combination:

$$Q_S = Q_D + Q_L + Q_{OBE} \quad (2)$$

Q_S = Combined action of dead, live, and OBE loads for use in evaluating serviceability performance

Q_{OBE}= Earthquake load effect from MDE ground motions including hydrodynamic and dynamic soil pressure effects

Live loads to be considered are those that are likely to be present during the OBE earthquake event.

3.0 EARTHQAUKE GROUND MOTIONS

The earthquake ground motions for design and evaluation of dams are generally characterized in terms of response spectra and acceleration time histories. Information on development of response spectra can be found in EM1110-2-6050 (1999). Information on development and selection of earthquake acceleration time histories and time history dynamic analysis of concrete hydraulic structures can be found in EM 1110-2-6051 (2003). General guidance and direction for the seismic design and evaluation of all civil works projects are provided in ER 1110-2-1806 (1995).

3.1 Standard Response Spectra

The manual provides guidance for constructing standard acceleration response spectra based on the most recent national seismic hazard data. The standard response spectra are used as a starting point for developing conceptual designs and performing evaluations, determining if the earthquake loading controls the design, and establishing the need for more refined analysis and the impact the earthquake loading might have on construction costs.

3.2 Site-Specific Response Spectra

Earthquake ground motions depend on source characteristics, source-to-site transmission path properties, and site conditions. All of these factors can be considered in detail in a site-specific ground motion study for developing site-specific response spectra. There are two basic approaches to developing site-specific response spectra: deterministic and probabilistic. In the deterministic approach, one or more earthquakes are specified by magnitude and location with respect to a site. Usually, the earthquake is taken as the Maximum Credible Earthquake (MCE), and assumed to occur on the portion of the source closest to the site. The site ground motions are then estimated deterministically, given the magnitude and source-to-site distance.

In the probabilistic approach, site ground motions are estimated for selected values of probability of ground motion exceedance in a design time period or for selected values of the annual frequency or return period of ground motion exceedance. A probabilistic ground motion assessment incorporates the frequency of occurrence of earthquakes of different magnitudes on the various seismic sources, the uncertainty of the earthquake locations on the various sources, and the ground motion attenuation including its uncertainty. Guidance for developing site-specific response spectra and for using both the deterministic approach and the probabilistic approach can be found in EM 1100-2-6050 (1999).

3.3 Acceleration Time Histories

Acceleration time-histories of ground motion for dynamic analysis of dams are developed using procedures described in EM 1110-2-6051 (2003). The overall objective is to develop a set (or sets) of time-histories that are representative of site ground motions that may be expected for the design earthquake(s) and that are appropriate for the types of analyses planned for the dam. The following steps are included in this process:

- Initially selecting recorded time-histories that are reasonably consistent with the tectonic environment of the site; design earthquake (magnitude, source-to-site distance, type of faulting); local site conditions; and design ground motion characteristics (response spectral content, duration of strong shaking, and special characteristics, e.g. near-source characteristics).

- Modifying time-histories selected above to develop the final set(s) to be used in dynamic analysis. Two approaches that can be used in this process are simple scaling of time-histories (by constant factors) so that a set of time-histories has spectral values that, on average, are at the approximate level of the design

response spectrum; and spectrum matching, which involves modifying the frequency content of a given time-history so that its response spectrum is a close match to the design response spectrum.

- Further modifying the time-histories for site response effects and spatial variations of ground motion, if it is desired to incorporate effects of site topography and wave passage and incoherence in the ground motions that would arrive beneath the dam.

3.4 Selection of Acceleration Records

Application of the above guidelines is straightforward when design earthquakes are expressed deterministically. However, the application of the guidelines is less straightforward when the design earthquake ground motions (typically the response spectrum) are derived from a probabilistic ground motion analysis (often termed a probabilistic seismic hazard analysis or PSHA). From this type of analysis, the design response spectrum for a design return period reflects the contribution of different earthquake magnitudes and distances to the probabilities of exceedance. Therefore, when the design response spectrum is probabilistically based, the PSHA should be de-aggregated to define the relative contributions of different magnitudes and distances to the ground motion hazard. Furthermore, the de-aggregation should be done for probability values or return periods that correspond to those of the design earthquake and for response spectral periods of vibration of significance for seismic structural response because the relative contributions of different magnitudes and distances may vary significantly with return period and period of vibration. The dominant magnitude and distance is then considered as representative in selecting time histories and defining strong motion duration.

For use in linear dynamic analysis, at least three time-histories (for each component of motion) should be used for each design earthquake. For use in nonlinear dynamic analysis, at least five time-histories should be used (for each component of motion) for each design earthquake. Fewer time-histories are required for linear dynamic analysis than for nonlinear analysis because the dynamic response of a linear structure is determined largely by the response spectral content of the motion, whereas the response of a nonlinear structure may be importantly influenced by the time domain character of the time-history (e.g., shape, sequence, and number of pulses) in addition to the response spectrum characteristics. Since these time domain characteristics may vary greatly for time-histories having similar spectral content, more time-histories are required for nonlinear analysis to capture the variability in response. If the nonlinear response is found to be significantly sensitive to the time-history characteristics for the records selected, then the set of time-histories should be expanded.

4.0 ANALYSIS METHODOLODY

The manual recommends progressive analysis methodology where the seismic evaluation is performed in phases in order of increasing complexity progressing from simple equivalent lateral force methods, to linear elastic response-spectrum and time-history analysis, to nonlinear methods, if necessary.

Gravity dams with simple geometry may initially be analyzed using the equivalent lateral force method, but generally 2D or 3D finite-element dynamic analysis will be required. Arch dams should always be analyzed using 3D finite-element idealization. For both gravity and arch dams, dynamic interactions with the foundation rock and the impounded water should be considered. Foundation rock may be idealized using simplified massless model, viscoelastic with inertia and damping effects, or a finite-element mesh with transmitting boundaries. The dam-water interaction effects may be represented by the Generalized Westergaard added-mass (Kuo, 1982), an incompressible fluid mesh (Kuo, 1982), or a compressible fluid mesh with energy loss capability at the reservoir bottom due to sediment accumulation (Hall and Chopra, 1980).

5.0 EVALUAITON PROCEDURES

Evaluation of seismic performance of concrete dams starts with utilization of a demand-to-capacity ratio (DCR) as a performance indicator, then

progresses to the use of performance threshold curves using both DCR and cumulative inelastic duration, and finally continues with the extent of irrecoverable movements caused by sliding and rotation, as appropriate. For concrete dams, DCR is defined as the ratio of stress demands to static tensile strength of the concrete and is used to assess the results of response-spectrum analysis. The performance threshold curves, discussed later, are used to assess the results of linear time-history analysis. They provide a measure of severity of the nonlinear response in terms of amount of cracking and joint opening. Finally, irrecoverable movements which are obtained by conducting nonlinear time-history analysis are used to assess stability condition of the dam under severe earthquake ground shaking.

5.1 Acceptance Criteria for Response-Spectrum Analysis

A linear-elastic response-spectrum analysis is generally the first step in the evaluation process. The earthquake demands in terms of stresses are computed and compared with the stress capacity of the concrete to assess whether the resulting DCR ratios meet the allowable values listed in Table 1. In cases where DCR limits for tensile stresses are exceeded, a linear-elastic time-history analysis is generally performed and evaluated, as discussed next.

5.2 Acceptance Criteria for Linear Time-history Analysis

The acceptance criteria for the linear-elastic time-history analysis of concrete dams are based on the use of performance threshold curves (Ghanaat, 2002 and EM 1110-2-6051, 2003). The dam response to the MDE is considered to be within the linear-elastic range of behavior with little or no damage if computed stress demand-capacity ratios are less than or equal to 1.0. The dam is considered to exhibit nonlinear response in the form opening and closing of contraction joints and cracking of the horizontal joints (lift lines) and the concrete if the estimated demand-capacity ratios exceed 1.0. Note that in the case of arch dams where the ability of contraction joints to resist tension is limited, the joints may open even if demand-capacity ratios are less than or equal to 1.0. However, the amount of contraction joint opening at a DCR $\leq$ 1, is expected to be small with negligible or no effects on the overall stiffness of the dam. For DCRs exceeding unity the performance is evaluated as follows:

5.2.1 Gravity Dams

The level of nonlinear response or cracking is considered acceptable if demand-capacity ratios are less than 2.0 and the percent of overstressed dam-section surface areas and the cumulative duration of stress excursions above the tensile strength of the concrete fall below the performance threshold curves given in Figure 2. Consideration should also be given to relation between the fundamental period of the dam and peak of the earthquake response spectra. If lengthening of the periods of vibration due to nonlinear response behavior causes the periods to move away from the peak of the spectra, then the nonlinear response would reduce seismic loads and improve the situation by reducing stresses below the values obtained from the linear time-history analysis. When these performance conditions are not met, then a nonlinear time-history analysis would be required to estimate the damage more accurately, as discussed in Section 5.3.1.

5.2.2 Arch Dams

The level of nonlinear response in the form of cracking and/or opening of contraction and lift joints is considered acceptable if DCR < 2 and the percent of overstressed dam surface areas and the cumulative inelastic duration of tensile stress cycles exceeding tensile strength of the concrete fall below the performance threshold curves given in Figure 3. The relation between the fundamental period of the dam and peak of the response spectra should also be considered to determine whether the nonlinear response behavior would increase or decrease the seismic demand. If these performance criteria are not met, then a nonlinear analysis would be required for more accurate estimate of the damage, as described in Section 5.3.2.

5.3 Evaluation and Acceptance Criteria for Nonlinear Time-history Analysis

5.3.1 Gravity Dams

While it is possible to model material and other sources of nonlinearity in analysis of gravity dams, the required parameters are either not known or well defined. For this reason the nonlinear dynamic analysis of a gravity dam should focus on capturing the potential failure modes that would have the most impact on the stability of the dam. A typical gravity dam is built as individual monoliths separated by vertical joints. Furthermore, construction of each monolith involves placement of concrete in lifts that produces horizontal joints whose tensile strength could be less than that of the parent concrete. Consequently, in a major earthquake it is likely that the vertical joints would open and close repeatedly and tensile cracking would occur along the lift lines, at the dam-foundation interface, and at the change of slope in the upper part of the dam where stress concentration occurs. The nonlinear performance evaluation of gravity dams therefore starts with a linear-elastic time-history analysis to identify overstressed regions that would experience cracking, followed by nonlinear dynamic analyses incorporating slippage and rotation with respect to opened joints and cracked sections, as well as post-earthquake analyses for static loads and after-shock excitations.

The results of nonlinear analysis will include sliding displacement and rotation demands that must be sufficiently small not to jeopardize safety of the dam during the main event as well as during the after shocks. This means that after the level of damage has been established for the main event, the damaged structure should be tested against the probable aftershocks that could be one to two magnitudes smaller than the main shock. In addition, post-earthquake static stability analyses should be carried out so that the ability of the damaged structure to resist the operating loads and the potential increased uplift can be demonstrated.

For example, a linear-elastic dynamic analysis may indicate that the gravity dam will experience high tensile stresses at the dam-foundation interface and that the dam does not pass the acceptance criteria set forth for the linear analysis. In subsequent nonlinear dynamic analyses gap-friction elements are introduced at the high tensile-stress region of the base to allow formation and propagation of cracks, which may extend through the entire base of the dam. The results may indicate that the dam would fully crack leading to sliding and rocking responses with a permanent displacement (offset) at the end of the shaking. The magnitude of the permanent sliding displacement is estimated and compared with operational and safety requirements. The performance of the dam is then considered satisfactory if the cracks and permanent sliding displacement do not lead to uncontrolled release of water, and that the post-earthquake stability of the dam under static loads is not compromised. A numerical example of linear and nonlinear time-history analyses and performance evaluation of a non-overflow gravity dam to illustrate this process is presented in Section 6.

5.3.2 Arch Dams

Arch dams are generally built as independent cantilever monoliths separated by vertical contraction joints. Since contraction joints cannot transfer substantial tensile stresses in the arch direction, the joints can be expected to open and close repeatedly as the dam vibrates in response to severe earthquake ground motions. Construction of arch dams also involves horizontal construction joints known as lifts that may exhibit lower tensile strength than the mass concrete. Consequently opening of contraction joints and cracking of lift joints are the most likely nonlinear mechanisms that could occur in arch dams. Such conditions can be modeled and analyzed using QDAP (Quest Structures, 2001) or other finite-element programs with nonlinear joint capabilities. As in the case of linear analysis the concrete arch and the foundation rock are discretized using standard 3D solid elements, but joints and fractures in the dam, at the dam-foundation interface, or within the foundation are represented by nonlinear 3D joint elements. Therefore the only nonlinear effects considered for the response of the dam are those associated with the opening, closing, and sliding along the joints and cracked sections. Since opening of the contraction joint and cracking of the lift joints

relieve high tensile stresses, the traditional stress-based criteria will not be applicable to the nonlinear results. Instead the magnitude of compressive stresses, the extent of joint opening or cracking, and the amplitude of non-recoverable movements of concrete blocks bounded by opened joints would control the overall stability of the dam and should be used to assess dam safety.

The nonlinear dynamic analysis of arch dams should also assess stability of potentially moveable blocks in the abutments if there are adversely jointed rock blocks directly beneath the dam. This problem is best handled as a coupled dynamic problem in which the moveable blocks are modeled as part of the dam finite-element model to allow joint slippage in the abutments and the effects it might have on the stability of the dam. The block joints can be modeled using 3D joint elements discussed above which resist bearing and shear but not tension. The sensitivity of the results to shear strength of the joints and strength degradation with movement and uplift pressures should be investigated.

6.0 EXAMPLE GRAVITY DAM

The purpose of this example is to demonstrate the application of manual guidelines to earthquake response assessment of gravity dams. The example problem is a 74.17 m (243.33 ft) high non-overflow gravity dam with crest thickness of 9.75 m (32 ft) and a base thickness of 53.83 m (176.6 ft). On the lower two-third, the dam is sloped at 1/10 on the upstream and at 7/10 on the downstream face. The dam is first analyzed using linear time-history method to demonstrate the linear-elastic acceptance criteria discussed in Section 5.2, and then evaluated by nonlinear time-history method to assess potential sliding and rocking responses under earthquake shaking in accordance with Section 5.3.1.

6.1 Earthquake Ground Motions

The example gravity dam was assumed to be located in the near field of a maximum earthquake event having a moment magnitude M_w of about 6-1/2. Four sets of recorded acceleration time-histories from three California earthquakes were selected in accordance with Section 3.4. These included the Pacoima Dam record from 1971 San Fernando earthquake, the Gilroy Array No. 1 record from 1989 Loma Prieta earthquake, the Newhall record from 1994 Northridge earthquake, and the 1971 Pacoima Dam record modified to match the design response spectra. The smooth design response spectra for the horizontal and vertical components of ground motion were constructed to be representative of median ground motions for an M_w 6-1/2 earthquake occurring at a distance of R = 5 km (3.1 miles). The ground motions were scaled such that the sum of ordinates for the response spectra of each natural record would match the sum for the smooth response spectra in the period range of 0.06 to 0.3 sec (see Figure 4). Time-histories of the horizontal components of the records are plotted in Figure 5. This figure clearly demonstrates the pulsive type motions contained in the San Fernando and Northridge records.

6.2 Linear Elastic Response

6.2.1 Finite Element Model

The linear-elastic time-history analysis of the example gravity dam was carried out using a 2D model of the dam and foundation rock with a concrete modulus of elasticity of 40,679 MPa (5.9×10^6 psi), a Poisson's ratio of 0.19, and a unit weight of 158 pcf. The foundation rock was assumed massless but its modulus and Poisson's ratio were assumed to be respectively 39,990 MPa (5.8×10^6 psi) and 0.19. The inertia forces of the impounded water were represented by added hydrodynamic mass values in accordance with the generalized Westergaard method. The finite-element model is shown in Figure 6.

6.2.2 Evaluation of Linear Response

The gravity dam model was analyzed for the combined effects of static plus seismic loads. The static loads included the gravity, hydrostatic pressures due to a headwater depth of 73.15 m (240 ft), and uplift pressures. The earthquake loads consisted of the inertia forces generated by earthquake ground motions described above. A linear uplift pressure distribution from full

headwater to zero tailwater was assumed. The uplift pressure was also assumed not to change during the earthquake ground shaking. The results of analyses include envelopes of maximum stresses, time history of stresses, time history of displacements, and time history of reaction forces at the dam-foundation contact. The envelopes of maximum stresses are used to assess severity and extent of overstressed regions (Figure 7). The stress time histories are used to compute cumulative duration of stress excursions for comparison with the acceptance limits (Figure 8). Finally, time histories of reaction forces are used to compute instantaneous factors of safety to assess stability condition of the dam (Figure 9).

The results of linear analyses indicate that high tensile stresses generally develop at the heel and toe of the dam as well as at upper elevations near the change of slopes, but they are largest at the heel of the dam (Figure 7). Recognizing that the tensile strength of the dam-rock interface or of the fractured rock immediately below the interface is lower than that of the intact concrete, the cracking is expected to initiate at the heel of the dam and propagate toward the toe. The instantaneous factors of safety for an assumed friction coefficient of unity (Figure 9) indicate that factor of safety repeatedly falls below unity during the earthquake ground shaking, an indication that the sliding might occur along the base.

The results of linear-elastic time-history analyses were also compared with the acceptance criteria established in Section 5.2.1. Figure 10 shows that the dam section overstressed areas exceed the acceptance limit for three of the earthquake records; only overstressed areas for the Loma Prieta record fall below the acceptance curve. Figure 11 compares cumulative inelastic duration of stress cycles at the heel of the dam with the acceptance curve. It is obvious that all cumulative duration for stresses at the heel of the dam are above the acceptance threshold set for the linear-elastic analysis. Similar results for stresses near the toe of the dam showed cumulative duration for stresses at this location fall below the acceptance threshold. These results suggest that the cracking would initiate from the heel of the dam but may or may not propagate through the entire base of the dam; thus nonlinear time-history analyses are needed to evaluate the crack propagation and the effects it may have on sliding of the dam, as discussed next.

6.3 Nonlinear Response Analysis

The results of linear analyses indicate that high tensile stresses develop at the base of the dam, on the upstream face of the dam, and on the downstream face near the change of slope. The magnitudes of stresses are greater at the base of the dam than they are at the upper elevations. For this reason and also because tensile strength of the dam-rock contact and the rock below is expected to be lower than that of the concrete, the nonlinear response in the form of tensile cracking is likely to start at the base. The nonlinear analysis of the dam was therefore formulated to capture this nonlinear mechanism. In this example, gap-friction elements are introduced at the base of the dam to simulate cracking and the sliding and rocking responses that might follow.

6.3.1 Nonlinear Finite-Element Model

Finite-element model for the nonlinear analysis consists of the dam monolith and gap-friction elements. The foundation rock is not included in the model in order to reduce computational efforts. The tensile cracking at the base of the dam is modeled by introducing gap-friction elements between the dam and the rigid foundation. The gap-friction elements are nonlinear elements that can resist bearing and shear parallel to the bearing plane but not tension. The friction forces follow the Coulomb theory and thus are directly proportional to bearing forces in the element. Figure 12 shows the dam finite-element model with 23 gap-friction elements at the base of the dam. Except for the nonlinear gap-friction elements, the rest of the dam is assumed to behave elastically.

6.3.2 Evaluation Loads and Parameters

The nonlinear dynamic analysis was conducted for the combined action of static and earthquake loads. The static loads included gravity, hydrostatic pressures, and uplift pressures, all of which were applied as initial loads. The uplift pressures were assumed to vary linearly from the headwater to

tailwater with no changes during the earthquake ground shaking. A zero tailwater was assumed. The earthquake loads included the same four acceleration time-history records discussed previously.

The gap-friction elements used in this example have friction properties for shear deformation in the horizontal direction and gap behavior in the axial or vertical direction. The gap properties usually include zero tension resistance but the element can be preloaded so that the element could start with a certain amount of tension resistance. In this example, zero cohesion with zero tensile strength and a friction angle of 45 degrees were assumed for sliding along the dam-foundation contact surface.

6.3.3 Evaluation of Nonlinear Response

Stress results in Figure 13 show significant reduction in tensile stresses due to tensile cracking at the base of the dam (compare Figure 13 with Figure 7). Note that magnitudes of stresses within the body of the dam have also dropped significantly. This confirms the assumption that tensile cracking at the base of the dam would preclude tensile cracking elsewhere by relieving high tensile stresses within the body of the dam.

It was also found that the crack propagates through the entire base of the dam followed by sliding of the dam in the downstream direction. Figure 14 shows time histories of sliding displacements for all joints across the base of the dam. The sliding displacement varies from joint to joint due to deformations of the flexible dam. The sliding displacements are slightly higher for nodes closer to the heel and reduce toward the toe. For a rigid dam sliding displacements are the same for all nodes across the base. Figure 15 displays horizontal displacement history for a crest nodal point, where the permanent displacement at the end of the record is evident. The results show an overall permanent displacement of about 0.8 inches. Although this permanent displacement is relatively small and does not appear alarming, the main concern is the post-earthquake stability condition of the dam under static loads. The post-earthquake static sliding factor of safety for the example dam was found to fall below unity. This is because the uplift forces have increased due to formation of crack at the base of the dam. Based on these results the dam should be retrofitted and its shear resistance increased to remedy the situation.

7.0 CONCLUDING REMARKS

The paper presents an overview of an engineering manual for performance-based design and evaluation of concrete hydraulic structures as it relates to concrete dams. The manual introduces procedures that show how to design or evaluate a hydraulic structure including dams to have a predictable performance for specified levels of seismic hazard. Three seismic performance levels including serviceability, damage control, and collapse prevention are introduced. The analysis and evaluation procedures as well as the acceptance criteria for each performance level are described and demonstrated. The performance criteria presented in the manual employs demand-capacity ratios, damage control thresholds, and nonlinear response behavior as well as the post-earthquake stability condition to assess dam safety. This is a departure from the traditional simple stress checks in which the predicted elastic stress is compared with the expected concrete strength.

8.0 ACKNOWLEDGEMENTS

This work was sponsored by the Civil Works Projects of the US Army Corps of Engineers, Washington, D.C. We appreciate the cooperation of the authorities at the Chief's office, which permitted the preparation and presentation of this paper.

9.0 REFERENCES

EM 1110-2-6050 (1999), "Response Spectra and Seismic Analysis for Concrete Hydraulic Structures," US Army Corps of Engineers, Washington, D.C.

EM 1110-2-6051 (2003), "Time-History Dynamic Analysis of Concrete Hydraulic Structures," US Army Corps of Engineers, Washington, D.C.

EM 1110-2-6053 (2007), "Earthquake Design and Evaluation of Concrete Hydraulic Structures," US Army Corps of Engineers, Washington, D.C.

ER 1110-2-1806 (1995), "Earthquake Design and Evaluation of Civil Works Projects," US Army Corps of Engineers, Washington, D.C.

Ghanaat, Y. (2002), "Seismic Performance and Damage Criteria for Concrete Dams," Proceedings of the 3rd US-Japan Workshop on Advanced Research on Earthquake Engineering for Dams, San Diego, California, June 22-23, 2002.

Hall, J. F., and Chopra, A. K. 1980. "Dynamic Response of Embankment, Concrete Gravity and Arch Dams Including Hydrodynamic Interaction," Report No. UCB/EERC-80/39, Earthquake Engineering Research Center, University of California, Berkeley.

Kuo, J. S. -H. 1982. "Fluid-Structure Interactions: Added Mass Computations for Incompressible Fluid," Report No. UCB/EERC-82/09, Earthquake Engineering Research Center, University of California, Berkeley.

Quest Structures (2001), "QDAP, a web-based nonlinear dam analysis program" developed by Quest Structures, see www.WebDams.com.

Table 1. DCR Allowable Values for Response-Spectrum Analysis of Concrete Dams

Action In terms of stresses	Performance Objectives	
	Damage Control (MDE)	Serviceability (OBE)
Tension due to flexure	1.5	1.0
Diagonal tension due to shear.	0.9	0.8
Shear due to sliding.	1.0	0.8

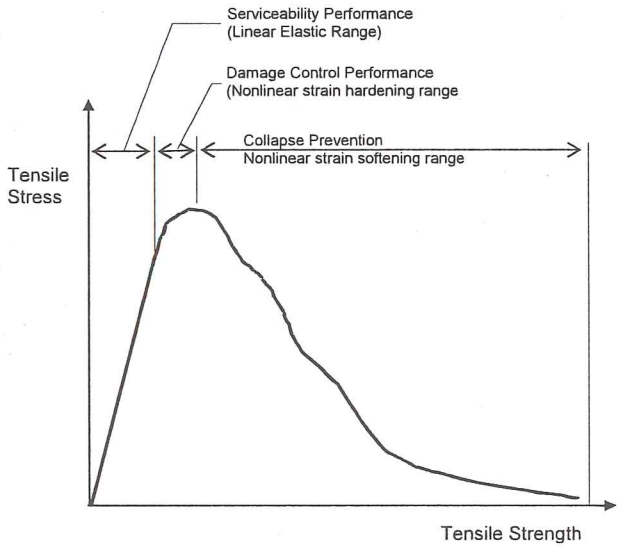

Figure 1. Stress – Strain relationship for plain concrete structures illustrating three performance levels

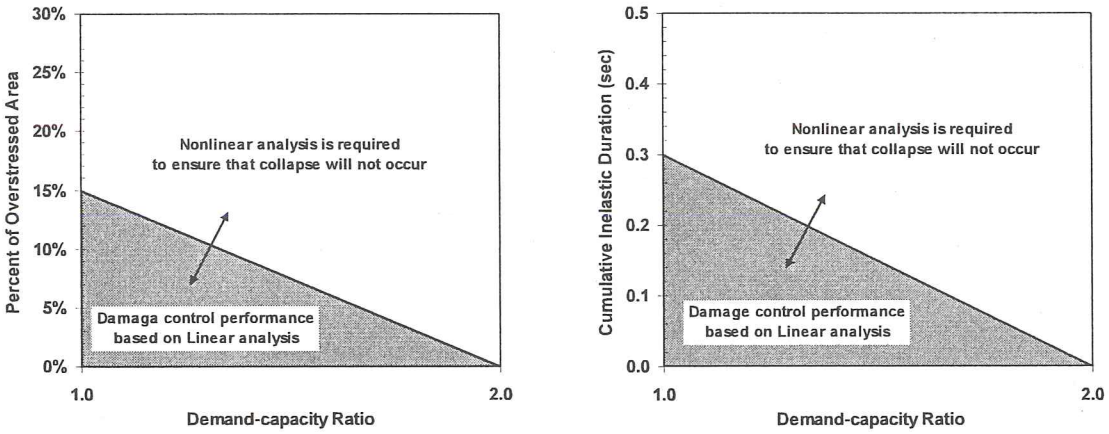

Figure 2. Performance threshold curves for concrete gravity dams

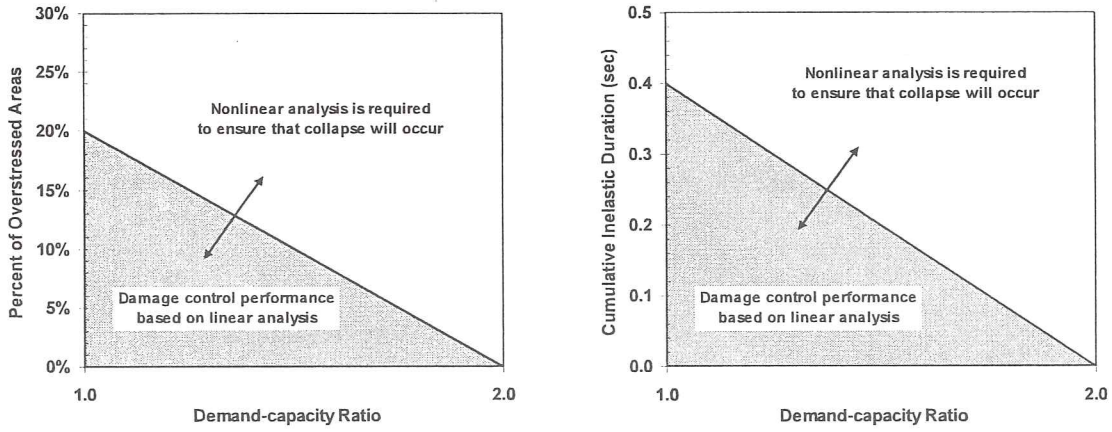

Figure 3. Performance threshold curves for concrete arch dams

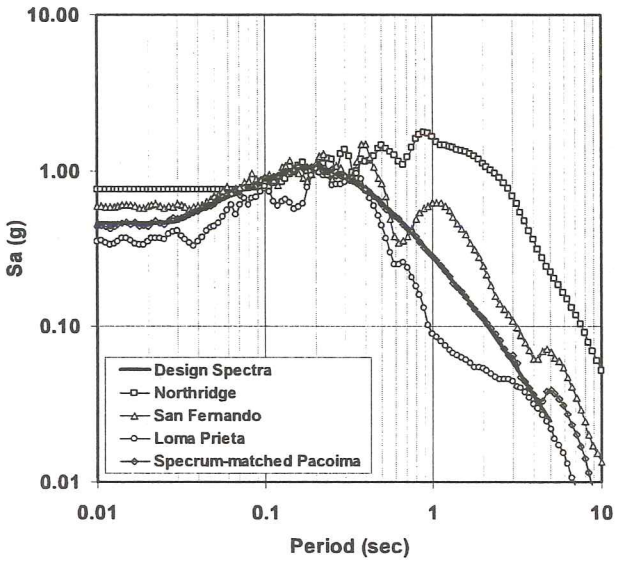

Figure 4. Comparison of design response spectra with spectra of scaled records

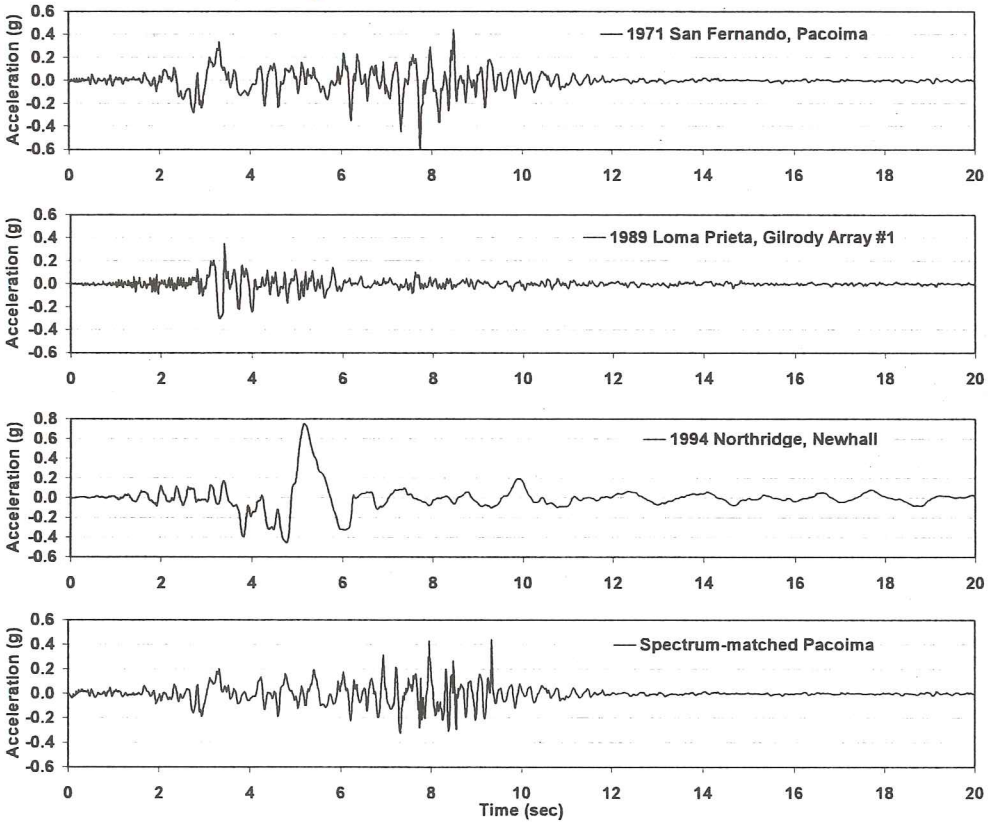

Figure 5. Horizontal component of earthquake input acceleration time histories

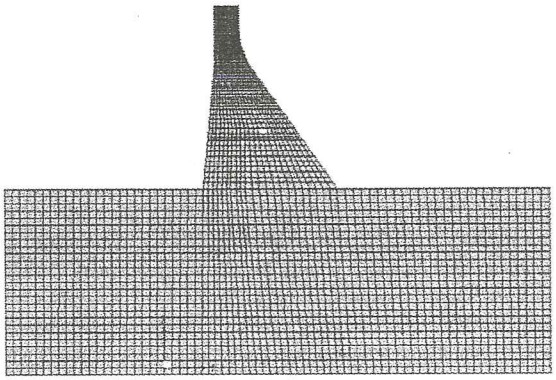

Figure 6. Dam-foundation finite-element model

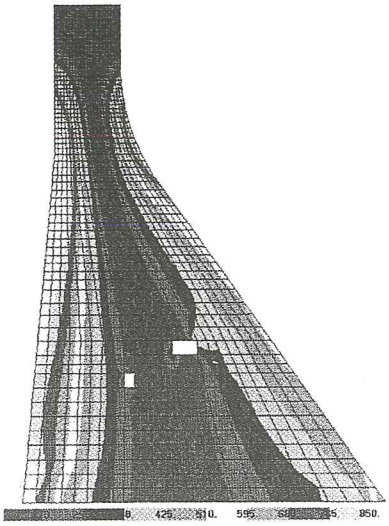

Figure 7. Envelopes of maximum vertical stresses for San Fernando record (linear model) (1 MPa = 145 psi)

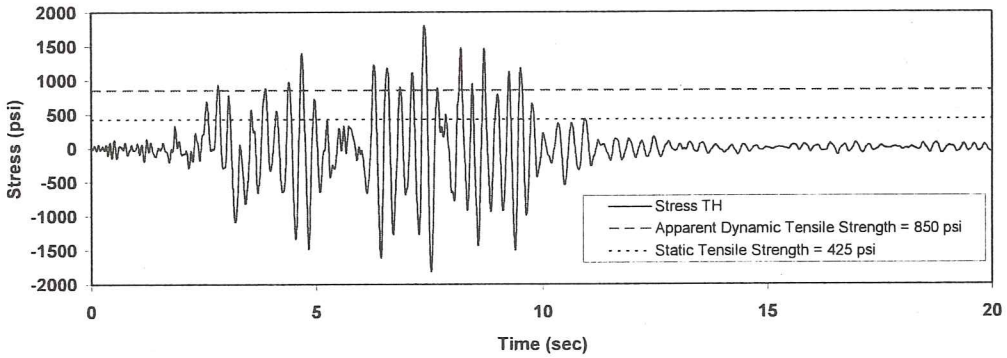

Figure 8. Time history of maximum vertical stresses at the heel of the dam for San Fernando record.

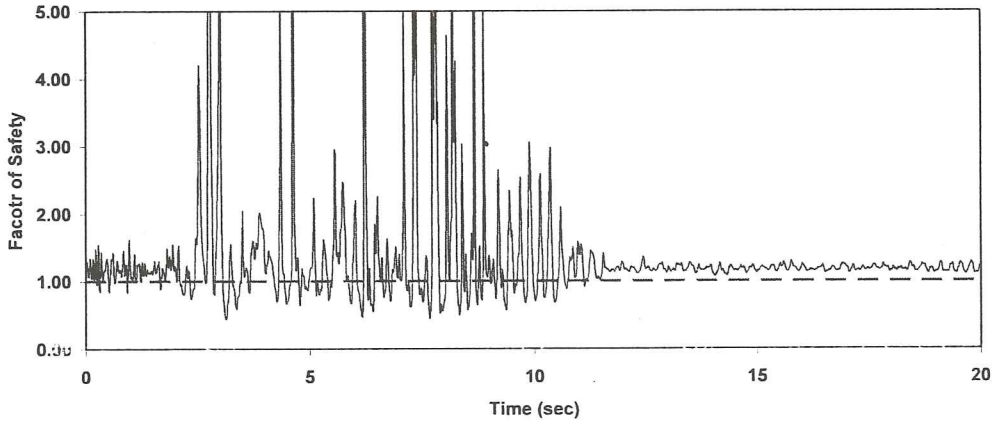

Figure 9. Instantaneous factors of safety for San Fernando record.

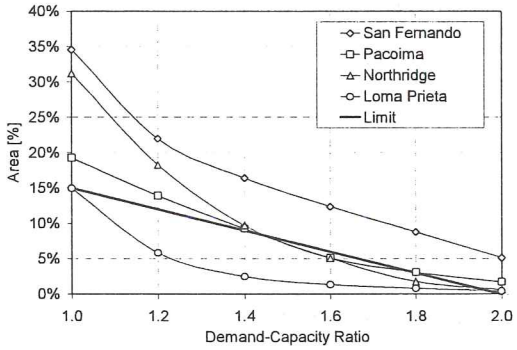

Figure 10. Comparison of percentage of overstressed areas with acceptance limits

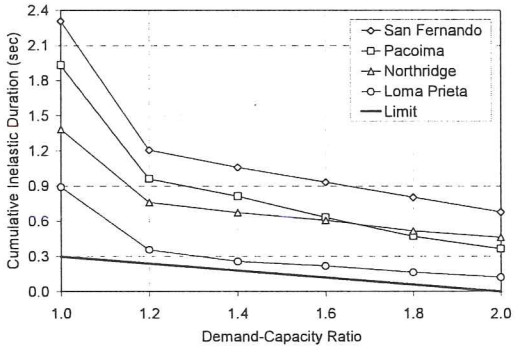

Figure 11. Comparison of cumulative duration of stress cycles with acceptance limits for stresses at the heel of the dam

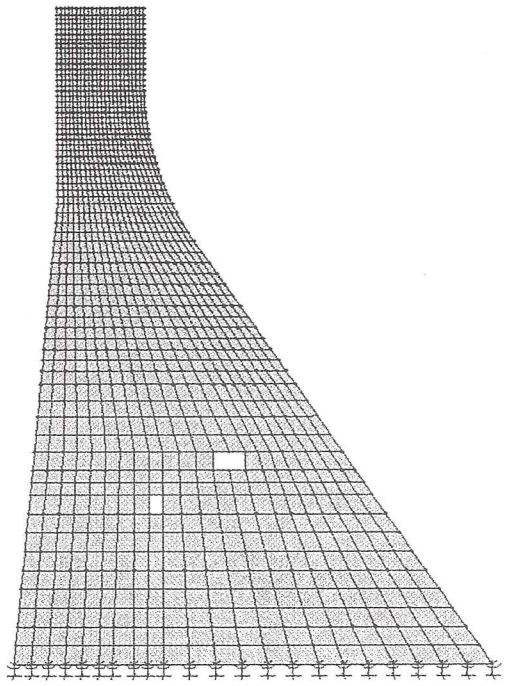

Figure 12. Dam finite-element model with gap-friction elements

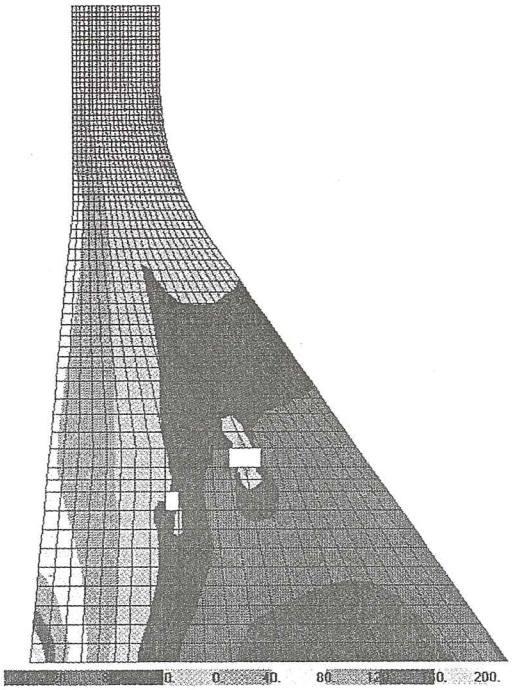

Figure 13. Envelopes of maximum vertical stresses for San Fernando record from nonlinear analysis (1 MPa = 145 psi)

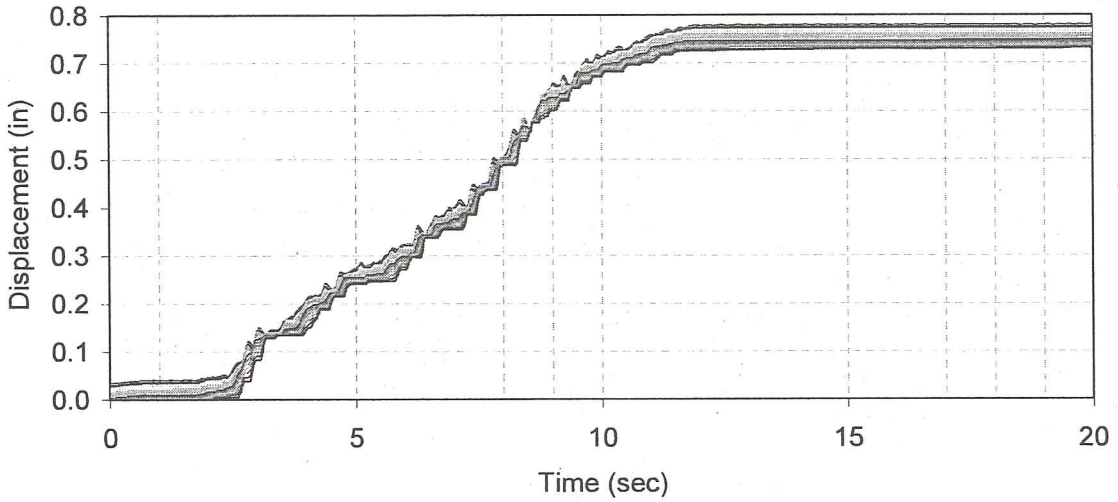

Figure 14. Time history of static plus seismic sliding displacements for San Fernando record (1 in. = 25.4 mm)

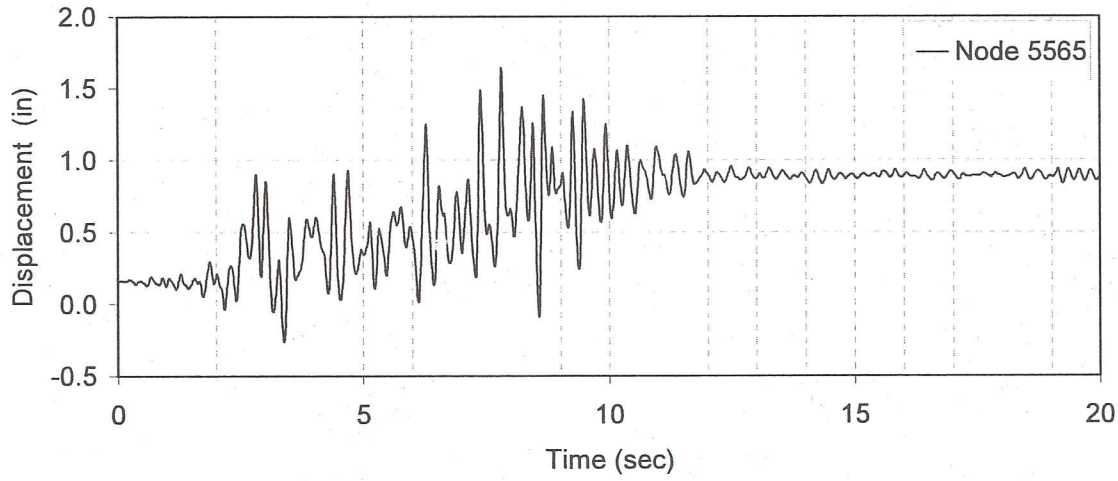

Figure 15. Time history of total horizontal displacement of dam crest for San Fernando record (1 in. = 25.4 mm)

Outline of "*Guidelines for Seismic Performance Evaluation of Dams During Large Earthquakes (Draft)*"

by

Nario Yasuda[1], Kazuhito Shimamoto[2], Yoshikazu Yamaguchi[3] and Takashi Sasaki[4]

ABSTRACT

On March 2005, the River Bureau of the Ministry of Land, Infrastructure and Transport issued "Guidelines for Seismic Performance Evaluation of Dams during Large Earthquakes (Draft)." The Draft Guidelines describe the methods for systematically evaluating the seismic safety of dams subjected to large earthquake motions, including establishment of scenario earthquakes and required seismic performance of dam bodies and appurtenant structures. Before practical application of the Guidelines, we require further study for verification with existing dams. Therefore, the Guidelines are used as "Draft" during trial implementation for verification.

The Draft Guidelines are composed of four chapters," Basic matters"," Required seismic performance"," Methods for evaluating dam bodies" and " Methods for evaluating appurtenant structures." The chapter of "Basic matters" describes the definitions of technical terms, the seismic safety to be evaluated, etc. The chapter of "Required seismic performance" describes the procedure for setting scenario earthquake for seismic performance evaluation. Especially, it also shows "Earthquake motions with lower-limit acceleration response spectrum for evaluation." The chapter of " Methods for evaluating dam bodies" describes that the seismic performance of the dam body is evaluated basically by dynamic analysis and additionally by cumulative pertinent damage processes analysis . The chapter of " Methods for evaluating appurtenant structures" shows the basic concept for evaluating gates, pier, intake facility, control devices and so on.

Keyword: Earthquake-proof design ,Large earthquakes, Seismic performance evaluation, Technical guideline.

1. INTRODUCTION

On March 2005, the "*Guidelines for Seismic Performance Evaluation of Dams during Large Earthquakes*" [1] (hereinafter referred to as the "Guidelines") was announced by the River Bureau of the Ministry of Land, Infrastructure and Transport (MLIT).

The guidelines show three important matters to evaluate the seismic performance of dams against large earthquakes.

i) The definition of earthquake motions that should be taken into consideration in evaluations

1 Head, Water Management and Dam Division, River Department, National Institute for Land and Infrastructure Management (NILIM), Ministry of Land, Infrastructure and Transport(MLIT), Tsukuba-shi, Ibaraki-ken 305-0804 Japan

2 Senior Researcher, ditto

3 Team Leader, Dam Structure Research Team, Hydraulic Engineering Research Group, Public Works Research Institute (PWRI), Tsukuba-shi, Ibaraki-ken 305-8516 Japan

4 Former Deputy Team Leader, ditto (Director, Isawa Dam Construction Work Office, MLIT)

ii) The concepts of the required seismic performance of dams.
iii) The methods of seismic performance evaluation of dam bodies and appurtenant structures

The Guidelines were applied as a "trial implementation" to verify the applicability in the technical viewpoint. Verification was conducted at several existing dams to find out various problems in working-level and solve them.

In the following section, the Guidelines are introduced as shown in Table 1.

2. BASIC MATTERS IN SEISMIC PERFORMANCE EVALUATION

Chapter 1 of the guidelines shows basic thoughts of the seismic performance evaluation. Those are intent and purpose of the guidelines, the definition of terms, scope of application, a definition of the seismic performance required and evaluation conditions.

At first, we mainly describe the intent and purpose of guidelines, the definition of terms, a definition of the seismic performance required and so on.

2.1 The Intent and Purpose of the Guidelines

In the beginning of the guidelines, it shows that "the guidelines showed a standard way of thinking to evaluate of the seismic performance of dams for *level 2 earthquake motions.*"

The purpose of evaluation is to confirm the seismic performance safety for the large earthquakes of dams designed in a current design standard.

The Guidelines are based on the knowledge available at present, and do not prevent the use of new and more rational evaluation methods when new knowledge about the earthquake motion prediction and dynamic response analysis is acquired.

2.2 Definitions of Terms

The definitions of terms used in the Guidelines are as follows:

1) Earthquake motions

Ground vibration generated when seismic waves are transmitted through the ground during an earthquake

2) *Level 2 earthquake motions*

Motions having the maximum-scale level of intensity conceivable at the dam site, at the present and in the future

(The level of earthquake motion was proposed by Japan Society of Civil Engineering [2]. "*Level 1 condition*" demands a structure to suffer no damage even if *level 1 earthquake motion* acts. "*Level 2 condition*" demands to consider the damage process and evaluation of the seismic performance of the structure when it rarely suffers the damage by very strong earthquake motion. Level 2 condition is approximately corresponding to the concept of Maximum Credible Earthquake (MCE).)

3) Dam body

The dam body and the adjacent foundation ground

4) Appurtenant structures

Various structures and facilities that are located on or near the dam body serve as portion of the dam functionally but are not included in the main body physically

5) Dynamic response analysis

The general analyses used in estimating and assessing the responses of structures and the ground during an earthquake

2.3 Required Seismic Performance

The required seismic performance of dams against *Level 2 earthquake motions* was defined as follows:

i) Dam's function to store reservoir water should be maintained even after suffering damage; and

ii) Any damage suffered should be limited to the repairable extent.

The first definition means that there would be no uncontrollable release of stored reservoir water. This definition was stipulated due to concerns that if a dam were damaged so severely by an earthquake and an uncontrollable discharge of stored water were to occur, the damage to the people in the lower reaches of the river could be socially unacceptable.

In 2002, Ministry of Land, Infrastructure and Transport announced "*Basis of Structural Design for Buildings and Public Works*."[3] It showed a basic direction of development and revision of the technical standard to affect the structure design.

The second definition is based on the concept of the so-called limit state design. "*Basis of Structural Design for Buildings and Public Works*" provides the concepts of three limit states. They are "*Serviceability limit*", "*Restorability limit*", "*Ultimate limit*." Furthermore, the Basis requires that any design criteria should be revised to set the goal of seismic design so as to restrict the damage suffered during an assumed earthquake to one state among the above-mentioned three limit.

For the *level 2 earthquake motions*, it is not realistic to the use *Serviceability limit* to make a demand.

However, dams are very important for flood control and water use in river basins. When a dam suffers earthquake damage to such an extent that it cannot be repaired using available technologies at a reasonable cost and within a reasonable period of time, facilities for replacement of the dam functions would be extremely difficult to find or reconstruct without delay.

Therefore, it is necessary for the damage of dams by the earthquake to be confined to the restorable range.

The application of guidelines doesn't depend on reservoir capacity and scale of dams. In Japan dams are usually constructed in precipitous river basins where a large number of people and properties are concentrated. If, by chance, the dam should break, the consequences would be devastating to the people in the lower reaches.

2.4 Water Level Condition

In evaluating the seismic performance of dams, an important factor is the stored water level, which determines the load conditions including hydrodynamic pressure. The Guidelines state that the reservoir water level to be considered in seismic performance evaluation for *Level 2 earthquake motions* is basically the normal water level (NWL), which is the highest water level in non-flood season.

The Guidelines also state that the dam should also be evaluated for seismic performance using the other water level (e.g., lowest water level in arch dams) in which dam is structurally susceptible to effects of earthquakes.

The guidelines may not take into consideration about water levels which temporarily occur during floods, such as the Surcharge Water Level, because the possibility of *Level 2 earthquake motions* occurring during floods is very low.

3. EARTHQUAKE MOTIONS FOR SEISMIC PERFORMANCE EVALUATION

The guideline shows that the seismic performance evaluation of dams for the large earthquake uses "*Level 2 earthquake motions*" defined as "earthquake motion having maximum-scale level of intensity conceivable at the dam site at the present and in the future."

Chapter 2 of the Guidelines explains how to set *Level 2 earthquake motions* for evaluation.

3.1 How to Set *Level 2 Earthquake Motions*

Under the Guidelines, *Level 2 earthquake*

motions should be determined by thoroughly investigating and collecting information about past earthquakes, active faults and plate boundaries near the dam site. *Level 2 earthquake motions* for each dam are determined as the estimated earthquake motions at each dam site and caused by selected earthquakes that could have the largest impact on the dam (*Scenario Earthquakes*). In other words, *level 2 earthquake motions* to use for evaluation are earthquake motions occurring in dam site by "*Scenario Earthquakes*".

For determination of the *Scenario Earthquakes* for each dam, information such as location and magnitude of past earthquakes, active faults and plate boundaries that might suggest to the occurrence of future earthquakes, should be gathered from reports provided by various earthquake research organs. The results of the Quaternary fault survey, which is to be carried out in determining the sites for dam construction in Japan, should also be checked.

The *Scenario earthquakes* for each dam should be selected by comparing the estimated earthquake motions at the site caused by potential earthquakes that might occur near the dam site. The effects of individual potential earthquakes is basically estimated by comparison of acceleration response spectrum evaluated using the *Distance attenuation formula for dams* on acceleration response spectrum [4], which is a set of empirical equations derived from earthquake motions observed at locations corresponding to rock foundation ground at numerous dams in Japan.

However, if the damage process by extremely strong earthquake is taken into account, for example, earthquakes at plate boundaries, which have much longer duration than those at active faults, may have a greater final impact on dams compared to earthquakes at active faults even if the acceleration response spectrum for an active fault earthquake is larger than that of a plate boundary earthquake. Thus, there is a situation in which two or more *Scenario earthquakes* should be selected.

The Guidelines state several methods for estimating earthquake motions at dam sites other than the empirical method mentioned above, such as the quasi-empirical method (e.g., methods using Green's function) and the theoretical method. However, appropriate modeling of the fault rupture process or the transmission process of seismic motions from the fault to the site becomes necessary when applying these methods to estimate earthquake motions at a dam site and there is a limited number of faults for which such data is available. Therefore, there are still problems to use these methods, and the further studies are necessary. Thus, Guidelines state that earthquake motions for evaluation should be estimated basically by using an empirical method such as the *Distance attenuation formula of acceleration response spectra for dams.*

3.2 *Lower-limit Acceleration Response Spectrum for evaluation*

The Guidelines provide "*Lower-limit acceleration response spectrum for evaluation*" shown in Table.2 and Fig. 1 that should be considered as the mandatory minimum *Level 2 earthquake motions*. The reason for stipulating this minimum spectrum is that the earthquake motion used for seismic performance evaluation should be determined taking into consideration the possibility of an earthquake occurring directly at an active fault under the dam site even when no active faults are found by the observation of the ground surface in an earthquake-prone country such as Japan. This spectrum has been estimated from the response spectrum of earthquake motions generated at the ground surface of rock foundation by an earthquake that could occur just under the dam site. Modifications on the spectrum have been

provided to consider the dynamic response of dams and observed response of existing dams during severe earthquakes.

This spectrum is earthquake motion equivalency to occur when an inland earthquake of magnitude 6.5 (Japan Meteorological Agency magnitude, *Mj*.) just under the dam site of the dam. This spectrum considers a cover rate of 84% that increased normal deviation value to the mean including unevenness of occurring earthquake motion. When it thought at 50% cover rate equivalent to the mean, it is *Mj*=7.3 equivalency. This spectrum was calculated, using the above-mentioned *the Distance attenuation formula of acceleration response spectra for dams*, and assumed various fault planes right under the site of the dam.

When the spectrum of earthquake motion calculated by the above-mentioned earthquake motion setting method is compared with Lower-limit Acceleration Response Spectrum for evaluation,, the calculated spectrum is used for evaluation. Therefore, we perform evaluation of all dams with larger earthquake motion than Lower limit spectrum, evaluating of dams based on this guidelines.

4. METHODS FOR EVALUATING DAM BODIES

Chapter 3 of the Guidelines shows how to evaluate the seismic performance of concrete dams and embankment dams, against *Level 2 earthquake motions as follows*.

Dynamic response analyses appropriate for the structural properties of the dam shall be conducted to evaluate the seismic performance of the dam main body. It shall be confirmed that the dam will continue to store reservoir water even when the main body suffers damage, and that the damage is limited to a repairable extent.

When the damage of the dam body is expected by dynamic analysis using *Level 2 earthquake motions*, we should estimate the state and degree of damage, identify available repair methods, and estimate the cost and time needed to restore the required seismic performance. When the repair method, cost and period are judged to be reasonable, the damage suffered can be regarded as repairable.

4.1 Concrete Dams

Concerning the seismic performance evaluation of concrete dams, the Guideline states, "As a result of linear dynamic analysis, when the estimated stress in the dam is smaller than the strength of the concrete materials, the dam will not suffer damage and preserve the required seismic performance." The Guideline also states, "If some damage would be expected in the dam body, dynamic response analysis in which the damage process during the earthquake can be simulated should be carried out, and if only limited damage is expected, the dam could be evaluated as maintaining the required seismic performance.

This way of thinking, whereby consideration is given to the damage extent of dams during earthquakes, is a stance never taken before in technical standards or guidelines for dams in Japan.

Fig.2 shows the flow chart of the seismic performance evaluation for concrete gravity dams based on the Guidelines.

In the case of concrete gravity dam, the two-dimensional dynamic response analysis is carried out for the maximum cross section of the dam.

Therefore, we would regard that the dam's function of water storage will be maintained in case that "limited damage" is the following states.

1) The dam body is not divided by continuous tensile cracks between the upstream and downstream surfaces.

2) Stress that may cause compressive or shearing fracture of the main body is not generated or is generated only locally.

The condition for tensile failure, which requires that dam body is not divided by continuous tensile cracks generated between the upstream and downstream surfaces, was established as the condition including the margin for safety. This is because the dam's function of water storage will be maintained even when continuous tensile cracks are generated, unless the entire upper block of the dam body destabilizes. Therefore, when continuous tensile cracks between the upstream and downstream surfaces are expected, further investigation should be conducted including analyses to confirm the stability of the upper block of the dam body. The time-history response analysis such as a smeared crack model is available and a kind of nonlinear dynamic analysis for simulating tensile cracks.

Fig.3 shows the flow chart of the seismic performance evaluation for concrete arch dams based on the Guidelines.

The basic points for analysis of the arch dam are common to that for a gravity dam in many respects, except several points.

In the evaluation of the arch dam, three-dimensional analysis is required structurally and simulates the transmission of arch thrust between adjacent monoliths and to the abutments considering the behavior of transverse and perimeter joints.

So, the nonlinear dynamic analysis is available for arch dams.

Conclusively, we would regard that the dam's function of water storage will be maintained in case that "limited damage" is the following states.

1) The dam body is not divided due to the opening of joints or continuous tensile cracks generated between the upstream and downstream surfaces.

2) Stress that may cause compressive or shearing fracture of the main body is not generated or is generated only locally.

In nonlinear dynamic analysis considering the behavior of joints, the estimated opening of the joints must also be confirmed not to exceed a range obtained from the structure of keys and water stops.

4.2 Embankment Dams

Once reservoir, water should overflow from the crest of an embankment dam, a catastrophe such as dam failure might occur. The Guidelines states that the seismic performance evaluation of embankment dams should be conducted by confirming that the settlement of crest embankment during an earthquake is small, the overflow of reservoir water is not caused. Moreover no risk of seepage failure after the earthquake must be verified. The flow chart of seismic performance evaluation for embankment dams is shown in Fig. 4.

As seen in the figure, dynamic analysis based on equivalent linear method can be used to evaluate embankment dams at first. Static analysis including embanking and impounding processes to calculate the state of stress and deformation prior to the earthquake must be performed beforehand. When the results of above-mentioned analysis show the possibility of sliding failure, then plastic deformation analysis is required to estimate the amount of deformation or settlement caused by an earthquake. The allowable amount of deformation is basically within the freeboard height. Safety against seepage failure should be carefully investigated when possible sliding planes penetrating the core zone to the downstream are expected in rock-fill dams with earth core, and when possible sliding planes starting at points lower than the water level and reaching to the downstream are expected in

earth-fill dams.
Furthermore, the liquefaction potential should also be examined, although this investigation is required only in exceptional cases such as rock-fill dams on un-solidified sedimentary stratum, or earth-fill dams with insufficiently consolidated body or on foundation of liquefiable sandy soil.

5. METHODS FOR EVALUATING APPURTENANT STRUCTURES

Chapter 4 of the Guidelines shows how to evaluate the various appurtenant structures including dam gates, crest piers and so on.
Not all of the structures require evaluation, but structures that are crucial for ensuring the seismic performance of dams, that is to say, structures that may cause the uncontrolled release of stored water by earthquake damage, should be evaluated. Moreover, the structures needed to ensure the safety of the dam by urgently lowering the water level and restricting rises of lowered water level are required for evaluation.
The main gates of principal outlet with a large capacity below NWL should be evaluated whether there is a risk of buckling or plastic deformation, leading to a defect. Additionally, the facilities equivalent to the main gates for lowering the water level must also be evaluated.
Crest piers that support the gates or bridges above the gate should also be evaluated whether or not to collapse or fall.
Evaluation of appurtenant structures is carried out by the dynamic response analysis method, or the other suitable methods.

6. CONCLUSIONS

The outline of the new Japanese guidelines for seismic performance evaluation of dams was introduced. The Guidelines provide the method for determining the largest-scale earthquake motions for each dam considering *Scenario Earthquakes*, define the required seismic performance against this earthquake motion and mention the methods used to evaluate the seismic performance of concrete dams, embankment dams and various appurtenant structures.
During three or four years of trial implementation for evaluation, we apply the guidelines to several existing dams and verify the applicability in the technical viewpoint. Studies were conducted at several MLIT dams to find out various problems in working-level and find the means to solve them, and after then, guidelines become formal.
Further efforts should be made to strengthen and consolidate the applicability of the present guidelines through evaluating existing dams.

7. ACKNOWLEDGEMENT

This paper revised a paper of *the 75th Annual Meeting of ICOLD* (2007). The title of the original paper is "Trial Implementation of New Japanese Guidelines for Seismic Performance Evaluation of Dams during Large Earthquakes." [5]
In closing, we would like to express our sincere thanks to Prof. Tatsuo Ohmachi (Tokyo Institute of Technology), Chairman of the committee for preparation of the Guidelines, for their advice and encouragement also to all relevant parties for their cooperation. And especially we would like to express our deepest gratitude to Mr. Masafumi Kondo (Japan Dam Engineering Center (JDEC)) for helping.

8. REFERENCE

1. River Bureau of MLIT, *Guidelines for Seismic Performance Evaluation of Dams during Large Earthquakes* (2005)
2. JSCE, Proposal on Earthquake Resistance for Civil Engineering Structures (2000)
3. MLIT, *Basis of Structural Design for*

Buildings and Public Works (2002)
4. Matsumoto, N., Yoshida, H., Sasaki, T. and Annaka, T. Response Spectra of Earthquake Motion at Dam Foundations, *Proceedings of the 21st Congress of ICOLD* (2003)
5. Shimamoto, K., Sasaki, T. and Kondo, M., Trial Implementation of New Japanese Guidelines for Seismic Performance Evaluation of Dams during Large Earthquakes, *The 75th Annual Meeting of ICOLD* (2007) (printing)

Table 1 Composition of the Guidelines

Chapter	Section
1. Basic matters	1.1 Intent of Guidelines 1.2 Definition of terms 1.3 Scope of application 1.4 Basic concepts of evaluation 1.5 Seismic performance required 1.6 Water level condition for evaluation
2. Earthquake motion for seismic performance evaluation	2.1 Selection of *Scenario earthquakes* 2.2 Setting of *Level 2 earthquake motions* for evaluation
3. Methods for evaluating dam bodies	3.1 Policy for evaluation of dam bodies 3.2 Evaluation of concrete dams 3.3 Evaluation of embankment dams
4. Methods for evaluating appurtenant structures	4.1 Selection of structures to be evaluated 4.2 Evaluation of appurtenant structures

Table 2 *Lower-limit acceleration response spectrum for evaluation* (attenuation constant = 5%)

Range of natural period T (sec)	Acceleration response spectrum S_A (gal)
$0.02 \leq T < 0.1$	$S_A = 400/0.08 \times (T-0.02) + 300$
$0.1 \leq T \leq 0.7$	$S_A = 700$
$0.7 < T \leq 4$	$S_A = 700 \times (T/0.7)^{-1.642}$

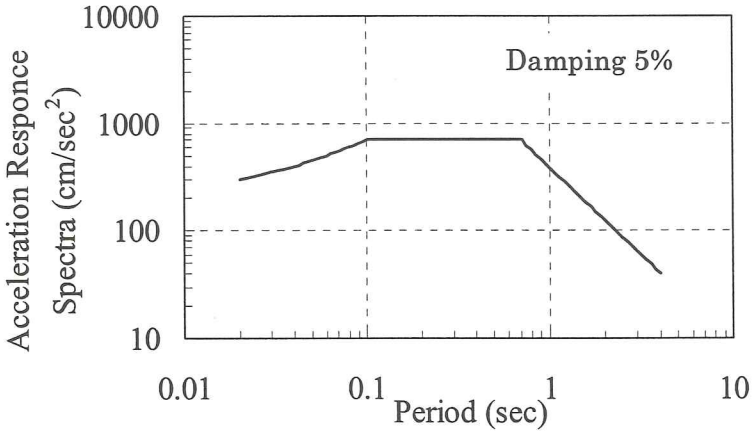

Fig. 1 *Lower-limit acceleration response spectrum for evaluating seismic performance*

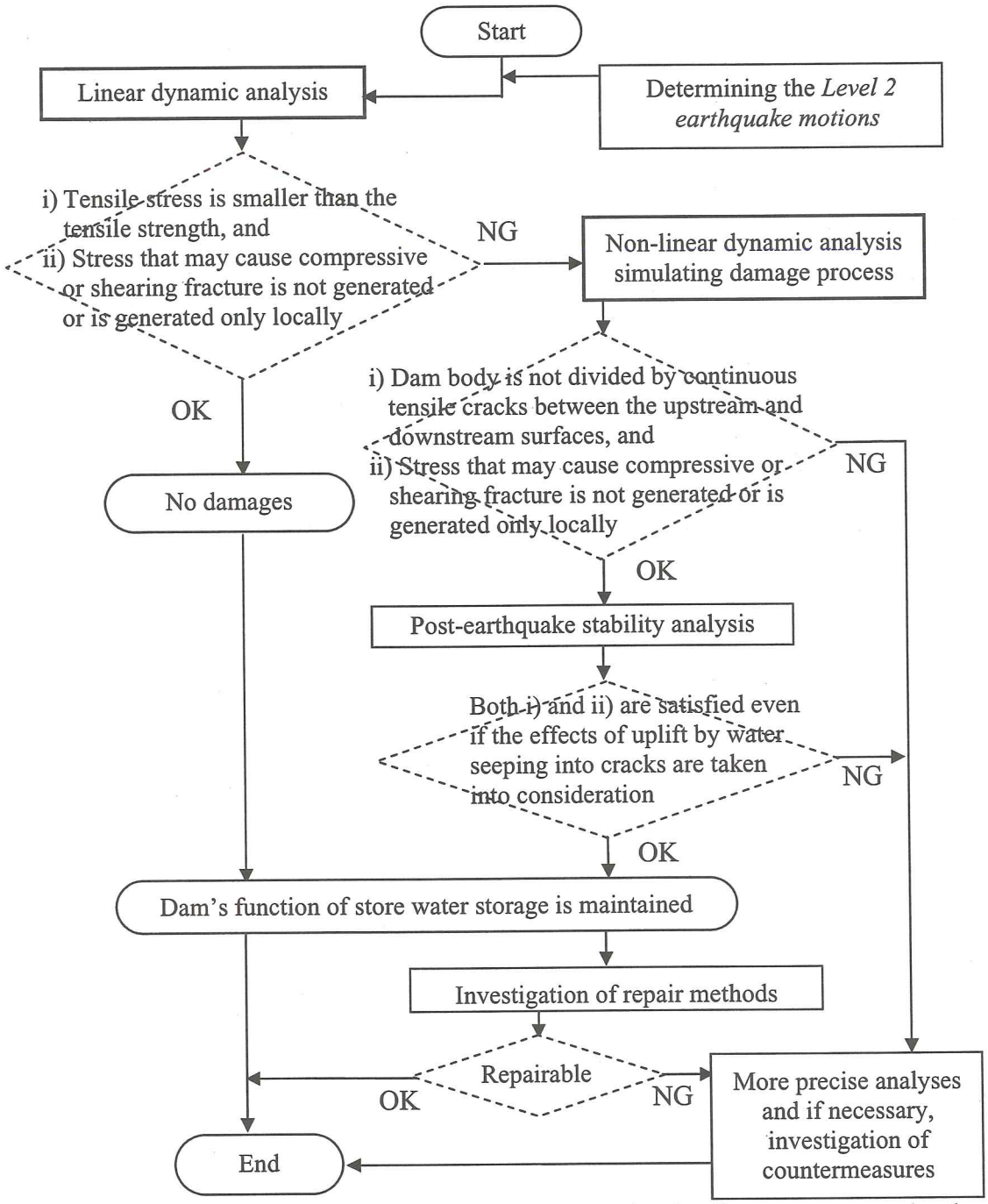

Fig. 2 Flow chart of seismic performance evaluation for concrete gravity dams

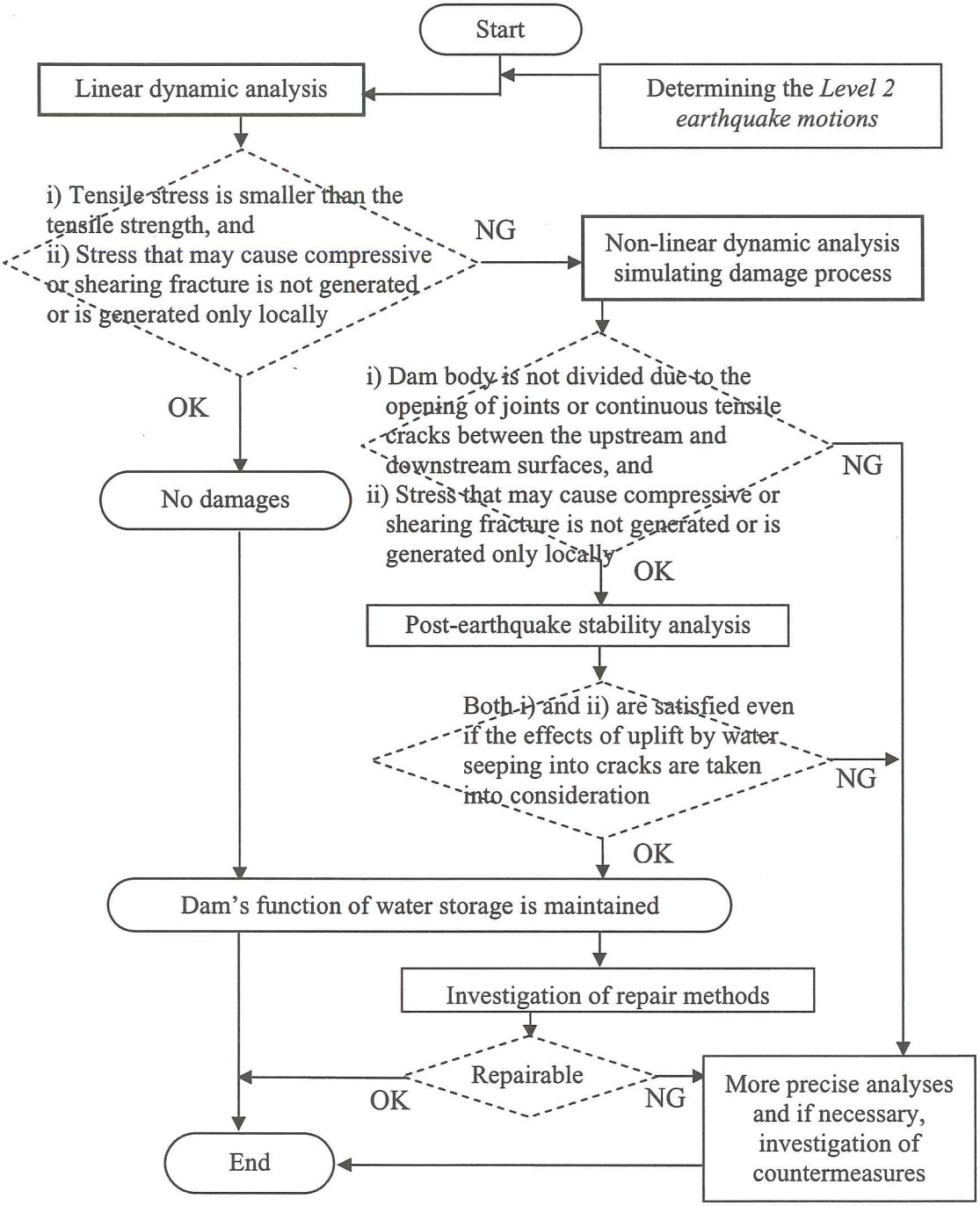

Fig. 3 Flow chart of seismic performance evaluation for concrete arch dams

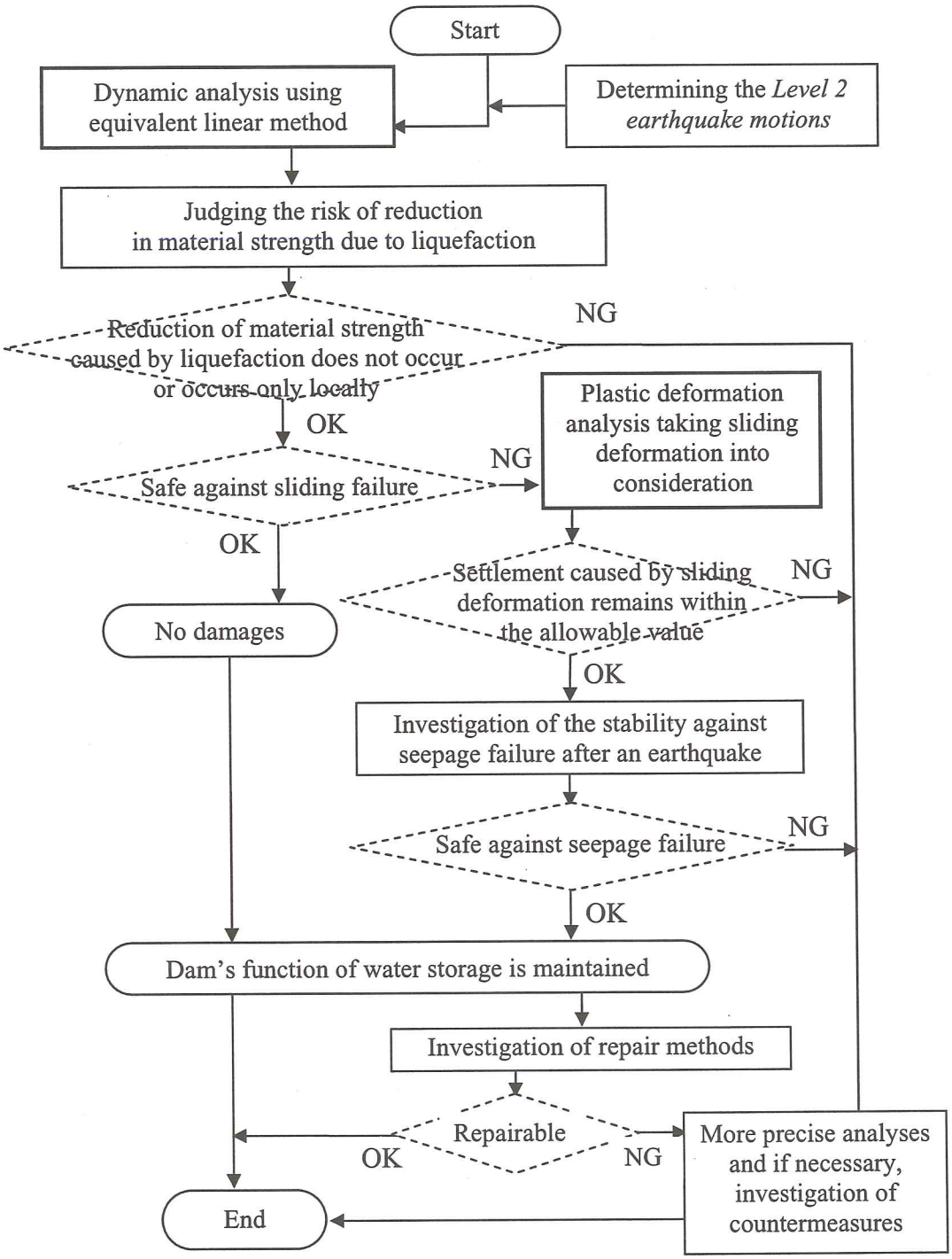

Fig. 4 Flow chart of seismic performance evaluation for embankment dams

Lessons Learned from Analysis of the New Orleans Hurricane Protection System

By

Interagency Performance Evaluation Task Force
Reported by Michael K. Sharp

ABSTRACT

This report, Performance Evaluation of the New Orleans and Southeast Louisiana Hurricane Protection System, is the final report of a series concerning the in-depth analysis of the New Orleans and Southeast Louisiana Hurricane Protection System conducted by the Interagency Performance Evaluation Task Force (IPET). The IPET was established by the Chief of Engineers to determine the facts concerning the performance of the hurricane protection system in New Orleans and Southeast Louisiana during Hurricane Katrina. The analyses conducted by the IPET and the information presented in this report are designed to answer five principal questions that comprised the IPET mission:

- The System: What were the pre-Katrina characteristics of the hurricane protection system (HPS) components; how did they compare to the original design intent?

- The Storm: What was the surge and wave environment created by Katrina and the forces incident on the levees and floodwalls?

- The Performance: How did the levees and floodwalls perform, what insights can be gained for the effective repair of the system, and what is the residual capability of the undamaged portions? What was the performance of the interior drainage system and pump stations and their role in flooding and unwatering of the area?

- The Consequences: What were the societal-related consequences of the flooding from Katrina to include economic, life and safety, environmental, and historical and cultural losses?

- The Risk: What were the risk and reliability of the hurricane protection system prior to Katrina, and what will they be following the planned repairs and improvements?

The knowledge gained in answering these questions 1) was applied directly to the design and construction of immediate and longer term repairs, 2) was used to assess the integrity of and plan remedial actions for the sections of the hurricane protection system not severely damaged, 3) is being used in the ongoing efforts to enhance the capabilities of the system to achieve 100-year levels of protection, and 4) provide analytical methods and a body of knowledge to assist in planning and designing more effective protection measures in the future. The IPET analytical tools and information bases are being transitioned to the Louisiana Coastal Protection and Restoration Study (LaCPR), to assist in developing effective approaches for higher levels of protection.

The nine volumes of the final report provide a detailed documentation of a broad, multi-disciplinary analysis of the hurricane protection system and its performance during Hurricane Katrina. The frequent professional interaction and review comments provided by the American Society of Civil Engineers (ASCE) External Review Panel and the strategic oversight of the National Research Council (NRC) Committee on New Orleans Regional Hurricane Protection Projects have made substantial contributions to the conduct of the analysis and development of the results described in this report. This volume, Volume I, Executive Summary and Overview, provides an overview of the IPET and its efforts, a synopsis of the performance of the hurricane protection system during Katrina and a summary of the principal findings and lessons learned. All are described in more detail in Volumes II–IX. Since the hurricane protection system is only

designed to manage flooding in the metropolitan New Orleans basin, wind-based consequences and any direct consequences exterior to the hurricane protection system are excluded from this report. In addition, the IPET did not examine organizational and jurisdictional issues that impacted the effectiveness of the physical hurricane protection system. These issues are being examined by a separate team in the Hurricane Performance Decision Chronology Study whose results will be reported separately.

This report and all other IPET-produced documents are available on the IPET Web site, *https://IPET.wes.army.mil.*

1.0 HURRICANE KATRINA AND ITS IMPACT

In 2005 the world watched Hurricanes Katrina, Rita, and Wilma devastate portions of the Gulf Coast of Louisiana and Mississippi. The Corps of Engineers, in conjunction with other federal, state, and local partners, mounted an unprecedented, multi-faceted effort to assist in the recovery and rebuilding of the areas affected by these massive storms. The devastation from Hurricane Katrina in New Orleans and vicinity was particularly unprecedented. Because of the extent of the damage to the HPS itself and the consequences of the subsequent flooding, it was imperative to understand what happened and why. Only through this knowledge could the levees and floodwalls be repaired and rebuilt to provide more effective protection in the future. This report provides a detailed accounting of the IPET work to determine why the hurricane protection measures performed as they did and how to provide more effective protection for the future. The area of principal study is shown in Figure 1 and represents the bulk of New Orleans and Southeast Louisiana. This overview includes a brief historical perspective of hurricane protection in New Orleans, a description of the IPET organization and its activities, and an overview of what happened during Katrina in the context of the five IPET mission questions and the analyses accomplished to answer those questions.

2.0 HISTORICAL PERSPECTIVE

Geologic History and Setting: The following is a brief overview of the geologic setting in New Orleans and its influence on the HPS. A more detailed summary of the geologic history of the New Orleans region and the implications of the geologic conditions on the HPS is provided in Appendix I-5. There is also significant discussion of geologic issues on the HPS in Volume III and extensive information on geology presented in Volume V.

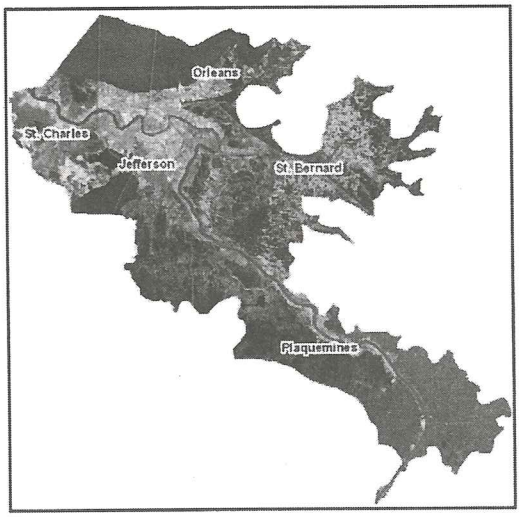

Figure 1. Principal area of analysis.

The geologic history of the New Orleans area significantly influences the engineering properties of the foundation soils beneath the levees. Geologic and engineering data gathered from the different levee failures identify a spatially complex geomorphic landscape, caused by Holocene sea level rise, development of different Mississippi River delta lobes, and the distributary channels associated with delta development. Overlying the Pleistocene surface beneath the New Orleans area are predominantly fine-grained, shallow water depositional environments and related sediments associated with bay sound (or estuarine), nearshore-gulf, sandy beach, lacustrine, interdistributary, and paludal (marsh and swamp) environments. These environments define the New Orleans area history during the Holocene, and comprise the levee foundation for the different failure areas. A relict barrier beach ridge is present

in the subsurface along the southern shore of Lake Pontchartrain. This relict beach blocked the filling of the lake with fluvial-deltaic sediments, impacted the supply and texture of sediment being deposited by advancing distributary channels, and influenced the engineering properties of these soils. Marsh and swamp soils beneath the failure area at the 17th Street Canal are much thicker than those beneath the London Avenue Canal because of the influence of the beach complex, and are thickest in the Inner Harbor Navigation Canal area.

Additionally, man's activities in New Orleans during historic time contributed to the spatial complexity of this area and affected the engineering properties of the foundation soils. Man's activities included construction of drainage and navigation canals, pumping groundwater drainage, hydraulic filling of the Lake Pontchartrain lake front, and construction of levees to prevent the river from flooding low-lying areas. Man's activities, combined with the geologic setting and subsidence in this region are responsible for the unique landscape that created the New Orleans area. Historic settlement and subsidence in the New Orleans area has been most severe on the back barrier side of the relic Pine Island Beach (along the south shore of Lake Pontchartrain).

Subsidence did not contribute materially to the foundation failures of the I-wall/levee structures on the outfall canals. However, subsidence has impacted the datum of many of the benchmarks in the city upon which engineering decisions and design were based and affected levee and floodwall height and the level of flood protection. This did influence the amount of overtopping that occurred, which contributed to erosion behind floodwalls and on the back sides of levees that eventually led to their breaching.

Geographic History and Setting: Located in the low-lying Mississippi River delta in Louisiana, large portions of New Orleans lie near or below sea level, which has posed complex flood management problems since the city's founding in 1718. Historically, the greatest natural threat posed to residents and property in the New Orleans area has been from hurricane-induced storm surges, waves, and rainfall. Until the early twentieth century, construction was largely limited to the slightly higher ground along old natural river levees and bayous, since much of the rest of the land was low, swampy, and subject to frequent flooding. In 1899, the Sewerage and Water Board of New Orleans was created; it remains responsible for draining the city. The topography of New Orleans makes drainage a major challenge, with the same natural and artificial levees designed to keep water out having the unintended effect of confining rainwater and sewage in the city. This led to perhaps one of the most sophisticated and comprehensive drainage systems in the world.

The drainage system created by the Sewerage and Water Board allowed the city to expand outward from the higher ground close to the river into the lower elevations towards and near Lake Pontchartrain. The development of these areas in the early 1900s caused the water table to drop dramatically, which in turn enabled development of additional new neighborhoods such as Lakeview. In addition to the lakeside portions of the city, development in the other areas surrounding the metropolitan area led to a seven-fold total increase in urban acreage during the twentieth century.

The Sewerage and Water Board today drains over 61,000 acres in New Orleans and neighboring Jefferson Parish of almost 13 billion cu ft (cubic feet) of water per year. The drainage system includes 90 miles of covered canals, 82 miles of open canals, and a multitude of pumping stations. However, pumping of groundwater from underneath the city has accelerated the subsidence that the area was already prone to because of its natural alluvial floodplain geology. The subsidence increases the flood risk, should the levees be breached or precipitation exceed pumping capacity, because the New Orleans bowl is becoming deeper as time and subsidence progress.

The geographic location of New Orleans makes the city particularly vulnerable to hurricanes. Fortunately, New Orleans has been impacted by only a few large storms. New Orleans

was hit by major storms in the 1909 and 1915 Atlantic hurricane seasons. Much of the city flooded in September 1947 due to the Fort Lauderdale Hurricane. The next major threat came in the 1960s with Hurricanes Betsy and Camille.

In 1965 the city was severely damaged by Hurricane Betsy. The catastrophic flooding of the city's Lower 9th Ward, 75 fatalities and substantial loss of property, made Betsy the nation's first billion dollar storm. Although Camille came close to New Orleans, it had much more impact in Mississippi and caused relatively minor damage in New Orleans proper. There has not been severe flooding in New Orleans from a hurricane since Betsy. The city did experience severe flooding May 8, 1995, when heavy rains suddenly dumped over 12 in. (inches) of water on New Orleans in a short time period, overwhelming the pumps. Betsy was the stimulus for the Flood Control Act of 1965 which was the initial authorization for the HPS in place today.

Hurricane Protection System History: Over time, three hurricane protection projects have been designed and partially constructed in New Orleans and the Southeast Louisiana region: Lake Pontchartrain and Vicinity Project, the West Bank and Vicinity Project, and the New Orleans to Venice Project. The Lake Pontchartrain and Vicinity Hurricane Project is discussed in more detail below because of its central role in Hurricane Katrina. All of these projects are discussed in detail in Volume III of this report.

The Lake Pontchartrain and Vicinity Hurricane Project was intended to protect areas around the lake (in Orleans, Jefferson, St. Bernard, and St. Charles Parishes) from flooding caused by a storm surge or rainfall associated with a hurricane that would be roughly the same as what is today classified by the Saffir-Simpson Scale as a fast-moving Category 3 hurricane. The basis for this was the SPH developed for the Corps by the Weather Bureau (now the National Weather Service). The SPH is a steady-state storm based on an analysis of meteorological parameters of past large hurricanes. The assumption of steady-state precludes the consideration of some of the dynamic behaviors we now know characterize hurricanes such as decreasing in intensity and increasing in diameter as they approach shore. It also precludes consideration of the dramatic impact of large storms in generating surge and waves long before they reach landfall. For the initial definition of the SPH used in design of the New Orleans hurricane protection structures, hurricanes were considered that occurred during the period 1900 to 1956. Central Pressure Index (CPI) was the primary intensity criterion and the 1-percent recurrence CPI (100-year) was chosen for the initial SPH definition. When the additional consideration of the likelihood of a storm of that size hitting the area near New Orleans is added, it was estimated to be equivalent a 200- to 300-year recurrence event. The SPH was intended to represent the most severe meteorological conditions considered "reasonably characteristic" for the region. A maximum wind speed was also associated with the SPH; for Lake Pontchartrain and Vicinity, it was assumed to be 100 miles per hour.

Following Hurricane Betsy in 1965, the wind speed criterion was revised but all other characteristics remained the same. The 1965 version of the SPH was used for the design of both the Lake Pontchartrain and Vicinity and New Orleans to Venice Projects. In 1979, NOAA issued a report that significantly revised the SPH criteria, and this became the basis for the design of the West Bank and Vicinity Project. All activities with respect to the Lake Pontchartrain and Vicinity continued to use the original SPH criteria through the time of Hurricane Katrina.

Although federally authorized, the Lake Pontchartrain and Vicinity Project was to be a joint federal, state, and local effort, with the federal government paying 70 percent of the costs and the state and local interests paying 30 percent. The local interests included the State of Louisiana Department of Transportation and Development, the Sewerage and Water Board, and the local levee boards. The Corps of Engineers was assigned responsibility for project design and construction, and the local interests were responsible for operation and maintenance of the levees and flood control structures. This was one of the first major cost-sharing projects for the Corps of Engineers.

During the first 17 years of the project, it was focused on what has become known as the "barrier plan." The barrier plan included a series of levees along the lake front, concrete floodwalls along the IHNC, and a variety of control structures, including barriers and flood control gates located at The Rigolets and Chef Menteur Pass areas that connect Lake Pontchartrain to Lake Borgne. These structures were intended to prevent storm surges from entering Lake Pontchartrain and overflowing the levees along the lake front. A number of project delays and cost increases occurred as a result of technical issues, environmental concerns, legal challenges, and local opposition to various aspects of the project.

A December 1977 court decision enjoined the Corps from constructing the barrier complexes and certain other parts of the project until a revised environmental impact statement was prepared and accepted. The Corps conducted a "Re-Evaluation Study," published in 1984, in response to the court order and examined the feasibility of providing protection mostly by means of raising and strengthening levees and floodwalls. The exact treatment of the outfall canals was not resolved. Based on this study, the Corps recommended shifting to the "high level plan" originally considered in the early 1960s. Follow-on efforts examined the use of butterfly surge gates and pump stations at the lake ends of the canals and the use of parallel protection levees and floodwalls along the length of the canals as the sole protection measure. The Energy and Water Development Act of 1992 mandated the use of parallel protection and set the stage for the construction of the levee and I-wall structures that were in place prior to Katrina. Note that the original authorization for protection occurred in 1965 time frame and the final resolution of how to provide protection for a large portion of the metropolitan area of New Orleans was not determined until 1992, over a quarter of a century later.

The construction of the HPS was accomplished in many separate steps over a long period of time. The first major structures constructed were the levee and floodwall structures within the IHNC (late 1960s and early 1970s). The levees and structures along the east side of St. Bernard Parish from Bayou Bienvenue to Bayou Dupre were built in the same time frame with periodic enhancements. The initial levee lifts were placed by hydraulic fill from 1967 to 1970, and subsequent lifts were added from 1972 to 1987. Sheet-pile closures at bayous and pipelines were placed in 1992. Construction of the floodwalls along the outfall canals occurred from 1993 to 1999. There were 10 flood-proof bridges and 4 fronting protections (associated with pump plants along the canals) also included in the effort. At the time of Katrina, nine of the bridges had been constructed. The fronting protection for the London Avenue (number 4) and 17th Street (number 6) pump stations were completed prior to Katrina. The protection for Pump Station No. 7 on Orleans Canal and Pump Station No. 3 on London Avenue Canal remained to be done. The lack of the fronting protection for Pump Station No. 7 left a section of legacy wall significantly lower than the adjacent floodwalls, providing a route for water to enter the city without overtopping adjacent floodwalls. This omission left a weak link which compromised the local level of flood protection. Ironically, work on this area was terminated due to lack of funding.

Some components of the system were not scheduled to be completed until 2015, primarily the West Bank and Vicinity Project. At no time has the entire New Orleans and Vicinity area had a reasonably uniform level of protection around its perimeter. At no time has any individual parish or basin had the full authorized protection planned for in 1965.

As of May 2005, the Lake Pontchartrain and Vicinity Project included about 125 miles of levees, major floodwalls, flood-proofed bridges, and a mitigation dike on the lake's west shore. Progress on the project varied by area: 90 percent complete in Orleans Parish, 70 percent complete in Jefferson Parish, 90 percent complete in the Chalmette area, and 60 percent complete in St. Charles Parish. In 2002, a pre-feasibility study on whether to strengthen hurricane protection along the Louisiana coast was completed. A full feasibility study was estimated to take 5 years to complete. A major Emergency Response Exercise

in July 2004 used the hypothetical Hurricane Pam to examine the ramifications of a storm much like Katrina. The results projected losses in excess of what happened in Katrina, including massive overtopping and breaching of levees.

The history of this HPS has been one of continuous incompleteness. This situation was a product of the overall water resources development process, the magnitude of the investments needed to accomplish such projects, the piecemeal allocation of resources, the time and complex processes required to resolve differences in local and federal priorities, and the traditional step-by-step construction process for structures such as levees in subsidence-prone areas such as New Orleans. The affordability of protection appeared to be a major issue between local and federal authorities.

3.0 PRINCIPAL FINDINGS AND LESSONS LEARNED

This section presents the principal findings and lessons learned from the IPET efforts. The information here represents a big-picture perspective of an extensive amount of work and does not attempt to include detail or supporting technical data or arguments. More detailed findings and lessons learned are provided in each volume of the IPET report along with extensive supporting information on the analyses upon which they were based.

3.1 PRINCIPAL FINDINGS

3.1.1 The System

Impact of Datum Misinterpretation: Spatial and temporal variations of 0.2 to 3 ft were found between the geodetic datum (land elevation reference) and local mean sea level (water level reference datum, LMSL). Some flood control structures in the region were authorized and designed relative to a water level datum (mean sea level), but constructed relative to the geodetic vertical datum incorrectly assumed to be equivalent to the water level datum. This resulted, in the case of the outfall canals, in structures built approximately 1 to 2 ft below the intended elevation. Updating of the reference elevation points for the region, although underway, was not completed. The use of out-of-date reference elevation points left decision makers without an accurate understanding of the actual elevations of the hurricane protection structures.

Impact of Subsidence: The variable and considerable subsidence in the New Orleans area was reflected in the performance of the system in Katrina. It was well known that the New Orleans area experiences significant subsidence, and structures such as levees had some increases in their initial design elevations as compensation. The amount of elevation loss for critical hurricane protection structures was not well quantified prior to Katrina. The IHNC structures, for example, are more than 2 ft below their intended design elevations, mostly from subsidence over the 35-year life of the project. This resulted in a significant loss of protection capability in areas such as the IHNC. The lack of knowledge of accurate elevations was directly tied to the incomplete update of the geodetic reference datum and LMSL.

The hurricane protection system consists predominantly of levees and levees with cantilevered I-type floodwalls. In locations where the right of way did not permit these options and at gated closure structures, there are segments of T-walls. T-walls are inverted "T" shaped concrete structures supported on pre-cast prestressed concrete or steel H-piles. As with I-walls, a continuous steel sheet-pile wall is embedded in the bottom of the above ground concrete wall to reduce seepage under the structure. The vast majority of the total miles of structures were conventional levees, the majority of floodwalls were I-wall structures with selected areas, specifically at transitions to major structures such as pumping plants and gated structures, having T-walls.

All of the structures are constructed on weak and compressible soils. Stability and settlement of structures are generally critical design issues. The geology of the area was relatively well known and borings taken were reasonably adequate for characterizing the variety of conditions in the area,

but the spacing could miss local anomalies in soil type and strength. See Appendix I-5 and Volume V for more details on the geology of the area and its impact on performance.

The majority of the structures in the HPS were generally built as designed, and design approaches were consistent with local practice. A number of samples were taken of materials used in the construction of the structures, particularly concrete from the floodwalls and steel from sheet piles. These samples were tested by independent laboratories and all test results conformed to accepted standards. Sheet-pile lengths were confirmed by physically pulling them from the ground.

The levee and I-wall structure designs along the 17th Street and London Avenue Outfall Canals and for a portion of the Inner Harbor Navigation Canal (IHNC) were inadequate. Several factors significantly impacted the performance of these structures during Katrina. The 17th Street Canal structures had the most significant issues. First, the foundation soil strengths were derived from widely spaced borings and at times using average values that do not capture the high variability inherent in this type of geology. Second, an assumption of uniform shear strengths for soils, based on the greater strengths under the centerline of the levee, beneath the 17th Street Canal levee and floodwall resulted in an overestimation of the subsurface strength at the levee toe. Third, the shear strength of the clay soils under the 17th Street Canal levee and floodwall assumed for design were higher than warranted from the measured data available at the time. These same soil strength assumptions were not made in other sections of the system where more conservative strength values were used.

The levee and I-wall designs for the outfall canals and IHNC did not consider deflection of the I-wall to the extent that hydrostatic pressure would reach to the base of the sheet piles. This deflection and pressure basically split the levee into two pieces resulting in the protected side attempting to resist the forces for which the entire structure was designed. This played a major role in all four of the I-wall foundation failures. At London Avenue, the deflections provided a direct pathway for the high hydrostatic pressures for the elevated flood waters in the canals to enter the underlying porous relic beach sands and rapidly propagate to the back side of the levee. The pressure caused massive subsurface erosion of the sand under the levee as well as uplift on the protected half of the levee reducing its ability to resist the forces placed on the floodwall and sheet pile. This resulted in failure of the levee-floodwall system.

The original design criteria developed through use of the Standard Project Hurricane (SPH) in 1965 and used for the outfall canals in the late 1980s, was not representative of the hurricane hazard at the time of the design. The Standard Project Hurricane is defined as a hypothetical hurricane intended to represent the most severe combination of hurricane parameters that is reasonably characteristic of a specified region, excluding extremely rare combinations. In 1979 the National Oceanic and Atmospheric Administration (NOAA), updated the SPH definition by increasing the maximum sustained wind speed to 115 mph from the original 100 mph. The Corps chose to continue to use the original SPH definition developed for the Lake Pontchartrain and Vicinity Project for use on the outfall canals. The 1979 definition of the SPH was used for design of the West Bank and Vicinity protective structures.

The system did not perform as a system. The hurricane protection in New Orleans was designed and developed in a piecemeal fashion, resulting in inconsistent levels of protection. In addition to the use of different SPHs for individual projects, the designs for specific structures were influenced by the local conditions. For example, the levee and I-wall system designed for the Orleans Canal was more conservative than that for the 17th Street Canal. The Orleans Levee was broader and the I-wall freeboard (height above the levee crest) less. Soil strength assumptions were also more conservative, using the weaker values at the toe instead of the stronger values under the centerline as assumed for the 17th Street Levees.

Levee and I-walls were designed to provide protection up to the estimated water elevations for the SPH. They were not designed to withstand overtopping. There was no armoring or uniform use of erosion resistant soils in the levee sections. Levee materials ranged from highly resistant to scour to poorly resistant, resulting in significant variations in the protection levels afforded nearby areas. Similarly, I-walls were not protected against erosion if overtopping occurred. Given overtopping, evacuation was the only alternative to reduce exposure to flooding.

The system was not scheduled for completion until 2015. Sections that are not completed represent anomalously low areas, often accompanied by transitions from one type of structure to another. These ended up being weak spots, more vulnerable to overtopping and then erosion.

A majority of the pump stations are not part of the HPS and were not designed to provide capability during large storms. Most pump operators are routinely evacuated prior to hurricanes striking the area because of a lack of a safe haven to ride out the storm. Many of the larger pumping stations have mechanisms to prevent backflow through the pumps if they are not being operated. In some cases these require manual activation.

3.1.2The Storm

Katrina generated a storm surge and wave environment unparalleled in the history of New Orleans. Hurricane Katrina was a very large Category 3 storm when it passed the New Orleans area on the morning of August 29th. Twenty-four hours earlier this storm had been the largest Category 5 and most intense (in terms of central pressure) storm on record within the northern Gulf of Mexico. During Katrina, at a location due east of the Mississippi River delta and just offshore in deep water, NOAA Buoy 42040 recorded the highest significant wave height ever measured in the Gulf of Mexico (55 ft). That observation matched the largest significant wave height ever recorded by a sensor within NOAA's buoy network, in any ocean. The large size of Katrina throughout its history, combined with the extreme waves generated during its most intense phase, enabled this storm to produce the largest storm surges that have ever been observed within the Gulf of Mexico (up to 28 feet in Mississippi), as determined from analyses of historical records.

Hurricane Katrina generated water levels that for much of the system significantly exceeded the design criteria. Katrina surge levels were up to 20 ft along the east side of the HPS, substantially higher, up to 5 or 6 ft, than the design levels for all areas along the eastern and southern portions of the HPS. The surge levels were roughly equivalent to design criteria along the southern shore of Lake Pontchartrain. Katrina-generated wave heights were approximately equal to the design criteria with the exception of Plaquemines Parish where Katrina-generated waves were significantly higher. Wave periods, however, especially along New Orleans East, St. Bernard, and Plaquemine Parishes, were approximately three times that estimated for the design criteria. The waves impacting the levees were 15- to 16-second-long period ocean storm waves that caused much more runup and overtopping than shorter period waves.

Local wave generation can contribute significantly to wave conditions within outfall and navigation canals in the New Orleans area. Local wave generation in the outfall canals during Katrina generated higher wave conditions over much of the length of the canal than were associated with the waves entering the canals from primary generation areas (either Lake Pontchartrain or the Gulf of Mexico). In the most extreme case examined here, wave heights of over 4 ft were generated within the GIWW/MRGO canal entering the IHNC from the east. The IHNC design assumed 1-ft waves. Detailed hydrodynamic analyses showed that dynamic forces were a significant portion (20 to 30 percent) of the total forces experienced by many of the levees and floodwalls. The dynamic forces considered in the original design were significantly less.

Overtopping by waves generated very high velocities over the crest and back sides of the

levees, leading to a high potential for scour and erosion. Velocities from 10 to 15 ft/sec were calculated for the back sides of the levees along St. Bernard Parish, while the front sides of the levees experienced velocities of about one-third of those on the back side. Since erosion potential is related to the cube of velocities, the erosion potential on the back side of the levees was up to 27 times greater. The exception was in the east/west-trending leg of the GIWW near the I-10 Bridge, where wave energy and currents were almost parallel to the orientation of the levees and while overtopping occurred, the back side velocities were not severe. Examination of these levees that failed due to erosion determined that all failures were caused by erosion of the crest and back face.

The southeast trending leg of the Mississippi River Gulf Outlet (MRGO) had little influence on the water levels in the IHNC during Katrina. The relative size of the channel with respect to the very large flow area available when the marsh areas have been inundated by surge, make the amount of water conveyed through the channel a relatively small part of the total. During Katrina, MRGO was far from the "hurricane highway" moniker with which it has been branded. Model results show that this is the case for very large surge-generating storms in this area. This finding agrees with those of an independent study conducted for the State of Louisiana.

There was no evidence of significantly reduced surge levels and wave heights in areas adjacent to wetlands and marshes. Surge elevations and wave energy along the HPS were impacted mostly by the relative orientation of structures with respect to the direction of the wind and oncoming surge and wave energy. For example, areas on the south side of St. Bernard Parish were sheltered from the dominant east to west movement of wind and water, resulting in reduced storm water levels and less damage. It is likely that the presence of marshes had an impact on surge and wave conditions during the earlier parts of the storm, but the massive size of the storm and propagation of surge and waves ahead of landfall had inundated the surrounding marshes with significant water long before the peak of the storm hit. The exact impact of marshes on surge and waves remains unquantified.

Measurements of temporal variation in wave and water level conditions, and wind, through the peak of the storm were extremely scarce. Of the few sensors deployed in the high impact zone, nearly all were damaged or malfunctioned. None of the self-recording instruments that were in place to record water levels successfully captured water level changes through the peak of the storm in the high impact zone. All malfunctioned prior to the peak.

3.1.3 The Performance

Of the 50 major breaches experienced by the HPS during Katrina, all but four were due to overtopping and erosion. For floodwalls, the overtopping caused erosion behind the walls that eventually caused instability and wall failure. For levees, the scour eroded the back sides and tops of the levees due to high velocities of the overtopping waves in areas of erosion-susceptible soils creating breaching. Areas with high quality levee materials performed well in the face of water conditions that exceeded their design criteria. Structures at authorized design elevations would have reduced the amount of overtopping.

There was no evidence of systemic breaching caused by erosion on face or water sides of the levees exposed to surge and wave action. The water velocities on the face side were only one-third of those experienced at the crest and back or protected side of the levees. The levees largely performed as designed, withstanding the surge and waves until overtopping, at which time they became highly vulnerable to erosion and breaching, especially those constructed by hydraulic fill.

Four breaches, all in the outfall canals and IHNC and all involving I-walls, occurred before water levels reached the top of the floodwalls. All were caused by foundation failures induced by the formation of a gap along the canal side of the floodwall. All of these structures were built over a layer of marsh sediments, in two cases underlain by clays and in the other two underlain by relict beach sand deposits. Along the outfall canals, the

subsurface conditions dictated the specific mechanics that, coupled with the high hydrostatic pressures introduced to depth by the gap along the face of the sheet pile, led to instability and failure. The sites underlain by sand experienced significant uplift pressures, seepage and, in one case, a massive piping of subsurface sand from under the levee to the protected side. This action undermined the floodwall.

In the case of the sites underlain by clays, the formation of the gap to the base of the sheet piles introduced high loads along the depth of the wall which could not be resisted by the weak clays. At the IHNC site, the fact that the ground surface elevations beyond the levee toe were significantly below those in the design cross sections contributed to the failure. Soil strength assumptions used in the design of the 17th Street structures were too optimistic. The formation of the gap and the associated hydrostatic pressures introduced at depth, along with effectively splitting the levee into two parts, resulted in a significant reduction in the factor of safety of the structure. This failure mechanism, in particular the gap formation to the bottom of the sheet piles, was not considered in the original design of these structures.

Three other sites within the IHNC experienced I-wall breaches due to overtopping and scour behind the walls which reduced the stability of the structures. These breaches added to the flooding in Orleans (East Bank) and the Lower Ninth Ward. The storm surge levels in the IHNC exceeded the design levels, and lower structure elevations, reduced over 2 ft by 35 years of subsidence, contributed to the amount of overtopping that occurred.

Transitions between types and levels of protection and between protection structures and other features created vulnerabilities to erosion and breaching and reduced the effectiveness of the protection. Some of the transitions are associated with changes in the organization responsible for the structures, some are due to incompletion of the authorized construction, and others are associated with necessary penetrations through the levee/floodwall system.

In spite of being subjected to design-exceeding conditions and forces, many sections of the HPS performed well. These tended to be sections with materials resistant to erosion and more conservative designs. The Orleans Canal levee-floodwalls are similar to those on the 17th Street and London Avenue Canals, yet they did not fail. The northern section of Orleans Canal is underlain by clays similar to the 17th Street breach site and the southern section is underlain by sand similar to the London Avenue breach sites. Investigations showed that the levees were more conservative in design, having broader base and less floodwall freeboard. In addition, more conservative soil strength values were assumed in their design.

Levee sections constructed from quality clay materials were much less susceptible to erosion from overtopping. They performed well in spite of being subjected to conditions significantly beyond their design criteria. There was a direct correlation between the character of the levee materials and their performance.

Flooding from Katrina covered approximately 80 percent of the New Orleans metropolitan area. For Orleans East and St. Bernard Parishes, approximately two-thirds of the volume of flooding can be attributed to water flowing through breaches. The one-third due to overtopping and the very large amount of rainfall would itself have caused a significant level of interior flooding.

The three breaches in the outfall canals and I-wall/levee failures along the west side of the IHNC were responsible for approximately 70 percent of the flooding in Orleans East Bank. The remainder was due to the heavy rainfall (up to 14 in. in 24 hr) and overtopping.

Because of inoperability, pump stations played no significant role in the reduction in flooding during Katrina. Sixteen percent of the total pumping capacity was operating during the storm, equivalent to approximately 18,000 cfs. The distribution of operating pumps across four parishes, however, reduced the impact of the pumping. Their inoperability, due to a

combination of the necessary evacuation of operators, loss of power, loss of cooling water, and flooding, impacted the ability to unwater the city after the storm. Temporary pumps were useful after Katrina, but provided only a small fraction of the capacity needed. Reverse flow through some pumps added to the flooding in at least one parish. While methods are available to prevent reverse flow, they are dependent on human implementation and electrical power.

The maintained condition of the levees was an additional negative factor in the performance of the system. While the presence of trees and other features on the levees could not be directly related to the failures of the outfall canal structures, it is likely that they were enablers in the overall breaching process. The presence of large trees on the levees was particularly troublesome and could easily have accelerated the failure process.

All features must be included in the performance assessments of a system. There are other features, such as the CSX railroad closure gate, that are not an integral part of the HPS but are sources of vulnerability and require independent action to manage during a hurricane event.

3.1.4 The Consequences

Loss of life was concentrated by age, with 70 percent of deaths being people over the age of 70. There were 727 fatalities in the five parishes examined. The poor were disproportionately affected. Loss of life also correlated to elevation, in terms of depth of flooding, especially with regard to the poor, elderly, and disabled, the groups least likely to be able to evacuate without assistance.

Katrina caused direct property losses (excluding Plaquemines Parish) of over $20 billion, approximately 78 percent ($16 billion) of which was attributed to residential losses. The next largest component was the 11.5 percent ($2.4 billion) attributed to commercial losses. There was an additional $7.0 billion in losses attributed to public infrastructure, including the HPS itself. The most significant infrastructure impact was incurred by the HPS ($2.0 billion) followed by roadway networks and assets of the regional electrical distribution\transmission grid. Together, the damages to these categories of infrastructure totaled approximately $2.0 billion. This estimate is followed by damages to public transit assets of approximately $700 million, followed by damages to rail lines, airport facilities, gas and water distribution, telecommunications assets, and assets for waterborne transportation totaling an additional $1.7 to $1.9 billion.

Approximately half of the direct economic losses, excluding public and utilities infrastructure, can be associated with breaching of levees and floodwalls. The remaining losses alone, attributable to rainfall and overtopping, constitute the largest losses experienced in any disaster in the New Orleans vicinity. Losses and, in many respects, recovery can also be directly correlated to depth of flooding and thus to elevation. In some areas flooded by Katrina, where water depths were small, recovery has been almost complete. In areas where water depths were greater, little recovery or reinvestment has taken place.

Combined with the significant and far-reaching impact of Hurricane Katrina regarding initial displacement of population, workforce, and businesses, the impacts to infrastructure and affiliated public welfare and services will contribute to slowed phasing of recovery with regard to return of populace and business activities. Orleans Parish alone is estimated to have lost over 60 percent of its population and St. Bernard Parish nearly 80 percent. On the other hand, St. Charles and Tammany Parishes have increased in population since before the storm.

In terms of the social consequences of the Katrina event specifically, the social organization of the community and region has been compromised by the mass exodus of the population, the structural damage, and the demands to respond and rebuild. The flooding caused a breakdown in New Orleans' social structure, a loss of cultural heritage, and dramatically altered the physical, economic, political, social, and psychological character of the

area. These impacts are unprecedented in their social consequence and unparalleled in the modern era of the United States. The flooding disproportionately impacted the poor, the elderly, and the disabled.

The performance of the levees protecting New Orleans is a key to its social, cultural, and historic conditions. The immediate physical damage made large portions of the city uninhabitable, with thousands of residential, commercial, and public structures destroyed. Basic infrastructure facilities, such as power, water, sewer, and natural gas lines, were made inoperable and continued to be out of service for months after the event. Many victims not only lost their homes, but also their schools, health care, places of worship, places of trade, and jobs. The forced relocations disrupted family and friend networks. As a result, the event not only had an immediate impact on the well-being of the population of those living and working in the metropolitan area, but also resulted in basic changes in the social organization of all aspects of that population.

The available information indicates that if environmental harm has come from the Katrina flooding of greater New Orleans, it was associated with past regional land and water development. Like many other cities, the soils and sediments of land and waters in New Orleans and other delta urban areas are contaminated with metals and organics at concentrations that often exceed health standards in areas of most dense development. The flooding of greater New Orleans removed some contamination from greater New Orleans and transported it to Lake Pontchartrain and Violet Marsh with pumped floodwater where it added a small increment to estuarine sediments. The IPET analysis did not look at local redistribution of contaminants within individual drainage basins. Katrina and Rita resulted in the loss of approximately 300 square kilometers of wetlands and marshes, all independent of the performance of the levees and floodwalls. Loss of wetlands regionally appears to fit a pattern of loss associated with past regional development as well. Overall, any sustained environmental loss from flooding and flood management is indicated to be very small in the context of long-term impacts from development in the region.

3.1.5 The Risk

Risk assessment provides a viable means to understand the relative vulnerability of protected areas. The combination of the likelihood of storm water levels (surge and waves), the likelihood of structural failure at different water levels and dynamic loadings, the likelihood of flooding based on the expected performance of the system, and the consequences of that flooding provides a comprehensive information set on residual risk. This information defines the relative vulnerability of each area as well as the sources of that vulnerability.

Performing a meaningful risk assessment requires an accurate inventory and characterization of all components of the HPS. This includes the information and assumptions used in the design, the physical properties including accurate dimensions and elevations, materials and strengths, and maintained condition. This is a substantial task but provides a foundation for true system-wide analysis.

The effectiveness of the protection system depends on human factors as well as engineered systems. These factors, such as timely gate closures, operating gates, and pumping station operability, must be included in the overall assessment to reach accurate conclusions.

It is critical to estimate the inherent uncertainty in the individual components of the risk assessment and in the final risk products. Risk assessment combines a variety of data types and incorporates numerous models. Each of these has an inherent degree of uncertainty, in their values, in the ability of the models to replicate the processes they represent, and in the end products themselves. The level of uncertainty must be estimated and incorporated in an overall uncertainty analysis to understand the variance associated with the risk assessment results. This provides some measure of the confidence one can have in using the risk data.

3.2 PRINCIPAL LESSONS LEARNED

The principal lessons learned from the IPET analyses are presented below by mission question. Detailed lessons learned are provided in Volumes II to VIII. In addition to the lessons learned that relate directly to the mission questions, there was a cross cutting topic, knowledge and expertise, that warranted discussion and is presented at the end of this section of the report.

3.2.1 The System

Correct elevations and reference datum are essential. All hurricane and flood control protection structures should be designed, constructed, and maintained relative to an up-to-date local sea level reference datum. Areas experiencing variable subsidence, such as New Orleans, are likely to have systematic datum and elevation accuracy issues that need frequent attention. It is important to have appropriate monitoring stations (for tide and subsidence) in place and associated up-to-date guidelines for the application of this information to existing and new projects. In subsidence-prone areas, designs should consider multiple elevation increases over the life cycle of the structure.

Systems planning and design methods are needed. Planning and design methodologies need to allow for examination of system-wide performance. It is obvious from the IPET analysis that the piecemeal development of the New Orleans Hurricane Protection System provided a system in name only. This is especially true of the sections that have not been completed, transitions between types of protection that differ in capability (thereby representing weak points), and differences in the relative levels of reliability that created areas with greater likelihood of failure. The system-based approach should have a time dimension to allow consideration of the potential changes in requirements or conditions over the life of the project and to examine approaches to build in adaptive features and capabilities. Subsidence, changing population demographics, and the changing patterns of hurricane intensity and frequency are obvious examples of the time-dependent challenges hurricane protection systems face. All components that contribute to the performance of the overall system must be treated as an integral part of the system. Pump stations are one example in New Orleans. For any given drainage basin, the protection is only as robust as the weakest component of the system protecting that area and how effectively the various components that are interdependent operate together.

Frequent update to guidance and review of projects is critical. Design methods and designs need frequent review to determine whether they represent best practice and knowledge. Designs in coastal flood damage reduction projects need to include the concepts of resilience, adaptation, and redundancy to accommodate unanticipated conditions or structural behaviors. Design should be based on a system-wide understanding of the processes affecting the system and the interaction and interdependencies of the system components. This is especially true for the characterization of the hazard where modern probabilistic methods should be used.

The SPH process is outdated. More comprehensive probabilistic methods that consider a broader variety of storm characteristics and storm generated conditions should be used as a basis for planning and design. The Joint Probability Method – Optimized Sampling approach described in Volume VIII is recommended as a technically credible approach.

3.2.2 The Storm

Surge and waves are the hazard, not the storm. Meteorological designations such as the Saffir-Simpson scale by themselves are not adequate to characterize the distributed surge and wave conditions that a HPS will face. Katrina, a Category 3 storm at landfall, generated surges of 24 to 26 ft at Biloxi, MS. In the vicinity of Biloxi, the surge produced by Camille was 15.8 ft, the highest surge that had ever been recorded at that location prior to Katrina. In other words, Katrina (a Category 3 storm at landfall) generated substantially higher surges than Camille (a Category 5 storm at landfall) in the area where they both made a direct hit.

Sophisticated modeling using physics-based codes with high spatial resolution and accurate windfield input is necessary to depict the variable hydrodynamic environments created by large storms. Similarly, the traditional methods of assessing the frequency of occurrence of hurricanes, dependent primarily on historical data, are too simplistic to capture important characteristics of the hurricane hazard such as time- and space-dependent storm intensity and track patterns. The wave and storm surge modeling (using the Corps' WAM, STWAVE, and ADCIRC prediction models) provided considerable insight into how water surrounding such a complex physical system responds to an equally complex hurricane wind system. The hurricane protection system in Southeast Louisiana is very long and expansive, having a highly irregular layout. These factors coupled with a translating counter-clockwise rotating wind field about the center of a hurricane produced a complicated pattern of wave and storm surge development and evolution. Propagation of an evolving storm surge wave influences the water depth, which in turn exerts strong influence on the local wave field. The wave field is not only a function of what is locally generated by the wind. It is also heavily influenced by wave conditions generated by the hurricane while it was still well off the coast. Those waves propagated into the region well ahead of the storm's arrival.

Current models have uncertain accuracy in treating the effects of wetland and marsh environments on storm surge and waves. Sensitivity tests showed that wave and surge model computations are somewhat sensitive to the methods used to characterize frictional resistance of wetlands and to the values of frictional resistance assigned to different types of wetland landscape. Results showed that storm surge is reduced in some areas, whereas it is increased in others. Likewise, wave height is reduced in some areas and increased in others. Wave height increases are primarily due to the fact that increased water depths associated with increases in storm surge enable larger local wave heights to be sustained.

Resolution of wave setup is a critical element in the estimation of design levels of levees in this area. Hurricane Katrina produced extremely energetic wave conditions along the entire coast of Louisiana. Significant offshore wave heights along the Southeast Louisiana coast ranged from 55 ft due east from the tip of the Mississippi River delta to 20 to 25 ft just north of the Chandeleur Island chain, with peak wave periods of approximately 15 to 16 sec. Considerable wave breaking took place seaward of the Chandeleur Islands. High resolution (as fine as 300 ft) was added to the ADCIRC grid mesh to resolve areas of intense wave breaking along the barrier islands, the periphery of the coastal wetlands fronting Southeast Louisiana, and along the periphery of Lake Pontchartrain. The STWAVE model was run at fine resolution. The high resolution adopted and the use of coupled wave and surge models were able to capture the contribution of wave setup to storm surge away from coastal structures, a contribution of up to 2.5 ft depending on location. But even though the ADCIRC model contained contributions of both direct forcing and wave-related radiation stresses in its estimates of storm surge heights, local wave setup not resolved by the ADCIRC grid contributed 1.5 to 2 ft of additional setup along exposed levees in St. Bernard Parish, Plaquemines Parish, and New Orleans East, as well as along the south shore of Lake Pontchartrain. This additional setup contribution was estimated using Boussinesq wave modeling applied with much higher resolution.

Only 10 to 15 percent of high-water marks were considered to be reliable measures of peak storm water level. Of the many hundreds of high-water marks collected in Louisiana and Mississippi, a relatively small percentage of high-water marks were rated to be reliable measures of storm surge (the peak still water level that was experienced during the storm). The most reliable marks were those measured in the interior of structures on walls, in places where oscillatory wave motions were minimized.

3.2.3 The Performance

Designs need to better consider unknowns. The design approaches taken for the outfall canals

were not conservative enough to deal with the unknowns, in this case the excessive floodwall deflection not considered in the design. Floodwall design methods need to consider a broader spectrum of possible behaviors, and resilience to overtopping should be considered as a fundamental performance characteristic. Research is needed to understand the full performance limits of structures and to discover new approaches for creating adaptive designs. The unanticipated failure mode defined for the I-walls from this analysis does not represent the only possible failure mode for these structures. Numerous other modes were considered in their design, and other yet undefined modes are likely to occur at some point in the future. Designers need to consider a broad range of failure modes, including some approaches beyond traditional or standard practice.

Design methods and assumptions need continuous review and update. Design methods should be clearly based on physical behavior of engineering components and systems and should be reviewed periodically to determine if they represent the latest knowledge, practice, and technology. Similarly, existing projects should be periodically reviewed to ensure that their original design has not been compromised by changing hazard or changing knowledge base.

Planning methods should facilitate examination of system-wide performance. In addition, hurricane protection systems should be deliberately designed and built as integrated systems to enhance reliability and provide consistency in levels of protection. Components such as the interior drainage and pumping need to be an integral part of the system because of the important role they can play in limiting the amount and duration of flooding. Resilience in pumping capacity is especially important.

Resilience to catastrophic breaching can provide huge benefits in reduced loss of life and property. It is clear that a resilient HPS can provide enormous advantages. Resilience, in this case, refers to the ability to withstand, without catastrophic failure, forces and conditions beyond those intended or assumed in the design. For our purposes, resilience refers to the ability to withstand higher than designed water levels and overtopping without breaching. As demonstrated in this analysis of Katrina, approximately two-thirds of flooding and half of the losses were the result of breaching, i.e., the significant loss of protective elevation in structures. While overtopping alone from Katrina would have created dramatic flooding and losses, the difference is staggering in many regards. Reductions in losses of life, property, and infrastructure; associated reductions in the displacement of individuals, families, and the workforce, coupled with reduced disruption to businesses and social and cultural networks and institutions, would have a dramatic impact on the ability of a community and region to recover. Added to this is the savings of the time and funding needed to rebuild the protection system itself, which would accelerate the pace of recovery. Resilience is not a national priority in the development of hurricane protection systems, and resilience was not an element in the New Orleans HPS design.

3.2.4 The Consequences

Losses and recovery are flood depth dependent. Losses from a hurricane event creating water levels that exceed design criteria can be expected to be significant, but could be much less if the HPS can withstand overtopping without catastrophic breaching. While the reduction in direct property losses can be substantial and readily estimated (over $10 billion for Katrina), it is the more difficult to quantify reduction in the indirect economic and cultural losses that may be most relevant to the ability of the affected area to recover. In addition, the perceived character and expected performance of the HPS itself is a significant factor in the choices people will make with respect to re-population and re-investment.

Damages and loss of life were both directly tied to depth of flooding, which in turn is inversely tied to the elevation of the location or subbasin. Areas with lower elevations experienced the most severe losses and, all else being equal, will harbor the highest probabilities of experiencing flooding into the future.

System-based planning should include all aspects of hurricane response. A broad and system-based planning capability can increase the effectiveness of integrating evacuation, recovery, and reconstruction aspects into the HPS. In particular, a risk-based approach can provide an effective means to examine approaches to manage both the probability of an adverse event and the exposure to losses as well as the consequences. Spatial analysis of consequences and the ability to relate consequences to physical performance are powerful tools for making difficult decisions concerning hurricane protection.

3.2.5 The Risk

The comprehensive risk assessment was ongoing at the time of the release of this edition of Volume I. The following are insights gained in the development and execution of the risk assessment. More specific results and lessons learned will be provided in an amended version of this Volume and a completed Volume VIII when the risk results have been validated and published.

Risk supports system-wide planning. A risk-based planning and design approach would provide a more viable capability to inform decisions on complex infrastructure such as hurricane protection systems. The traditional approach, as used for the New Orleans protection measures, is component-performance-based, uses standards to define performance, and relies on factors of safety to deal with uncertainty. It is difficult to examine the integrated performance of multiple components, and standards are usually limited to past experience. Risk-based planning is system-based, requiring that the entire system be described in consistent terms and explicitly including uncertainty. Component performance is related to system performance as well as the consequences of that performance.

Risk expands the criteria for decision making. The risk-based approach is well suited for consideration of a variety of measures of merit. Factors such as loss of life, environmental losses, and cultural consequences can be included in decision making without reducing everything to one measure such as dollars. As applied for the IPET assessment, it allows aggregation and de-aggregation of information to address issues at different scales, providing a useful tool for collaborative planning between responsible agencies at different levels. It also allows for a more comprehensive consideration of hazards. Instead of a single definition derived from limited historical data, a joint probability approach can consider events that reflect historical information as well as a variety of possible events, providing a more robust basis for considering the spectrum of hurricanes that may occur. Most importantly, risk and reliability allows decision makers to understand the relative levels of vulnerability that specific areas face, the nature of the consequences (e.g., loss of life, economic loss, or environmental loss), and to understand the source of the vulnerability. As such, it is an excellent tool for understanding the effectiveness of alternative approaches to reduce risk, which can be managed by changing the performance of the protection system or changing the nature or degree of related consequences.

Traditional methods of hurricane frequency analysis are not adequate to describe the hurricane hazard for risk assessment. Risk assessment requires a stage (water level)-frequency of occurrence (or exceedence) relationship for a multitude of locations around the HPS, the number depending on the variation of the surge and wave conditions. The SPH, or any design hurricane, is only a single representative storm, having a certain combination of characteristics, with an estimated frequency of occurrence; one storm out of a population of hurricanes that are possible, some of which are more severe than the SPH. Relatively little information regarding risk is available from this treatment of the storm threat. Considering a larger set of historical storms, such as in a strict application of the Empirical Simulation Technique, is an improvement; but it also limits consideration of what might occur in terms of combinations of hurricane characteristics to what has occurred. Using the Empirical Simulation Technique with track variations of historical storms adds some hypothetical storms to the historical record, but also adds the challenge of assigning frequencies to these storms. The Joint Probability Method – Optimal Sampling, coupled

with high-resolution surge and wave models, was deemed the most rigorous and tractable means to characterize the hurricane hazard for the New Orleans risk assessment. It most thoroughly considers the spectrum of hurricanes that might occur. The period of record from 1950 to the present was defined as the most accurate interval for assessing hurricane characteristics. One will always be limited to a degree by the length of the historical record.

4.0 KNOWLEDGE AND EXPERTISE

Awareness and exploitation of emerging knowledge are critical. The history of the planning, design, and performance of the HPS in New Orleans points out a dilemma. While new pieces of knowledge were available over time that were relevant to the ultimate performance of the I-walls on the outfall canals, the pieces were not put together to solve the puzzle of the failure mechanism that occurred. The Corps' own testing of sheet-pile stability (E-99) in the mid 1980s was not directed at the behavior of I-walls, but with hindsight, some of the behavior observed was indicative of the deflection of a structure that designers essentially assume to be rigid. Similarly, late in the 1980s, research papers published in part through the Corps laboratories discussed the high hydrostatic pressure issue with regard to a gap forming in conjunction with sheet-pile structures. Work, not directly related to levee or floodwalls, in England discussed the deflection and hydrostatic pressure problem for retaining walls. How do these puzzle parts get pieced together to create knowledge for designers and how do designers and reviewers get access to this information? How does the research or testing community become aware of applications, perhaps different from their original purpose, for their new knowledge?

Constant renewal of planning and design criteria and guidance are critical. Part of the solution to this dilemma relates to the amount of overall effort and resources put into the search for new knowledge and capabilities to deliberately update design criteria and planning capabilities. Awareness and capability are gained best when there is both technology push (research creating new knowledge and capabilities) and requirements pull (designers/constructors seeking and pulling information from the research and professional communities). The solution is not more research or more outreach alone, it is the ability of the design/construction and research communities to work together in an environment enabling collaboration and experimentation with new knowledge and approaches to old and new problems. There has been a distinct loss in energy and resources expended in this area, particularly in the domain of hurricane and flood protection and specifically in the geotechnical fields that are at the heart of the levee and floodwall performance issues in Katrina. The focus on standards may, in fact, also deter this process. Standards imply stability and constancy, when in fact the concept of guidelines may be more appropriate, allowing and encouraging customization and adaptation as new knowledge emerges. In either case, standards and/or guidelines need to be refreshed at a greater frequency as the generation of new knowledge continues to accelerate.

Maintaining expertise is critical. The other dimension to this issue is expertise. As technology accelerates and engineering practice evolves at an increasing pace, it becomes more difficult to maintain the level of technical expertise necessary to cope with the ever more complex issues faced in water resources. This is true for the government and the private sectors. Government agencies are especially challenged in an era of outsourcing and competition for experienced professionals. Significant measures are needed to reemphasize technical expertise and renew that expertise as water resources practice evolves. These measures must be part of the culture of organizations and cover the entire profession to ensure that the total team addressing priority issues such as hurricane protection are working from the latest knowledge and professional practice.

Calculation Method of Hydrodynamic Pressure in Seismic Response Analysis of Gates

by

Takashi Sasaki[1], Tomoya Iwashita[2] and Yoshikazu Yamaguchi[3]

ABSTRACT

In order to maintain dam storage functions, it is essential to guarantee the safety of the dam body and appurtenant structures which are use to control the flow of water from the dam reservoir, i.e. gates and so on.

This report describes a study on basic characteristics of hydrodynamic pressure acting on gates during an earthquake based on numerical analysis that considered vibration of dam bodies and gates, and based on its results, proposes a method of calculating hydrodynamic pressure during an earthquake in the seismic performance evaluation analysis of gates.

KEYWORDS: Gates, Hydrodynamic Pressure, Guideline, Seismic Performance Evaluation,

1. INTRODUCTION

The Guidelines for Seismic Performance Evaluation of Dams during Large Earthquakes (Draft) [1] (Below "The Guideline") issued by the Ministry of Land, Infrastructure and Transport in March of 2005 stipulates two requirements concerning seismic performance that a dam must ensure under level-2 earthquake motions: "It shall maintain its water storage function," and, "damage caused shall be within a repairable range." In order to maintain dam storage functions, it is essential to guarantee the safety of the dam body and other parts of its structure including gates. So the Guideline divides the objects for a evaluation into dam body (body of the dam and parts of the foundation in contact with the dam body) and appurtenant structures etc. (structures and systems of various kinds that are installed on or around the dam body to maintain the functions of the dam) and stipulates the fundamental concepts of the evaluation methods for each.

When an actual seismic performance evaluation is done, gates of discharge systems are generally selected as appurtenant structures etc., which needed to maintain the dam's water storage function. Gates include those installed on the dam crest, those installed at high elevations inside the dam body and there are several types of gates, so the evaluation analysis method for gates is studied considering the characteristics of each gate. Gates, even those installed in dam bodies, generate vibrations separate from those of the dam body, so the analysis model used must be one capable of correctly representing the vibration properties of the gate itself. And hydrodynamic pressure from the reservoir during an earthquake acts on the gates in the same way it acts on the dam body. Because the self-weight of a gate is low, the hydrodynamic pressure acting on a gate from the reservoir has a greater impact on the dynamic behavior of structures than that acting on the dam body. Many research activities concerning hydrodynamic pressure during an earthquake that is generated by vibration of the dam body have been reported [2], but there have been little studies of hydrodynamic pressure accompanying the vibration of gates.

This report describes a study of basic characteristics of hydrodynamic pressure acting on gates during an earthquake based on numerical analysis that considered vibration of dam bodies and gates, and based on its results, proposes a method of calculating hydrodynamic pressure during an earthquake in the seismic performance evaluation analysis of gates.

---

1 Former Deputy Team Leader, Dam Structures Research Team, Hydraulic Engineering Research Group, Public Works Research Institute, Tsukuba-shi, Ibaraki-ken, 305-8516 Japan
2 Deputy Team Leader, ditto
3 Team Leader , ditto, Dr. Eng.

2. CONCEPT OF SEISMIC PERFORMANCE EVALUATION OF GATES

The Guideline provision regarding appurtenant structures that have been selected for evaluation stipulates that, "It shall be confirmed that even if the appurtenant structures etc. are damaged, the water storage function of the dam will be maintained by seismic response analysis or other appropriate method performed according to the functions and structural properties of the appurtenant structures etc."

It is technologically possible to analyze a dam body and to simultaneously model and perform seismic response analysis of its gates. But an example of an FEM model of the dam body and an example of an FEM model of a radial gate are shown on the left side and right side respectively of Fig. 1, and in order to appropriately represent the vibration properties of a gate, it must be modeled with elements with much more precise dimensions than those of the dam body. So practically, the seismic response analysis of the dam body and the gate should be done separately. In this case, first the seismic response analysis of the dam body is done, then the response acceleration is calculated at the locations where the gate is installed (for example, the location of the trunnion if it is a radial gate installed in the dam body and the location of the rollers if it is a roller gate). The response acceleration can be handled as input earthquake motion for the seismic response analysis of the gate. It is evaluated by obtaining the stress or deformation produced in each member of the gate by seismic response analysis. The seismic response analysis must consider the gate's self weight and the hydrostatic pressure as the static load, and must also appropriately consider the inertia of the gate itself and the impact of the hydrodynamic pressure acting on the gate during an earthquake.

3. OUTLINE OF STUDY OF HYDRODYNAMIC PRESSURE ACTING ON GATES

3.1 Hydrodynamic Pressure in Present Design Method in Japan

Under the present design method in Japan [3], the gate is designed considering the static seismic load (inertia) that is represented by the design seismic coefficient in the same way as in the design of the dam body, and the hydrodynamic pressure that is calculated using Westergaard's hydrodynamic pressure equation [4] that is shown in equation (1).

$$p_d = 0.875 W_o \cdot k\sqrt{H \cdot h} \quad \cdots\cdots\cdots\cdots \quad (1)$$

Where:

p_d : Hydrodynamic pressure (kN/ m^2)

W_o : Unit weight of the water (kN/m^3)

k : Design seismic coefficient

H : Depth from the reservoir water surface to the foundation (m)

h : Depth from the reservoir water surface to the point of action of hydrodynamic pressure.

But Westergaard's hydrodynamic pressure equation is an equation induced by hypothesizing that the dam body is a rigid body. Observations of dam behaviors during earthquake have revealed that in fact, the higher on the dam body, the larger the vibrations produced. Applying Westergaard's equation to evaluate the hydrodynamic pressure on a gate is equivalent to assuming a situation in which the gate vibrates the same way as the dam body or ignoring the impact of the vibration of the gate itself.

3.2 Concept of Hydrodynamic Pressure on a Dam Body in Seismic Response Analysis

Studies of hydrodynamic pressure acting on dam bodies during earthquakes generally treat the stored water as a compressible (non-cohesive) fluid body. When the compressibility of stored water is considered, the hydrodynamic pressure is affected by the frequency of the input earthquake motion, causing the resonance phenomenon under certain frequencies. But if the energy absorption at the bottom of the reservoir is also considered, the resonance phenomenon becomes gentler [5] and the actual earthquake motion includes a variety of frequency components, so the resonance phenomenon in reservoir water is not remarkable. So even if it is handled as a non-compressible (non-cohesive) fluid body, analysis that is approximate but provides adequate precision can be performed. The hydrodynamic pressure equation and solution that

Westergaard studied obtains hydrodynamic pressure in a case where originally it is treated as a compressive non-cohesive fluid body, but the so-called Westergaard's hydrodynamic pressure equation that is regularly used for dam design represents the distribution of hydrodynamic pressure in a case where the frequency of the input earthquake motion is fixed at about 4/3Hz, and can be almost approximated by the hydrodynamic pressure distribution obtained assuming a non-compressive fluid body in a case of rigid body vibration of the dam body.

And when performing non-linear analysis to consider damage to the dam body [6] in particular, the modeling of the reservoir should be as simple as possible for the sake of more efficient calculation. For this reason, dynamic analysis of dam bodies is even now conducted while considering the hydrodynamic pressure during an earthquake based on Westergaard's hydrodynamic equation.

3.3 Study Based on Numerical Experiments Concerning Hydrodynamic Pressure Acting on Gates

The following two points should be considered to study hydrodynamic pressure acting on a gate compared with that on a dam body.

- Hydrodynamic pressure at the gate location, that is not the sum of all hydrodynamic pressure acting on the overall dam body
- Impact for hydrodynamic pressure by the occurrence of the vibration in the gate along with the vibration of the dam body

The above two points were studied separately in this report.

In Chapter Four, first the relationship of the form of vibration of the dam body with the distribution of hydrodynamic pressure is studied. The hydrodynamic pressure in gate parts is affected by vibration of dam near the gate location along with the vibration of the entire dam body, and clarifying the degree of this impact is the object of this study. The study was performed for input motion of a sinusoidal wave.

Chapter Five is a study of the characteristics of the hydrodynamic pressure acting on the gate in a case where vibration unrelated to the dam body vibration is generated in the gate. In this study, the vibration of the gate under an actual earthquake motion is studied along with vibration with a sinusoidal wave.

4. RELATIONSHIP OF DAM BODY ACCELERATION DISTRIBUTION WITH HYDRODYNAMIC PRESSURE DISTRIBUTION ACTING ON DAM BODY

4.1 Outline

Stored water is modeled as a non-compressive (non-cohesive) fluid body to study the relationship of the acceleration distribution of the fluid body with the hydrodynamic pressure that acts on the dam body.

In a case where Westergaard's hydrodynamic pressure equation is used to calculate the hydrodynamic pressure, the local hydrodynamic pressure (hydrodynamic pressure at the gate location) is calculated by considering only vibration at this location (vibration at the location of the gate).

So when the stored water is assumed to be a non-compressive fluid body, the hydrodynamic pressure distribution produced by vibration of the dam body is calculated at the same time as the hydrodynamic pressure based on Westergaard's hydrodynamic pressure equation and the results of the two calculations are compared.

4.2 Analysis Conditions

The objects of the analysis are the dam body and the reservoir as shown in Fig. 2. But an actual analysis considers only the vibration on the upstream side of the dam body without modeling the dam body itself, and inputs the acceleration value to the reservoir. In a case where the stored water is assumed to be a non-compressive fluid body, there is no frequency dependency on the hydrodynamic pressure during an earthquake and there is no phase difference with the input earthquake motion frequency, so the hydrodynamic pressure results are represented by the maximum amplitude of the hydrodynamic pressure. And the upstream surface of the dam body is divided into 20 equal parts to obtain the hydrodynamic pressure at 21 nodes.

In the analysis, the hydrodynamic pressure matrix is calculated based on finite element analysis of the reservoir model assuming it is non-compressive, and then it multiplies this matrix by the acceleration distribution vector on

the upstream surface of the dam body to obtain the hydrodynamic pressure during an earthquake that acts on the upstream surface of the dam body. In this paper, this method is called "case considering the overall dam body response." The method of calculating the hydrodynamic pressure based on Westergaard's hydrodynamic pressure equation is called "case where only the local dam body response is considered" in this paper.

4.3 Analysis Results

4.3.1 Results of Calculation of Hydrodynamic Pressure Distribution

(1) Hydrodynamic pressure during an earthquake in a case of rigid vibration of a dam body.

Figure 3 shows the hydrodynamic pressure amplitude distribution acting on the upstream surface of a dam body in a case where the same horizontal vibration (acceleration amplitude of $1m/sec^2$) occurs on the entire upstream surface of a dam body. It shows that the value considering only local dam body response is slightly higher than the value considering the entire dam body response at the top and in the bottom of the dam body, but overall, their form is almost identical.

(2) Hydrodynamic pressure during an earthquake in a case where vibration equivalent to the characteristic vibration shape of the dam body occurs

Figures 4 to 7 show the hydrodynamic pressure amplitude distribution acting on the upstream surface of the dam body in a case where the upstream surface of the dam body is vibrating horizontally (crest acceleration amplitude of $1m/sec^2$) based on the acceleration distribution of the 1st, 2nd, 4th and 5th order shapes of the characteristic vibration modes of the dam body. The 3rd vibration shape is generally excited by the vertical earthquake motion, so it is not considered.

Looking at the hydrodynamic pressure distribution shape equivalent to the 1st mode shape reveals that the value considering only local dam body response is larger at the top and inversely it is smaller near the bottom than the value considering the overall dam body response. But no large difference is found with the overall values. Looking at the hydrodynamic pressure distribution shape equivalent to the 2nd mode shape reveals that the value considering only local dam body response is generally larger than the value considering the overall dam body response. The hydrodynamic pressure equivalent to the 4th order and 5th order mode shape reveals the same tendency, and as the order advances, this tendency becomes greater. This means that in the case of vibration in which the low order vibration of the dam body is dominant, even if the hydrodynamic pressure during an earthquake is calculated considering only local dam body response, it seems to be possible to evaluate it with a certain degree of accuracy, but it can be stated that in a case where it is necessary to focus on the high order vibration of the dam body, it is not appropriate to evaluate the hydrodynamic pressure considering only local dam body response.

4.3.2. Comparison of Maximum Value and Total Forces of Hydrodynamic Pressure

Table 1 summarizes the maximum absolute value and the sum of the horizontal forces produced by the hydrodynamic pressure in all cases studied in the previous part of this report. The table shows that there is little difference between the totals of the horizontal forces considering the entire dam body response and considering only the local dam body response. The local maximum value shows that it is over-estimated based on the concept of considering only local dam body response. This occurs because the higher order the vibration of the dam body, the more remarkable this tendency.

4.4 Summary

The above study has revealed the following facts.

In the case of vibration with the low order vibration of the dam body dominant, it is possible to evaluate the hydrodynamic pressure during an earthquake considering even only the local dam body response, but when it is necessary to focus on the high order vibration of the dam body, considering only local dam body response may result in excessive hydrodynamic pressure, so it is necessary to evaluate the hydrodynamic pressure considering the overall dam body response.

5. HYDRODYNAMIC PRESSURE DURING AN EARTHQUAKE CONSIDERING CHARACTERISTIC VIBRATION OF A GATE

5.1 Outline

So the hydrodynamic pressure during an earthquake in a case where a gate produces local characteristic vibration that differs from that of the dam body is studied. This study was divided into the following two parts.

a. Study of hydrodynamic pressure in a case where the gate produces sinusoidal wave vibration

b. Study of hydrodynamic pressure in a case where simulated earthquake response of the gate is produced

This study was an analysis performed considering the dam body to be a rigid body and under the hypothesis that the gate produces vibration different from that of the dam body. Regarding a), as in Chapter Four, it was hypothesized that the stored water is non-compressive fluid body, but regarding b), the characteristics of hydrodynamic pressures of both a non-compressive fluid body and a compressive fluid body were studied.

5.2 Study for Sinusoidal Wave Vibration

5.2.1 Analysis Conditions

Analysis conditions are same as Chapter 4.

5.2.2 Analysis results

Figure 8 is the hydrodynamic pressure amplitude in a case where only one point at a medium elevation on the dam body vibrates horizontally with acceleration amplitude of $1m/sec^2$. The figure shows that the hydrodynamic pressure considering only the local dam body response is much larger than the value that considers the overall dam body response. This occurs because in the actual phenomenon, vibration at a certain point affects hydrodynamic pressure acting on other points.

Although it is not shown here, an analysis performed separately has shown that as in the case where vibration occurs only in the upper part of the dam body or at a low elevation, considering only the local dam body response evaluates the hydrodynamic pressure higher than in a case where the entire dam body response is considered.

Table 2 shows the maximum absolute value and the sum of the horizontal forces. The table shows that there is little difference between the totals of the horizontal forces considering the entire dam body response and considering only the local dam body response. But, the maximum value could be over-estimated based on the concept of considering only local dam body response.

5.3 Study for Earthquake Response Vibration (Case of Non-compressive Fluid Body)

5.3.1 Analysis Conditions

Results of dynamic analysis of the separately executed dam body and conduit gate are used to calculate the hydrodynamic pressure acting on the gate during an earthquake by the overall dam body vibration and by the relative gate vibration different from the overall dam body vibration. The hydrodynamic pressure was obtained using the hydrodynamic pressure matrix that hypothesizes a non-compressive fluid body by a method considering the overall dam body response and by a method considering only local dam body response based on Westergaard's added mass (Westergaard's hydrodynamic pressure equation).

The response acceleration at the gate location was obtained from the dynamic time history analysis for the dam model with a height of 67m, with a maximum input acceleration of 851gal. The location of a gate is 23m form the foundation. And, that response acceleration was used as an input motion for the gate structural model, the response acceleration of the gate was calculated.

Figure 9 shows the dam body response acceleration at the location of the gate pin, in other words the input earthquake motion to the pin in the earthquake response analysis of the gate that was obtained based on the results of the dynamic analysis of the dam body.

In this study, the dam body was vibrated rigidly at the acceleration shown in Fig. 9. Figure 10 shows the acceleration time history of the gate vibrations corresponding to the dam body. This is average horizontal acceleration of the upstream surface of the gate, and it is a value obtained by subtracting the overall dam body vibration from the vibration acceleration of the gate. The maximum acceleration of the relative gate

vibration is about four times the maximum acceleration of the dam body vibration. Figure 11 shows the response spectrum of the acceleration time histories in Fig. 9 and Fig. 10. Those spectra were normalized by the maximum acceleration of each acceleration time histories. From this figure, it is shown that the vibration of gates has smaller component in low frequency range than that of the overall dam body vibration.

Figure 12 is a schematic diagram of the positions of the dam body and the gate hypothesized for this study. Here the gate is hypothesized, but the gate structure itself is not modeled. It is assumed that the gate location conforms to the front surface of the dam body without considering the conduit pipe at the front surface of the gate.

The acceleration distribution of the overall dam body and the corresponding hydrodynamic pressure distribution are shown in Fig. 13, and the relative gate acceleration and the corresponding hydrodynamic pressure are shown in Fig. 14. Assuming that the gate is small as compared with a height of the dam, the gate vibration was caused to correspond to the vibration at one node.

5.3.2 Analysis Results

Figures 15 to 17 show the hydrodynamic pressure time history at nodes corresponding to the gate under the overall dam body vibration shown in Fig. 9 and the relative gate vibration shown in Fig. 10. Figure 15 shows the hydrodynamic pressure under the overall dam vibration, Figure 16 shows the hydrodynamic pressure under the relative gate vibration, and Fig. 17 shows the hydrodynamic pressure under the combined gate vibrations (overall dam body vibration + relative gate vibration), showing values calculated (1) considering the overall dam body response and (2) considering only the local dam body response. Figure 15 shows that hydrodynamic pressure values under the overall dam body vibration were little different when obtained by the two methods (1) and (2). But Fig. 16 shows that the hydrodynamic pressure under the relative gate vibration that was obtained by method (2) was a very high value, and that it is difficult to calculate the local hydrodynamic pressure by considering only the local dam body response by ignoring the overall dam body response. And Fig. 15(a) and Fig. 16(a) show that the hydrodynamic pressure under the relative gate vibration based on method (1) is much lower than the hydrodynamic pressure under the overall dam body vibration. Comparing Fig. 15(a) to Fig. 17(a) shows that the hydrodynamic pressure on the gate under the combined vibration is almost equal to the hydrodynamic pressure under overall dam body vibration.

The above findings show that to calculate the hydrodynamic pressure acting on a gate during an earthquake when performing earthquake response analysis of a gate, it is possible to calculate the hydrodynamic pressure considering overall dam body response while ignoring the relative gate vibration.

5.4 Studies for the Earthquake Response Vibration (Case of Compressive Fluid Body)

5.4.1 Analysis Conditions

This part of the report explains the properties of the hydrodynamic pressure acting on a gate during an earthquake for a case where the entire dam body undergoes rigid body vibration and for a case where only the gate vibrates, while considering the stored water to be a compressive fluid body.

The object of the analysis consists of the dam body and the reservoir water that are shown schematically in Fig. 18. The analysis model was modeled two dimensionally.

The material physical properties analyzed are shown in Table 3. The material physical property of the reservoir bottom is almost equivalent to the acoustic impedance ratio $\beta = 5$. The acoustic impedance ratio indicates the reflectivity of the reservoir bottom, is generally between $\beta = 1$ to 5, and the smaller the value of β, the lower the reflexivity of the reservoir bottom, with $\beta = 5$ correspondent to hard rock.

The boundary conditions are, on the reservoir far side, a cohesive boundary that approximately represents limitless surroundings, while the water surface boundary of the reservoir is a free water surface condition.

Linear dynamic analysis is performed based on the frequency response analysis method and the maximum frequency considered in analysis is 20Hz. Figure 19 shows excitation points for a case where only the gate is vibrated and a case

where the entire dam body is rigidly vibrated.

5.4.2 Analysis Results

Figure 20 shows the hydrodynamic pressure time history under the overall dam vibration, and Fig. 21 shows the hydrodynamic pressure time history under the relative gate vibration. Figure 22 shows the total hydrodynamic pressure under the combined vibration. From Fig. 20 and Fig. 22, it is revealed that the hydrodynamic pressure can be evaluated considering only the overall dam vibration, that is to say, ignoring the relative gate vibration even if the compressibility of the stored water is considered.

Figure 23 shows that the hydrodynamic pressure acting on the gate in a case where the compressibility of the stored water was considered and in a case where ignoring the compressibility of the stored water. From this figure, there are not so large differences in the overall wave forms and the maximum value for the non-compressive water is larger than that for the compressive water. This fact indicates the treatment of the stored water as non-compressive body is good and rational assumption to calculate the hydrodynamic pressure acting on a gate.

6. CONCLUSIONS

The following summarizes the results of a study of hydrodynamic pressure acting on dam bodies and on gates during an earthquake performed by numerical analysis of the vibration of dam bodies and gates.

1) In the case of vibration with low order vibration of a dam body dominant, the hydrodynamic pressure can be evaluated by considering even only the local dam body response.

2) In a case where it is necessary to focus on high order vibration of a dam body, or under local vibration such as vibration of a gate, if hydrodynamic pressure is evaluated considering only local dam body response, the hydrodynamic pressure is over-evaluated.

3) The hydrodynamic pressure on a gate produced by the relative gate vibration is smaller than that by overall vibration of the dam body.

According to the above findings, regarding the hydrodynamic pressure acting on a gate during an earthquake, the hydrodynamic pressure acting on the upstream surface of a dam body is calculated by a method that considers the overall dam body response but does not consider the characteristic vibration on a gate itself, and the hydrodynamic pressure at the gate location obtained from this result can be considered to be the hydrodynamic pressure acting on the gate. When the dynamic analysis of the gate is performed separately from the dam body analysis, the time history of the hydrodynamic pressure obtained by the above concept can be applied as the external force on the gate.

For this study, the hydrodynamic pressure for the overall dam body response was obtained using a hydrodynamic pressure matrix, but if the hydrodynamic pressure is obtained through dynamic analysis of the dam body based on a method that considers the overall response of the dam body, it is possible to do so applying this to the dynamic analysis of the gate as it is, regardless of whether it is considered to be a non-compressive fluid body or a compressive fluid body.

7. REFERENCES

1) River Bureau, Japanese Ministry of Land, Infrastructure and Transport: Guidelines for Seismic Performance Evaluation of Dams during Large Earthquakes (Draft), 2005.3. (in Japanese)

2) C . N. Zanger: Hydrodynamic Pressures on Dams Due to Horizontal Earthquake Effects, Engineering Monographs, No.11, U.S. Bureau of Reclamation, 1952.

3) Japanese Government Ordinance and Ministry of Construction Ordinance for Structural Standard for River Administration Facilities, 2000. (in Japanese)

4) H . M. Westergaard ; Water Pressures on Dams during Earthquakes, *Trans. ASCE*, Vol.98, 1933.

5) T. Hatano and T. Nakagawa: Analytical Solution of Hydrodynamic Pressure with Reflective Conditions at Reservoir Bottom during Earthquakes. *Journal of the Japan Society of Civil Engineers*, No.229, 1974.

6) Y. Yamaguchi, R. Hall, T. Sasaki, E. Matheu, K. Kanenawa, A. Chudgar and D. Yule: Seismic Performance Evaluation Of Concrete Gravity Dams, *Proceedings of 13WCEE*, No.1068, 2004.

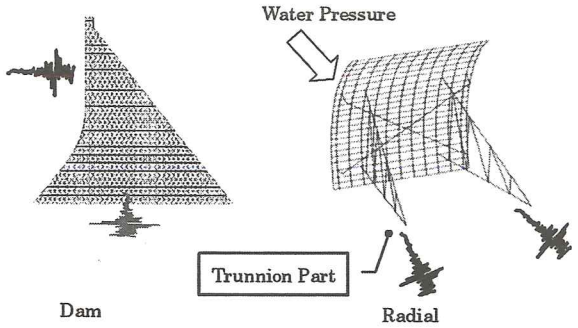

Fig. 1 Example of an Analysis Model of a Gate (Radial Gate)

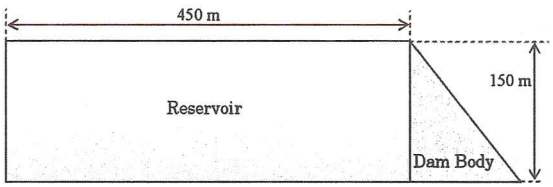

Fig. 2 Objects of the Analysis

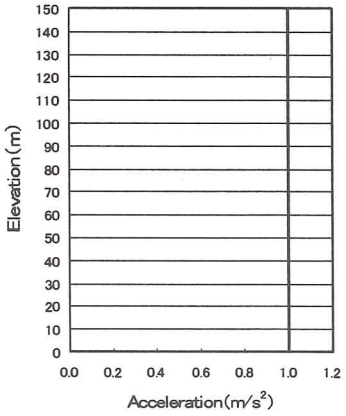

(a) Acceleration distribution

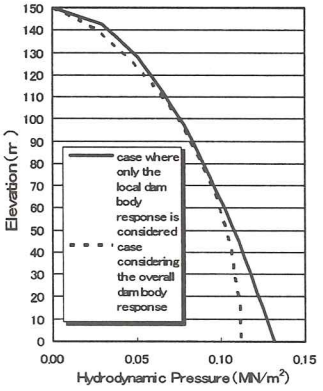

(b) Hydrodynamic pressure distribution

Fig. 3 Case of Uniform Rigid Vibration of the Dam Body

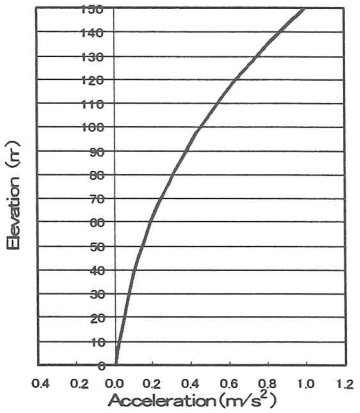

(a) Acceleration distribution

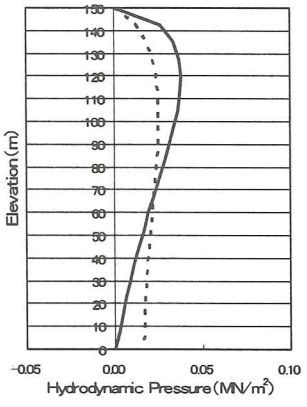

(b) Hydrodynamic pressure distribution

Fig. 4 Case of 1st Mode Vibration Shape of the Dam Body

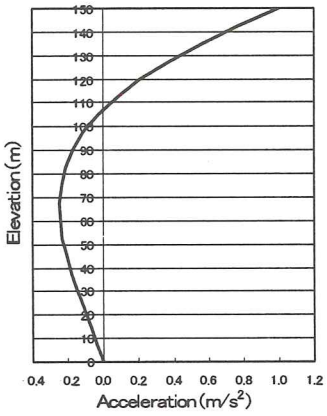

(a) Acceleration distribution

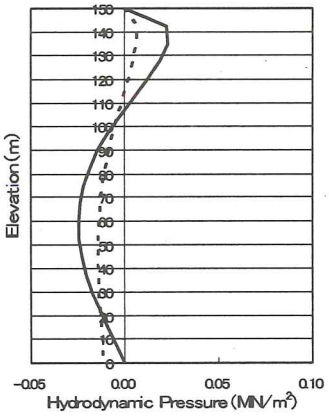

(b) Hydrodynamic pressure distribution

Fig. 5 Case of 2nd Mode Vibration Shape of the Dam Body

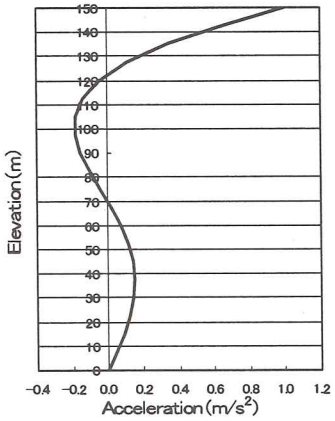

(a) Acceleration distribution

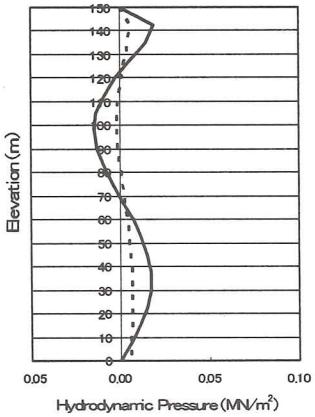

(b) Hydrodynamic pressure distribution

Fig. 6 Case of 4th Mode Vibration Shape of the Dam Body

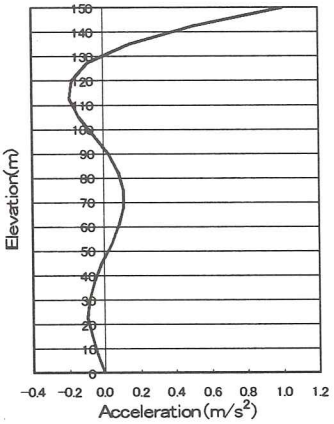

(a) Acceleration distribution

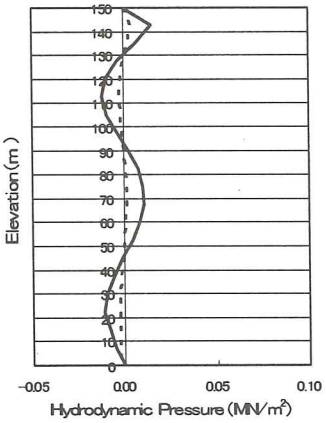

(b) Hydrodynamic pressure distribution

Fig. 7 Case of 5th Mode Vibration Shape of the Dam Body

Table 1 Comparison of Maximum value and Horizontal Total Forces of Hydrodynamic Pressure Acting on the Upstream Side of the Dam Body

Case	Considering overall dam body response (A)		Considering only local dam body response (B)		B / A	
	Max. value	Total force	Max. value	Total force	Max. value	Total force
Uniform rigid body vibration	0.111	12.19	0.131	13.08	1.18	1.07
1st mode vibration shape	0.025	3.04	0.038	3.26	1.50	1.07
2nd mode vibration shape	-0.014	-1.09	-0.025	-1.07	1.76	0.98
4th mode vibration shape	0.006	0.46	0.019	0.55	3.20	1.20
5th mode vibration shape	-0.003	-0.13	0.015	-0.14	-5.39	1.14

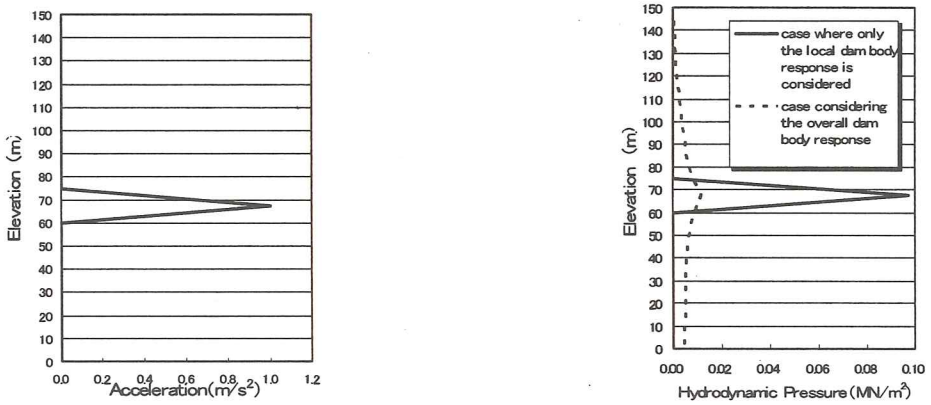

(a) Acceleration distribution (b) Hydrodynamic pressure distribution

Fig. 8 Case of Vibration of one Point at Medium Elevation

Table 2 Comparison of Maximum value and Horizontal Total Forces of Hydrodynamic Pressure Acting on the Upstream Side of the Dam Body

Case	Considering overall dam body response (A)		Considering only local dam body response (B)		B / A	
	Max. value	Total force	Max. value	Total force	Max. value	Total force
One point vibration at a medium elevation	0.012	0.72	0.097	0.73	8.36	1.02

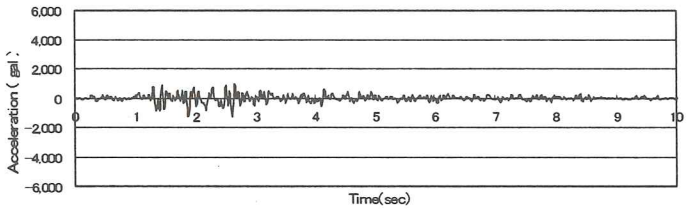

Fig. 9 Acceleration Time History of the Overall Dam Body Vibration

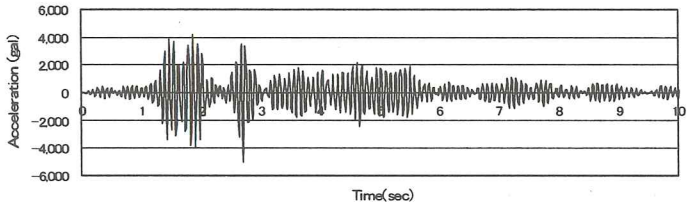

Fig. 10 Acceleration Time History of Relative Vibration of Gate

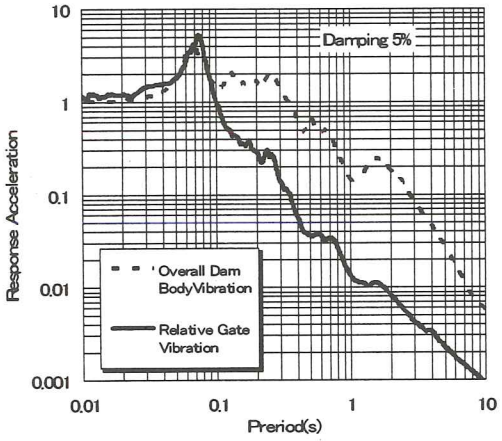

Fig.11 Normalized Response Spectrum of Acceleration

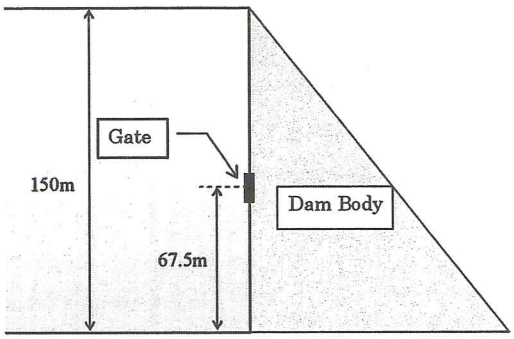

Fig. 12 Schematic Figure of the Dam Body and Gate Locations

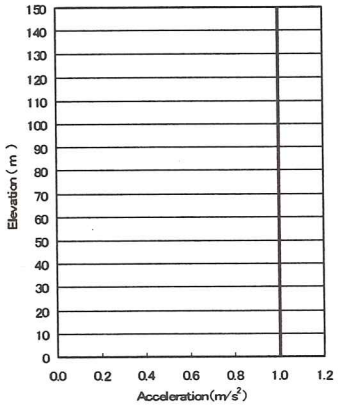

(a) Acceleration distribution

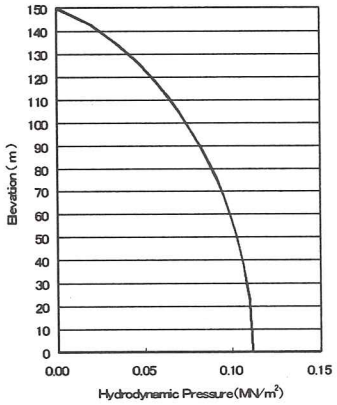

(b) Hydrodynamic pressure distribution

Fig. 13 Overall Dam Body Vibration Distribution and Corresponding Hydrodynamic Pressure Distribution

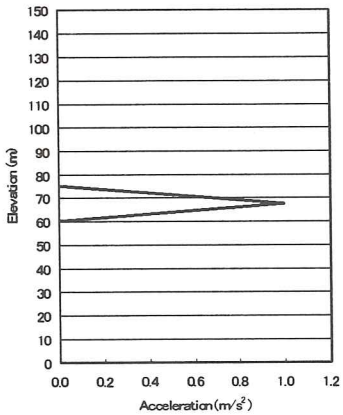

(a) Acceleration distribution

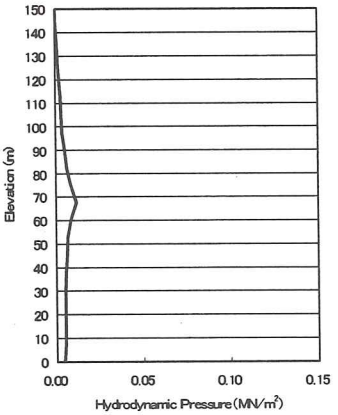

(b) Hydrodynamic pressure distribution

Fig. 14 Relative Gate Vibration Distribution and Corresponding Hydrodynamic Pressure Distribution

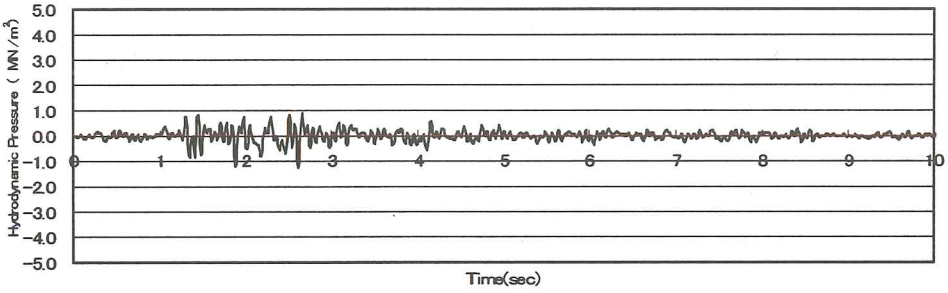

(a) Case considering the overall dam body response

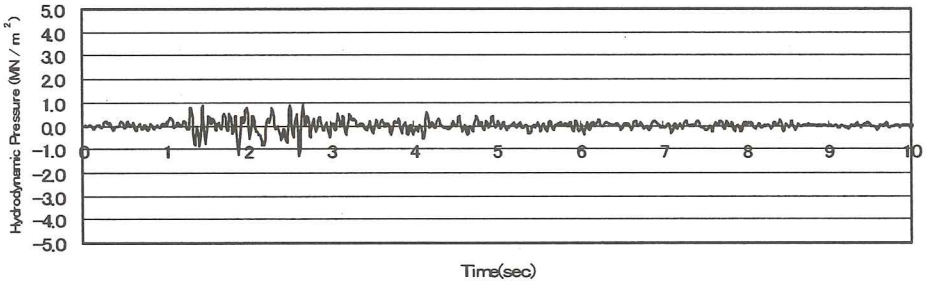

(b) Case considering the local dam body response

Fig. 15 Hydrodynamic Pressure Time History of the Gate under Overall Dam Body Vibration

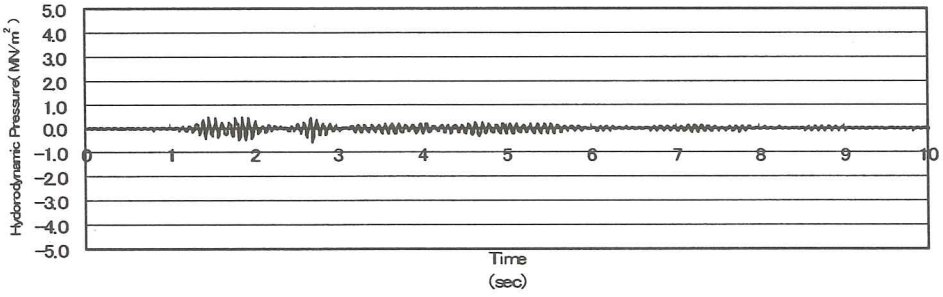

(a) Case considering the overall dam body response

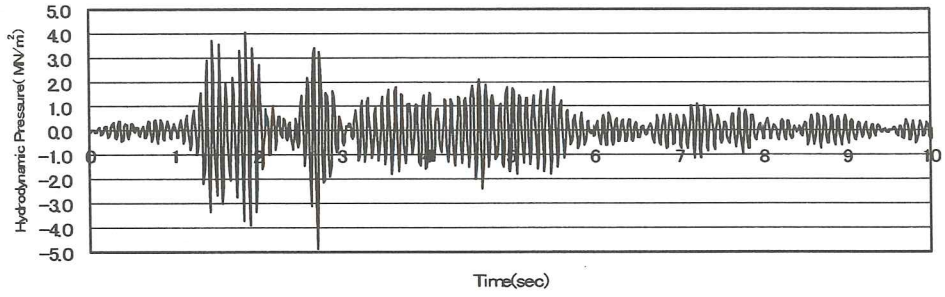

(b) Case considering the local dam body response

Fig. 16.Hydrodynamic Pressure Time History of the Gate under Relative Gate Vibration

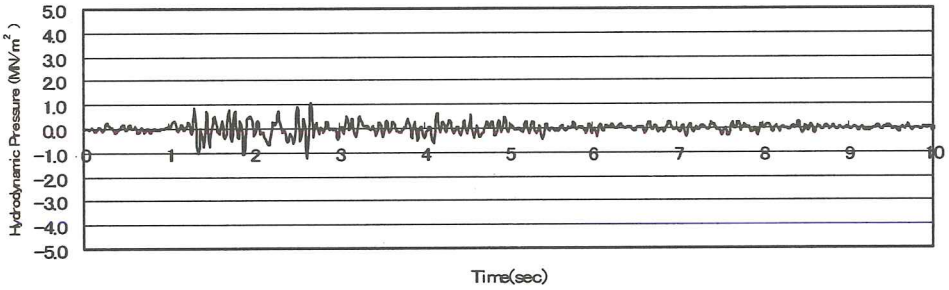

(a) Case considering the overall dam body response

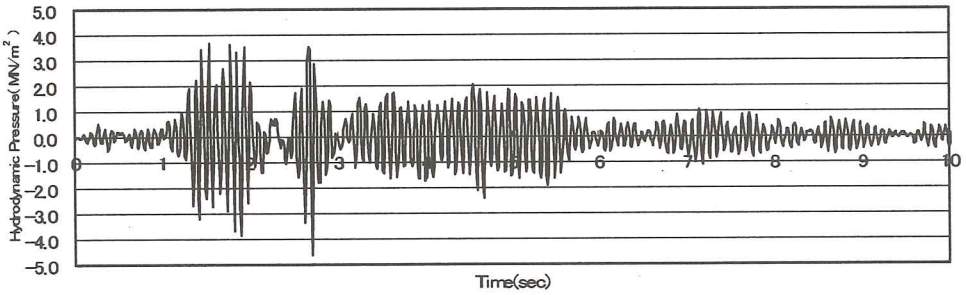

(b) Case considering the local dam body response

Fig. 17 Hydrodynamic Pressure Time History of the Gate under Combined Vibrations

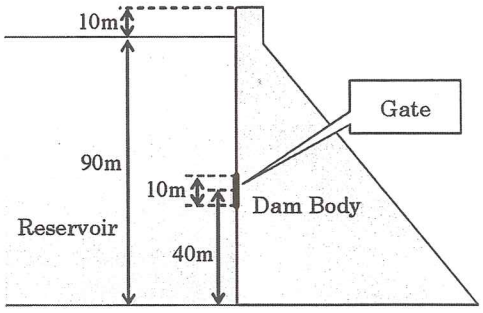

Fig. 18 Object of the Analysis

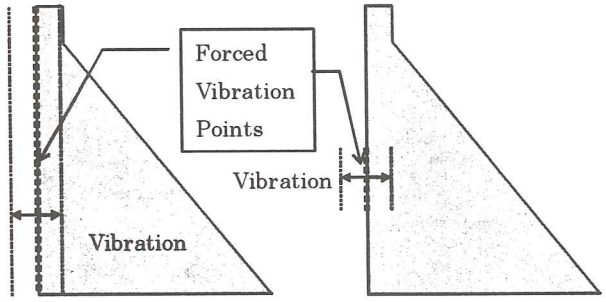

Fig. 19 Forced Vibration of Multiple Nodes

Table 3 Material Property Values

Item	Reservoir
Unit weight(kN/m^3)	9.80665
Underwater P wave velocity (m/s)	1.40E+03

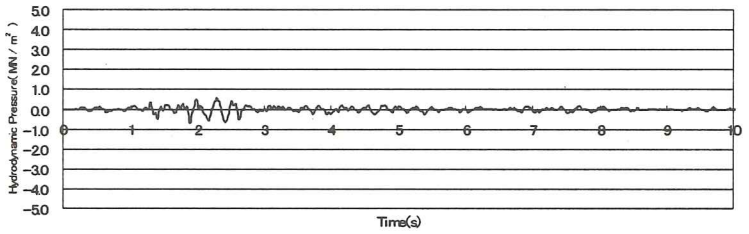

Fig. 20 Hydrodynamic Pressure Time History under Overall Dam Body Vibration

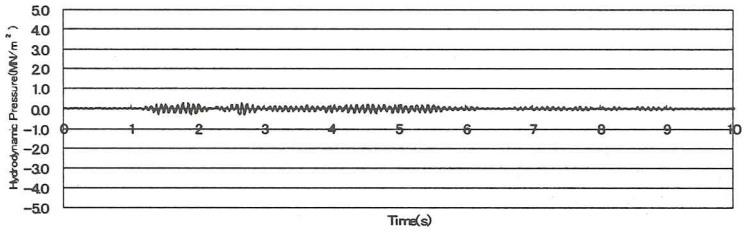

Fig. 21 Hydrodynamic Pressure Time History under Relative Gate Vibration

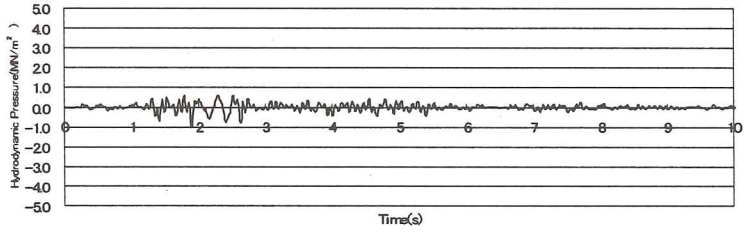

Fig. 22 Time History of Hydrodynamic Pressure under Combined Vibration

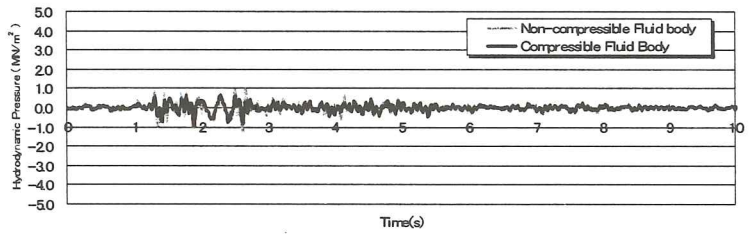

(a) All time range

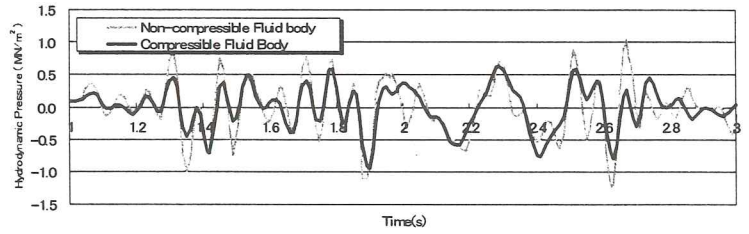

(b) From 1.0 sec to 3.0 sec

Fig. 23 Time History of Hydrodynamic Pressure under Combined Vibration
– Comparison of Non-compressible Fluid and Compressible Fluid –

3D Nonlinear Transient Analysis of Concrete Dams

by

Victor E. Saouma[1] and Yoshihisa Uchita[2] and Yoshinori Yagome[3]

ABSTRACT

Concrete dams, by virtue of the lack of reinforcement, and the potential for well predefined cracks (along lift joints and the rock/concrete interfaces, or in-between monoliths, not to mention within the solid concrete or rock mass) are indeed prime candidates for fracture mechanics. This paper will highlight laboratory tests, numerical models, validation experiments, and case studies. Numerous laboratory tests have been conducted to characterize fractured concrete under varying conditions (such as dynamic load, effect of water pressure inside the crack, cyclic loads) and will be reported. Other laboratory tests were conducted on a concrete dam model mounted on a shaking table inside a centrifuge to assess the accuracy of our numerical predictions. Finally, a numerical model (Merlin) for the nonlinear (implicit and explicit) 3D nonlinear transient analysis of concrete dams has been under continuous development for the past 15 years. The computational challenges encountered will be highlighted.

It will also be pointed out that, though nonlinear fracture mechanics has an important role to play in the seismic safety assessment of a concrete dam, it is only one major player amongst many other important ones whose participation is equally essential to the comprehensive analysis.

1 INTRODUCTION

Japan, which is geographically located on the intersection of three major faults, is one of the most seismically active regions in the world and as such has taken a leadership role in research and development to mitigate the destructive forces unleashed by a seismic tremor. Recognizing the computational power currently available, the advances in various related disciplines, the authors have developed a vision of what a modern analysis should entail. They seek not only to advance the State of the Art, but as importantly, to transform it into their State of the Practice, (Uchita, Noguchi and Saouma 2005).

Few organizations have previously embraced such a broad and challenging set of objectives. In the U.S., the Electric Power Research Institute (EPRI) has indeed funded for five years the third co-author to develop a fracture mechanics based methodology to assess dam safety. However, the impact of this research remained minimal. More recently, the European Community has funded a five years network program on the integrity assessment of large dam (NW-IALAD), but its objective was limited to the identification of the State of the Art/Practice as opposed to focused research.

Building on the American experience developed by the first author, and the seismic expertise and needs of the Japanese dam owners, an international collaboration was initiated seven years ago. Our approach is one which takes a holistic approach to a very complex and coupled multi-physics problem. First we identify the State of the Art, advance it need be, publish those results in the scientific literature to share it with others, develop a computational tool which can effectively and efficiently analyze the simplest and most complex structures, and last but not least assess the reliability of this tool through complex model testing.

This paper will share our collective experience in this adventure. However, before we proceed, it should be emphasized that a peculiarity of concrete dams is the simplicity or complexity with which they can be analyzed. In the simplest case, a spreadsheet is all what is needed, at the other end of the spec-

[1]University of Colorado, Boulder,USA
[2]Tokyo Electric Power Company, Japan
[3]Tokyo Electric Power Service Company, Japan

trum a supercomputer (or massively parallel one) is essential. What causes this dichotomy is simple. As for most structures, design is limited to linear elastic analysis, generous safety factors, and simple calculations compounded by engineering common sense. Risk analysis on the other hand, is much more complex. The Federal Energy Regulatory Commission (FERC) for instance stipulates that a potential failure mode analysis (PFMA) must be undertaken. Hence, a nonlinear finite element analysis must be conducted to determine whether the dam can sustain a given flood, earthquake, blasting, aging of its concrete or a combination of the above. The stakes hinging on the outcome of such an evaluation are enormous.

Unfortunate recent events (Tsunami in the Far-East, and breakdown of levees in New Orleans) have shown the destructive nature of unleashed water. Our responsibility is to make sure that this does not occur through dam failure

2 TESTING

Nonlinear finite element analysis is much dependent on the constitutive models (stress-strain or stress-displacements) adopted. These must not only be rigorously derived, but must be based and validated by laboratory tests.

Material testing for dam much differs from "traditional" material testing for buildings. Major difference is in size of specimens, and in type of application specific tests. The resistance to crack growth of concrete, and concrete-rock joints in large specimens (5 by 5 ft and 3" MSA), Fig. 1 was first investigated, (Brühwiler, Broz and Saouma 1991). Also investigated was the relationship between crack opening and internal uplift pressures during both static and dynamic loads, (Slowik and Saouma 2000). Finally, prevailing ourselves of the existing testing capbilities, a large scale direct tension test was conducted on a 762 by 254 mm section, (Slowik, Saouma and Thompson 1996) and yielded an unexpectedly high fracture energy of 280 N/m, Fig. 2 3.

It is often desirable to extract directly in-situ key physical parameters of the concrete; this was attempted through the use of special probe which records radial displacements while it pressurizes a borehole. First, laboratory tests were conducted, then field tests performed, Figure 3.

Another example of tests particularly relevant to concrete dams is the response of joints subjected to reverse cyclic loads, Figure 4. As the earthquake shakes the rock/concrete interfaces, there is a degradation of the interface resistance to crack formation/propagation. These tests are essential prior to the development of a constitutive joint model to be used in strong earthquakes.

3 MATHEMATICAL MODELING

Mathematical modeling of a double curvature arch dam subjected to a strong earthquake is indeed one of the most challenging civil engineering problems. It is a tightly coupled multi-physics problem. One must understand the 1) thermally induced initial stresses in the arch dam, 2) nonlinear mechanical response of joints and cracks, 3) hydrodynamic forces exerted on the dam, 4) staged construction and residual stresses, 5) dynamic flow of water inside a crack, 6) Wave propagation from the epicenter to the dam, 7) "Soil-Structure" interaction, 8) Structural model, and last but not least 9) the dynamic structural response of this massive concrete structures.

Whereas a thermal transient analysis may not be particularly challenging, determination of the thermally induced thermal stresses, simulation of the construction process, and of the joint grouting is a delicate computational task which may not be easily accomplished with commercial codes.

Joints and cracks do constitute the primary, if not the only source of nonlinearity in the stress analysis of a dam. Whereas most commercial codes, as well as researchers, focused on the so-called smeared crack model, we felt all along that the discrete crack model should be one adopted. In the smeared model, the mesh is fixed, and Gauss points constitutive models are modified to reflect the presence of a crack. A major limitation of this model, and despite years of research, is the difficulty to capture the localization of the crack. In the discrete crack model, the mesh topology reflects the presence of the crack/joint and a special interface element is inserted along the crack. In the context of dam, where few cracks/joints exist, and which location is known a priori, there is little doubt that the discrete crack model should be adopted. Hence, much of our effort dwelt on improving this model. When used along the concrete/rock

discontinuity in a dynamic analysis, this model indeed captures the nonlinear response of the joint through crack opening and normal stress distributions which account for possible (small) cohesive tensile stresses, Figure 5.

Our focus on discrete crack may have started with (Saouma 1980), really took roots in modern plasticity approach through the model developed in (Cervenka, Chandra and Saouma 1998) which was extensively used for actual nonlinear dam analysis, and culminated most recently with the extension of our previous model to account for reverse cyclic loads, (Puntel, Bolzon and Saouma 2006).

During an earthquake, joints open and cracks may form. Currently, there is much controversy as to whether water can flow into the newly formed crack, and what the dynamic uplift is. There is some strong experimental evidence that during crack opening and closure, we have respectively a decrease or an increase of uplift pressure. Hence during crack propagation, not only is the new crack surface subjected to an internal uplift pressure, but the magnitude of the pressure is a function of the rate of crack opening displacements (as a first approximation), Fig. 6.

Earthquake records (accelerograms) are usually measured or determined at the surface. Yet the analysis requires modeling the rock foundation (and its mass), at the base of which accelerations are applied. Again, in simpler analyses the surface acceleration is simply applied at the base; however a more rigorous approach would require deconvolution of the signal under the assumption of a linear elastic rock foundation. This is done by first applying the (surface) recorded signal at the base, through a preliminary finite element analysis compute the induced acceleration on the surface, transfer those two accelerations from the time to the frequency domain, and compute the transfer function. In the general three dimensional case, there will be 9 transfer functions which constitute the convolution matrix. The inverse of that matrix times the input accelerations will give the deconvoluted one. Hence, we the deconvoluted one is applied at the base of the foundation, the induced acceleration at the surface will be nearly identical to the one recorded, Fig. 7.

Whereas many simpler analyses ignore the foundation mass, this must be accounted for in a rigorous nonlinear analysis. A major complication becomes modeling of the so-called free-field as the seismic wave will artificially and numerically be reflected by the lateral edges of the model. This problem was long recognized. In the context of a finite element (as opposed to boundary element) analysis, this problem is most efficiently addressed through application of boundary conditions which would absorb these waves (thus we often talk of "Silent" boundary conditions, or of radial damping). The classical (and partial) solution to this problem is the application of Lysmer dashpots. However, in this model, the free field is assumed to be rigid. A more rigorous model, developed by Miura and Okinaka (1989) consists in a separate analysis of each of the free fields (2 in 2D and 4 in 3D) for each of the 3 components of the earthquake record. The determined velocities are then applied as initial boundary conditions to the dam which must also have the traditional lysmer support, Figure 8.

Free field modeling require that there is no vertical support below the foundation (to avoid the vertical reflection of waves), hence in our analysis we first perform a static analysis with gravity load, and then the program can automatically replace the vertical reactions by equal nodal forces for the restart in the Dynamic analysis.

While conceptually simple, this can be a potentially "labor intensive" task as velocities must be extracted for each time steps from many different files and then inserted in the main analysis input file.

Amongst the many "fine-grain" issues in the structural model (and not previously discussed), we list the need to have an initial static analysis, followed by a Restart (and resetting of displacements to zero) of the dynamic analysis with dynamic elastic properties. In the dynamic analysis, one needs to avoid the effect of "rocking" (reflection of the elastic waves with the vertical supports of the gravity load) by replacing static reactions with point loads in the dynamic analysis. Concrete and rock should also have different Rayleigh damping coefficients. Different joint models should be used if we expect a pure mode I (simpler) or mixed mode crack propagation. Highly fissured and fragmented rock (as is the case in Japan) should have a nonlinear model, and major rock joints should be modeled.

Whereas until fairly recently, transient analysis was considered to be computationally impossi-

ble (and hence most analyses were linear and performed in the frequency domain) , this is clearly no longer the case. With modern computers, time history analysis of even small dams is becoming the norm. Time integration can be either implicit or explicit. Dynamic crack opening and closures can induce numerical problems, and integration schemes may have to be refined. In Fig. 9 it is apparent that the both the Newmark β and Hughes α methods yield identical results as long as the discrete crack is not activated, when it is Hughes time integration method is more suited to dissipate the high frequency content of the response. More recently, we have modified our code to accommodate explicit (which being conditionally stable requires very small time steps) method. A major advantage of the explicit time integration is that the global structural stiffness matrix need not be assembled, and hence the code can be relatively easily parallelized to run on multiple CPU's. This was done through the MPI library, whereas we used METIS for domain decomposition. It is our strong expectation that complex 3D nonlinear analysis of dam-foundation-reservoir system can most effectively be analyzed in parallel on a network of computers connected by 1 GB Ethernet network. A special purpose 2D-3D finite element mesh generator, Kumo-no-su, for concrete dams with the capability of supporting all the above features was developed, (Saouma 2007).

4 ANALYSIS

The kernel of our computational tools is the finite element code. It is a 3D nonlinear dynamic finite element code which has been under continuous development for over 12 years. Being (as all other programs) developed "in-house" we do have the source code and the flexibility to easily modify it to address new needs of the Dam Engineering profession. Merlin, (Saouma, Červenka and Reich 2006) has a library of over 25 constitutive models, 30 element types, different algorithms for nonlinear analysis (including indirect control/Line Search). In addition to stress analysis, it can also solve transient heat transfer analysis (to determine temperature field for AAR analysis), and steady state seepage analysis (to determine initial uplift pressure in complex geological formation). Implemented in Merlin are all the desirable features previously discussed, and others (such as a comprehensive model for AAR largely based on the experimental work undertaken at the Laboratoire Central des Ponts et Chausss in France).

Whereas much of the earlier emphasis was on discrete crack models, Merlin can combine localized failure (discrete cracks) with distributed failures (smeared cracks).

Not surprisingly, computational time on a Pentium IV of a 3D nonlinear analysis with dam reservoir can take well over two weeks. Hence, to address this severe constraint, an explicit version of the program was developed, and the parallelized using the MPI library (http://www-unix.mcs.anl.gov/mpi/). Hence, not only seismic analysis of a dam with reservoir could be performed in a matter of hours, but also analysis of dams subjected to impact or explosives could be possible. In turn, the preprocessor can perform domain decomposition using METIS (http://www-users.cs.umn.edu/ karypis/metis).

5 IMPORTANCE of POSTPROCESSING

Whether running a simple or complex analysis, Engineers no longer limit themselves to scrutinizing pages of output data file. Not only graphical postprocessors are essential, but those must be "jazzed-up" to satisfy the wishes of a new generation grown with electronic games. Last but not least, the Engineer should be able to "data-mine" the information needed to prepare analysis reports. This was accomplished in our case with our in-house program Spider, (Haussman and Saouma 2006). As this tool was developed by Engineers for Engineers, it truly responds to all our needs. Hence, Spider accepts input data from:

Eigenvalue analysis: display and animation of mode shapes. User selects the mode shape, and spider will display it in static mode, or through an animation. Animation can then be saved into an .AVI file.

Time History analysis: real time display of displacements and accelerations while the (very long) numerical simulation is under way. User can select in real time node and degree of freedom for which accelerations are to be displayed (histogram at the bottom, bar chart and

numerical values on the top), through a graphical user interface. Furthermore, the user can select two accelerograms and seek the evaluation of the transfer function between the two signals (FFT and transfer function all being internally computed), or plot accelerations and FFT's, Fig. 11.

.AVI files showing the animation of the dam's response are also possible. Finally, Spider is also setup to read various analysis results and automatically determine the deconvoluted earthquake accelerogram which should be applied.

Nonlinear finite element analysis: Provides practically all the major and (minor) features we found in other finite element postprocessors. Aside from the usual displays of meshes, contour lines, contour surfaces, carpet plots, vector plots and principal plots, Spider provides a number of other features. Display of individual groups, possibility to slice the structure; provide different types of displays for a sliced structure, and many more options, Fig. 12. Of particular relevance to dam engineering, Spider can display contour lines for the factors of safety, surface plots of the joint stresses, displacements and uplift pressures.

It should be noted that Spider is in no way "hard-wired" to Merlin, and that it can be used as a stand-alone post-processor to other finite element codes. User has to supply a .pst file, .rtv or .eig (standard post-processor, real time view, or eigenvalue) file

6 VALIDATION

Society can no longer afford the failure of a major infrastructure before it revises its mathematical predictive models. This is particularly true for dams where increased sophistication in modeling and narrowing factors of safety (economic hardship) imposes upon us to verify the accuracy of the mathematical models through controlled laboratory testing. All model testing must satisfy Buckingham's laws of similitude; for most ordinary structures, this is seldom a concern however for dams it is. Hence, for a dam model n times smaller than the corresponding prototype, we must increase the gravitational forces by a factor of n. Furthermore, a 10 seconds earthquake hitting the prototype should be modeled by a 10/n model excitation (hence if n. is 100, that 10 sec. earthquake must be applied in 0.1 sec!).

Whereas we do not, yet, advocate the use of centrifuges to assess the safety of an actual dam, we certainly recognize the values of such a test to validate numerical models. Indeed, this may very well constitute the only safe and reliable way to verify the accuracy of a numerical code for dam engineering. Preliminary centrifuge tests of dams were performed in Boulder in the early 90's through our EPRI project. Most recently, we have examined first the development of uplift pressure beneath the dam, and assessed the accuracy of our models, Fig. 15, (Gillan, Saouma and Shimpo 2004).

Building on the experience gained from the previous test, a new test program was initiated to dynamically excite and crack impounded dams inside a centrifuge, (Uchita, Shimpo and Saouma 2005). Hence, the facility of the centrifuge facility of the Obayashi Corporation was used. A model, representative of Japanese gravity dams, was cast with a very shallow foundation, Fig. 16.

Beside strain gages, the dam was instrumented with crack gages, laser based displacement transducers, and accelerometers. Whereas no attempt was made to model uplift, the impounded dam was to be excited by a series of harmonic excitations (five cycles each), with increasing magnitudes. Following each excitation, a "white-noise" excitation is applied, and through the determination of the transfer function between base and crest, damage (cracks) was detected.

Again, the objective was not to test a particular dam, but rather to test a generic and representative geometry which could be used to assess our computer program Merlin. As with the uplift investigation, numerical prediction of crack propagation, and crest acceleration was very satisfactory, Fig. 17

7 CONCLUSIONS

Historically, Dam Engineering has constituted some of the most complex and challenging engineering problems. Hence, solutions initially developed for dams were subsequently extended to other Engineering disciplines. Furthermore, given what is at stake,

we no longer can satisfy ourselves with simple engineering approaches, instead we must take advantage of the latest developments and lead the way in Civil Engineering research and development.

Nonlinear fracture mechanics plays a crucial role in the seismic safety assessment of concrete dams, it is by far the largest source of nonlinearity. Joints are present between monoliths, between the rock and the concrete and potentially in the rock foundation as joints or in the dam as cracks. Nevertheless, it should be made clear that as important as fracture mechanics is, it is only one "player" amongst many others which should also be accounted for.

8 ACKNOWLEDGMENTS

The research reported in this paper could not have been possible without the precious assistance of numerous collaborators: Prof. Brühwiler, Prof. Slowik, Dr. Puntel, and particularly Dr. Ćervenka. Their contributions is gratefully acknowledged. The extensive software development was made possible through the invaluable assistance of Mr. Takashi Shimpo and Mr. Yoshinori Yagome. Financial support for the research was made possible orginally by the Electric Power Research Institute (EPRI), and for the past seven years by the Tokyo Electric Power Company (TEPCO) through the Tokyo Electric Power Service Company (TEPSCO).

9 REFERENCES

References

Brühwiler, E., Broz, J. and Saouma, V.: 1991, Fracture model evaluation of dam concrete, *ASCE, Journal of Civil Engineering Materials* **4**, 235–251.

Cervenka, J., Chandra, J. and Saouma, V.: 1998, Mixed mode fracture of cementitious bimaterial interfaces; part ii: Numerical simulation, *Engineering Fracture Mechanics* **60**(1), 95–107.

Gillan, C., Saouma, V. and Shimpo, T.: 2004, Centrifuge tests of concrete dams, *International Journal of Water Power and Dam Construction* pp. 38–41.

Haussman, G. and Saouma, V.: 2006, Spider, a 3d interactive graphics finite element post-processor; user's manual, *Technical report*, Report Submitted by the University of Colorado to the Tokyo Electric Power Service Company. `http://civil.colorado.edu/~saouma/Spider`.

Miura, F. and Okinaka, H.: 1989, Dynamic analysis method for 3d soil-structure interaction systems with the viscous boundary based on the principle of virtual work, *Japanese Journal of Civil Engineering* pp. 395–404.

Puntel, E., Bolzon, G. and Saouma, V.: 2006, A fracture mechanics based model for joints under cyclic loading, *ASCE J. of Engineering Mechanics* **132**(11), 1151–1159.

Saouma, V.: 1980, *Finite Element Analysis of Reinforced Concrete; a Fracture Mechanics Approach*, PhD thesis, Cornell University, Department of Structural Engineering.

Saouma, V.: 2007, KumoNoSu, a 3d interactive graphics mesh generator for merlin; user's manual, *Technical report*, Report Submitted by the University of Colorado to the Tokyo Electric Power Service Company. `http://civil.colorado.edu/~saouma/Kumo`.

Saouma, V., Červenka, J. and Reich, R.: 2006, Merlin finite element user's manual, *Technical report*, Electric Power Research Institute (EPRI), Palo Alto; Tokyo Electric Power Service Company (TEPSCO), Tokyo. `http://civil.colorado.edu/~saouma/Merlin`.

Slowik, V. and Saouma, V.: 2000, Water pressure in propagating cracks, *ASCE J. of Structural Engineering* **126**(2), 235–242.

Slowik, V., Saouma, V. and Thompson, A.: 1996, Large scale direct tension test of concrete, *Cement and Concrete Research* **26**(6), 949–954.

Uchita, Y., Noguchi, H. and Saouma, V.: 2005, Dam safety research, *International Water Power & Dam Constuction* pp. 16–22.

Uchita, Y., Shimpo, T. and Saouma, V.: 2005, Dynamic centrifuge tests of concrete dams, *Earthquake Engineering and Structural Dynamics* **34**, 1467–1487.

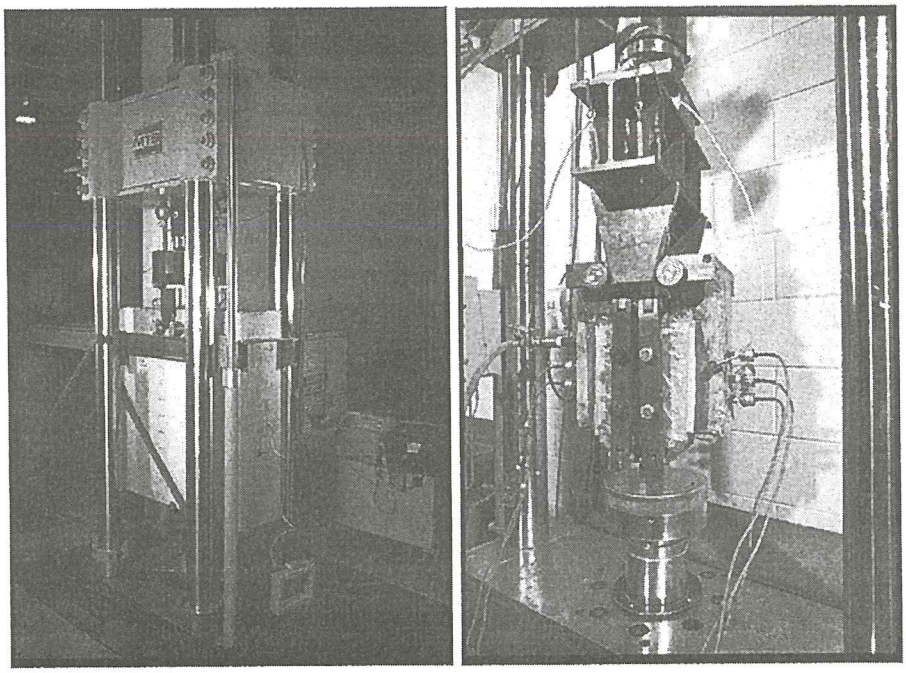

Figure 1: Large Dry and Small Wet Wedge Splitting Tests

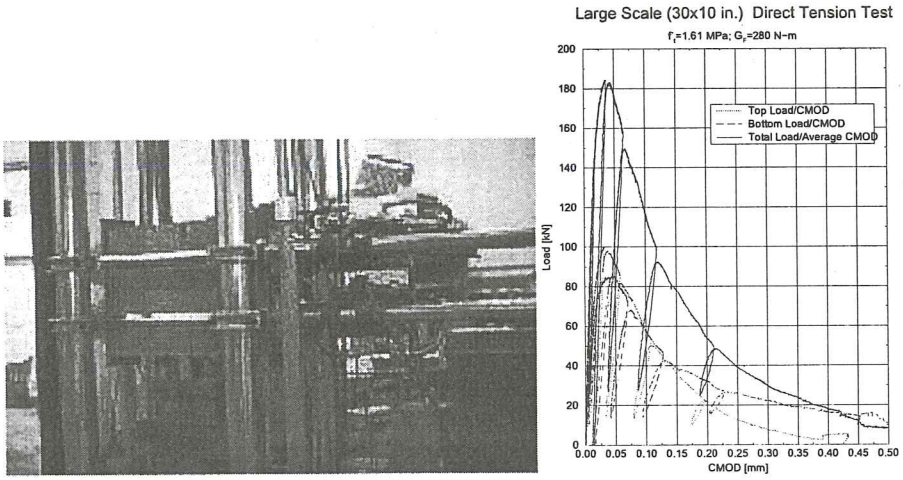

Figure 2: Large Scale Direct Tension Test

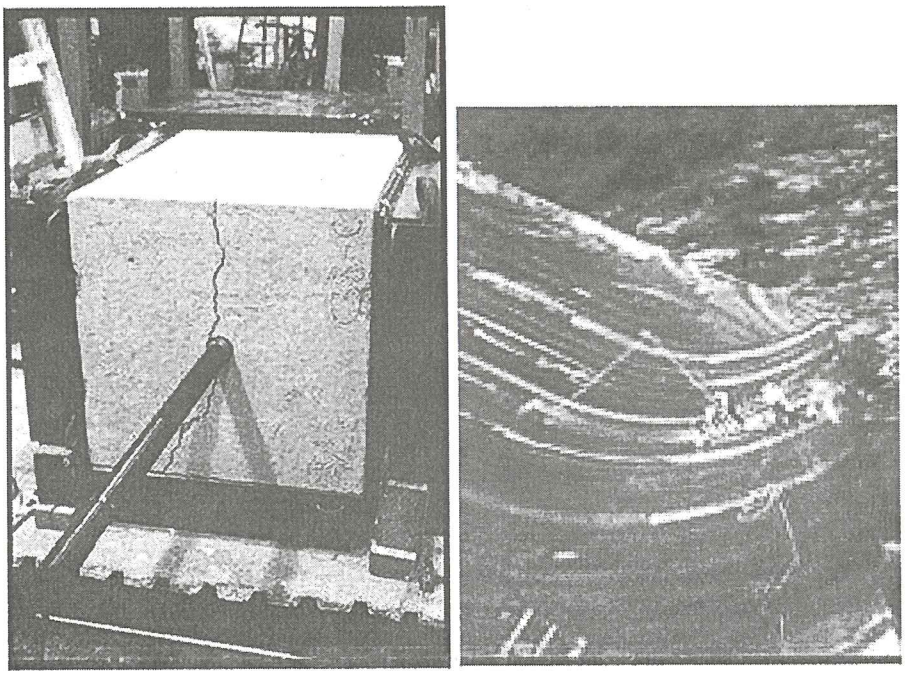

Figure 3: Use of Pressurized Probes to Determine in-situ Concrete Properties in a Dam

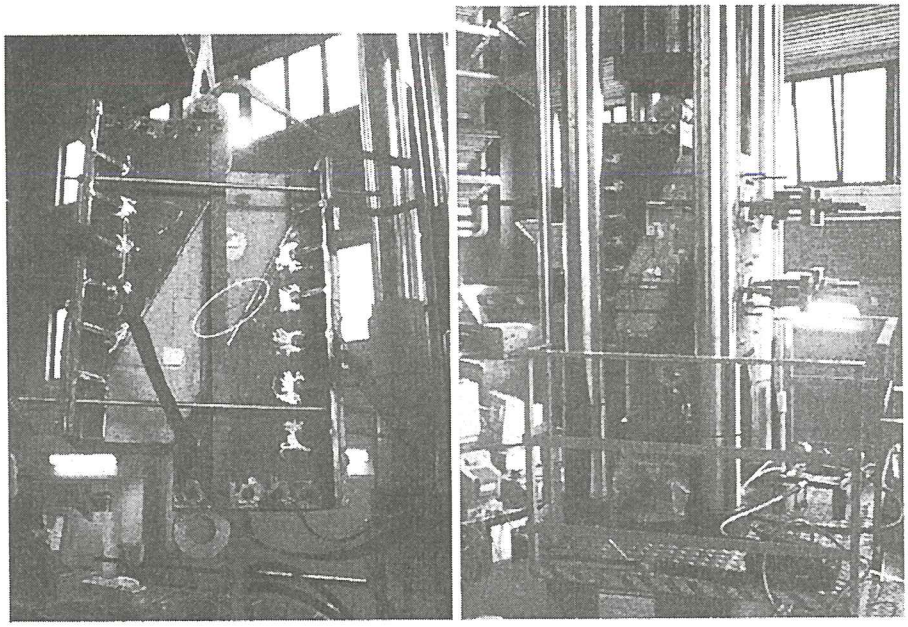

Figure 4: Large Scale Testing of Concrete Joints Subjected to Reverse Cyclic Loading

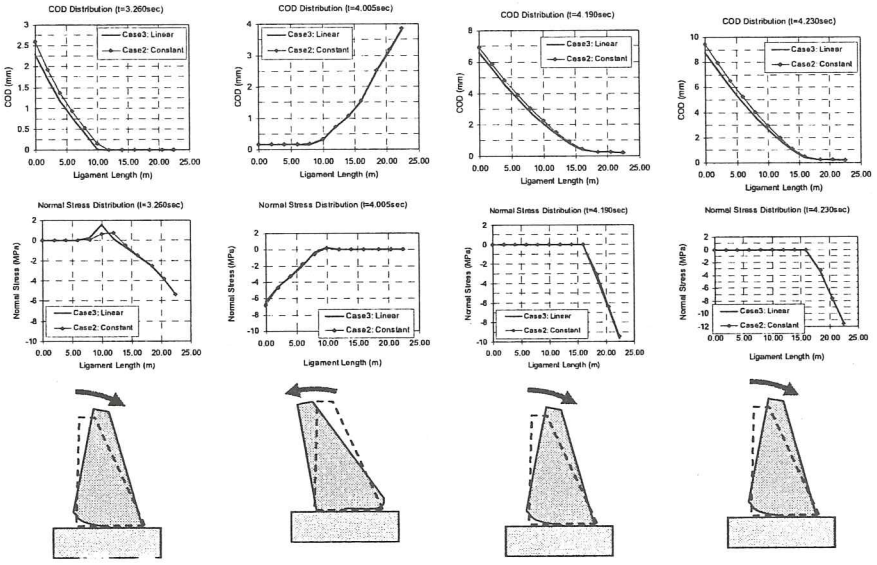

Figure 5: Special Interface Elements Simulating Cohesive Crack Joints During Seismic Excitation. Note Out of Phase Crack Opening Displacements and Cohesive Stresses

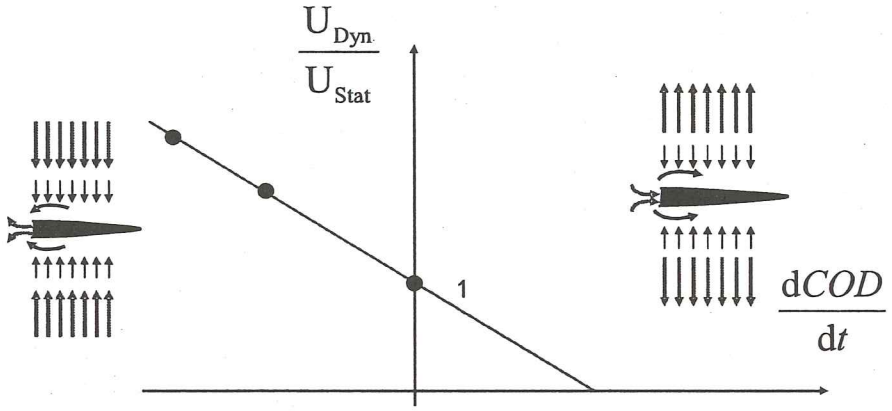

Figure 6: Dynamic Uplift in a Joint

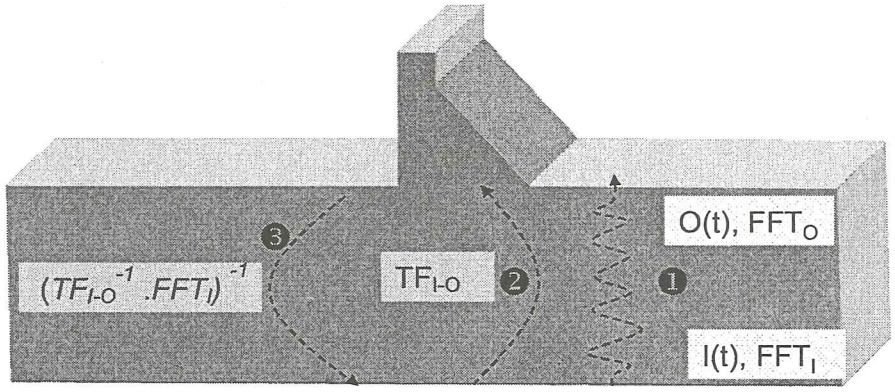

Figure 7: Deconvolution of Seismic Record

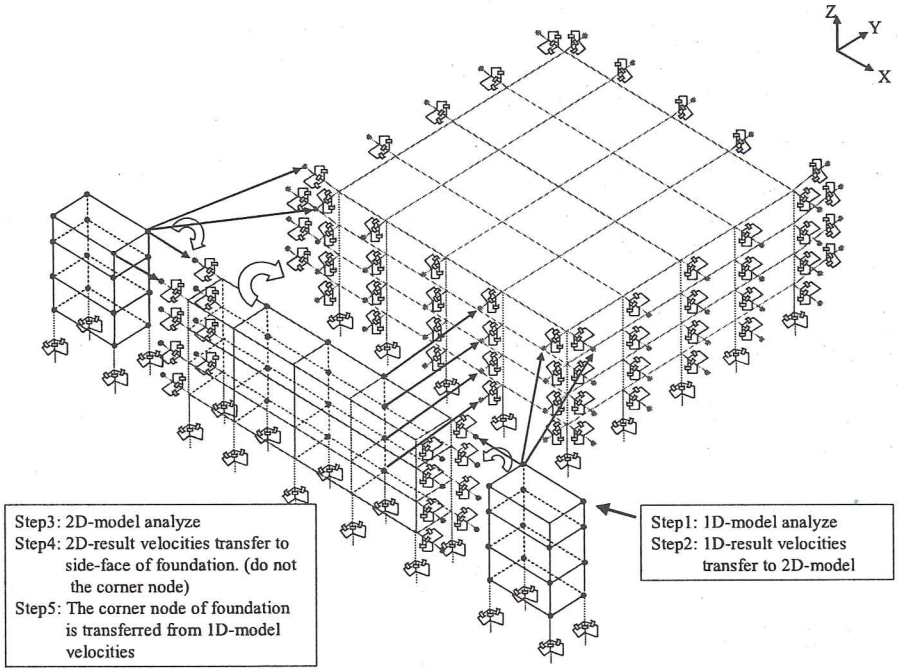

Figure 8: Finite Element Discretization of the free field; Outline of Procedure

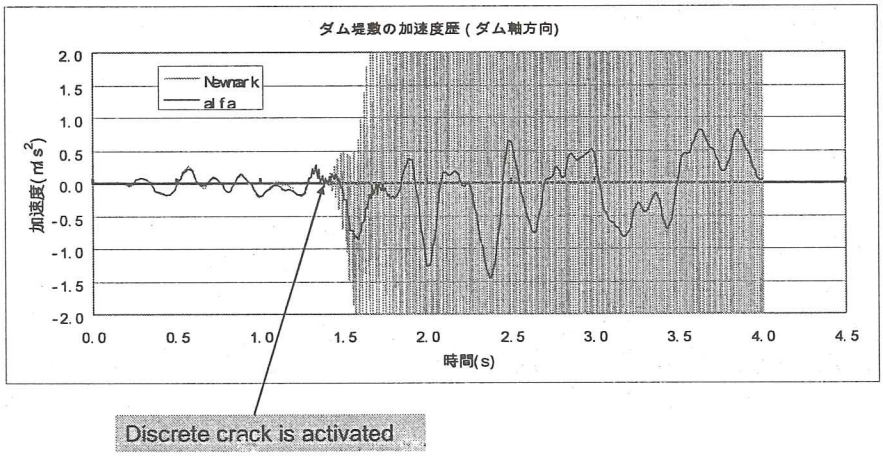

Figure 9: Effect of Time integration Scheme on Dynamic Response with Discrete Cracks

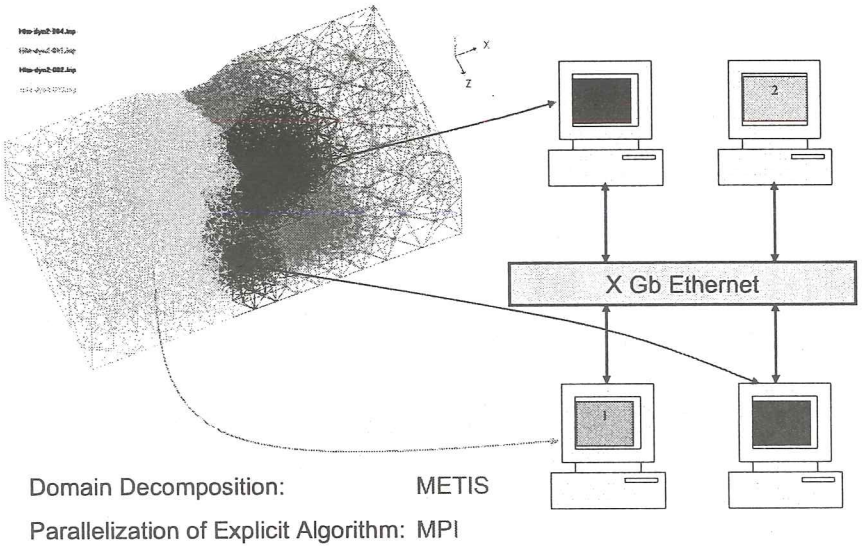

Figure 10: Explicit Distributed Computation of an Arch Dam

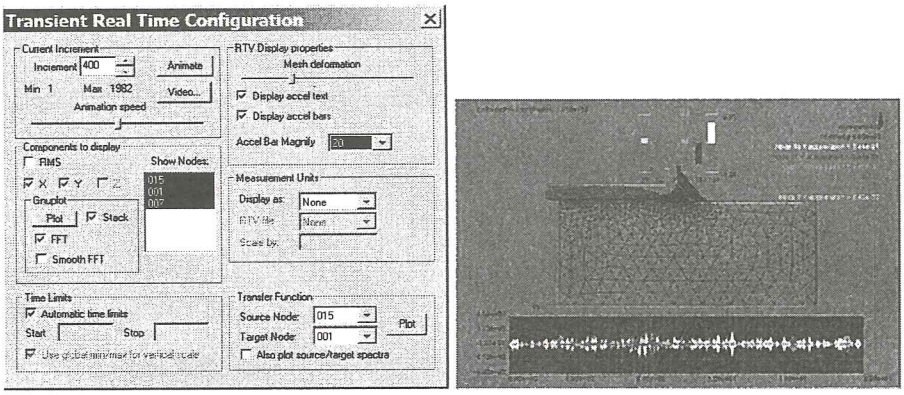

Figure 11: Real Time Display of Nonlinear Seismic Analysis of a Dam

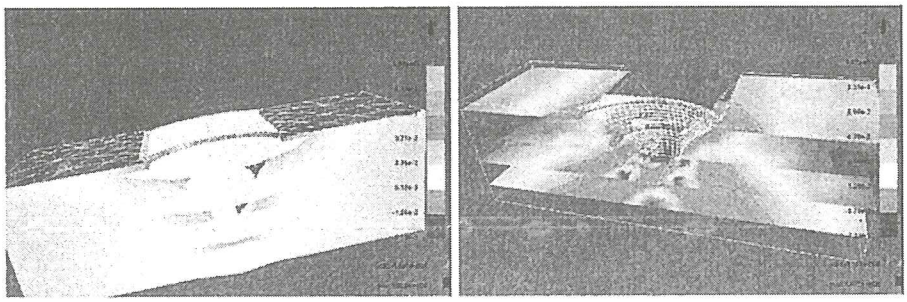

Figure 12: Postprocessing visualization

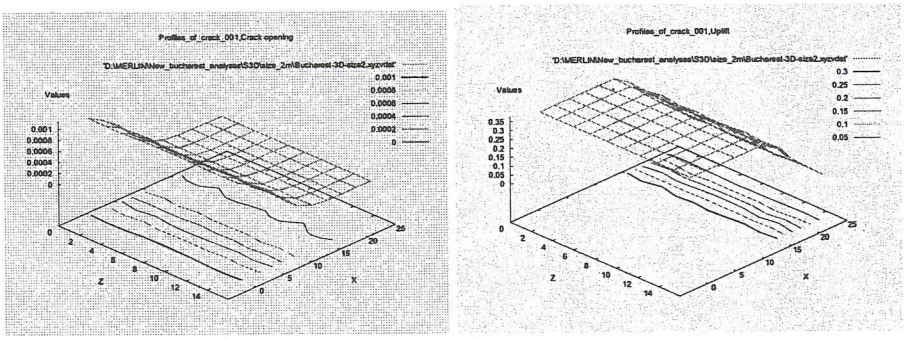

Figure 13: 3D Crack Opening Displacement Profile of a Joint, and Corresponding Nonlinear Uplift Pressures

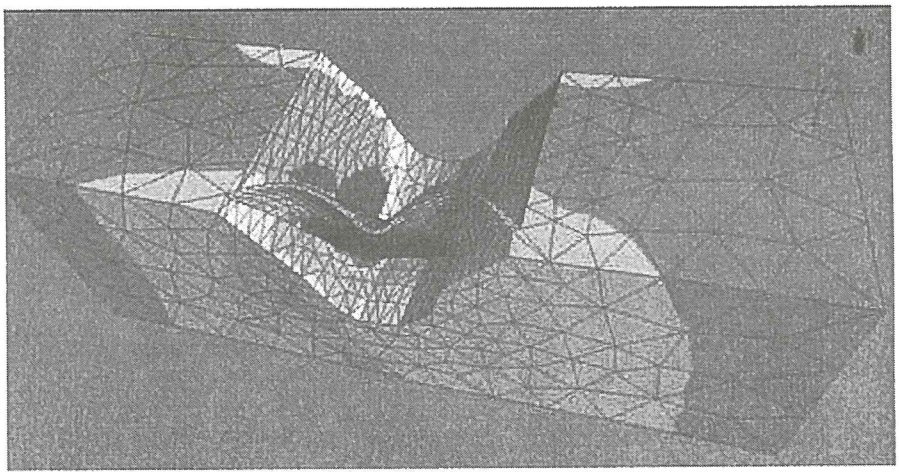

Figure 14: Example of Joint Sliding During and Earthquake

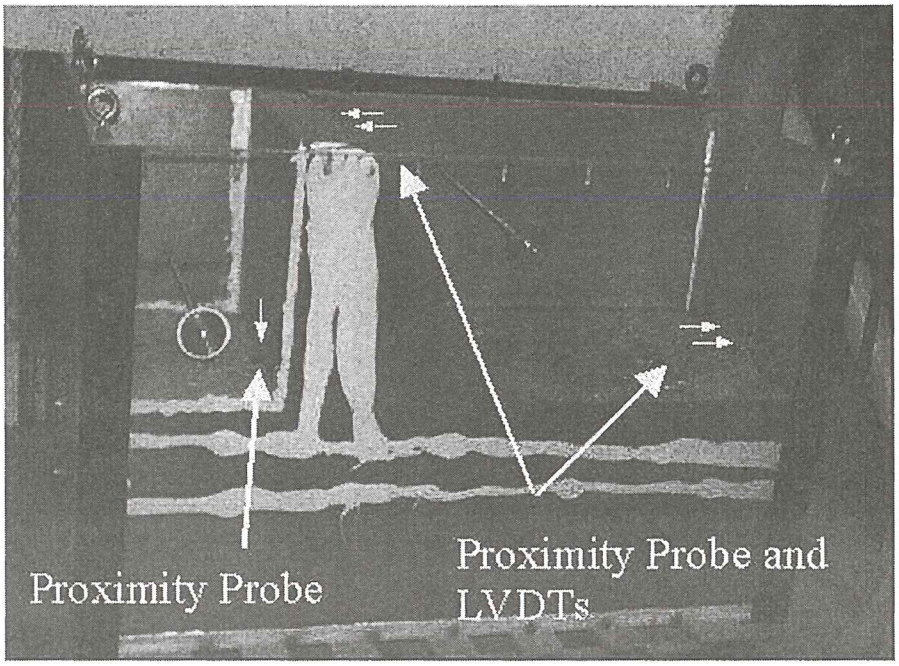

Figure 15: Aluminum container showing dam model and accompanying instrumentation

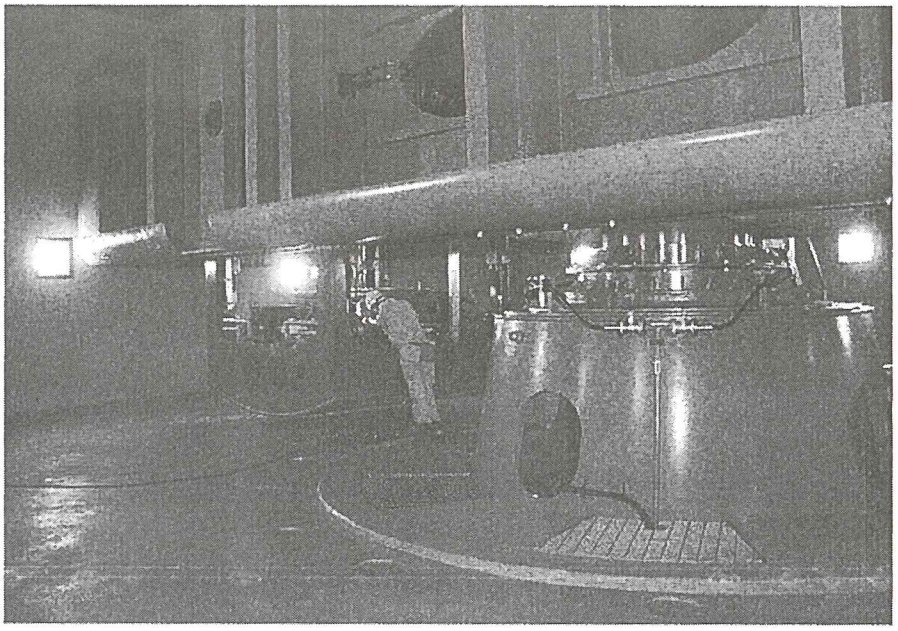

Figure 16: Centrifuge Facility at Obayashi Corporation, and Gravity Dam model

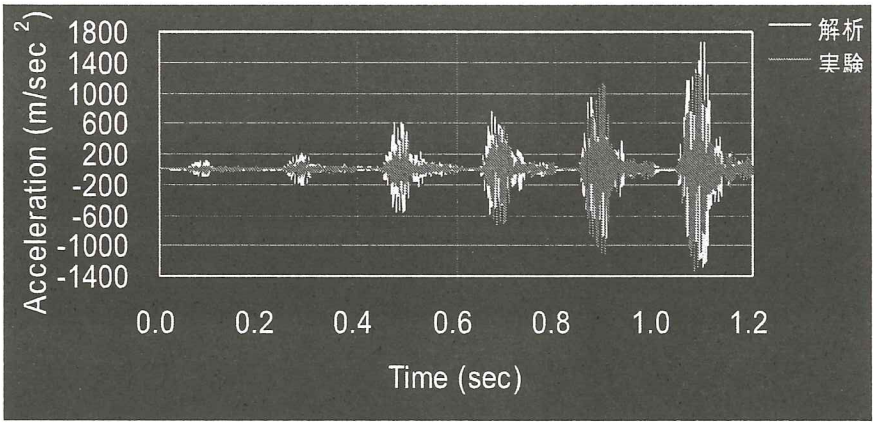

Figure 17: Crest Acceleration of Dam Model: Yellow Predictive Analysis, Orange: Experiments

THEME 5

Fire Performance of Structures

Ultimate Temperature of Steel Columns subject to Thermal Elongations of Adjacent Beams at Fire

by

Fuminobu Ozaki

ABSTRACT

The present paper focuses on structural fire resistance of heated steel columns, in particular the columns subjected to thermal elongations of adjacent beams at fires. Behavior of the steel column at the fire is minutely investigated by making full use of a refined finite element analysis taken a 3-D non-linear thin plate element into account. From results obtained by numerically parametric calculations, it is clarified that the above thermal elongation is not a sensitive factor affected the fire resistance of the steel column and its ultimate temperature can be estimated by verification methods which has been proposed in the Recommendation for Fire Resistant Design of Steel Structures (AIJ, 1999).

KEYWORDS: FEM, Local buckling, Overall buckling, Steel column, Thermal elongation of beam, Ultimate temperature

1. INTRODUCTION

Recent studies on the fire resistance of steel structures have focused on the stability of steel members and steel structures during fires [1-5]. To investigate the structural stability of structures exposed to fire, the fire load-bearing capacities of key members (beams, columns and connections) and other factors involved in their stability should be investigated since their collapse may lead to the collapse of the entire structure. The overall structural stability during fires of the combined members needs to be understood. Since the fire stability of members is closely related to the fire stability of the frames, the fire stability of both should be known to determine the fire resistance of a structure.

Overall and local buckling of steel columns are one of the key causes that destabilize a structure. Especially, the fire resistance of columns positioned within frames is affected by elongation of adjacent beams. When beams are heated during a fire, the beams expand lengthwise and push adjacent heated columns. The longer the beam, the further it elongates, which may cause local buckling of adjacent columns at their upper and lower ends. Structures with long beam spans have increased in recent years and could suffer excessive elongation during fires. In most structures, the collapse of a fire compartment room is controlled by applying fire proofing materials to steel members to prevent excessive elongation and using fire resistant columns. Methods for controlling the heat input into beams have been found to be effective for preventing elongation, but the necessary structural fire resistance of columns is not understood and this question has not yet been clearly resolved.

In the present study, a numerical analysis by the finite element method was conducted to investigate factors involved in the destabilization of steel columns at high fire temperatures, such as the possibility of local buckling when pushed by elongating beams, the behaviors of steel columns after local buckling, and the possibility of local buckling inducing failure of the columns, and to determine the temperature at which the columns collapse [1]. The results of the numerical analysis were also used to investigate the validity and feasibility of existing methods for assessing the fire resistance of steel columns.

In Japan, various attempts have been made to ensure the fire safety of steel structures, such as the method for assessing the collapse temperature at which steel columns suffer local buckling proposed in " Recommendation for Fire Resistant Design of Steel Structures "[6]. The validity of the method has been investigated by

COE Post doctoral Researcher
Center for Fire Scie. and Tech., Tokyo Univ. of Science
Yamasaki2641 Noda-shi Chiba 278-8510, Japan

conducting non-linear finite element analysis [7] using two-dimensional beam elements, in which several numerical assumptions are made, such as the deteriorating stress-strain relationship after local buckling is given as a known value and the beam element models are restricted to two-dimensional behaviors on a plane. Actual steel columns have cross sections in which steel plates are combined, so local buckling involves the three-dimensional behavior of collapse of the sectional form. To investigate the validity of the method for determining the collapse temperature, a precise numerical analysis is needed. This paper describes a non-linear finite element analysis using three-dimensional thin plate elements (shell element) to investigate the precise behaviors of steel columns during local buckling at high temperatures. The validity of the analysis was examined by comparing the results with those of high-temperature experiments of short steel columns in the past.

2. COMPARISON OF NUMERICAL ANALYSIS RESULTS FOR SHORT STEEL COLUMNS AND EXPERIMENTAL RESULTS IN THE PAST

Hirashima et al. conducted compressive tests of heated stub columns at a constant temperature and under increasing load [8]. In their experiment, weld assembly square hollow columns were used. A cross section of the specimen is shown in Figure 1, and its specifications are listed in Table 1. The plate width of the specimen was B, the plate thickness was t, and the total length was H. Specimens of width to thickness ratios (B/t) of 25 and 30 were used. The length to width ratio (H/B) was 3 in all specimens. In the experiment by Hirashima et al., splice plates were welded on the corners to prevent the weld joints from breaking during the experiment (Figure 1). The thickness of the splice plates (t_s) was 9 mm, which was thicker than the plates constituting the specimens (t). Therefore, the experimental results should have been affected by the splice plates. The models of the rectangular specimens used for numerical analysis are shown in Figure 2(a) and 2(b). The finite element models were constructed using the three-dimensional thin plate elements

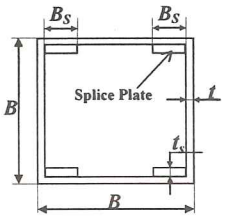

Fig-1 Section of Specimen

Table 1 Specifications of Specimen

	B/t = 25	B/t = 30
Plate Width B	150	135
Plate Thickness t	6	4.5
Height of Specimen H	450	405
S. Plate Width B_s	25	25
S. Plate Thickness t_s	9	9

(Unit : mm)

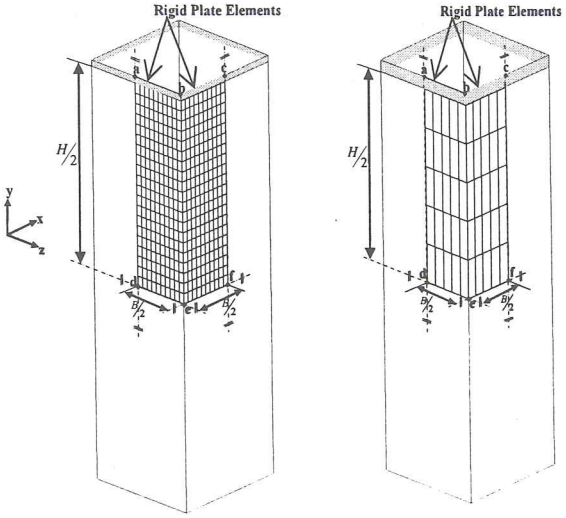

(a) Model A (b) Model B

Fig-2 Analytical Models of Stub Columns

proposed in Reference 9). Details of the models are described in the reference; an overview is given below:

1) The plate elements were rectangular. There were eight nodes per element: four on the corners and four in the middle of each side. The nodes on the corners had two degrees of freedom along the parallel direction, two degrees of freedom along the out-of-plane rotational direction, and two degrees of freedom along the in-plane rotational direction, making a total of seven degrees of freedom. The nodes in the middle of the sides had one degrees of freedom along the parallel direction. Each element had a total nodal degrees of freedom of 32.

2) The strain in the elements was determined according to Green's strain tensile [10] to cope with geometrical non-linear problems. The multi-axial elasto-plastic constitutive law followed the Prandtl-Reuss law [11] and was used to derive the increment stress-strain relationship under plane stress.

3) The equation of equilibrium of force for the plate elements was determined using the principle of virtual work. The discretization into finite elements, and derivation of incremental control equation (incremental relationships between the node force and node displacement) were determined.

Assuming the specimens were symmetrical right and left and up and down, partial analytical models A and B, each consisting of two steel plates, shown in Figure 2(a) and 2(b) were analyzed. The number of elements differed between Models A and B. Model A was divided into 400 elements of equal size, and Model B was divided into 50 elements of equal size. The other analytical conditions were all the same. Models A and B were used for the following reasons.

Generally, local buckling deformation in the columns tends to concentrate at points of buckling. At the points of local buckling, the plate deforms toward the out-of-plane, showing very complicated stress conditions. Thus, at least a certain number of elements are needed to precisely analyze the behavior of plates during local buckling. On the other hand, the calculation load jumps when the number of three-dimensional plate elements is increased. For example, parametric numerical analysis of the behaviors of steel columns during fire, which is described in a following paragraph, requires an enormous amount of calculation and long calculation time. The three-dimensional plate elements used in this numerical analysis can precisely analyze the non-linear behaviors of plates using the least number of elements because each element has a nodal degrees of freedom of 32, enabling the displacement function inside the element to be set more precisely than for plate elements that have only four nodes [12]. This was expected to reduce calculation loads. To examine the advantage, Model B shown in Figure 2(b) was also used as an analytical model.

The relationships between stress σ and strain ε at high temperatures used in the analysis are shown in Figure 3. The stub column specimens were made of JIS SM490 steel, and the test results are shown with solid lines in the figure. The dashed lines in the figure denote the σ-ε relationships used in the numerical analysis, which were derived by approximating the test results (solid lines) to the σ-ε relationships of steels stated in the Recommendation for Fire Resistant Design. Young's modulus of the steel at high temperatures was the values stated in Reference 6). Figure 3 shows that the stress jumped at a strain of 0.5% at temperatures above 500°C. This was because the strain speed changed from 0.3%/min to 10%/min at 0.5% strain. This sudden rise in stress was not incorporated in the σ-ε relationships (dashed lines) used for the numerical analysis. At strains of over 0.5%, the forms of the σ-ε relationships (dashed lines) were determined so as to agree with the experimental stress values at 10% strain. This method was based on the same concept used by Hirashima et al. for determining the σ-ε relationships. Hirashima et al. reported no specific values for the loading speed (strain velocity) during their short column experiment at high temperatures but only that the loading was continued for about 100 minutes. The loading speed estimated from the duration of loading was slower than that used for the coupon tests at high temperatures (0.3%/min).

The sections where the splice plates were welded were modeled as plate elements that had

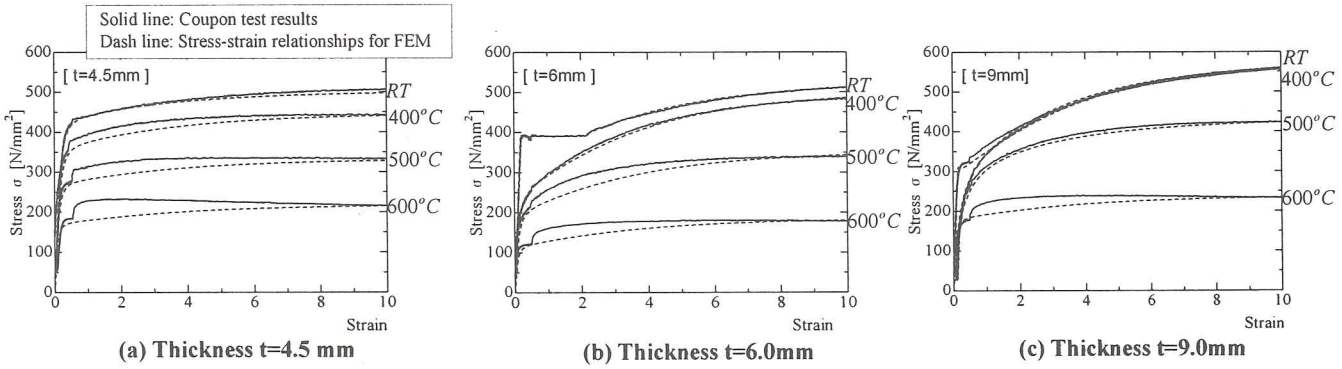

(a) Thickness t=4.5 mm (b) Thickness t=6.0mm (c) Thickness t=9.0mm

Fig-3 Stress and strain relationships

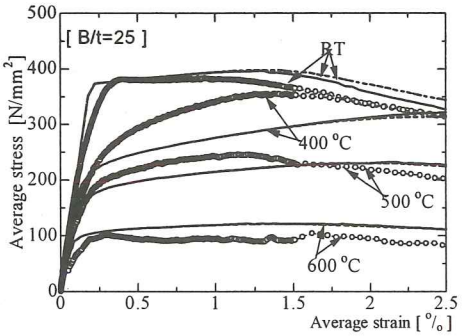

(a) B/t=25

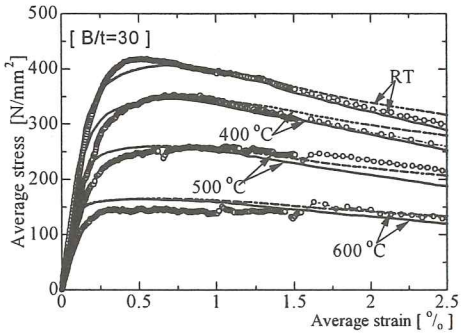

(b) B/t=30

Fig-4 Comparison between experimental and analytical results

a thickness of the sum of the plate thickness t of the specimen and the plate thickness t_s of the splice plate. Since both ends of the specimen were connected to an accelerator via steel blocks, rigid plate elements were added to the upper ends of Models A and B, and the rotational freedom along the upper sides ab and bc was restricted. The initial imperfections were given by applying minute uniform load on the sides de and ef at the center of the specimen in Figure 2 toward the out-of-plane direction of the plates. The uniform load was adjusted so as to produce initial out-of-plane deflection of -B/1,000 and B/1,000 at points d and f in the middle of the specimen, respectively, in all analytical cases. The load imperfections were given in this analysis because it was easier than giving configuration imperfections. The stub column specimens tested were suspected of having produced local temperature distribution and strain restriction, and the specimens before load application at the high temperature were likely to have received any minute load imperfections by heat and other stresses as well as configuration imperfections. The displacement at point b on the upper end along the member axis (displacement along the y direction in Figure 2) was controlled, and uniform compressive load was applied on the specimen via rigid plate elements. Analysis was conducted for specimen temperatures ranging from ambient temperature to 600°C.

The experimental results and the results of the numerical analysis are shown in Figure 4 for stub columns of square hollow section. The X axis of the figure shows the average strain of the specimens, and the Y axis shows the average stress. The former is the value determined by dividing the total length H of the specimen by compressive deformation δv, and the latter is the value determined by dividing the compressive force P applied on the specimen by the total cross sectional area A of the specimen including the area of the splice plates. The open circles in the figure denote the experimental results, and the solid and dashed lines are the analytical results of Models A and B, respectively. Figure 4(a) and 4(b) show that the experimental and analytical results agreed with each other quite well in all cases although not perfectly. Especially at B/t = 30 (Figure 4(b)), the ultimate strength of the specimens and their behaviors after the peak agreed very well. When the analytical values of Models A and B (solid and dashed lines) in Figure 4(a) and 4(b) are compared, the results of Model B (dashed line) were slightly higher than those of Model A (solid line). Model B, which had smaller elements than Model A, showed coarser deformation at the points of local buckling than in Model A. However, as shown in Figure 4(a) and 4(b), the analytical data of Model B agreed well with the experimental results.

3. ESTIMATING THE ULTIMATE TEMPERATURE OF STEEL COLUMNS UNDER THE EFFECTS OF ELONGATING BEAMS

The following three methods were used to estimate the temperature at which steel columns collapse. The methods have been proposed for estimating ultimate temperatures. The relationships with this study and the importance of the methods are described below.

3.1 THEORETICAL BUCKLING TEMPERATURE T_B OF COLUMNS BY THE

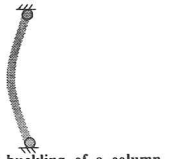

Fig-5 Overall buckling of a column with pin supports at the upper and lower ends

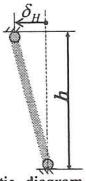

Fig-7 Schematic diagram of a column with local buckling at both upper and lower ends

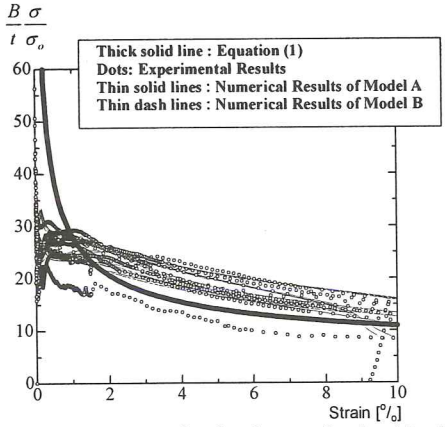

Fig-6 Residual strength of stub columns after local buckling

The Recommendation for Fire Resistant Design of Steel Structures by AIJ proposes equations for estimating the ultimate temperatures at which a steel column compressively collapses by local buckling (hereinafter referred to as the "AIJ equations"). The recommended equations estimate the residual strength σ of the steel column after local buckling by:

$$\frac{\sigma}{\sigma_o}=\left(\sqrt{\frac{6.35}{\varepsilon}}+3\right)\frac{t}{B} \qquad (1)$$

where, σ_o is the stress determined from the relationship between σ and ε in the tensile region. Equation (1) was proposed by Suzuki and Segawa et al. for estimating the residual strength of rectangular steel after local buckling [14]. They performed a number of compression tests of stub columns at high temperatures, extracted and analyzed the dynamic significance of behaviors during local buckling, and found that the equation (1) estimated by a lot of experimental results did not much depend on test temperature, the ratio of width to thickness, and material properties. The residual strengths of the steel columns after local buckling, which were calculated using Equation (1), are shown in Figure 6 together with the experimental and analytical results of the stub columns described in Section 2. The horizontal axis ε of both experimental and analytical results is differently evaluated before and after the ultimate strength. Before the ultimate strength, strain was assumed to be uniformly distributed throughout the specimens ($\Delta\varepsilon = \Delta\delta_V / H$, Δ denotes differences). After the ultimate strength, strain was assumed to concentrate at points of local buckling, which spread over the plate width B ($\Delta\varepsilon = \Delta\delta_V / B$) [8]. Figure 6 shows that all the experimental and analytical results converged into almost a single curve and Equation (1) for calculating residual strength after local buckling gives a curve that lies along the lower limit of the experimental and analytical values.

The AIJ equations assume that a strain ε_0 of 0.01 is generated along the edge on the tensile side of a column section where local buckling occurs and a strain ε_1 of 0.04 is generated along

TANGENT MODULUS THEORY

The temperature at which the steel column buckles during fire can be estimated from theoretical buckling temperature T_B using the tangent modulus theory [5,6]. To estimate T_B, the effective buckling length of the column at high temperatures should be determined. The Euro Code [13] recommends to use 0.5 as the effective buckling length coefficient γ of a steel column at high temperatures for columns when there are members of ordinary temperatures adjacent to both the upper and lower ends and to use 0.7 for columns on the top story. On the other hand, the Recommendation for Fire Resistant Design of Steel Structures by AIJ proposes to use 1.0 regardless of the boundary conditions of the column at both ends since elongation of adjacent beams may cause local buckling of the column at the upper and lower ends and loosen the rotational restriction of the column [6]. Assuming that the column loses bending strength at the points of local buckling but retains the capacity to sustain axial load, the said points can be assumed to be pin supports (Figure 5). In this case, the buckling length coefficient is 1.0. In this paper, the coefficient was decided to be γ = 1.0 by considering the possibility of local buckling.

3.2 ULTIMATE LOCAL BUCKLING TEMPERATURE T_{LB1} OF STEEL COLUMNS IN THE RECOMMENDATION FOR FIRE RESISTANT DESIGN OF STEEL STRUCTURES BY AIJ

the edge on the compression side. The strain distribution in a cross section is given by a line. The strain on the compression side of the section is increased by elongation of adjacent beams. The recommended equations assume a strain ε_1 of 0.04 for the edge on the compression side by considering the effects of the beams. Using Equation (1), the stresses in the section are integrated, and the temperature of the members at which the resultant value is equal to the axial compressive stress of the column, which is the external force, is determined. The temperature is the ultimate local buckling temperature of the column [6] and is hereinafter referred to as T_{LB1}.

3.3 ULTIMATE LOCAL BUCKLING TEMPERATURE T_{LB2} OF COLUMN UNDER EFFECTS OF ELONGATING ADJACENT BEAMS

Joint translation angles are formed on columns when adjacent beams elongate. Joint translation angles are larger in longer spans and at higher member temperatures. Excessive joint translation angles induce early local buckling and accelerate the deterioration of the column after buckling. The theoretical buckling temperature T_B and the ultimate local buckling temperature T_{LB1} of the AIJ equation are ultimate temperatures determined by the date on the only column and are independent of joint translation angles. Thus, when the joint translation angle is excessively large, the column may collapse at a temperature lower than the ultimate temperatures.

Suzuki and Nakayama et al. have proposed an equation for calculating the ultimate local buckling temperature of a column under the effects of elongating beams (hereinafter referred to as the "original Suzuki Equation") [7]. A schematic diagram of local buckling of a column by the elongation δ_H of an adjacent beam is shown in Figure 7. Local buckling was assumed to occur at the upper and lower ends of the column and to rotate like a hinge. The original Suzuki equation assumed local buckling only at the upper end of a column, but large δ_H may also cause local buckling at the lower end. Thus, a column was assumed to have two local buckling hinges. The equation for calculating the ultimate temperature by assuming two hinges is hereinafter referred to as the "modified Suzuki equation". The length of the hinge that becomes plastic was assumed to be equal to the buckling wavelength at the buckling points, and the wavelength was assumed to be equal to the sectional plate width B. The resultant difference between the strain ε_1 on the compression side and the strain ε_0 on the tensile side becomes equal to the hinge rotation θ:

$$e = \theta = \frac{\delta_H}{h} = \alpha T \frac{L}{h} \qquad (2)\ [7],$$

where, L is the total span length of the heated beam, α is the elongation coefficient of steel (= 12×10^{-6} 1/°C), h is the height of the column in the story, and T is the material temperature. Thus, the modified Suzuki equation for determining the strain ε'_1 on the compression side is:

$$\varepsilon'_1 = \varepsilon_o + e = \varepsilon_o + \alpha T \frac{L}{h} \qquad (3).$$

The strain ε_0 on the tensile side is given as 0.01 as in the recommended equation. The process of determining the ultimate temperature is the same as that used in the recommended equation. The ultimate local buckling temperature determined by the modified Suzuki Equation is referred to as T_{LB2}.

4. NUMERICAL ANALYSIS OF A COLUMN AFFECTED BY AN ELONGATING BEAM

4.1 MODEL USED FOR NUMERICAL ANALYSIS

The model used for numerically analyzing a column under the effect of an elongating beam is shown in Figure 8. The model is a part of the frame model formed by removing the exterior columns and beams of several spans from the model of the frame in the story where there is a fire (Figure 9). A uniform compressive force P was applied on the column, and the member temperatures T of the column and beam were raised uniformly. The boundary conditions at the lower end of the column were fixed. The heated beam in Figure 8 was assumed to be rigid at ordinary and high temperatures and to expand horizontally as the temperature rose for a length of δ_H. The effective buckling length coefficient γ was 0.5 (theoretical value for a column with

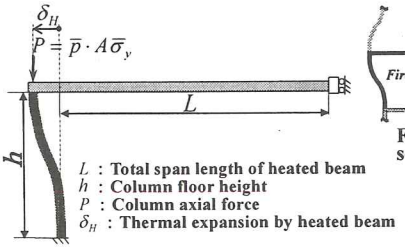

Fig-8 Numerical analysis model of a column affected by an elongating beam

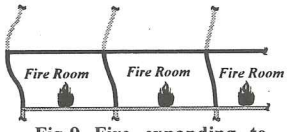

Fig-9 Fire expanding to several spans

Table-2 Parameters of Numerical analysis

$\bar{p}$	0.1、0.3、0.5
B/t	20 (□−500×500×25) 25 (□−500×500×20) 33 (□−500×500×15)
L/h	1～15

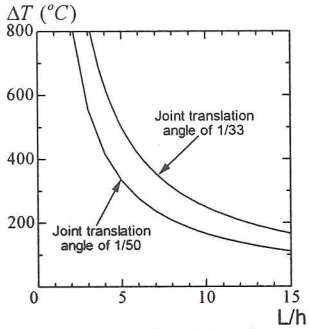

Fig-10 Relationship between L/h and ΔT

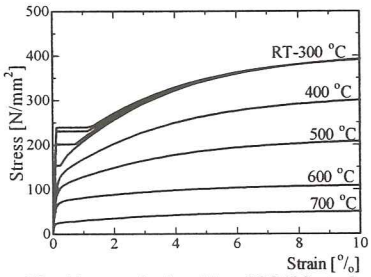

Fig-11 σ–ε relationship of SS400 steel

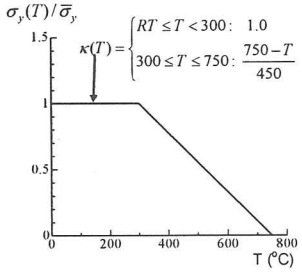

Fig-12 Reduction factor of SS400 Steel

both ends fixed) when no local buckling occurred. During an actual fire in a frame, the upper and lower ends of buckling columns on the story of the fire are believed to be strongly restricted by members on the other stories, which are at ordinary temperatures (Figure 9).

Parameters used for the numerical analysis are shown in Table 3. Three axial force ratios $\bar{p}$, three column width to thickness ratios B/t, and beam to column length ratios L/h ranging from 1 to 15 were used as the analytical parameters. The column height h was fixed to 4,500 mm, and L/h was varied by changing the span length of the heated beam. The width to thickness ratio was varied (B/t = 20, 25, and 33) by fixing the plate width B of the square cross section and changing the plate thickness t. B/t = 33 is the limit width to thickness ratio of square hollow steel columns (JIS SS400) of Class FA at ordinary temperatures [15]. Since the floor column height h and the sectional plate width B were set uniform and only plate thickness t was changed, the height to width ratio λ of the column was almost uniform in all analytical cases (λ = 0.25). Therefore, the three columns were similarly resistant against overall buckling. The analytical case with a large L/h value assumed a fire in a space with a long beam span and a fire spreading to a large space on a story by burning partition walls (Figure 9). The relationships between L/h and temperature rises ΔT are shown in Figure 10. The figure shows that, for example, for L/h = 15, a temperature rise of about 110°C causes a joint translation angle $\Delta\delta_H/h$ of 1/50.

The steel was assumed to be JIS SS400. Its σ–ε relationships at high temperatures are shown in Figure 11. These are the σ–ε relationships proposed by the Recommendation for Fire Resistant Design of Steel Structures. At each temperature, the 1% stress σ_y corresponds to $\kappa(T)\bar{\sigma}_y$ (Figure 12). $\bar{\sigma}_y$ is the standard yield strength of steel at ordinary temperature. The analysis considered no effects from the creep of steel at high temperatures to examine the validity and feasibility of the method for estimating the ultimate temperature described in the previous section. In the evaluation method, the effects of creep should be investigated separately or the effective yield strength of steel at high temperature should be reduced when the effect is considered (Figure 12). Thus, the effects of creep of steel columns at high temperature are not discussed in this paper but will be separately reported. The aforementioned three-dimensional plate elements were used as the finite element model, which was a square hollow section consisting of four steel plates. Each plate was divided into elements using the methods described in Section 2 for dividing Model B of a stub column specimen into elements. In the column model shown in Figure 8, the plates were divided into 10 and 30

elements of equal sizes along the sectional and axial directions, respectively. The total number of elements was 1,200. Actual loading models should have been different between the beam-column model shown in Figure 8 and the stub column model shown in Figure 2, the former of which should have been more complicated that the latter. Although the analysis was a pure compression analysis, the minute elements of the plates after local buckling were under very complicated stress conditions and showed three-dimensional non-linear behaviors of in-plane and out-of-plane deformation. The numerical analysis of Model B of the stub column precisely reproduced the complicated non-linear behaviors of plates. Therefore, the element division method used for Model B was used for the column model shown in Figure 8. The numerical analysis case of B/t = 25, $\overline{p}$ = 0.3, and L/h, which is discussed in the following section, was analyzed using the element division method used for Model A in Figure 2. The analysis results in an ultimate temperature difference of only 2°C from the result of an analysis conducted using the element division method of Model B.

4.2 RESULTS OF THE NUMERICAL ANALYSIS OF A COLUMN AFFECTED BY AN ELONGATING BEAM

The results of the numerical analysis of all parametric study cases are shown in Figures 13 to 15. Figures 13, 14, and 15 show the results of B/t = 20, 25, and 33, respectively. The X axis of the figures is the beam to column length ratio L/h, and the Y axis is material temperature T. The dark dots in the figures are the collapse temperatures of the column given by numerical analysis of three-dimensional plate elements (hereinafter referred to as the "numerical ultimate temperature"). For analytical cases in which local buckling occurred in the process of heating, the member temperatures at which the local buckling occurred are shown with double circles. Local buckling temperatures are the member temperatures when out-of-plane buckling waveforms were produced in a plate at the upper or lower end of the column. The numerical ultimate temperatures determined by using a two-dimensional non-linear beam element model as a finite element model are also shown with open triangles in Figures 13 to 15. The same partial frame model (Figure 8) was used for the numerical analysis using the beam element model to the calculated ultimate temperature. The same analytical parameters (Table 3) and σ–ε relationships (Figure 11) were also used. The beam element model is not for analyzing the local buckling behaviors and considers no drop in strength by local buckling. Thus, the collapse mode was overall buckling of the columns for all cases. Figures 13 to 15 also show theoretical ultimate temperatures of various kinds. The ultimate local buckling temperature T_{LB2} determined by the modified Suzuki equation is shown as a solid line. The ultimate local buckling temperature T_{LB1} determined by the AIJ equation is shown as a dashed line. The theoretical buckling temperature T_B for an effective buckling length coefficient γ of 1.0 is shown as a dotted line. The trends shown by the series of parametric numerical analyses and comparisons with the theoretical ultimate temperatures are discussed in the following section.

[1] First, an analytical case of a column affected by an elongating beam is described. The analytical results of B/t = 25 and $\overline{p}$ = 0.3 are shown in Figure 16(a) and 16(b). Figure 16(a) is for L/h=1, and Figure 16(b) is for L/h = 15, both of which show the deformation when the columns collapsed. The elongation δ_H of the beam at the upper end of the column is produced along the +y direction in the figure. The temperature history of vertical displacement (displacement along the x direction in Figure 16) of the column head calculated from the two analyses is shown in Figure 17. Figure 17 shows upward extension of the column of L/h = 1 by itself thermal expansions. On the other hand, the column of L/h = 15 shows a drop in vertical displacement at the column head as the temperature rose since the settlement of the head by inclination was larger than the extension of the column. On the column of L/h = 15, local buckling occurred at the plates on the compression side at the upper and lower ends of

[Legends for Figures 13 to 15]

● : Numerical ultimate temperatures(using three-dimensional plate elements)

◎: Numerical local buckling temperatures(using three-dimensional plate elements)

△: Numerical ultimate temperatures(using two-dimensional beam elements)

Solid lines: T_{LB2}

Dash lines: T_{LB1}

Dotted line: T_B

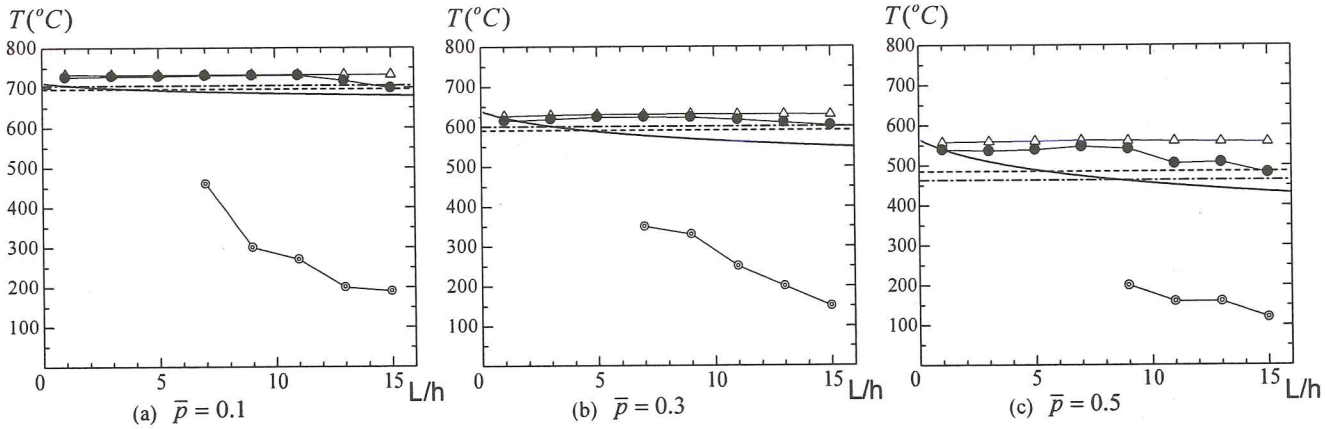

(a) $\overline{p} = 0.1$ (b) $\overline{p} = 0.3$ (c) $\overline{p} = 0.5$

Fig-13 Numerical Results [B/t=20]

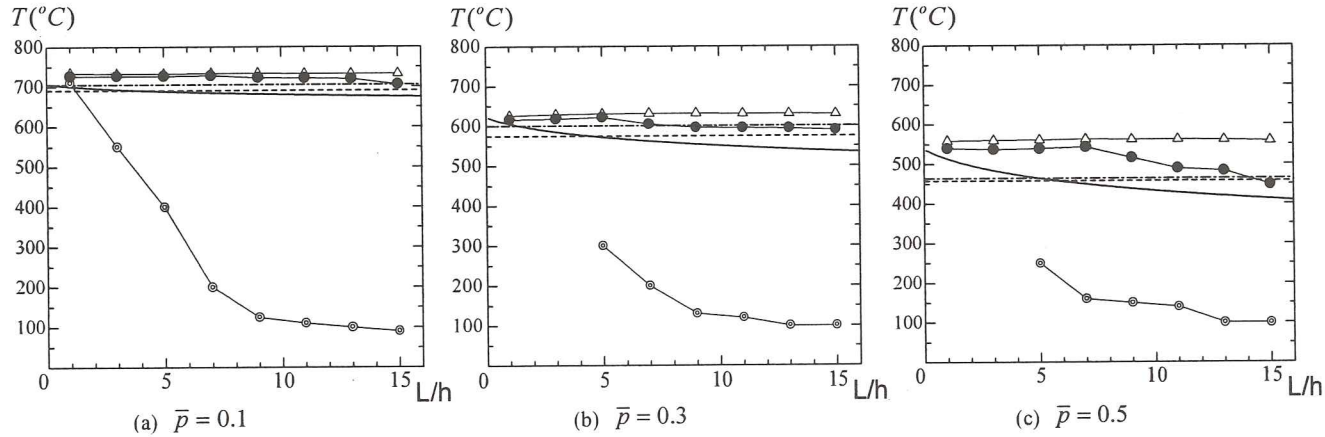

(a) $\overline{p} = 0.1$ (b) $\overline{p} = 0.3$ (c) $\overline{p} = 0.5$

Fig-14 Numerical Results [B/t=25]

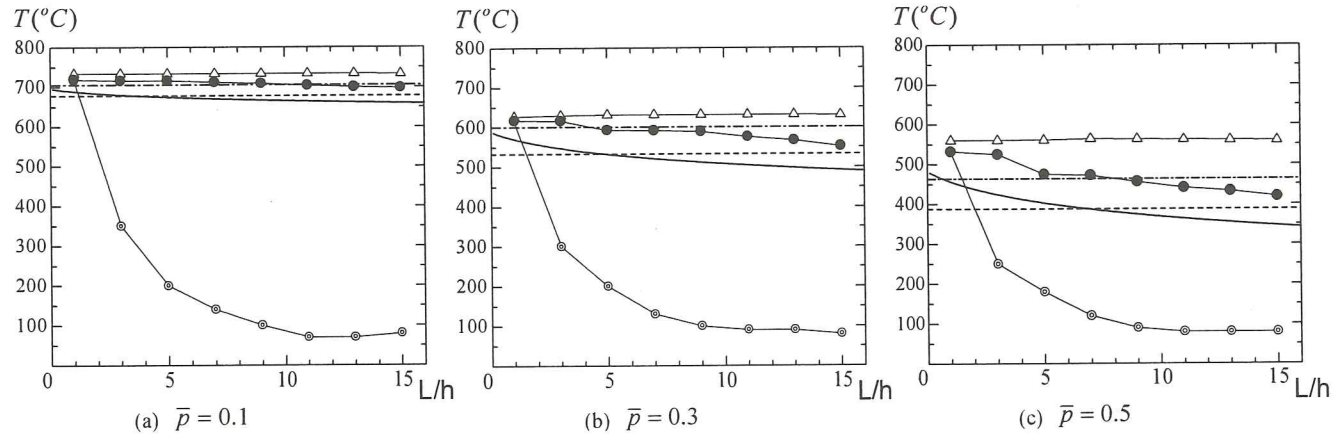

(a) $\overline{p} = 0.1$ (b) $\overline{p} = 0.3$ (c) $\overline{p} = 0.5$

Fig-15 Numerical Results [B/t=33]

the column at a member temperature of about 100°C. The column could sustain the fixed axial force P even after the local buckling, and the member temperature rose further. In both analyses, immediately before the collapse of the columns, the column head suddenly sank, and

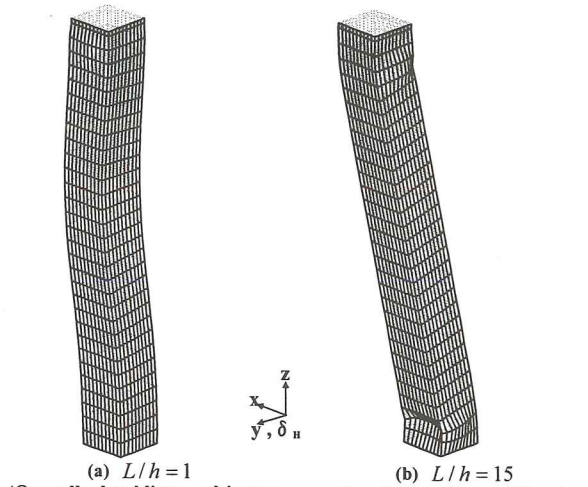

(a) $L/h=1$
(Overall buckling, ultimate temperature: 616°C)
Magnification of deformation: 5

(b) $L/h=15$
(local buckling, ultimate temperature: 616°C)
Magnification of deformation: 2

Fig-16 Deformation of a column at collapse (analytical result for $B/t=25$, $\bar{p}=0.3$)

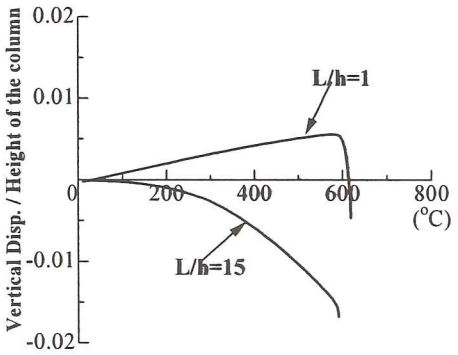

Fig-17 Displacement of column head along the material axis ($B/t=25$, $\bar{p}=0.3$)

the columns became unable to sustain the axial force and collapsed. This member temperature was the ultimate temperature of the column, and is the limit member temperature at which the column can keep the equilibrium of forces. The ultimate temperature of the column of L/h = 1 was 616°C, and that of the column of L/h = 15 was 590°C. In Figure 17, the ultimate temperature is around the member temperature at which the column head showed a sudden vertical displacement. The mode of collapse was overall buckling in the column of L/h = 1 (Figure 16(a)) and was compressive collapse at the points of local buckling in the column of L/h = 15 (Figure 16(b)). As Figure 17 shows, the entire column of L/h = 1 suffered buckling deformation and showed jumps in the settlement of the head near the ultimate temperature. On the other hand, in the column of L/h = 15, local buckling waveforms concentrated at the upper and lower ends of the column, and the settlement of the head at around the ultimate temperature was smaller than that of L/h = 1. Figure 16 shows a bow-shaped buckling deformation of the column of L/h = 1 and local buckling deformation of the column of L/h = 15. The parametric study of the analytical cases showed that the mode of collapse of columns in which local buckling occurred during the process of heating was compressive collapse by local buckling and that of columns in which no local buckling occurred was overall buckling.

[2] Figures 13 to 15 showed that local buckling occurred during the process of heating in many cases analyzed (○). The temperature at which local buckling occurred was lower in cases of longer beam elongation, i.e. with larger beam to column ratio L/h. Especially, when both L/h and the width to thickness ratio B/t were large, local buckling occurred at temperatures below 100°C (Figure 15). However, the local buckling did not cause the column to collapse immediately. The steel column kept stable residual strength even after it suffered local buckling (Figure 6) up to high temperatures. As the temperature rose, the joint translation angle gradually increased and accelerated the strain at the points of local buckling on the compression side, and the column ultimately collapsed by compressive fracture at the points of local buckling. The numerical analysis showed that the ultimate temperatures of columns (●) gradually dropped as L/h and B/t increased. The relationship between the column axial force ratio $\bar{p}$ and calculated ultimate temperature showed lower calculated ultimate temperatures for larger column axial force ratios $\bar{p}$. The case in which the ultimate temperature of a column (●) was almost the temperature at which local buckling occurred (◎) (for example, when $\bar{p}$ = 0.1 and L/h = 1) was when local buckling occurred at the upper end of the column when the column suffered overall buckling deformation.

[3] Ultimate temperature values estimated using two-dimensional beam element models (Δ) and

three-dimensional plate element models (●) were more different for columns of larger beam to column ratio L/h and larger width to thickness ratio B/t. The difference was likely attributable mainly to the occurrence of local buckling. Columns with small L/h and B/t were estimated to collapse by overall buckling in both analyses. On the other hand, columns with large L/h and B/t values were estimated to collapse by local buckling when analyzed using three-dimensional plate models. Figure 15(c) shows that the difference in estimated ultimate temperature was as large as about 130°C for the column of B/t = 33.

[4] When the column axial force ratio $\overline{p}$, the width to thickness ratio B/t and the joint translation angle (= L/h) increased, the column was exposed to larger loads and several structural conditions, and both the temperature at which local buckling occurred and ultimate temperature lowered. However, the increases in L/h caused sharp drops in the temperature at which local buckling occurred (◎), and the drop in the numerical ultimate temperature (●) was small. For example, an analysis of a steel column with small B/t and $\overline{p}$, which is widely used in actual frames, is shown in Figures 13(b) and 14(b), revealing that local buckling occurred when the heated span was long (◎) but the ultimate temperature (●) changed little even at large L/h. Columns of small width to thickness ratios (B/t) showed small drops in strength after local buckling, resulting in small drops in ultimate temperature. This trend was also estimated from Equation (1), which gives the residual strength of a steel column after local buckling. Equation (1), which is shown with a thick line Figure 6, shows that compressive strain ε in the section of a column increased largely by an elongating beam but the corresponding drops in residual strength were small at large ε values. Thus, the ultimate temperature of a column is likely to be a stable index of fire resistance, which is little affected by elongation of beams during fire.

[5] The theoretical ultimate temperatures (T_B, T_{LB1} and T_{LB2}) of a column were investigated. The ultimate local buckling temperature T_{LB1} of steel columns in the Recommendation for Fire Resistant Design of Steel Structures (dashed line) and the theoretical buckling temperature T_B (dotted line) were constant regardless of the beam to column ratio (L/h). On the other hand, the ultimate local buckling temperature determined by the modified Suzuki Equation T_{LB2} (solid line) gradually dropped as L/h increased. The three temperatures were similar in columns with small width to thickness ratios B/t, but differed in columns with large B/t values. The reductions were large in the ultimate local buckling temperature in the Recommendation (T_{LB1}) and in the ultimate local buckling temperature determined by the modified Suzuki equation T_{LB2} (Figure 15). In columns of small L/h values, the temperature of the modified Suzuki Equation T_{LB2} (solid line) was higher than the temperature in the Recommendation T_{LB1} (dashed line); and the relationship was the opposite in columns of large L/h values. In the ultimate temperature estimation method, the range in which T_{LB2} (solid line) is lower than T_{LB1} (dashed line) is when $\varepsilon'_1 > \varepsilon_1$ (= 0.04) (Equation (3)). From Equation (2), this means that a joint transition angle δ_H/h of at least 0.03 is generated in the column. From Figures 13(a) to 15(a), most columns of $\overline{p}$ = 0.1 were within this range, but their ultimate temperatures were high because their original axial forces were small.

[6] When the numerical ultimate temperatures (●) of the columns were compared with their theoretical ultimate temperatures T_B (dotted line), the former was larger than the latter in columns of small L/h values. As described in Section 3.1, the coefficient of effective buckling length γ was assumed to be 1.0 for estimating the theoretical temperature T_B by considering the occurrence of local buckling. However, columns with small L/h values showed no local buckling, and thus their coefficients of effective buckling length should have been smaller than 1.0. The difference caused the calculated temperature to be larger than the theoretical temperature. On the other hand, columns of large L/h values suffered local buckling at their upper and lower ends, loosening the bending constraints at the ends. Columns of even larger

L/h values showed larger drops in strength by local buckling, resulting in calculated ultimate temperatures lower than their theoretical ultimate temperatures T_B. Figures 13 to 15 show that most calculated ultimate temperature values were higher than the ultimate local buckling temperatures T_{LB1} and T_{LB2} (solid and dashed lines). The Recommendation for Fire Resistant Design of Steel Structures assesses the fire resistance of columns after local buckling by making some assumptions, and estimates the ultimate temperatures on the safe side for a number of actually used steel columns.

5. SUMMARY

When beams are heated during fire, the beams elongate and push adjacent columns. The longer the span of the heated beam, the larger the elongation of the beam, and the more vulnerable the adjacent hot columns to local buckling. However, local buckling does not cause the steel column to collapse immediately, but the column keeps stable residual strength after the occurrence of local buckling, making the column advantageous in terms of fire resistance. The temperature at which local buckling occurs is strongly affected by the joint translation angle of the column (= elongation of adjacent beams), and assessing the fire resistance of the column at the temperature may result in underestimation of the load bearing capacity of the column. On the other hand, the ultimate temperatures of columns, which were the upper member temperature at which a column could keep equilibrium of forces, did not much depend on the size of joint translation angles under most structural and loading conditions analyzed and were much higher than the temperatures at which the columns suffered local buckling. This trend was especially clear in columns that consisted of thick plates and received small compressive forces along the action axis, which are widely used at seismic designs of Japanese steel buildings, and the columns showed no large drops in ultimate temperature even with large joint translation angles. Methods proposed for estimating the ultimate temperatures of columns were verified by conducting parametric numerical analyses, and were verified to be reliable.

This study investigated square hollow steel columns of the FA class in structural classification by Japanese seismic codes. Columns of larger width to thickness ratios, such as those of FB class, may show larger drops in strength after local buckling and thus larger drops in ultimate temperature than in columns of FA class, and thus the safety should be thoroughly examined. Excessive elongation of beams during fire may also threaten fire compartment room. Therefore, comprehensive studies on these topics, investigation of local buckling behaviors during fire, and high-temperature experiments of members need to be conducted.

6. ACKNOWLEDGMENTS

The author thanks Associate Professor Takeo Hirashima of Chiba University for providing valuable experimental data of short square hollow steel columns at high temperatures. The calculation codes of the finite element models used in the numerical analyses were prepared when the author was working in the Institute of Structural Engineering, Swiss Federal Institute of Technology Zurich (ETH Zurich), and the author thanks Professor Mario Fontana of the Institute for precious advice. This study was conducted as a part of a COE study project of the Tokyo University of Science entitled "Center for Advanced Fire Safety Science and Technology For Buildings (representative: Takao Wakamatsu) and was also partly supported by a grant-in-aid program of the Japan Society for the Promotion of Science entitled "Progressive study on destabilization of steel columns during fire and their collapse at high temperatures (representative: Fuminori Ozaki, project number: 18860069)".

7. REFERENCES

1) Suzuki, H.: ULTIMATE TEMPERATURES OF STEEL FRAMES SUBJECTED TO FIRE, J. of Structural and Construction Eng. Transactions of AIJ, Vol. 477, 1995 (in Japanese).
2) Okabe, T.: BUCKLING STRENGTH OF STEEL COLUMN MODELS(SM490) WITH

RECTANGULAR CROSS-SECTION AT HIGH TEMPERATURE, J. of Structural and Construction Eng. Transactions of AIJ, Vol. 515, 1999 (in Japanese).
3) Okabe, T. and Abe, T.: BUCKLING STRENGTH OF STEEL COLUMNS USING STRUCTURAL STEEL (SN490B) AT HIGH TEMPERATURE, J. of Structural and Construction Eng. Transactions of AIJ, Vol. 585, 2004(in Japanese).
4) Okabe, T. and Abe, T.: COLLAPSE BEHAVIOR OF STEEL COLUMNS SUBJECTED TO INDUCED JOINT TRANSLATION ANGLE AND CONSTANT AXIAL LOAD AT HIGH TEMPERATURE, J. of Structural and Construction Eng. Transactions of AIJ, Vol. 587, 2005 (in Japanese).
5) Suzuki, H., Nara R. and H. Fujita: STABILITIES OF STEEL FRAMES SUBJECTED TO FIRE, J. of Structural and Construction Eng. Transactions of AIJ, Vol. 571, 2003(in Japanese).
6) Architectural Institute of Japan: Recommendation for Fire Resistant Design of Steel Structures 1999 (in Japanese).
7) Nakayama, H. and Suzuki H. et al.: Ultimate Temperature of Steel Frames Subject to Fire Part.11, Summaries of Technical Papers of Annual Meeting(Fire Safety), AIJ, 1995 (in Japanese).
8) Hirashima T. et al.: A STUDY ON STRENGTH-DEFORMATION CAPACITY OF STEEL MEMBERS AT ELEVATED TEMPERATURE, J. of Structural Eng., Vol. 46B, 2000, (In Japanese).
9) OZAKI F., NIEDEREGGER P., KNOBLOCH M. and FONTANA M.: STUDIES ON LOCAL BUCKLING OF HEATED STEEL COLUMNS WITH BOX SECTIONS BY USING FINITE ELEMENT ANALYSES, Proceedings of 4th International Workshop Structure in Fire,2006
10) Zienkiewicz O.C. and Taylor R.L.: The Finite Element Method, Butterworth Heinemann, 2000.
11) Hill R.: The Mathematical Theory of Plasticity, Clarenden Press, Oxford, 1950.
12) Nakagawa, H. et al.: Ultimate Temperature of Steel Frames Subject to Fire Part.13, Summaries of Technical Papers of Annual Meeting(Fire Safety), AIJ, 1995(in Japanese).
13) European Committee for Standardisation : prEN 1993-1-2:2003 (Eurocode3 Design of steel structures, Part1.2 : General rules, Structural fire design), 2003
14) Segawa, T. and Suzuki H. et al.: Ultimate Temperature of Steel Frames Subject to Fire Part.13, Summaries of Technical Papers of Annual Meeting(Fire Safety), AIJ, 1992(in Japanese).
15) Architectural Institute of Japan: Recommendation for Stability Design of Steel Structure Second Edition, 2000 (in Japanese)

Recent Advances in Fire-Structure Analysis

By

Dat Duthinh[1], Kevin McGrattan[1], and Abed Khaskia[2]

ABSTRACT

One of the recommendations of the National Construction Safety Team for the Federal Building and Fire Safety Investigation of the World Trade Center Disaster (NIST NCSTAR 1, 2005) is to enhance the capability of available computational software to predict the effects of fires in buildings, for use in the design of fire protection systems and the analysis of building response to fires. This paper presents two new interfaces in fire-thermal-structural analysis. The first interface uses adiabatic surface temperatures to provide an efficient way of transferring thermal results from a fire simulation to a thermal analysis. It assigns these temperatures to surface elements of structural members based on proximity and directionality. The second interface allows the transfer of temperature results from a thermal analysis modeled with solid elements to a structural analysis modeled with beams and shells. The interface also allows the reverse, namely the geometric updating of the thermal model with deflections and strains obtained from the structural analysis. This last step is particularly useful in intense fires of long duration, where significant deflections and strains could cause damage to insulation and displace the structure to a different thermal regime. The procedures can be used for a variety of fire simulation, thermal and structural analysis software.

KEYWORDS: Adiabatic surface temperature; finite elements; fire; insulation; plate thermometer; strains; structural analysis; thermal analysis.

1.0 INTRODUCTION

Following the investigation of the collapse of the World Trade Center, the National Construction Safety Team (NCST) recommended, among other things, that efforts be made to enhance the capabilities of computational methods to study the effect of realistic fires on buildings, all the way to the burn-out and cooling phases, or to collapse. The recommendation was partially attributable to the difficulties experienced by the investigators in interfacing the fire, thermal, and structural models that were used to study various collapse hypotheses. This paper describes two recent advances in interface development; the first facilitates the exchange of information between a computational fluid dynamics fire model and a finite-element thermal model; the second transfers information both ways between the thermal model and a structural model. The goal of developing these tools, verified by experiments, is to assist the engineering community and the standards organizations in taking fire into account as a potential structural load.

2.0 ASTM E 119 STANDARD FIRE TEST

In the United States, the design of fire resistance in buildings has been traditionally achieved by prescriptive means. For this purpose individual structural members are subjected to standard time-temperature curves, e.g., ASTM E 119 (2007), and coated with sufficient insulation as the case may be, to prevent them from reaching a certain temperature deemed detrimental to their performance. While this approach is simple and has worked well, as

[1] National Institute of Standards and Technology (NIST), Building and Fire Research Laboratory (BFRL), 100 Bureau Drive, Gaithersburg, MD 20899 USA

[2] Mallett Technology, Laurel, MD 20707 USA

shown by the rarity of structural collapse due to fire of engineered structures designed according to current building and fire codes, it offers no guidance on the actual behavior and the margin of safety of a structure in fire. The main problem, of course, is that a prescriptive time-temperature curve does not reflect the actual temperature of various structural members exposed to a realistic fire that varies in time and space. To compound the difficulty, actual structures have many redundancies, and the increase in structural demand due to thermal expansion coupled with material softening due to heating may not necessarily lead to imminent collapse if alternate load paths still exist. These problems point to the need to treat fire as a realistic structural load.

3.0 FIRE-THERMAL INTERFACE

In a sense, the time-temperature curve such as ASTM E 119 *is* the fire model. The fire-structural *interface* is thus nothing more than the specification of the bounding gas temperature at all solid surfaces. However, in a performance-based design environment, it should be possible to model potential fire scenarios and pass spatially and temporally resolved temperatures to the structural model. This will involve much more information than just a single time-temperature curve, requiring some form of interface for data transfer.

A proposed interface makes use of the adiabatic surface temperature (AST), an output of the fire model, to serve as the boundary condition for the thermal model. Adiabatic surface temperatures are the virtual equivalent of temperatures measured by plate thermometers placed in the vicinity of the surfaces of interest. This concept was first proposed by Wickstrom (1994) as a means of better controlling the temperature of furnaces in fire tests. The plate thermometer is a thin metallic plate with insulated backing on the face opposite the surface of interest. It responds with negligible time lag to radiative and convective heat fluxes from the furnace, and thanks to its geometry, in the same proportion as what the surface of interest sees. Heat transfer to the plate thermometer is described by:

$$\varepsilon_{pt}(q_{inc} - \sigma T_{pt}^4) + h_{pt}(T_g - T_{pt}) = 0$$

where q_{inc} = incident radiative heat flux, h = convective heat transfer coefficient, T_g = gas temperature, ε = emissivity (assumed equal to absorptivity), σ = Stefan-Boltzman constant, and subscript *pt* refers to plate thermometer. The net heat transfer to a surface can be approximated as:

$$q \approx \varepsilon_s \sigma (T_{pt}^4 - T_s^4) + h_s (T_{pt} - T_s)$$

where subscript *s* refers to the surface. This is approximately equal to the more exact heat transferred from a fire to the surface:

$$q = \varepsilon_s \sigma (T_f^4 - T_s^4) + h_s (T_f - T_s)$$

where subscript *f* refers to the fire. For this interface, the fire analyst calculates the time history of the AST, or what a perfect plate thermometer in the vicinity of the structural member would measure, at nodes defined by spatial coordinates and orientation. In doing so, he provides the thermal analyst the required input for heat transfer analysis (Wickstrom, 2005) in a convenient form, thus eliminating the need for a radiation analysis that accounts for the presence of all radiating structural members and fire at various locations in the compartment.

The interface allows for two independent fire and thermal models, whose geometries may not coincide perfectly. This is a useful feature since the spatial resolution of fire models is typically coarser than that of thermal models. The only condition is that the AST nodes must not be contained within a solid material. For example, for a hollow tube, AST nodes that radiate to the outside surface of the tube must be outside, and AST nodes that radiate to the inside of the tube must be inside. Any AST

nodes contained within the thickness of the tube walls are deemed to be erroneous and are not read. Since the idea is to simulate plate thermometers near the surface, the interface searches for the closest AST node in the half-space facing the surface element, within a distance defined by the user. When it finds one, it checks for orientation by ensuring that the dot product of the orientation vector associated with the AST node and the vector normal to the surface element is positive. If that is not the case, the interface expands its search to the next closest AST node. This directional check only becomes relevant when the discrepancy in geometry between the fire and the thermal models is rather large, e.g., when web members of a truss are modeled as vertical planes in the fire model, whereas they are faithfully modeled as inclined round bars in the thermal model. To resolve other possible ambiguities in assigning the correct AST nodes, e.g., in the case of two parallel adjacent trusses placed closely next to each other, the interface also allows the user to intervene and manually select a set of relevant AST nodes and/or shift the entire thermal model to better center it with the AST nodes.

3.1 Comparison with experiments

Experimental verification involves a compartment fire performed at NIST (NCSTAR 1, 2005). Figs. 1 and 2 show the actual fire and the simulation model. Figs. 3 and 4 show the AST nodes used in the thermal analysis of the column and one of the trusses (A) and Figs. 5 and 6 compare temperatures measured and calculated with two different software codes. The calculations use the same insulation thickness and properties as in the experiments. Satisfactory agreement is achieved for the column, whose simple geometry allows close matching of AST nodes with their corresponding surfaces. As expected, for the web members of the truss, agreement between measurements and calculations is less close due to differences in model geometries mentioned previously.

4.0 THERMAL-STRUCTURAL INTERFACE

The second interface discussed in this paper is that between the thermal and the structural models. In the case of one of the software codes used in the WTC investigation, for example, the transfer of temperatures from a thermal model to a structural model, or the transfer of deflections and strains from a structural model to a thermal model (this latter step was not done in the investigation) can only be performed with compatible elements, e.g., solid to solid or shell to shell. These types of elements are prevalent in thermal analyses, and are often used in structural analysis as well, especially in smaller structures where a manageable number of solid or shell elements may suffice. For larger, more complex structures, such as the WTC towers, the use of beam elements to model the columns, floor and hat trusses is desirable to keep the structural model to a reasonable size. A procedure for efficient, general and automatic transfer of results between thermal and structural analyses is therefore needed. Temperature results would be transferred from the thermal to the structural analysis, so the effects of thermal expansion and evolution of material properties with temperature can be determined over time; conversely, structural deflections and strains would be transferred back to the thermal model. This last step is especially important in the case of intense fires of long duration, where significant structural deflections and strains may cause local damage to the insulation and move the structure to a different thermal regime. Furthermore, structural deflections may lead to changes in boundary conditions, such as new openings, that may affect the fire. This feedback would affect not just the thermal analysis, but the fire analysis as well. This last aspect is, however, beyond the scope of this paper. The interface requires that the thermal and structural models be geometrically compatible, within the tolerances specified by the finite-element program (default) or the user, and use compatible coordinate systems.

4.1 Temperature transfer

In the thermal model, the temperature field is interpolated between corner nodes, linearly or quadratically depending on the finite elements. For shell elements in the structural model, temperatures are input as element body loads at the corners of the outside faces of the element and at the corners of the interfaces between layers, where, for the purpose of temperature transfer, additional transfer nodes are created. The structural model nodes at the outside faces and the transfer nodes between layers are then mapped onto the thermal model, and temperatures at these locations interpolated from the temperatures at the nodes of the thermal model.

For beam elements in the structural model, at each end node of the beams, temperatures are input as element body loads in the form of a mean temperature and two temperature gradients in the element Y and Z directions (X is the longitudinal beam direction). The actual input at each beam end takes the form of three temperatures at (x, 0, 0), (x, 1, 0) and (x, 0, 1), where x is either 0 or L (length of beam element). The location of the temperature transfer nodes depends on the cross section. A number of commonly used cross sections, either singly or doubly symmetric, are supported by the newly developed interface macros (Fig. 7). If later or different versions of the software transfer temperatures directly to beams at specific points, rather than through a mean and two gradients, the present interface would still work with minor adaptation.

4.2 Deflection transfer

Solid element nodes from the thermal model are first mapped onto the undeformed structural model. Displacements $\boldsymbol{u}'$ at the mapped nodes are calculated from structural displacements $\boldsymbol{u}$ and rotations $\boldsymbol{r}$ from the nearest beam or shell nodes by the kinematic vector equation (in bold), where $\boldsymbol{d}$ is the distance between the mapped node and the undeformed nearest structural node: $\boldsymbol{u}' = \boldsymbol{u} + \boldsymbol{r} \times \boldsymbol{d}$, where $\times$ denotes the vector cross-product.

4.3 Strain transfer

Since strain transfer is done solely for the purpose of determining insulation damage, it is not available at this stage for shells, which are typically used to model uninsulated slabs. For structural beams, strain results are available at both beam ends at the corner nodes of cross sectional cells created automatically by the structural software for various common sections. The strains ε_{xx} (X is the beam longitudinal axis) at various nodes on these section perimeters are mapped onto the thermal model and used to calculate by interpolation the strains at any nodes of the interface between steel and insulation. The interpolation is linear over three dimensions, and uses the thermal solid element shape functions. Currently, the user can input a failure criterion, such as the tensile strain at the interface between steel and insulation exceeding 5 %. When the criterion is reached for a given finite element, the insulation is assumed to fail and its thermal properties degraded over its entire thickness. This criterion may be refined as experimental data become available.

4.4 User-defined, multi-material beam section

For the cases where the mechanical properties of the insulation are known to the level that they can be incorporated into the structural analysis, the thermal-structural interface makes available a cross section whose geometry and mesh can be defined by the user, who may assign different materials (e.g., steel or insulation) to various cells. Cross-section cells are used for thermal body load calculations by area averaging, and the user controls the accuracy by defining the number and distribution of cells. The user also defines the insulation failure criteria and intervenes to degrade the insulation elements that have failed before updating the thermal analysis. The geometry of the user-defined section is currently limited to a quadrilateral.

4.5 Test case

As an example, a floor slab supported by an open web truss is tested. The truss is made of three different sections modeled with beam elements, and the floor slab is modeled with three-layered shell elements. The thermal model uses solid elements and, in addition, link elements to tie together the various members at the corners for thermal conduction. Insulation is present in the thermal model, but not in the structural model. A thermal flux of 10 kW/m^2 is applied to the bottom surface of the insulated lower chord and concrete slab, except where it is in contact with the top chord, while a lower flux of 5 kW/m^2 is applied to the other surfaces, except the top of the slab, where a convection boundary with a film coefficient of 25 W/(m^2• °C) applies.

Fig. 8 shows the temperature contours for steel and concrete from the thermal model at 1800 s. The temperature transfer macro is invoked after the thermal analysis is completed. Fig. 9 shows the temperature body loads as transferred by the macro for the full model and the slab. Differences in the temperature contours between the thermal and the structural models are due to the different mesh densities. In addition to the thermal body loads, the truss dead weight is activated along with symmetrical boundary conditions along the long edges of the concrete slab and simple supports where the truss meets the slab ends. Large deflection solution of the model results in deflections shown in Fig. 10. The deflection transfer macro is invoked and results in an updated thermal model. Fig. 11 shows the deflected thermal model, detection and removal of failed insulation based on strains ε_{xx} at 1800 s and insulation failure criterion $\varepsilon_{xx} > 5$ % at the interface with steel. The continuity of temperatures, deflections and strains appears satisfactory. Further verification of the software code against theoretical and experimental results is in progress and will be reported in a forthcoming publication.

5.0 CONCLUSIONS

This paper presents two user-friendly interfaces that complement existing fire-thermal-structural analysis software. The first interface uses adiabatic surface temperatures to provide an efficient way of transferring thermal results from a fire simulation to a thermal analysis. It assigns these temperatures to surface elements of structural members based on proximity and directionality. The second interface allows the transfer of temperature results from a thermal analysis modeled with solid elements to a structural analysis modeled with beams and shells. The interface also allows the reverse, namely the geometric updating of the thermal model with deflections and strains obtained from the structural analysis. This last step is particularly useful in intense fires of long duration, where significant deflections and strains could cause damage to insulation and displace the structure to a different thermal regime. The procedures can be used in a variety of fire simulation, thermal and structural analysis software.

6.0 REFERENCES

ASTM (2007): "E 119-07: Standard test methods for fire tests of building construction and materials," American Society for Testing and Materials International, W. Conshohocken, PA

NIST NCSTAR 1 (2005), "Final Report on the Collapse of the World Trade Center Towers," National Institute of Standards and Technology, Gaithersburg, MD, September

Wickstrom, U. (1994): "The plate thermometer- a simple instrument for reaching harmonized fire resistance tests," Fire Technology **30**, 2, May, pp. 195-208

Wickstrom, U. (2005): "Heat transfer calculations in fire safety engineering," Proposal to SPFE Standards Committee on Calculating Fire Exposure to Structures, June

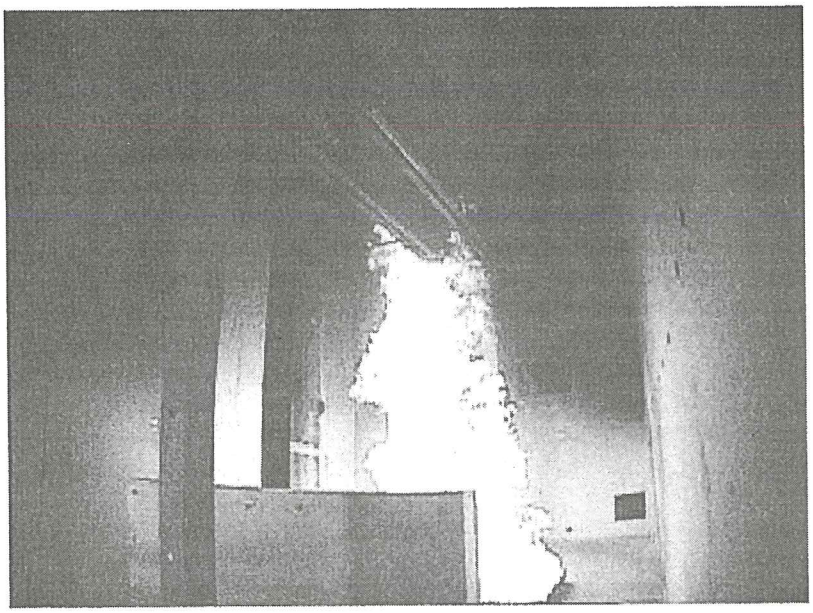

Fig. 1 Fire experiment

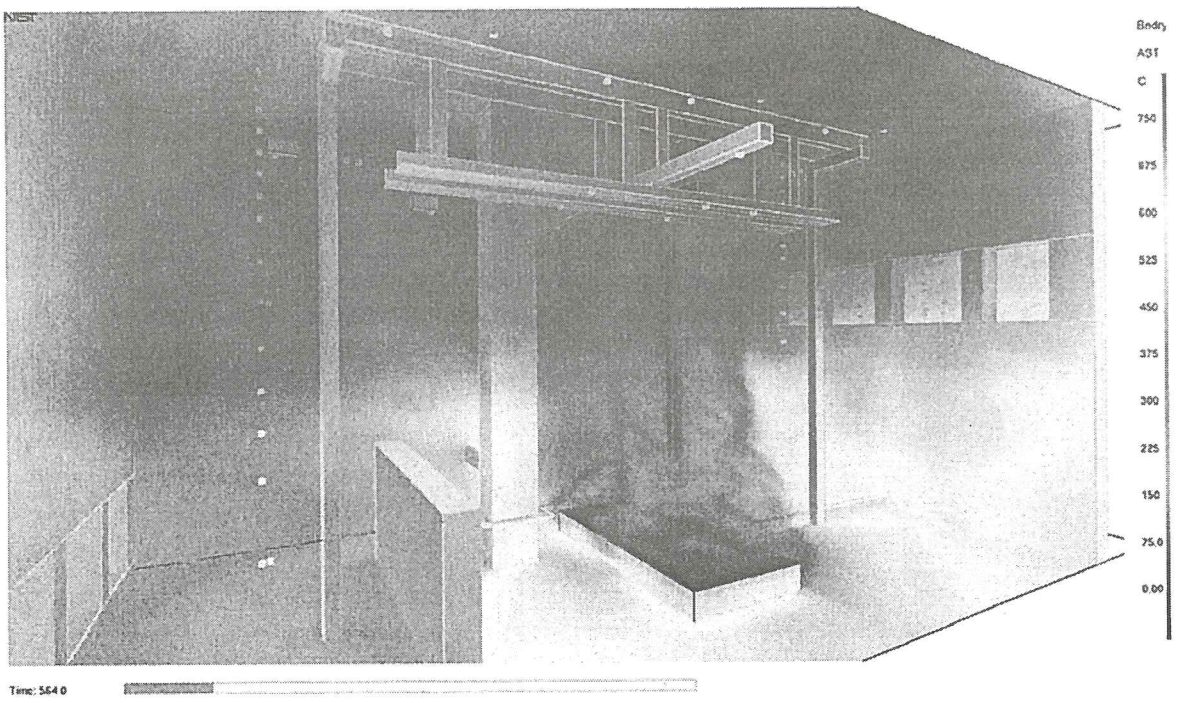

Fig.2 Fire simulation

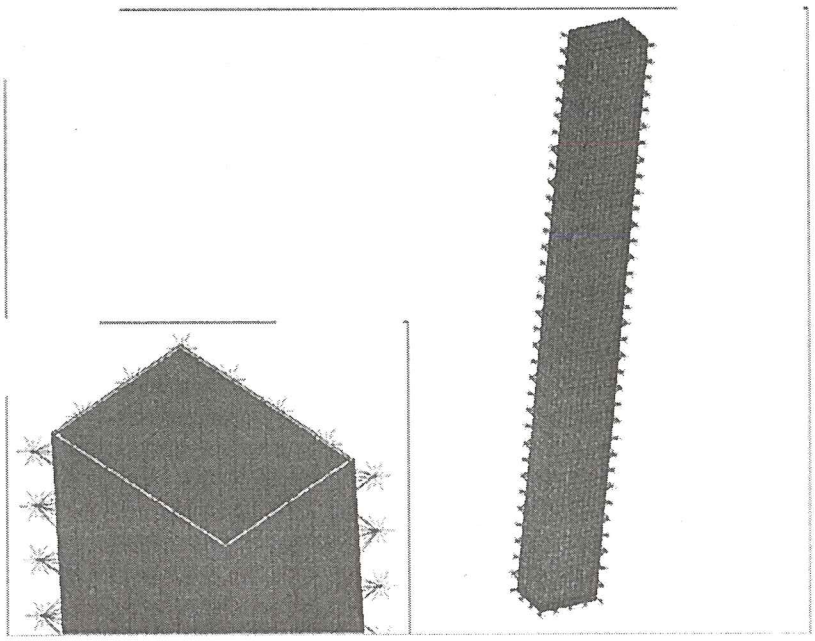

Fig.3 AST nodes for inside and outside faces of column

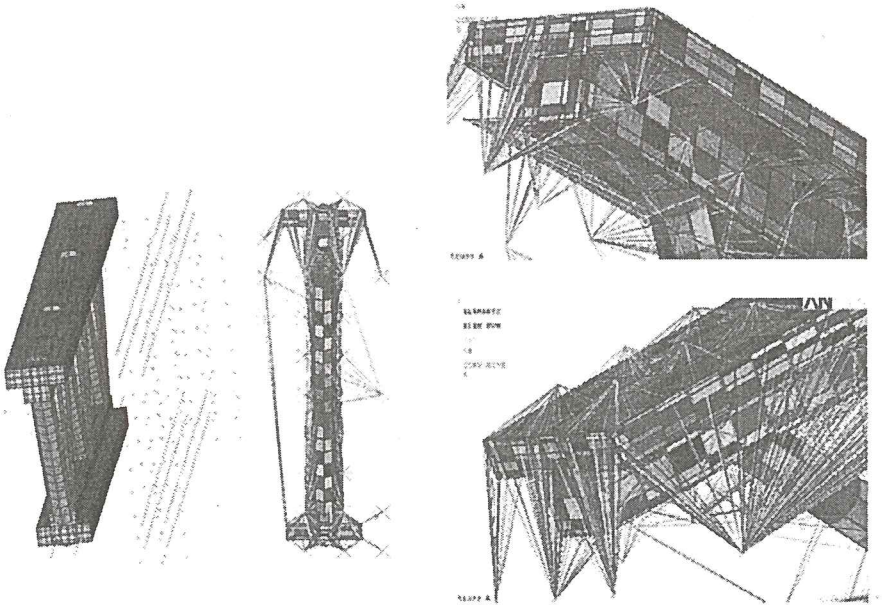

Fig.4 AST nodes for truss

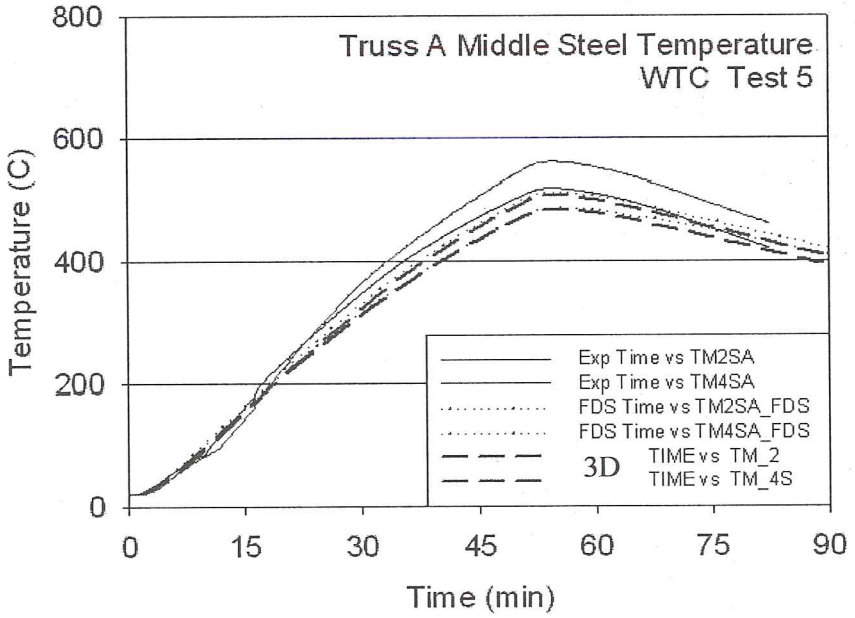

Fig.5 Comparison of measured and calculated temperatures for truss A, middle location, steel

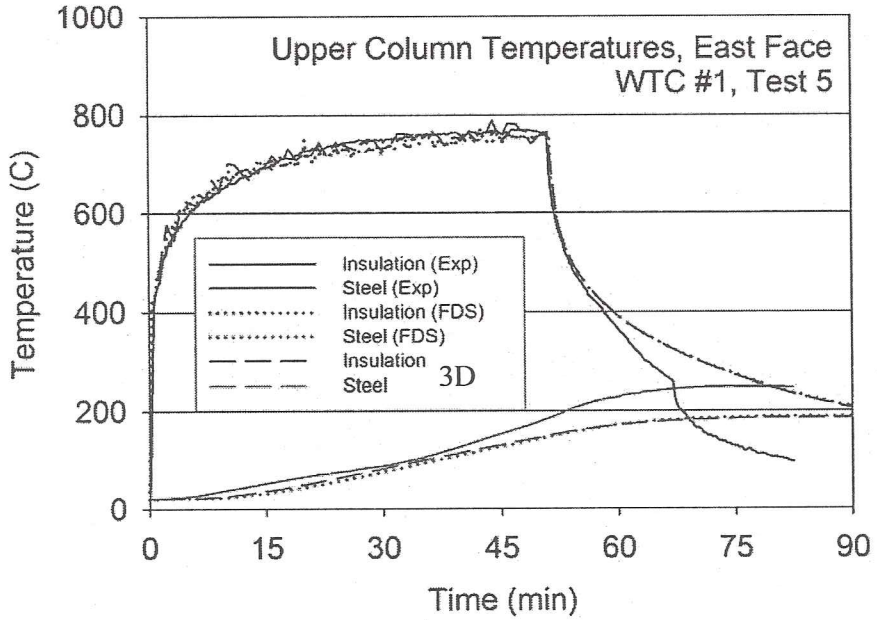

Fig. 6 Comparison of measured and calculated temperatures for column, upper location

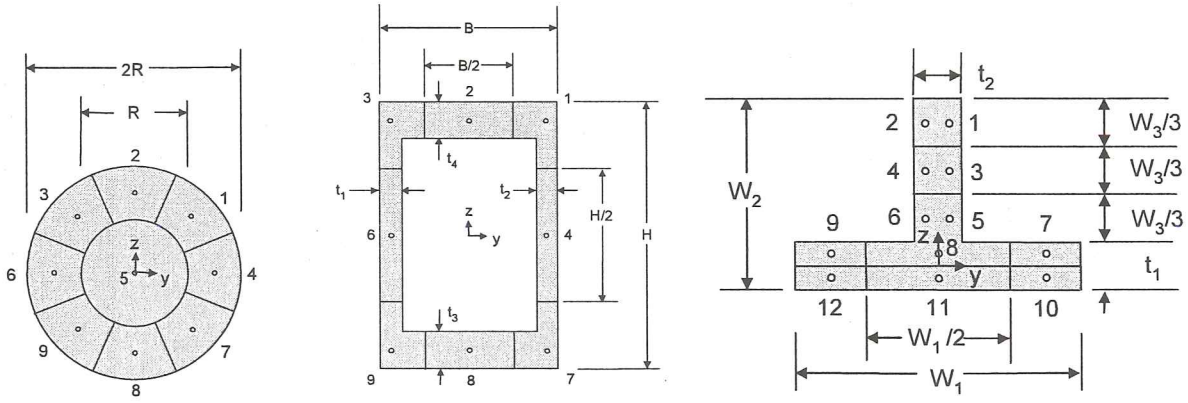

Fig. 7 Some common beam cross sections and their transfer points

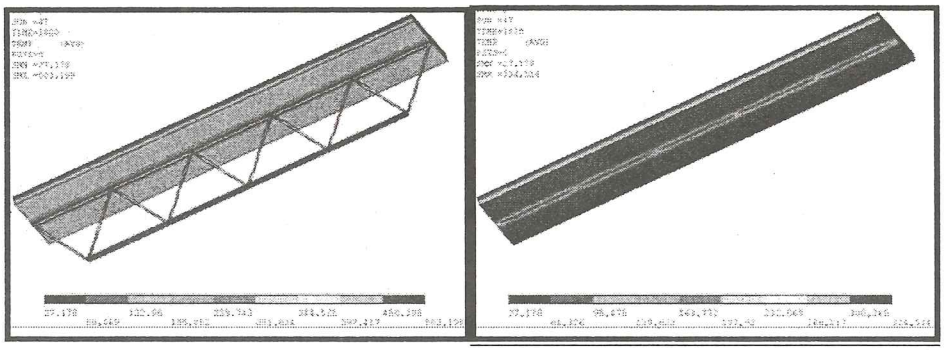

Fig. 8 Temperature results (°C) from thermal model, shown without insulation

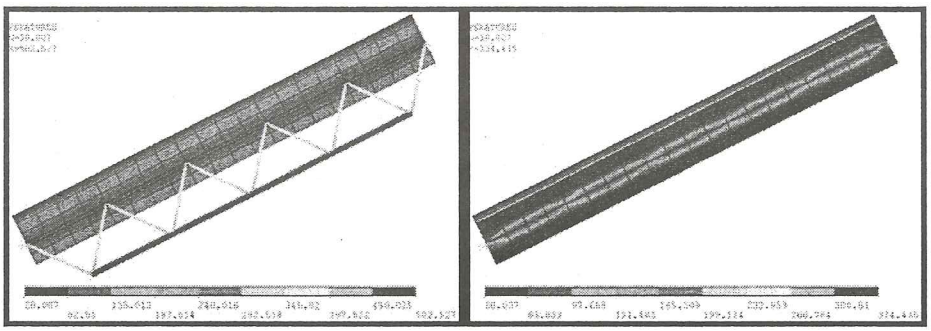

Fig. 9 Structural model – temperatures (°C) input as body loads

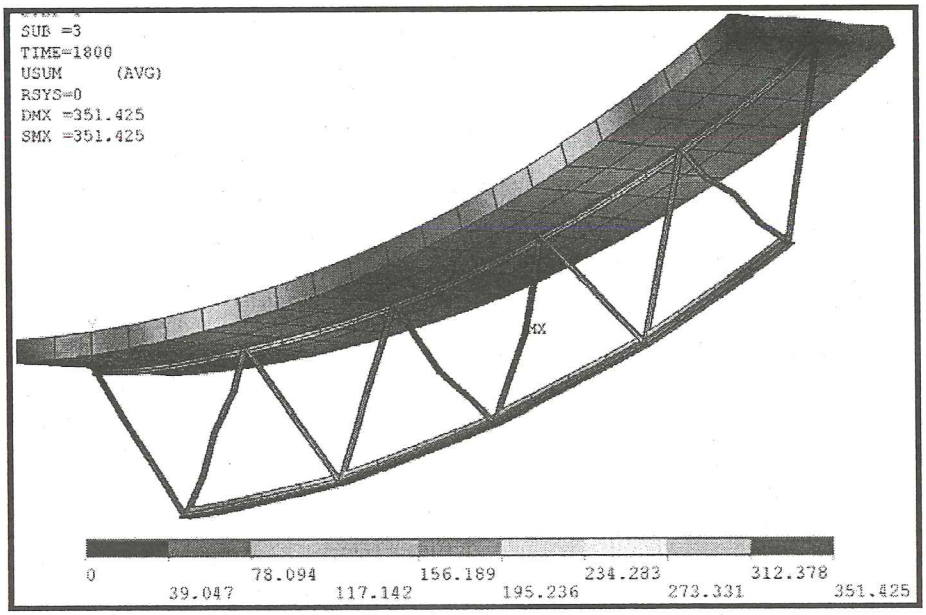

Fig. 10 Structural model – deflections (mm) under thermal loads and dead weight

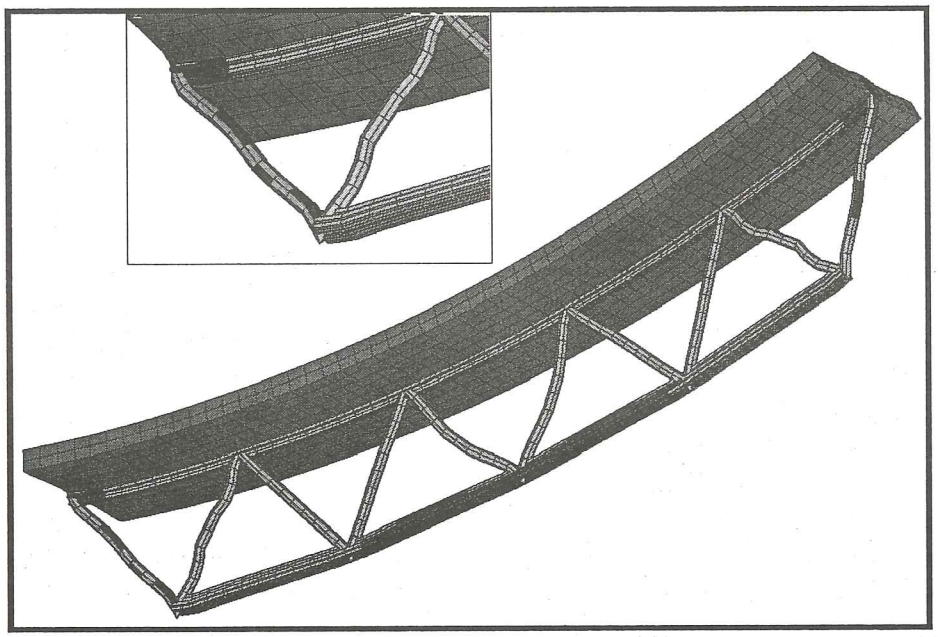

Fig. 11 Thermal model – updated geometry based on structural deflections and failed insulation (red)

Numerical Analysis of Fire Resistance Tests of Press-formed Steel Columns (BCP325)

by

Takeshi Okabe[1] and Mamoru Kohno[2]

ABSTRACT

A numerical simulation of the fire resistance test of large steel columns is presented. The experimental investigation into the fire resistance properties of axially loaded large steel box columns was described in References [1, 2] by the authors. In this paper, a procedure for a one-dimensional finite element of nonlinear numerical analysis was applied to simulate thermal deformation, described as an elastic-plastic-creep, of steel columns as they are subjected to high temperatures. The results of the calculations clearly show that numerical analysis can be used to provide accurate predictions of the deformation characteristics of columns at high temperatures when an appropriate mechanical model and creep strain data of steel materials at high temperatures are used.

KEYWORDS: Steel column, Press formed, Creep deformation, Fire resistance test, Tall building

1. INTRODUCTION

Few full-scale fire resistance tests applying actual axial forces have been conducted on steel columns used for tall buildings, and the fire safety of such columns is not thoroughly understood. One of the authors conducted loaded fire resistance tests of full-scale square steel tubes which were welded, assembled, and press formed. The results showed that the steel columns retained high heat resistance when their fire protection was sound but that compromised fire protection caused sharp drops in fire ratings [1, 2].

The authors also simulated the loaded fire resistance tests of weld-assembled square steel tube columns (Series A of Reference [1]) by a numerical analysis in which the behaviors of steel at high temperatures were considered. The results verified the analytical and physical experimental methods [3]. The numerical analysis, in which the behaviors of steel at high temperatures were considered, was shown to be effective in predicting the behaviors of the columns during loaded fire resistance tests, but creep data of steel at high temperatures need to be corrected for accurate behavior prediction.

This paper, a supplement to Reference [3], describes a simulation analysis of thermal elastic-plastic-creep deformation using the one-dimensional finite element method, which was conducted to reproduce the high axial-force loaded fire resistance tests (Series B) of cold press-formed square steel tube columns described in Reference [2] and to compare the experimental and analytical results.

This study is valuable since few tests have been conducted by applying loads and heat to full-size press-formed square steel tube columns until they collapse. In addition, as indicated in Reference [3], creep properties of steel at high temperatures are crucial for simulating the deformation behaviors of steel columns in detail. In this study, a numerical analysis was conducted using experimental creep data of steel to examine the validity of the method used for a simulation of the experimental behavior of steel columns at high temperatures.

This study aims to provide basic data and information about loaded fire resistance tests

1 Assoc. Prof., Graduate School of Science and Technology, Kumamoto University, Kumamoto-shi, Kumamoto-ken 860-8555, Japan

2 Research Coordinator for Quality Control of Building, Building Department, National Institute for Land and Infrastructure Management, Tsukuba-shi, Ibaraki-ken 305-0802, Japan

and numerical analyses to enhance fire safety in the design of buildings.

2. LOADED FIRE RESISTANCE TEST OF PRESS-FORMED SQUARE STEEL TUBE COLUMNS

An overview of the loaded fire resistance tests (Series B) conducted in Reference [2] is shown in Fig. 1 and Table 2, and the specifications of the specimens are shown in Table 1. The mechanical properties of the steel in the mill-sheet are shown in Table 3.

A high-performance column furnace at the Building Research Institute of Japan was used for the experiments. Press-formed square steel columns, BCP325, were used for test specimens. Two of the four columns were fabricated by using JIS G 3136 SN490B grade steel (conventional steel), and the remaining two columns were made of JIS G 3136 SN490B FR (fire-resistant) grade steel. The specified design strength is 325 MPa for both grades. The four columns had identical geometrical dimensions: the length was 4.3 m, the cross-section was 600 mm^2, and the plate thickness was 28 mm.

The columns were coated with a fire protection made of a ceramic fiber blanket which is a 1-hour rated protection material. According to the estimation in Reference [2], the columns corresponded to those used for the lowest stories of high-rise buildings of about 40 stories.

In the experiment, thermocouples were installed at the levels and positions shown in the middle figure of Fig. 1, and central compressive load was applied with the two spheres. As shown in Table 2, axial forces equal to 0.6 times and 1.0 times the long-term allowable axial force of the column were applied. Heat was applied along the standard fire temperature curve (ISO-834) and the temperature curve of hydrocarbon combustion. By the end of the experiment, all specimens showed buckling collapse.

3. METHODS OF NUMERICAL ANALYSIS

As in Reference [3], a method of thermal elastic-plastic creep deformation analysis by the one-dimensional finite element method was used. The analysis was based on a finite displacement formulation of the one-dimensional finite element procedure proposed by Fujimoto et al. [4] and was modified for thermal elastic-plastic creep deformation analysis [5, 6] by incorporating a mechanical model of steel at high temperatures [7].

The analytical method assumed that planes were retained and did not consider local buckling and lateral buckling. The members were divided into beam elements along the member axis. The cross-section of the column was divided along the center line of plate elements into small segments, and the areas of small elements were concentrated in the center of the segments. In the segments, both stress and strain were assumed to be uniform.

The analytical method used is a combined non-linear analysis method that simultaneously considers geometrical and material non-linearity. The method has been shown to be valid in past studies [11-14].

3.1 Analytical Model

The analytical model of the steel columns in the test apparatus is shown in the right figure in Fig. 1. In the column furnace, a column is a pin supported by two spheres at the top and bottom ends of a loading system. The buckling length of column specimens was 4.6 m. In the analytical model shown in Fig. 1, the columns were assumed to have the initial crookedness of a sinusoidal wave with a central value of $L/1000$, where L is the length of the columns. The model was divided along the length of the column into 44 beam elements, and the cross-section was divided into 22 elements as shown in Fig. 2.

In analyzing the columns, the axial loads were maintained at a constant level, and the heating time was increased by increments. The analysis continued until an equilibrium solution could no longer be found, signifying that the columns had failed. As the creep effect is a transient phenomenon, a transient analysis was carried

out for a more realistic modeling of steel columns.

3.2 Temperature Distribution Model

In the experiment described in Reference [2], the temperature of column specimens was measured at nine sections (Levels A to I) using thermocouples (Fig. 1). Of the sections, the temperature was measured on both the surface and the back of the sections on Levels C, E, and G and was measured only at the surface on the other levels.

In this analysis, the surface temperature measured during the experiment was assumed to be the temperature in the middle of the plate thickness of the steel tube since the surface temperature was measured throughout the specimen and differed little from the temperature at the back, except at the corners, where it differed by 20 to 30 °C. Temperatures between the measured values were linearly interpolated along the sectional direction by assuming that the temperature distribution along the plate thickness direction was uniform and that temperature changed linearly along the length of the column.

3.3 Model of Steel Behaviors at High Temperatures

In order to model the behaviors of steel at high temperatures, the relationship between the stress and strain of steel at a certain temperature, a creep equation at high temperatures, and an equation of thermal expansion should be known [7].

3.3.1 Relationship between Stress and Strain of Steel at a Certain Temperature

In References [1] and [2], static tensile tests were conducted, and the stress-strain curves at ambient temperature, 400 °C, 500 °C, 600 °C, and 700 °C were obtained. In order to represent these stress-strain curves mathematically, Eqs. (1) and (2) were adopted (Fig. 3). The yield plateau in the stress-strain relationship of conventional steel SN490B is expressed by Eq. (1) in Fig. 3, and the other curve sections are expressed by Eq. (2).

The coefficients in Eqs. (1) and (2) were obtained directly by applying the least squares method to the digitalized stress-strain data. Since fire-resistant steel SN490B-FR showed no clear yield plateau even at ambient temperature, the relationship at all temperatures was expressed by Eq. (2). Thus, SN490B needed six coefficients, and SN490-FR needed four coefficients.

3.3.2 Effects of Cold Press Forming

Cold press forming is likely to cause changes in the stress-strain relationships of steels and increase their strength. However, no experimental studies have been conducted on the effects of cold press forming at high temperatures. In this study, the effects of cold press forming on the stress-strain relationships determined in Section 3.3.1 were handled in the following manner.

To show a trend of plastic processing erasing the yield plateau, the data for ordinary steel at 200 °C, shown in Table 4, were obtained from the data of SN490B at 300 °C, given in Reference [14], since the studies described in References [1, 2] did not obtain the stress-strain relationship of SN490B at temperatures below 400 °C.

The stress-strain curves drawn using the data from Table 4 are shown in Fig. 4. In general, for steel plates not subjected to plastic processing, the yield stage disappears at temperatures above 200 °C. On the other hand, the yield plateau in Fig. 4 disappeared at 100 °C. Since tensile tests of the fire-resistant steel resulted in a curved relationship between stress and strain, the disappearance of yield stage by plastic processing was not considered.

To consider the increases in strength by cold press forming, values 1.1 times larger than the yield strength values obtained by tensile tests were used for the structural calculations.

Cold press forming causes changes in the quality of materials at corners and has been reported to increase the yield point up to 1.4 to 1.6 from that of flat plate sections [9] although

the value should differ by the degree of processing. Since corners account for less than 30% of the entire sectional area of a square steel tube, the mean yield strength of the entire section should be less than 1.15 times larger than that of the original flat steel plate.

In the calculations, the authors decided to use values 1.1 times larger than the yield strength of the original steel plates. Figs. 4 and 5 show the stress-strain relationships calculated using values 1.1 times larger than the yield strength of the original steel plates and the data given in Tables 4 and 5.

3.3.3 Creep-strain Equation at High Temperatures

The creep-strain equation at high temperatures should, in principle, be determined by conducting creep tests of steel column specimens at high temperatures and processing the data as for a stress-strain relationship. However, because creep tests at high temperatures require time, labor, and advanced skills, they are difficult to conduct. In this study, data of past studies were used [8, 10].

In References [8] and [10], the results of creep tests at high temperatures of SM50A and NSFR490A, respectively, were approximated using the least squares method to determine the coefficients of Eq. (3):

$$\varepsilon_c = 10^{a/T+b}(\sigma/9.81)^{c/T+d}\, t^{eT+f} \qquad (3),$$

where ε_c is creep strain (%), t is time (minutes), σ is stress (N/mm2), and T is absolute temperature (K). The material constants of SM50 were as follows: $a = -8.48 \times 10^3$, $b = 4.50$, $c = 3.06 \times 10^3$, $d = 2.28 \times 10^{-1}$, $e = 2.00 \times 10^{-3}$, $f = -1.10$.

The material constants of NSFR490A were $a = -4.205 \times 10^4$, $b = 37.615$, $c = 1.407 \times 10^4$, $d = -9.264$, $e = -1.584 \times 10^{-4}$, $f = 0.851$.

Since no experimental studies have been conducted on the creep strain of SN490B at high temperatures, the creep-strain equation of SM50A, which should have similar creep properties, was used.

To examine the accuracy of the creep-strain equation (Eq. (3)), the time history of the term of time t^{eT+f} in Eq. (3) is shown in Fig. 6, and the creep-strain curves of SM50 and NSFR490A, given by References [8] and [10], are shown in Fig. 7. In Fig. 7, the dashed lines show the experimental values of the creep tests at high temperatures, and the solid lines show the values calculated using Eq. (3). The stress levels in Fig. 7 were converted into SI units. Fig. 6 shows the basic form of the term of time t^{eT+f} in the creep-strain equation (3) at certain high temperatures (400 to 700 °C), and Fig. 7 shows the quantitative correlation between the experimental and calculated results.

As shown in Fig. 6, the primary creep decreased and the secondary creep increased in SM50 steel as the temperature rose from 400 to 600 °C. On the other hand, NSFR4909A showed large secondary creep regardless of temperature.

As shown in the upper figure of Fig. 7, the calculated values of SM50 were slightly larger than the experimental values at 450 °C but reproduced well the increases in the primary creep. At 500 °C, the experimental results showed large secondary creep, although the calculated results still showed the primary creep to be larger than the secondary creep. The relationship as a whole showed experimental values taking over the calculated values in the middle of the course. At 550 °C and with large stresses, the calculated strain values were smaller than the experimental values.

On the other hand, NSFR490A in the bottom figure of Fig. 7 showed smaller calculated values at 550 °C since the experimental values, which resulted in large primary creep, were approximated using a function that resulted in large secondary creep. At 600 °C and 650 °C, the relationship between the experimental and calculated values was complicated. Even at the same temperature, the relationship was reversed by stress level, and the experimental values showed tertiary creep.

Since the correlation between the experimental and calculated creep values of the steels at high temperatures was complicated, their qualitative

and quantitative correlations need to be thoroughly understood in order to use the values for calculations.

3.3.4 Equation of Thermal Expansion

$$\varepsilon_T = 5.04\times10^{-9}\theta^2 + 1.13\times10^{-5}\theta \qquad (4),$$

where θ is temperature (°C).

4. RESULTS AND DISCUSSION

4.1 Tests of Conventional Steel Columns B-CS06 (Fig. 8) and B-CS10 (Fig. 9)

The conventional steel column B-CS06 (Fig. 8) was heated by the ISO 834 standard fire temperature curve, and B-CS10 (Fig. 9) was heated by the hydrocarbon fire curve. The existing load ratios to sustained allowable load were 0.6 for B-CS06 and 1.0 for B-CS10. The mean axial stress values, which were calculated by simply dividing the axial load by sectional area, were 143.3 N/mm^2 and 236.5 N/mm^2, respectively.

The upper figures in Figs. 8 and 9 show the steel temperatures measured at points on Level E (experimental values), the middle figures show column elongations (experimental and calculated values), and the bottom figures show the deflection W at the middle of the columns (calculated values). To examine the effects of the accuracy of the creep-strain equation at high temperatures, three cases were calculated using values 40% larger and smaller than the value determined by Eq. (3). In the middle figures, open circles denote the experimental values, solid lines denote values calculated by considering creep at high temperatures, and dashed lines denote calculations made by disregarding the creep strain.

As shown in the upper figures, the temperature distribution was almost uniform throughout the cross-section when the columns were heated. The steel temperatures of B-CS06 and B-CS10 rose almost linearly by 150 °C to 200 °C per hour.

The calculated values for B-CS06 with consideration of creep strain at high temperatures (solid line) reproduced the experimental values very accurately. The 40% fluctuation of the creep strain at high temperatures corresponded to a collapse time of about 10 minutes. The values calculated by disregarding creep strain at high temperatures (dashed lines) continued rising until immediately before the collapse and differed from the actual contraction observed in the experiment.

The results show that, at high temperatures, creep strain needs to be considered to correctly reproduce the actual behaviors during collapse (contraction of displacement U) and that disregarding creep strain results in predicting collapse time on the dangerous side.

The calculated values for B-CS10 (Fig. 9) with consideration of creep strain at high temperatures (solid line) reproduced the experimental results except that the calculated contraction behavior occurred slightly earlier than the actual contraction (open circles). Since the 40% reduction in creep strain at high temperatures matched the experimental values, Eq. (3) for calculating creep strain at high temperatures may tend to overestimate the creep strain of SN steel under large stresses.

The values calculated by disregarding creep strain at high temperatures (dashed lines) continued rising until immediately before the collapse and differed from the actual contraction observed in the experiment, suggesting that creep strain at high temperatures cannot be disregarded if the experimental collapse behavior is to be reproduced. However, the calculated collapse time (dashed line) nearly agreed with the actual collapse time.

The bottom figures in Figs. 8 and 9 show that the calculated deflection W at the middle of the columns started to increase when axial displacement U started to contract.

4.2 Tests of Fire-resistant Steel Columns B-FR06 (Fig. 10) and B-FR10 (Fig. 11)

A fire-resistant steel column B-FR06 (Fig. 10) was heated by the ISO834 standard fire temperature curve, and B-FR10 (Fig. 11) was

heated by the hydrocarbon fire curve. The existing load ratios to sustained allowable load were 0.6 for B-FR06 (Fig. 10) and 1.0 for B-FR10 (Fig. 11). The mean axial stress values, which were calculated by simply dividing the axial load by sectional area, were 143.3 N/mm^2 and 236.5 N/mm^2, respectively.

The upper figures in Figs. 10 and 11 show the steel temperatures measured at points on Level E (experimental values), and the middle and bottom figures show the column elongation (experimental and calculated values). The middle figures show the results of calculations made using values 40% larger and smaller than the ε_c value determined by Eq. (3). In the bottom figures, ε_c values 0.01, 0.1, 0.4, and 1.0 times the value determined by Eq. (3) were used.

The middle figures are calculations made to examine the effects of the accuracy of the creep-strain equation at high temperatures. The bottom figures show attempts to indirectly correct the equation using the results of loaded fire resistance tests of steel columns. In the middle and bottom figures, open circles denote the experimental values, solid lines denote values calculated by considering creep strain at high temperatures, and dashed lines denote calculations done by disregarding creep strain.

As shown in the upper figures, the temperature distribution was almost uniform throughout the cross-section when the columns were heated. The steel temperatures of B-FR06 and B-FR10 rose almost linearly by 150 °C to 200 °C per hour.

The calculated values with consideration of creep strain at high temperatures (solid line) reproduced the overall experimental behaviors after the contraction of axial deformation up to collapse. The 40% fluctuation of the creep strain at high temperatures caused smaller effects than in conventional steel (middle figures of Figs. 8 and 9). The experimental behaviors (open circles) shown in the middle figures in Figs. 10 and 11 and the behaviors calculated by considering creep strain at high temperatures (solid lines) differed in two respects.

The first difference was that the drops in elongation observed in the experiment at steel temperatures above 400 °C were not reproduced in the calculation. The other was that the calculation resulted in sudden collapse after axial deformation started to contract.

The first difference can be explained using creep curves of fire-resistant steel at 550 °C (lower figure of Fig. 7). In this study, the mean stresses of the columns were 143.3 to 236.5 N/mm^2, but at a stress level of 550 °C, the values calculated using Eq. (3) were much smaller than the experimental values.

In the lower figure of Fig. 7, the experimental values of fire-resistant steel (dashed lines) at 550 °C showed primary creep strain at the start of the experiment, followed by a gradual transition to secondary creep. On the other hand, the values calculated using the approximation equation did not reproduce the modes at the start of the experiment. Such a creep equation resulted in the underestimation of primary creep strain and thus resulted in almost no contraction of axial deformation (deceleration of elongation) by creep strain at high temperatures in the calculations shown in the middle figures of Figs. 10 and 11.

On the other hand, the latter difference was possibly attributable to an overestimation of the strain by Eq. (3), which yielded strain values larger than the actual strains of the columns.

As described in Section 3.3.3, the constants of Eq. (3) for calculating creep strain at high temperatures for analyzing fire-resistant steel NSFR490A were derived by "approximating the results of the ordinary creep test by the least squares method" (Reference [10]), not by conducting a creep experiment of SN490B-FR at high temperatures. Thus, the constants should be corrected by considering the significance of the constants of such a creep equation rather than by discussing in detail the differences between the experimental and calculated values in the middle figures of Figs. 10 and 11. In this study, the coefficients of Eq. (3) were indirectly corrected by analyzing the results of loaded fire resistance tests of steel tube columns.

The bottom portions of Figs. 10 and 11 show

calculations made by setting the scale of Eq. (3) low (0.01 to 1.0) in an attempt to address the problem. When the creep strain ε_c value obtained by Eq. (3) was reduced, the collapse time was prolonged. At ε_c equal to 0.1 of the value of Eq. (3), the collapse time almost matched the experimental collapse time. Thus, the creep strain of fire-resistant steel SN490B-FR is possibly much smaller than the creep strain of NSFR490A, from which Eq. (3) was derived.

4.3 Collapse Time

The experimental and calculated collapse time values of all cases investigated in this study are compared in Fig. 12. In the figure, open circles denote the values calculated by disregarding the creep strain at high temperatures, and dark squares denote the values calculated by considering the creep strain at high temperatures, as determined using Eq. (3). The experimental collapse time was the time when the columns failed to sustain their axial load constant, and the calculated collapse time was when the convergence calculation could no longer be applied.

The figure shows that the calculated and experimental values differed by less than 10%. The analytical values calculated by considering the creep strain at high temperatures (dark squares) were on the safer side than the experimental values, and the values calculated by disregarding the creep strain (open circles) were on the dangerous side.

5. CONCLUSIONS

A non-linear numerical simulation analysis of the one-dimensional finite element method was conducted on loaded fire resistance tests of full-scale press-formed square steel tube columns, and the analytical results were compared with the experimental results. The study revealed the following:

(1) The calculation of the behaviors of BCP columns (B-CS06 and B-CS10) using conventional steel SN490B correctly reproduced the behaviors observed during the experiments and was found to make predictions on the safe side. Thus, the one-dimensional finite element calculation method used in this study appears to be valid. An equation for calculating creep strain at high temperatures for SM50A steel also appears to be feasible for predicting the behaviors of SN490 steel at high temperatures.

(2) Numerical analysis of B-FR06 and B-FR10 using fire-resistant steel NSFR490B columns did not reproduce the axial displacement behaviors of the columns before contraction and predicted much earlier collapse than the experiments did even when creep at high temperatures was considered. This problem may have occurred because the equation used to calculate creep strain at high temperatures underestimated the first-stage creep up to 550 °C and overestimated the creep at temperatures above 600 °C.

(3) A comparison of all the experimental and calculated collapse time values showed that the calculated values differed from the experimental values by less than 10%. The analytical values calculated by considering the creep behaviors at high temperatures were on a safer side than the experimental values, and the values calculated by disregarding the behaviors were on the dangerous side.

A simulation analysis of the results of loaded fire resistance tests of full-scale, press-formed square steel tube columns by numerical analysis showed the importance of obtaining creep property data of steel at high temperatures. To accurately predict the behaviors of steel structures and buildings at high temperatures, the creep properties of SN490C and fire-resistant steel should be experimentally confirmed.

6. REFERENCES

1. Kohno, M. and Masuda, H.: Fire-resistance of Large Steel Columns under Axial Load, Proc. of CIB-CTBUH International Conference on Tall Buildings, 2003.

2. Kohno, M., Sakumoto, Y., and Fushimi, M.: Effects of Large Section Size and Fire Resistant Steel on Redundancy Improvement of Steel High-rise Buildings in Fire, Proc. of the CTBUH 2004 Seoul Conference, 2004.
3. Okabe, T. and Kohno, M.: Numerical Simulation of Fire Resistance Test of Large Steel Columns under Axial Load, Journal of Structural Engineering, Vol. 51B, 2005.
4. Fujimoto, M., Wada, A., Shirakata, K., and Kosugi, T.: Non-linear Analysis of Braced Steel Frames, J. of Structural and Construction Engineering, Trans. of A.I.J., No. 209, 1973.
5. Furumura, F., Ave, T., Okabe, T., and Kim, W. J.: A Uniaxial Stress-strain Formula of Structural Steel at High Temperature and its Application to Thermal Deformation Analysis of Steel Frames, J. of Structural and Construction Engineering, Trans. of A.I.J., No. 363, 1986.
6. Furumura, F., Migita, K., Takeo, A., Okabe, T., and Kim, W. J.: Elasto-plastic Creep Thermal Deformation Behavior of Plastic Designed Steel Frames, J. of Structural and Construction Engineering, Trans. of A.I.J., No. 368, 1986.
7. Furumura, F., Ave, T., Kim, W. J., and Okabe, T.: Nonlinear Elasto-plastic Creep Behavior of Structural Steel under Continuously Varying Stress and Temperature, J. of Structural and Construction Engineering, Trans. of A.I.J., No. 353, 1985.
8. Fujimoto, M., Furumura, F., and Ave, T.: Primary Creep of Structural Steel (SM50A) at High Temperatures, J. of Structural and Construction Engineering, Trans. of A.I.J., No. 306, 1981.8.
9. Kuwamura, H., Akiyama, H., Yamada, S., and Jung-Cheng, C.: Experiment on the Mechanical Properties and Their Improvement of Cold Press-Bent Steel Plates, J. of Structural and Construction Engineering, Trans. of A.I.J., No. 444, 1993.2.
10. Sakumoto, Y., Yamaguchi, T., Ohashi, M., and Saito, H.: High-temperature Properties of Fire-resistant Steel FR Buildings, ASCE, Journal of Structural Engineering, Vol. 118, No.2, 1992.
11. Sakumoto, Y., Yamaguchi, T., Okada, T., Yoshida, M., Tasaka, S., and Saito, H.: Experimental Study for Fire Resistance of Fire Resistant Steel Columns, J. of Structural and Construction Engineering, Trans. of A.I.J., No. 434, 1992.
12. Okabe, T., Sakumoto, Y., Okabda, T., and Yamaguchi, T.: Calculation of Fire Resistance Tests on Concrete-filled Steel Tube Columns using FR Steel, Journal of Structural Engineering, Vol. 40B, 1994.
13. Hirayama, H. et al.: Fire Resistance of Protected Steel Column, Summaries of Technical Papers of Annual Meeting, Architectural Institute of Japan, A-2, 2000.
14. Okabe, T. and Ave, T.: Buckling Strength of Steel Columns using Structural Steel (SN490B) at High Temperature, J. of Structural and Construction Engineering, Trans. of A.I.J., No. 585, 2004.11.

Table 1 Parameters of Steel Columns (Reference [2])

	Symbol (Unit)	Series B
Section Shape	Press Formed □-600 × 600 × 28	
Specified Design Strength	F (N/mm^2)	325
Cross-sectional Area	A (mm^2)	6.00×10^4
Length	L (mm)	4 300
Second Inertia	I (mm^4)	3.14×10^9
Slenderness Ratio	λ	18.8
Shape Factor	Hp/A (m^{-1})	39.0
Weight	W (kg)	2.03×10^3

Table 2 Summary of Experiment Series B (Reference [2])

Symbol	Steel Grade	Fire Protection	Applied Load (Ratio*)	Heating Curve
B-CS06	SN490B CP325	Ceramic fiber blanket 30 mm (Fireguard C-60)	8.60 MN (0.6)	ISO-834
B-FR06	SN490B-FR BCP325		8.67 MN (0.6)	ISO-834
B-CS10	SN490B BCP325		14.19 MN (1.0)	Hydrocarbon
B-FR10	SN490B-FR BCP325		14.45 MN (1.0)	Hydrocarbon

* Load ratio to the sustained allowable load.

Table 3 Mechanical Properties (mill sheet)

Test Piece (Plate 28 mm)	σ_{yRT} (N/mm^2)	σ_{uRT} (N/mm^2)	Elong.$_{RT}$ (%)
SN490B	363	522	31
SN490B-FR	389	577	24

Table 4 Coefficients of Stress-strain Curves (SN490B)

Temp. (°C)	$\frac{E_T}{E_{RT}}$	$\frac{\sigma_{0T}}{\sigma_{yRT}}$	n_{oT}	$\frac{E_T - E_{pT}}{E_{RT}}$	$\frac{\sigma_T}{\sigma_{yRT}}$	n_T
RT	1.000	1.000	82	0.992	1.246	0.849
200	0.887	0.752	3.32	0.869	1.046	1.073
400	0.865	0.568	4.719	0.844	0.846	1.480
500	0.710	0.050	4.719	0.698	0.703	1.499
600	0.549	0.050	4.719	0.545	0.475	1.766
700	0.307	0.050	4.719	0.306	0.258	2.721

T: temperature, RT: ambient temperature, E: Young's modulus, σ_y: yield strength

Table 5 Coefficients of Stress-strain Curves (SN490B-FR)

Temp. (°C)	$\frac{E_T}{E_{RT}}$	$\frac{E_T - E_{pT}}{E_{RT}}$	$\frac{\sigma_T}{\sigma_{yRT}}$	n_T
RT	1.000	0.989	1.151	2.077
300	0.933	0.924	1.280	1.387
400	0.894	0.885	1.204	1.485
500	0.833	0.832	1.185	1.409
600	0.809	0.809	0.864	1.870
700	0.608	0.608	0.433	1.567
800	0.238	0.238	0.216	3.109

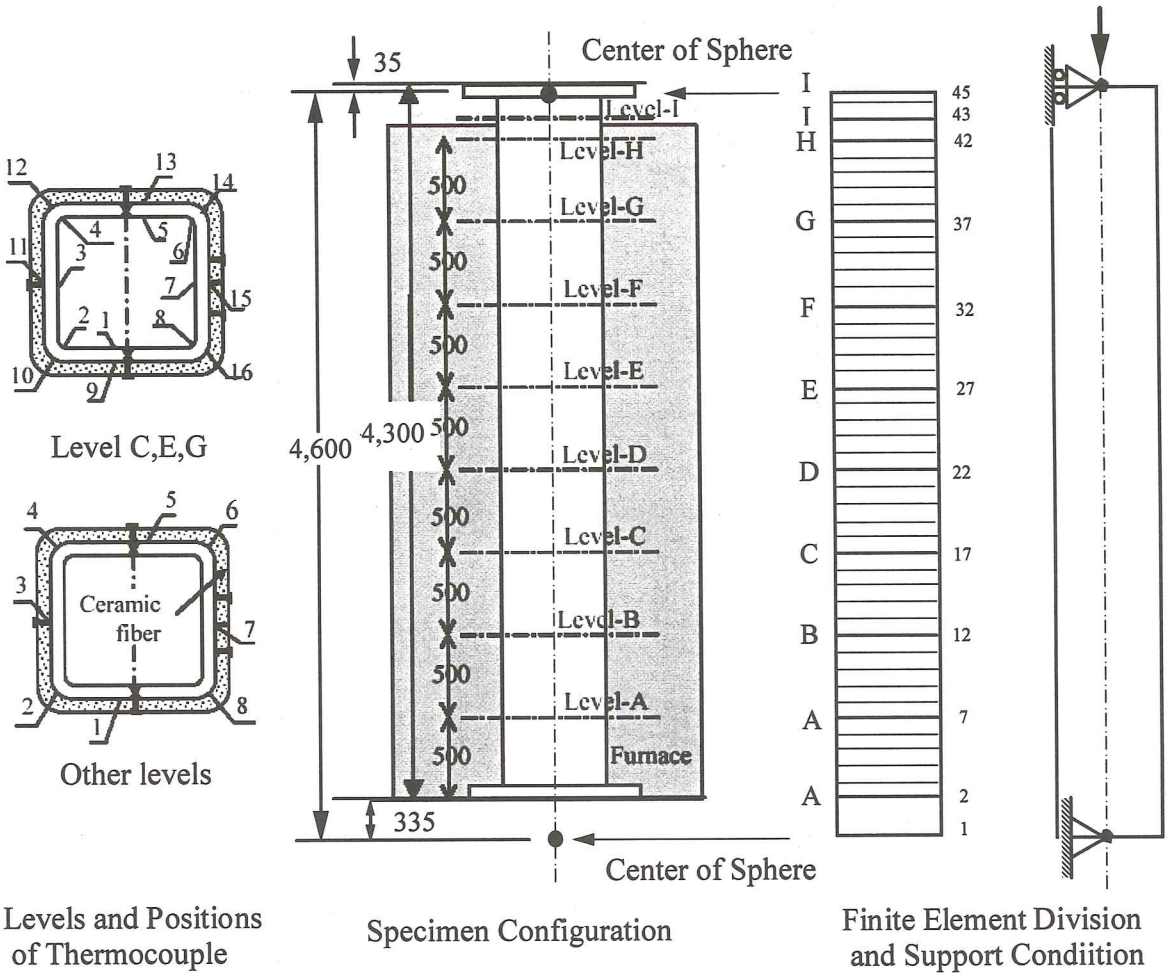

Fig. 1 Analytical Model of Fire Resistance Test

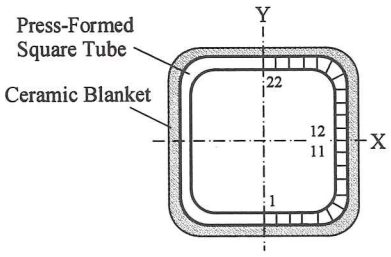

Fig. 2 Sectional Division

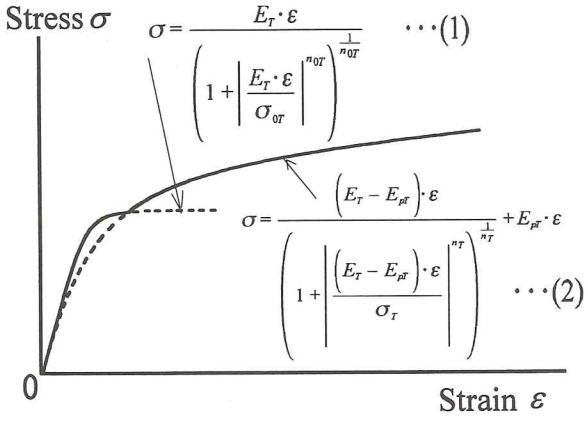

Fig. 3 Equations of Stress-Strain Relationship

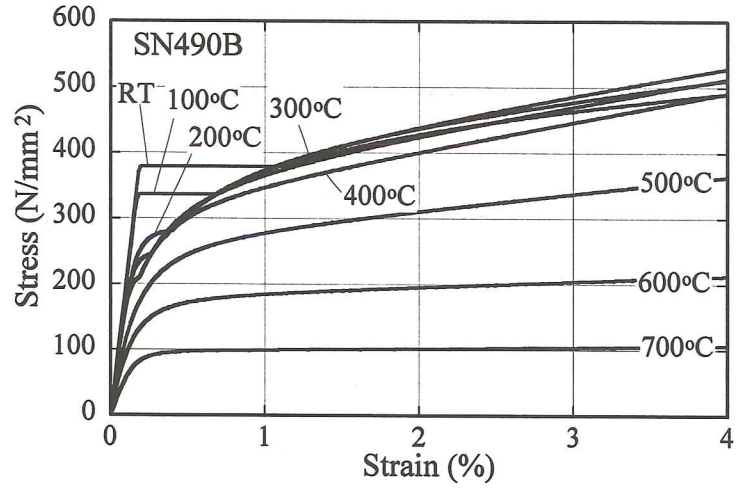

Fig. 4 Stress-Strain Relationship (SN490B)

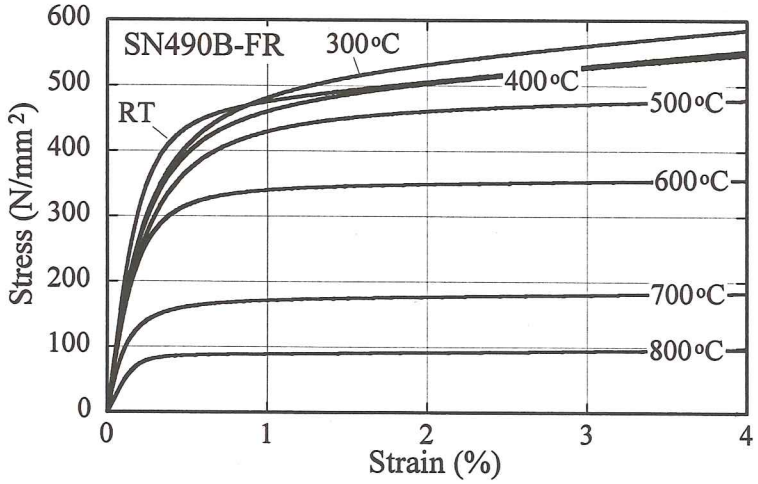

Fig. 5 Stress-Strain Relationship (SN490B-FR)

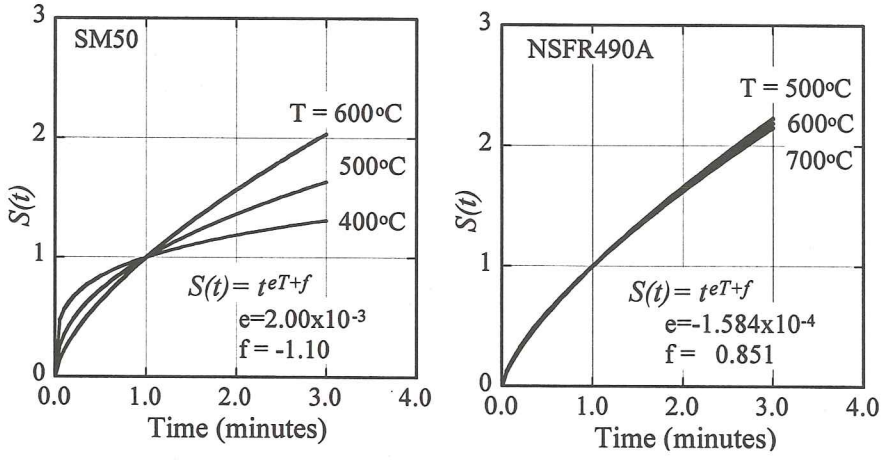

Fig. 6 Profile of time term t^{eT+f}

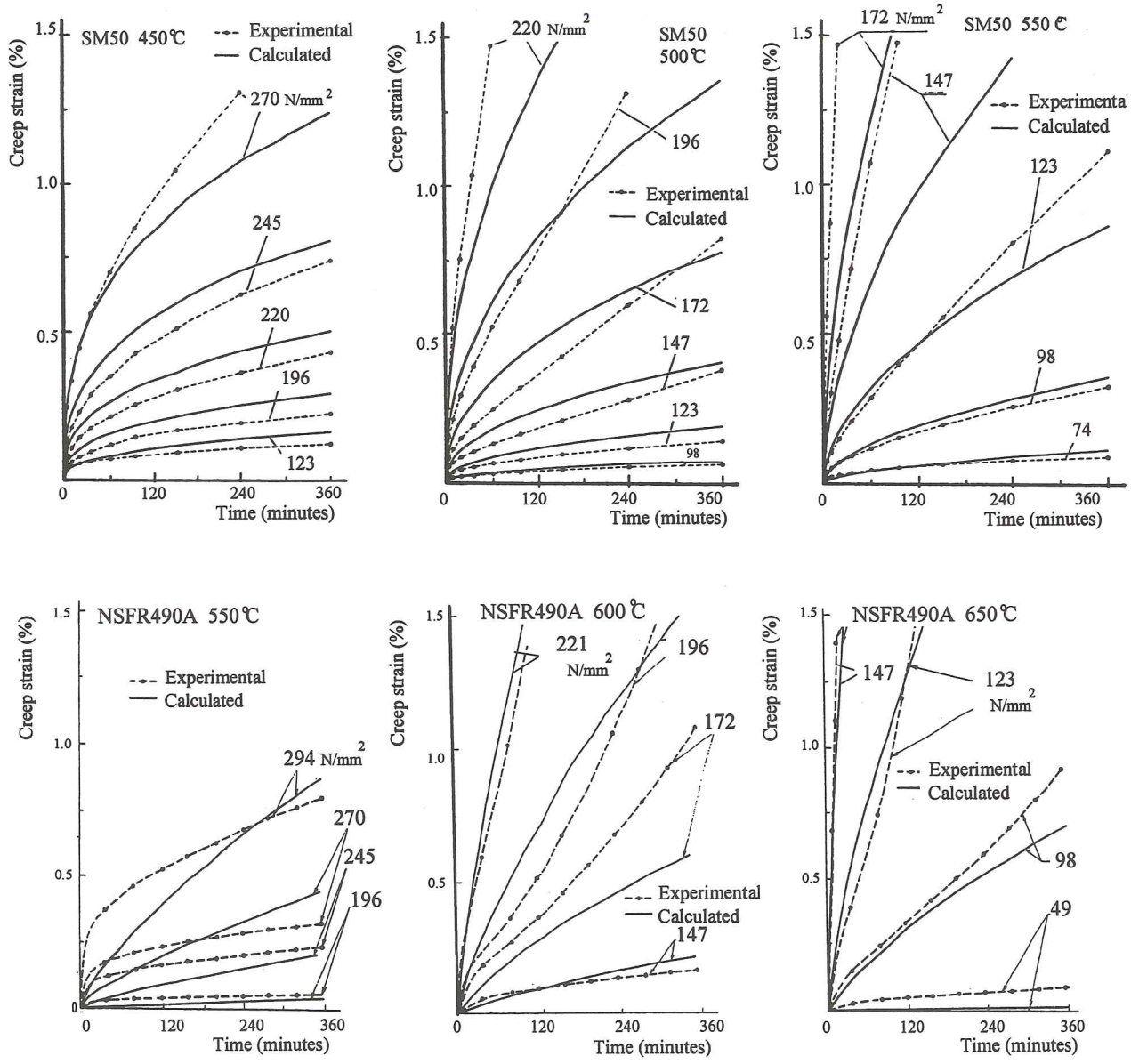

Fig. 7 Experimental creep strain (References [8, 10])

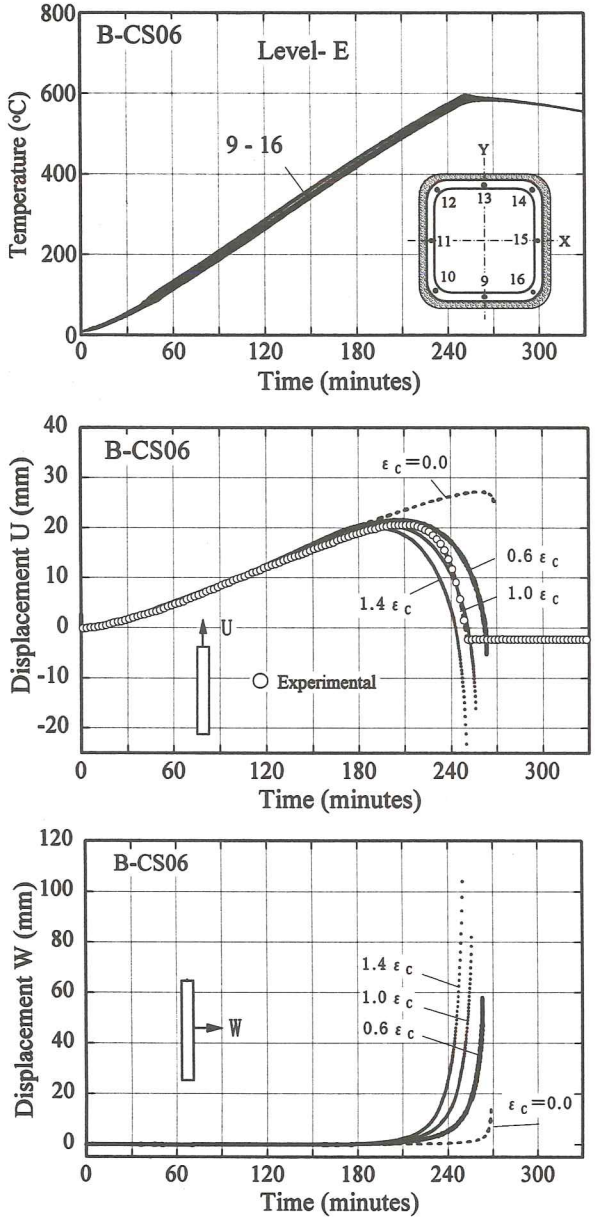

Fig. 8 Experimental and Calculated Values (B-CS06)

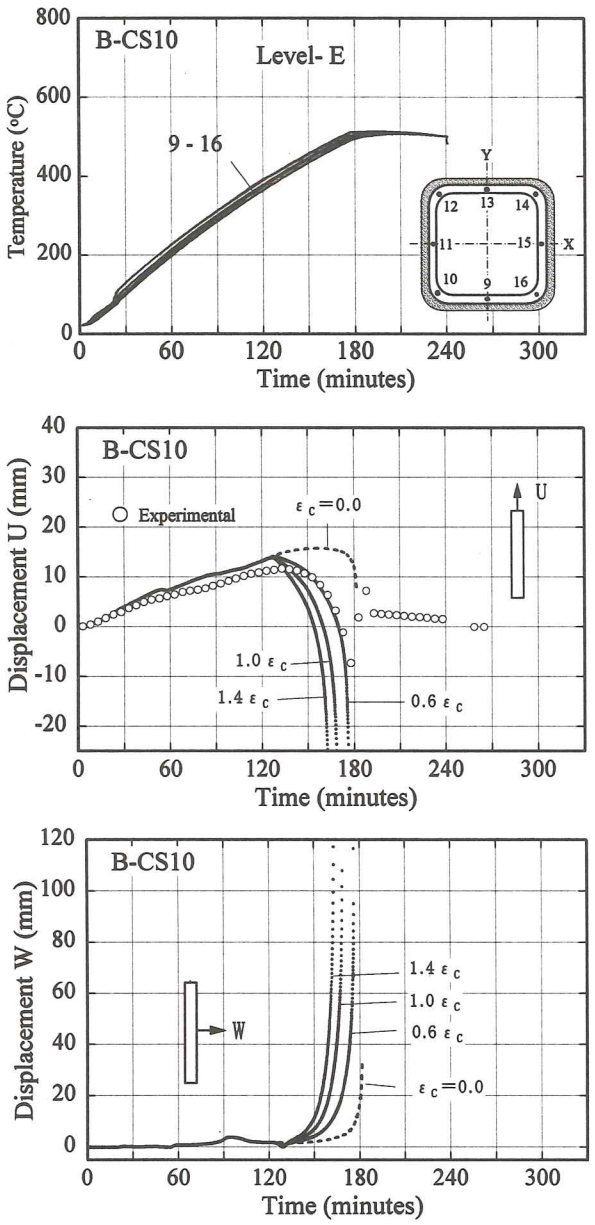

Fig. 9 Experimental and Calculated Values (B-CS10)

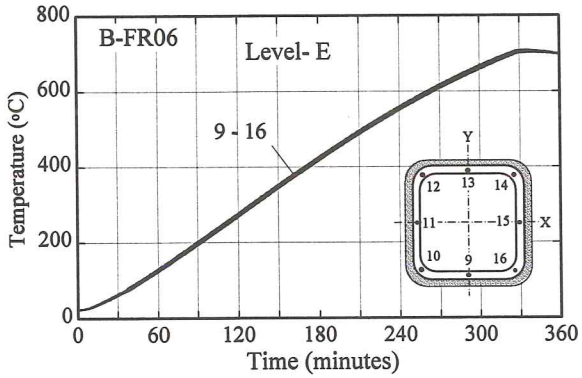

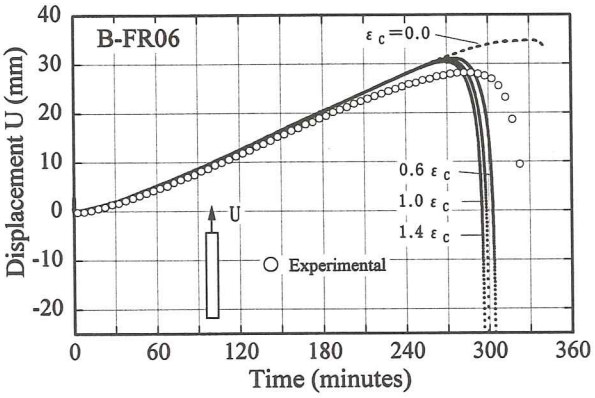

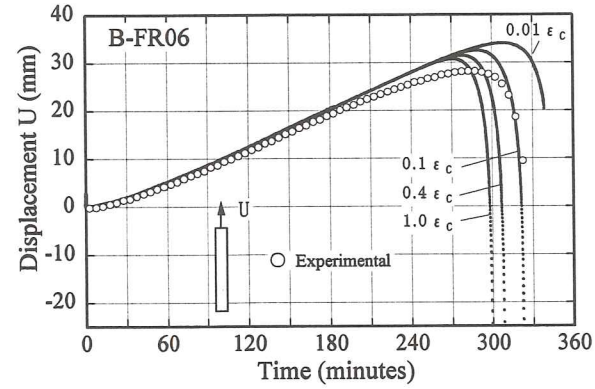

Fig. 10 Experimental and Calculated Values (B-FR06)

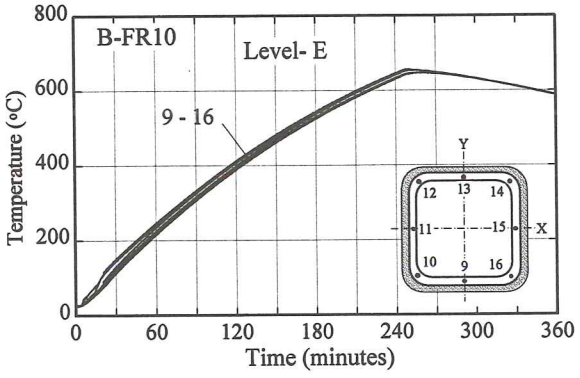

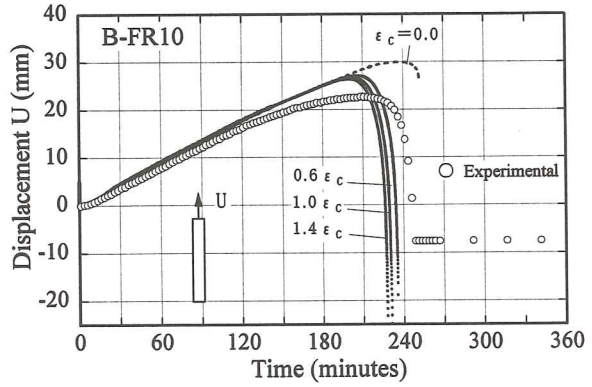

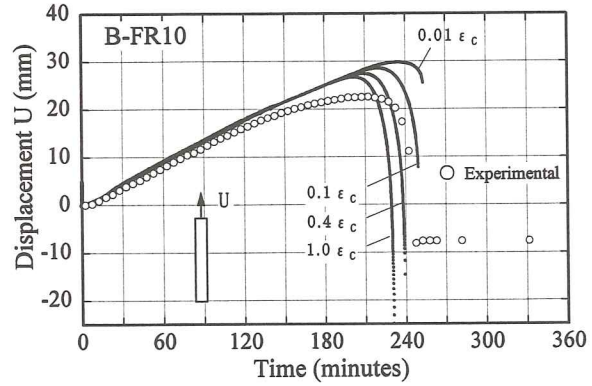

Fig. 11 Experimental and Calculated Values (B-FR10)

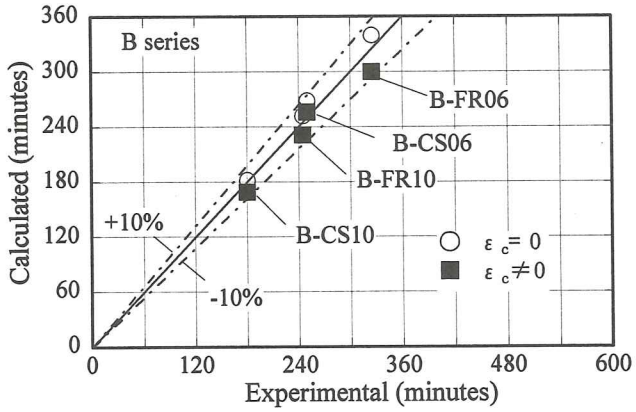

Fig. 12 Collapse Time

Fire Resistance Proficiency Testing of Gypsum/Steel-Stud Wall Assemblies

by

William L. Grosshandler[1]

ABSTRACT

This paper summarizes the results of a proficiency test program conducted in 2006 by the North American Fire Testing Laboratories (NAFTL) consortium. Gypsum/steel-stud wall assemblies, nominally rated at 1-h, were tested by six different organizations employing nine different furnace facilities following the guidance provided in ASTM E119-00. The program was completed successfully and forms the basis for future proficiency programs aimed at testing additional structural materials, elements, and systems subjected to fire test standards referenced in building codes.

KEYWORDS: structural fire resistance, fire tests, gypsum walls, proficiency programs

1.0 INTRODUCTION

In the aftermath of the World Trade Center collapse, a possible building code requirement that highrise structures withstand a complete burnout is being discussed in the U.S. Compartmentation and the integrity of bearing and non-bearing walls play a role in the severity and rate of spread of the fire, and thus the fate of the structure in a burnout scenario.

The ability of a structural element or system to withstand a fire is rated by subjecting the element, or a representative section of the system, to the heat of a furnace. Wall systems approximately 3 m by 3 m (10 ft by 10 ft) in area are evaluated by mounting them in a fixture and exposing them to a flame in a furnace with a prescribed temperature rise. (A photograph of a typical wall furnace is shown in Fig. 1.)

ASTM E 119-00: *Standard Test Methods for Fire Tests of Building Construction Materials* is often cited in the U.S. model building codes; NFPA 251 and UL 263 are equivalent test methods. ISO 834-1 is the similar international standard, although it is never used in U.S. construction. Details on these and other test methods used to characterize the fire resistance of walls and other building elements are reviewed elsewhere (e.g., Grosshandler, 2002; Grosshandler, 2006). While there are some differences among the test protocols, the general procedures and many of the measurements prescribed in all four test methods are similar.

The fire resistance of the wall assembly in an actual building fire is assumed to be related to the length of time necessary for the test specimen to meet any one of several failure criteria:

- the maximum temperature increase on the unexposed side of the wall exceeds 181 °C (325 °F);
- the average temperature increase on the unexposed side of the wall exceeds 139 °C (250 °F);
- a breach occurs in the wall that allows hot gases from the furnace to penetrate and ignite a cotton target on the unexposed side of the wall; or
- the wall is unable to maintain its design load.

The fire resistance rating of the wall system is defined as the time (to the next lowest half-hour increment for times up to two

[1] Fire Research Division, Building and Fire Research Laboratory, National Institute of Standards and Technology, Gaithersburg, Maryland, 20899-8660, USA

hours, and to the next lowest hour for longer times) when any of the criteria indicated are exceeded. It is expected that a 2-h rated wall would resist failure in a real fire for a longer period of time than a similarly functioning 1-h rated wall, and this is invariably the case. What can not be expected, however, is that a 2-h rated wall would necessarily withstand an actual fire in a building for two hours, or that the wall would necessarily fail after two hours. The inability of the fire resistance rating to act as an absolute predictor of performance in an actual fire was recognized from the beginning when the forerunner of ASTM E119 was published in 1918. Over the years, however, the reference to fire resistance ratings in common time units has become erroneously interpreted to relate closely (or at least conservatively) to the actual time that a wall would be expected to resist a fire.

The shortcomings of the current methods for rating the fire resistance of wall systems are numerous; some are obvious and have been recognized for years:

- The maximum size of the wall system is limited by the size of the furnace.
- The load conditions for the test article may not adequately mimic field use.
- The thermal environment of the furnace does not mimic a real fire.
- The tests reveal no fundamental information about the performance of the specimen and provide little guidance on how to improve performance.
- The furnaces themselves are not standardized; hence, the same specimen could receive different ratings if tested in two different facilities.
- Ratings are based upon a single test, with no way to quantify the uncertainty or safety factor.

In spite of severe shortcomings, these test methods continue to be used throughout the world because (i) a massive data base has been established and is in continual use, (ii) history suggests that the test methods are conservative, and (iii) alternative methods have not been developed yet that are acceptable to the major parties involved.

2.0 NAFTL PROFICIENCY TEST PROGRAM

Designing structures to withstand the hazard posed by an unconfined building fire requires that the standard fire resistance tests be reliable and consistent, independent of the laboratory performing the test. Ascertaining the consistency of testing in North America is the focus of this paper.

2.1 North American Fire Testing Laboratories Consortium[2]

The North American Fire Testing Laboratories (NAFTL) consortium was formed in 2004 to provide a forum for the exchange of technical information, to conduct studies, and to develop industry consensus positions relating to the full range of fire tests; e.g., reaction to fire, fire suppression, fire resistance and fire detection. The organization is open to any North American-based independent commercial laboratory engaged in fire testing or research. Current members include Southwest Research Institute (SwRI), Underwriters Laboratories (UL); FM Approvals, Intertek, NGC Testing, and Western Fire Center. NIST, the National Research Council of Canada (NRC-C), and the Fire Testing Laboratory of the Bureau of Alcohol, Tobacco, and Firearms (ATF) are non-voting associate members of NAFTL.

The operations of the member laboratories of NAFTL are certified according to ISO 17025. As part of the certification process, organizations must demonstrate to a certifying body that they are proficient in conducting fire testing services offered to their customers, a task which is difficult for a test like ASTM E119. For this reason, and to gain a better understanding of the test itself as a means to overcome the shortcomings previously enumerated,

[2] http://www.naftl.org/

NAFTL organized a proficiency test program for ASTM E119-00 using a common structural element: a gypsum/steel-stud wall assembly.

2.2 Participants and Objectives

A total of nine different laboratories representing six different organizations participated in the proficiency test program. They included Intertek (three locations), UL (two locations), SwRI, NGC, Western Fire Center, and NRC-C. All of these laboratories routinely operate large-scale furnaces that rate the fire resistance of structural elements such as building partitions and non-load-bearing walls.

The guidance provided in ASTM E119-00 is imprecise with regard to the details on the design of the testing furnace, and the guidance allows some leeway in how the sample is to be prepared and instrumented, as well as the way the test is to be conducted. Thus, it is not surprising that different laboratories develop different standard operation procedures that are still within the constraints of the prescribed test method. In addition, the dimensions and materials used in constructing the test article often differ, and may not be within the control of the fire testing laboratory. When differences in ratings occur of ostensibly the same test article, it is not possible to attribute the cause of the difference to the test article itself, to the differences in furnace design and instrumentation, or to the differences in operational procedures. In order to assess these differences and how they might lead to uncertainty in the fire resistance rating of a product, proficiency testing is necessary using a standardized product, with the results of the testing accumulated and analyzed by a qualified independent party.

The objective of the current proficiency test program is to compare the behavior of different vertical furnaces and identify operational parameters that influence the performance of a generic non-load-bearing wall assembly undergoing an ASTM E119-00 resistance to fire test. The testing was conducted in accordance with the standard operating protocol of each participant.

The data from each test were collected in a common format and sent to the American Council of Independent Laboratories (ACIL), who acts as the secretariat for NAFTL. ACIL removed all identifying information from the data and delivered it to NIST, who was the qualified independent party responsible for analyzing and reporting the data.

The outcome from this proficiency test program is being used by the participating organizations to assess the relative performance of their furnaces. The data collected are also being used by NIST to help develop the needed relationship between furnace behavior and actual fires.

3.0 TEST PROCEDURES

3.1 Wall Assembly Description

The wall assembly was designed to be non-load bearing, nominally 1-h fire resistance rated, and consisting of a 15.9 mm (5/8 in) thick type X gypsum board (ASTM C36/1396), 3 m by 3 m (10 ft by 10 ft) with taped, staggered vertical seams, on each side of steel studs located on 0.41 m (16 in.) centers. The gypsum board was purchased by the individual laboratories in a single lot from the manufacturer since it was desired to have as little variation as possible in the gypsum board. All laboratories used the same steel studs (25 gauge) and fasteners (32 mm (1 ¼ in) long Type S drywall screws). The walls were constructed using each laboratories' established practice. The tests were documented and, in several cases, witnessed by NIST research staff.

3.2 Instrumentation

The furnace and wall assembly were instrumented according to the provisions in ASTM E119-00. Additional thermocouples (type K) were located as indicated in Fig. 2

to measure the temperature within the wall cavity. A thermal imaging camera was used in several of the tests to view the unexposed side of the wall assembly. The actual instrumentation employed and its placement on the specimen was documented by each laboratory.

3.3 Conduct of Test

The instrumented specimen was mounted on the vertical wall furnace and prepared for testing using the standard procedure of the respective laboratory. The furnace was controlled to follow the standard time-temperature curve specified in ASTM E119-00. Temperatures of the specimen and furnace were collected at least once a minute. A video record of the entire test was made, along with photos of observed damage to the specimen when it occurred.

The test was designed to continue until all of the following conditions were met:

- at least one thermocouple used in standard practice by the laboratory on the unexposed side of the specimen reached a temperature 181 °C (325 °F) above its initial temperature;
- the average temperature of thermocouples used in standard practice by the laboratory on the unexposed side of the specimen reaches 139 °C (250 °F) above its initial average temperature; and
- a crack opens up in the specimen large enough and hot enough to ignite cotton waste.

The hose stream test (which is specified in ASTM E119-00) was not applied to the specimen.

3.4 Data Treatment

Each laboratory prepared a standard ASTM E119-00 data sheet for the tests conducted. In addition, the following data were compiled:

- temperature vs. time for all specimen thermocouples
- temperature vs. time for the standard specimen thermocouples
- temperature vs. time for the furnace control thermocouples

These data were collected by ACIL and sent to NIST for analysis, without identifying which data set belonged to which laboratory. Proficiency is based upon how much an individual lab differed from the following composite results of the group:

- time for the first thermocouple to reach 181 °C (325 °F) above its initial temperature
- time for the average temperature to reach 139 °C (250 °F) above its initial average
- time for a crack to open up sufficient to ignite a cotton swab
- T vs. t for the peak temperature
- T vs. t for the average temperature

4.0 TEST RESULTS

4.1 Average Furnace Temperatures

The temperature of the furnace is determined from the average of multiple shielded, slow time-response thermocouples located within the furnace cavity. Most furnaces are controlled manually, with an experienced operator increasing or decreasing the fuel flow to different burners to maintain uniformity at the temperature specified in ASTM E119-00. The standard time-temperature curve is shown in Fig. 3 as the dotted red line. At five minutes, the furnace temperature is required to be 538 °C (1000 °F); at fifteen minutes it must be 759 °C (1399 °F); the target temperature at one hour is 927 °C (1700 °F); and at 2 hours the temperature is 1010 °C (1850 °F).

The temperatures of the nine laboratory furnaces, designated A1 through A9, are also plotted in Fig. 3. The vertical bars represent one standard deviation around the mean of the nine tests. During the start-up period, several of the furnaces tend to either

lag or over-correct, but by fifteen minutes into the test, eight of the nine furnaces fall close to a single curve. Furnace A3 lags the group until about 40 minutes into the test.

The Standard requires that the integral of the temperature over time be within 7.5 % of the specified curve for tests lasting more than one hour. For the nine furnaces in the proficiency test program, the areas under the temperature curves were all within 2 % of the area specified in ASTM E119-00.

4.2 Peak Wall Temperatures

Because each furnace has a unique design and method of temperature control, it is not possible to predict which of the thermocouples positioned on the side of the wall that is unexposed to the flames will be the hottest. For most of the current testing, the temperature increase indicated by TC6 was within one minute of being the hottest, and for ease of comparison, this temperature increase is plotted in Fig. 4 for the nine furnace tests. Note that the ambient temperature (which varied between 17 °C and 33 °C (62 °F to 92 °F)) has been subtracted from the temperature of TC6. The dotted line in Fig. 4 represents the failure criteria (181 °C (325 °F)) specified in ASTM E119-00. The first laboratory to reach the limit is A7, at 62 minutes; laboratory A9 is the last, with TC6 reaching the limit more than 10 minutes later.

The highest temperature increases measured on the unexposed surface of the wall assembly at any given time (regardless of thermocouple location) are plotted on the vertical axis in Fig. 5 against the average of the nine tests on the horizontal scale. If all of the tests were identical, the data would fall on the solid line. Up to about 93 °C (200 °F), the tests are well correlated; however, at higher values the maximum temperature increases at any given time diverge greatly, ranging from more than 55 °C (100 °F) higher to 55 °C (100 °F) lower for mean high temperature increases equal to the limiting temperature in ASTM E119-00 (the vertical dotted line at 181 °C (325 °F) indicates the limit).

4.3 Average Wall Temperatures

The average of the thermocouples measuring the temperatures on the unexposed side of the wall specimen is shown in Fig. 6 for the nine furnace tests; Fig. 7 is a plot of the standard deviation of these temperatures around the mean. The average temperatures are well grouped for the first 55 minutes of the test, with standard deviations less than 6 °C (10 °F), except for a short period of time during start-up. At 70 minutes, the individual average unexposed face temperature increases deviate from the overall mean by as much as 139 °C (250 °F).

4.4 Fire Resistance Ratings

The key output of ASTM E119-00 is the fire resistance rating. In all nine furnace tests, this wall design received a rating of 1-h. For five of the laboratories, the failure time was based upon the average temperature increase on the unexposed face exceeding 139 °C (250 °F). The maximum allowed individual temperature on the backside of the wall (181 °C (325 °F)) was the failure limit for the remaining four laboratories. In no case was the wall breached in less than 70 minutes. The wall was not designed to be loaded; hence, the failure to maintain a load was not examined.

The chart in Fig. 8 indicates the time that the specimen failed for each of the furnace tests. The overall average time was 65 minutes, with a standard deviation of 3 minutes. Laboratory A6 exceeded the average by more than one standard deviation, and laboratory was less that the average by more than one standard deviation.

Table 1 displays these times, as well as the failure criteria. The far right column indicates additional temperature failure criteria that occurred within one minute of the first failure. Note that the fire resistance rating, shown in the second column, is the same for all nine laboratories: 1-h.

5.0 CONCLUSIONS

Round-robin testing programs have been attempted in the past to identify uncertainties in the results and deficiencies in the ASTM E119-00 test method. A proficiency test program, in contrast, focuses upon the laboratory rather than the test method. The results of the proficiency program can be used by the participating laboratories to satisfy the requirements for ISO 17025 certification. The proficiency test program undertaken by the NAFTL consortium and described here is the first ever to target a fire resistance test of this magnitude.

The following conclusions can be drawn from the results of this effort:

- The participating laboratories, using their individual standard operating procedures, were able to arrive at an identical 1-h rating for the gypsum wall specimen.
- The variability among laboratories in measured time-to-failure for a 1-h rated gypsum wall, based upon ASTM E119-00, should not be expected to be better than plus/minus 5 minutes.
- The variability in individual peak temperature increase measurements at similar locations on different 1-h rated gypsum wall assemblies is likely to be at least plus/minus 22 °C (40 °F) for times greater than one hour.
- Individual temperature increases measured on the unexposed side of a 1-h rated gypsum wall diverge quickly among laboratories as the specimens approach failure, differing by as much as 166 °C (300 °F) at the average time of failure.
- The proficiency test program conducted by the NAFTL consortium will assist the participating laboratories in maintaining ISO 17025 certification, and will act as a model for future proficiency programs for additional fire test methods.

6.0 ACKNOWLEDGEMENT

The author acknowledges the hard work by S. Manzello and A. Maranghides of NIST in coordinating and observing the furnace tests, the cooperation of the participating laboratories, and the assistance of E. Van Aken of ACIL, who sanitized the data.

7.0 REFERENCES

ASTM E 119-00: "Standard Test Methods for Fire Tests of Building Construction Materials," ASTM International, West Conshohocken, PA, 2000.

ASTM C1396-04: "Standard Specification for Gypsum Wallboard," ASTM International, West Conshohocken, PA, 2005.

Grosshandler, W. (ed.), 2002, "Fire Resist. Determination and Perf. Prediction Research Needs Workshop: Proc.," NISTIR 6890, Nat. Inst. of Stds. and Technology, Gaithersburg, Sept.

Grosshandler, W., 2006, "The Response of Structures to Fire -- Advances and Challenges in Predicting Behavior," *Proceedings of the 13th International Heat Transfer Conference*, Sydney.

ISO/IEC 17025:1999(E), "General Requirements for the Competence of Testing and Calibration Laboratories," International Organization for Standardization, Geneva, 1999.

ISO 834: "Fire resistance tests -- Elements of Building Construction," Parts 1-9 International Organization for Standardization, Geneva.

NFPA 251: "Standard Methods of Test of Fire Endurance of Building Construction Material" NFPA Int'l, Quincy, MA, 1999.

UL 263: "Fire Tests of Building Construction and Materials," Underwriters Laboratories, Northbrook, IL, 1998.

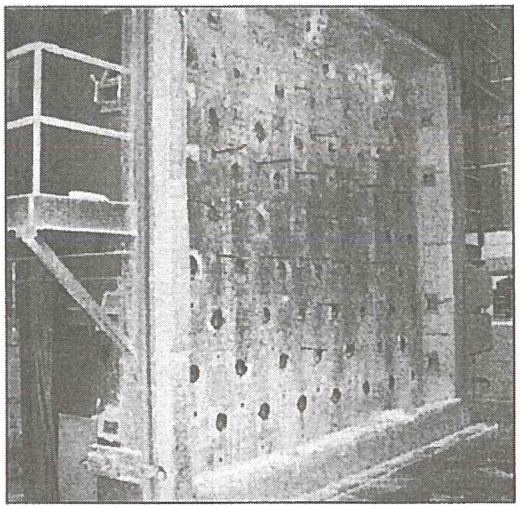

Figure 1: Photograph of the interior of a typical wall furnace showing multiple gas burners (courtesy of Underwriters Laboratories).

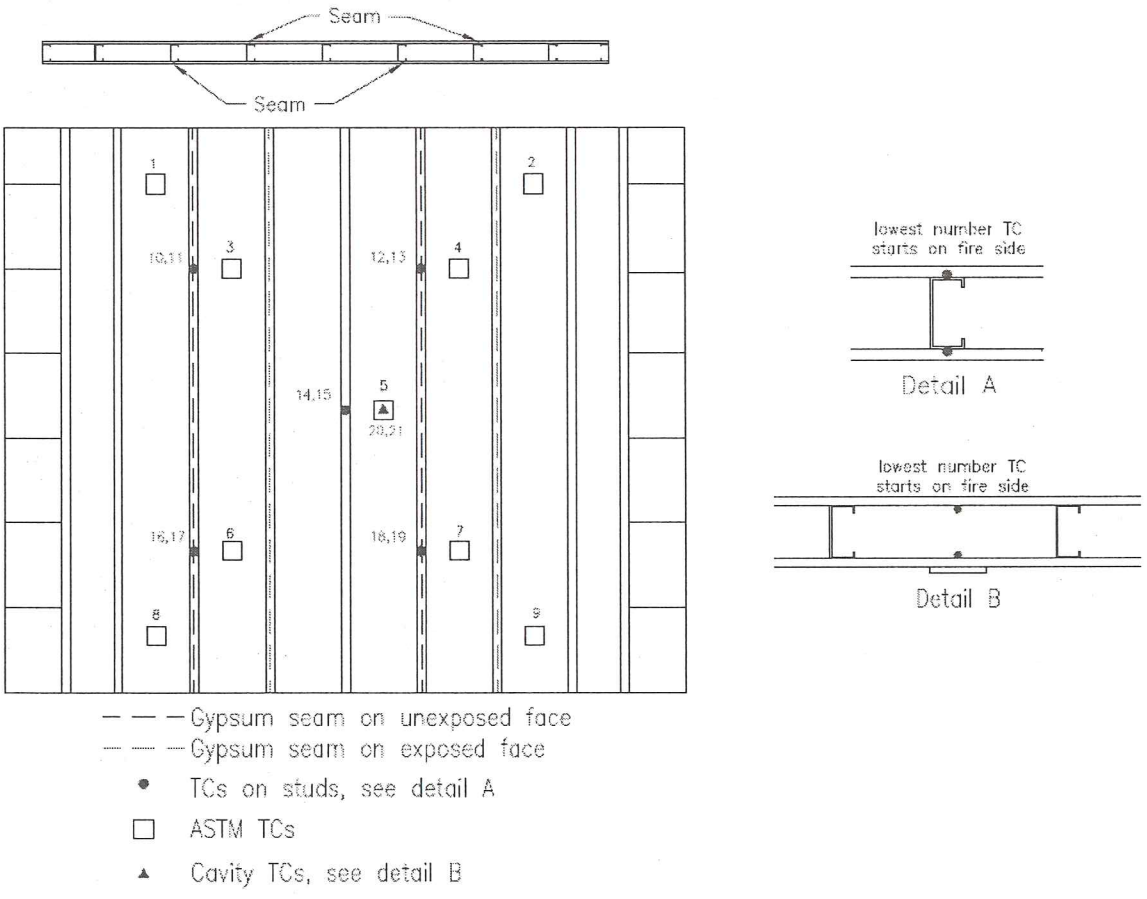

Figure 2: Gypsum/steel-stud wall assembly and location of thermocouples

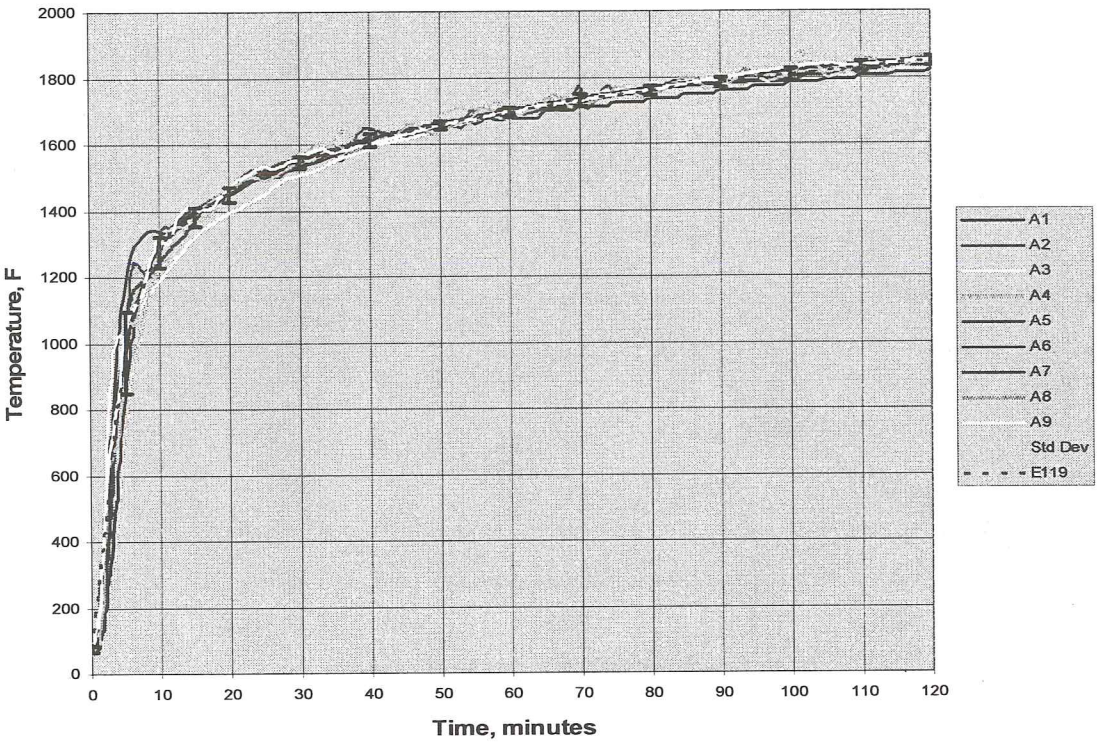

Figure 3: Average furnace temperatures

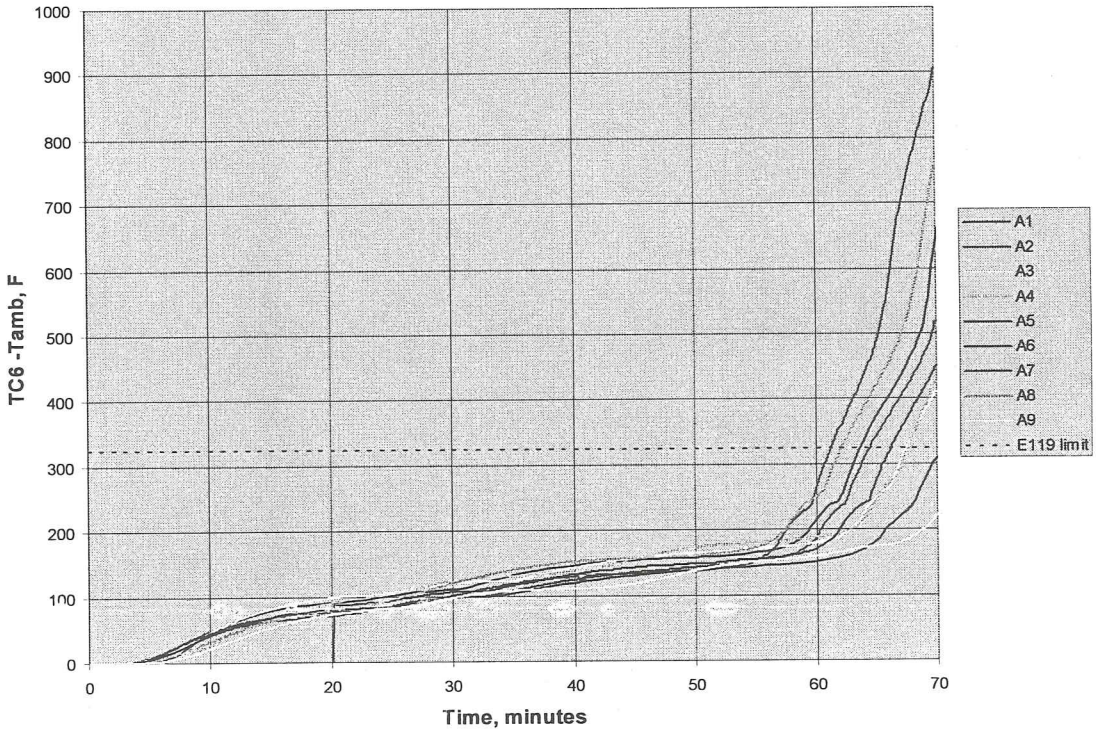

Figure 4: Peak temperature increase on unexposed side of wall (TC 6)

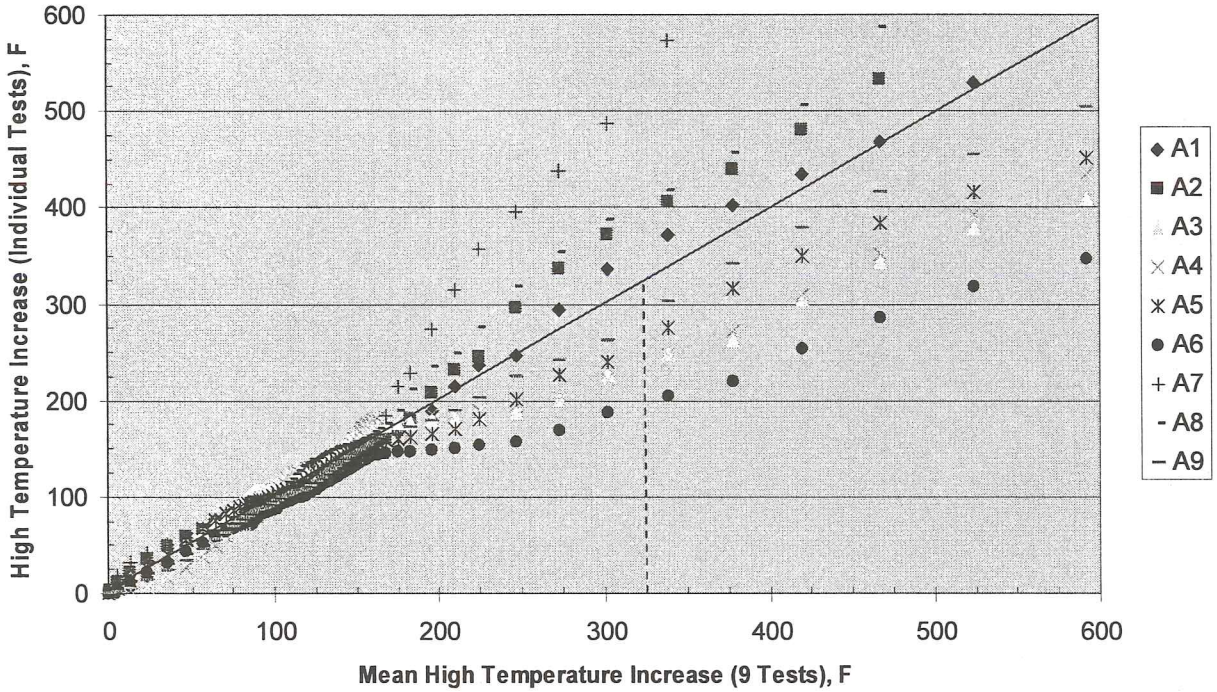

Figure 5: Highest temperature increases on unexposed side of wall, plotted vs. the nine-test average

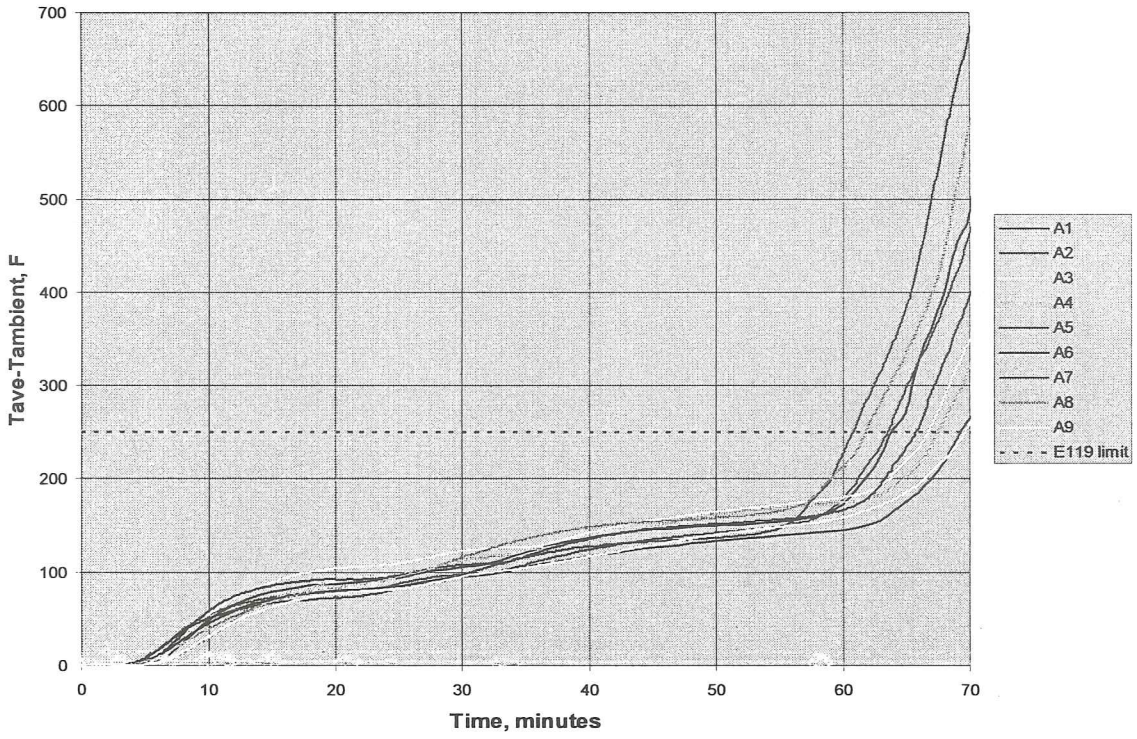

Figure 6: Average thermocouple temperature increase on unexposed side of wall

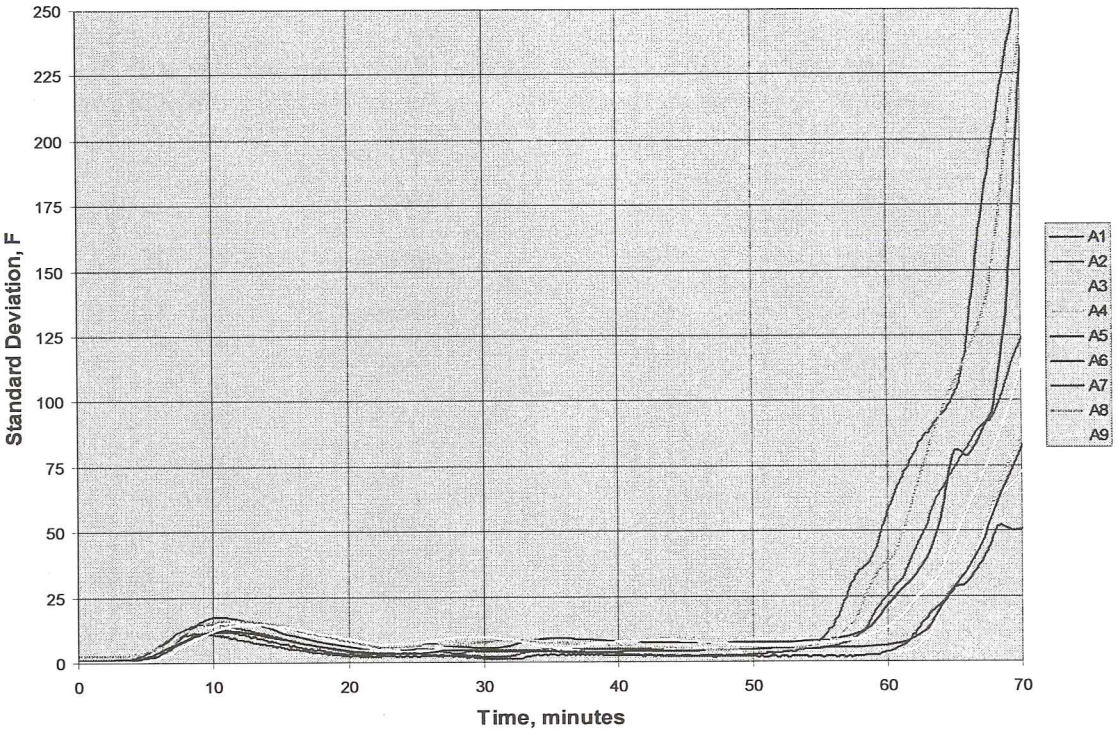

Figure 7: Standard deviation of average temperatures on unexposed side of wall

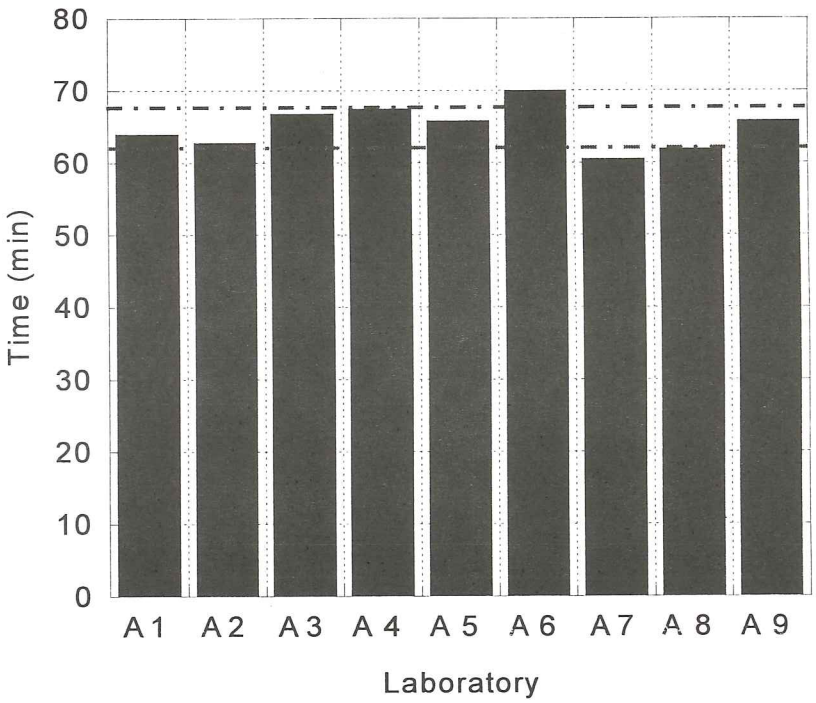

Figure 8: Time to First Failure Criteria in Each of Nine Furnace Tests; $t_{average}$ = 65.0 min. Dotted lines represent standard deviation of +/- 3.0 min.

Table 1: Summary of Failure Criteria

Laboratory	Fire Resistance Rating	Time to First Failure, minutes	Failed Thermocouple Reading	Other TC's Failing Within 1 Minute
A1	1 hour	64	average	TC3, 5, 7
A2	1 hour	62.8	TC3	average
A3	1 hour	66.8	average	TC4, 6, 8
A4	1 hour	67.5	average	TC3, 6, 8
A5	1 hour	65.8	average	TC6
A6	1 hour	70	TC3	TC4, 5, 6, 7, average
A7	1 hour	60.6	TC7	TC3, 5, 6, average
A8	1 hour	61.9	average	TC3, 4, 6
A9	1 hour	65.8	TC5	none

THEME 6

Geotechnical Engineering and Ground Motion

Correlation between aspects of slope failures and surface displacement triggered by the 2005 northern Pakistan earthquake

by

Hiroshi P. Sato[1], Hiroshi Une[1] and Mikio Tobita[1]

ABSTRACT

Northern Pakistan earthquake (Mw7.6) of October 8, 2005 occurred in the Kashmir region controlled by Pakistan. The previous studies reported 1) some uplift (on the northeast side) and dextral strike-slip crustal deformation occurred on the exsisting active fault (Balakot-Garhi fault), 2) 3-D crustal deformation map was produced using ENVISAT/Synthetic Aperture Radar (SAR) amplitude images, 3) the earthquake-induced 2,424 slope failures were identified from the interpretation using SPOT5 (System pour l'Observation de la Terre 5) stereo-images, almost all of them occurred on the hanging wall of the fault and near the fault. In this study area, which is 4km-wide zone from the fault on the hanging wall, we calculated 2-D (horizontal) deformation aspect from the 3-D crustal deformation map, we selected 979 large slope failures whose size is 15.8m by 15.8m and more, and we overlaid the large failures' slope aspect on the horizontal crustal deformation aspect. As a result, many large slope failures faced SW and S direction, and it was found that this anisotropic aspect is correspondent to that of planar crustal deformation. This fact infers that aspect of slope failures may be mainly controlled by the direction of the displacement of the earth surface.

KEYWORDS: SPOT5, ENVISAT, SAR, Pakistan, earthquake, slope failures, crustal deformation

1. INTRODUCTION

Northern Pakistan earthquake (Mw7.6) of October 8, 2005 occurred in the Kashmir region in the northwestern part of the Himalayas. The epicenter is north-northeast direction and 105 km away from Islamabad.

The crustal deformation was spatially mapped with Synthetic Aperture Radar (SAR) data from the European Space Agency's ENVISAT [1], and it was revealed that the newly deformed area occupies a 90-kilometer-long northwest-southeast trending strip. Heavily damaged area north of Muzaffarabad has the maximum deformation up to six-meter uplift as observed by the satellite. The detected crustal deformation was along the active fault and all observations were consistent with previously known directions of past fault movements.

There is the known active fault (Balakot-Garhi fault, Fig.1) stretching NW-SE direction near the epicenter, some uplift (on the NE side) and dextral (right-lateral) strike-slip activities were revealed [2]. According to the fault model optimal calculation in a homogeneous elastic half-space as formulated by [3], three planes of dip-slip reverse fault were reported [4].

Furthermore, many slope failures were triggered by the earthquake [5], and 2,424 slope failures were detected in the area of 55km by 51km including Muzaffarabad [6]. Almost all of the slope failures were located on the hanging wall of Balakot-Garhi fault.

Purpose of this study is to clarifythe relation between the slope aspect of slope failures triggered by the earthquake and the direction of crustal movement by the earthquake.

2. STUDY AREA

The study area is 4km-wide zone of the hanging wall from the Balakot-Garhi fault, whose area is 245.7km^2. More than 4km away from the fault,

[1] Geography and Crustal Dynamics Research Center, Geographical Survey Institute, Tsukuba-shi, Ibaraki-ken 305-0811 Japan

the number of the slope failures is remarkably reduced.

3. METHODS

3.1 SPOT5 image interpretation

After the earthquake, SPOT5 (System pour l'Observation de la Terre 5) panchromatic images were taken on October 20 and 27, 2005. The incident angle of October 20 and 27 images is at the left side of 26.4 degree and at the right side of 30.4 degree, respectively.

To delineate the interpreted slope failures and record their planar location, in advance, orthographic (ortho-) images were prepared. In other words, SPOT5 images were geometrically corrected using 34 ground control points (GCPs) and 90m-resolution Shuttle Radar Topography Mission- (SRTM-) digital elevation model (DEM). Next, we interpreted SPOT5 stereo-images in the study area, and delineated the slope failures on the orhto-image.

Before the earthquake, SPOT5 panchromatic images were taken on March 2, 2004. As referring it, the slope failures existed before the earthquake were removed, and the slope failures were selected.

3.2 Calculation of slope aspect at the slope failure.

The slope failures were overlaid on the 15m-resolution DEM derived from TERRA/ASTER data [7]. The ASTER has a stereoscopic capability in the along-track direction mainly for DEM generation. To fit the size of slope failure in area with ASTER-DEM resolution, those whose area are less than 15.8m by 15.8 m were removed, and relatively large slope failures were selected. As a result, the number of the selected slope failures in the study area was 979.

3.3 3-D crustal deformation analysis

Tobita et al (2006) [1] clarified the 3-D components of the crustal deformation by the earthquake using multiple SAR image matching [8]. Three pairs of ENVISAT/SAR images, i.e., those taken on 17 September 2005 and 22 October 2005 from descending orbit, which means the SAR sensor looked down on the study area from the east sky, taken on 19 September 2005 and 24 October 2005 and 3 September 2005 and 12 November 2005 from ascending orbit, which means the SAR sensor looked down on the study area from the west sky. The two components such as azimuth (longitudinal) and line of sight (crosswise) components of crustal deformation were independently calculated from the above three pairs of the SAR image, next, Cartesian (easting, northing, and upward) components were calculated by least square method, finally, horizontal and vertical components of the crustal deformation were obtained from the Cartesian components.

4. RESULTS AND DISCUSSION

Ratio of the aspect of the slope failures is shown as black solid bold line in Fig.2(a), indicating concentration of S and SW aspect. Black solid thin line in Fig.2(a) shows the ratio of the aspect of all slopes of the mountain in the study area. In general, SW, W, and NW facing slopes exist in this area. By comparing these, it is recognized that the slope failures occurred prominently on the S and SW facing slopes.

Fig.2(b) shows the ratio of the direction of the horizontal component of the crustal deformation in the study area., which concentrates in S and SW direction. The similarity of prominence of aspect of slope failures and direction of horizontal crustal deformation suggests that the failures were triggered by not the ground motion but the displacement of the earth surface by the crustal movement itself.

The crustal deformation detected by the SAR technology [1][4] shows the mixture of the deformation triggered by the main shock but also by the aftershocks and aftereffect, but according to the interview for afflicted people living near the Balakot-Garhi fault, main crustal deformation was formed at a burst (Prof. Takashi Nakata, Hiroshima Technology University, Japan, personal communication). This suggests that almost all amount of surface displacement occurred at the main shock and the

slope failures were triggered.

Earthquake-induced slope failures are often explained as follows: when driving force derived from seismic acceleration in unit area exceeds sediment shear stress on the slope, they occur [9], and it is valid that many slope failures were triggered by the acceleration of S-wave, which is transverse wave and almost all of the seismic-wave energy is occupied by S-wave energy. However, the seismic wave directivity by the 2005 north Pakistan earthquake is not reported because an installed strong-motion seismograph network is not known in the study area. Even if the strong motion were recorded, the result would show that the motion oscillated from one direction to the opposite direction, but black solid bold line in Fig.2(a) does not show the prominent slope ratio of both S-SW and N-NE. In the case of Mikawa earthquake (M6.8) occurred on 13 Jan 1945 in SE Japan, the houses built on the hanging wall of low-angle reverse fault were heavily damaged, and it was reported that direction of the collapsed houses coincided with the direction of the horizontal crustal deformation [10]. It infers that the prominent aspect of many slope failures in this study may be controlled not by the ground motion of S-wave but by some other factors such as the decline of friction by the rapid displacement of the ground toward the particular direction.

5. CONCLUSIONS

Digital elevation model was able to be directly produced by satellite remote sensing image, and slope aspects in wide area were able to be effectively calculated compared with existing topographic map. In a wide study area, neither had it been possible until crustal deformation was mapped by the SAR technology at uniform resolution, nor had it been possible to correlate slope aspect of failures to direction of horizontal crustal deformation.

There is scarce example to correlate them, but if many example of the correlation between them will be stocked, it will be revealed whether the prominent aspect of slope failures has relation to horizontal direction of crustal deformation or not. In the case that the correlation is approved, this knowledge may be useful information to reduce earthquake-induced slope failure disaster against human-related facilities by considering slope aspect and the past crustal deformation directions triggered by the past earthquakes.

5. REFERENCES

1. Tobita, M., Nishimura, M., Ozawa, S. and Fujiwara, S.: Crustal deformation of 2005 northern Pakistan earthquake detected by SAR (2) SAR image matching and 3D deformation map. Abstract of Japan Geoscience Union Meeting 2006, 2006. http://www.jpgu.org/publication/cd-rom/2006cd-rom/pdf/D124/D124-017_e.pdf (accessed on 13 Apr 2007)
2. Kumahara, Y., Nakata, T.: Active faults in the epicentral area of the 2005 Pakistan earthquake. Research Center for Regional Geography, Hiroshima University, Japan, 54pp., 2006.
3. Okada, Y.: Surface deformation due to shear and tensile faults in a half-space, Bulletin of the Seismological Society of America, 75, 1135-1154.
4. Fujiwara, S., Tobita, M., Sato H.P., Ozawa, S., Une, H., Koarai, M., Nakai, H., Fujiwara, M., Yarai, H., Nishimura, T. and Hayashi F.: Satellite data gives snapshot of the 2005 Pakistan earthquake, EOS, Transactions of American Geophysical Union, 87, 73-77.
5. Sato, H.P., Koarai, M., Une, H., Hasegawa, H., Iwahashi, J., Kamiya, I. and Ishitsuka, Y.: Interpretation of landslide distribution triggered by the northern Pakistan earthquake on 8 October 2005 using 2.5m-resolution SPOT 5 stereo-imagery, Extended Abstracts of International Conference on Earthquake in Pakistan, 94-98, 2006. http://www.gsp.gov.pk/international_conference.pdf (accessed on 13 Apr 2007).
6. Sato, H.P., Hasegawa, H., Fujiwara, S., Tobita, M., Koarai, M., Une, H. and Iwahashi, J.: Interpretation of landslide distribution triggered by the 2005 northern Pakistan earthquake using SPOT5 imagery, Landslide, 4, in press.

7. Urai, M., Nakamura, R., Kawabata, D., Tsuchida, S., Iwasaki, A.: Landslides observation with ASTER caused by the 2005 Pakistan Earthquake, Extended Abstracts of International Conference on Earthquake in Pakistan, 115-116, 2006. http://www.gsp.gov.pk/international_conference.pdf (accessed on 13 Apr 2007).
8. Tobita, M., Murakami, M., Nakagawa, H., Yarai, H., Fujiwara, S., Rosen, P.A..: 3-D surface deformation of the 2000 Usu eruption measured by matching of SAR images, Geophysical Research Letters, 28, 4291-4294, 2001.
9. Chigira, M.: Dry debris flow of pyroclastic fall deposits triggered by the 1978 Izu-Oshima-Kinkai earthquake: the "collapsing" landslide at Nanamawari, Mitaka-Iriya, southern Izu Peninsula, Journal of Natural Disaster Science, 4(2), 1-32.
10. Ando M., Kawasaki, I.: Acceleration near low-angle reverse fault – asymmetricity of seismic damage on hanging and foot walls, Proceedings of autumn meeting on Seismological Society of Japan, p.107, 1973.

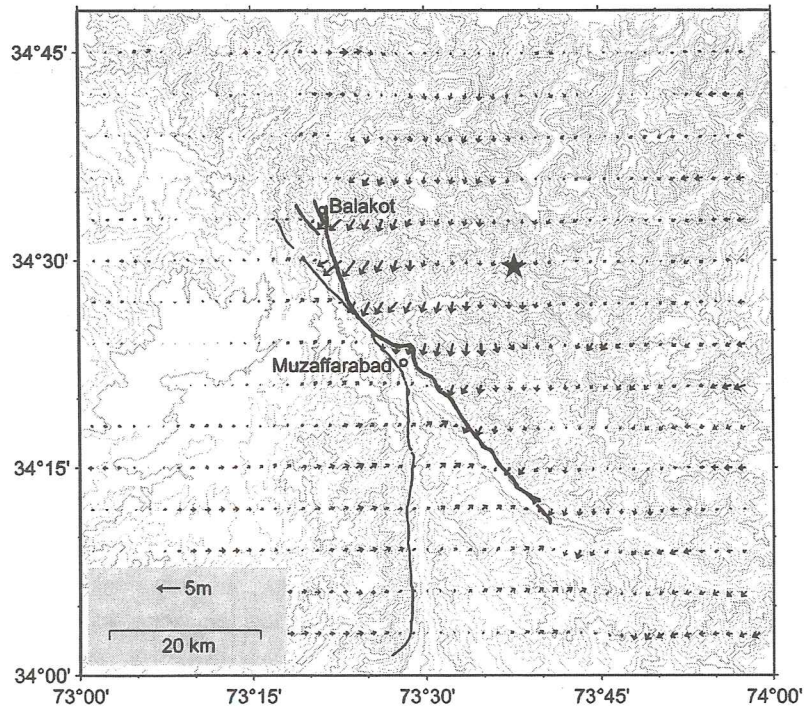

Fig.1 Detected crustal deformation using ENVISAT/SAR data (wavelength of 5.6 cm, C-Band) [1]. The star means epicenter of the earthquake. Arrow indicates 2-D (horizontal) deformation (amount and direction). Black solid bold and thin lines are Balakot-Garhi fault and Jhelum fault [2], respectively.

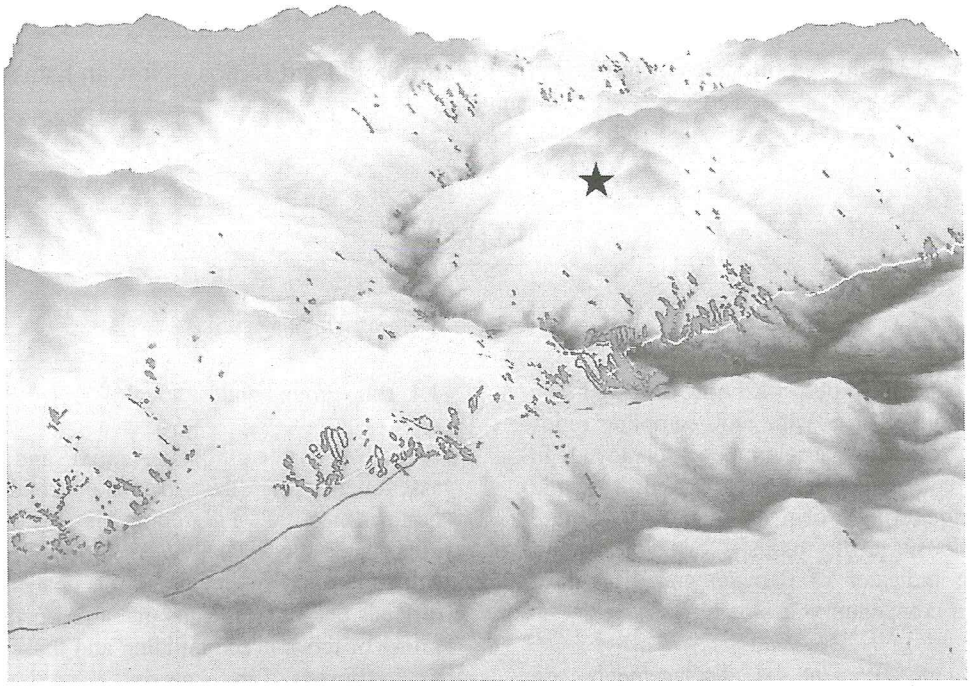

Fig.2 Bird-eye view from the east direction around the epicenter (black star). Polygons are slope failures interpreted using SPOT5 stereo-imagies. Pale and dark lines are Balakot-Garhi fault and Jhelum fault [2], respectively.

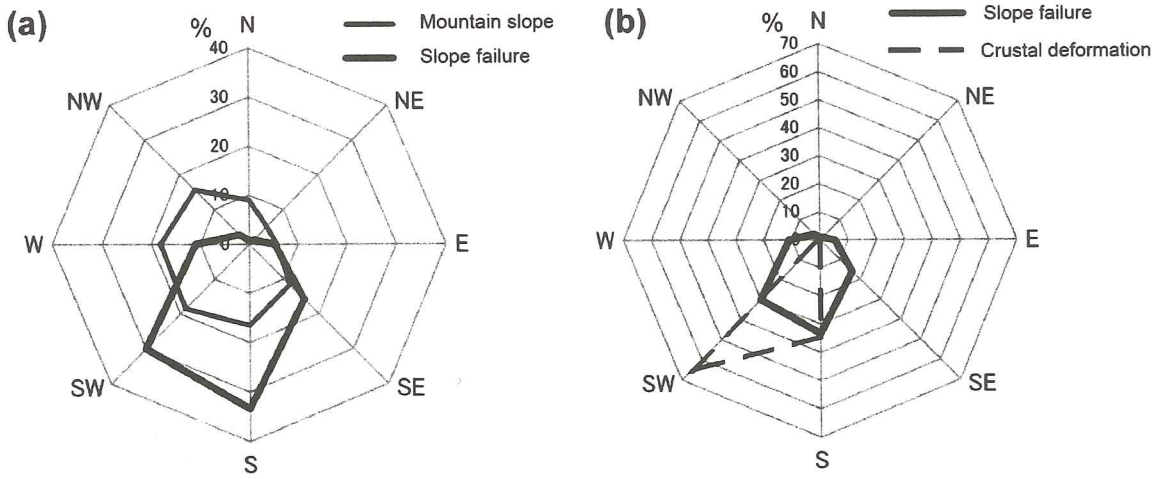

Fig. 3 (a) Relation of slope aspect count ratio between mountain slope and large slope failures on the hanging wall within 4 km from Balakot-Garhi fault, (b) Relation of slope aspect count ratio between slope failures and horizontal crustal deformation.

Response Health Monitoring of Buildings Using Threshold Drift Ratios – Now an Established Method

by

M. Çelebi[1]

ABSTRACT

In earlier papers, we described how observed data from differential GPS with high sampling ratios and from classical accelerometer deployed in structures can be configured to establish seismic health monitoring of structures. In these configurations, drift ratios[1] are the main parametric indicator of damage condition of a structure or component of a structure.

Real-time measurement of displacements are acquired either directly using GPS or by double integration of accelerometer time-series data. Recorded sensor data is then related to the performance level of a building. Performance-based design method stipulates that for a building the amplitude of relative displacement of the roof of a building (with respect to its base) indicates its performance.

Experience with both types of sensor deployments (GPS and accelerometers) indicate that they are reliable and provide pragmatic alternatives to alert the owners and other authorized parties to make informed decisions and select choices for pre-defined actions following significant events. Furthermore, recent adoption of such methods by financial and industrial enterprises is testimony to their viability.

KEYWORDS: real-time, health monitoring, buildings, GPS, displacement, drift ratio, acceleration, accelerometer, internet communication, data acquisition.

[1] Drift ratio is defined as relative displacement between any two floors divided by the difference in elevation of the two floors. Usually, this ratio is computed for two consecutive floors.

1. INTRODUCTION

1.1. Background and Rationale

Following an earthquake, rapid and accurate assessment of the damage condition or performance of a building is of paramount importance to stakeholders [owners, leasers, permanent and/or temporary occupants, and city officials and rescue teams that are concerned with safety of those in the building and those that may be affected in nearby buildings and infrastructures]. Until recently, assessments of damage to buildings following an earthquake were essentially carried out by inspections of city-designated engineers following procedures similar to ATC-20 tagging requirements *(ATC* 1989). Tagging usually involves visual inspection only and is implemented by colored tags indicative of potential hazard to occupants - green indicating the building can be occupied; that is the building does not pose a threat to life safety, yellow indicates limited occupation (that is, hazardous to life safety but not to prevent limited entrance to retrieve possessions), and red indicating entrance prohibited (that is, hazardous to life). However, one of the impediments to accurately assessing the damage level of structures by visual inspection is that some serious damage may not be visible due to the presence of building finishes and fireproofing. In the absence of visible damage to the building frame, most steel or reinforced concrete moment-frame buildings will be tagged based on visual indications of building deformation, such as damage to partitions or glazing. Lack of certainty regarding the actual deformations that the building experienced may

[1] Earthquake Hazards Team, USGS (MS977), 345 Middlefield Rd., Menlo Park, Ca, 94025

typically lead an inspector toward a relatively conservative tag. In such cases, expensive and time-consuming intrusive inspections may be recommended to building owners (e.g., it is known that, following the [M_w=6.7] 1994 Northridge, CA earthquake, approximately 300 buildings ranging in height from 1 to 26 stories were subjected to costly intrusive inspection of connections (FEMA352, SAC 2000)).

However, as described in this paper, an alternative to tagging is now available to owners and their designated engineers by configuring real-time response of a structure instrumented as a health monitoring tool. As Porter and others (2006) state, most new methods do not utilize real-time measurements of deformations of a building for assessments of building's performance during an event with the exception outlined by Çelebi and Sanli (2002) and Çelebi and others (2004). In these applications, differential GPS (Çelebi and Sanli, 2002) with high sampling ratios and classical accelerometer deployed structures (Çelebi and others, 2004) are configured to obtain data in real-time and compute drift ratios as the main parametric indicator of damage condition of a structure or one or more components of a structure. The rationale here is that a building owner and engineers are expected to use the response data acquired by a real-time health monitoring system to justify a reduced inspection program as compared to that which would otherwise be required by a city government for a similar non-instrumented building in the same area[2]. It is possible that depending on the deformation pattern and associated damage indicators observed in a building, it could also be possible to direct the initial inspections toward specific locations in the building that experienced large and potentially damage-inducing drifts during an earthquake.

Examples of and data from either type of sensor deployment (GPS or accelerometers) indicate that these methods are reliable and provide requisite information for owners and other parties to make informed decisions and select choices for pre-defined actions following significant events. Furthermore, recent additional adoptions of such methods by financial and industrial enterprises validate its usefulness.

1.2. Requisites

The most relevant parameter to assess performance is the measurement or computation of actual or average story drift ratios. Specifically, the drift ratios can be related to the performance- based force-deformation curve hypothetically represented in Figure 1 [modified from Figure C2-3 of *FEMA-274* (ATC 1997)]. When drift ratios, as computed from relative displacements between consecutive floors, are determined from measured responses of the building, the performance and as such "damage state" of the building can be estimated as in Figure 1.

Measuring displacements directly is very difficult and, except for tests conducted in a laboratory (e.g., using displacement transducers), has not yet been feasibly achieved for a variety of real-life structures. For structures with long-period responses, such as tall buildings, displacement measurements using GPS are measured directly at the roof only; hence, drift ratio then is an average drift ratio for the whole building. Thus, recorded sensor data is related to performance level of a building; hence, related to performance-based design which stipulates that for a building the amplitude of relative displacement of the roof of a building (with respect to its base) indicates its performance.

For accelerometer based systems, the accelerometers must be strategically deployed at specific locations on several floors of a building to facilitate real-time measurement of the actual structural response, which in turn is used to compute displacements and drift ratios as the indicators of damage.

Table 1 shows typical drift ratios for steel moment resisting framed buildings. The table is developed from FEMA 352 (SAC 2000). For

[2] The City of San Francisco, California, has developed a "Building Occupancy Resumption Program" (BORP, 2001) whereby a pre-qualified Occupancy decision making process as described in this paper may be proposed to the City as a reduced inspection program but in lie of detailed inspections by city engineers following a serious earthquake.

reinforced concrete framed buildings, the lower figures may be more appropriate to adopt.

Table 1. Summary of Suggested Typical Threshold Stages and Ranges of Drift Ratios

Threshold Stage	1	2	3
Suggested Typical Drift Ratios (%)	0.2-0.3	0.6-0.8	1.4-2.2

2. AN TWO APPROACHES FOR MEASURING DISPLACEMENTS

2.1. Use of GPS for Direct Measurements of Displacements

Until recently, use of GPS was limited to long-period structures (T>1 s) because differential GPS systems readily available were limited to 10-20 sps capability[3]. Currently, the accuracy of 10-20 Hz GPS measurements is ± 1 cm horizontal and ± 2cm vertical. Furthermore, with GPS deployed on buildings, measurement of displacement is possible only at the roof.

A schematic and photos of an application using GPS to directly measure displacements is shown in Figure 2. In this particular case, two GPS units are used in order to capture both the translational and torsional response of the 34-story building in San Francisco, CA. At the same locations as the GPS antennas, tri-axial accelerometers are deployed in order to compare the displacements measured by GPS with those obtained by double-integration of the accelerometer records. Both acceleration and displacement data streaming into the monitoring system is shown also in Figure 2.

To date, strong shaking data from the deployed system has not been recorded. However, ambient data obtained from both accelerometers and GPS units are analyzed (Figures 3a-d). Sample cross-spectra (Sxy) and coherency and phase angle plots of pairs of parallel records (N-S component of north deployment [N_N] vs. N-S component of south deployment [S_N], from accelerometers are shown in Figures 3e-f. The same is repeated for the differential displacement records from GPS units (Figures 3g-h). Frequency of 0.24-.25 Hz seen in Sxy plots from both acceleration and displacement data belong to the expected fundamental frequency for a 34-story building. A second frequency at 0.31 Hz (from acceleration data) Hz is belongs to the torsional mode.

At the fundamental frequency at 0.24 Hz, the displacement data exhibits a 0° phase angle; however, the coherencies are lower (~0.6-0.7). The fact that the fundamental frequency (0.24 Hz) can be identified from the GPS displacement data, amplitudes of which are within the manufacturer specified error range, and that it can be confirmed by the acceleration data, is an indication of promise of better results when larger displacements can be recorded during strong shaking.

2.2. Displacement via Real-time Double Integration

A general flowchart for an alternative strategy based on computing displacements in real-time from signals of accelerometers strategically deployed throughout a building is depicted in Figure 4, and described by Çelebi and others (2004). Although ideal, deploying multiple accelerometers in every direction on every floor level is not a feasible approach not only because of the installation cost, but also from the point of view of being able to robustly, and in near real-time, (a) stream accelerations, (b) compute and stream displacements and drift ratios after double integration of accelerations, and (c) visually display threshold exceedences, thus fulfilling the objective of timely assessment of performance level and damage conditions.

A schematic of a recently deployed health monitoring system which utilizes these principles is shown in Figure 5 (Çelebi and others, 2004). The distribution of accelerometers provides data from several pairs of neighboring floors to facilitate drift computations. The system server at the site (a) digitizes continuous analog data, (b) pre-processes the 1000 sps digitized data with low-pass filters (c) decimates the data to 200 sps and streams it locally, (d) monitors and applies server

[3] Recently, up to 50 sps differential GPS systems are available on the market and have been successfully used (Panagitou et al, 2006).

triggering threshold criteria and locally records (with a pre-event memory) when prescribed thresholds are exceeded, and (e) broadcasts the data continuously to remote users by high-speed internet. Data can also be recorded on demand to facilitate studies while waiting for strong shaking events.

A "Client Software" remotely acquires acceleration data to compute velocity, displacement and drift ratios. Figure 6 shows two PC screen snapshots of the client software display configured to stream acceleration or velocity or displacement or drift ratio time series. The amplitude spectrum for one of the selected channels is periodically recomputed and clearly displays several identifiable frequency peaks. In the lower left, time series of drift ratios are shown.

Corresponding to each drift ratio, there are 4 stages of colored indicators. When only the "green" color indicator is activated, it indicates that the computed drift ratio is below the first of three specific thresholds. The thresholds of drift ratios for selected pairs of data must also be manually entered in the boxes. As drift ratios exceed the designated three thresholds, additional indicators are activated with a different color (Figure 4). The drift ratios are calculated using data from any pair of accelerometer channels oriented in the same direction. The threshold drift ratios for alarming and recording are computed and determined by structural engineers using structural information and are compatible with the performance-based theme, as previously illustrated in Figure 1.

A set of low-amplitude accelerations (largest peak acceleration ~ 1 % g) recorded in the building during the December 22, 2003 San Simeon, Ca. earthquake (Mw=6.4, epicentral distance of 258 km are exhibited in Figure 7 for one side of the building. The figure (center) also shows accelerations at the roof and corresponding amplitude spectra for the (a) two parallel channels (Ch12 and Ch21), (b) their differences (Ch12-Ch21), and (c) orthogonal channel (Ch30). The amplitude spectra depicts the first mode translational and torsional frequencies as 0.38 Hz and 0.60Hz respectively. The frequency at 1.08 Hz belongs to the second translational mode. At the right (Figure 7), a 20 s window of computed displacements (20 s into the record) reveals the propagation of waves from the ground floor to the roof. The travel time is extracted as about 0.5 seconds. Since the height of the building is known (262.5 ft [80m]), travel velocity is computed as 160 m/s. One of the possible approaches for detection of possible damage to structures is by keeping track of significant changes in the travel time, since such travel of waves will be delayed if there are cracks in the structural system (Safak, 1999).

3. MONITORING SINGLE STRUCTURE VS. CAMPUS STRUCTURES

Rather than having only one building monitored, there may be situations where some owners desire to monitor several buildings simultaneously, such as on industrial campus. Figure 8 schematically shows a campus-oriented monitoring configuration. Depending on the choice of the owner and consultants, a campus system may have building specific or central monitoring systems and as such is highly flexible in configuration. As can be stipulated, potential variations and combinations of alternatives for a campus-wide monitoring system are tremendous. There can be central controlled monitoring as well as building specific monitoring or both. A wide variety of data communication methods can be configured to meet the needs (Figure 8).

4. CONCLUSIONS

An Capitalizing on advances in global positioning systems, in computational capabilities and methods, and in data transmission technology, it is now possible to configure and implement a seismic monitoring system for a specific building with the objective of rapidly obtaining and evaluating response data during a strong shaking event in order to help make informed decisions regarding the health and occupancy of that specific building. Using GPS technology and/or double-integrated acceleration, displacements and, in turn, drift ratios are obtained in real-time or near real-time. Drift ratios can be related to damage condition of the structural system by using

relevant parameters of the type of connections and story structural characteristics including its geometry. Thus, once observed drift ratios are computed in near real-time, technical assessment of the damage condition of a building can be made by comparing the observed with pre-determined threshold stages. Both GPS and double-integrated acceleration applications can be used for performance evaluation of structures and can be considered as building health-monitoring applications. Although. To date, these systems were not tested during strong shaking events, analyses of data recorded during smaller events or low-amplitude shaking are promising.

5. REFERENCES

Çelebi, M., and Sanli, A. (2002). GPS in Pioneering Dynamic Monitoring of Long-Period Structures, Earthquake Spectra, Journal of EERI, Vol. 18, No. 1, pp 47–61, Feb. 2002.

Çelebi, M., Sanli, A., Sinclair, M., Gallant, S., and Radulescu, D. (2004). Real-Time Seismic Monitoring Needs of a Building Owner and the solution – A Cooperative Effort, Journal of EERI, Earthquake Spectra, v.19, Issue 1, pp.1-23.

Applied Technology Council (ATC), 1989. Procedures for Post-Earthquake Safety Evaluation of Buildings, ATC-20, Redwood City, CA.

FEMA-352: Recommended Post-earthquake Evaluation and Repair Criteria for Welded Steel Moment-Frame Buildings (SAC 2000).

SAC Joint Venture, 2000. Recommended Post-earthquake Evaluation and Repair Criteria for Welded Steel Moment-Frame Buildings, prepared for the Federal Emergency Management Agency, FEMA 352, Washington, D.C.

Porter, K., Mitrani-Reiser, J., Beck, J. L., and Ching, J., 2006, Smarter Structures: Real- time loss estimation for instrumented buildings, 8NCEE (paper no. 1236), San Francisco, Ca. April 18-22, 2006.

Building Occupancy Resumption Program (BORP), 2001. City and County of San Francisco, Department of Building Inspection, Emergency Operation Plan, (Rev. 2001). [www.seaonc.org/member/committees/des_build .html).

Applied Technology Council (ATC). (1997). NEHRP Commentary on the Guidelines for the Seismic Rehabilitation of Buildings, prepared for the Building Seismic Safety Council, published by the Federal Emergency Management Agency, FEMA 274, Washington, D.C.

Panagitou,M., Restrepo, J.I., Conte, J. P., and Englekirk, R. E., 2006, Seismic Response of Reinforced Concrete Wall Buildings, 8NCEE (paper no. 1494), San Francisco, Ca. April 18-22, 2006.

Safak, E. (1999). Wave-propagation formulation of seismic response of multistory buildings, ASCE, Journal of Structural Engineering, vol. 125, no. 4, April 1999, pp. 426-437.

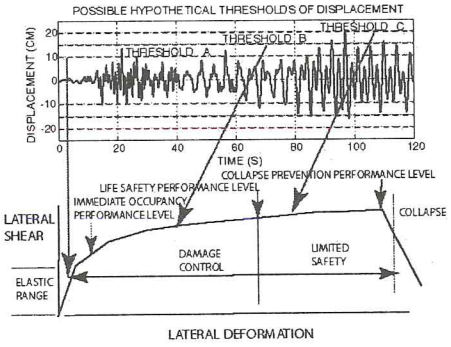

Figure 1. Hypothetical displacement time-history as related to performance [modified from Figure C2-3 of *FEMA-274* (ATC 1997)].

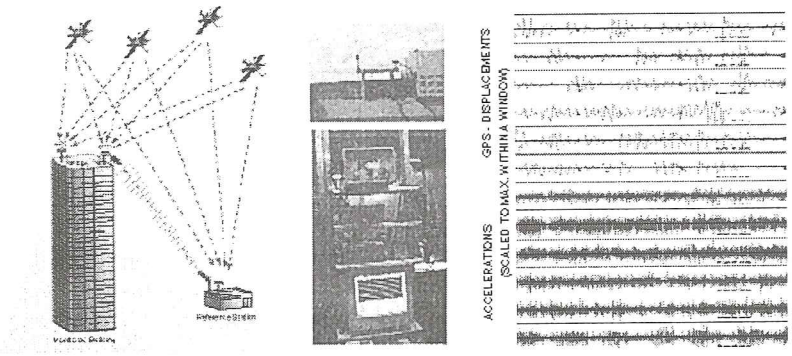

Figure 2. (Left)- Schematic of the overall system using GPS and accelerometers (San Francisco, CA.): (Center)- GPS and radio modem antenna and the recorders connected to PC, (Right)- streaming acceleration and displacement data in real-time.

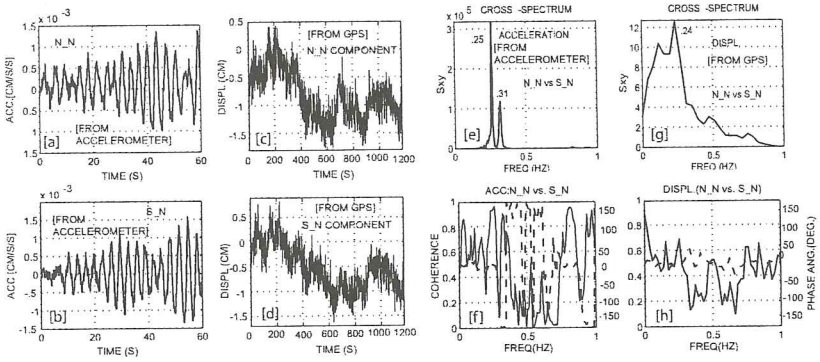

Figure 3. [a,b] 60 second windowed accelerations and [c,d] 1200 second windowed GPS displacement data in the north-south orientation and at N (North) and S (South) locations. Cross-spectra (Sxy) and associated coherency and phase angle plots of horizontal, and parallel accelerations [e,f] and GPS displacements [g,h]. [Note: In the coherency-phase angle plots, solid lines are coherency and dashed lines are phase-angle].

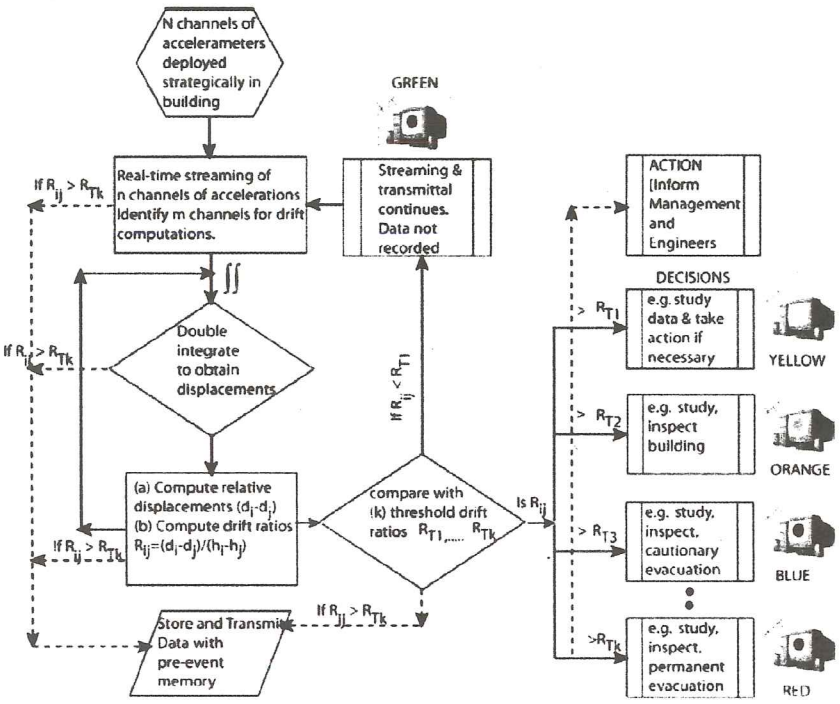

Figure 4. Flow-chart for observation of damage levels based on threshold drift ratios.

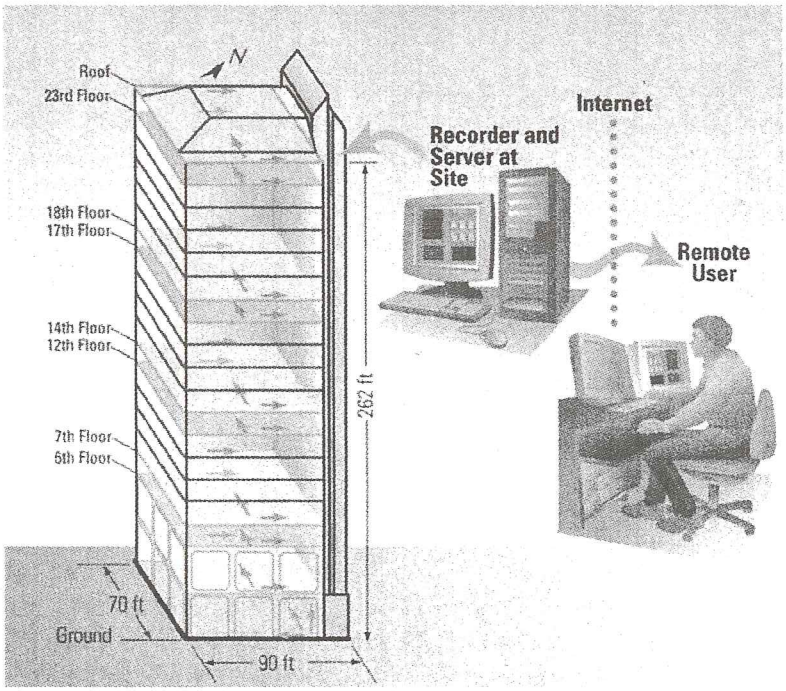

Figure 5. Schematic of real-time seismic monitoring of the building.

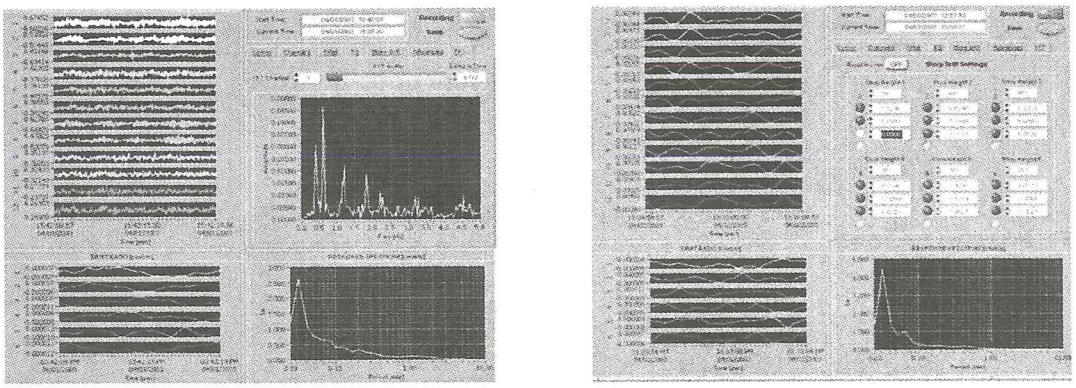

Figure 6. Screen snapshots of sample client software displays: (left) acceleration streams and computed amplitude and response spectra, and (right) displacement and corresponding drift ratios and alarm systems corresponding to thresholds.

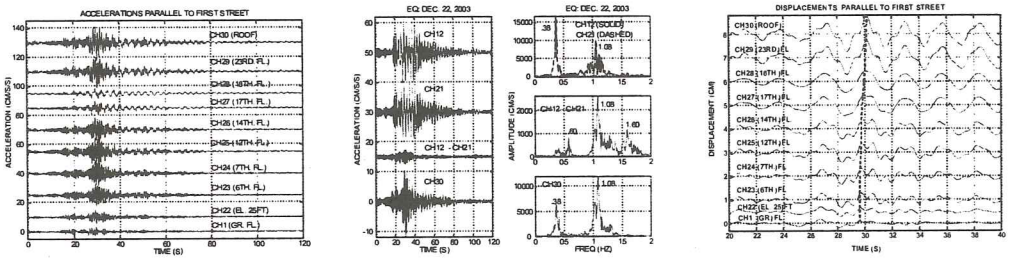

Figure 7. Accelerations (left) at each instrumented floor on one side of the building [San Simeon EQ. of 12/22/2003], (center) from parallel channels (CH12, CH21) at the roof, their difference (CH12-CH21), and orthogonal CH30, and corresponding amplitude spectra indicate fundamental frequency at 0.38 Hz. (right) A 20-s window starting 20-s into the record of computed displacements shows propagating waves with travel time of ~ 0.5 s (onsets indicated by dashed line) from the ground floor to the roof.

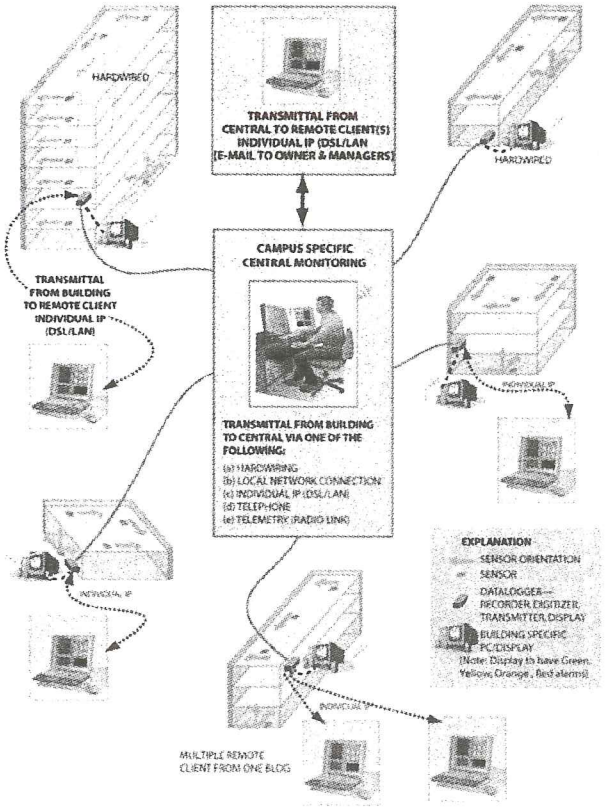

Figure 8. A schematic of campus oriented monitoring system. Each building within a campus may have its own monitoring system or there may a central monitoring unit.

Development of Seismic Design Criteria for River Facilities against Large Earthquakes

by

Hideki SUGITA[1] and Keiichi TAMURA[2]

ABSTRACT

This paper introduces the fundamental concept of seismic design of river facilities against large-scale earthquakes described in the "Performance-based Seismic Design Criteria for River Facilities (Draft)" recently compiled by the MLIT on 2007.3. River facilities include levees, self-supporting structural levees, sluiceways, water gates, weirs and drainage pumping station. As background, characteristics of damage induced in river facilities by past earthquakes, and the history of revision of the "Technical Criteria for River Works and Sabo Works (Draft) Volume of Design" are also briefly reported.

KEYWORDS: Earthquake Damage, Large Earthquake, River Facilities, Seismic Design Criteria

1. INTRODUCTION

River facilities are divided into earth structures such as general levees and high-standard levees, and structures consists of reinforced concrete and steel components. The latter structures are further classified into works attached to levees or to river beds, such as revetments, dikes, and groundsills, and into structural groups such as sluiceways, water gates, weirs, and drainage pumping stations. The seismic design of these various structures basically conforms to the "Technical Criteria for River Works and Sabo Works (Draft) Volume of Design, 1997, the Ministry of Construction". However, since only the Level 1 (moderate-scale) earthquake ground motion was taken into account in the criteria, seismic design procedure against Level 2 (large-scale) earthquake ground motion had been urgently required. Under the circumstances, the MLIT (Ministry of Land, Infrastructure and Transport) established and carried a "Committee for countermeasures against large earthquakes of River Facilities" during 2004 to 2007, and compiled the "Performance-based Seismic Design Criteria for River Facilities (Draft)" in March 2007.

This paper presents fundamentals of the "Performance-based Seismic Design Criteria for River Facilities (Draft)". And as a background, characteristics of damage induced in river facilities by past earthquakes, and the history of revision of the "Technical Criteria for River Works and Sabo Works (Draft) Volume of Design" are also briefly described.

2. EARTHQUAKE DAMAGE FEATURES

The relationship between levee height and levee crown settlement in cases of earthquake damage induced by major earthquakes after the 1981 Nobi Earthquake is summarized in **Figure 1**. General river levees have been suffered damage such as settlements, longitudinal and transversal cracks, or sliding destruction reputedly. It can be said that the seismic resistance of levees is based on the condition of foundation ground, since obvious damage has occurred on soft ground. Furthermore, since sand boiling phenomena have been found in most cases, soil liquefaction of foundation is considered to be the main factor of the damage. Cases of damage are rarely found in soft cohesive soils.

Although the amount of levee crown settlement changes according to the foundation condition or the scale of the seismic motion, those difference conditions are not considered in summarizing **Figure 1**. According to this figure, the amount of levee crown settlement is generally about 75% of the levee height at most.

[1] Team Leader, Ground Vibration Team, Earthquake Disaster Prevention Research Group, PWRI, 1-6 Minamihara, Tsukuba-shi, Ibaraki-ken 305-8516 Japan

[2] Research Coordinator for Earthquake Disaster Prevention, NILIM, Tsukuba-shi 305-0804 Japan

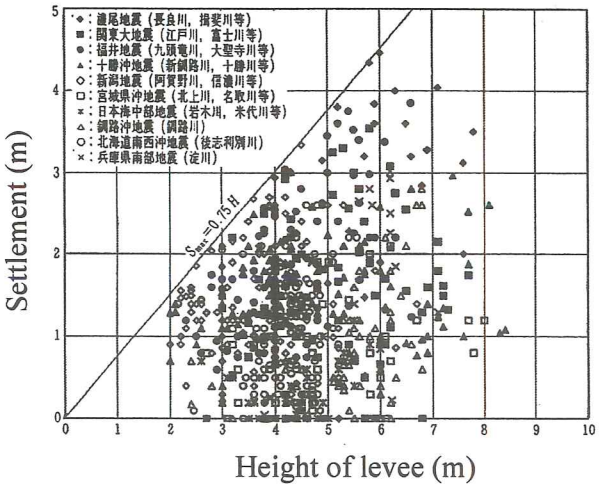

Figure 1 Relationship between Levee Height and Settlement of Crown in Past Earthquake[1)]

Table 1 shows cases of earthquake damage induced in river structures consist of reinforced concrete and steel components after the 1964 Niigata Earthquake. Since there are not enough remaining records from the very old days, the data from **Figure 1** cannot be directly compared with that in **Table 1**. According to **Table 1**, however, the number of seismic damage to structures is obviously small compared with the number of damage events to river levee. The reason for this is thought to be because the moderate-scale ground motion has been taken into the seismic design for river structures of reinforced concrete and steel components from years ago. In cases of damage, considerable sluiceway box culvert damage has been reported. This is because, unlike with the design of the sluiceway gate column, seismic-resistant design considering seismic load has not been applied in the case of the sluiceway box culvert. If the levee is largely deformed, then only the joints set between each box culvert cannot absolves the deformation of the surrounding ground. That causes joint separation, cracks of box culvert and breakage of supporting pile foundation.

Although cases of damage to water gates or weirs are rarely found, the Myoken weir suffered extensive damage by the 2006 Mid-Niigata Earthquake as shown in **Picture 1**. The strong-motion accelerograph installed at the Myoken Weir control office measured the maximum value of the acceleration time-history waveform as more than 1500 gals, and the acceleration response spectrum exceeded the ground motion observed at the Kobe Marine Observatory on the occasion of the 1995 Kobe

Table 1 Major Cases of Damage to River Structures by Past Earthquakes

Earthquake	Structure	Damage
1964 Niigata EQ	Structural Levee	Gap of Joint
	Sluiceway	Spread of Joint Breakage of Culvert
I978 Miyagi offshore EQ	Weir	Deformation of Gate
	Sluiceway	Damage of Column
	Weir	Deformation of Gate
1983 Mid Nihonkai EQ	Sluiceway	Crack of Culvert
	Sluiceway	Crack of Culvert
	Sluiceway	Spread of Joint
	Sluiceway	Spread of Joint
	Water Gate	Tilting of Retaining Wall
1997 Kushiro offshore EQ	Sluiceway	Spread of Joint
	Sluiceway	Spread of Joint Damage of Drainage Inlet
1993 Hokkaido Nansei-oki EQ	Sluiceway	Spread of Joint Breakage of Culvert
1995 Hyogoken Nanbu EQ	Structural Levee	Tilting of Retaining Wall, Damage of Pile Foundation
	Water Gate	Damage of Column
	Weir	Deformation of Gate
	Tunnel River	Breakage of Joint Crack of Culvert
	Tunnel River	Crack of Lining
2003 Tokachi offshore EQ	Sluiceway	Tilting of Column
2004 Mid Niigata EQ	Weir	Damage of Column
	Sluiceway	Spread of Joint
	Pump Station	Damage of Flexible Joint

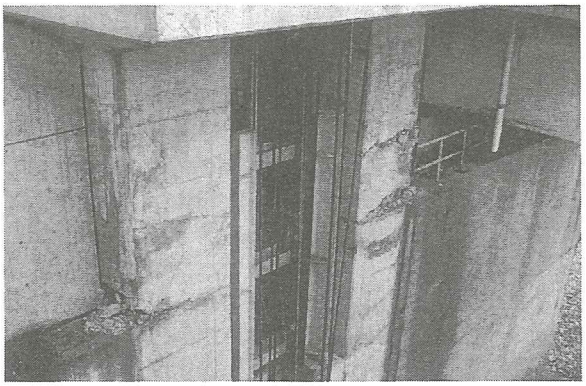

Picture 1 Damaged Gate Column of Myoken weir by 2004 Mid-Niigata Earthquake

Earthquake especially in the short natural period range. This fact indicates that even river structures consisted with reinforced concrete and steel components may suffer severe damage when strong ground motion greatly exceeds the design seismic load (moderate-scale ground motion) developed at the site.

3. HYSTORY OF SEISMIC DESIGN

The "Technical Criteria for River Works and Sabo Works (draft)" was first published in 1958 in order to compile the technologies for the construction river works and sabo works at that time. The criteria were divided into five volumes in 1972, i.e. survey, plan, design, construction and maintenance in order to correspond to the rapid economic growth and social changes that began around 1955. In the 1985 revision of the criteria, the seismic load equivalent to the moderate-scale of earthquake ground motion was first introduced into the design of river structures consists of reinforced concrete and steel components.

In the 1995 Kobe Earthquake, levees located downstream of Yodo-river was settled approx. 3m. The fact endorsed recognition of seismic strength of levees that had low-lying areas behind them. The Ministry of Construction (at that time) established a "Committee for seismic strengthening of levees (chairman: Prof. Kazuya Yamamura of Nihon Univ.)" soon after the earthquake and proposed the fundamental policy for the seismic strengthening of levees located zero-meter area (area below sea level). In the 1997 revision of the criteria, seismic design of levees was introduced taking into account the proposal. Since the revision of criteria, seismic inspection and seismic strengthening has been initiated across the nation.

The settlement of levee has been estimated based on the experimental relationship between the settlement and safety factor derived from the seismic coefficient method as shown in **Table 2**. This is because a theoretical method to estimate the seismic deformation, i.e. the finite element method was not yet well prepared at that time. In the criteria, design seismic coefficient has been given as between 0.10 and 0.18 according to the regional classification and the levee scale, whereas large-scale earthquake ground motion is not considered. Behind the decision of seismic coefficient, political circumstances are taken into account, i.e. restoration of earth structures is generally easy, and countermeasure against heavy rain is prior to the measures against large-scale earthquake from the frequency point of view.

Table 2 Relationship between Levee Settlement and Seismic Safety Factor

Safety Ratio F_{sd}		Settlement (maximum)
$F_{sd}(kh)$	$F_{sd}(\Delta u)$	
$1.0 < F_{sd}$		0
$0.8 < F_{sd} \leqq 1.0$		(Levee Height) ×0.25
$F_{sd} \leqq 0.8$	$0.6 \leqq F_{sd} \leqq 0.8$	(Levee Height) ×0.50
—	$F_{sd} \leqq 0.6$	(Levee Height) ×0.75

4. CRITERIA AGAINST LARGE-SCALE EQ

In recent, technical review of the probability and damage scenarios of large-scale earthquake such as Miyagiken-oki Earthquake, Tokyo inland Earthquake, Tokai Earthquake, Tonankai Earthquake and Nankai Earthquake has been conducted by the Central Disaster Prevention Council of Government. However, as mentioned before, only moderate-scale earthquake ground motion is considered in the conventional criteria. Therefore, it was urgently required to prepare new criteria that include counter earthquake measures for river facilities against large-scale earthquake. Under these circumstances, the MLIT established and carried the "Committee for countermeasures against large earthquakes of river facilities (chairman: Prof. Yasushi Sasaki of Hiroshima Univ.)" during 2004 to 2007 and compiled the "Performance-based Seismic Design Criteria for River Facilities (draft)" in March 2007. The criteria covers moderate-scale (Level 1) and large-scale (Level 2) earthquake ground motion.

4.1 Contents

The criteria shall be applied to check the seismic performance of river facilities including levee, self-supporting structural levee, water gate,

sluiceway, weir and drainage pumping station. Contents of the draft criteria are shown in **Table 3**. Among river structures that could affect flood control or water utilization due to their earthquake damage, inverted siphons and underground tunnel river shall be treated in accordance with the technical guidelines for similar structures such as roads and sewage systems.

Table 3 Contents of Draft Criteria

Volume	Contents
Common	Basic Principle of seismic performance design, Common Items such as Design Load
Levee	Seismic Performance Design of Levee*
Self-supporting Structural Levee	〃 Seif-supporting Structural Levee
Water Gate, Sluiceway and Weir	〃 Water Gate, Sluiceway and Weir
Drainage Pumping Station	〃 Drainage Pumping Station

*High-standard levees are not included in this draft principle, since they are at present separately reviewed

4.2 Basic Policy to Check Seismic Performance

In checking the seismic performance of river facilities, required seismic performance and earthquake ground motion shall be appropriately determined and seismic analysis method shall be appropriately adopted. The seismic analysis method can be classified into the dynamic response analysis method and static analysis method. The dynamic response analysis generally requires precise modeling of actual dynamic phenomena, detailed input data and technically difficult decisions. On the other hand, the static analysis method can be conducted more easily by simplifying the actual dynamic phenomena. In the draft criteria, mainly specify the static analysis method considering its practical use, however seismic performance check shall be appropriately conducted considering the response characteristic of the structure and required analysis accuracy.

The water level for checking the seismic performance of river facilities shall be, in principle, the highest daily water level under usual condition. The water level was defined in accordance with the water level that has been considered for the seismic inspection practice and seismic strengthening practice supposing that the earthquake and heavy rain would not occur simultaneously from the statistic point of view. Around the river mouth area, the highest tidal water level and the amount of wind wave shall be considered. Furthermore, tsunami supposed to be occurred following the earthquake, estimated tsunami height shall be considered in addition.

4.3 Earthquake Effect

As the effect of the earthquake, the inertia force caused by the structure's weight, earthquake ground deformation, earthquake earth pressure, dynamic water pressure and the effect of soil liquefaction shall be considered. There are many kinds of structures, including earth structure such as levee, aboveground structure such as water gate or weir, and structures installed in the ground such as drainage pumping station. Some structural components may contact surrounding soil or water. The effect of the earthquake shall be appropriately considered depending on each structure and each structural component.

4.4 Earthquake Ground Motion

Level 1 earthquake ground motion and Level 2 earthquake ground motion shall be considered in the checking of the seismic performance. Definition of the Level 1 earthquake ground motion is the ground motion occurs with high probability during its service period. Level 1 earthquake ground motion was determined to follow the ground motion that has been adopted in the conventional seismic design according to the seismic coefficient method.

Definition of the Level 2 earthquake ground motion is the maximum credible ground motion at each site from the present to the future. As the Level 2 earthquake ground motion, Level 2-1 ground motion which assumes a large-scale earthquake occurs at the plate boundary and Level 2-2 ground motion which assumes an inland earthquake shall be considered. Level 2 earthquake ground motion was determined by referring the "Draft Guideline for the Seismic Design of Civil Structures, Japan Society of Civil Engineering, 2001.9" and the "Design

Fundamentals for Constructing Civil Structures and Architectural Structures, MLIT, 2002.10". Level 2-1 ground motion is characterized as a repeated motion with large amplitude for a long duration time, whereas Level 2-2 ground motion is characterized as a motion with extremely large amplitude for a short duration time. Above mentioned two types of ground motion shall be considered to check the seismic performance of river facilities, because the dynamic response of structure is affected by the characteristics of amplitude, natural period, duration time and repetition.

4.5 Required Seismic Performance Level

Required seismic performance level of various river facilities and various structural components were defined according to the flowchart shown in **Fig. 2**. In the flowchart, emphasis is placed on whether or not the structure is important for the water utilization or flood control, whether or not the structural component is one of the major components that consists the structural flame, and whether or not an alternative measures are available when the component lose its function.

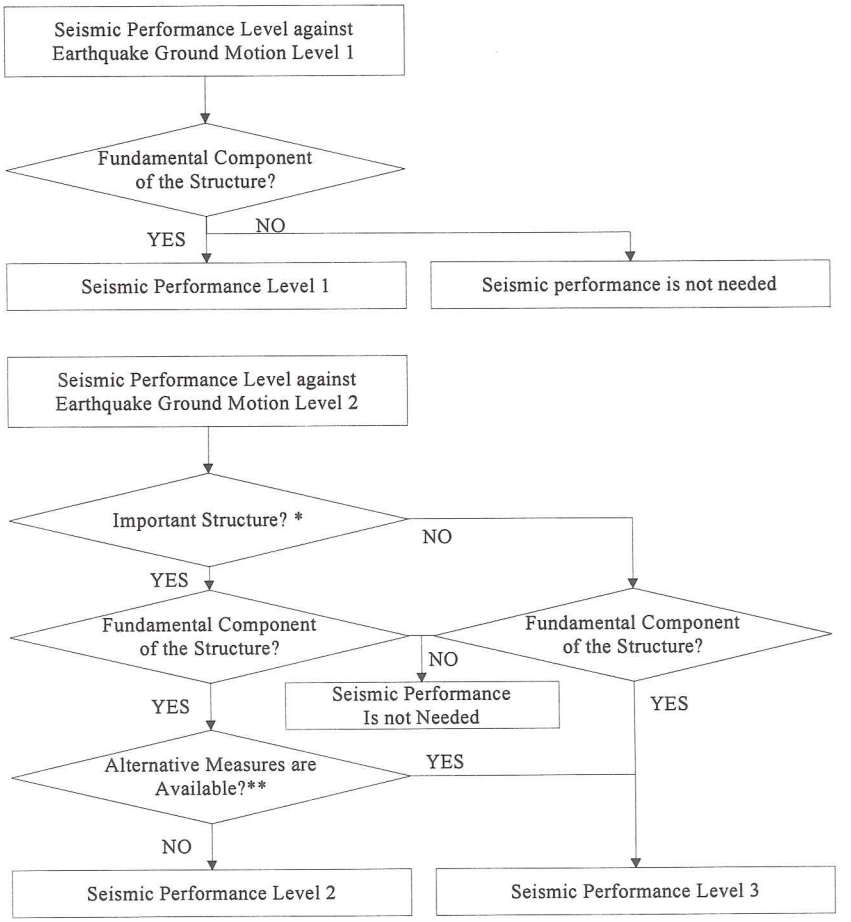

*Important Structure:	Important for flood control or water utilization. 1) When the structure lose control, flood damage may be induced by the water level defined in the seismic design criteria for checking the seismic performance. 2) When the structure lose control, difficulty of water utilization may be induced by the water level defined in the seismic design criteria for checking the seismic performance.
** Alternative Measures are Available	1) When the structure lose control, weir , water gate and sluiceway can be closed by supplemental gate or using square timbers. 2) When the structure lose control, the drainage pump can be replaced by supplemental handy pump in the drainage pumping station

Fig.2 Determination of Required Seismic Performance

Table 4 Required Seismic Performances for River Facilities

Structure	Type	Importance Classification	Earthquake Ground Motion	
			Level 1	Level 2
Levee		※	Not Required	Level 2
		Other Area	Not Required	Not Required
Self-supported Structural Levee	RC Retaining Wall	※	Level 1	Level 2
		Other Area	Level 1	Level 3
	Sheet Pile	※	Not Required	Level 2
		Other Area	Not Required	Level 3
Weir	Flip-top Gate	Very Important	Level 1	Level 2
		Others	Level 1	Level 3
	Steel Reverse Gate	Very Important	Level 1	Level 2
		Others	Level 1	Level 3
Water Gate Sluiceway		Very Important	Level 1	Level 2
		Others	Level 1	Level 3
Drainage Pumping Station		Very Important	Level 1	Level 2
		Others	Level 1	Level 3

※ Area that the ground level is lower than the water level defined in the seismic design criteria for checking the seismic performance

Table 5 Required Seismic Performances for structural components

Structure	Type	Component	Earthquake Ground Motion	
			Level 1	Level 2
Levee		Main Body	Not Required	Level 2
Self-supported Structural Levee	RC Retaining Wall	Main Body, Foundation	Level 1	Level 2
	Sheet Pile	Main Body	Not Required	Level 2
Weir	Flip-top Gate	Slab, Weir Column, Gate Column, Foundation, Gate Beam	Level 1	Level 2
		Gate, Operation Room, Maintenance Deck	Level 1	Level 2*
		Apron, Liner Facility, Revetment, Fish Way, Others	Not Required	Not Required
	Steel Reverse Gate	Slab, Weir Column, Foundation, Gate	Level 1	Level 2*
		Apron, Liner Facility, Revetment, Fish Way, Others	Not Required	Not Required
Water Gate Sluiceway		Slab, Weir Column, Gate Column, Foundation, Gate Beam, Culvert	Level 1	Level 2
		Gate, Operation Room, Maintenance Deck	Level 1	Level 2*
		Apron, Liner Facility, Revetment, Fish Way, Parapet Wall, Others	Not Required	Not Required
Drainage Pumping Station		Pump, Foundation	Level 1	Level 2
		Pump Rated Device, Building	Level 1	Level 2*
		Others	Not Required	Not Required

* Alternative Measures are Available in order to Secure Structural Function

Here, three kinds of seismic performance level were defined. Seismic performance level 1 means that the structure or component does not loose the soundness as a river facility. Seismic performance level 2 means that retains the function as a river facility against the water level defined in the criteria for checking the seismic performance. And seismic performance level 3 means that the earthquake damage is limited and the recover of the damage can be made within a short time.

Table 4 shows the required seismic performance for each river facility. **Table 5** shows the required seismic performance for each structural component of the structure that is important for the water utilization and flood control.

5. SEISMIC PERFORMANCE OF LEVEE

5.1 Basic Policy to Check Seismic Performance

Levees are constructed to prevent running water from overflowing. In the zero-meter area much settlement of levee may induce flood disaster. On the other hand, it is not necessarily rational that development of any settlement of levee is not allowed after a large-scale earthquake. Based on these characteristic of earth structure, therefore, required seismic performance of levee was defined as level 2 that means levee retains its function against the water level defined for checking seismic performance although some amount of settlement may be developed.

In the checking of seismic performance of levee, soil liquefaction shall be considered as the earthquake effect. This is because severe damages of levee in the past earthquake were induced by the soil liquefaction of their foundation ground.

5.2 Analysis Method

The static analysis method can be adopted to check the seismic performance of levee because it is relatively simple structure. For the checking of seismic performance of levee by the static analysis method, first seismic coefficient in the horizontal direction shall be determined, and then probability of soil liquefaction at sandy layer shall be checked. Next, seismic deformation of the levee shall be estimated in proportion to the degree of soil liquefaction, and check whether or not the levee height after the earthquake will exceed the water level defined in the criteria for checking the seismic performance. As a simple and precise static analysis method to estimate the seismic deformation of the levee, the finite element method assuming that the levee deforms in cooperation to the reduction of shear stiffness can be adopted. Also, the estimation method of fluidic deformation of the levee assuming that the liquefied soil layer is a viscous fluid can be adopted.

5.3 An Example of Static Analysis by FEM

As an example, static analysis of levee using the above-mentioned finite element method is shown in here. The levee specifications and a sectional view are shown in **Fig. 3** and **Table 6**.

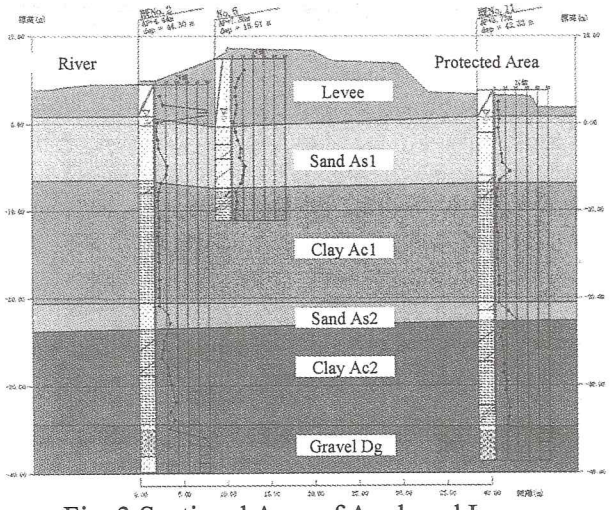

Fig. 3 Sectional Area of Analyzed Levee

Table 6 Analyzed Levee Specifications

Levee Height (River Side)	Levee Height (opposite)	Width of Levee Crown	Width of Levee
6.9m	5.2m	9.0m	55.4m
Slope (River Side)	Slope (Opposite)	Altitude of Levee Crown	Highest tidal Water Level
1:1.6	1:2.0	AP+8.7m	AP+2.1m

Ground conditions of the levee are supposed to be horizontally laminated. From the surface, the

ground consists of sandy soil with approx. 2m thickness, alluvial sandy soil As1 with approx. 6-7m thickness which shows 1-11 N-value, soft clay soil Ac1 with approx. 14m thickness which shows 1-5 N-value, and alluvial sandy soil As2 with approx. 4m thickness which shows 11-20. Below the As2, alluvial clay soil Ac2 and gravel soil is accumulated. According to the boring data, the ground of river side and protected side are both classified soil type III. On the basis of the soil type, the design horizontal seismic coefficient for Level 2-1 and Level 2-2 ground motion are determined 0.40 and 0.60, respectively. As the result of checking the probability of soil liquefaction against two kinds of seismic coefficient, all the alluvial sandy layer As1 is found to be liquefied.

The analysis method estimates the deformation of levee by assuming that the levee deforms in accordance with the reduction of shear stiffness due to soil liquefaction. In this case study, reduction of shear stiffness in the liquefied layer was determined based on the relationship between the liquefaction resistant ratio F_L, cyclic triaxial strength ratio R_L and the degree of reduced shear stiffness. The averaged cyclic triaxial strength ratio was adopted for the R_L. Here, it is necessary to consider the settlement associated with the volume compression separately from the analytical solution. This is because the analysis method does not consider the settlement of levee associated with the volume compression induced by the propagation of excess pore water pressure generated in the liquefied layer during the earthquake.

In this case study, both Level 2-1 and Level 2-2 ground motion were considered. In the case of Level 2-1 ground motion, the analytical solution was 163.0cm, settlement associated with volume compression was 38.3cm, and the total settlement of levee crown was estimated as 201.3cm. In the case of Level 2-2 ground motion, the analytical solution was 171.4cm, settlement associated with volume compression was 38.3cm, and the total settlement of levee crown was 209.7cm. **Fig. 4** shows the deformation of the levee against Level 2-2 ground motion.

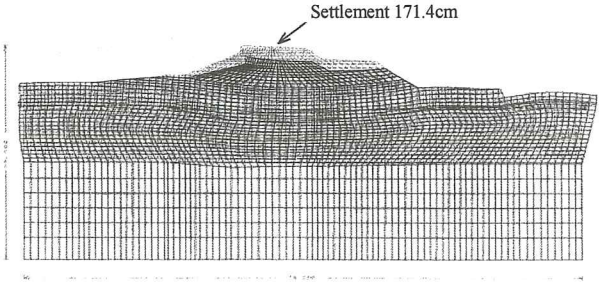

(a) Solution of Finite Element Method

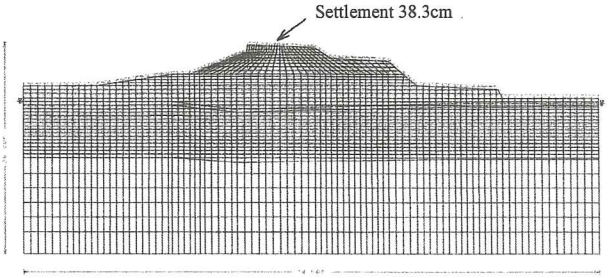

(b) Volume Compression of Liquefied Layer

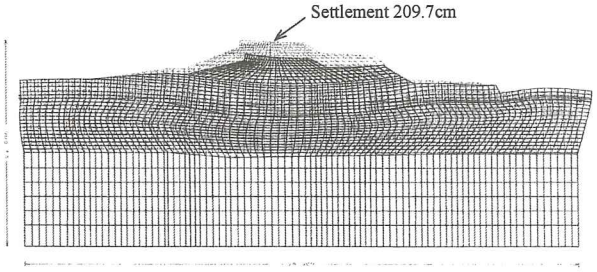

(c) Total Deformation

Fig. 4 Deformation of Levee against L2-2 EQ

6. CONCLUDING REMARKS

The fundamentals of the "Performance-based Seismic Design Criteria for River Facilities (Draft)" were introduced briefly. From the fiscal year of 2007, new structures will be constructed based on the criteria. Seismic inspection will be conducted in nationwide and seismic upgrading of existing structures which have insufficient seismic performance will be carried out one by one from the viewpoint of importance for flood control and water utilization.

7. REFERENCES

1. Committee on Earthquake Countermeasure for River Facilities: *Committee Report*, 1996

Extraction of Damages by Tsunami from ALOS Image at South Java in 2006

by

Mayumi Noguchi[1], Keiko Suzuki[1] and Toshio Kitahara[2]

ABSTRACT

ALOS (Advanced Land Observation Satellite) is a Japanese satellite launched in January 2006. It has three different sensors for precise land coverage observation. GSI (Geographical Survey Institute of Japan) has carried out geoinformation research such as crustal deformation and topographical and disaster-related mapping in order to fulfill one of the missions of ALOS.

In the southern offing from Java Island, an earthquake of magnitude 7.7 occurred on July 17, 2006. A tsunami generated by the earthquake attacked the coast of Java and caused extensive damage.

In this study, we try to extract the damage caused by the tsunami using an ALOS/AVNIR-2 (Advanced Visible and Near Infrared Radiometer type 2) image in order to evaluate the applicability of ALOS imagery in tsunami disaster. Damaged areas revealed on the basis of NDVI (Normalized Difference Vegetation Index) of the AVNIR-2 image well match the interpretations from IKONOS images. As a result, it is shown that AVNIR-2 data is applicable to grasp an overview of damage caused by tsunami.

KEYWORDS: ALOS/AVNIR-2, Disaster Map, NDVI, Tsunami

1. INTRODUCTION

The Advanced Land Observation Satellite "Daichi" (ALOS) was launched on January 24, 2006. It was developed to contribute mapping, precise regional land coverage observation, disaster monitoring and resources surveying. ALOS has three sensors to achieve its objectives of cartography, regional observation, disaster monitoring, resources surveying and technology development.

The three sensors are the Panchromatic Remote-sensing Instrument for Stereo Mapping (PRISM) which has three sets of optical systems for the precise measurement of land elevation, the Advanced Visible and Near Infrared Radiometer type 2 (AVNIR-2) for the precise observation of land coverage, and the Phased Array type L-band Synthetic Aperture Radar (PALSAR) that enables day-and-night and all-weather land observation.

The Geographical Survey Institute of Japan (GSI) undertakes joint research on understanding geographical information with the Japan Aerospace Exploration Agency (JAXA). We have examined the applicability of ALOS data in evaluating damage by natural disasters both in Japan and abroad.

In this study, we try to extract of damage by tsunami using an ALOS/AVNIR-2 image in order to evaluate the applicability of ALOS imagery in tsunami disaster.

2. STUDY AREA

An earthquake of magnitude 7.7 occurred in the southern offing from Java Island on July 17, 2006, and the tsunami generated by this earthquake attacked the coastal area (Fig. 1).

The tsunami damaged the southern coastal area of Java Island along a 300km long stretch. There were many places where the tsunami reached the height more than 5m. This disaster killed over 500 people.

[1] Technical Official, Disaster-Prevention Geographical Division, Geographical Survey Institute, Tsukuba-shi, Ibaraki-ken 305-0811 Japan

[2] Head, Disaster-Prevention Geographical Division, Geographical Survey Institute

We studied the area around Pangandaran, the most severely stricken area. According to various news sources, the tsunami swept areas up to 3km inland from the beach, and the number of victims was more than 300 in Pangandaran. The study area is indicated by the red box in Fig. 1.

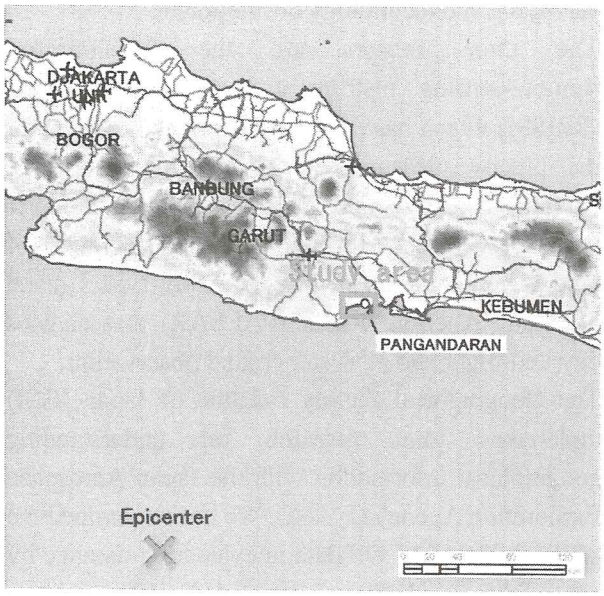

Fig. 1 Map around Study Area
(quoted from GSI Homepage [1])

3. IMAGE SPECIFICATIONS

AVNIR-2 is a visible and near infrared radiometer for observing land and coastal zones. It enables us to provide better landcover and landuse maps for monitoring regional environments.

AVNIR-2 has a 10m spatial resolution and a cross-track pointing function for prompt observation of disaster. The pointing angle of AVNIR-2 is -44 to +44 degrees. The AVNIR-2 specifications are shown in Table 1 [2].

Only one AVNIR-2 image taken after the earthquake was used in this study because there is no image taken before the earthquake. This image was taken on July 21, four days after the earthquake. The image specifications are shown in Table 2.

The study area is located in the vicinity of the center of the image.

Table 1 AVNIR-2 Specifications

Number of Bands	4
Wavelength (μm)	Band 1 : 0.42-0.50 Band 2 : 0.52-0.60 Band 3 : 0.61-0.69 Band 4 : 0.76-0.89
Spatial Resolution	10 m (at Nadir)
Swath Width	70km (at Nadir)
S/N	>200
Number of Detectors	7000/band
Pointing Angle	-44 to +44 degree
Bit Length	8bits

Table 2 Image Specifications

Observation Date	2006/07/21
Pointing Angle	8.0 deg
Left Top LAT/LON	7.274°S/108.447°E
Right Top LAT/LON	7.410°S/109.095°E
Left Bottom LAT/LON	7.892°S/108.315°E
Right Bottom LAT/LON	8.029°S/108.964°E

4. METHODS

In the flood area of seawater by tsunamis, it is known that a great change in the land cover occurs because of the force of currents, stagnant water and the inflow of earth and sand. In particular, vegetation can provide information of the flood area because the affects of weakening due to vegetation being washed away, fallen trees and salt remain for some time [3]. Therefore, the damaged area is identified on the basis of vegetation activity in this study. The Normalized Difference Vegetation Index (NDVI) is used as a index of vegetation activity.

Tsunami-damaged areas are usually identified by comparing images taken before and after a disaster. Because only an image taken after the disaster was available in our case, we designed a method to extract the damaged area using only one image and tested it.

First, one of the IKONOS images of the damaged area available on the CRISP (Centre for Remote Imaging, Sensing and Processing) website [4] was

used as the reference data, and we investigated the characteristics of ALOS data in the damaged area. The afflicted area (the area where vegetation is recognized to be washed away) and the flood area (the area of assumed inundation) are selected from the ALOS image by comparing the IKONOS image (true color) and ALOS images (both true and false color). Next, the thresholds of NDVIs are determined from their ranges in each area (Fig. 2). The whole study area is classified into 3 areas on the basis of the NDVI thresholds. Town areas are removed from the extracted areas because these areas show very low NDVI originally. Finally, boundary lines of the afflicted area and the flood area are mapped (Fig. 3).

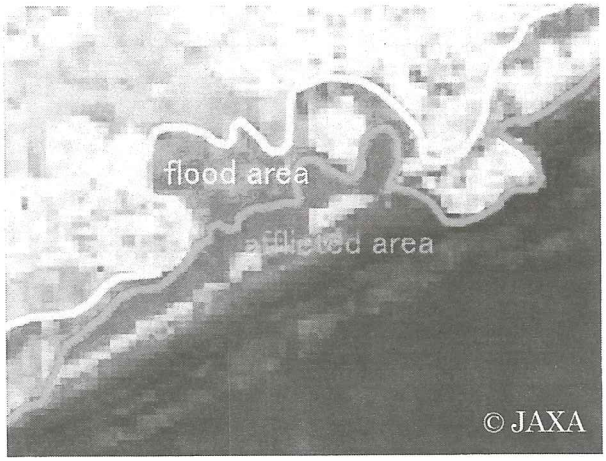

Fig. 2 NDVI Image of Reference Area

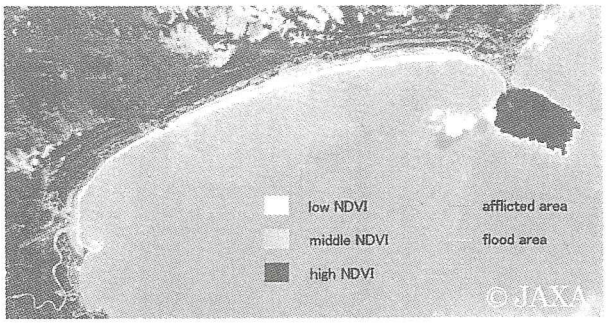

Fig. 3 Three Classifications of NDVI

5. RESULTS

The extraction result is overlaid on the ALOS false color composite image and a Tsunami Disaster Map (see Appendix) is made. The map contains additional information; roads and rails are taken from the Peta Rupabumi Digital Indonesia 1:25,000 "Cijulang", "Pajaten" and "Pananjung" by Bakosurtanal, and place names are taken from the Indonesia 1:250,000 "Garut" by U.S.Army Map Service.

When the extraction result is compared with IKONOS images of damaged points which are different from the CRISP reference data, the places where damage is obvious in IKONOS images can be extracted from the AVNIR-2 image almost completely. Moreover, the flood area extracted in this study well matches the potential tsunami-affected area in the UNOSAT (Fig. 4) [5]. It is shown that the extraction of damaged area in this study is appropriate.

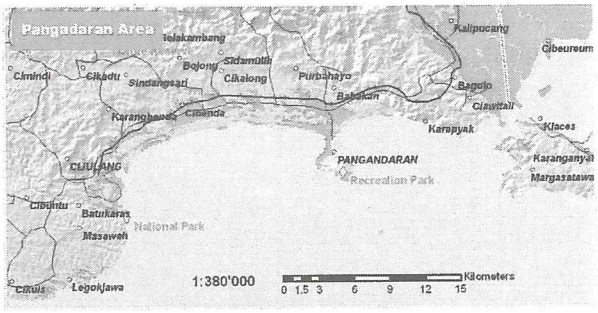

Fig. 4 Potential Tsunami-Affected Areas (quoted from UNOSAT [5])

As a result, it is concluded that ALOS/AVNIR-2 imagery is available to grasp an outline of tsunami disaster. Considering the advantage of the pointing function, AVNIR-2 is expected to contribute immensely to early investigations at tsunami disaster.

6. SUMMARY

The estimation of the tsunami damaged area by using the ALOS/AVNIR-2 image well matches the data of damaged area from other sources. AVNIR-2 is superior in mobility and it is expected to be effective for early investigations at tsunami disaster.

7. REFERENCES

1. GSI, Map of Java Island and its Vicinity by Global Map, http://www.gsi.go.jp/BOUSAI/java-2/index.html, 2006
2. JAXA, About ALOS – AVNIR-2 –, http://www.eorc.jaxa.jp/ALOS/about/avnir2.htm, 1997
3. Takeda, A. and Tsuji, Y.: Discrimination of Flooded Areas Due to Tsunami By Using Satellite Image Data, Research Report of National Disaster Prevention Center, No. 41, 1988.
4. CRISP, Tsunami in Java, Indonesia (17 Jul 2006), http://www.crisp.nus.edu.sg/coverages/tsunami20060717/index.html, 2006
5. UNOSAT, South Coast of Java, Indonesia: Potential Tsunami-Affected Areas, http://www.unosat.org/, 2006

Appendix

Tsunami Disaster Map

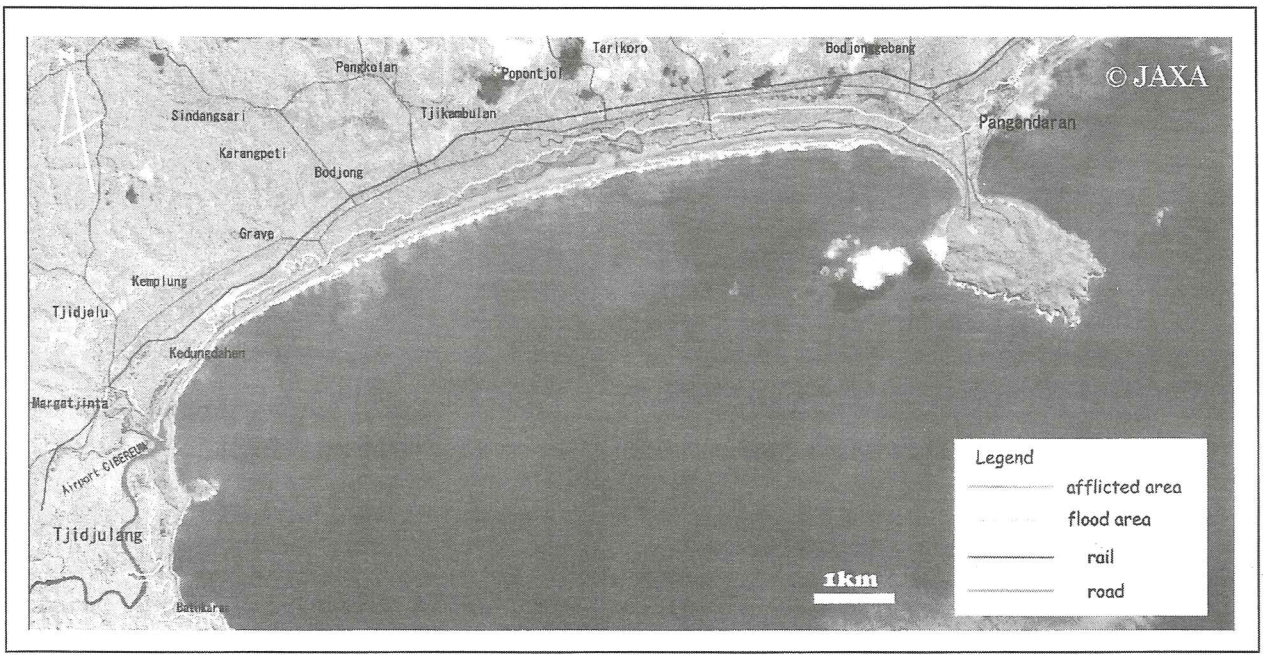

THEME 7

Next-Generation Building and Infrastructure Systems

Damping Ratio Estimation of an Existing 8-story Building Considering Soil-Structure Interaction Using Strong Motion Observation Data

by

Koichi Morita[1]

ABSTRACT

In this study, damping ratio of an exiting 8-story SRC building using the strong observation data is identified. Strong motion observation is continually carried out since just after the completion of the building. Damping ratio are identified with the effect of interaction and without the effect. The effect of the dynamic interaction of the building to damping ratio will be discussed.

KEYWORDS: Amplitude Dependence,
Damping Ratio,
Health Monitoring,
Identification Method

1. INTRODUCTION

Damping ratio is one of the important indexes to predict the response of the building. Damping ratio value used for structural design does not always agree with the measured value, though those of natural frequency and participation function agree with the measured value. Although the consideration of the structure classification is done, the first damping ratio has been set at 2% and 3%, etc. regardless of the condition of the building. This setting seems to base on experience and practice in the past, and the reason which is clearly physical is not shown. It is very difficult to evaluate the damping ratio by the theoretical method, so, in the present state, the tendency of damping ratio should be grasped by the observations and measurements.

The database of building damping ratio is made on various experiments and observations results carried out in the past, and the statistical examination of damping ratio has been made. [1] This data is analyzed from many points such as characteristics of buildings, and the influential factor to damping ratio is analyzed. The correlation is being found on some factors, but clear tendency cannot be found out because of large dispersion. From these results, large dispersion is included in damping ratio. It seems to become a situation in which structural designers must use the practice value.

Many kinds of experimental method and evaluation technique for estimating damping ratio has been proposed. It has also been indicated that the identified results of damping ratio change by the setting of conditions such as technique itself and band pass filter, curve fitting and so on. In case of damping database, such difference from technique cause large dispersion. The authors carried out microtremor observation in same observation method and evaluation method to exclude the dispersion from method. Though the correlation between the aging number and damping ratio is shown as strong, clear tendency cannot be shown because of large dispersion of damping.

In the other research, very much observation is carried out on one building continually, and damping ratio tendency are grasped. On one building, tendency such as amplitude dependence and aging of damping are examined. Tendency of the natural frequency is very clear, but damping ratio is included large dispersion.

As the characteristics of the damping ratio, the amplitude dependence is mentioned. Many examples of the experimental studies which noticed the amplitude dependence of damping are observed. On the amplitude dependence, damping ratio will increase as amplitude increases, or there is some leveling off in this increase. It has also been indicated that the effect of the non-structural members is large. Authors collected the data on amplitude dependence of damping ratio on many buildings. Damping ratio increases to some drift angle, after that leveling-off can be found out.

As a factor of the damping ratio of the building,

[1] Senior Researcher , Building Research Institute, Tsukuba-shi, Ibaraki-ken 305-0802, Japan

the underground dissipation by the dynamic soil-structure interaction is mentioned. It is necessary to measure vertical motion of the input layer at more than 2 points in order to remove the effect of the rocking. The case for such measurement is few, and the evaluation example of damping ratio considering soil-structure interaction effect is very little.
In this study, damping ratio of an exiting 8-story SRC building using the strong observation data is identified. Strong motion observation is continually carried out since just after the completion of the building. Damping ratio are identified with the effect of interaction and without the effect. The effect of the dynamic interaction of the building to damping ratio will be discussed.

2. OUTLINE OF TARGET BUILDING AND INSTALLED SENSORS

2.1 Building Characteristics

The target building is Urban Disaster Prevention Research Center in National Institute for Land and Infrastructure Management (NILIM) that was completed in March 1998. Outline of building characteristics are shown in Table1.

2.2 Installed Sensors

The sensors are installed with 11 locations (33 channels) in the building. The sensor configuration is shown in Fig. 2 and 3. (Kashima 2004) In addition to these accelerometers, maximum response memory sensors of story displacements are installed. In this study, only accelerometers installed at ground(A01), basement, 1st , 2nd, 5th and 8th story are used for system identification.

3. THREE TYPES OF DAMPING RATIO

3.1 Three Types of Damping Ratio Identified in This Study

Using the data of strong motion seismometer shown in Figure 1, damping ratio is identified. In this study, three types of damping ratio considering the interaction effect are identified as following;

1) the SRB type damping ratio h_{SRB} including basement horizontal motion and the rotation motion. (input motion is ground motion.)
2) the RB type damping ratio h_{RB} including the rotation motion. (input motion is basement floor motion.)
3) the B type damping ratio h_B including only the building motion. (input motion is basement floor motion plus rocking motion.)

3.2 Types of Damping Ratio by Experimental Methods

The types of damping ratio are different by the experimental methods. The types of the damping ratio by experimental methods are shown in Tables 2.
In the past experiments, most damping ratio are estimated in SRB or RB type, and the B type damping ratio is very rare. The example just after the completion of the building is frequent in the time of the observation.

3.3 Type of Damping Ratio in Response Analysis

In the response analysis, the damping ratio of B type is indicated in the case of first damping ratio 2%. From this fact, the damping ratio generally used by the analysis indicates the B type. By facing, the damping ratio by the experimental observation can be called being SRB type or RB type.

4. OUTLINE OF SYSTEM IDENTIFICATION

In this monitoring system, accelerometer data of basement, 1st, 2nd, 5th and 8th story are used.
Parameter identification based on the ARX model is applied for input-output data of vibration measurements. The ARX model structure is the simple linear difference equation

$$\begin{aligned} &y(t)+a_1 y(t-1)+\ldots+a_{na} y(t-na) \\ &=b_1 u(t-nk)+\ldots+b_{nb} u(t-nk-nb+1) \end{aligned}, \quad (1)$$

which relates the current output y(t) to a finite number of past outputs y(t-k) and inputs u(t-k). The structure is thus entirely defined by the three integers na, nb, and nk. na is equal to the number of poles and nb-1 is the number of zeros,

while nk is the pure time-delay (the dead-time) in the system. From this model structure, the coefficients aj and bj are estimated.
If A and B are expressed as,

$$A(q) = 1 + \sum_{j=1}^{n_a} a_j q^{-j} \quad , \qquad (2)$$

$$B(q) = \sum_{j=1}^{n_b} b_j q^{-j+1-n_k} \quad , \qquad (3)$$

${}_z p_j$ is the root of A(z)=0 and ${}_z r_j$ is the residue of a partial fraction expansion of $B(z)/A(z)$.
Natural frequency f_j and damping ratio h_j are expressed as the following.

$$f_j = \frac{\sqrt{(\log|{}_z p_j|)^2 + (\arg {}_z p_j)^2}}{2\pi\Delta t} \quad , \qquad (4)$$

$$h_j = \frac{-\log|{}_z p_j|}{2\pi f_j \Delta t} \quad , \qquad (5)$$

When model numbers change as na=70 to 80 (even numbers), nb=na+1, and nk=0, we select the numbers in which Akaike's Information Criteria (AIC) [2] is estimated as small.

5. IDENTIFICATION RESULTS

5.1 Tendency of Damping Ratio in All Data

430 strong motion records from June 1996 to December 2006 are used for identification. For all strong motion records (all duration time), three types damping ratio are identified, and the relationship between the aging number is shown in Figure 2 to 4. In all these figures, there are some dispersions in damping ratio. The SRB and RB type damping ratio decrease in about initial 3 years. The tendency changed to the increase afterwards can be seen. The B type damping ratio in Figure 4 has also large dispersion, but tends to increase as the aging year increases. In Figure 5, ratio between two damping ratios in which SRB or RB damping is divided by B type is shown. According to this figure, ratio between two damping tends to decrease as the aging.

5.2 Secular Change of Damping Ratio

In 5.1, since the result of various amplitude levels is included, the dispersion increases. Then, the result of extracting only the data over 30cm/s2 at the maximum response acceleration is shown in Figure 6, in order to reduce the effect by the amplitude level. The SRB and RB type damping ratio similarly decrease in initial 3 years, and tendency is changed to the increase afterwards. Just after completion, the ratio between two damping takes the value of about 2 to 4, as shown in Figure 7. The ratio between two damping tends to decrease to some aging, after some point the ratio approaches to 1. The result of extracting only the data of about 5cm/s2 (4.5 ~ 5.5) at the largest response acceleration is shown in Figure 8, in order to reduce the effect of the amplitude level. The SRB and RB type damping ratios decrease in initial 3 years, and tendency is changed to the increase afterwards. The B type damping ratio tends to increase as aging. The ratio between two damping is shown in Figure 9. Just after the completion of building, the value of ratio is about 2 to 6. The tendency in the decrease is traced with the aging, and the ratio tends to approach 1 when it becomes to some extent aging number. Similar tendency can be observed in other response levels.

5.3 On Amplitude Dependence of Damping Ratio

From 5.1 and 5.2, damping ratio and those ratios change according to the aging number. In order to reduce these effects, the data in which aging number is from 4.5 to 5.5 years are extracted and tendency is shown in Figure 10.
SRB and RB damping ratios tend to increase, as acceleration increases. The B type damping ratio tends to decrease with the acceleration level. The ratio of two damping tends to increase with the increase of the level of the response acceleration shown in Figure 11.

6. CONCLUSIONS

Using the strong motion record data of an existing building, damping ratios are identified. . As a result of evaluating the three types of damping ratio (SRB,RB,B type) considering the dynamic soil-structure interaction effect, conclusions of this study are shown in the below:

1) Most becomes SRB or RB type for the damping ratio based on experiment and observation reported in past research. On the other hand, the damping ratio in the design stage indicates the B type.

2) SRB and RB type damping tend to decrease in initial about 3 years, and are changed to the increase afterwards. .

3) The B type damping ratio tends to increase by the aging.

4) In initial time, the ratio in which SRB or RB type damping is divided by B type takes the value of about 2 from 4. It tends to approach 1 constant value with the aging.

5) As the acceleration level is higher, SRB and RB type damping ratio tend to be larger. As the acceleration level is higher, B type damping ratio tends to be smaller.

6) As the acceleration level is higher, the ratio in which SRB or RB type damping is divided by B type takes larger value.

7. REFERENCES

1. N. Satake, K. Suda, T. Arakawa, A. Sasaki, Y. Tamura : Damping Evaluation using Full-Scale Data of Buildings in Japan, Journal of Structural Engineering, Vol. 129, No. 4,, pp. 470-477, 2003.4
2. Akaike, H., 1973. Information theory and an extension of the maximum likelihood principle, 2nd Inter. Symp. On Information Theory (Petrov, B.N. and Csaki, F. eds.), Akademiai Kiado, Budapest 267-281

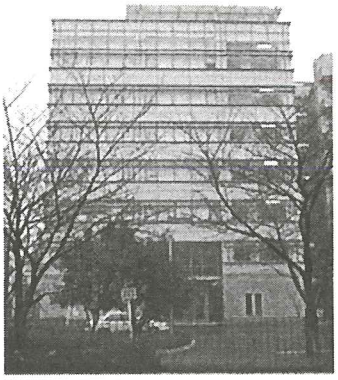

Figure 1. Exterior of Target Building

Table 1. Outline of Building Characteristics.

Structure type	steel encased reinforced concrete
Number of story	8-story
Height	30.9m
Total building area	5050m^2
Foundation type	mat foundation

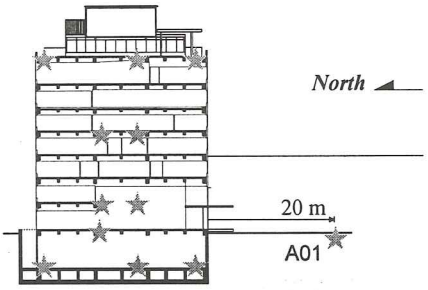

Figure 2. Vertical Sensor Configuration

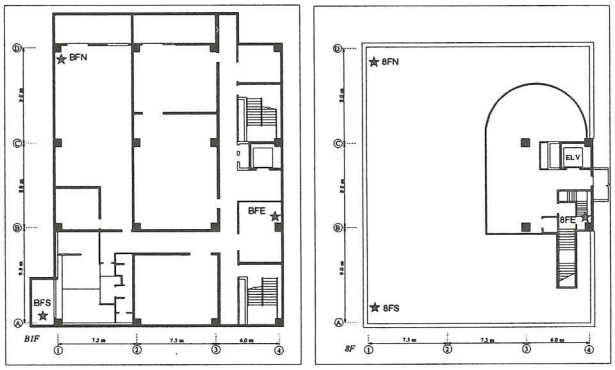

Figure 3. Sensor Configuration at Basement Floor and 8th Floor

Table 2. Type of Damping Ratio by Experimental Method.

Experimental method	Estimation method	Type
Free vibration test	logarithmic decrement etc.	SRB
Forced vibration test	Resonance curve	SRB
Microtremor observation, Wind observation	Random decrement	SRB
Microtremor observation & Strong motion observation(only horizontal)	Transfer function etc.	RB
Microtremor observation & Strong motion observation(including up-down components)	Transfer function etc.	B

Table 3. Type of Damping Ratio in Response Analysis.

analytical method	Type
time history response analysis	B
response spectrum method	B

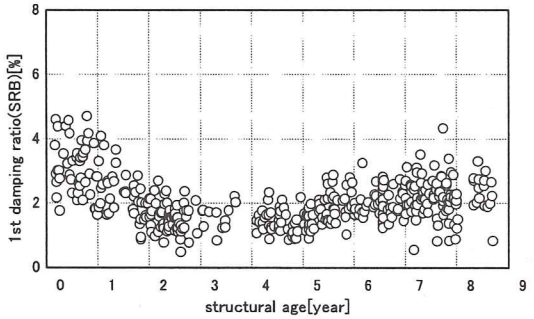

Figure 4. Secular Change of Damping Ratio (SRB)

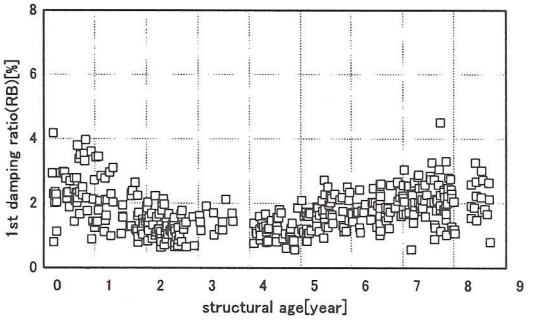

Figure 5. Secular Change of Damping Ratio (RB)

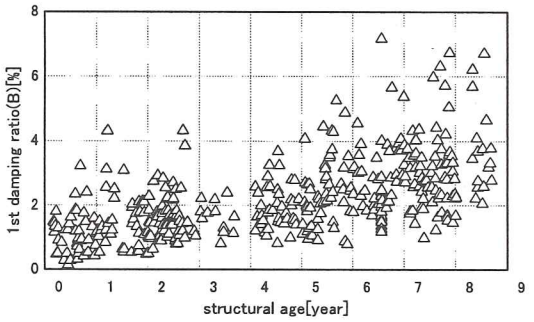

Figure 6. Secular Change of Damping Ratio (B)

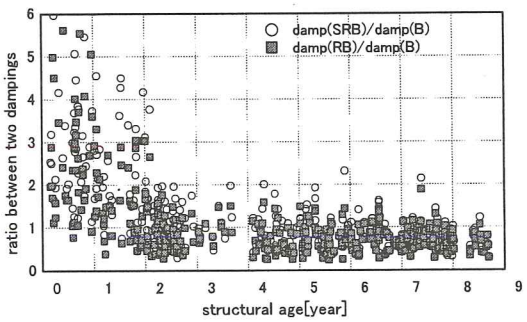

Figure 7. Secular Change of Ratio between Two Damping

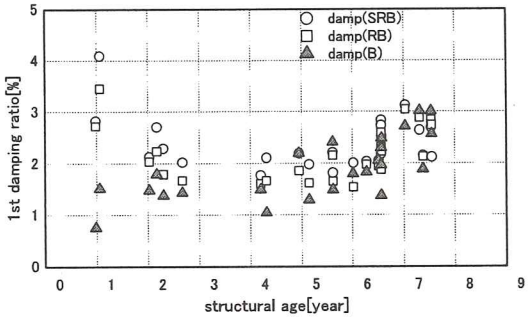

Figure 8. Secular Change of Damping Ratio (Peak response is more than 30cm/s2)

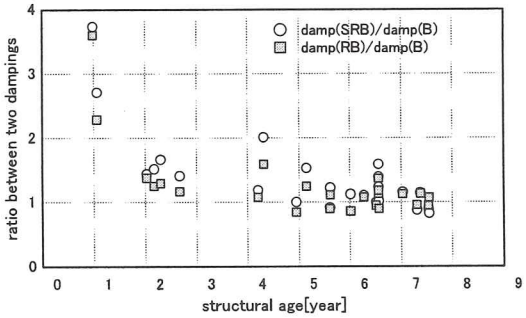

Figure 9. Secular Change of Ratio between two damping (Peak response is more than 30cm/s2)

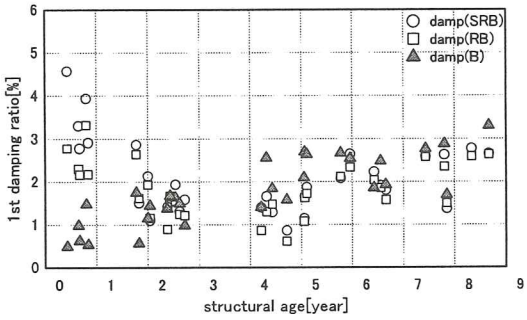

Figure 10. Secular Change of Damping Ratio (Peak response is about 5cm/s2)

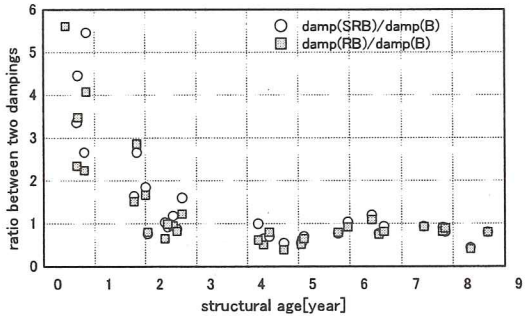

Figure 11. Secular Change of Ratio between Two Damping (Peak response is about 5cm/s2)

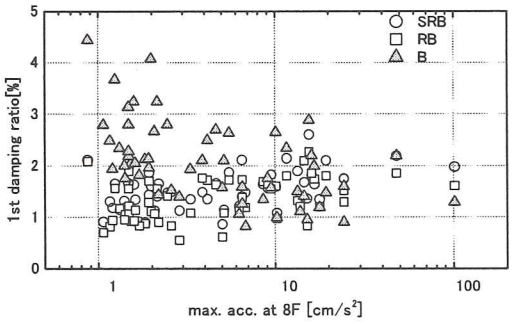

Figure 12. Amplitude Dependence of Damping Ratio (Aging number is about 5 years)

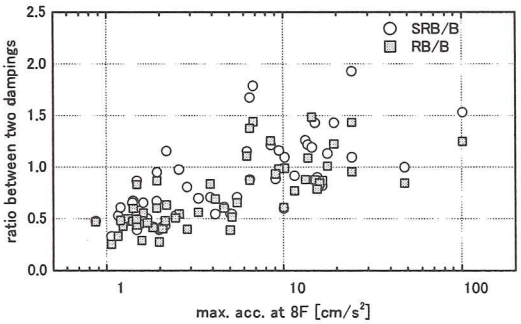

Figure 13. Amplitude Dependence of Ratio between Two Damping (Aging number is about 5 years)

Smart Sensing Technology: A New Paradigm for Structural Health Monitoring

by

B.F. Spencer Jr.,[1] T. Nagayama,[2] J.A. Rice,[3] and G.A. Agha[4]

ABSTRACT

The computational and wireless communication capabilities of smart sensors densely distributed over structures can provide rich information for structural monitoring. While smart sensor technology has seen substantial advances during recent years, interdisciplinary efforts to address issues in sensors, networks, and application specific algorithms are needed to realize their full potential. This paper first reports on research that addresses each of these issues and then integrates this research to provide a new structural health monitoring (SHM) system that is suitable for implementation on a network of smart sensors. Experimental verification is provided using Intel's Imote2 installed on a three-dimensional truss structure. The Imote2 is employed herein because it has the high computational and wireless communication performance required for advanced SHM applications. The efficacy of this SHM system is then demonstrated from sensing, network, and SHM algorithm perspectives.

KEYWORDS: smart sensors, structural health monitoring, damage detection, distributed computing, data aggregation

1.0 INTRODUCTION

The investment of the United States in civil infrastructure is estimated to be $20 trillion. Annual costs amount to between 8-15% of the GDP for most industrialized countries (US Census bureau 2004; Jensen 2004). This investment is likely to increase. Indeed, much attention has been focused in recent years on the declining state of the aging infrastructure in the U.S. These concerns apply not only to civil engineering structures, such as the nation's bridges, highways, and buildings, but also to other types of structures, such as the aging fleet of aircraft currently in use by domestic and foreign airlines. The ability to continuously monitor the integrity of civil infrastructure in real-time offers the opportunity to reduce maintenance and inspection costs, while providing for increased safety to the public. Furthermore, after natural disasters, it is imperative that emergency facilities and evacuation routes, including bridges and highways, be assessed for safety. Addressing all of these issues is the objective of structural health monitoring (SHM).

To efficaciously investigate damage, a dense array of sensors will be required for large civil engineering structures (Spencer et al 2004; Gao 2005). To illustrate this point, consider the task of locating a few strategic sensors in structures such as the 2 km long Akashi-Kaikyo Bridge or the 443 m tall Sears Tower in Chicago so that these sensors can detect randomly occurring damage; such a task is intractable, if not impossible. To effectively detect arbitrary damage in structures, especially complicated structures, a dense array of sensors distributed over the entire structure will be required.

Some efforts have been made toward in-depth monitoring that can provide detailed information

[1] Nathan M. and Anne M. Newmark Endowed Chair in Civil Engineering, Dept. of Civil and Environmental Engineering, University of Illinois at Urbana-Champaign, Urbana, IL 61801, USA
[2] Assistant Professor, Dept. of Civil Engineering, University of Tokyo, Tokyo 113-8656, Japan
[3] Ph.D. Student, Dept. of Civil and Environmental Engineering, University of Illinois at Urbana-Champaign, Urbana, IL 61801, USA
[4] Professor, Dept. of Computer Science, University of Illinois at Urbana-Champaign, Urbana, IL 61801, USA

on civil infrastructure. The Tsing Ma Bridge and Kap Shui Mun Bridge in Hong Kong are monitored with 326 channels of sensors in total, producing about 65 MB of data every hour (Wong 2004). The expense of installing traditional monitoring systems, however, has limited significantly wider-spread implementation (Farrar 2001; Celebi 2002; Lynch and Loh 2006). For example, the total system cost, including installation, of the monitoring system on the Bill Emerson Memorial Bridge in Cape Girardeau, Missouri, USA is about $1.3M for 86 accelerometers, which makes the average installed cost per sensor a little over $15,000 dollars (Hartnagel 2006). Costs for other bridge installations are of a similar magnitude. Smart sensors with wireless communication capability are reported to reduce installation effort to a great extent (Lynch et al. 2005) and help to realize a dense array of sensors.

Though networks of densely deployed smart sensors have the potential to improve SHM dramatically, limited resources on smart sensors preclude direct application of traditional monitoring strategies on smart sensor networks which typically require centralized, synchronized data acquisition. Such an approach for SHM requires a tremendous amount of data to be sent to such a central station and is not scalable to large numbers of sensors.

Noting that damage in structures is an intrinsically local phenomenon, SHM applications using smart sensors may be realized even for structures of substantial size. Responses from sensors close to the damaged site are expected to be more heavily influenced than those remote to the damage. If data is locally processed, communication requirement will remain reasonable. Several other characteristic of smart sensors also need to be investigated with respect to application specific requirements. For example, time synchronization accuracy may not be suitable for some applications, and packet loss may severely affect the performance of SHM systems. By understanding both the structure and the smart sensor network, implementable SHM systems deployed on a dense array of smart sensors can be realized.

This paper addresses several critical problems toward realization of a SHM system employing smart sensors. Following a brief review of smart sensors and a description of the proposed system framework, middleware services such as data aggregation, reliable communication, and synchronized sensing are presented. These services are then used to develop a scalable SHM strategy for implementation on smart sensor networks. The efficacy of this strategy is then demonstrated using Intel's Imote2 smart sensor implemented on a three-dimensional truss structure.

2.0 SMART SENSORS

The essential difference between a standard sensor and smart sensor is the latter's flexible communication and information processing capability. Each sensor has an on-board microprocessor that can be used for digital signal processing, self-diagnostics, self-identification, and self-adaptation functions. Furthermore, all smart sensor platforms have thus far employed wireless communication technology.

Some of the first efforts in developing the smart sensors for application to civil engineering structures were presented by researchers at Stanford University (Straser and Kiremidjian 1996, 1998; Kiremidjian et al. 1997). Since these early efforts, numerous researchers have developed smart sensing platforms. Lynch and Loh (2006) cited over 150 papers on wireless sensor networks for SHM conducted at over 50 research institutes worldwide.

The first available open hardware/software smart sensor platform, which allows users to customize hardware/software for a particular application, was the Berkeley Mote. The third generation of Mote, the Mica, was released in 2001 (Hill and Culler 2002), having improved memory capacity and using a faster microprocessor than its predecessors. Subsequent improvements to the Mica platform resulted in the Mica2, Mica2Dot, and MicaZ. Moreover these sensors have been made commercially available (Crossbow 2007).

Several SHM applications with smart sensors have been studied using both scale models and full-scale

structures (e.g., Lynch et al 2002; Aoki et al. 2003; Tanner et al. 2003, Chung et al. 2004; Nagayama et al. 2004; Nitta et al. 2005; Ou et al. 2005). Sensor calibration and demonstration of data acquisition and computational capability have been performed with the ultimate goal of life-long monitoring of civil infrastructure using a dense array of smart sensors.

While smart sensor technology has seen substantial advances during recent years (Hill and Culler 2002; Adler et al. 2005; Kling et al. 2005), interdisciplinary research efforts to address issues in sensors, networks, and application specific algorithms are needed to realize their potential. Some identified research gaps are summarized in Table 1.

3.0 FRAMEWORK

3.1 Network topology

Most of the SHM applications with smart sensors can be categorized into two groups, neither of which has fully exploited the smart sensor's capability.

In the first group, the smart sensors emulate traditional wired sensors, with all data being synchronously collected for processing at a centralized location (see Figure 1a). Centralized SHM algorithms can then be applied to this data. This approach allows for direct application of a wealth of traditional SHM algorithms. As the number of smart sensors increases, however, the measurement data to be centrally collected exceeds the network bandwidth, regardless of whether homerun or hopping communication is adopted. Forwarding data to the base station may take a prohibitively long time and consume a lot of power. Introducing faster communication speeds offered by nodes with ample power sources is one approach. Chintalapudi, et al. (2006) utilizes a tiered approach, with lower tier nodes and powerful upper tier nodes. Assuming that the upper tier nodes have sufficient power, the limitation on the communication speed among upper tier nodes is removed; power consumption at lower tier nodes is moderate. However, installing powerful nodes is sometimes impractical or can reduce the advantages of smart sensors; the need for powerful nodes with associated power sources may increase the installation cost. In terms of the network, dependency on such nodes limits the ability of the network to automatically reconfigure should a powerful node cease to function. The limited communication bandwidth and battery power hinders the application of a centralized data acquisition approach to a large smart sensor network.

The second group of the algorithms assumes that each smart sensor measures and processes data independently without sharing information among the neighboring nodes (Sohn et al. 2002; Lynch et al. 2005; Nitta et al. 2005). Since only the processed data is sent back to base station, communication requirements are quite modest. Consequently, this approach is scalable to a large number of smart sensors (see Figure 1b). However, the independent node approach does not utilize available information from neighboring nodes; all spatial information (e.g., mode shapes) is discarded. The inability to incorporate spatial information limits the effectiveness of this approach.

A hierarchical system is considered to resolve the limitations of these two approaches (see Figure 1c). Smart sensors are conceptually divided into interacting communities of sensors. Data processing is coordinated and distributed among sensors. The Distributed Computing Strategy for SHM (DCS) (Gao 2005) is an example of such a hierarchical SHM system. Communication and data processing in DCS take place mainly in local sensor communities, reducing requirements on transmission of large amounts of data. Structural analysis of DCS takes into account measurements at multiple locations, making use of available spatial information. The DCS has the features that make it possible to be deployed on a dense array of smart sensors.

3.2 Proposed architecture

A homogeneous configuration of hardware is chosen, as opposed to a tiered system approach employing resource demanding upper level nodes and less powerful lower level nodes. In addition to

smart sensors, a PC is needed in this architecture as the interface to the users. A homogeneous configuration results in simpler programming and deployment of smart sensor nodes. Systems with homogeneous configurations can be programmed so that failure of one node does not result in failure of the system; roles of a non-functioning node can be taken over by neighboring nodes as conceptually shown in Figure 2.

In terms of functionality, smart sensor nodes in the proposed system are differentiated as follows: (i) base station, (ii) manager nodes, (iii) cluster heads, and (iv) leaf nodes. All the sensors deployed on a structure, in principal, work as leaf nodes. Leaf nodes receive commands from the other nodes and perform preprogrammed tasks such as sensing, data processing, and acknowledgement. The collection of leaf nodes in a neighborhood make a local sensor community. One of the nodes in each local sensor community is assigned as a cluster head and handles most of the communication and data processing in the community. In addition to tasks inside the community, the cluster head communicates with cluster heads of neighboring communities to exchange information. One of the cluster heads also functions as the manager sensor. When intra-cluster RF communication signals reach nodes in neighboring sensor communities, the manager deals with time sharing among sensor communities to avoid RF interference. The manager also exchanges packets directly with leaf nodes to manage operations in which all the leaf nodes participate; sensing, which is triggered by the manager sensor, is an example. The base station node is the gateway between the smart sensor network and the PC. The PC, which provides the user interface, sends commands and parameters to the smart sensor networks via the base station. The PC also receives data and calculation results from the base station. While the base station can communicate directly with any node in communication range, most communication involving the base station is routed through the manager or cluster heads, with the exception being the transmission of a large amount of data or calculation results from leaf nodes to the PC for debugging purpose.
The smart sensor platform employed in this work is Intel's Imote2 (Adler et al. 2005). The Imote2 (Figure 3) is a new smart sensor platform developed by Intel for data intensive applications. The main board of the Imote2 incorporates a low-power X-scale processor, the PXA27x, and an 802.15.4 radio (ChipCon 2420). The processor speed may be scaled based on the application demands, thereby improving its power usage efficiency. One of the important characteristics of the Imote2, which separates it from previously developed wireless sensing nodes, is the amount of data which can be stored on the node. The Imote2 has 256 KB of integrated SRAM, 32 MB of external SDRAM, and 32 MB of Strataflash memory (Intel Corporation 2005), which is particularly important for the large amount of data required for real-time, dynamic monitoring of structures. Table 2 gives a comparison of the Imote2 to the Mica2, a third generation of Mica motes developed at Berkeley.

The sensors used with the Imote2 are interfaced to the main board via two connectors. This interface provides a significant amount of built-in flexibility for the type of sensors which may be utilized. Some of the options available for I/O are I2C (which allows interface to an unlimited number of channels), 3 SPI ports (serial data ports limited to one channel per port) and multiple GPIO (general purpose I/O) pins.

Intel has created a basic sensor board to interface with their Imote2. This basic sensor board can measure 3-axes of acceleration, light (TSL2561), temperature, and relative humidity (SHTx). All of the sensors on this board are digital, thus no analog to digital converter (ADC) is required (Adler et al. 2005). STMicroelectronics manufactures the 3-axis digital accelerometer (LIS3L02DQ) which has a ±2g measurement range and a resolution of 12-bits or 0.97 mg (STMicroelectronics 2005a).

The LIS3L02DQ's has a built-in ADC which is followed by digital filters with selectable cutoff frequencies. These cutoff frequencies are user defined by setting a decimation factor, which also dictates the sampling rate of the accelerometer. The sampling rate and cutoff frequency versus the decimation factor is given in Table 2, as specified by the manufacturer. The digital output interface

may be either SPI or I2C (STMicroelectronics 2005b).

TinyOS is employed as the operating system on many smart sensors, including the Imote2. This operating system has a small memory footprint and is therefore suited to the limited resources of wireless sensors. TinyOS has a large user community and many successful smart sensor applications. However, some features pose limitations for SHM applications. Primarily, TinyOS does not support real time operations and thus has only two types of execution threads: 1) tasks and 2) hardware event handlers. This concurrency model leaves only a small amount of control to the user in the assignment of priority to commands; execution timing cannot be arbitrarily controlled. The subsequent section will show that this feature of TinyOS must be carefully considered when designing an SHM implementation.

4.0 MIDDLEWARE SERVICE DEVELOPMENT

In this section, the basic functionalities of smart sensors essential to SHM applications are studied and realized. Among these functionalities are data aggregation, reliable communication, and synchronized sensing. These functionalities are developed on the Imote2 platform.

4.1 Data aggregation

The amount of data transferred in SHM applications is considerable. Long vibration records will be acquired from densely distributed smart sensors. If they are collected at a single sink node using multi-hop communication, the associated time easily exceeds the time necessary for any other smart sensor task. Distributed estimation of the correlation function has been proposed as a type of model-based data aggregation (Nagayama et al. 2006). When the excitation can be assumed to be broadband and the structural response stationary, the correlation function between the output measurements can be used to determine modal parameters by virtue of the Natural Excitation Technique (NExT) (James et al. 1992). This data aggregation method, which is scalable to networks of a large number of smart sensors, is described herein.

Correlation functions are, in practice, estimated from finite length records. Power and cross spectral density (PSD/CSD) functions are estimated first through the following relation (Bendat and Piersol 2000):

$$G_{xy}(\omega) = \frac{1}{n_d T} \sum_{i=1}^{n_d} X_i^*(\omega) Y_i(\omega) \qquad (1)$$

where $G_{xy}(\omega)$ is the CSD estimation between two stationary random process, $x(t)$ and $y(t)$. $X(\omega)$ and $Y(\omega)$ are the Fourier transform of $x(t)$ and $y(t)$; the * denotes the complex conjugate. T is the length of the sample records, $x_i(t)$ and $y_i(t)$. In estimating the spectral densities, windowing of the time histories is common practice to suppress the phenomena of spectral leakage. Window functions are multiplied by the time histories, $x(t)$ and $y(t)$, prior to the Fourier transform. When $n_d = 1$, the estimate has a large random error. The random error is reduced by computing an ensemble of the estimates from n_d different or partially overlapped records. The normalized RMS error $\varepsilon[|G_{xy}(\omega)|]$of the spectral density function estimation is given as

$$\varepsilon\left[\left|G_{xy}(\omega)\right|\right] = \frac{1}{\left|\gamma_{xy}\right|\sqrt{n_d}} \qquad (2)$$

γ_{xy} is the coherence function between $x(t)$ and $y(t)$, indicating the degree of linearity between them. Through the averaging process, the estimation error is reduced. Averaging of 10-20 times is common practice. The estimated spectral densities are then converted to correlation functions by inverse Fourier transform.

An implementation of correlation function estimation for a small community of sensors in a centralized data collection scheme is shown in Figure 4, where node 1 works as a reference sensor. Assuming n_s nodes, including the reference node, are measuring structural responses, each node acquires data that is sent to the reference node. The reference node calculates the spectral density. This procedure is repeated n_d times and averaged. After averaging, the inverse FFT is taken to calculate the correlation function. All the calculations take place at the reference nodes. When the spectral density is estimated from discrete time history records of

length N, the amount of data to be transmitted through the radio is $N \times n_d \times (n_s - 1)$.

In the next scheme, data flow for correlation function estimation is examined and data transfer is reorganized to take advantage of the computational capability on each smart sensor node (see Figure 5). After the first measurement, the reference node broadcasts the time record to all the nodes. On receiving the record, each node calculates the cross spectral density between its own data and the received record. This spectral density estimate is locally stored. The nodes repeat this procedure n_d times. After each measurement, the stored value is updated by taking a weighted average between the stored value and the current estimate. In this way, Eq. (1) is calculated on each node. Finally the inverse FFT is applied to the spectral density estimate locally. The resultant correlation function is sent back to the reference node. Because the subsequent modal analysis such as ERA uses, at most, half of the correlation function data length, $N/2$ data is sent back to the reference node from each node. The total data to be transmitted in this scheme is, therefore, $N \times n_d + N/2 \times (n_s - 1)$.

As the number of nodes increases, the advantage of the second scheme, in terms of communication requirements, becomes significant. The second approach requires data transfer of $O(N \times (n_d + n_s))$, while the first one needs to transmit to the reference sensor node data of the size of $O(N \times n_d \times n_s)$. For example, a parameter set $\{N, n_d, n_s\} = \{1024, 20, 10\}$ necessitates the second approach to transfer 25,088 data points while the first one involves transmit of 184,320 data points; the reduction factor achieved by the distributed implementation is more than seven. The distributed implementation leverages knowledge regarding the application to reduce communication requirements as well as to utilize CPU and memory efficiently in a smart sensor network.

The data communication analysis above assumes that all the nodes are in single-hop range of the reference node. This assumption is not necessarily the case for a general SHM application. However, Gao (2005) proposed a Distributed Computing Strategy (DCS) for SHM which supports this idea. Neighboring smart sensors within single-hop communication range make local sensor communities and perform SHM in the communities. In such applications, the assumption of nodes being in single-hop range of a reference node is reasonable, while data processing results such as damage location may need to be transferred to the base station using multi-hop communication.

4.2 Reliable communication

RF communication is not reliable unless lost packets are specifically addressed. Packets may not be transmitted properly. When the distance between nodes is too long, packets may not reach the destination. Multiple nodes trying to send packets at the same time cause packet collisions. SHM applications employing smart sensors suffer from this packet loss. If packets carrying commands are lost, destination nodes fail to perform certain tasks. The sender is unsure whether the destination nodes have received commands. If packets carrying measurement data are lost, destination nodes cannot fully reconstruct the sender's data. Therefore, packet loss may cause a system to be in an unknown state and may degrade measurement signals.

When smart sensor applications come to involve more and more complicated internode data processing and are assigned more and more tasks by commands sent through packets, the commands need to be reliably delivered. Otherwise, smart sensors cannot assess the current state of neighboring nodes without intricate logic, resulting in extremely complicated programs. Reliable communication of short messages is clearly a necessary feature for an SHM system with complicated internode data processing.

Compared to the need for reliable communication of short messages, the need to transfer large amounts of data is not apparent. In many SHM research attempts, data loss has not been addressed, and the loss of a few data points has often been considered acceptable. The effect of data loss on SHM applications are assessed by Nagayama, et al. (2007). Packet loss is shown to degrade signals in the same way as observation noise, therefore

reliable communication is preferable to maintain data quality. Also when loss of a large block of packets is expected, such as when devices using the same frequency range pass by, resending of data is preferable.

A reliable communication protocol suitable for sending a large amount of data, as well as a protocol to send a single packet, is proposed. Each of these protocols supports multicast as well as unicast data transmission; SHM applications benefit from multicast transmission. One example is the distributed correlation function estimation. Multicasting of commands is commonly observed in smart sensor systems. Because of limited space, only the reliable multicast protocol for long data is briefly explained herein.

The proposed reliable communication protocol is based on a modification of the Automatic Repeat reQuest (ARQ) protocol. ARQ is an error control method which repeats the sending of packets based on requests from the receiver. On reception of packets without error, the receiver replies with a positive acknowledgement (ACK). If an error is detected, the receiver sends a negative acknowledgement (NACK) and a request for retransmission. There are several ARQ protocols.

The radio component on the Imote2 is in either listening mode or in transmission mode. During transmission, the Imote2 cannot receive packets. Without careful implementation of ARQ, the receiver may send acknowledgments while the sender is in transmission mode. Packet loss and retransmission are expected to be more frequent if transmission and reception are deeply interwoven. Scheduling interwoven transmission and reception may result in long wait times. In the proposed protocol, the sender transmits all the packets without expecting an acknowledgement. The receiver stores all the received data in a buffer. Once the sender transmits the last packet of data, the sender repeatedly transmits a packet indicating the end of data until acknowledgement packets from the receivers are received. These acknowledgment packets also contain information about missing packets. Only missing packets are resent. At the end of transmitting missing packets, a packet requesting acknowledgment is sent again. If no receiver reports missing packets, the sender signals the end of data transfer to the receivers and itself, disengaging them from this round of reliable communication. In this way, the number of acknowledgement and retransmission can be greatly reduced (see Figure 6).

This protocol is designed to send 64-bit double precision data, 32-bit integers, or 16-bit integers. Many ADCs on traditional data acquisition systems have a resolution less than 16 bits, supporting the need for transfer of 16-bit integer format data. Some ADCs have a resolution better than 16 bits, necessitating data transfer in 32-bit integer format. Once an acceleration record is processed, the outcome may require more bits. Onboard data processing such as FFTs and SVDs are usually performed in a double precision format. Even when the effective number of bits is smaller than 32, debugging of onboard data processing greatly benefits from transfer of double precision data; data processing results on Imote2s can be directly compared with those on a PC, which are most likely in a double precision format. Transfer of 64-bit double precision data is supported based on such needs.

4.3 Synchronized sensing

Time synchronization errors in a smart sensor network can cause inaccuracy in SHM applications. Time synchronization is a middleware service common to smart sensor applications and has been widely investigated. Each smart sensor has its own local clock, which is not synchronized initially with the other sensor nodes. By communicating with the surrounding nodes, smart sensors can assess relative differences among their local clocks. For example, Mica2 motes employing the Timing-sync Protocol for Sensor Network (Ganeriwal et al. 2003) are reported to synchronize with each other to an accuracy of 50 μsec; different algorithms and hardware resources may result in different precision. Whereas time synchronization protocols have been intensely studied, requirements on synchronization from an application perspective have not been clearly addressed. The effect of time synchronization error on SHM applications is studied by Nagayama et al. (2007).

In this section, the accuracy of Flooding Time Synchronization Protocol (FTSP) (Maroti et al. 2004; Mechitov et al. 2004), realized on the Imote2, is evaluated for the SHM application. Time synchronization among smart sensors, however, does not necessarily offer synchronized measurement signals; other critical issues must be considered. Finally synchronized sensing is realized utilizing resampling.

The Imote2s are programmed as follows to evaluate time synchronization error. A beacon node transmits a beacon signal every four seconds. The others eight nodes estimate global time using the beacon packet as provided in FTSP. Two seconds after the beacon signal, the beacon node sends another packet requesting replies. The receivers get time stamps of the reception of this packet and convert them to global time stamps. The receivers take turns in reporting back these time stamps. With perfect time synchronization, the time stamp of the packet reception should give the same global time at all the nodes. This procedure is repeated more than 300 times. These time stamps from the eight nodes are compared with each other. Figure 7 shows the difference in the global time stamp using one of the eight nodes as a reference. The difference is generally less than 10 μsec, indicating the time synchronization error of about 10 μsec. Scattered peaks are not necessarily indicators of large synchronization error; they may also be due to delays associated with global time stamping after the packet requesting replies are received.

The time synchronization error estimated above is considered small for SHM applications. A delay of 10 μsec corresponds to 0.072 degree phase delay for a mode at 20 Hz. Even at 100 Hz, the corresponding phase delay is only 0.36 degree.

While global clock estimates two seconds after sending the beacon signal are found to be accurate, local clocks drift over time. Large clock drift necessitates frequent time synchronization to maintain a certain level of accuracy.

The same program is utilized to estimate clock drift. On reception of the packet requesting replies, the receivers get offsets of their own timestamps instead of global time stamps. The offsets are sent back to the beacon node and then to a PC. If the clocks on the nodes are ticking at a consistent rate, the offsets should be constant over a long period of time. This experiment, however, did not show constant offsets. Figure 8 shows the offsets of nine receiver nodes. One of them stopped responding around 45 second, exhibiting a short line on the figure. Here, the maximum clock drift among this set of Imote2 nodes is estimated to be around 50 μsec per second. This drift is small but not negligible if measurement takes a long time. For example, after a 200-second measurement, time synchronization error may become as large as 10 msec.

One solution to address this clock drift problem is frequent time synchronization. The drawback of this approach is that time synchronization may not perform well when other tasks (e.g., sensing) are running. Time synchronization requires precise time stamping as previously explained. Sensing also requires precise timing and needs higher priority in execution. Scheduling more than one high priority tasks is challenging, especially for operating systems such as TinyOS which have no support for real-time control. If the time synchronization interval necessary to address the clock drift is shorter than the sensing time, a different solution must be sought.

Another approach is to compensate for the difference in clock rate. The slopes of the lines in Figure 8 approximately indicate the clock drift that needs to be compensated. If time synchronization offset values can be observed for a certain amount of time, the slope can be estimated using a least squares approach.

Several issues must be addressed to achieve synchronized sensing. Issues observed on the Imote2 platform include uncertainty in sensor start-up time, difference in sampling rate among sensor nodes, and fluctuation in sampling frequency over time (Nagayama et al. 2006). These issues are addressed by resampling of measured time histories based on time stamps marked after a fixed number of data points are collected.

The polyphase implementation of resampling Oppenheim et al. (1999) by an arbitrary non-integer rational factor addresses the problem of data sampled at inaccurate frequencies. The measured time history $x[m]$ is first upsampled by about one-hundred zeros. Then, lowpass a filter $h[i]$ is applied to yield an upsampled signal $y[j]$. The outcome $z[k]$ of the resampling process is calculated by interpolating this upsampled signal.

$$\begin{aligned} z[j] &= y[p_l](p_u - p_j) + y[p_u](p_j - p_l) \\ &= \sum_{m=\lceil (p_l - N+1)/L_a \rceil}^{\lfloor p_l / L_a \rfloor} h[p_l - L_a m]x[m]\cdot(p_u - p_j) + \\ &\quad + \sum_{m=\lceil (p_u - N+1)/L_a \rceil}^{\lfloor p_u / L_a \rfloor} h[p_u - L_a m]x[m]\cdot(p_j - p_l) \end{aligned} \quad (3)$$

$$p_j = jM_r + l_i$$

$$p_l = \lfloor jM_r + l_i \rfloor$$

$$p_u = p_l + 1$$

L_a is the factor of upsampling, N is the length of filter coefficients, and M_r is the non-integer factor of downsampling. $\lceil\ \rceil$ and $\lfloor\ \rfloor$ represent ceiling and floor function respectively. The initial delay, represented by l_i, is determined based on the global timestamp and takes into account the inaccuracy in sampled timing. The factor, L_a / M_r, determines the rate of sampling rate conversion. The sampling rate conversion is first tested in Matlab as shown in Figure 9 and subsequently implemented on the Imote2. The resampling process implemented on the Imote2 is found to yield acceleration signals with synchronization accuracy better than 50 μsec.

5.0 EXAMPLE IMPLEMENTATION

The Distributed Computing Strategy (DCS) for SHM (Gao 2005) is implemented on Imote2s using the developed middleware services. The SHM system realized on the Imote2s is then experimentally verified using a three-dimensional truss structure.

5.1 Distributed Computing Strategy for SHM

Gao (2005) proposed a Distributed Computing Strategy (DCS) for SHM that meshes well with the hierarchical architecture necessary to realize the potential of a dense network of smart sensors. The DCS approach is an extension of the DLV method (Bernal 2002) that does not require central collection of the measurement data. Instead, DCS shares data among the neighboring nodes to utilize spatial information. Due to this local data sharing with a limited number of neighboring nodes, the total amount of data to be transmitted throughout the network is kept small. Therefore, this algorithm is scalable to a large number of sensors densely deployed over large structures. While DCS does not require measurements at all the DOFs, the method's performance is improved by sensing at many DOFs; DCS benefits from a dense array of smart sensors. Computer analysis and experimental validation on a simulated wireless network showed that DCS is a promising SHM scheme (Gao 2002). While DCS has been shown promising as an SHM algorithm for smart sensor networks, the strategy has not been implemented on smart sensor platforms.

Gao (2005) explains two methods to normalize mode shapes in DCS. One of them utilizes input force measurements while the other measures only vibration outputs under known mass perturbation. Because no Imote2 sensor board with force measurement is available and because the input force of a full-scale structure is difficult to measure, DCS employing the mass perturbation method is chosen as the algorithm to be implemented. Bernal (2006) proposed a stochastic DLV (SDLV) localization approach. This variant of the DLV method does not require normalization of mode shapes. The absence of the need for normalization greatly simplifies the SHM strategy. Therefore, the SDLV approach is also implemented on networks of Imote2s.

The DCS implementation is comprised of various steps, including numerical calculation functions, middleware services, and the damage detection algorithm. The major numerical calculation functions utilized in DCS for SHM are: singular value decomposition (SVD), complex eigensolver, Fast Fourier transform (FFT), quick sort, and complex matrix inverse. These functions are either developed from scratch or functions written in C language are adapted. The performance of these functions is examined on the Imote2; execution of

these functions on the Imote2 yields identical outputs as those from Matlab functions with the precision of double data type. Required middleware services for DCS include: data aggregation, reliable communication, and synchronized sensing. The services described earlier are adapted for this purpose. The algorithm to locate damage involves NExT, ERA, and DLV. These techniques are coded as C-functions and adapted to TinyOS.

Implementation of DCS for SHM including these functions requires further consideration of the limited hardware resources. The memory space on the Imote2 is limited, and the CPU speed is slower than that of a PC. For example, the size of the Hankel matrix utilized in ERA may exceed the available memory space on the Imote2s. The matrix size must be limited so that the matrix fits in the available memory. Fortunately, application of DCS on a PC to experiment data has shown that modal parameters can be estimated with sufficient accuracy using a reduced-size Hankel matrix. Additionally, estimation of the stresses induced by the DLVs may involve structural analysis of the whole truss, which requires large amounts of memory and calculation time. Instead, a matrix to convert input force to stress is calculated on a PC in advance and injected to the cluster heads; cluster heads need to simply compute the product of the matrix and the DLVs rather than to run the entire structural analysis. Through these considerations, DCS can be ported to the Imote2.

Imote2s are preprogrammed to autonomously accomplish the DCS. All the necessary parameters such as node ID, sensor direction, and data length are initially injected to the network from the base station. The base station sends these parameters to the manager sensor or cluster head sensors, which forward a part of the parameters to the leaf nodes. After this parameter injection, the PC connected to the base station does not need to give input to the Imote2 network. Tasks are preassigned to each command which is sent by the reliable communication protocol.

Several functionalities, which may not be necessary for complete SHM systems, are considered important for debugging purposes and are implemented as well. Measured acceleration time histories are sent back to the base station so that processing of the time history in the network can be compared to equivalent data processing on a PC. Intermediate results of DCS such as modal parameters, DLVs, and accumulated stress are also sent back to the base station for the same reason. In addition, critical communication packets among sensor nodes are directed to the base station using the multicast reliable communication protocol so that important communication is logged at the base station for debugging. These functionalities help development and performance evaluation for the smart sensor system.

5.2 Experimental setup

A 5.6 m long, three-dimensional truss structure at the Smart Structures Technology Laboratory (SSTL) of the University of Illinois at Urbana-Champaign (http://sst.cee.uiuc.edu/) is employed for experimental validation (see Figure 10). The length of each bay of the truss is 0.4 m. The truss sits on two rigid supports. One end of the truss is a pinned support, and the other is a roller support. The pinned end can rotate freely with all three translations restricted. The roller end can also move in the longitudinal direction.

The truss is excited vertically by a Ling Dynamic Systems permanent magnetic V408 shaker. A band-limited white noise is sent from the computer to the shaker to excite the truss structure up to 100 Hz. The shaker is connected to the bottom of the outer panel using a stinger.

Ten Imote2s mounted on nodes of the truss measure acceleration in three directions. The three axes of the Imote2 accelerometers are aligned with longitudinal, transverse and vertical directions. The acceleration data is acquired at a nominal sampling rate of 560 Hz and resampled to 280 Hz. Six Imote2s mounted on six front panel nodes of two consecutive bays of the truss constitutes a local sensor community and monitor structural damage within the bays. The ten Imote2s in total make three overlapping sensor communities.

A horizontal element on the lower cord is replaced with a thinner element to simulate damage to the

truss. This replacement results in 52.7 % cross section loss in elements 20 and 8 in the mass perturbation-based DCS method experiment and SDLV-based DCS method experiment, respectively (see Figure 11). The cross section loss reduces stiffness in the element and is expected to be detected as damage by the DCS method.

5.3 Experimental results

Through the resampling process, measured acceleration signals are synchronized to each other. The phase of the cross spectral densities indicates the synchronization accuracy. The slope of the phase indicates time synchronization error. As shown in Figure 12, the time synchronization error is approximately 30 μsec.

Modal parameters are determined from these measured acceleration signals. The NExT method is used to estimate the cross spectral densities and convert them to correlation functions. The Hanning window is employed in spectral density estimation. Figure 13 shows cross spectral densities between the vertical acceleration signal of a cluster head node and the longitudinal and vertical acceleration signals of other nodes in the community. As expected, the spectral densities estimated on the Imote2s show clear peaks corresponding to structural modes. The acceleration signals are also processed on a PC to validate the numerical operation on the Imote2s. The spectral densities estimated on the Imote2s in a distributed manner are found to be identical (within the numerical precision of double data type) to those calculated on the PC. Natural frequencies, damping ratios, mode shapes, EMAC, initial modal amplitude, etc. are identified from the cross spectral densities by cluster head nodes running ERA. These identified parameters are numerically the same as those identified on a PC.

First, the mass perturbation-based DCS method is considered. Here, the network of Imote2s installed at nodes 7, 9, 11, 13, 15, 17, 19, 21, 23, and 25 (see Figure 11) estimates the mass normalization constants prior to commencement of monitoring by measuring the acceleration responses of the truss with and without known mass perturbation. Then Imote2s are installed at nodes 8 to 13. The modal parameters identified before and after element replacement are input to the DLV method to locate the simulated damage. The normalized accumulated stress estimated by the cluster head node, node 10, is shown in Figure 14. This local sensor community monitors elements 15 to 23. The DLV method identifies damaged elements as those with small accumulated stress. Element 20, which was replaced with a thinner bar, has a normalized accumulated stress smaller than a predetermined threshold value, 0.3. While the small normalized accumulated stress successfully localized damage in this experiment, false positive/negative damage localization is sometimes observed in other cases.

The damage localization algorithm is then changed to the SDLV method, and the damaged element is sought. Ten Imote2s are installed from nodes 2 to 11. Nodes 4, 6, and 8 become cluster heads and form local sensor communities around them. Each local sensor community consists of a cluster head and five surrounding nodes. Figure 15 shows the normalized accumulated stress calculated by the three adjacent cluster heads. In this experiment, element 8 is replaced with the thinner element. As shown, the Imote2s in these local sensor communities successfully detected the damaged element.

The SDLV results from the respective communities are shared among neighboring cluster heads to make judgment on damage. If neighboring nodes are consistent, the damage detection results are reported to the base station and the cluster heads switches to the sleep mode. If inconsistency is observed, the neighbors retake data and apply the series of data processing again. Figure 16 shows the report from the cluster heads to the base station after applying the SDLV-based DCS method and exchanging damaged element information among the communities. Element 8 is identified as the only damaged element. The damage localization at the three cluster heads is consistent and the flag to indicate retaking data is set to zero.

6.0 CONCLUSION

A hierarchical, distributed SHM system employing smart sensors has been developed and experimentally verified on the Imote2 smart sensor platform. To realize this SHM system required various issues and algorithms to be addressed. Middleware services including data aggregation, reliable communication, and synchronized sensing were realized on Imote2s. These services as well as numerical functions and algorithms were combined to produce the SHM system. Experimental verification using the three-dimensional truss demonstrated the efficacy of the SHM system developed herein. More details about this research can be found in Nagayama (2007).

7.0 ACKNOWLEDGEMENTS

The authors gratefully acknowledge the support of this research by the National Science Foundation under NSF grants CMS 03-01140 and CMS 06-00433, Dr. S.C. Liu, Program Manager. The second and third authors would also like to acknowledge the support of a Vodafone-U.S. Foundation Graduate Fellowship.

6.0 REFERENCES

Adler, R., Flanigan, M., Huang, J., Kling, R., Kushalnagar, N., Nachman, L., Wan, CY., and Yarvis, M. "Intel mote 2: an advanced platform for demanding sensor network applications." Proc. 3rd int. conference on Embedded networked sensor systems, 298 - 298. (2005)

Aoki, S., Fujino, Y., and Abe, M. "Intelligent bridge maintenance system using MEMS and network technology." Proc., SPIE – Smart Systems and NDE for Civil Infrastructures, 5057, 37-42. (2003)

Bendat, J. S., and Piersol, A.G. Random data: analysis and measurement procedures, John Wiley and Sons, Inc. (2000)

Bernal, D. "Load vectors for damage localization." J. of Engineering Mechanics, 128(1), 7-14. (2002)

Bernal, D. "Flexibility-based damage localization from stochastic realization results." J of Engineering Mechanics, 132(6), 651-658. (2006)

Celebi, M. "Seismic instrumentation of buildings (with emphasis on federal buildings)." Special GSA/USGS Project, an administrative report, United States Geological Survey, Menlo Park, CA. (2002)

Chintalapudi, K., Paek, J., Gnawali, O., Fu, T., Dantu, K., Caffrey, J., Govindan, R., and Johnson, E. "Structural Damage Detection and Localization Using NetSHM." Proc 5th International Conference on Information Processing in Sensor Networks: Special track on Sensor Platform Tools and Design Methods for Networked Embedded Systems (IPSN/SPOTS'06), Nashville, TN, (2006)

Chung, H.-C., Enomoto, T., Shinozuka, M., Chou, P., Park, C., Yokoi, I., and Morishita, S. "Real time visualization of structural response with wireless MEMS sensors." Proc., 13th World Conference on Earthquake Engineering, No. 121, 1-10. (2004)

Crossbow Technology, Inc. <http://www.xbow.com> (Mar. 2, 2007).

Farrar, C. R. "Historical overview of structural health monitoring." Lecture Notes on Structural Health Monitoring using Statistical Pattern Recognition. Los Alamos Dynamics, Los Alamos, NM. (2001)

Ganeriwal, S., Kumar, R., and Srivastava, M. B. "Timing-sync protocol for sensor networks." Proc., 1st International Conference On Embedded Networked Sensor Systems, Los Angeles, CA, 138 - 149. (2003)

Gao., Y. Structural health monitoring strategies for smart sensor networks, Ph.D. Dissertation, University of Illinois at Urbana-Champaign, IL (2005)

Hartnagel, Bryan A. Personal Communication, August 22 (2006)

Hill, J., and Culler, D. "Mica: A wireless platform for deeply embedded networks." *IEEE Micro.*, 22(6), 12-24. (2002)

James, G. H., Carne, T. G., Lauffer, J. P., and Nord, A. R. "Modal testing using natural excitation." Proc., 10th Int. Modal Analysis Conference, San Diego, CA..(1992)

Jensen, S. "Summary Outlook to 2005 for the European Construction Market."

http://www.cifs.dk/scripts/artikel.asp?id=775&lng=2. (2005)

Kiremidjian, A. S., Straser, E. G., Meng, T. H., Law, K. and Soon, H. "Structural damage monitoring for civil structures." Proc., Int. Workshop on Structural Health Monitoring, Stanford, CA, 371-382. (1997)

Kling, R., Adler, R., Huang, J., Hummel, V., and Nachman, L. "Intel Mote-based Sensor Networks." Structural Control Health Monitoring, 12:469–479. (2005)

Lynch, J. P., Law, K. H., Kiremidjian, A. S., Carryer, E., Kenny, T. W., Patridge, A., and Sundararajan, A. "Validation of a wireless modular monitoring system for structures." Proc., SPIE - Smart Structures and Materials: Smart Systems for Bridges, Structures, and Highways, San Diego, CA, 4696(2), 17-21. (2002)

Lynch, J. P. and Loh, K. "A summary review of wireless sensors and sensor networks for structural health monitoring." Shock and Vibration Digest, 38(2), 91-128. (2006)

Lynch, J. P., Wang, Y., Law, K. H., Yi, J.-H., Lee, C. G., and Yun, C. B. "Validation of a large-scale wireless structural monitoring system on the Geumdang bridge." Proc., the Int. Conference on Safety and Structural Reliability, Rome, Italy. (2005)

Maroti, M. Kusy, B., Simon, G., and Ledeczi, A. "The flooding time synchronization protocol." Proc., 2nd International Conference On Embedded Networked Sensor Systems, Baltimore, MD, 39-49. (2004)

Mechitov, K., Kim, W., Agha, G., and Nagayama, T. "High-frequency distributed sensing for structure monitoring." Proc., 1st Int. Workshop on Networked Sensing Systems, Tokyo, Japan, 101–105.(2004)

Nagayama, T. Structural health monitoring using smart sensors, Ph.D. Dissertation, University of Illinois at Urbana-Champaign, IL (2007)

Nagayama, T., Rice, J.A., and Spencer, Jr., B.F. "Efficacy of Intel's Imote2 wireless sensor platform for structural health monitoring applications." Proc., Asia-Pacific Workshop on Structural health Monitoring, Yokohama, Japan. (2006)

Nagayama, T., Ruiz-Sandoval, M., Spencer Jr., B. F., Mechitov K. A., Agha, G. "Wireless strain sensor development for civil infrastructure." Proc., 1st Int. Workshop on Networked Sensing Systems, Tokyo, Japan, 97–100. (2004)

Nagayama, T. Sim, S.H., Miyamori, Y., Spencer Jr., B.F. "Issues in Structural Health Monitoring Employing Smart Sensors." Smart Structures and Systems (in review)

Nagayama, T, Spencer, B.F., Agha, G., and Mechitov, K. "Model-based Data Aggregation for Structural Monitoring Employing Smart Sensors." 3rd International Conference on Networked Sensing Systems (INSS). (2006)

Nitta, Y., Nagayam, T., Spencer Jr., B. F., and Nishitani, A. "Rapid damage assessment for the structures utilizing smart sensor MICA2 MOTE." Proc., 5th Int. Workshop on Structural Health Monitoring, Stanford, CA., 283-290. (2005)

Oppenheim, A.V., Schafer, R.W., Buck, J.R. "Discrete-Time Signal Processing." Prentice Hall. (1999)

Ou, J. P., Li, H. W., Xiao, Y. Q., Li, Q. S. "Health dynamic measurement of tall building using wireless sensor network." Proc., SPIE - Smart Structures and Materials, 5765(1), 205-215. (2005)

Sohn, H., Worden, K., and Farrar, C. R. "Statistical damage classification under changing environmental and operational conditions." J. Intelligent Material Systems and Structures, 13, 561-574. (2002)

Spencer Jr., B.F., Ruiz-Sandoval, M.E., and Kurata, N. "Smart sensing technology: opportunities and challenges." J. of Structural Control and Health Monitoring, 11:349–368. (2004)

STMicroelectronics, LIS3L02DQ Data Sheet. (2005)

STMicroelectronics, Application Note AN2041. (2005)

Straser, E. G. and Kiremidjian A. S. "A modular visual approach to damage monitoring for civil

structures." Proc., SPIE - Smart Structures and Materials, San Diego, CA, 2719, 112-122. (1996)

Straser, E. G. and Kiremidjian A. S. "A modular, wireless damage monitoring system for structures." The John A. Blume Earthquake Engineering Center Technical Report, 128. (1998)

Tanner, N. A., Wait, J. R., Farrar, C. R., and Sohn, H. "Structural health monitoring using modular wireless sensors." J., Intelligent Material Systems and Structures, 14(1), 43-56. (2003)

U.S. Census Bureau. "Value of construction Put in Place." http://www.census.gov/const/www/c30index.html. (2004)

Wong, K.-Y. "Instrumentation and health monitoring of cable-supported bridges." Structural Control and Health Monitoring, 11(2), 91-124. (2004)

Table 1: Research gaps.

Network	Sensor node	Algorithms
Scalability	Power available	Scalability
Time synchronization	Power needed to meet performance requirements.	Distributed
Data loss	Computational speed	Data aggregation
Power efficiency	Communication bandwidth	Minimize power
Localization	Environmental hardening	Sensor fusion
adaptive network	Resolution/range	Data protocols
Fault tolerance	Sensor type	
interoperability	Digital vs analog	
middleware		

Table 2: Comparison between Mica2 and Imote2.

	Mica2	Imote2
Microprocessor	ATmega128L	XScalePXA271
Clock speed (MHz)	7.373	13-416
Active Power (mW)	24 @ 3V	44 @ 13 MHz, 570 @ 416 MHz
Program flash (bytes)	128 K	32 M
RAM (bytes)	4 K	256 K + 32 M external
Nonvolatile storage (bytes)	512 K	32 M (Program flash)
Size (mm)	58 x 32 x 7	48 x 36 x 7

Table 3: Accelerometer user specified sampling rates and cutoff frequencies

Decimation factor	Cutoff frequency (Hz)	Sampling rate (Hz)
128	70	280
64	140	560
32	280	1120
8	1120	4480

Table 4: Natural frequencies identified on Imote2s.

Mode	Natural frequency (Hz)
1st	19.638
2nd	40.846
3rd	61.888
4th	66.714
5th	70.344
6th	93.606

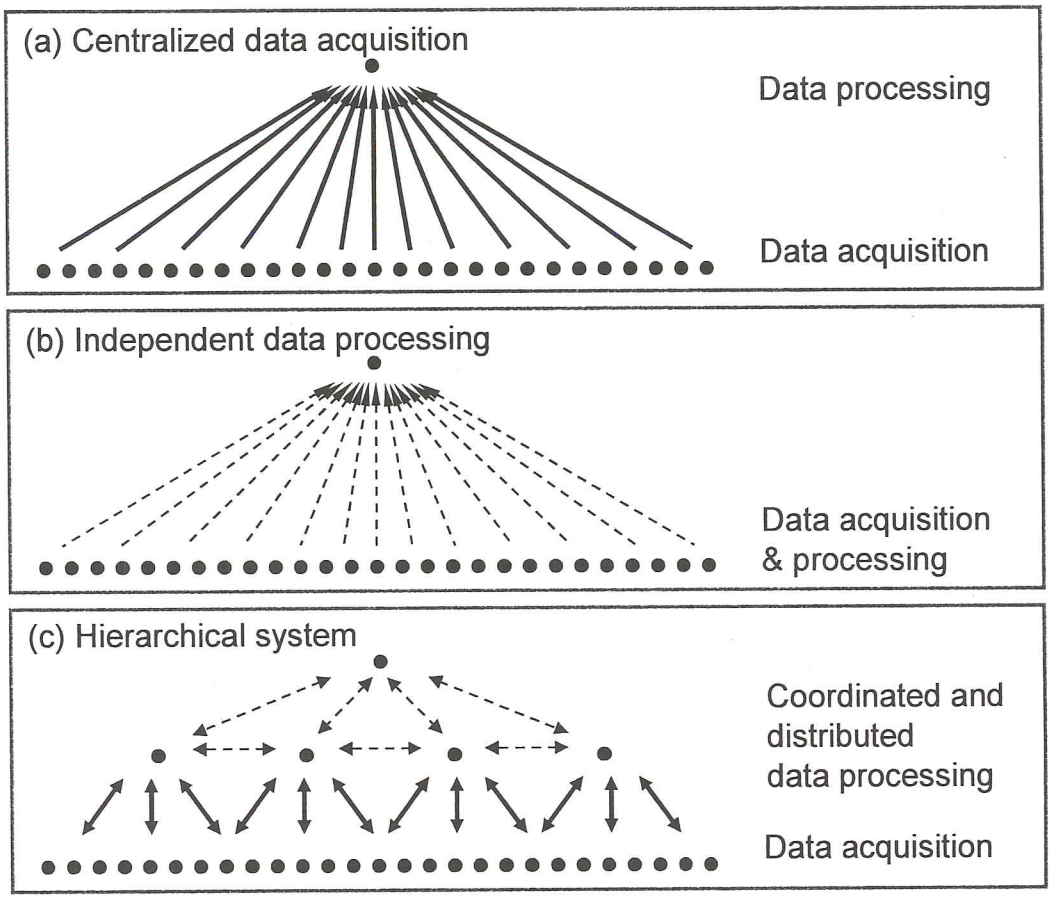

Figure 1: Smart sensor topologies.

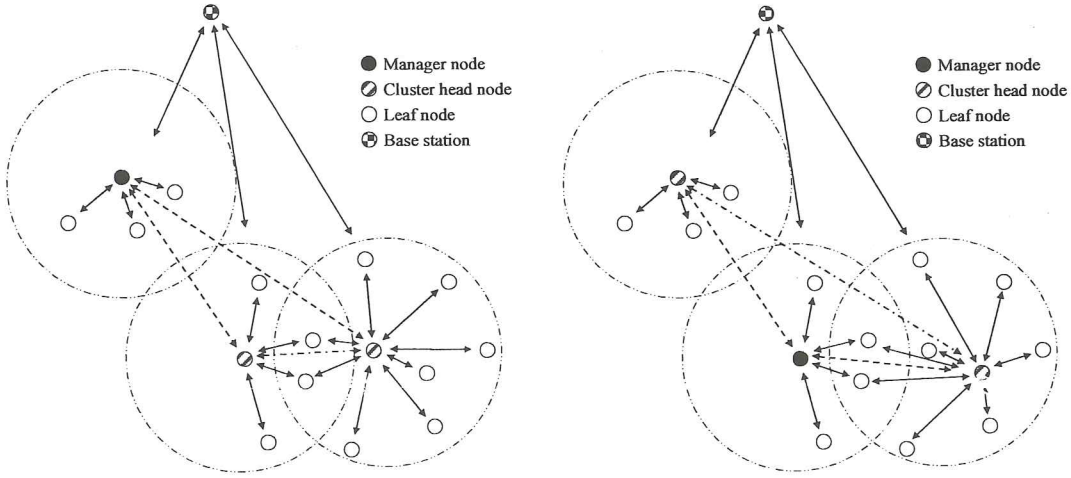

Figure 2: SHM system architecutre with interchangeable

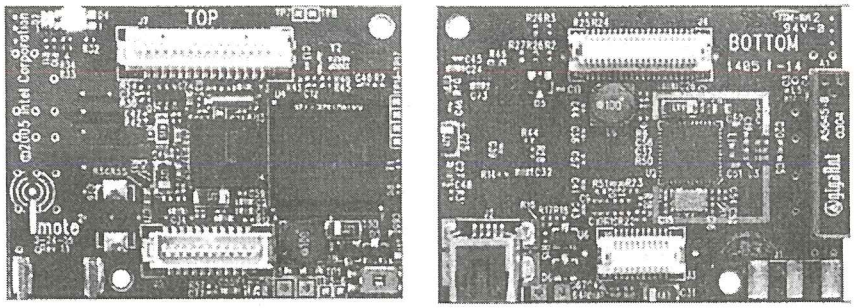

Figure 3: Intel's Imote2. Top view and bottom view

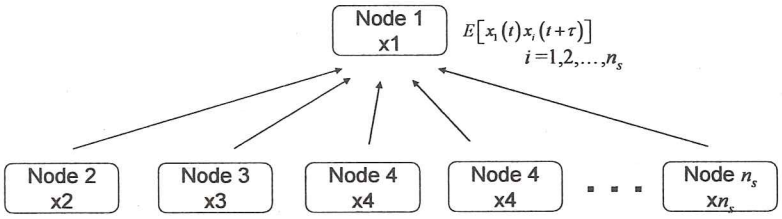

Figure 4: Centralized NExT implementation.

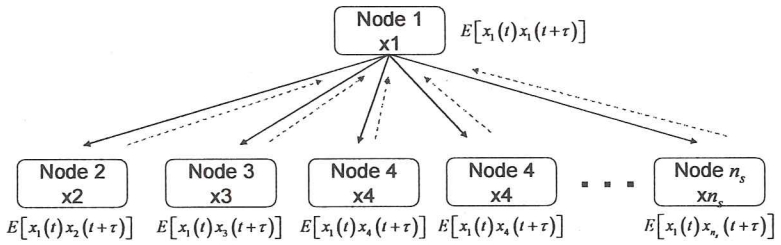

Figure 5: Distributed NExT implementation.

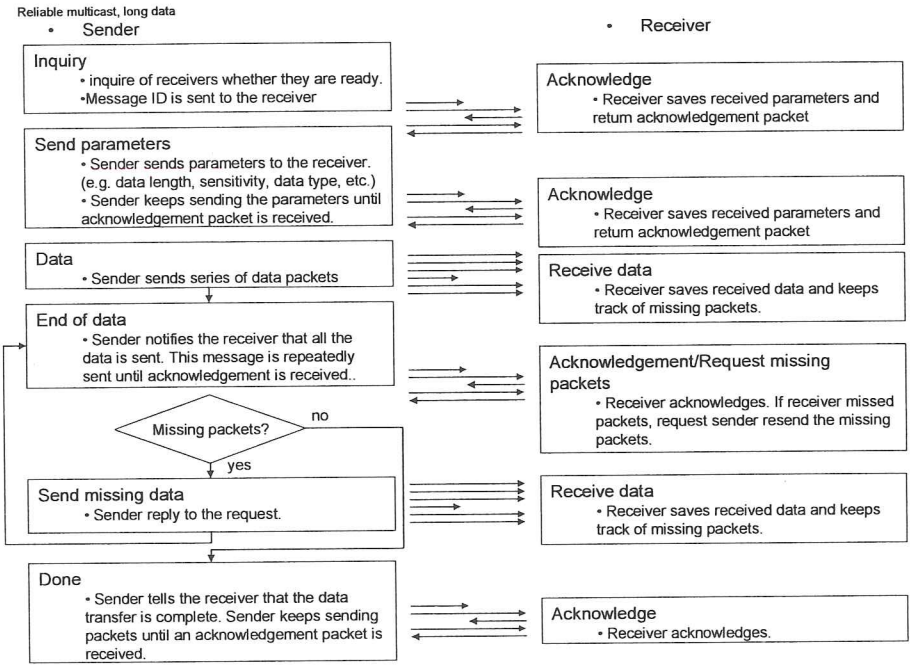

Figure 6: Reliable communication protocol for long data records.

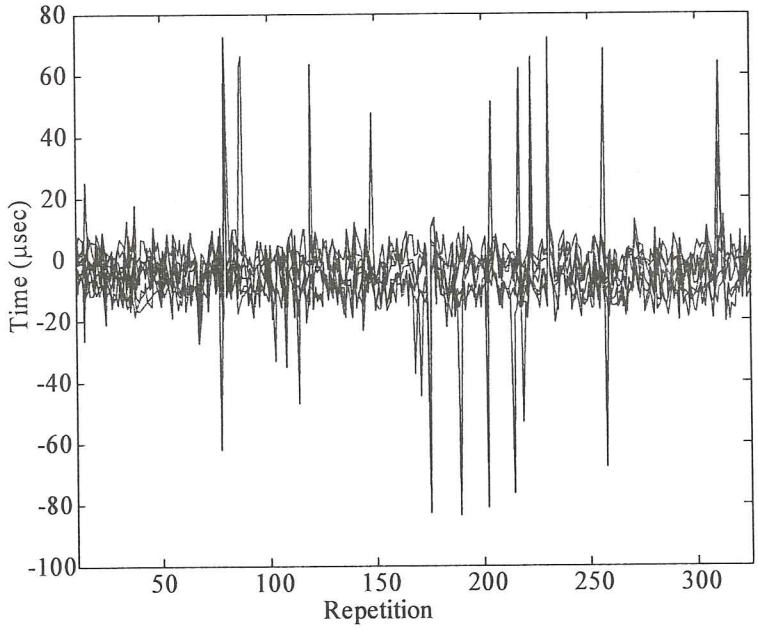

Figure 7: Time synchronization

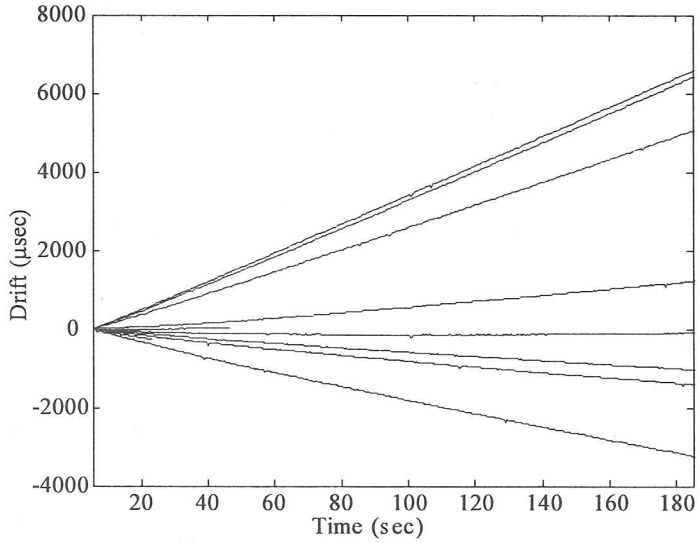

Figure 8: Drift estimation.

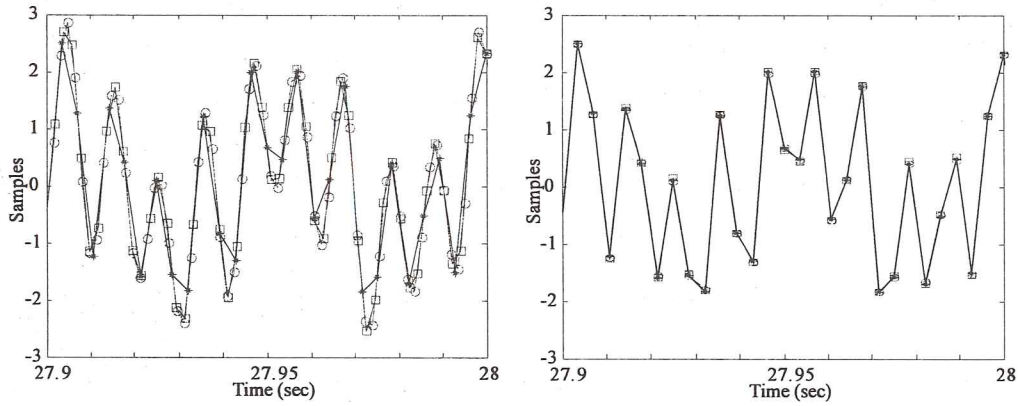

Figure 9: Signals before and after resampling.

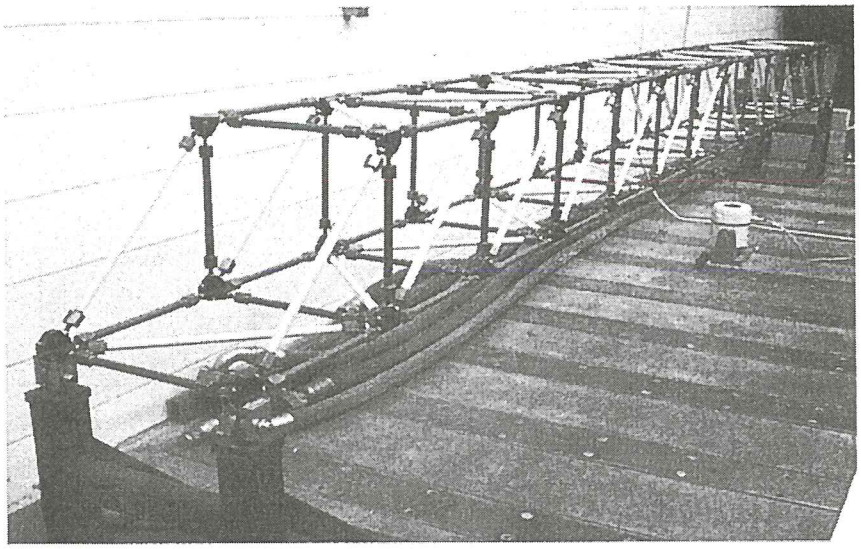

Figure 10: Three dimensional truss model.

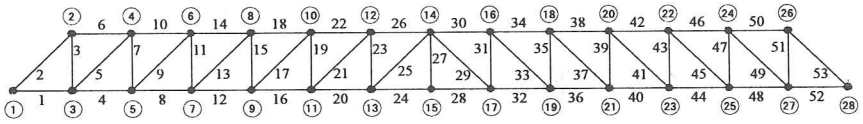

Figure 11: Node and element IDs of the truss.

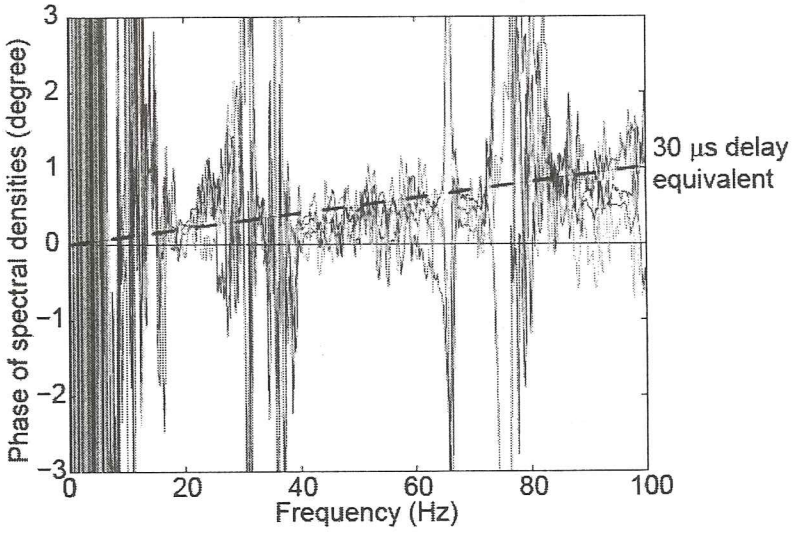

Figure 12: Phase of spectral densities.

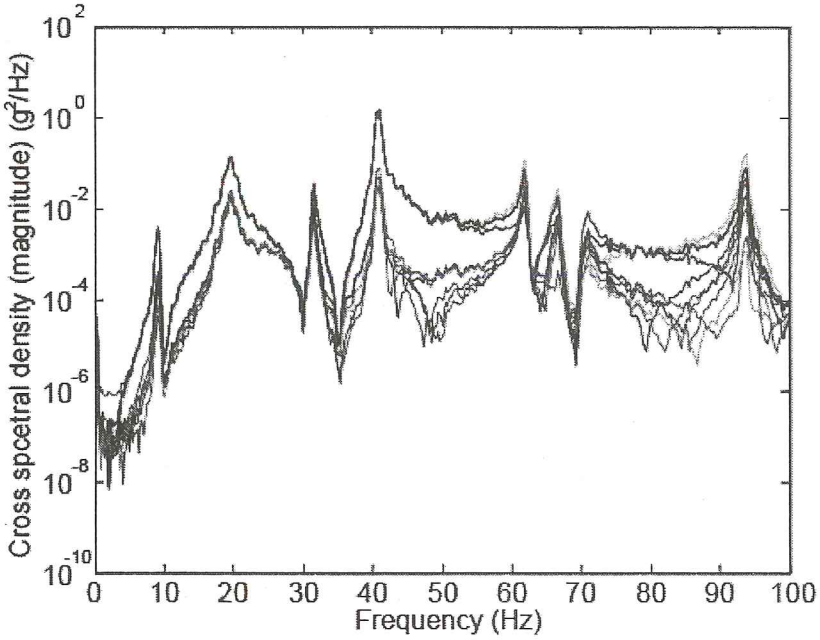

Figure 13: Cross spectral densities.

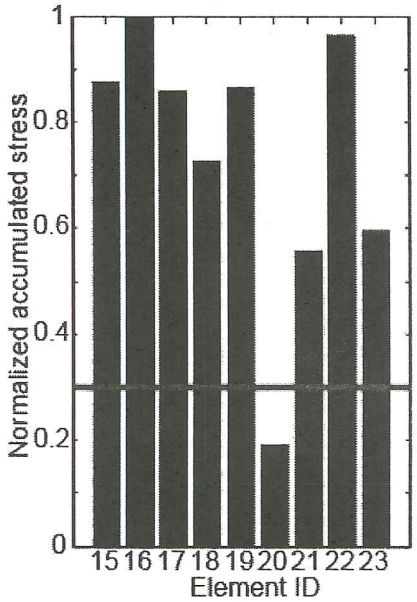

Figure 14: Normalized accumulated stress from mass perturbation-based DCSmethod.

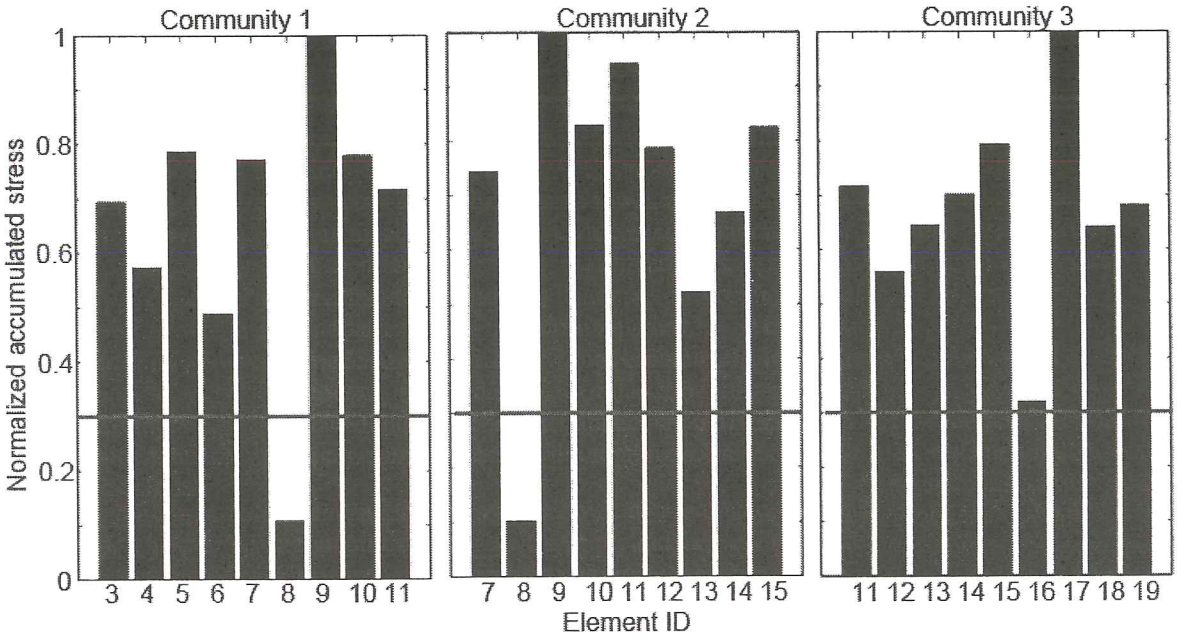

Figure 15: Normalized accumulated stress from SDLV-based DCS method.

```
Node ID 67 RETAKE 0
ID 67 # of Damaged Element:  1
Damaged Element ID: 8

Node ID 81 RETAKE 0
ID 81 # of Damaged Element:  1
Damaged Element ID: 8

Node ID 73 RETAKE 0
ID 73 # of Damaged Element:  0
```

Figure 16: Report on damaged elements.

THEME 8

Wind Engineering

Comparative Inter-Laboratory Study of Wind Loading on Low Industrial Buildings

by

Bogusz Bienkiewicz[1], Munehito Endo[1], Joseph A. Main[2], and William P. Fritz[3]

ABSTRACT

Results of an ongoing inter-laboratory comparative study of approach flow and wind pressures on low buildings are presented. The wind tunnel data generated at six wind engineering laboratories during a pilot project initiated and coordinated by the National Institute of Standards and Technology was employed. Variability in the laboratory wind loading on low buildings was investigated. The largest variability in the laboratory wind pressures and in the associated wind-induced internal loading in structural frames of generic low buildings was found for suburban wind exposure, for which an average coefficient of variation of 26.6 % was observed. This variability was primarily attributed to differences in the approach flows employed in physical modeling of wind pressures on tested buildings, carried out by the participating laboratories. The variability in the approach flows resulted in a large measure from the differences in the along-wind turbulence intensity implied by different empirical models, defining the target wind exposures and used by the laboratories.

KEYWORDS: wind loading, low buildings, wind tunnel testing

1.0 INTRODUCTION

The consistency of wind loading on low buildings inferred from wind tunnel testing has been of concern to wind engineering researchers and practitioners, structural engineers and code writers. The National Institute of Standards and Technology (NIST) has initiated and coordinated a pilot project addressing this issue. Two representative low buildings of rectangular plan and two wind exposures were selected for the study and a number of wind engineering laboratories were invited to carry out wind tunnel testing to determine wind loading on the buildings.

To ensure consistency in laboratory settings, most of the experimental conditions were specified by the coordinating team at NIST. They included: geometrical scale, data sampling rate and record length, number of data records and locations of pressure taps. Ultimately, six laboratories (four from North America, one from Japan and one from Europe) provided datasets, of which a total of seven have been deposited at and analyzed by NIST. These sets consisted of time series and statistical summaries of coefficients of external pressure acquired at specified taps. Information on modeling and statistical properties of approach wind was also provided.

The above data were employed in calculations of internal forces (bending moment, shear force, etc.) in representative frames of metal buildings of geometry modeled in the wind tunnel tests, Fritz et al. [1]. The results of this analysis indicated large differences in the forces calculated using the datasets generated at different laboratories. The largest variability was found for a building of a relatively low height (a prototype eave height of 6.1 m), placed in the suburban wind exposure, Fritz et al. [1]. These discrepancies were tentatively attributed to a number of experimental factors and assumptions made during wind tunnel testing.

[1] Wind Engineering and Fluids Laboratory, Department of Civil and Environmental Engineering, Colorado State University, Fort Collins, CO 80523-1320, USA

[2] Building and Fire Research Laboratory, National Institute of Standards and Technology, Gaithersburg, MD 20899-8611, USA

[3] Wells Fargo Bank, Columbia, MD 21046, USA (formerly, Building and Fire Research Laboratory, National Institute of Standards and Technology)

However, it has been recognized that a systematic investigation would be required to provide definite explanation of the origins of this variability and to develop means to reduce/eliminate these discrepancies. The overall objective of the paper is to present a progress report on an ongoing collaborative study addressing the above variability, its origins and related issues.

2.0 BUILDINGS AND TEST SETUP

The two buildings selected for the inter-laboratory study, see Figure 1, had the same planar dimensions, 30.5 m by 61 m, and the same slope of the gable roof, 2.39° (1/2 in 12). The main difference between the buildings was the eave height: 6.1 m and 9.8 m.

Selection of the pressure tap locations was based on a layout developed by the Boundary Layer Wind Tunnel Laboratory, at the University of Western Ontario, for wind tunnel testing carried out as part of the NIST/Texas Tech University Windstorm Mitigation Initiative. In view of varying capabilities – number of data channels of pressure measurement systems available at different laboratories – a subset of that layout (comprising of a smaller number of taps) was chosen and assigned to the laboratories participating in this study. The selected taps were located in rows 1 through 5, as is schematically depicted in Figure 1.

3.0 RESULTS

The primary focus of the investigation presented in the paper was an inter-laboratory comparison of the modeled approach flows, acquired building point pressures and the wind-induced internal forces (bending moments) computed in main wind force resisting system (MWFRS). The considered system (MWFRS) is shown in Figure 2. This system was also employed by Whalen et al. [2], in investigation of wind-induced internal forces. In the present structural analysis, the frame geometry was simplified, as is depicted in Figure 3, and the influence lines were employed in calculations. Coefficients α and β were used to control respectively the frame stiffness and aspect ratios.

Representative results of this effort are presented herein. Letter labeling – A through F – is used to denote the source (participating laboratories) of the compared approach wind, wind-induced external point pressure and other referenced information provided by the laboratories. While uncertainty estimates were not provided by each laboratory, estimates based on repeated tests from one particular laboratory indicate a coefficient of variation (COV) of approximately 2 % in the mean wind speed and a COV of approximately 3 % in the mean and standard deviation of pressure coefficients. Error bars are not shown in figures as they are smaller than the plotting symbols.

Regarding the approach flow, it was found that significantly different experimental set-ups were used by the laboratories to simulate a given target wind exposure. This is illustrated in Figure 4, where the wind tunnel configurations employed to generate the suburban wind exposure at three representative laboratories (denoted A, B and C) are displayed. For this exposure, the experimental setups were found to exhibit the largest differences.

The impact of the differences in the setups depicted in Figure 4 can be inferred from Figures 5 and 6, where the vertical profiles of the along-wind mean velocity and turbulence intensity are displayed, for the two approach flows modeled at four representative laboratories. As can be seen in Figure 5, the inter-laboratory discrepancy in the mean velocity profiles is moderate, with the power-law exponents ranging from 0.139 through 0.191 (target value of 0.143) and from 0.165 through 0.234 (target value of 0.22) for the open and suburban wind exposures, respectively. It can be seen in Figure 6 that the spread among the compared turbulence intensity profiles is significantly larger. The largest discrepancy is observed for the (modeled) suburban exposure.

It should be pointed out that the participating laboratories used different empirical models to define the target profiles for the approach flows modeled in boundary-layer wind tunnels. Representative comparisons of these models are depicted in Figure 7 and they include: ASCE 7 [3], Eurocode [4], AIJ [5], AS1170.2 [6] and NBCC [7] (from Zhou and Kareem [8]), and two variants of ESDU model (from [9] and [10]). It can be seen

that the spread in these profiles is overall similar to that exhibited by the profiles of the simulated (laboratory) approach flows, shown in Figure 6.

Representative wind-induced mean roof pressures at tap rows 1 through 3 (compare Figure 1), acquired at five or six (one case) laboratories are depicted in Figure 8. The resulting wind-induced mean bending moments in frame F1 (compare Figure 2), normalized by the square of the rooftop mean velocity, are shown in Figure 9. Overall, the displayed mean roof pressures and the bending moments show similar trends. A comparison of the results originating from different laboratories reveals a scatter among the data, which is primarily attributed to the level of turbulence of the modeled approach flows. It can be seen in Figure 8 that the highest level of the inter-laboratory discrepancy occurred in suburban exposure – the exposure that exhibited the largest discrepancy in the turbulence intensity of the modeled approach flow, see Figure 6. A similar trend, although the magnitude of the inter-laboratory discrepancy is lower, can be observed for the bending moments, in Figure 9.

The time series of the roof pressures and bending moments were subsequently employed to predict the peak pressures and bending moments. The peak estimation procedure proposed by Sadek and Simiu [11] was employed in this analysis. Representative results are presented in Figures 10 and 11, for suburban approach flow. The 90th percentile pressure peaks at two locations in a roof corner region (taps P1 and P2 in Figure 1) are displayed in Figure 10. The 90th percentile peak bending moments in two frames (frames F1 and F2 in Figure 2) are shown in Figure 11.

The data depicted in Figures 10 and 11 indicate significant inter-laboratory scatter in the peak wind loading and the resulting internal force (bending moment). This variability is quantified in Figures 12 and 13, using the coefficient of variation (COV). It can be seen that the COV computed for suburban exposure is significantly larger than that for open exposure. The overall COV of roof pressures and bending moments are compared in Table 1 with the COV of turbulence intensity.

The results in Table 1 show that in open exposure the inter-laboratory variability in the roof pressure and the frame bending moment was moderate, with the average coefficient of variation of approximately 13 % for the building of lower height (6.10 m) and 10 % for the building of larger height (9.75 m). The variability was approximately twice as large in suburban exposure. This increase can be attributed to an increased variability in the turbulence level (turbulence intensity) displayed in Table 1. It is postulated that the inter-laboratory variability in the internal loading reported by Fritz et al. [1] is in a large measure caused by the variability in the approach flow turbulence employed in physical modeling of wind pressure on tested buildings, carried out by the participating laboratories.

4.0 CONCLUDING REMARKS

Results of an ongoing inter-laboratory comparative study of approach flow, wind pressures on low buildings and internal wind-induced loading are presented. The largest variability in the laboratory wind pressures and in the associated (computed) wind-induced internal loading (bending moment) in structural frames of generic low buildings was found for suburban wind exposure. This variability was primarily attributed to differences in the approach flows employed in physical modeling of wind pressures on tested buildings, carried out by the participating laboratories. The variability in the approach flows resulted in a large measure from the differences in the along-wind turbulence intensity implied by different empirical models, defining the target wind exposures and used by the laboratories. A follow-up comparative inter-laboratory study is planned to address a number of issues identified in the ongoing efforts.

5.0 ACKNOWLEDGEMENTS

The authors would like to express gratitude to Dr. E. Simiu of the National Institute of Standards and Technology for initiating and managing the inter-laboratory wind tunnel project and for his contributions to the ongoing investigation. All of the participants in the inter-laboratory comparative

study are gratefully acknowledged, including Bo Cui of the Clemson Wind Load Test Facility at Clemson University; Olivier Flamand of the Centre Scientifique at Technique du Bâtiment (CSTB) in Nantes, France; Eric Ho of the Boundary Layer Wind Tunnel Laboratory at the University of Western Ontario; Hitomitsu Kikitsu of the Building Research Institute in Tsukuba, Japan; and Chris Letchford of the Wind Science and Engineering Research Center at Texas Tech University.

6.0 REFERENCES

[1] W.P. Fritz, B. Bienkewicz, O. Flamand, E. Ho, H. Kikitsu, C.W. Letchford, and C. Bo, International comparison of wind tunnel estimates of wind effects on an industrial building model: test-related uncertainties, UJNR, Proc. The 4th U.S.-Japan Workshop on Wind Engineering, July 20-22, Tsukuba, Japan, 2006, 12 pp.

[2] T. Whalen, E. Simiu, G. Harris, J. Lin, and D. Surry, The use of aerodynamic database for the effective estimation of wind effects in main wind-force resisting systems: application to low buildings, J. Wind Eng. Ind. Aerodyn. 77&78 (1998) 685-693.

[3] ASCE 7-02, Minimum Design Loads for Buildings and Other Structures, American Society of Civil Engineers, New York, USA, 2002.

[4] Eurocode, Eurocode 1: Basis of Design and Actions on Structures. Part 2-4: Actions on Structures–Wind Actions, European Prestandard, ENV-1991-2-4, 1995.

[5] AIJ, Recommendations for Loads on Buildings, Architectural Institute of Japan, Tokyo, Japan, 1996.

[6] AS1170.2, Australian Standards: SAA Loading Code, Part2 – Wind Loads, AS1170.2-89, Australia, 1989.

[7] NBCC, Commentary B–Wind Loads, User`s Guide-NBC 1995 Structural Commentaries, Canadian Commission on Building and Fire Codes, National Research Council of Canada, Ottawa, Canada, Part 4, 9-42, 1996.

[8] Y. Zhou, A. Kareem, Definition of wind profiles in ASCE 7, J. Struct. Engrg. 128 (8) (2002) 1082-1086.

[9] T.C.E. Ho, D. Surry and D. Morrish, NIST/TTU Cooperative Agreement – Windstorm Mitigation Initiative: Wind Tunnel Experiments on Generic Low Buildings, Tech. Rep. BLWT-SS20-2003, The Boundary Layer Wind Tunnel Laboratory, The University of Western Ontario, London, Ontario, Canada, May 2003, 105 pp.

[10] O. Flamand, Measurement of time series of pressures on a low-rise building for the NIST, Tech. Rep. ENCAPE 03.146 C-V0, CSTB, Nantes, France, 2003, 12 pp.

[11] F. Sadek and E. Simiu, Peak non-Gaussian wind effects for database-assisted low-rise building design, J. Eng. Mech. 128 (5) (2002) 530-539.

Table 1. Overall inter-laboratory variability of approach flow, point pressure and frame bending moment

Building height (m)	Exposure (O=open S=Suburban)	Turbulence intensity (%)					COV (%) for Cp (peak) [Cp (mean)]		COV (%) for M1 (peak) [M1 (mean)]		Average COV (%)
		Max ($\hat{M}$)	Mean	Min ($\check{M}$)	Δ ($\hat{M}-\check{M}$)	COV	Tap P1	Tap P2	Frame F1	Frame F2	
6.10	O	21.1	19.8	18.2	2.9	6.2	16.5 [11.7]	11.6 [9.0]	14.7 [12.7]	21.3 [15.7]	14.2
6.10	S	31.2	27.4	24.9	6.4	9.9	25.8 [33.7]	22.9 [21.3]	21.9 [31.6]	21.7 [45.2]	28.0
9.75	O	20.7	18.8	16.7	4.0	10.1	20.4 [8.8]	10.4 [8.4]	13.7 [5.9]	13.1 [7.5]	11.0
9.75	S	32.4	27.0	23.8	8.6	13.8	26.9 [31.3]	24.3 [19.7]	24.6 [23.4]	22.2 [29.5]	25.2

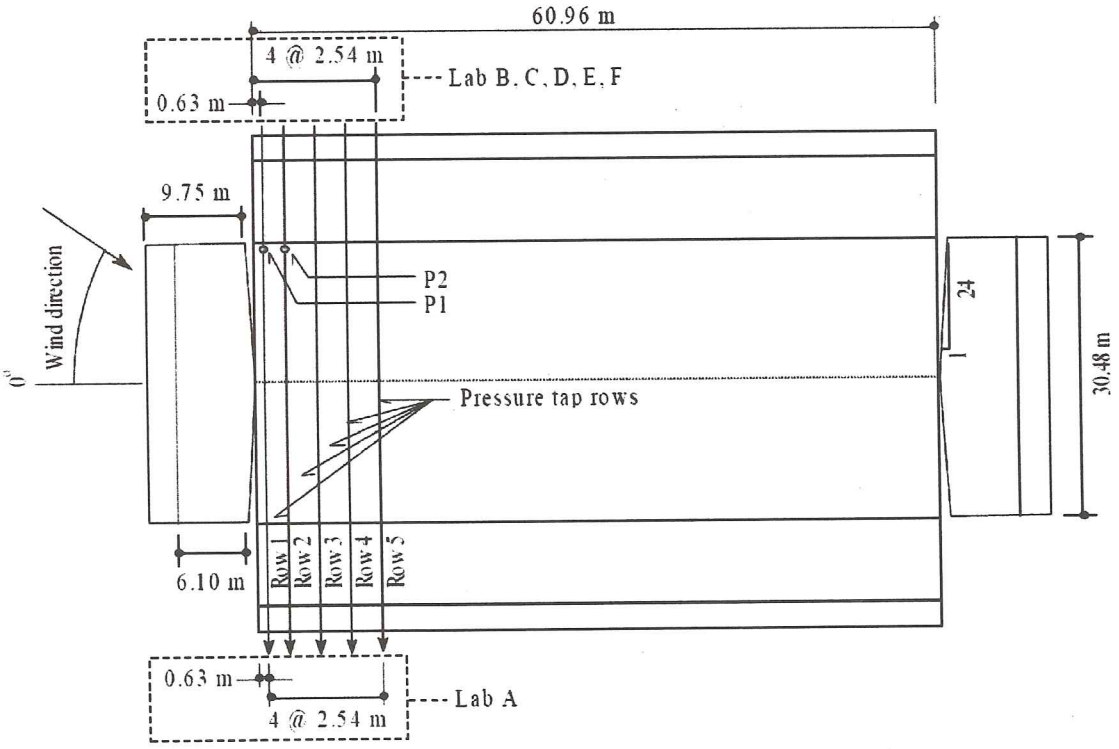

Figure 1. Geometry of prototype low buildings and pressure tap locations.

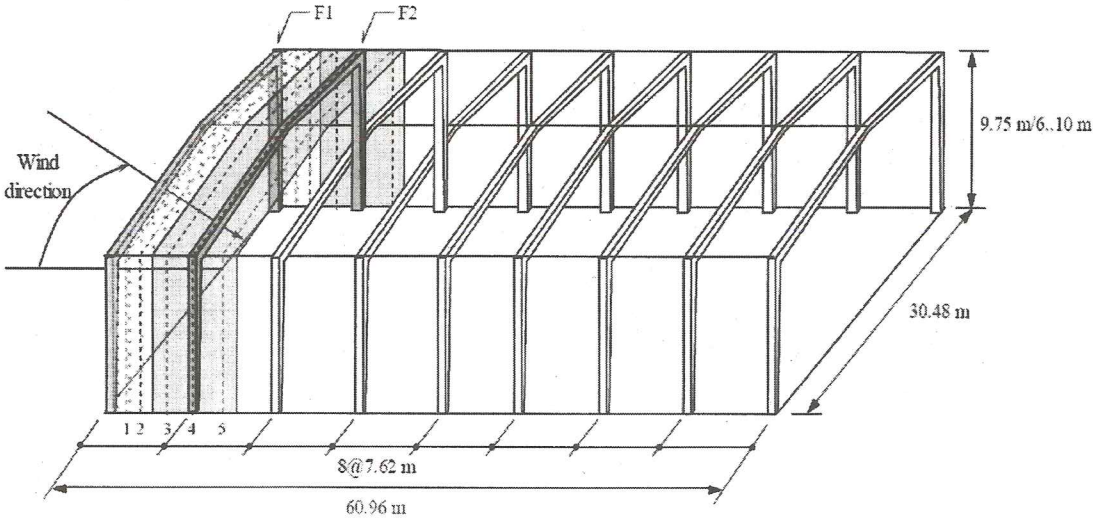

Figure 2. Geometry and main wind force resisting system (MWFRS) of low building.

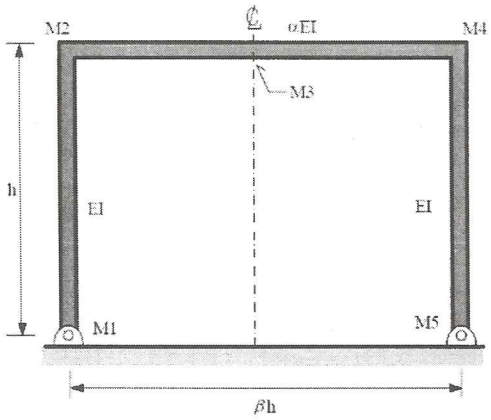

Figure 3. Simplified geometry of structural frame.

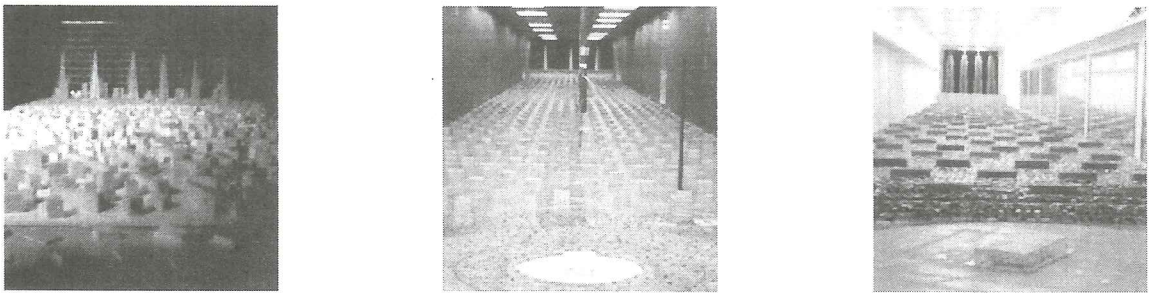

Figure 4. Wind tunnel setups to generate suburban wind exposure in three representative laboratories.

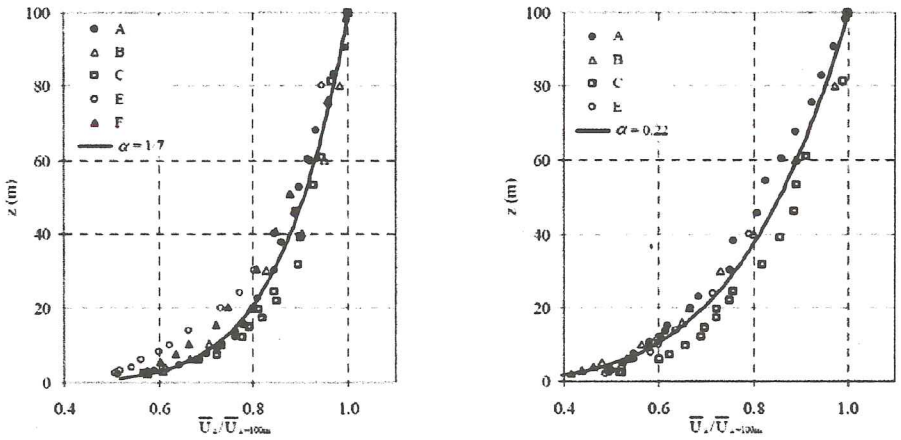

(a) Open exposure (b) Suburban exposure

Figure 5. Comparison of laboratory and target mean wind speed profiles.

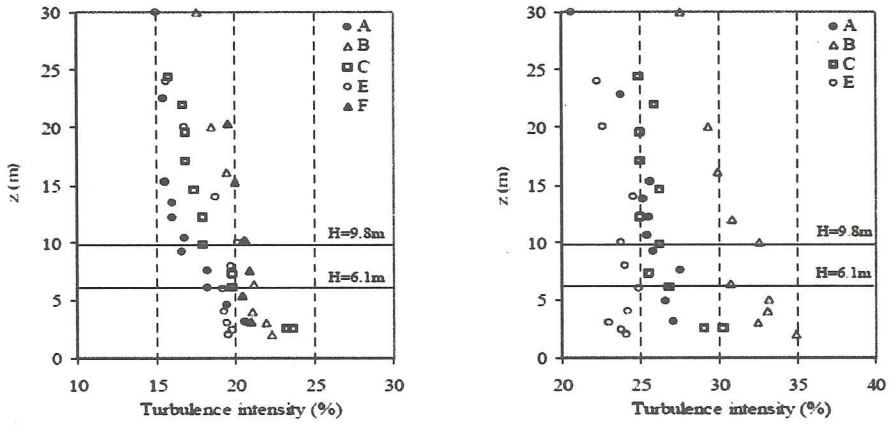

(a) Open exposure (b) Suburban exposure

Figure 6. Comparison of laboratory along-wind turbulence intensity profiles

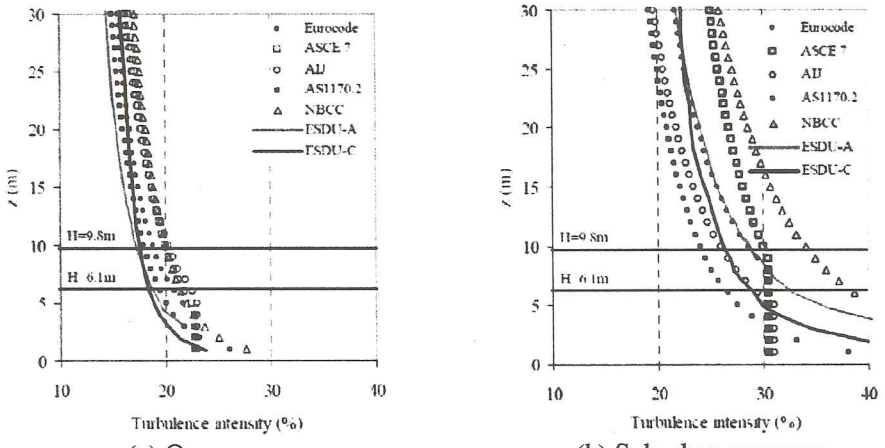

(a) Open exposure (b) Suburban exposure

Figure 7. Comparison of empirical models for along-wind turbulence intensity profiles.

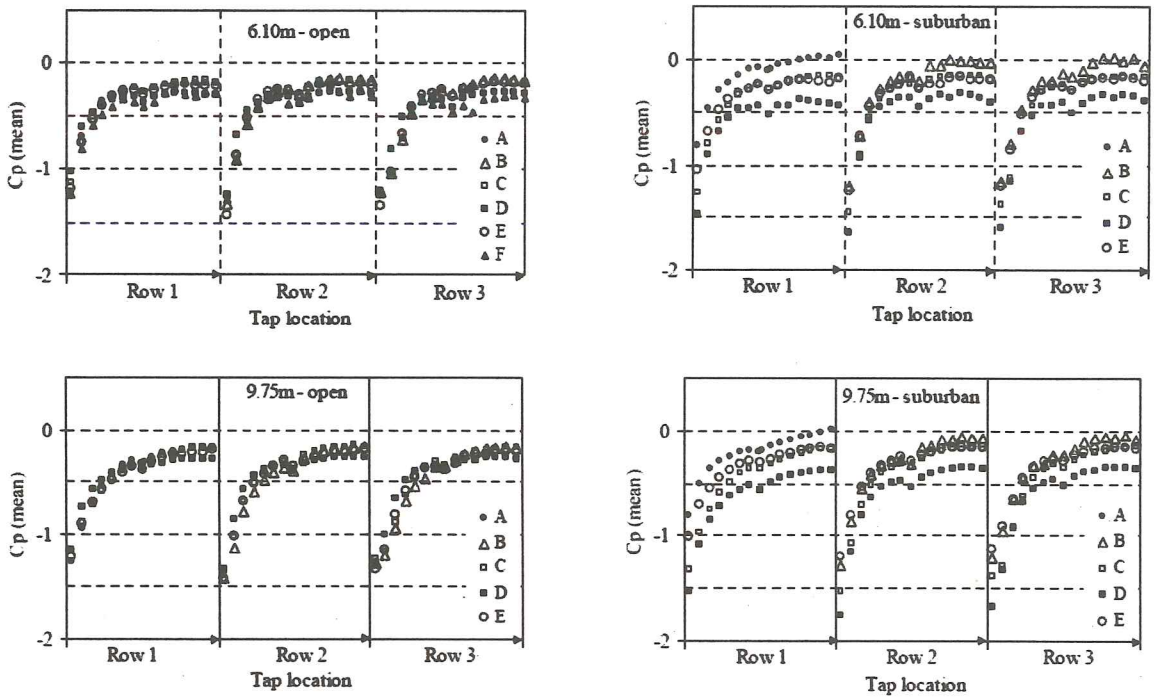

Figure 8. Representative mean roof pressure coefficient, wind normal to ridge (wind direction 90°).

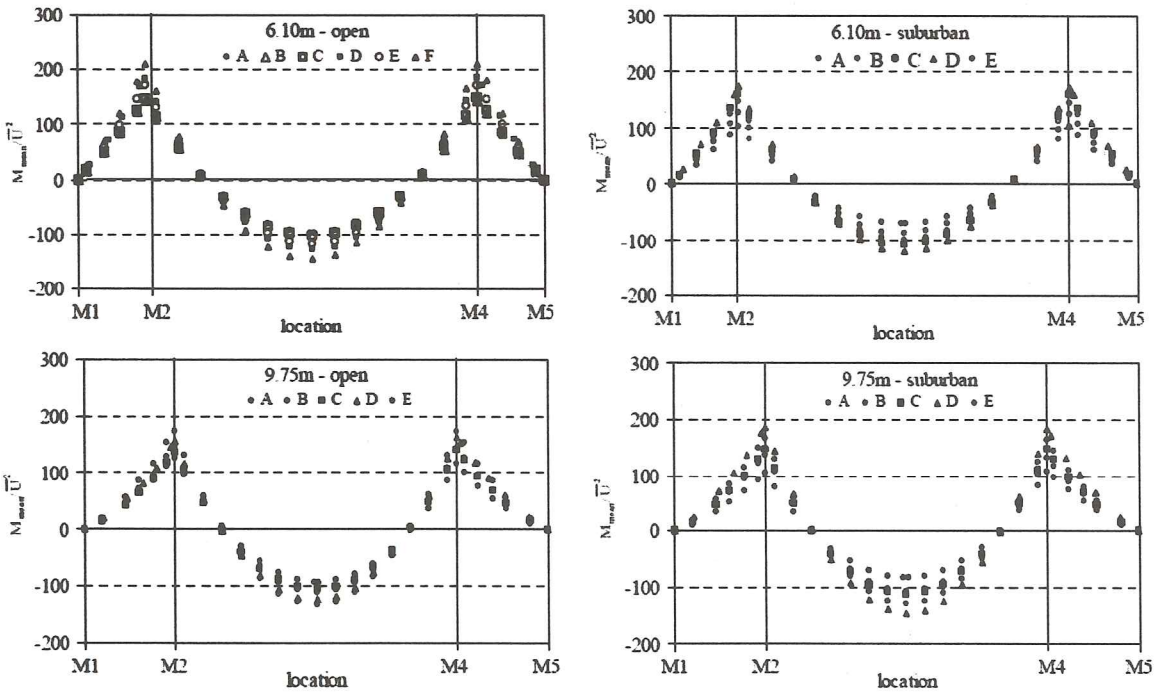

Figure 9. Mean bending moment in frame F1, wind parallel to ridge (wind direction 0°).

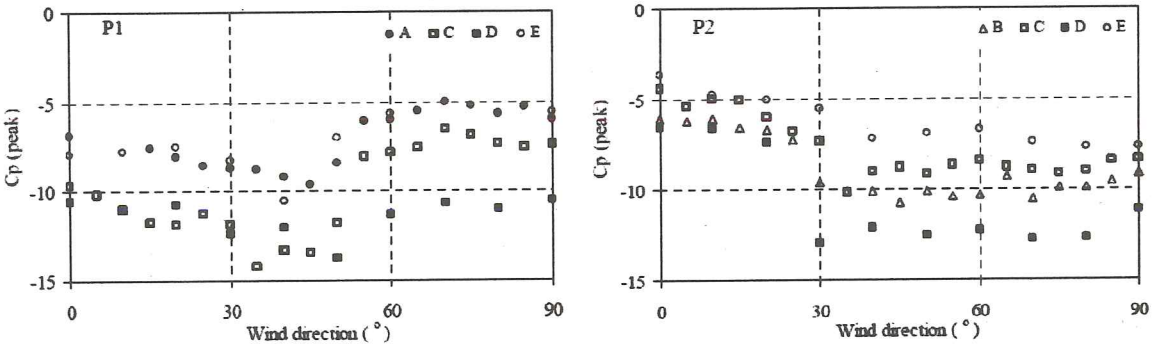

Figure 10. The 90th percentile roof peak pressure, building height 6.10 m, suburban exposure.

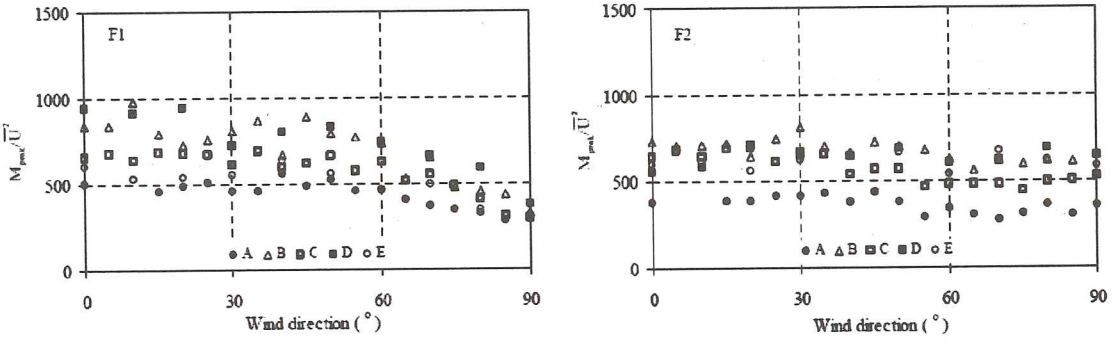

Figure 11. The 90th percentile peak bending moment, location M2, building height 6.1 m, suburban exposure.

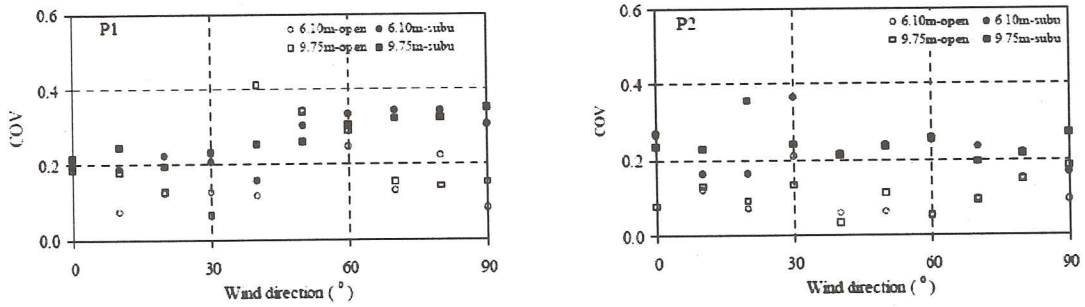

Figure 12. Comparison of COV for 90th percentile peak pressure.

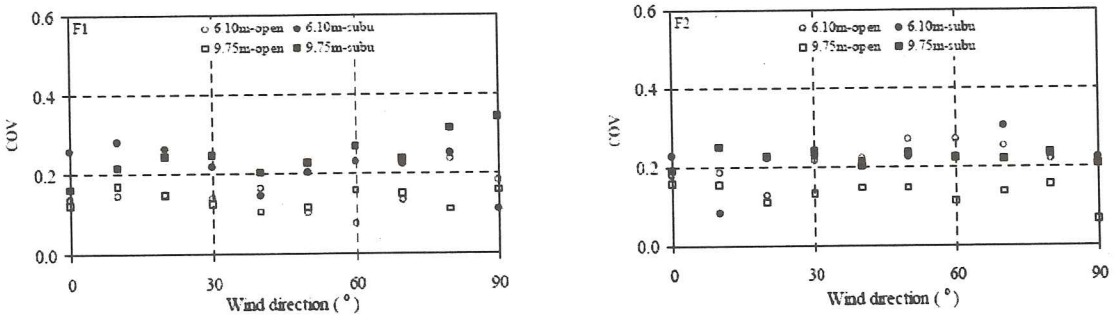

Figure 13. Comparison of COV of 90th percentile peak bending moment, location M2.

Damage to Buildings Induced by Tatsumakis in Nobeoka City, Miyazaki and Saroma Town, Hokkaido in 2006

by

Yasuo Okuda[1], Hitomitsu Kikitsu[2] and Tomonori Murakami[3]

ABSTRACT

Two big tatsumakis occurred in Miyazaki and Hokkaido in 2006. A tatsumaki damaged more than 1,200 houses in Nobeoka city, Miyazaki with an approach of Typhoon Shanshan on September 17, 2006. Another tatsumaki killed 9 persons in Saroma town in Hokkaido on November 7, 2006. BRI investigated damage to houses in Nobeoka city in Miyazaki and Saroma town in Hokkaido.

Collision of flying debris to claddings and scattering of roof materials in houses were very remarkable in two tatsumaki damage. Borderline of each damaged area by tatsumaki was very clear. Damage state of each house was applied to a high wind damage scale that the authors proposed and applied typhoon damage to houses in 2004.

1. INTRODUCTION

The gust wind occurred in Miyazaki, Oita and Kochi prefectures with an approach of Typhoon Shanshan on September 17, 2006. A large tatsumaki (F2) occurred in Nobeoka city Miyazaki. The gust wind damage such as tatsumakis occurred in some places in Hokkaido when a cold front passed over Hokkaido on November 7, 2006. Another large tatsumaki (F3) occurred and killed 9 persons in Wakasa region of Saroma town in Hokkaido. BRI investigated damage to buildings in Nobeoka city in Miyazaki and Saroma town in Hokkaido.

2. METEOROLOGICAL CONDITION AT TIME OF TATSUMAKI OUTBREAK

Fukuoka meteorological observatory reported that Typhoon Shanshan approached Kyushu district on September 17 and made landfall in the vicinity of Sasebo city, Nagasaki at past 18:00. The atmospheric pressure in the center of typhoon Shanshan was about 950hPa at the time of the landing and the maximum wind velocity were about 40m/s. The maximum wind velocity 46m/s was recorded in Nomozaki of Nagasaki city. The maximum instantaneous wind speeds were recorded 53.4m/s in Fukue city and 50.3m/s in Saga city. Fig.1 shows the track of typhoon Shanshan which is similar with the track of typhoon Mireille in 1991 or typhoon Songda in 2004 which brought the serious damage in Japan. At about 14:00 before typhoon Shanshn made landfall, a tatsumaki occurred in Nobeoka city, Miyazaki located in about 300km east-northeast from the typhoon center (See Fig.2). The gust wind damage occurred not only at Nobeoka city but also at Nichinan city and Hyugashi city in Miyazaki, at Usuki city and Ooita city in Ooita, and at Aki city in Kochi, with approach of typhoon Shanshan.

1 Chief Research Engineer, BRI
2 Senior Research Engineer, BRI
3 Cooperative Researcher, BRI

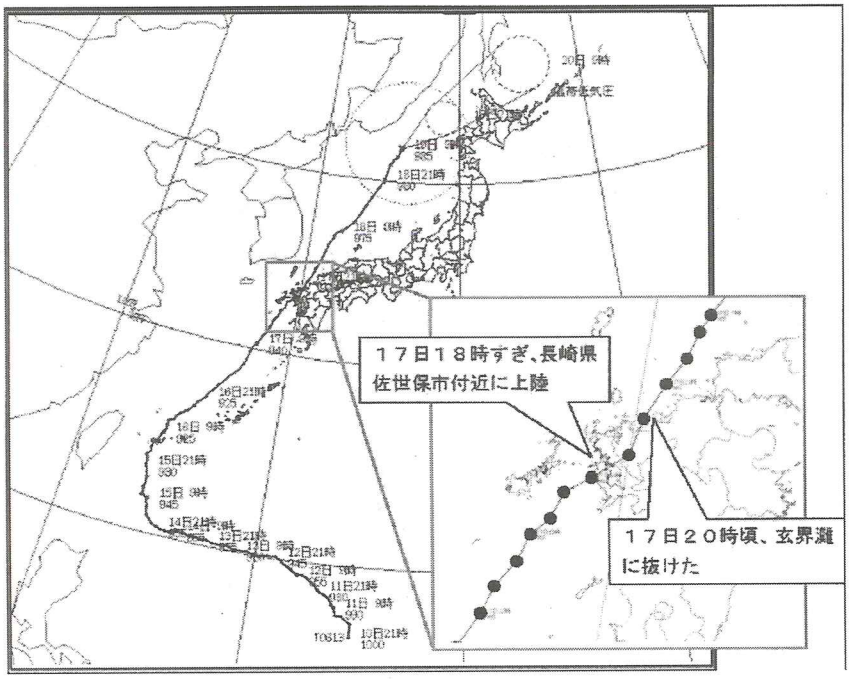

Fig.1 Track of Typhoon Shanshan (JMA)

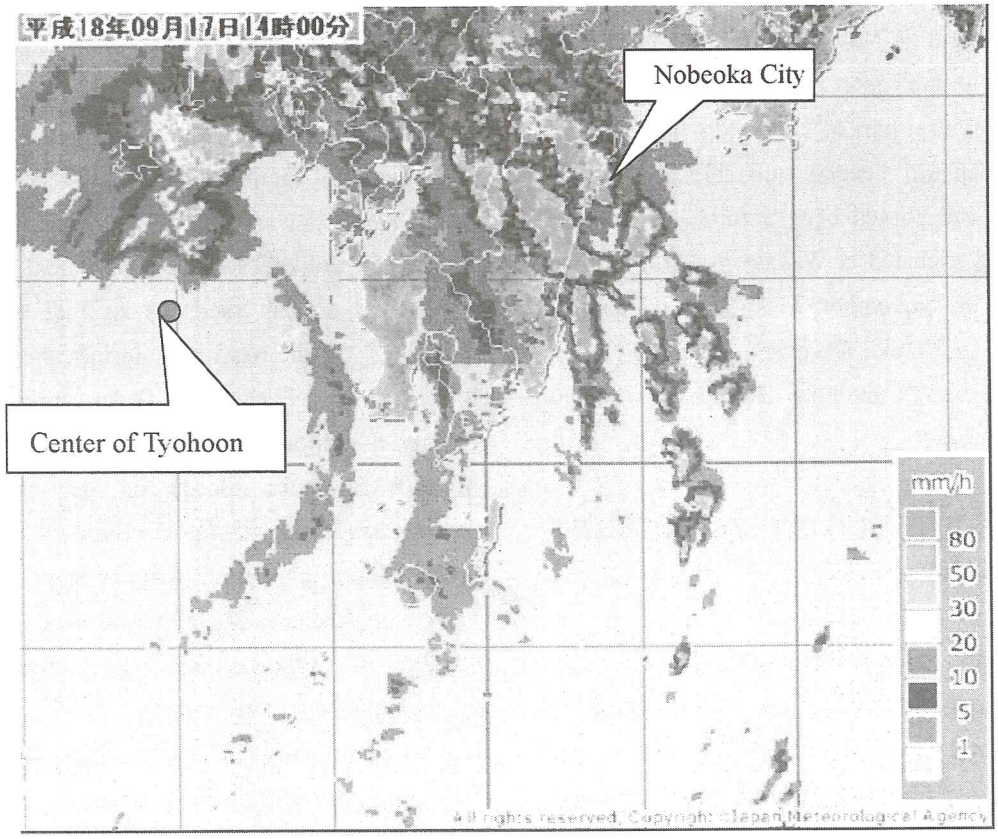

Fig.2 Center of Typhoon Shanshan and Nobeoka Tastumaki Outbreak at 14:00 on September 17 (JMA)

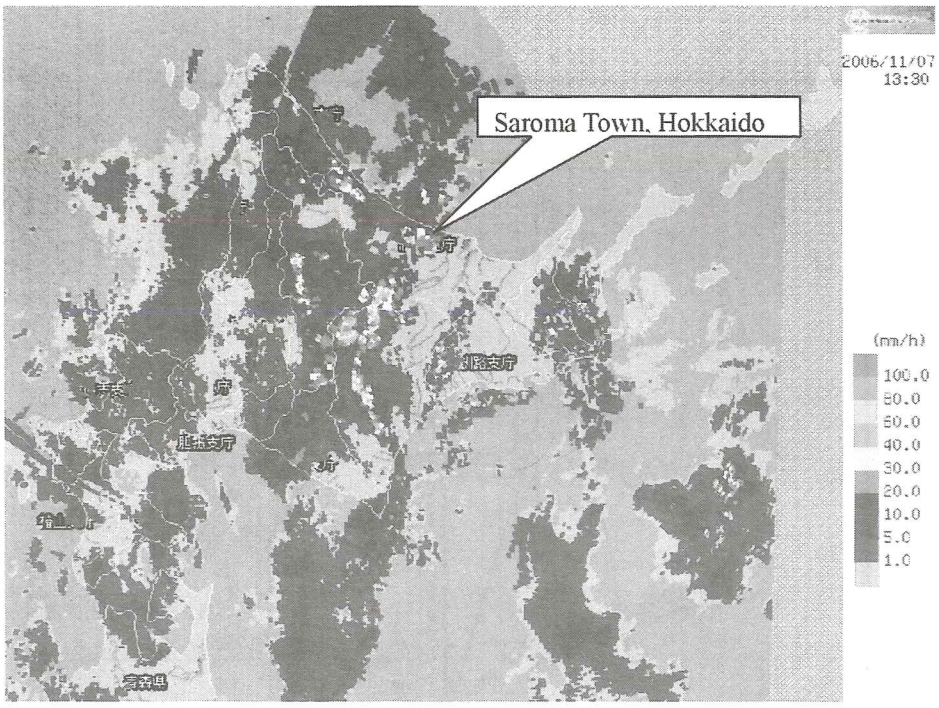

Fig.3 Rain band over Saroma town, Hokkaido at Tatsumaki Outbreak (JMA)

A depression was developing in the vicinity of Soya Channel on November 7, and a cold front spread from the center of the depression passed over the central part of Hokkaido. The state of the atmosphere became unstable. An active thundercloud passed over Saroma town and a gust wind occurred at Wakasa in Saroma town at 13:30 on November 7. Another tatsumakis occurred in Hidaka town and Toyotomi town, Hokkaido on the same day and Okushiri Island on November 9.

3. DAMAGE TO BUILDINGS INDUCED BY TATSUMAKIS

This section shows the main outlines about damage to buildings by tatsumakis on which the authors obtained information during the post disaster investigations. In the following, damage of commercial facility in Nobeoka city and that of temporary working office and houses in Saroma town are described, respectively.

3.1 Damage to Commercial Facility

A commercial facility of mass grocery retailer in Nobeoka city experienced serious damage and which induced lots of economical loss of goods and display racks as well as external claddings. On the roofing materials, there were lots of marks of attack by flying debris. This facility is supposed to locate just in the course of the tatsumaki. Based on the observed damage state, the sudden decrease of internal pressure had generated first because of the peeled-off steel roofing materials and then the damage of indoor goods was supposed to become extensive very much.

Figs. 4 to 10 show the main damage state of this commercial facility. This retailer rapidly began repairing just after the disaster and only five days was needed for resuming business.

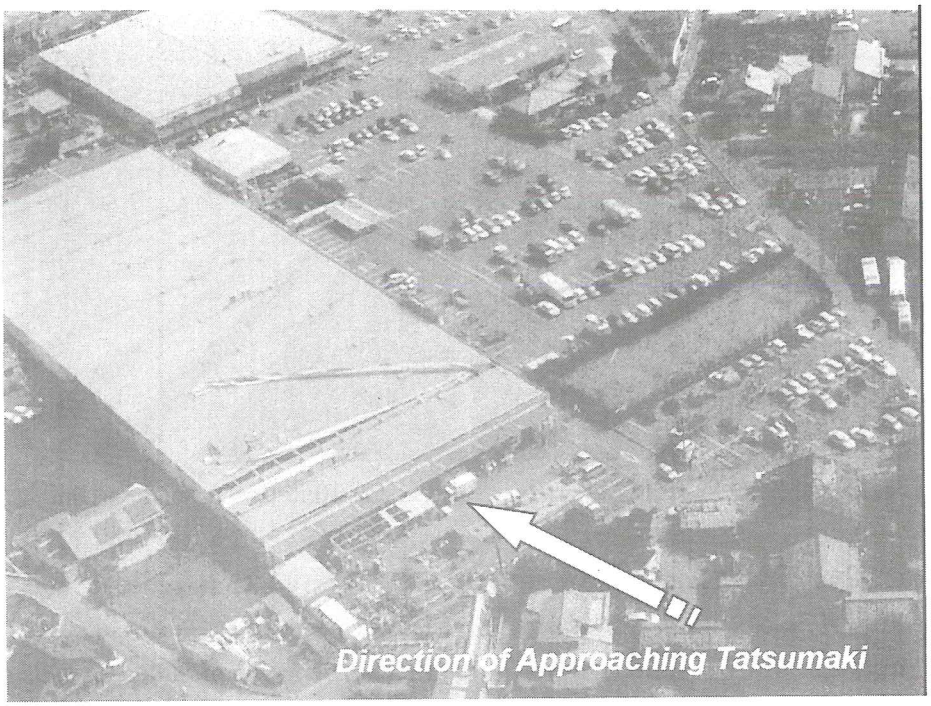

Fig.4 Damage State after Disaster

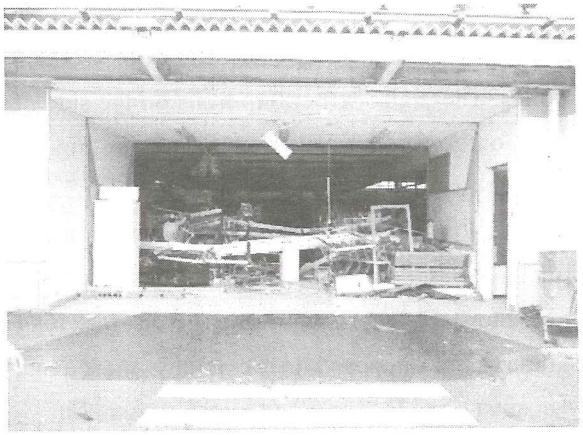

Fig.5 Overturning of Sash in Entrance



Fig.6 Overturning of Sash in Entrance



Fig.7 Damage State of Commercial Goods



Fig.8 Breakage of Window in Entrance

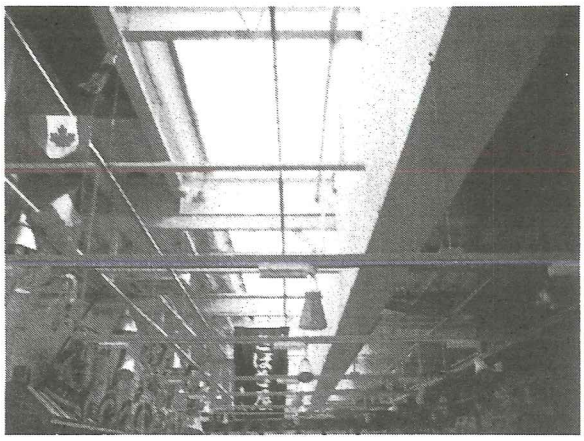

Fig.9 Peeled-off Steel Roofing Materials

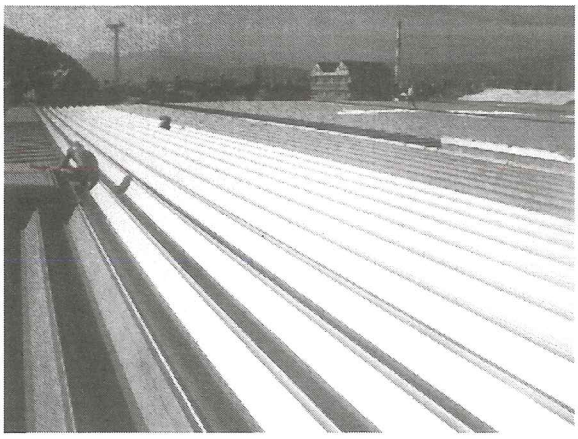

Fig.10 Repaired Steel Roofing Materials

3.2 Damage to Temporary Working Office

In Wakasa region of Saroma town, two of three temporary working offices were severely collapsed by the approaching tatsumaki (See Fig.11). Office A was flown off to the north direction and the other office C was collapsed to the same direction. Series of wooden piles of them were still left on these sites and lots of broken structural elements such as lattice girder were observed to be scattered in the neighboring site (See Figs. 12 and 13). The left temporary working office (office B) which was connected to the office C by connecting corridor had several breakages of windows, but was observed to experience not so severe damage compared to those collapsed.

There were marks of pulled-up nails on the top of the wooden piles of offices A and C as shown in Fig.14 and these nails were considered to fasten floor joists with wooden piles. There also left crump irons on the side of the outer wooden piles as shown in Fig.16, which were considered to fasten ground sill with outer wooden piles. Based on the result of the serious damage, the pull-out performance of these fasteners with the given fastening interval is supposed to be totally inadequate against wind load induced by the tatsumaki.



Fig.11 Damaged Temporary Working Offices



Fig.12 Collapse of Offices A and C (See Fig. 11)



Fig.13 Scattered Structural Elements and Others

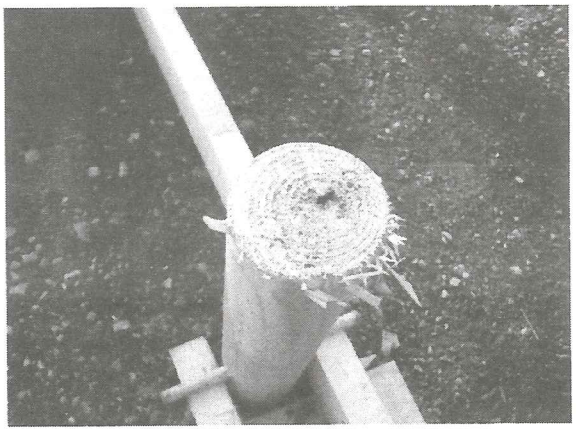

Fig.14 Wooden Pile of Office A



Fig.15 Wooden Piles of Office A



Fig.16 Clump Iron Left on Wooden Pile

3.3 Damage to Houses and Warehouses

Houses in Wakasa region of Saroma town are mainly built by conventional method of timber construction and lots of them experienced severe damage by the tatsumaki. According to the survey by Saroma town office, the damage of houses accounts for 12 of total collapse, 8 of partial collapse and 18 of partial damage, respectively. As the main damage state, breakage of external claddings such as wall and window by flying debris and flown-off roofing materials were observed. As for the damage state of the totally collapsed houses and warehouses, structural elements such as columns and bearing walls were collapsed and the whole roofing system including roofing material, ridge, rafter and vertical roof strut was flown off. Figs. 17 to 24 show main examples of damaged houses by the tatsumaki.

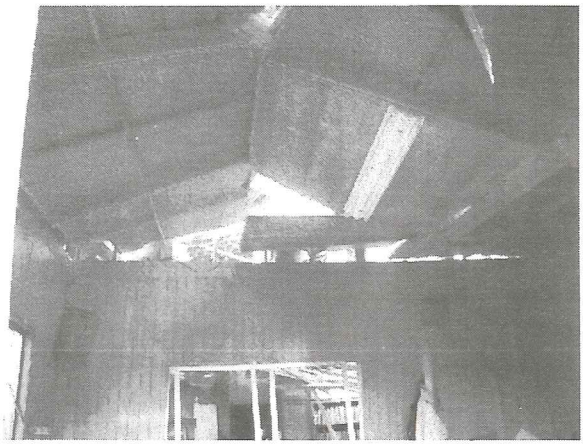

Fig.17 Damage to Ceiling

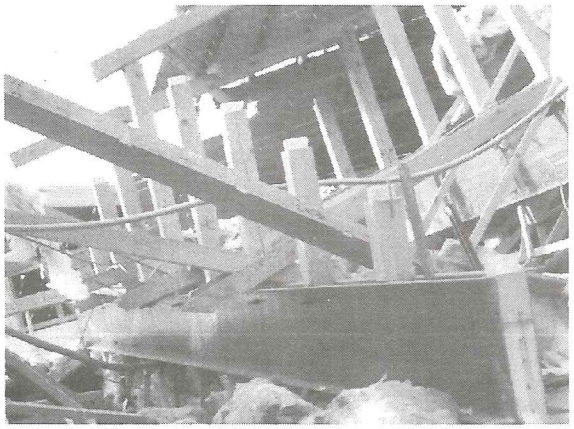

Fig.18 Out-of-joint between Vertical Roof Strut and Purline



Fig.19 Damage to Roofing Materials



Fig.20 Damage to Roofing System and Part of Wall



Fig.21 Severe Damage to External Cladding by Flying Debris



Fig.22 Damage to Wall by Flying Debris

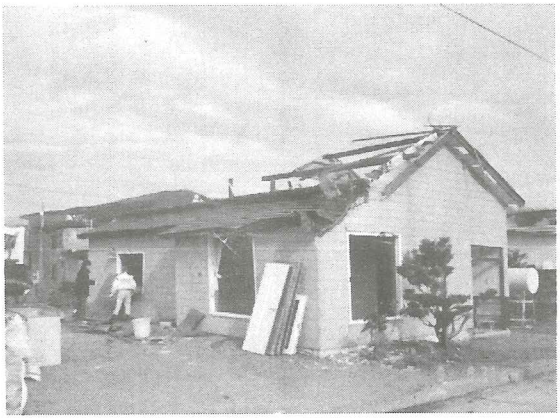

Fig.23 Damage to Roofing System

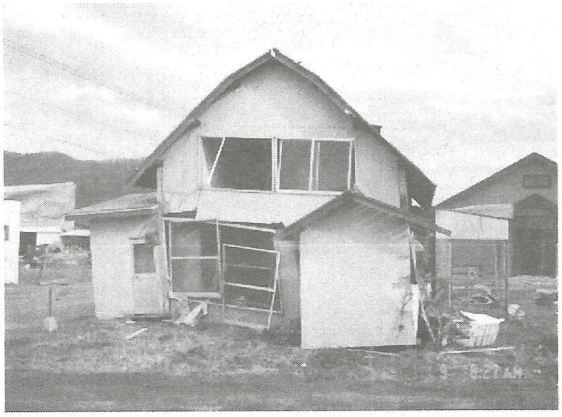

Fig.24 Residual Deformation of External Cladding

4. CHARACTERISTICS OF DAMAGE STATE AND DISTRIBUTION OF BUILDINGS DAMAGED BY TATSUMAKIS

4.1 Characteristics of Damage State of Buildings

Damage of building envelopes such as roofing materials and walls can be generally observed as typical wind-induced disaster of buildings. Recently in Japan, it has been often pointed out that peeled-off external claddings may become flying debris and attack neighboring buildings and structures as a consequent disaster. These modes of damage are also true in the damage by the effect of tatsumakies. Figs. 25 to 32 show several examples of damage to building envelopes such as external claddings induced by flying debris.



Fig.25 Damage to Wall by Flying Debris



Fig.26 Damage to Wall by Flying Debris



Fig.27 Damage to Wall by Flying Debris

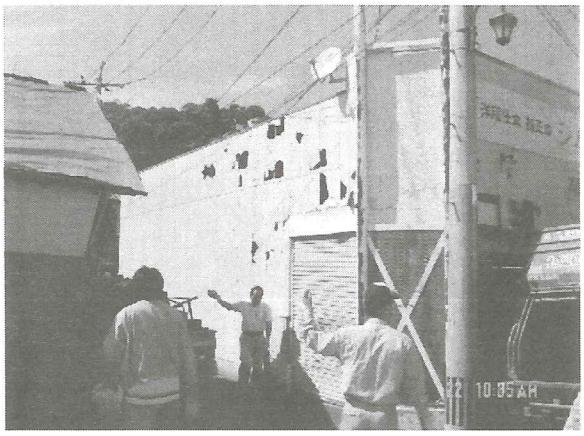

Fig.28 Damage to Wall by Flying Debris



Fig.29 Separation of Wall



Fig.30 Separation of Wall



Fig.31 Damage to Windows and Sash



Fig.32 Damage to Wall

4.2 Distribution of Buildings Damaged by Tatsumakis

The authors presented high wind damage scale which can associate the degree of damage state with several numerical ranks. Researchers or local government officials, who carry out post disaster investigation, can make use of this scale in order to easily grasp overall disaster by high wind including the effect of tatsumakis. Table 1 shows the high wind damage scale.

The authors applied observed damage states of each houses in Wakasa of Saroma town to the high wind damage scale shown in Table 1. The result is illustrated in Fig. 30. If the line which covers buildings ranked 4 or 5 is supposed to the route of the tatsumaki, how the tatsumaki went across the area can be estimated as shown in the figure. The width of disaster area was ranging from 100m to 250m and the damage area may be more extensive in the eastern side of the estimated route of the tatsumaki.

As the typical characteristics of disaster by tatsumaki, it can be pointed out that the width of the disaster area is narrower than that by typhoon and the estimated boundary between damaged area and non-damaged one is very clear. Figs. 34 and 35 are examples of the clear boundary between damaged and non-damaged houses.

Table 1 High Wind Damage Scale

Rank	Damage state
1	Antenna or gutter on the roof is broken. Twigs are folded and lots of leaves are scattered. 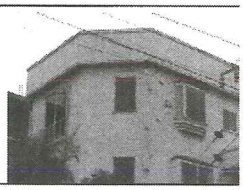
2	Roof tiles are shifted. Roofing materials such as roof tile, shingle and steel roof are blown off from edge of eaves or gable (less than 30% of total area of the roof). Thick branches are folded.  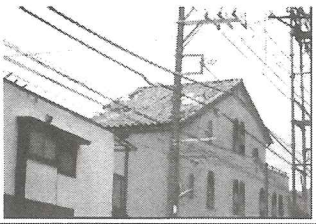 
3	Roofing materials such as roof tile, shingle and steel roof are blown off and extensive area of sheathing roof board can be exposed (30% and more of total area of the roof). Windows and nonstructural external walls are partially broken. Thick trees are fallen down.   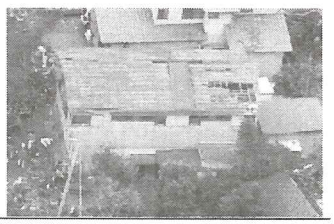
4	Rafters and purline of roof are broken. Roofing system is collapsed. Lots of windows are broken. 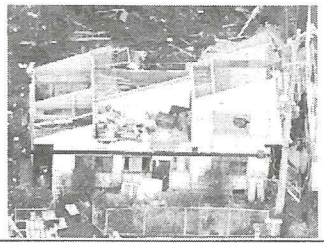  
5	Houses are totally collapsed. 

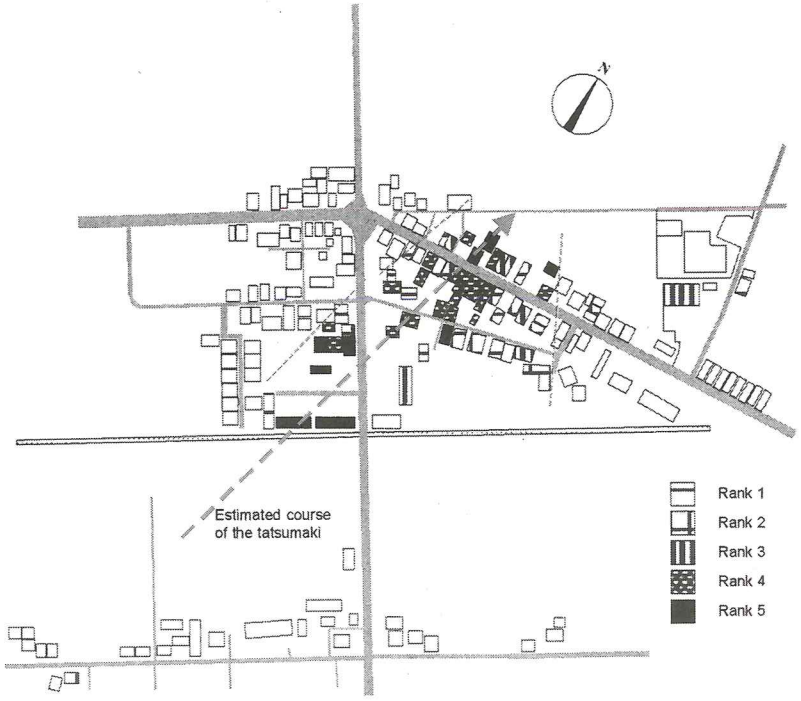

Fig.33 Distribution of Damaged Buildings in Wakasa of Saroma Town



Fig.34 House with Collapsed Roofing System and House with Small Damaged Roofing Material



Fig.35 House with Peeled-off Roof and Non-damaged House

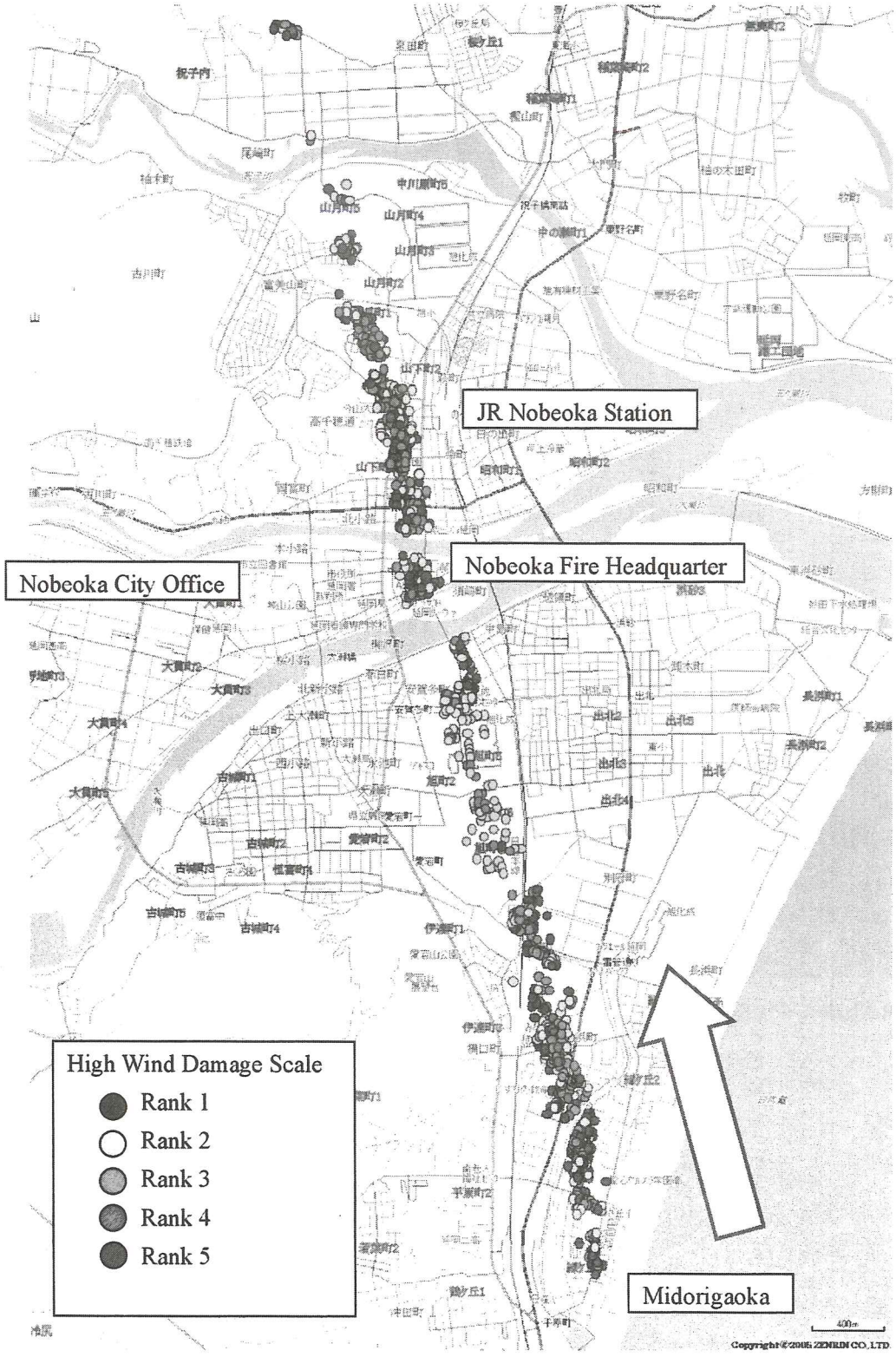

Fig. 36 Distribution of Damaged Buildings in Nobeoka City

The damage is almost distributed for about

7.5km in a straight line to run through a center of Nobeoka city. A Tatsumaki generated on the sea in the offing of Midorigaoka, Nobeoka city and moved up to the north from the south. According to the Meteorological Agency, movement speed of a tornado estimates it with about 90km/h. A Tatsumaki struck Nobeoka Fire Headquarter and all windows of the building were broken.

5. WIND LOAD OF TATSUMAKI AND FLYING DEBRIS IN BUILDING STANDARD LAW

Basic wind velocity Vo in Building Standard Law of Japan[1] is provided from records of the maximum wind velocity (10 minute averaged velocity) observed at weather stations in Japan, and is not considered of gust wind such as a tatsumaki. "Tornadoes have not been considered in developing the basic wind speed distributions" in ASCE[2], because the wind-resistant design for almost buildings that considered action of a tornado is not economical. However, tornadic gust wind speed map corresponding to annual probability of 10^{-5} are illustrated in Appendix of ASCE for special buildings.

It is not explicitly written how walls can be designed against flying debris in Building Standard Law of Japan. On the other hand, in ASCE, it is demanded that shutter or glass should be used of which the strength is confirmed by examinations for flying debris according to buildings or building site.

6. CONCLSIONS

BRI investigated the damage to buildings by two tatsumakis. Collision of flying debris to claddings and scattering of roof materials in houses were very remarkable in tatsumaki damage. Borderline of each damaged area by tatsumaki was very clear. Damage state of each house was applied to a high wind damage scale that the authors proposed and applied typhoon damage to houses in 2004.

REFERENCES

1. The Building Standard Law of Japan 2004, The Building Center of Japan, 2004

2. Minimum Design Loads for Buildings and Other Structures: 6.Wind Loads, ASCE 7-05, 2005

Parametric Study of Flutter Derivatives of Bridge Cross Sections and Their Implications on the Aeroelastic Stability of Flexible Bridges

by

Partha P. Sarkar[1], Luca Caracoglia[2], Fred L. Haan, Jr.[3]

ABSTRACT

Results of various experimental flutter derivative extraction techniques are compared in this paper. The motivation for this work emerged from the U.S.-Japan Benchmark Study on Bridge Flutter Derivatives that Iowa State University (ISU) in the US and the Public Works Research Institute (PWRI) in Japan initiated in 2002. In the first part, a systematic analysis of laboratory results was conducted; this included free and forced-vibration wind tunnel methods, which are routinely employed by researchers or designers. Data from US and Japanese laboratories were compared considering both streamlined and bluff deck sections. In the second part, a sensitivity study was performed to examine the implications of the perceived dissimilarities among flutter-derivative data sets on the aeroelastic instability of long-span bridges. It was found that flutter derivative uncertainty did not directly relate to flutter velocity. Flutter derivative uncertainties were estimated anywhere between negligibly small values to as much as 50%. The resulting flutter velocities, however, depended heavily on the type of bridge and mode of flutter. Flutter velocity uncertainty values were estimated from as small as 5% to as large as 30% depending on various conditions.

KEYWORDS: bridge aerodynamics, free and forced vibration, bridge flutter-derivative benchmark study, flutter speed calculation.

1.0 INTRODUCTION

The motivation for this work emerges from the U.S.-Japan Benchmark Study on Bridge Flutter Derivatives that Iowa State University (ISU) in the US and the Public Works Research Institute (PWRI) in Japan initiated in 2002. Five bridge cross sections were proposed to be tested: (1) Rectangle (2:1 section), (2) Π-section (or edge girder section), (3) Streamlined Box Girder, (4) Slotted Box Girder, and (5) Original Tacoma Narrows. Sarkar et al. (2006) reported good comparison between the ISU free vibration data and PWRI forced vibration data (Sato, 2004) of all the eight flutter derivatives of the Streamlined Box Girder and Slotted Box Girder sections associated with their vertical-torsional motion except for some minor discrepancies.

Section model tests of the decks of long-span bridges have long been conducted as part of the design process for new bridges. Over the years, numerous methods have been developed to extract the required aeroelastic and aerodynamic parameters from the tests. Although the technical implementation of each method can vary widely, all methods can be grouped into two broad categories—those involving free vibration tests and those involving forced vibration tests. Both methods have advantages for different scenarios. Free vibration systems do not force any prescribed motion on the model but rather allow the fluid structure interaction to drive the motion. Forced

[1] Professor and Wilson Chair, [3] Assistant Professor
Wind Simulation and Testing Laboratory, Department of Aerospace Engineering, Iowa State University, 2271 Howe Hall, Room 1200, Ames, IA 50011-2271 USA

[2] Assistant Professor, Department of Civil and Environmental Engineering, Northeastern University, 360 Huntington Avenue, Boston, MA 02115 USA

vibration systems, however, are sometimes able to deal with cases involving larger reduced velocities or higher turbulence intensities that would be very difficult with free vibration tests.

In the past, very few studies have been conducted to examine the equivalence of results from free and forced methods. The work described here relates to an effort to compare the results of forced and free vibration testing within the same laboratory as well as two different laboratories. This paper focuses on two rectangular sections and provides comparison between ISU data set with another data set from Japan (Matsumoto, 1996). Many researchers in the past have suspected flutter derivatives to be amplitude dependent but none has explored it completely. One degree-of-freedom (DOF) free-vibration tests in heaving motion were conducted for up to three different initial amplitudes. The results were compared with each other and with those from Japan. Recent comparison of flutter derivatives of a particular streamlined deck that were obtained using the forced vibration method (Haan, 2000) with those from free vibration (Gan Chowdhury and Sarkar, 2003) showed some differences at ISU. This motivated us to perform an uncertainty analysis to estimate the variation of flutter derivatives obtained from this forced-vibration method. Since this method uses phase angle between displacement and force or moment to calculate the flutter derivatives and the phase angle depends on many factors including instrumentation, sampling rate, and filters used, it was decided to estimate the errors that could arise as a result of these factors. Lastly, flutter-speed predictions for long-span bridges of various spans were considered in terms of the variation in flutter derivatives due to different methods, laboratories, and amplitudes. Flutter speeds corresponding to single-mode or multi-mode flutter for a streamlined and a rectangular section were estimated using a range of flutter derivatives obtained at ISU and from Japan.

2.0 EXPERIMENTAL FACILITIES

A test section was built to accommodate section model testing in the Bill James Wind Tunnel (see Figure 1) at Iowa State University's Wind Simulation and Testing Laboratory. The Bill James tunnel has a 0.91m by 0.76m test section and an 80m/s maximum velocity. Section models that are suspended by linear springs slide on guide rails with extremely low friction air bearings. For free vibration testing, models are free to move with three degrees of freedom (DOFs)—plunge, pitch, and sway. Figure 2 shows a picture of the model in this suspension system; further details can be found in Sarkar et al. (2004). For forced vibration tests, only pitching and plunging DOFs are employed. The forced vibration excitation system is mounted on a frame above the test section (see Figures 1 and 2). Rods extend into the test section to drive the model motion. These rods are removed for free vibration tests. The initial displacements for the free vibration tests are accomplished using a setup of electromagnets, strings and pulleys (Figure 3). Forced vibration tests require lift and moment to be measured simultaneously with vertical or angular position. In this case, lift and moment were calculated using pressure measurements on the models. The top and bottom surfaces of the models were instrumented with 16 pressure taps each. Pressures were measured with an electronic pressure scanner and the signals were corrected for the dynamic effects of the tubing. More details can be found in Section 4.0.

The results of testing one streamlined box girder model (B1) with semi-circular fairings for the edges, as shown in Figure 4, are presented in this paper. The first test involved B1 that had a B/D ratio (width to depth) of 14.3 and a length of 0.6 m, respectively. This model was used in tests at ISU that compared free and forced vibration methods of flutter derivative extraction. Two other models with bluff cross sections, "R2_1" and "R5_1," as shown in Figure 5, were also tested at ISU. These models were rectangle box girders with a $B/D = 2$ (R2_1) and $B/D = 5$ (R5_1). Each model had a span of 0.533 m. Two Plexiglas end plates were used to reduce aerodynamic end effects for all models.

For comparison purposes and within the scope of the benchmark study, results from another laboratory are included in this paper. Matsumoto (1996) extracted flutter derivatives with a forced vibration system. In this system, the unsteady

aerodynamic pressures acting on a section model were measured in two separate one-DOF tests. The aerodynamic forces and moments were obtained by integrating these pressures and four aerodynamic derivatives were estimated from each test using these aerodynamic forces or moments and forcing displacements measured at the same time.

3.0 ANALYTICAL APPROACH OF EACH METHOD

The methods for free vibration and forced vibration analysis employed for this study used the following formulation for the aeroelastic forces acting on a bridge deck:

$$L_{ae} = \frac{1}{2}\rho U^2 B\left[\begin{array}{l} KH_1^*\dfrac{\dot{h}}{U} + KH_2^*\dfrac{B\dot{\alpha}}{U} \\ +K^2H_3^*\alpha + K^2H_4^*\dfrac{h}{B}\end{array}\right] \quad (1)$$

$$M_{ae} = \frac{1}{2}\rho U^2 B^2\left[\begin{array}{l} KA_1^*\dfrac{\dot{h}}{U} + KA_2^*\dfrac{B\dot{\alpha}}{U} + \\ K^2A_3^*\alpha + K^2A_4^*\dfrac{h}{B}\end{array}\right]$$

where B is the bridge deck width, U is the mean wind velocity, ρ is the air density, K is the reduced frequency and h and α represent heaving and pitching displacements, respectively (with the dot representing a time derivative). The reduced frequency K is defined as $\omega B/U$ where ω is the frequency of vibration. The reduced frequency is proportional to the reciprocal of the reduced velocity, U_r, which is defined as U/nB where n is the frequency of oscillation in Hz ($\omega=2\pi n$).

The free vibration testing of the present work employs a new system identification method (Iterative least squares method or ILS method) that can efficiently extract up to eighteen flutter derivatives associated with three-DOF motion of a section model. This identification technique (Gan Chowdhury and Sarkar, 2003, 2004) uses experimentally obtained free-vibration displacement time histories generated by a section model supported by a three-DOF elastic suspension system (Sarkar et al., 2004) inside a wind tunnel test section. The ILS method extracts the flutter derivatives by using an iterative technique to identify the stiffness and damping matrices that are associated with the equations of motion at a given wind speed. The ILS method can also be applied to fewer DOF (two or one), if needed, by appropriately restraining the section model to vibrate along certain DOF(s). In fact, it is recommended that performing three different sets of two-DOF testing, namely, vertical-torsional, vertical-lateral, and lateral-torsional, instead of three-DOF testing, would be more efficient procedure for accurate extraction of all the eighteen derivatives. In this paper, results from one-DOF testing for the rectangular sections R2_1 and R5_1 for three initial amplitudes, A=9 mm, 17 mm and 26 mm, two cases of two-DOF testing (vertical-torsional and lateral-vertical) of B1 (Gan Chowdhury and Sarkar, 2003, 2004) and one case of one-DOF forced vibration testing (torsional) of B1 are presented. Details of the identification technique (ILS method) and experimental procedure for the free vibration method can be found in Gan Chowdhury and Sarkar (2003).

The analytical approach of the forced vibration technique is similar in principle to that described in Haan (2000) and Matsumoto (1996). Essentially, while driving the model in a prescribed sinusoidal motion, the pressure is measured on the top and bottom surfaces of the model in the streamwise direction. The pressure signals are integrated to obtain lift and moment time series. Phase relations between the motion (the angular and vertical position) and the aerodynamic forces (the lift and the moment) are estimated using a frequency domain approach. For an angular oscillation prescribed as:

$$\alpha = \alpha_0 \cos(\omega_\alpha t) \quad (2)$$

where α_0 is the amplitude of the angular oscillation and ω_α is the frequency of oscillation, the lift and the moment can be expressed as:

$$L = L_0 \cos(\omega_\alpha t - \phi_L)$$
$$M = M_0 \cos(\omega_\alpha t - \phi_M) \quad (3)$$

where L_0 and M_0 are the amplitudes of the fluctuating lift and moment, respectively, and ϕ_L and ϕ_M are the phase lags with respect to the angular position, α, of the lift and moment, respectively.

Given the above definitions, it can be shown that the flutter derivatives related to the pitching motion can be given as:

$$A_2^* = \frac{-M_0}{\alpha_0}\frac{\sin\phi_M}{qB^2K^2},\quad A_3^* = \frac{M_0}{\alpha_0}\frac{\cos\phi_M}{qB^2K^2}$$

$$H_2^* = \frac{-L_0}{\alpha_0}\frac{\sin\phi_L}{qBK^2},\quad H_3^* = \frac{L_0}{\alpha_0}\frac{\cos\phi_L}{qBK^2} \qquad (4)$$

where q is the dynamic pressure. Given a prescribed heaving motion such as $h = h_0\cos(\omega_h t)$ expressions for the heaving flutter derivatives, (A_1^*, A_4^*, H_1^*, H_4^*) can be derived as well. Both vertical lift, L, and heaving displacement, h, are defined as positive *downward*. To identify flutter derivatives for a range of reduced velocity values, the frequency of the motion of the model was held constant while the velocity of the tunnel was varied. In this paper, the pitching amplitude of B1 was 3 degrees and frequency of motion was 3.3 Hz. The heaving motion amplitude of Matsumoto's forced vibration tests of the rectangular sections with *B/D*=2 and 5 was 5 mm (Matsumoto, 1996).

4.0 CONSIDERATIONS ON UNCERTAINTY IN THE EXTRACTION OF FLUTTER DERIVATIVES THROUGH FORCED-VIBRATION METHOD

The phase angle between the model motion and the resulting self-excited forces plays a major role in the final value of the flutter derivatives, particularly for the A_2^* and H_2^* flutter derivatives. Contributions to phase angle uncertainty were estimated along with the corresponding influences to the flutter derivatives.

The phase angles ϕ_L and ϕ_M represent the phase lag between the maximum torsional displacement and the maximum value of lift and moment, respectively. These values were obtained by calculating a cross correlation function between the time series of angular position and lift (or moment). The time delay, τ, associated with the peak in the cross correlation function is the time delay from which the phase angle is calculated. The phase angle in degrees is calculated as $\phi = 360n\tau$, where n is the model oscillation frequency.

Three contributions to phase angle uncertainty were identified. First, the frequency response function of the pressure tubing has a finite uncertainty. Using a range of values for tubing length and sensor volume, the analytical expressions of Bergh and Tijdeman (1965) were used to calculate a range of tubing phase values at the body oscillation frequency. This range was used to estimate $u_{\phi_{tube}}$ to be $\pm 0.5°$ where $u_{\phi_{tube}}$ is the uncertainty in the phase resulting from tubing response.

The second contribution was from the finite sampling time of the pressure scanner. The pressure scanners sampling rate was 430 Hz (the maximum sustainable sampling rate). This means that the time delay calculations have a resolution of 1/430 seconds. This resolution was used as an estimate for $u_{\tau_{rate}}$, the uncertainty in the correlation time delay due to the finite sampling rate.

The third contribution originated from the non-simultaneous sampling of the pressure sensors. The pressure scanners interrogate each sensor sequentially, and therefore, there is a skew in time between one sensor sample and the next. The multiplexer scan rate is 50,000 Hz. The inter-channel scan rate then is found by dividing this rate by the 64 channels in the scanner, 781 Hz. The total delay between sampling the first and last channels is therefore 1/781 seconds. This value was used as the worst case estimate for $u_{\tau_{skew}}$, the uncertainty in the correlation time delay due to the non-simultaneous sampling of the pressure signals.

The impact of these *individual* contributions to flutter derivative values was estimated by calculating the flutter derivatives with these uncertainties added or subtracted from the phase values. The overall uncertainty in the phase angle was estimated in the conventional sum of squares approach shown below:

$$u_\phi^2 = \left[u_{\phi_{tube}}^2 + \left(\frac{\partial \phi}{\partial \tau} u_{\tau_{rate}} \right)^2 + \left(\frac{\partial \phi}{\partial \tau} u_{\tau_{skew}} \right)^2 \right] \quad (5)$$

where the $\frac{\partial \phi}{\partial \tau}$ derivative was estimated from the ϕ expression given earlier.

An example of uncertainty analysis associated with phase-lag effects can be found in Figures 7(a) to 7(d) for the B1 streamlined cross section, derived from ISU 1-DOF tests (torsional motion). Each plot is associated with a specific flutter derivative. These figures show the overall effects associated with the uncertainty in the definition of the phase angle (including tubing, sampling time and skew time). The reference ("Ref") curves (triangle symbol) were derived by averaging ten subsequent experimental realizations. In addition, upper ("Up") and lower ("Low") confidence bounds (square symbols) can also be seen; these corresponds to the error analysis associated with the overall phase angle effects. Figures analyzing the contribution associated with each individual component are available but were omitted for brevity. Moreover, a comparison with an equivalent set of free-vibration data is depicted.

One aspect of the uncertainty analysis that is immediately evident is the very low sensitivity of the A_3^* and H_3^* derivatives to phase uncertainty. In all cases, this sensitivity was negligible. This is due to the fact that the flutter derivatives are proportional to the cosine of the phase angle. A_2^* and H_2^* showed variations of as much as 20% and 50%, respectively, with these rather modest uncertainty estimates.

The other observation that can be made is that the sampling rate made the largest contribution to the uncertainty in the A_2^* and H_2^* flutter derivatives. Increasing the sampling rate appears to be the most effective way to reduce flutter derivative uncertainty.

5.0 FLUTTER DERIVATIVE COMPARISON

All eight flutter derivatives *H1*-H4** and *A1*-A4** for B1 that were extracted using the 2-DOF free vibration tests and the ILS method (Gan Chowdury and Sarkar, 2003, 2004) are plotted in Figures 6a and 6b for reference since these were used later for aeroelastic-instability sensitivity analysis. The comparison of *H1*, H4** and *A2*, A3** as extracted by 2-DOF Vertical-Torsional, Lateral-Vertical and Lateral-Torsional motions are shown in Figures 6c and 6d. Slight differences between the two sets are observed that could be because of the influence of amplitude of vibration of the second degree of freedom not directly associated with the direct flutter derivatives that are being compared. In other words, *H1** and *H4** are likely to be influenced by amplitudes of torsional and lateral motions while *A2** and *A3** are likely to be influenced by amplitudes of vertical and lateral motions.

As observed in Figure 7 and reported earlier (Sarkar et al., 2006), the flutter derivatives from free vibration and forced vibration of B1 generally compare well except it can be seen that *H2** falls below the lower confidence level of the forced-vibration test. One of the explanations that could be offered is that the data from the free vibration tests will also have an upper bound and a lower bound due to its sensitivity to various parameters including but not limited to number of degrees of freedom, sampling rate and sampling time, instrumentation and system identification method that were used to extract them. There is a good possibility that the upper bound of the free vibration data could overlap with the lower bound of the forced vibration data. The error analysis of the free vibration data has not been performed yet.

Figures 8 and 9 show some effect of amplitude on the flutter derivatives for the R2-1 and R5-1 bridge deck cases. It was observed for both the cross sections that the *H1** curve does not change

between A=9 mm and 17 mm cases. In Figure 8, however, for the R2_1 and A=26 mm case the negative magnitudes of $H1^*$ decreased with respect to the other two cases. Matsumoto's forced-vibration data with an amplitude of A=5 mm that is lower than the ISU cases is consistent with this observation. In this case, the negative magnitudes of $H1^*$ are greater than the ISU cases. However, the higher positive values of this data set than those of the ISU cases can not be explained. The general trend of all the $H1^*$ graphs is consistent including the zero crossing points. There is a clear trend in the ISU $H4^*$ values for R2_1 case as shown in Figure 8b. The positive peak value of $H4^*$ corresponding to different amplitudes does not change but the graphs tend to shift toward left for smaller amplitudes. The first zero crossing of the ISU, A=9 mm case compares well with Matsumoto's data. However, the positive peak values of ISU $H4^*$ fall short of Matsumoto's positive peak value. This trend is consistent with those observed for $H1^*$ in Figure 8a. In Figure 9, for R5_1 case, the comparison is generally good except some difference at higher reduced velocity in $H1^*$. The ISU data does not demonstrate any amplitude dependency in this case.

6.0 SINGLE AND COUPLED-MODE AEROELASTIC INSTABILITY SENSITIVITY ANALYSIS

A sensitivity study was conducted to understand the implications of the differences emerged during the experimental benchmark comparison on the wind-induced oscillation of long-span bridges. Two distinct cross sections were considered: Streamlined cross section with semi-circular fairings with B/D=14.3 (B1) and the bluff rectangular prism with B/D=2 (R2_1). Numerical simulations were carried out in order to identify the influence of the variations in the flutter derivatives, extracted from tests conducted either by different laboratories or under distinct operational conditions, on the critical velocity corresponding to the onset of dynamic instability. Both single-mode and coupled-mode aeroelastic vibration were analyzed (Scanlan and Tomko, 1971; Simiu and Scanlan, 1996).

Table 1 summarizes the different flutter derivative sets, which were separately considered during the simulations. For each cross section, the denomination refers to a particular experimental set, such as free (FV) or forced vibration (FFV), 2-DOF or 1-DOF, initial oscillation amplitude (A).

In relation to the B1 cross section, data derived from the tests conducted at ISU were exclusively employed, from which five simulation sets were extracted (Table 1): two sets corresponding to free-vibration tests exclusively (FV), and three sets associated with a combination of free and forced-vibration (FFV) experimental results.

With regard to the first two simulation scenarios sets associated with free-vibration tests, Figures 6(a) and 6(b) respectively show the H_q^* and A_q^* derivatives (q=1,..,4), labeled as set B1.A in Table 1 (2-DOF Vertical-Torsional tests). The second set (B1.B) was derived from the combination of the cross terms of B1.A and the direct terms related to two additional ISU sets (2-DOF L&T, L&V). In Figures 6(c) and 6(d) the comparison between sets B1.A and sets B1.B is presented (H_1^*, H_4^* and A_2^*, A_3^*, respectively) as a function of the reduced velocity, U/nB. Evident dissimilarities are limited to A_2^* and A_3^* in the reduced velocity range beyond 8.0, while they are much less pronounced for the other terms.

In relation to the simulation sets, Figures 7(a) to 7(d) present the B1-cross section derivatives H_2^*, H_3^*, A_2^* and A_3^* corresponding to the ISU 1-DOF forced-vibration experiments (torsional). In the figures free-vibration tests are included along with the sensitivity analysis to phase-angle errors, as indicated in Section 4.0. The corresponding simulation sets, derived from the derivatives in Figures 7 are indicated as B1.C to B1.E in Table 1; it must be observed that in the simulations flutter derivatives H_2^*, H_3^* and A_2^*, A_3^* were derived from a combination of the different curves related to the FFV sets (Figures 7), whereas the remaining curves were taken from the free-vibration data. A detailed description can be found in Table 1.

In relation to the R2_1 case, H_1^*, H_4^* data were exclusively considered, since this particular shape

exhibits susceptibility to heaving-mode aeroelastic instability (single-mode galloping). Simulation sets included both 1-DOF ISU free-vibration wind tunnel tests, conducted at different amplitudes, and forced-vibration experimental sets reproduced from Matsumoto (1996). In Figures 8(a) and 8(b) the sets corresponding to H_1* and H_4* are respectively depicted as a function of U/nB.

Three long-span bridge configurations were analyzed. Multimode or single-mode analysis methods (e.g. Jones and Scanlan, 2001) were employed for the solution to the aeroelstic instability problem. Numerical procedures for aeroelastic simulations were derived from previous studies (Caracoglia, 2001) and adapted to the specific examples.

The mass and rotational moment of inertia of the deck/vibrating structure were simulated through a constant quantity per unit length (m_0 and I_0, respectively). Influence of the mode shape on the aeroelastic instability solution was neglected at this stage: mode shapes were postulated as simplified sinusoidal forms. Lateral modes were not considered.

The simulated structures are: Br1, a medium-span suspension-bridge (main span L=1200 m, deck width B=28 m, $m_0=3.5\times10^4$ kg/m, deck torsional inertia $I_0=4.4\times10^6$ kg×m^2/m); Br2, a short-span cable-stayed bridge (L=500 m, B=38 m, $m_0=3.1\times10^4$ kg/m, $I_0=2.8\times10^6$ kg×m^2/m); Br3, a long-span suspension bridge (L=3000m, B=60 m, $m_0=3.1\times10^4$ kg/m, $I_0=2.8\times10^6$ kg×m^2/m). In the case of Br1, for which the deck bending and torsional stiffness is predominant in comparison with those provided by the cables, the simulated modes (vertical and torsional) are symmetric, while these are skew-symmetric for Br2 and Br3.

In all the three cases a constant values of mechanical damping equal to 0.3% was considered, independently of the selected mode. Moreover, in the case of coupled-mode instability, perfect similarity between bending and torsional eigen-functions was considered. All these quantities were calibrated through the analysis of similar existing structures.

Table 2 summarizes the results of the coupled-mode simulations conducted on bridge types Br1, Br2, Br3 by considering the flutter derivative sets B1.A to B1.E; simulation scenarios (i) to (xv) were considered. For each scenario, the table shows the lowest critical eigen-value solution corresponding to the critical velocity of binary flutter (simple harmonic motion), based on two-mode analysis (Jones and Scanlan, 2001). In the table, the frequencies corresponding to the selected modes are also indicated, along with the critical reduced frequency (K_{crit}), flutter-mode frequency and velocity.

In relation to sets B1.A and B1.B, it must be observed that the variation between the two sets was exclusively simulated through direct terms (i.e., H_1*, H_4* and A_2*, A_3*), while differences in the cross-terms were not examined (Table 1). In contrast, both the direct (i.e., A_2*, A_3*) and the cross-terms (i.e., H_2*, H_3*) were considered in the sets from B1.D to B1.E.

Figure 10 shows the typical trajectories of the flutter real and imaginary solution branches. Flutter eigen-values (ratio between simple-harmonic-motion and torsional-mode frequencies, f_{shm}/f_{tors}) as a function of the reduced frequency ($K=\omega B/U$) are indicated for Br1 and set B1.A (a), Br3 and set B1.B (b). The two-mode flutter solution is highlighted in both cases. In all cases flutter seems to be dominated by the vertical mode because of the nature of the aeroelastic terms (streamlined cross section).

From the analysis of Table 2, differences of the order of few percent to a maximum of 8% (e.g., case (ii) vs. case (i)) can be observed between B1.A and B1.B for all three simulated bridge examples. Differences in the flutter speed are more evident for a medium-span bridge, at least for the investigated scenarios. The critical values of the reduced velocity can be located between 7.4 (Br3, case (xv)) and 33.4 (Br1, case (ii)). The latter case is clearly beyond the interval of measured U/nB (Figure 1) and the solution to the flutter problem was only possible through extrapolation of the experimental data associated with free-vibration tests.

In contrast, a disparity in the results was observed between the free and forced-vibration sets. As an example a 30% reduction in the flutter speed can be seen in Table 2 between case (iv) and (i) for Br 1, even though this result is affected by the fact that H_1*, H_4* and A_1*, A_4* are interpolated for U/nB>15. Similarly, a reduction in the flutter velocity was observed for Br2 and Br3 even though less significant (e.g., 13% reduction between (xiii) and (xi)).In all cases the discrepancy can be related to the measurements of H_2* (variations in both magnitude and sign, Figure 2(a)), responsible for the modal coupling during flutter.

Moreover, it can be concluded from Table 2 that the phase angle effect, typical of the sets derived through forced vibration, appears to be of secondary importance. A 3% maximum difference in the critical velocity was in general observed among sets B1.C, B1.D and B1.E (e.g., (ix) vs. (x) for Br2).

In the second part of the sensitivity study, heaving-mode aeroelastic instability was analyzed. This is a phenomenon similar to single-mode galloping, usually associated with inadequate aerodynamic characteristics of H_1* for bluff cross sections (Figure 8(a)). Results are summarized in Table 3. In this case bridge types Br1 and Br2 were only considered. Since a single-mode dynamic instability is damping driven, the initial selection of the structural damping value is important and had a direct effect on the assessment of the critical threshold. Nevertheless, relative differences among the investigated cases are of more relevance in this study since these are associated with the differences in measured H_1* and H_4* (Figure 8), derived under distinct operational conditions. The analysis of the data sets showed in fact a difference of the order of 30% in some cases between ISU and Matsumoto (1996), especially for H_1*. It was concluded that this effect in combination with an apparent shift of the different curves along the U/nB axis was responsible for the deviations in the critical velocities (Table 3), with variations between 5% and 20% for Br1, and 9% and 15% for Br2. The latter tends to show a more pronounced dissimilarity in comparison with others (Figure 8).

It must be observed that relative variations in the H_4* derivative are responsible for the differences in terms of critical frequency (equivalent added or subtracted mass aerodynamic component) in the simulations.

From the analysis of Table 3, it can be concluded that the effects on the heaving-mode instability, related to dissimilarities in the experimental extraction of flutter derivatives, cannot be neglected in the case of a bluff deck section. These considerations are strictly applicable to the selected case studies, and are affected by the evident simplifications introduced during the investigations. A more careful assessment, for example performed on real structures, is therefore required for a more general characterization of these aspects.

7.0 SUMMARY

This paper presents some recent results associated with a research activity focused on the comparison between different wind tunnel measurement techniques for the extraction of flutter derivatives for bridge aeroelastic analyses. This research was motivated by a benchmark study initiative promoted by Iowa State University, extended to the Japanese investigators within the scope of the UJNR cooperative research efforts.

In the first part of the study a systematic analysis of laboratory results was conducted; this included free and forced-vibration wind tunnel methods, currently routinely employed by researchers or designers. Data from a US laboratory under distinct operational conditions were analyzed and compared with literature results (Japan). Both streamlined and bluff deck sections were considered.

In particular, it was concluded that for bluff cross sections (rectangular prisms) differences emerged from the experimental data could be possibly associated with the effects of amplitude dependency of the aeroelastic terms. Moreover, a non-negligible dependence on the laboratory environment or the operational conditions was noticed, even for streamlined cross-sections. This fact also suggests that uncertainty (i.e., error)

analyses (i.e., error estimation), as performed in this study for a set of derivatives derived through forced-vibration tests, should be carefully considered during wind tunnel operations and possibly included as a recommendation during preliminary bridge design.

In the second part of the research, a sensitivity study was performed on the implications of the perceived dissimilarities among flutter-derivative data sets on the aeroelastic instability of long-span bridges. A preliminary investigation was conducted on a restricted set of simulated bridges with simplified structural characteristics. Both bluff and streamlined deck cross sections were analyzed; single-mode (heaving) and coupled-mode instability for streamlined deck were considered. Results indicate that a variation of the order of ten to fifteen percent in the critical velocity was possible, either an increment or a decrement depending on the selected derivative set. This fact reaffirms the importance of uncertainty analysis of experimentally extracted flutter derivatives in the context of aeroelastic simulations. Moreover, effects such as phase-angle systematic errors, typical of the forced-vibration method, appear to be of secondary importance in comparison with other perceived dissimilarities (e.g., forced vs. free-vibration data sets), at least for streamlined sections. More investigation on perhaps more realistic or existing structures is necessary to fully quantify these implications and to provide a general guideline for designers or researchers.

8.0 ACKNOWLEDGMENTS

The contributions of technician, Bill Rickard, graduate students, Vasanth Balaramudu and Kevin Sehn, former graduate students, John Stronck and Arindam Gan Chowdhury, and many undergraduate students in the Department of Aerospace Engineering at Iowa State University, who contributed to this work, are gratefully acknowledged. We would like to acknowledge Dr. Hiroshi Sato at PWRI, Japan for providing insight to this work. The second author would like to acknowledge the partial support of Northeastern University, Office of the Provost, Research and Scholarship Development Fund (2006-2007), and start-up funding for new faculty members.

9.0 REFERENCES

Bergh, H., Tijdeman, H. (1965), "Theoretical and experimental results for the dynamic response of pressure measuring systems," Nationaal Lucht en uimtevaartlaboratorium, NLR-TR F.238.

Caracoglia, L. (2001), "Wind-Structure Oscillations on Long-Span Suspension Bridges," Ph.D. Dissertation, University of Trieste, Trieste, Italy.

Gan Chowdhury, A., Sarkar, P.P. (2003), "A New Technique for Identification of Eighteen Flutter Derivatives using a Three-Degree-of-Freedom Section Model," Engineering Structures, v. 25, n. 14, 1763-1772.

Gan Chowdhury, A., Sarkar, P.P. (2004), "Identification of Eighteen Flutter Derivatives of an Airfoil and a Bridge Deck," International Journal of Wind and Structures, Vol. 7, No. 3.

Haan, F.L., Jr. (2000), "The Effects of Turbulence on the Aerodynamics of Long-Span Bridges," Ph.D. Dissertation, University of Notre Dame, Notre Dame, Indiana.

Jones, N.P., Scanlan, R.H. (2001), "Theory and full-bridge modeling of wind response of cable-supported bridges," Journal of Bridge Engineering, ASCE, v6, n6, 365-375.

Matsumoto, M., Kobayashi, Y., Shirato, H. (1996), "The influence of aerodynamic derivatives on flutter," Journal of Wind Engineering and Industrial Aerodynamics, 60, 227-239.

Matsumoto, M. (1996), "Aerodynamic Damping of Prisms," Journal of Wind Engineering and Industrial Aerodynamics, v. 59, n. 2-3, 159-175.

Simiu, E., Scanlan, R.H. (1996), "Wind effects on structures," John Wiley and Sons, New York, NY, USA.

Sarkar, P.P., Haan, F.L., Stronck, J.M. and Balaramudu, V.K. (2006), "Forced and Free

Vibration Extraction of Flutter Derivatives: A Parametric Study-Based Comparison," Proc. Fourth UJNR Workshop on Wind Engineering, Tsukuba, Japan, July, 20-22.

Sarkar, P.P., Gan Chowdhury, A., Gardner, T.B. (2004), "A Novel Elastic Suspension System for Wind Tunnel Section Model Tests," Journal of Wind Engineering and Industrial Aerodynamics, v. 92, n. 1, 23-40.

Sato, H. (2004), Personal Communications, PWRI, Japan.

Scanlan, R.H. and Tomko, J.J. (1971), "Airfoil and Bridge Deck Flutter Derivatives," Journal of Engineering Mechanics, ASCE, v. 97, n. EM6, 1717-1737.

Table 1: Summary of the flutter-derivative data employed in the simulations (sections B1, R2_1).

Flutter Derivative Set	H_1*	H_2*	H_3*	H_4*	A_1*	A_2*	A_3*	A_4*
B1.A	ISU, FV-2 (V&T)	ISU, FV-2 (V&T)	ISU, FV-2 (V&T)	ISU, FV-2 (V&T)	ISU, FV-2 (V&T)	ISU, FV-2 (V&T)	ISU, FV-2 (V&T)	ISU, FV-2 (V&T)
B1.B	ISU, FV-2 (L&V)	ISU, FV-2 (V&T)	ISU, FV-2 (V&T)	ISU, FV-2 (L&V)	ISU, FV-2 (V&T)	ISU, FV-2 (L&T)	ISU, FV-2 (L&T)	ISU, FV-2 (V&T)
B1.C	ISU, FV-2 (V&T)	ISU, FFV-1 (T) "Ref"	ISU, FFV-1 (T) "Ref"	ISU, FV-2 (V&T)	ISU, FV-2 (V&T)	ISU, FFV-1 (T) "Ref"	ISU, FFV-1 (T) "Ref"	ISU, FV-2 (V&T)
B1.D	ISU, FV-2 (V&T)	ISU, FFV-1 (T) "Up"	ISU, FFV-1 (T) "Up"	ISU, FV-2 (V&T)	ISU, FV-2 (V&T)	ISU, FFV-1 (T) "Up"	ISU, FFV-1 (T) "Up"	ISU, FV-2 (V&T)
B1.E	ISU, FV-2 (V&T)	ISU, FFV-1 (T) "Low"	ISU, FFV-1 (T) "Low"	ISU, FV-2 (V&T)	ISU, FV-2 (V&T)	ISU, FFV-1 (T) "Low"	ISU, FFV-1 (T) "Low"	ISU, FV-2 (V&T)
R2_1.A09	ISU, FV-1 (V) A09	-	-	ISU, FV-1 (V) A09	-	-	-	-
R2_1.A17	ISU, FV-1 (V) A17	-	-	ISU, FV-1 (V) A17	-	-	-	-
R2_1.A26	ISU, FV-1 (V) A26	-	-	ISU, FV-1 (V) A26	-	-	-	-
R2_1.M	Matsumoto et al. (1996), FFV-1 (V)	-	-	Matsumoto et al. (1996), FFV-1 (V)	-	-	-	-

Notes: FV-1: free vibration (1-dof), FV-2: free vibration (2-dof), FFV-1: forced vibration (1-dof), V: vertical dof; T: torsional dof; L: lateral dof
Sections: B1 (streamlined cross section , $B/D = 14.3$); R2_1 (rectangular prism, $B/D = 2$). A: ampl. (A09=9, A17=17, A26=26mm)
Phase-angles: "Ref" (reference curve); "Up" (upper confidence level, Phi+dPhi in Figures 2); "Low" (lower confid. Level, Phi-dPhi in Figures. 2)

Table 2: Coupled-mode flutter simulations; sensitivity analyses.

Case Study (Bridge Type)	Flutter Derivative Set	Vertical Mode Freq. (Hz)	Torsional Mode Freq. (Hz)	2Mode Flutter $K_{crit}=\omega B/U$	2Mode Flutter Freq. (Hz)	2Mode Flutter Speed (m/s)
(i) Br1 (suspens., L=1200m)	B1.A	0.087	0.192	0.209	0.097	79.9
(ii) Br1	B1.B			0.188	0.094	85.9
(iii) Br1	B1.C			0.269	0.093	59.8
(iv) Br1	B1.D			0.266	0.093	60.3
(iv) Br1	B1.E			0.272	0.094	59.3
(vi) Br2 (cb.-stayed, L=500m)	B1.A	0.200	0.500	0.447	0.203	108.2
(vii) Br2	B1.B			0.449	0.202	107.7
(viii) Br2	B1.C			0.499	0.204	97.5
(ix) Br2	B1.D			0.493	0.203	98.5
(x) Br2	B1.E			0.505	0.204	96.6
(xi) Br3 (suspens., L=3000m)	B1.A	0.061	0.079	0.676	0.058	32.2
(xii) Br3	B1.B			0.721	0.059	30.9
(xiii) Br3	B1.C			0.848	0.060	26.7
(xiv) Br3	B1.D			0.833	0.060	27.2
(xv) Br3	B1.E			0.844	0.060	26.9

Table 3: Heaving-mode instability simulations; sensitivity analyses.

Case Study (Bridge Type)	Flutter Derivative Set	Vertical Mode Freq. (Hz)	Heaving-Mode $K_{crit}=\omega B/U$	Heaving-Mode $U_{R,crit}$ (1)	Heaving-Mode Crit. Freq. (Hz)	Heaving-Mode Crit. Speed (m/s)
(i) Br1 (suspens., L=1200m)	R2_1.A09	0.087	0.61	10.36	0.078	22.1
(ii) Br1	R2_1.A17		0.55	11.35	0.077	24.1
(iii) Br1	R2_1.A26		0.52	12.13	0.077	25.5
(iv) Br1	R2_1.M		0.57	11.05	0.069	20.9
(v) Br2 (cb.-stayed, L=500m)	R2_1.A09	0.200	0.61	10.34	0.160	62.9
(vi) Br2	R2_1.A17		0.55	11.32	0.159	68.5
(vii) Br2	R2_1.A26		0.52	12.07	0.156	71.8
(viii) Br2	R2_1.M		0.57	11.04	0.132	55.3

Note (1): $U_{R,crit}=2\pi/K_{crit}$

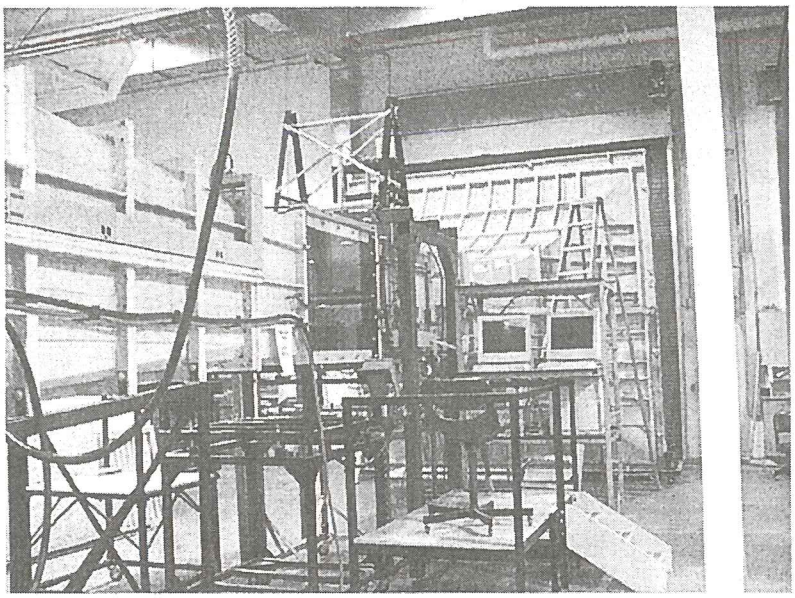

Figure 1: Bill James Wind Tunnel with forced-oscillation system installed on overhead frame.

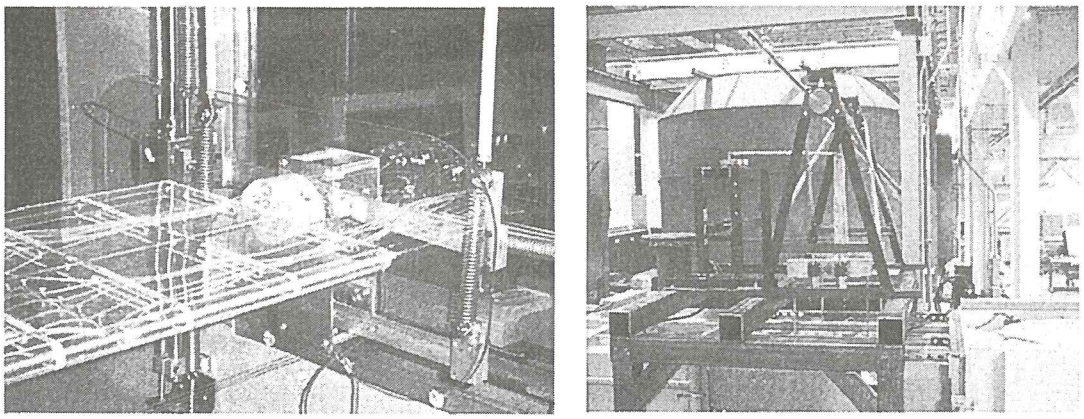

Figure 2: B1 Bridge model and model support structure (left) showing both spring mounts for free vibration and the push rods for forced vibration and forced oscillation system (right) showing motor and rocker arms used to actuate the push rods.

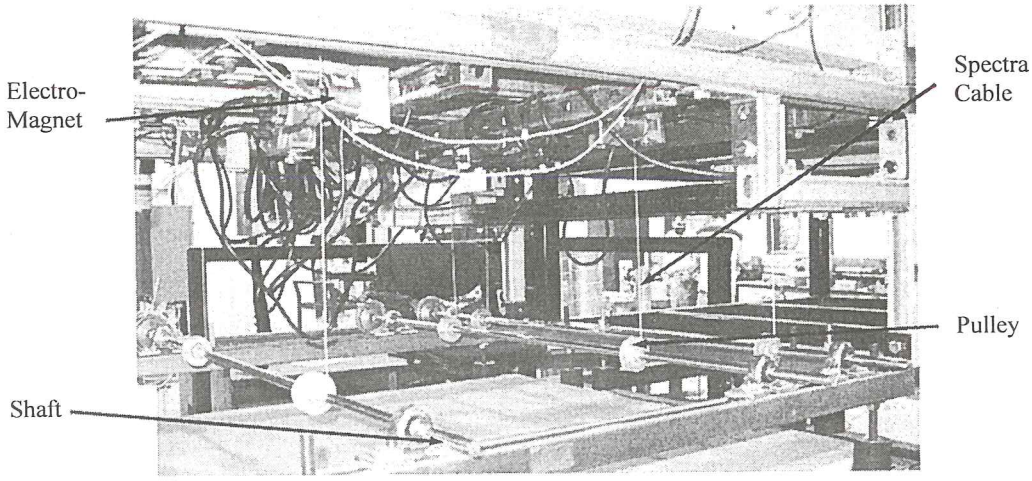

Figure 3: Free-vibration suspension system initial condition apparatus.

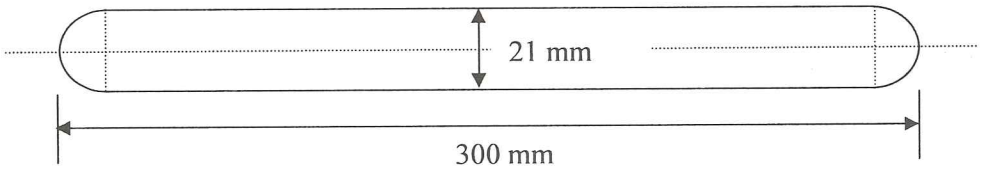

Figure 4: Diagram of streamlined bridge deck model, B1, used for comparing free and forced vibration methods of acquiring flutter derivatives in the Bill James Wind Tunnel at ISU.

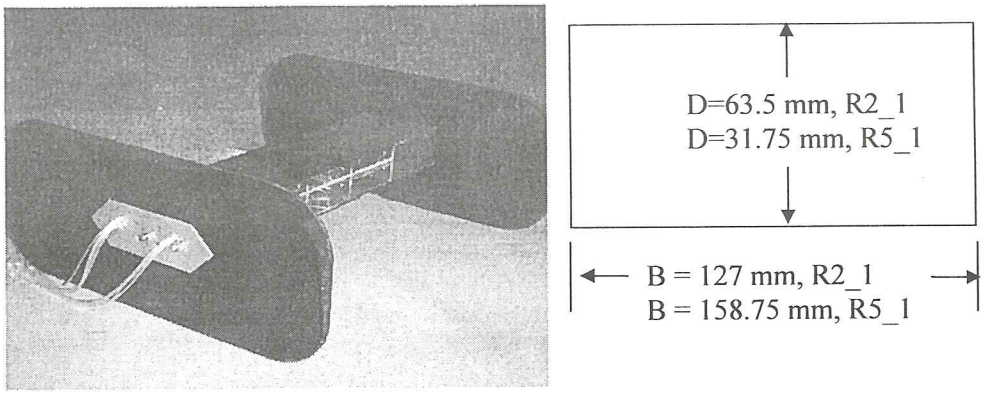

a. **b.**

Figure 5: a. Rectangular box girder section model, R2_1, b. Dimensions for the B/D =2 (R2_1) and B/D =5 (R5_1) models.

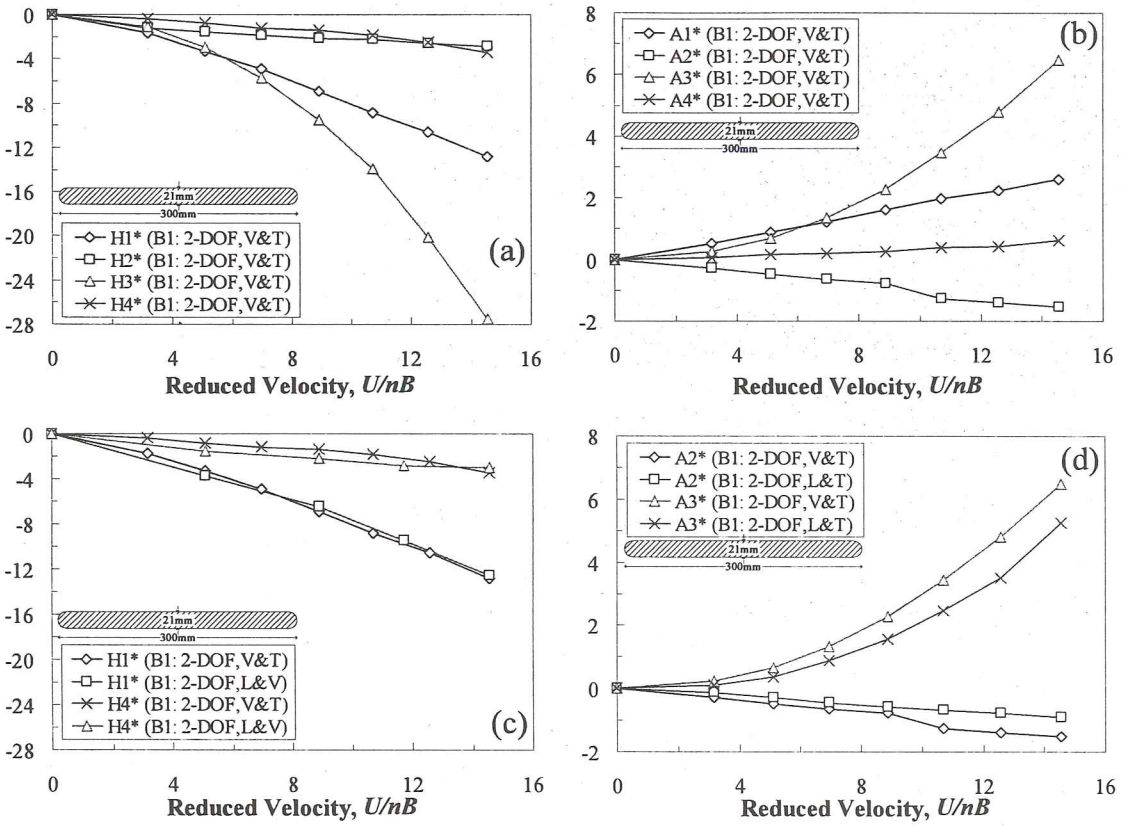

Figure 6: Flutter derivatives of B1 (ISU free-vibration tests) employed in the coupled-mode flutter simulations. H_q* (a) and A_q* (b) derivative set (q=1,..,4) corresponds to B1.A (2-DOF Vertical-Torsional); (c) H_1*, H_4* comparison between sets B1.A and B1.B (2-DOF Lateral & Vertical); (c) A_2*, A_3* comparison between sets B1.A and B1.B (2-DOF Lateral & Torsional).

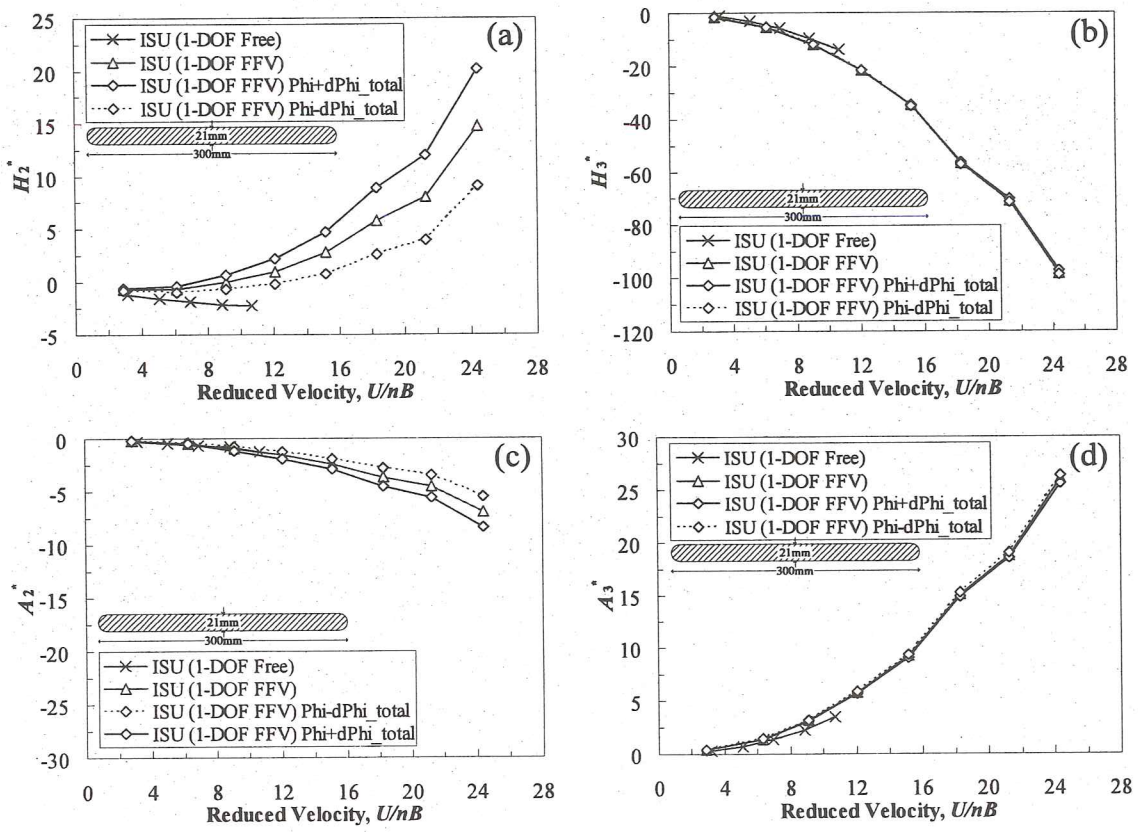

Figure 7: Flutter derivatives of B1 (ISU 1-DOF forced-vibration tests, Torsional or 1-DOF FFV), including sensitivity analysis to determine phase-angle errors. (a) H_2*, (b) H_3*, (c) A_2*, (d) A_3*. "(1-DOF FFV)": reference curves; "(1-DOF FFV) Phi+dPhi_total" upper confidence level; "(1-DOF FFV) Phi-dPhi_total" lower confidence level, and their comparison with the 1-DOF free vibration data.

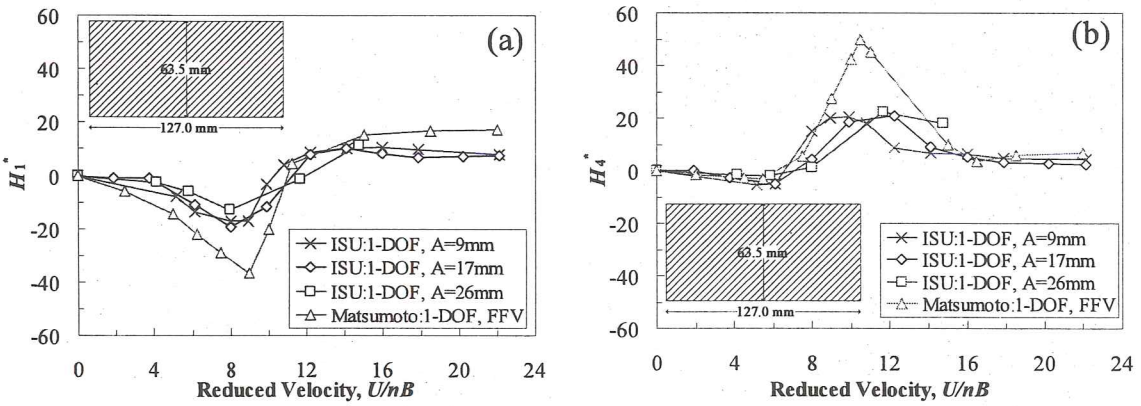

Figure 8: H_1* (a) and H_4* (b) flutter derivatives of the rectangular cross section R2_1 (AR 2:1) employed in the aeroelastic simulations. Comparison between the ISU 1-DOF vertical free-vibration experiments (A: initial amplitude) and the data reproduced from Matsumoto (1996), (FFV: forced vibration).

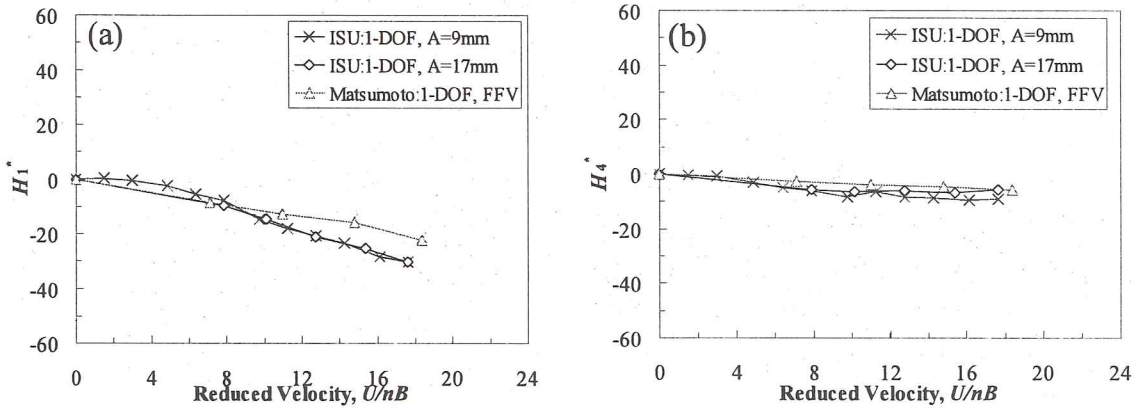

Figure 9: H_1* (a) and H_4* (b) flutter derivatives of the rectangular cross section R5_1 (AR 5:1). Comparison between the ISU 1-DOF vertical free-vibration experiments (A: initial amplitude) and the data reproduced from Matsumoto (1996), (FFV: forced vibration).

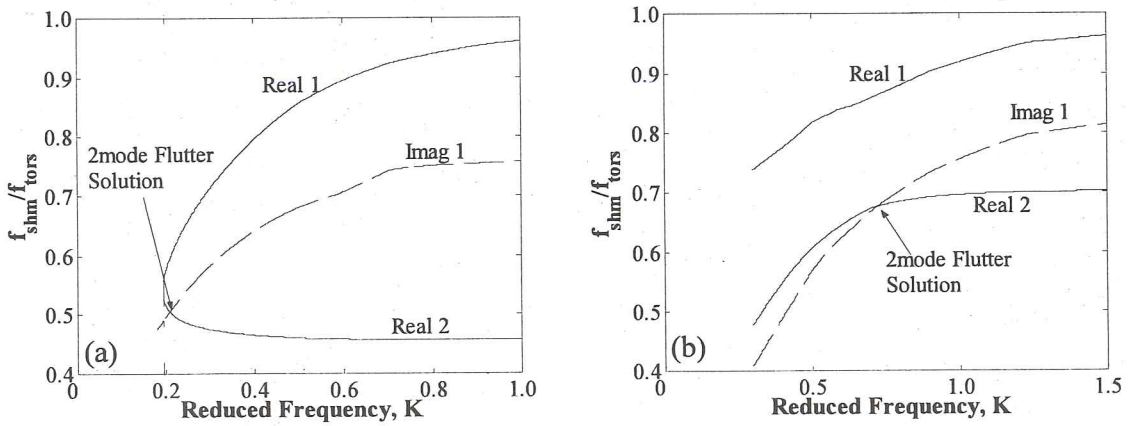

Figure 10: Example of coupled-mode flutter real and imaginary solution branches. Flutter eigen-value (ratio between simple-harmonic-motion and torsional-mode frequencies, f_{shm}/f_{tors}) as a function of the reduced frequency ($K=\omega B/U$). (a) Bridge type Br1, derivative set B1.A; (b) bridge type Br3, derivative set B1.B.

APPENDIX

TASK COMMITTEE REPORTS

Report of Task Committee A
GEOTECHNICAL ENGINEERING AND GROUND MOTION

Date: 14 May 2007

Place: National Institute for Land and Infrastructure Management, Tsukuba, Japan

Attendees:	U.S. Side --	Mehmet Celebi (Chair)	USGS
		Michael Sharp (Chair)	USACE
	Japan Side --	Keiichi Tamura (Chair)	NILIM
		Shojiro Kataoka	NILIM
		Shin Koyama	BRI
		Yasuhiro Shoji	NILIM

1. Objective and Scope of Work

The objectives of work include:

(1) To promote sharing of strong motion earthquake data among researchers and practicing engineers, and enhance the availability of technology for evaluating the destructive effects of earthquake motion, and

(2) To promote research on the dynamic behavior of soils, foundations and earth structures during earthquakes.

The scope of work includes:

(1) Exchange strong motion data regularly and identify significant issues.

(2) Exchange information on technological developments, state-of-the-art and practice related to strong motion recording, hazard mapping, soil-structure interaction, soil behavior and stability during earthquakes,

(3) Exchange field data related to geotechnical engineering, and

(4) Plan and conduct programs of cooperative research and/or workshops in coordination with the proposed or ongoing programs.

(5) Plan and form a cooperative post-earthquake survey team after a major event.

(6) Exchange information and conduct studies related to correlation of damage with ground motion.

2. Accomplishments

(1) The Fourth US-Japan Workshop on Soil-Structure Interaction was held in Tsukuba, Japan during March 28-30, 2007. This workshop was sponsored and hosted by BRI, and was also financially supported by USGS, USC and NSF. The work proceedings will be completed by the end of June 2007 and widely distributed. The workshop organizers were Dr. Okawa (BRI), Dr. Iiba (BRI), Dr. Todorovska (USC) and Dr. Celebi (USGS).

(2) The Japan-side Task Committee contributed to the issuing the Guidelines on Seismic Performance Verification of River Facilities (Draft), which include geotechnical works.

3. Future Plans

The future plans include:

(1) Plan a workshop on Real-Time Instrumentation of Densely Urbanized Areas and Instrumentation of Civil Engineered Structures including health monitoring. Temporary committee will include Dr. Fujiwara of NIED, Dr. Okawa of BRI, Mr. Shoji of NILIM, Dr. Borcherdt, Dr. Wald and Dr. Celebi of USGS. The committee will explore cooperation with other Task Committees.

(2) Explore the possibility of joint research and/or workshop on damage detection techniques. The responsible members will be Dr. Sugano (PARI), Dr. Todorovska and Dr. Celebi. Cooperation with

Task Committee B to have joint workshops will be explored.

4. Related Activities

(1) Dr. Eiji Kohama, Senior Research Engineer of the Port and Airport Research Institute (PARI) continues the research activities as a visiting researcher at the University of California, Berkeley (UCB).

(2) The Japan-side Task Committee members participated in the reconnaissance team organized by NILIM, PWRI, BRI and PARI in order to investigate damage to geotechnical works induced by the 2007 Noto Hanto Earthquake.

(3) Task Committee members and other invited seismologists and engineers will participate in a workshop on "Rotational Seismology and Engineering Applications" sponsored by USGS and to be held in Menlo Park, California during September 18-19, 2007.

Report of Task Committee B
NEXT-GENERATION BUILDING AND INFRASTRUCTURE SYSTEMS

Date: 14 May 2007

Place: National Institute for Land and Infrastructure Management, Tsukuba, Japan

Attendees:

U.S. Side -	Douglas Foutch (Co-Chair)	NSF
	Noël Raufaste (Acting Co-Chair)	NIST
	William Roper	GMU
	Josephne Malilay	CDC
	Fuyuen Yip	CDC
	Jennifer Rice	UI
Japan-side -	Takashi Kaminosono (Acting Co-Chair)	BRI
	Hiroshi Fukuyama (Co-Chair)	BRI
	Hitoshi Shiohara	Tokyo Univ.
	Taiki Saito	BRI
	Koichi Morita	BRI

1. Objective and Scope of Work

(1) Objective
The objectives of the Task Committee are to enhance the development and implementation of innovative and new 1) structural and non-structural materials; 2) enabling technologies such as structural health monitoring and multi-hazard performance based engineering; 3) evaluation, analysis, design, construction, and maintenance methods through cooperative individual and organized and networked analytical and experimental approaches for the next-generation building and infrastructure systems.
Opportunities during the next five years include topics on multi-hazard resilient buildings, embedded systems for the health and productivity of occupants, and collaborations with other researchers and practitioners.

(2) Scope-of-Work
a) Conduct joint workshops and joint meetings to identify research opportunities, new projects including multi-hazard risk reduction strategies and measures, and make recommendations for the UJNR Panel.
b) Encourage the development and application of new technologies, smart sensors, and intelligent materials to improve the health, safety, and productivity of construction workers and building occupants as well as reducing building impact on the environment.
c) Develop new materials and technologies for condition assessment, retrofit of existing buildings, and design of new buildings.
d) Coordinate development of databases, test procedures, and guidelines for interpretation of test results and their applications.
e) Coordinate joint research including the utilization of experimental facilities.
f) Enhance the exchange of information and personnel.

2. Accomplishments

(1) The key accomplishment was the Workshop on Technologies for Next Generation Buildings that initiated the Panel's charge for TCs to cluster with TC D, Wind Engineering, and TC I, Structural Fire Performance, and with other experts to improve productivity and reduce workshop costs (February 25-27, 2007).

(2) The Workshop resulted in a process to develop a five-year strategic research plan that addresses high-performance buildings' abilities to better resist the effects from extreme wind, earthquakes, and fire

loads and to effect informed decisions about design procedures that incorporate environmental quality and sustainability of occupant health and life cycle systems.

3. Future Plans

(1) Create an action plan (based on Figure 1) with targeted research activities, together with estimated schedule, milestones, and needed resources by fall of 2007. The plan will encourage cooperative research on infrastructure systems by partnering with TC G, Transportation Systems and other TCs.

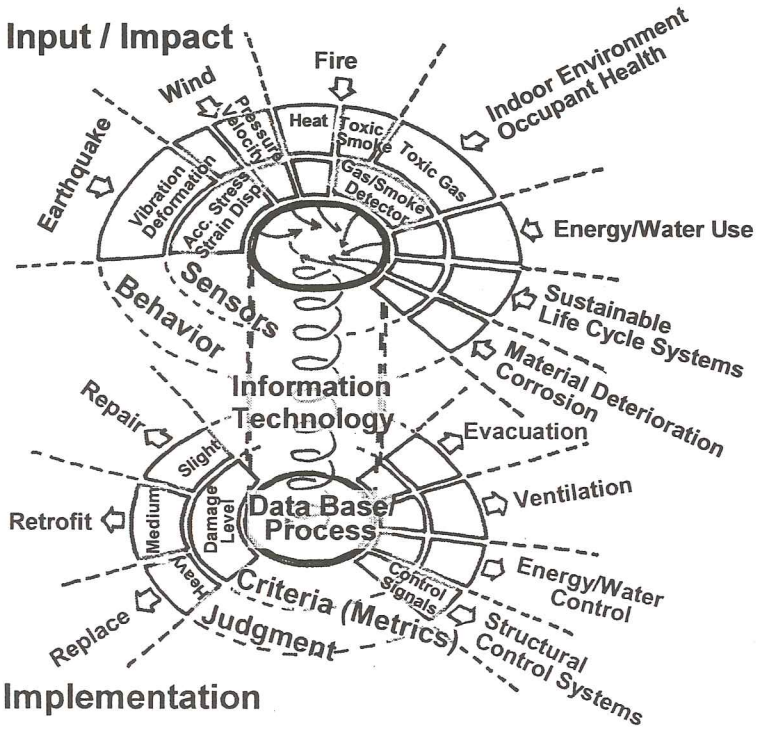

Figure 1

Diagram for creating high-performance buildings that better resist extreme winds, earthquakes, and fire loads resulting in informed decisions about design procedure incorporate environmental quality and sustainability of occupant health and life cycle systems. The initial TC focus is on sensors followed by subsequent actions to be determined during the next six months.

(1) Seek expanded membership from both sides with knowledge of sensors, information technology, and sustainability related expertise to collectively address technology for next generation buildings.

(2) Plan 2nd workshop with TC G, Transportation Systems, and other TCs as appropriate. Co-Chairs for TC B will contact Co-Chairs of other TCs to see if they are interested in partnering in this activity.

Report of Task Committee C
DAMS

Date: 14 May 2007

Place: National Institute for Land and Infrastructure Management, Tsukuba, Japan

Attendees:

U.S. Side --	Robert Hall (Chair)	USACE
	Anjana Chudgar	USACE
	Michael Sharp	USACE
	Victor Saouma	CU-Boulder
	Yusof Ghanaat	QUEST Structures
Japan Side --	Yoshikazu Yamaguchi (Chair)	PWRI
	Hitoshi Yoshida	PWRI
	Tomoya Iwashita	PWRI
	Hiroyuki Satoh	PWRI
	Kazuhito Shimamoto	NILIM

1. Objective and Scope of Work

To develop technical insights into better understanding of the response of dams to seismic effects, the T/C will plan, promote, and develop research initiatives to assist in assuring seismic safety and economical protective countermeasures against earthquake loading for these critical structures.

The scope of work includes:

(1) Develop methods of analysis for seismic design of dams including outlet works.
   a) Comparative analysis of design methods and evaluation criteria used by U.S. and Japan.
   b) Development of "Design Earthquake Ground Motions" for analysis and evaluation of dams.
   c) Assessment of models and numerical procedures used for seismic dynamic analysis.

(2) Perform research to better understand the dynamic characteristics of dam construction materials and site conditions.
   a) Strength and deformation characteristics of concrete, soil and rock materials during earthquakes.

(3) Evaluate observed performance of dams and outlet works during earthquakes.
   a) Develop a database that contains measured ground accelerations and dynamic response of dams and outlet works during earthquakes, and other related information necessary to evaluate their seismic behavior, such as experimental and/or analytical data with description of test and analysis procedures used.
   b) Investigation of damage mechanisms due to earthquake loading.
   c) Application of the analysis of the observed dynamic behavior to the improvement of design criteria.

2. Accomplishments

(1) Technical exchange and collaborative research on "***Non-linear response analysis of concrete dams***" has been conducted between the U.S. (U.S. Army Engineer Research and Development Center) and Japan (Public Works Research Institute). The non-linear response analyses were made using the results of the shaking table experiments for concrete dam models at PWRI in 2006. Both the U.S. Army Corps of Engineers and the U.S. Bureau of Reclamation have recently conducted similar tests at different scales and non-linear response analyses, and the joint comparison and evaluation of test and analysis results will be extremely beneficial to advance the state of the art in constitutive modeling of mass concrete structures.

(2) Technical exchange and collaborative research on "***Experimental characterization of non-linear tensile behavior of mass concrete***" has been conducted between U.S. (U.S. Army Engineer Research and Development Center & U.S. Bureau of Reclamation) and Japan (Public Works Research Institute).

3. Future Plans

(1) The Task Committee will hold the "***4th U.S.-Japan Workshop on Advanced Research on Dams***" on May 17, 2007 in Tsukuba, Japan. The main themes for the Workshop are non-linear response analyses and shaking table tests for concrete dams.

(2) The Task Committee will continue the current efforts focused on the development of improved mechanisms to facilitate the continuous exchange of results of research activities and general technical information related to dam earthquake engineering.

(3) The Task Committee will coordinate exchange visits of scientists and engineers from the U.S. and Japan. A series of case histories of mutual interest will be identified and prioritized and they will serve as the focus for this exchange program.

(4) The Task Committee will promote the development of joint research programs. The following topics have been identified as areas for future collaborative research:

a) ***Non-linear response analysis of concrete dams:***
The Task Committee will continue their collaboration in this research to include both analytical and experimental data.

b) ***Global stability analysis of concrete dams:***
The Task Committee will conduct a review of the minimum requirements for sliding and overturning stability currently in use in the U.S. and Japan. The Task Committee recognizes the importance of this collaborative effort, as the corresponding guidelines are currently subject to revision and update both in the U.S. and Japan. The results of this effort will be summarized and published. "***Engineer Manual No. 1110-2-2100: Stability Analysis of Concrete Structures***" published by The U.S. Army Corps of Engineers in December 2005 (4. (2)) contains this problem.

c) ***Criteria for seismic analysis progression:***
The Task Committee will review and compare the state of practice in the U.S. and Japan regarding current recommendations for progression of seismic analysis based on stages of increasing complexity. The results of this effort will be summarized and published.

d) ***Seismic evaluation of embankment dams:***
The Task Committee will review criteria and guidelines for post-earthquake stability and deformation analysis of embankment dams. The results of this effort will be summarized and published.

e) ***Dam-foundation interaction:***
The Task Committee will develop collaborating research efforts to review and develop improved numerical models for dam-foundation interaction.

The activities corresponding to the four areas indicated above will be addressed sequentially and the corresponding schedule will depend on the progress of the corresponding guidance documents, some of which are currently under discussion, development and/or review in the U.S. and Japan.

(5) Following large earthquakes in the U.S. or Japan, the Task Committee will assemble a joint reconnaissance team to investigate the performance of concrete dams, earth and rockfill dams, and outlet works.

4. Related Activities

(1) The Ministry of Land, Infrastructure and Transport, Japanese Government completed the ***"Guidelines for Seismic Safety Evaluation of Dams (Draft)"*** in March 2005. This document was applied to four existing dams during the fiscal year of 2005 and three other existing dams during the fiscal year of 2006 in order to verify and revise it.

(2) The U.S. Army Corps of Engineers has published the ***"Engineer Manual No. 1110-2-2100: Stability***

***Analysis of Concrete Structures*"** in December 2005. This document contains new criteria for stability analysis of concrete gravity structures.

(3) The U.S. Bureau of Reclamation published the ***"Research Topics to Validate the Seismic Response of Dams"***, whose object is to compile and independent list of research topics to validate the seismic response of dams, in January 2007.

Report of Task Committee D
WIND ENGINEERING

Date: 14 May 2007

Place: National Institute for Land and Infrastructure Management, Tsukuba, Japan

Attendees:			
	U.S. Side --	Joseph Main (Acting Co-Chair)	NIST
		Partha Sarkar	Iowa State University
		Luca Caracoglia	Northeastern University
	Japan Side --	Yasuo Okuda (Co-Chair)	BRI
		Jun Murakoshi (Co-Chair)	PWRI
		Masaaki Togashi	MRI
		Hitomitsu Kikitsu	BRI
		Yasushi Josen	PWRI

1. Objective and Scope of Work

To exchange technical information and to jointly plan, promote, and foster research and dissemination, in order to improve understanding of wind and its effects on structures, to establish more rational wind-resistant design procedures for structures, and to contribute collaboratively and synergistically to wind hazard mitigation. Specific objectives for the Task Committee include:

(1) Strategically and collaboratively, identify research needs in wind hazard mitigation in the areas of new technology, basic and applied research in wind and structural engineering, and in social and economic impacts of wind events.
(2) Facilitate cooperation and collaborative research between U.S. and Japanese researchers in wind engineering.
(3) Identify and exchange successes in wind engineering and wind hazard mitigation.

The scope of the US-Japan collaboration includes:

(1) Characterization of strong wind, especially boundary layer extreme winds.
(2) The study of wind effects including wind loading on and wind-induced response of structures.
(3) Performance of experimental and analytical research to predict wind effects.
(4) Performance of damage surveys, and wind hazard and risk assessments.
(5) Development of new technologies for wind hazard mitigation.

2. Accomplishments

(1) The 4th US-Japan Workshop titled as "New Challenges for Reduction of High-Wind Disasters" was held in Tsukuba on July 20-22, 2006. In the workshop, 29 researchers and engineers (U.S.:12, Japan:17) participated and 21 technical papers were presented on the issues of the prediction of disaster from wind, the influence of strong wind on buildings and bridges, and so on. The proceedings of the workshop were printed by BRI and PWRI in March 2007.
(2) A second phase of comparative analysis in the inter laboratory study of wind loading on low industrial buildings was initiated by Prof. Bogusz Bienkiewicz of Colorado State University following the 4th US-Japan Workshop. It was observed that different target empirical models for turbulence intensity were used by the participating laboratories, resulting in significant variability in the turbulence intensity, particularly for suburban terrain. This helps to account for the previously observed variability in point pressures and bending moments. These results are being presented by Joseph Main of NIST at the 39th UJNR Panel Meeting.
(3) A second phase of wind tunnel tests on streamlined and rectangular bridge deck sections were completed recently at Iowa State University (ISU) as part of the benchmark study on flutter

derivatives that was initiated at the 3rd U.S.-Japan workshop on wind engineering in 2002. Both free and forced-vibration tests were performed. Participants included Prof. Partha Sarkar and Prof. Fred Haan (ISU) and Prof. Luca Caracoglia (Northeastern University). Results were compared with those from PWRI (Dr. Hiroshi Sato) and Kyoto University (Prof. Masaru Matsumoto) and were presented at the 39th UJNR Panel Meeting.

3. Future Plans

(1) As a follow-up to the 4th U.S.-Japan Workshop on "New Challenges for Reduction of High-Wind Disasters" held in Tsukuba in July 2006, the 5th U.S.-Japan Workshop on Wind Engineering will be held in U.S. in fall 2009 or on January or February 2010.

(2) Seek additional opportunities to pursue collaborative research on the following topics:
   a) Wind characteristics and wind hazard mitigation.
      i) Wind characteristics in complex terrains.
      ii) Validation of wind models with full-scale data (opportunities for joint field studies).
      iii) Arrange for the hosting of colleagues interested in participating in quick-response post-storm damage assessments.
   b) Wind effects on buildings.
      i) Development of reliable and consistent aerodynamic loads and probabilistic methodologies for performance-based structural design.
      ii) Comparison of wind tunnel data sets and CFD results to full-scale measurements.
   c) Wind effects on bridges
      i) Prediction and mitigation of wind-induced vibration of stay cables.
      ii) Establish guidelines, criteria, and formats for sharing data from full-scale measurements, and identify potential collaborative instrumentation opportunities.
   d) Evolving Technologies
      i) Jointly evaluate need and costs, and to share preliminary investigation results relative to next-generation wind tunnels for the simulation of non-stationary winds (straight-line, tornado and microburst).
      ii) Structural control

(3) Exchange technical information on the following topics
   a) Wind characteristics and wind hazards
   b) Wind pressures, loadings and performance of buildings
   c) Wind-induced response of flexible, cable-suspended bridges and their components
   d) New prediction and mitigation techniques for wind effects

(4) Investigate opportunities for technical collaboration on the following topics
   a) Distribution of airborne chemical and biological agents
   b) Development of a distribution model for volcanic gas and dust
   c) Collaboration with fire engineering researchers by making use of unique facilities: Fire Research Wind Tunnel and Wind and Rain Test Laboratory
   d) Consider development of a compendium listing of relevant resources and facilities for wind engineering research

(3) Engage in more regular interaction and communication among Task Committee members. Use email (e.g., bi-monthly updates on activities) and exchange visits between full Panel meetings was suggested as a means of facilitating and coordinating collaborative activities.

(4) Continue to improve process, mechanisms, and funding for interaction on reconnaissance teams after future hurricane/typhoon impacts.

(5) Strategically and collaboratively construct a vision and plan for wind engineering research needs for the next decade, and formulate collaborative activities around those plans.

Report of Task Committee G
TRANSPORTATION SYSTEMS

Date: 14 May 2007

Place: National Institute for Land and Infrastructure Management, Tsukuba, Japan

Attendees:			
	U.S. Side --	W. Phillip Yen (Chair)	FHWA
		David Sanders	University of Nevada, Reno
	Japan Side --	Jiro Fukui (Chair)	PWRI
		Kazuhiko Kawashima	Tokyo Institute of Technology
		Shoichi Nakatani	PWRI
		Takashi Tamakoshi	NILIM
		Shigeki Unjoh	PWRI

1. Objective and Scope of Work

The objectives of work include:

(1) To plan, promote and foster research on the behavior of transportation facilities when subjected to wind and seismic forces, and

(2) To disseminate research results and provide specifications and guidelines based on the Task Committee's findings.

The scope of work includes:

(1) To investigate existing and new bridges design, the behavior of whole bridge systems and/or single component of a bridge without limitation on their size and function.

2. Accomplishments

(1) The 22nd US-Japan Bridge Engineering Workshop was held during 23 - 25 October 2006, at Seattle, WA, US. 24 U.S. and 24 Japanese participants attended the workshop. 41 technical papers were presented and discussed on the following main topics: a) Geotechnical Engineering, b) Health Monitoring and c) Advanced Seismic Technologies.

(2) The proceedings of the 22nd US-Japan Bridge Engineering Workshop were printed and will be distributed in May 2007. The program and papers of the workshop will be posted on the web-site of the UJNR at the PWRI (http://www.pwri.go.jp/eng/ujnr/tc/g/tc_g.htm)

(3) Both side conducted post earthquake damage evaluation studies, and the information has been exchanged.

3. Future Plans

(1) The 23rd US-Japan Bridge Engineering Workshop will be held in fall of 2007 in Japan. Specific program and itinerary will be proposed by the Japan-side Task Committee G with the concurrence of the US-side Task Committee. Main topics will be a) Seismic engineering, including damage assessment and prediction, b) Codes for new design and retrofit, including long term performance objectives and c) Multiple hazards, including design concepts and extreme events.

(2) Both sides agreed to develop and publish an accomplishment report of the past activities of Task Committee G.

(3) Following a devastating earthquake or hurricane (typhoon) in the US or Japan, the committee will form a joint reconnaissance team to investigate the performance of transportation systems.

(4) Exchange technical information on the following topics:

a) Seismic design and retrofit of highway bridges including the development of seismic response modification devices, smart materials, seismic retrofit for long-span bridges, and the development of damage evaluation methods using sensor systems.

b) Seismic and aerodynamic response of long-span bridges including suspension and cable stayed bridges, with emphasis on behavior of composite materials, cable inspection, vibration control, and corrosion protection.

(5) Both sides agreed to pursue the following two research topics as cooperative studies.

a) Performance Criteria – Limit States
- Relationship between performance criteria and structural response
- Relationship between damage and loss of function
- Realistic performance criteria
- Philosophical framework for Performance-based design and assessment

b) Three Dimensional Effects
- Effect of multi-dimensional input on superstructure and substructure
- Simplified, effective 3D modeling
- Total failure analytical modeling

And encourage the following research themes and share information:

a) High-performance materials
b) Input ground motion
c) Foundation – soil –structure systems
d) Assessment of component and system uncertainty
e) Seismic intervention
f) Size effects testing
g) Sequential failure of bridge systems

4. Related Activities

(1) Both side's committee members are participating NIED/NEES cooperative experimental research in full scale Bridge Column shaking table tests.

(2) FHWA will conduct a workshop on " Accelerated Bridge Construction Technology in Seismic Area" in spring, 2008.

Report of Task Committee H
STORM SURGE AND TSUNAMI

Date: 14 May 2007

Place: National Institute for Land and Infrastructure Management, Tsukuba, Japan

Attendees:

U.S. Side --	Solomon Yim (Chair)	OSU
Japan Side --	Takashi Tomita (Chair)	PARI
	Masaya Fukuhama	NILIM
	Katsuya Oda	NILIM
	Nadao Kohno	MRI

1. Objective and Scope of Work

The objectives of work include:

(1) To exchange scientific and technical information
(2) To jointly plan, promote and foster research and dissemination of knowledge
(3) To develop measures to prevent and mitigate damages from storm surges and tsunamis

The scope of work includes:

(1) Perform joint research on storm surge and tsunami occurrences, generation, propagation, and coastal effects. Develop database on storm surge, tsunami and wave measurements.
(2) Improve coordination of strategies and systems for observations of tsunamis and storm surges by field surveys, satellites, and in-situ measurements.
(3) Exchange results and status of storm surge and tsunami mitigation activities including analysis of the problem, planning, warning, and engineering approaches.
(4) Exchange information on development of technologies such as numerical models to predict propagation processes, land-fall locations, inundation and run-up heights, and wave characteristics, improved instrumentation, and use of satellite communication for detection and warning.
(5) Facilitate research result and technology development disseminations through exchange of literature, technical reports at joint meetings, special workshops, joint projects, and direct interaction among participants.
(6) Develop planning, design and construction guidelines in storm surge and tsunami flooding zones to serve as a model for international standards.
(7) Provide technical support to develop storm surge and tsunami mitigation programs worldwide.
(8) Encourage conduct of joint investigation following storm surge and tsunami events.

2. Accomplishments

(1) The 3rd International Workshop on Coastal Disaster Prevention was held on February 12-13, 2007 in Colombo, Sri Lanka organized by Port and Airport Research Institute (PARI), Coastal Development Institute of Technology (CDIT) and Ministry of Land Infrastructure and Transport (MLIT) in the Japan side, and University of Moratuwa, National Science Foundation and Disaster Management Centre in the Sri Lanka side. The Panel on Wind and Seismic Effects of UJNR supported the workshop together with the Japanese Section of International Navigation Association. Researchers and practitioners attended the workshop including the following: John R. Headland (Moffatt & Nichol Engineers, USA), Solomon Yim (Oregon State University, USA), Taro Arikawa (PARI, Japan), Koji Fujima (National Defense Academy, Japan), Yoshiyuki Kaneda (Japan Agency for Marine-Earth Science and Technology, Japan), Kentaro Kumagai (National Institute for Land and Infrastructure Management, Japan), Susumu Murata (CDIT, Japan), Yuji Nishimae (JMA, Japan), Shigeo Takahashi (PARI, Japan), Takashi Tomita (PARI, Japan), Subandono Diposaptono

(Ministry of Marine Affairs and Fisheries, Indonesia), Jose Miguel Montoya Rodriguez (Mexican Institute of Transport, Mexico), W.P.S. Dias (University of Moratuwa, Sri Lanka), S.S.L. Hettiarachchi (University of Moratuwa, Sri Lanka), Saman P. Samarawickrama (University of Moratuwa, Sri Lanka), and Ahmet C. Yalciner (Middle East Technical University, Turkey). Participants of 273 gathered from 13 countries: Greece, Indonesia, Japan, Malaysia, Maldives, Mexico, Myanmar, Philippine, Sri Lanka, Thailand, Turkey, USA, and Vietnam. After the workshop, Tsunami Hazard Map Seminar was continuously held in the same place.

(2) A US National Workshop on Tsunami Research Plan was held on July 25-26, 2006 in Corvallis, OR, USA organized by the US side co-chairs, Eddie Bernard of National Oceanographic and Atmospheric Administration (NOAA) and Solomon Yim of Oregon State University. It was co-sponsored by NOAA and the US National Science Foundation (NSF). Participants include all US side Storm Surge and Tsunami Task Committee members, Solomon Yim (OSU), Eddie Bernard (NOAA), Michael Briggs (USACE), Frank Gonzalez (NOAA), Laura Kong (ITIC), Philip Liu (Cornell University), and Harry Yeh (OSU). The Japan side chair, Takashi Tomita (PARI), was invited as a special participant (but was unable to attend due to prior a commitment).

3. Future Plans

(1) Create joint research between the US and Japan to develop and improve numerical models of storm surge and tsunami dynamics and to exchange experimental and field data. The following topics have been identified as areas of future research collaboration on storm surges and tsunamis:
   (a) field observation
   (b) characterization
   (c) physical experiment models
   (d) numerical simulation models
   (e) effects on coastal structures and damage estimations
   (f) design of protective structures for different levels
   (g) hazard maps development and warning system design
   (h) tsunami and storm surge information communication and warning systems development
   (i) risk assessment including hazard beyond designed levels

(2) Develop database for existing and planned experiments including description and parameters of experiments to maximize overall available experimental data for understanding of physical behavior, numerical model validation and structural design.

(3) Include the effects of global warming on atmospheric and oceanographic environmental conditions leading to changes in the probability of occurrence and intensity of typhoons, cyclones and hurricanes, and sea level rise. These changes in typhoon and sea level characteristics will directly influence the characteristics and induced damages of future storm surges and tsunamis.

(4) Hold the 4th International Workshop on Coastal Disaster Prevention in Japan, in fall 2007.

(5) The US side co-chair, Dr. Solomon Yim, will contact the co-chair, Dr. Eddie Bernard and the US side co-chair of T/C D, Mr. John Gaynor, regarding the study of storm surge, and the US side chair of T/C G, Dr. Phillip Yen, regarding storm surge and tsunami effects on bridges.

4. Related Activities

(1) Drs. Tomita and Yim participated in the UJNR post workshop technical tour of New Orleans and visited hurricane and storm surge damaged levees and residential areas on May 18-20, 2006.

(2) Drs. Tomita and Yim jointed the PIANC (International Navigation Association), MarCom Working Group 53 on "Recommendations with regard to the design and construction of maritime structures in tsunami prone areas." Dr. Yim participated in the 2nd meeting of the working group held on February 14, 2007 in Colombo, Sri Lanka.

(3) Drs. Tomita and Yim jointed the Tsunami Hazard Map Seminar which was held on February 14, 2007 in Colombo, Sri Lanka and which was organized by Ministry of Land, Infrastructure, and

Transport, Japan and Port and Airport Research Institute. In the Seminar, Dr. Tomita had a presentation on "Hazard Map to Build the Understandings and Awareness of Tsunami Disasters."

(4) Japan side T/C members have cooperative research activities in Technical Committee on Technologies to Estimate and Reduce Tsunami Damages, Japan Society of Civil Engineers.

(5) Drs. Yim and Yeh participated in a *NEES Training and Tsunami Modeling Workshop* hosted at Oregon State University, Corvallis, OR, on July 27-28, 2006.

(6) Dr. Tomita hosted the Workshop on Tsunami Disaster Mitigation on August 1-11, 2006 under the auspices of the Ministry of Land, Infrastructure and Transport, Japan and Port and Airport Research Institute. Researchers and practitioners participated including those from India, Indonesia, Maldives, Sri Lanka and Thailand, countries that suffered major damages from the 2004 Indian Ocean Tsunami.

(7) Dr. Yim conducted a survey of the damages of the Port of Crescent City and the Del Norte County, CA, on November 17-19, 2006.

(8) Dr. Yeh hosted and Drs. Yim and Philip Liu attended the *NSF Tsunami Workshop*, Hilo, HI, on December 26-28, 2006.

(9) Dr. Tomita participated in the 4th meeting of ASEAN-Japan Port Technology Group (PTG) on February 14, 2007 in Colombo, Sri Lanka, in order to discuss on tsunami hazard mapping in the affected countries by the 2004 Indian Ocean Tsunami and ASEAN countries, The PTG is in the ASEAN+Japan Transport Partnership Program of ASEAN+Japan Comprehensive Economic Partnership.

(10) Japan side T/C members contributed to the amendment of the technical standards for port and harbor facilities in which tsunami and storm surge protection function of breakwater was introduced and required performance were prescribed (the Ministerial Ordinance, the Notification and commentaries on them, enforced on April 1, 2007).

(11) Dr. Yim gave an invited presentation at the *Oregon Department of Transportation Bridge Design Conference,* in Salem, OR, on May 9, 2007 on "Tsunami Loads on Coastal Structures: A Case Study of Spencer Creek Bridge."

Report of Task Committee I
FIRE PERFORMANCE OF STRUCTURES

Date: 14 May 2007

Place: National Institute for Land and Infrastructure Management, Tsukuba, Japan

Attendees:

U.S. Side --	H. S. Lew (Acting Co-Chair)	NIST
	Stephen A. Cauffman (Acting Co-Chair)	NIST
Japan Side --	Mamoru Kohno (Co-Chair)	NILIM
	Tomohiro Naruse	NILIM

1. Objective and Scope of Work

The objectives of work include:

(1) Increase the availability of technology for evaluating the methods of fire/structural interaction that will be used to improve the performance of structures under fire loads.

(2) Promote post disaster investigations of fires following natural and technological disasters that enhance the Panel's core competencies in structural fire technologies.

(3) Encourage the development and sharing of research findings among the world's researchers and practitioners on the behavior of structural systems to fires.

The scope of work includes:

(1) Plan and conduct workshops and cooperative research on topics that improve the understanding of fire growth and service life predictions of the performance of structural components to fire loading.

(2) Exchange data on the performance of structural systems and components to fires and related modeling and simulation analyses.

(3) Exchange information on technological developments, state-of-art and practice related to the control of fire spread in buildings.

(4) Exchange information on technological developments related to the performance of structures exposed to fires.

(5) Exchange data on large fire analysis from natural and technological disasters to accurately simulate fire initiation and growth in urban environments.

(6) Develop the technical bases to revise structural-fire related codes, standards, and practice.

2. Accomplishments

(1) Added new members to the U.S. side: Prof. Paul Des Jardin Department of Mechanical Engineering State University of New York at Buffalo, Prof. Jay Gore Associate Dean of Engineering for Research and Entrepreneurship Purdue University West Lafayette.

(2) Planning for a TC workshop continued. Dr. Gross and Dr. Kohno have exchanged information for holding a workshop

3. Future Plans

The future plans include:

(1) Hold a workshop on Fire Performance of Structures in Japan during next 12 months. TC-I will explore a feasible mode of the workshop from such as physical meeting, web-based cyber meeting, or telecommunication. Possible topics for the workshop include:

- Current status of performance-based fire safety engineering. Japanese and U.S. experiences.

- Next generation design requirements. Reconstruction of performance requirements, and available and needed performance verification techniques.
- Evaluation of fire performance of existing steel and reinforced concrete structures including reality of connections and their expected performance in fire.
- Validation of numerical analysis methods by detailed simulations or full-scale experiments.
- Simplified calculation methods for predicting fire performances.
- Egress requirements for people with disabilities.

(2) Share Task Committee findings with the international research community.
(3) Explore the feasibility of creating a bi-lateral survey team to investigate fire-structure damage after major natural/technological disaster.

4. Related Activities

Collaborations ongoing between U.S. (NIST) and Japan (BRI) in Fire Spread at the Wildland-Urban Interface. Several U.S. researchers visited BRI and conducted fire wind tunnel tests.

NIST leads the Proficiency Testing of gypsum/steel stud walls according to ASTM E 119/ISO 834. Four Japanese testing laboratories have joined the program. TC-I is interested in the program and is exchanging information with them.

TECHNICAL SITE VISITS

HIGHLIGHTS OF THE TECHNICAL SITE VISITS

Technical Site Visits 17-19 May

1. Tokyo Metropolitan Expressway Route

The Metropolitan Expressway Company Limited, a privatized organization in 2005, is responsible for design, construction and management of Tokyo's Metropolitan Expressway. The delegation was briefed on investigation and techniques used to repair fatigue cracks in expressway steel bridge piers and orthotropic steel decks. Fatigue cracks are detected by magnetic particle testing procedure. Of 2011 piers tested, 566 had fatigue cracks. As temporary measure, holes are drilled at each end of the crack to prevent propagation of cracks that allowed traffic flow until permanent repairs. Monitoring is performed following a five year inspection plan. When visual inspection identifies serious cracks, annual inspections are performed for those selected fatigue cracks.

Modern Tokyo transportation relies on multiple highways that overlay the extinct canals and waterway systems of near the end of the Edo period (1603 – 1868). The delegation visited the Ohashi Junction of the Central Circular Shinjuku Route under construction designed to allow vehicles to pass through the central part of Tokyo by avoiding surface traffic congestion. A double loop reinforced concrete spiral ramp system is being constructed to connect the underground expressways with elevated highways. Completion of this Central Route is expected to reduce about half of the congestion on the expressways and expected to significantly reduce carbon dioxide emissions. The construction cost of the junction is $200 million.

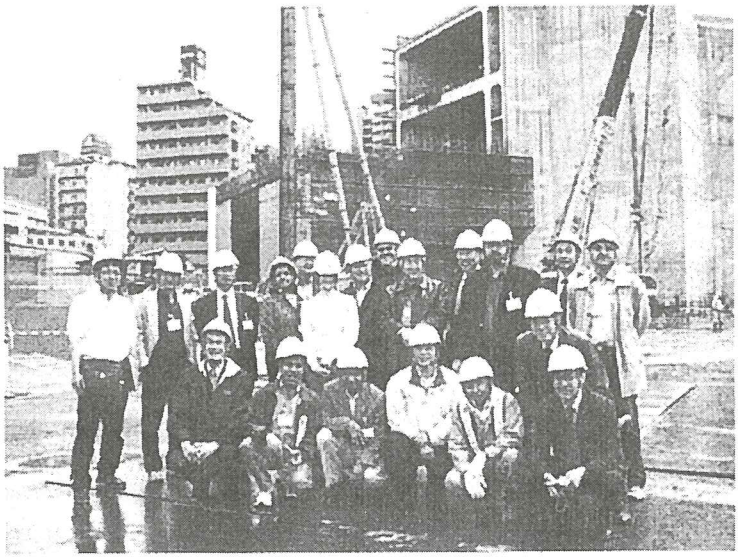

Figure 1: Group photo of members of the Panel Delegation at construction site of the Ohashi Junction of the Central Circular Shinjuku Route, Tokyo Metropolitan Expressway

2. Seismic Retrofit Project of Lower Murayama-Shimo Reservoir Dam (Tokyo Metropolitan Government Bureau of Waterworks).

This reservoir along with the nearby Yamaguchi and Murayama-Kami Reservoirs were built between 1916 and 1934. The dam for the Murayama-Shimo Reservoir is 587 m long and is an earthfilled dam (33 m high) made by compacting materials such as clay and sand. After the Great Hanshin-Awaji Earthquake in 1995, the dam was checked for seismic stability. Since heavily populated residential areas are downstream and the reservoir is able to gravity feed several purification plants, it was determined to be critical to the Tokyo area. Therefore a detailed seismic study was done and strengthening was determined to be necessary.

The dam consists of a shell, core, bomb shield and a counter weight fill. The strengthening consisted of adding drainage, reinforcing the counter weight fill with geogrid and covering the crest of the dam with a cement-stabilized soil layer. The geogrid prevents sliding of the counter weight. The cover on the crest of the dam is to prevent failure of the top of dam during overtopping.

As part of the project, the reservoir was drained a minimum level so that strengthening could be done. A minimum level was maintained in order to sustain local wildlife. The project is to be completed by March 2009 at an estimated cost of $90 million.

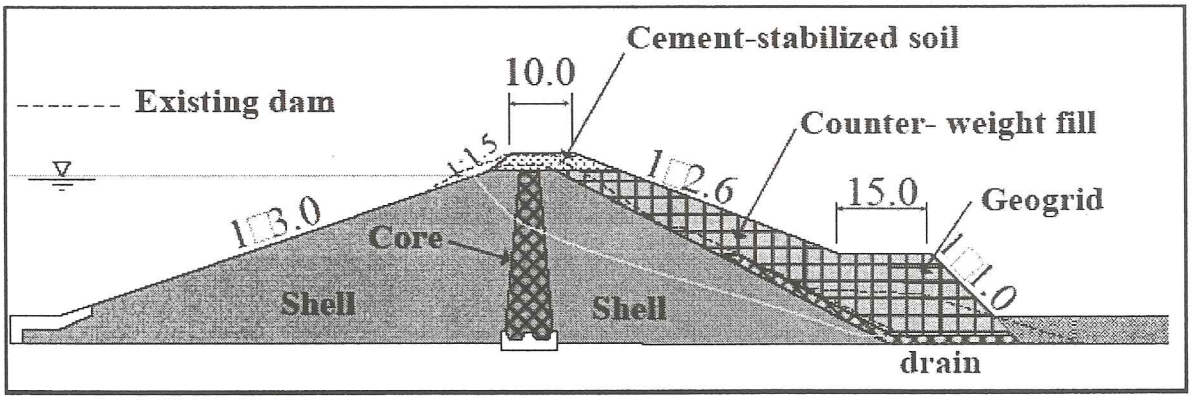

Figure 2: Dam strengthening (Courtesy, Tokyo Metropolitan Government Bureau of Waterworks)

3. Building Vibration Control System (Obayashi Corporation).

The delegation visited the thirty two story Shinagawa Intercity Tower A. The building is equipped with two unique Hybrid Mass Damper systems designed by the Technical Research Institute of Obayashi Corporation. The structure is 144.15 m tall with three basements, thirty stories and one penthouse.

The Hybrid Mass Damper (HMD) system is composed of three major components; 1) the Active Mass

Damper (AMD), 2) the Tuned Mass Damper (TMD) and 3) the Multi-Layer Laminated Rubber Bearings. In this application the HMD is secured above the AMD which is set on the passive mass of the TMD, supported with the Multi-Layer Laminated Rubber Bearing. The Multi-Layer Laminated Rubber Bearing has no frictional drag, and thus the TMD can move smoothly from a small external force level. The design also makes possible shifting smoothly from TMD to HMD according to the response level of the building.

The applied active control systems also make it possible to control multi-vibration modes including torsional modes of the building. The 200 ton TMD was tuned to the 1st natural frequency of the building. Methods were developed that allowed for a smooth transition between dampers based on the response of the building.

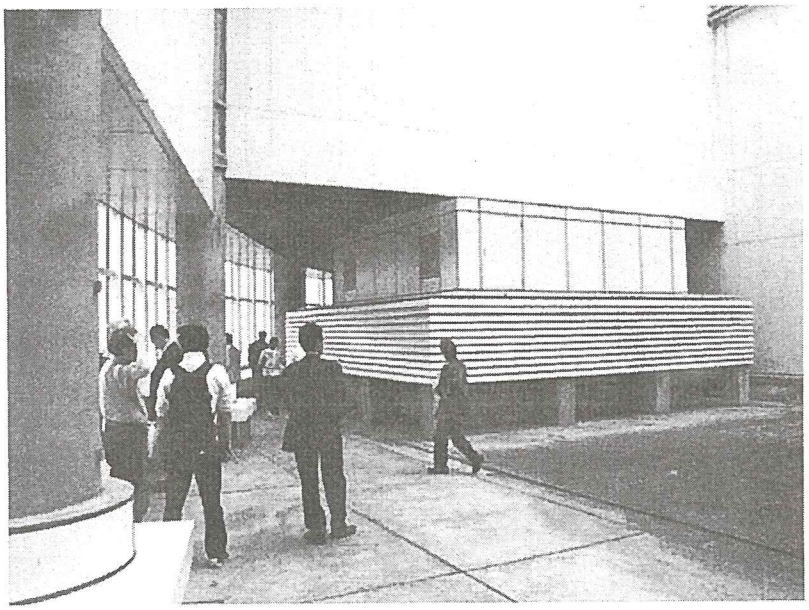

Figure 3: Members of the Panel Delegation are inspecting the Hybrid Mass Damper System in the Shinagawa Intercity Tower A Building

4. Karematsuzawa Bridge (Tohoku Regional Development Bureau).

The delegation visited the Karematsuzawa Bridge on the Sanriku National Highway under management of the Tohoku Regional Development Bureau near Kamaishi City, Iwate Prefecture. This 310 m long steel arch bridge, one of the longest arch bridges in Japan, was constructed over the gorge to straighten the 15 km section of a winding highway on steep topographic conditions. The bridge eliminated 46 sharp curves, and reduced a stretch of highway having a 9.6% grade to a 4% grade. The realigned highway and bridge significantly reduced vehicle accidents and driving time. The cost of this 15 km highway construction was $700 million.

The bridge's steel members were fabricated using weathering steel to reduce bridge maintenance. An issue that may exist is possible environmentally detrimental releases from steel's surface treatment or its interaction with adjoining materials. The delegation was briefed on the method (the cable erection method) used to construct the bridge over an 80 m deep gorge.

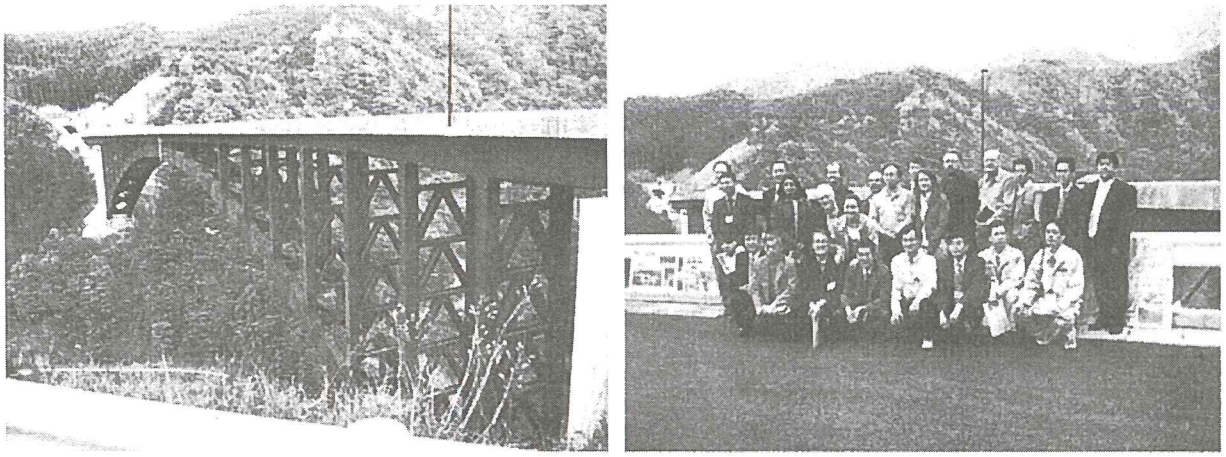

Figure 4: Overview of the Karematsuzawa Bridge (left) and group photo of members of the Panel Delegation at the site (right)

5. Kamaishi Port Tsunami Breakwater

The Pacific Ocean coast of Iwate Prefecture in northeast Honshu has a long history of tsunami attacks that have killed thousands of citizens and destroyed various coastal villages. The delegation visited Kamaishi Port to discuss the recently completed deep breakwater structure at the mouth of Kamaishi Bay with the representatives of the Kamaishi Port Office of the Port and Airport Department of Tohoku Regional Development Bureau. The planning of the breakwater started in 1978 and was completed in spring 2007. The breakwater consists of two dikes with a central opening for large ships. The dikes are comprised of trapezoidal and rectangular caissons. The total length of the breakwater system is 2260 m long. A second smaller breakwater (seawall) closer to the port harbor deflects remaining waves. The breakwater is the largest in Japan constructed in 63 m of water (the deepest water site in the world) with a 30 m high caisson designed with parallel slits to reduce wave force. Its 700 million ton base rock rubble foundation with armor stone layer on the outside face acts as a seismic countermeasure.